

Standard cover to be inserted

THREE BEAM TRANSITION CRASH TESTS

January 2005

**U.S. Department of Transportation
Federal Highway Administration**

FOREWORD

Numerous concrete bridge parapets and tubular bridge railings have been successfully crash tested and meet the current standards of National Cooperative Highway Research Program (NCHRP) *Report 350*.⁽¹⁾ Likewise, several guardrail systems have been tested to *NCHRP Report 350* guidelines and meet the requirements for placement on the National Highway System. The Federal Highway Administration (FHWA), in its continuing effort to promote and provide safer longitudinal traffic barriers for all the Nation's roadways, recognizes that more information is needed on the transitions between guardrails and bridge railings.

Seven transition designs were selected for this study by the State representatives for State Planning and Research (SP&R) Pooled Fund Study No. 2-134, "Testing New Bridge Rail and Transition Designs." The objective was to crash test and evaluate several transitions in accordance with National Cooperative Highway Research Program (NCHRP) *Report 350*.

Engineers and architects who design aesthetically compatible bridge structures will find this report useful.

Michael F. Trentacoste
Director, Office of Safety
Research and Development

Notice

This document is disseminated under the sponsorship of the U.S. Department of Transportation in the interest of information exchange. The U.S. Government assumes no liability for the use of the information contained in this document. This report does not constitute a standard, specification, or regulation.

The U.S. Government does not endorse products or manufacturers. Trademarks or manufacturers' names appear in this report only because they are considered essential to the objective of the document.

Quality Assurance Statement

The Federal Highway Administration (FHWA) provides high-quality information to serve Government, industry, and the public in a manner that promotes public understanding. Standards and policies are used to ensure and maximize the quality, objectivity, utility, and integrity of its information. FHWA periodically reviews quality issues and adjusts its programs and processes to ensure continuous quality improvement.

1. Report No. FHWA-RD-04-115		2. Government Accession No.		3. Recipient's Catalog No.	
4. Title and Subtitle Thrie Beam Transition Crash Tests				5. Report Date January 2005	
				6. Performing Organization Code	
7. Author(s) Dean C. Alberson, Wanda L. Menges, Roger P. Bligh, Akram Y. Abu-Odeh, C. Eugene Buth, and Rebecca R. Haug				8. Performing Organization Report No. 401021-F	
9. Performing Organization Name and Address Texas Transportation Institute The Texas A&M University System College Station, TX 77843-3135				10. Work Unit No. (TRAIS)	
				11. Contract or Grant No. DTFH61-00-C-00012	
12. Sponsoring Agency Name and Address Office of Safety and Traffic Operations Research and Development Federal Highway Administration 6300 Georgetown Pike McLean, VA 22101-2296				13. Type of Report and Period Covered Final Report: May 2000–April 2004	
				14. Sponsoring Agency Code	
15. Supplementary Notes Research Study Title: Thrie Beam Transition Crash Tests Name of Contracting Officer's Technical Representative (COTR): Mr. Charles F. McDevitt (HRDS-4)					
16. Abstract <p>The objective of this study was to crash test and evaluate these transitions according to requirements of <i>NCHRP Report 350</i>. The scope of this study is as follows: "This study will crash test a series of thrie beam transitions from guardrails to bridge rails in accordance with the appropriate test levels of National Cooperative Highway Research Program (<i>NCHRP Report 350</i>). These transition designs were selected by the State representatives for State Planning and Research (SP&R) Pooled Fund Study No. 2-134, "Testing New Bridge Rail and Transition Designs." The following transitions were tested under this project:</p> <ul style="list-style-type: none"> • Ohio Nonsymmetrical Type 2 W-beam to Thrie Beam Transition. <ul style="list-style-type: none"> < With 12-gauge nonsymmetrical transition section. < With 10-gauge nonsymmetrical transition section. • Ohio Type 1 Thrie Beam Transition to Concrete Parapet. <ul style="list-style-type: none"> < Type 1 without curb. < Type 1 with asphalt curb. • Thrie Beam Transition to Wisconsin Type "M" Tubular Steel Bridge Rail. • New York State Department of Transportation (DOT) Modified Box Beam Transition to Four-Rail Steel Bridge Rail. <p>All designs were tested to <i>NCHRP Report 350</i> Test Level 3, except the Ohio Type 1 Thrie Beam Transition to Concrete Parapet with Asphalt Curb, which was tested to Test Level 4.</p>					
17. Key Words Bridge rail, transition, thrie beam, guardrail, longitudinal barrier, aesthetic, crash testing, roadside safety			18. Distribution Statement No restrictions. This document is available to the public through the National Technical Information Service, 5285 Port Royal Road, Springfield, VA 22161		
19. Security Classif. (of this report) Unclassified		20. Security Classif. (of this page) Unclassified		21. No. of Pages 368	22. Price

SI* (MODERN METRIC) CONVERSION FACTORS

APPROXIMATE CONVERSIONS TO SI UNITS

Symbol	When You Know	Multiply By	To Find	Symbol
LENGTH				
in	inches	25.4	millimeters	mm
ft	feet	0.305	meters	m
yd	yards	0.914	meters	m
mi	miles	1.61	kilometers	km
AREA				
in ²	square inches	645.2	square millimeters	mm ²
ft ²	square feet	0.093	square meters	m ²
yd ²	square yard	0.836	square meters	m ²
ac	acres	0.405	hectares	ha
mi ²	square miles	2.59	square kilometers	km ²
VOLUME				
fl oz	fluid ounces	29.57	milliliters	mL
gal	gallons	3.785	liters	L
ft ³	cubic feet	0.028	cubic meters	m ³
yd ³	cubic yards	0.765	cubic meters	m ³
NOTE: volumes greater than 1000 L shall be shown in m ³				
MASS				
oz	ounces	28.35	grams	g
lb	pounds	0.454	kilograms	kg
T	short tons (2000 lb)	0.907	megagrams (or "metric ton")	Mg (or "t")
TEMPERATURE (exact degrees)				
°F	Fahrenheit	5 (F-32)/9 or (F-32)/1.8	Celsius	°C
ILLUMINATION				
fc	foot-candles	10.76	lux	lx
fl	foot-Lamberts	3.426	candela/m ²	cd/m ²
FORCE and PRESSURE or STRESS				
lbf	poundforce	4.45	newtons	N
lbf/in ²	poundforce per square inch	6.89	kilopascals	kPa

APPROXIMATE CONVERSIONS FROM SI UNITS

Symbol	When You Know	Multiply By	To Find	Symbol
LENGTH				
mm	millimeters	0.039	inches	in
m	meters	3.28	feet	ft
m	meters	1.09	yards	yd
km	kilometers	0.621	miles	mi
AREA				
mm ²	square millimeters	0.0016	square inches	in ²
m ²	square meters	10.764	square feet	ft ²
m ²	square meters	1.195	square yards	yd ²
ha	hectares	2.47	acres	ac
km ²	square kilometers	0.386	square miles	mi ²
VOLUME				
mL	milliliters	0.034	fluid ounces	fl oz
L	liters	0.264	gallons	gal
m ³	cubic meters	35.314	cubic feet	ft ³
m ³	cubic meters	1.307	cubic yards	yd ³
MASS				
g	grams	0.035	ounces	oz
kg	kilograms	2.202	pounds	lb
Mg (or "t")	megagrams (or "metric ton")	1.103	short tons (2000 lb)	T
TEMPERATURE (exact degrees)				
°C	Celsius	1.8C+32	Fahrenheit	°F
ILLUMINATION				
lx	lux	0.0929	foot-candles	fc
cd/m ²	candela/m ²	0.2919	foot-Lamberts	fl
FORCE and PRESSURE or STRESS				
N	newtons	0.225	poundforce	lbf
kPa	kilopascals	0.145	poundforce per square inch	lbf/in ²

*SI is the symbol for the International System of Units. Appropriate rounding should be made to comply with Section 4 of ASTM E380. (Revised March 2003)

TABLE OF CONTENTS

<u>Section</u>	<u>Page</u>
INTRODUCTION	1
PROBLEM	1
BACKGROUND	1
OBJECTIVES	2
TEST PARAMETERS	5
TEST FACILITY	5
TEST ARTICLES	5
TEST CONDITIONS	5
EVALUATION CRITERIA	5
OHIO THRIE BEAM TRANSITION AT THE 12-GAUGE NONSYMMETRICAL TYPE 2 TRANSITION SECTION	7
TEST ARTICLE—TEST 401021-4	7
CRASH TEST 401021-4 (NCHRP REPORT 350 TEST NO. 3-11)	8
Test Conditions	8
Test Vehicle	8
Soil and Weather Conditions	8
Impact Description	14
Damage to Test Article	14
Vehicle Damage	14
Occupant Risk Factors	19
Rail Instrumentation Results	19
Assessment of Test Results	19
Conclusions	22
OHIO THRIE BEAM TRANSITION AT THE 10-GAUGE NONSYMMETRICAL TYPE 2 TRANSITION SECTION	23
TEST ARTICLE—TEST 401021-6	23
CRASH TEST 401021-6 (NCHRP REPORT 350 TEST NO. 3-21)	24
Test Conditions	24
Test Vehicle	24
Soil and Weather Conditions	24
Impact Description	30
Damage to Test Article	30
Vehicle Damage	30
Occupant Risk Factors	35
Rail Instrumentation Results	35

TABLE OF CONTENTS (continued)

<u>Section</u>	<u>Page</u>
Assessment of Test Results	35
Conclusions	38
OHIO TYPE 1 THRIE BEAM TRANSITION TO CONCRETE PARAPET	39
TEST ARTICLE—TEST 401021-1	39
CRASH TEST 401021-1 (NCHRP REPORT 350 TEST NO. 3-11)	44
Test Conditions	44
Test Vehicle	44
Soil and Weather Conditions	44
Impact Description	47
Damage to Test Article	47
Vehicle Damage	47
Occupant Risk Factors	52
Rail Instrumentation Results	52
Assessment of Test Results	52
Conclusions	55
OHIO TYPE 1 THRIE BEAM TRANSITION TO CONCRETE PARAPET WITH ASPHALT CURB	57
TEST ARTICLE—TEST 401021-5 AND 2a	57
CRASH TEST 401021-5 (NCHRP REPORT 350 TEST NO. 3-11)	63
Test Conditions	63
Test Vehicle	63
Soil and Weather Conditions	63
Impact Description	63
Damage to Test Article	66
Vehicle Damage	66
Occupant Risk Factors	66
Rail Instrumentation Results	71
Assessment of Test Results	71
Conclusions	74
CRASH TEST 401021-2a (NCHRP REPORT 350 TEST NO. 4-22)	75
Test Conditions	75
Test Vehicle	75
Soil and Weather Conditions	75
Impact Description	79
Damage to Test Article	79
Vehicle Damage	79

TABLE OF CONTENTS (continued)

<u>Section</u>	<u>Page</u>
Occupant Risk Factors	84
Rail Instrumentation Results	84
Assessment of Test Results	84
Conclusions	87
THREE BEAM TRANSITION TO WISCONSIN	
TYPE “M” TUBULAR STEEL BRIDGE RAIL	89
TEST ARTICLE—TEST 401021-3	89
CRASH TEST 401021-3 (NCHRP REPORT 350 TEST NO. 3-21)	89
Test Conditions	89
Test Vehicle	89
Soil and Weather Conditions	106
Impact Description	106
Damage to Test Article	106
Vehicle Damage	109
Occupant Risk Factors	109
Results from Instrumentation of Test Article	109
Assessment of Test Results	112
Conclusions	115
COMPUTER SIMULATION OF THE NYSDOT BOX-BEAM TRANSITION	
AND MODIFIED BOX-BEAM TRANSITION	117
INTRODUCTION	117
TASK B1	117
TASK B2	120
TASK B3	125
TASK B4	131
Snagging Potential of Door Edge with Box-Beam Splice	132
Tire Interaction with Rub Rail	132
Vehicle Frame Rail Deformation	135
Sensitivity and Stochastic Issues	137
MODIFIED NYSDOT	
BOX-BEAM TRANSITION TO FOUR-RAIL BRIDGE RAIL	139
TEST ARTICLE—TEST 401021-7	139
CRASH TEST 401021-7 (NCHRP REPORT 350 TEST NO. 3-21)	143
Test Conditions	143
Test Vehicle	143

TABLE OF CONTENTS (continued)

<u>Section</u>	<u>Page</u>
Soil and Weather Conditions	148
Impact Description	148
Damage to Test Article	148
Vehicle Damage	151
Occupant Risk Factors	151
Assessment of Test Results	151
Conclusions	156
SUMMARY AND CONCLUSIONS	157
ASSESSMENT OF TEST RESULTS	157
Ohio Nonsymmetrical Type 2 W-Beam to Thrie Beam Transition	157
Ohio Type 1 Thrie Beam Transition to Concrete Parapet	157
Thrie Beam Transition to Wisconsin Type “M” Tubular Steel Bridge Rail	162
Modified NYSDOT Box-Beam Transition to Four-Rail Steel Bridge Rail	162
CONCLUSIONS	166
REFERENCES	167
APPENDIX A. CRASH TEST PROCEDURES AND DATA ANALYSIS	169
ELECTRONIC INSTRUMENTATION AND DATA PROCESSING FOR THE TEST INSTALLATION	169
ELECTRONIC INSTRUMENTATION AND DATA PROCESSING FOR THE TEST VEHICLE	178
ANTHROPOMORPHIC DUMMY INSTRUMENTATION	182
PHOTOGRAPHIC INSTRUMENTATION AND DATA PROCESSING	183
TEST VEHICLE PROPULSION AND GUIDANCE	183
APPENDIX B. TEST VEHICLE PROPERTIES AND INFORMATION	185
APPENDIX C. SEQUENTIAL PHOTOGRAPHS	205
APPENDIX D. VEHICLE ANGULAR DISPLACEMENTS AND ACCELERATIONS	227
APPENDIX E. RAIL INSTRUMENTATION TRACES	309

LIST OF FIGURES

<u>Figure</u>		<u>Page</u>
1	Details of the Ohio 12-gauge nonsymmetrical Type 2 thrie beam transition	9
2	Details of the Ohio 12-gauge nonsymmetrical Type 2 thrie beam transition—notes	10
3	Ohio transition before test 401021-4	11
4	Vehicle/installation geometrics for test 401021-4	12
5	Vehicle before test 401021-4	13
6	Vehicle trajectory path after test 401021-4	15
7	Installation after test 401021-4	16
8	Vehicle after test 401021-4	17
9	Interior of vehicle for test 401021-4	18
10	Details of the Ohio 10-gauge nonsymmetrical Type 2 thrie beam transition	25
11	Details of the Ohio 10-gauge nonsymmetrical Type 2 thrie beam transition—notes	26
12	Ohio nonsymmetrical transition before test 401021-6.	27
13	Vehicle/installation geometrics for test 401021-6	28
14	Vehicle before test 401021-6	29
15	Vehicle trajectory path after test 401021-6	31
16	Installation after test 401021-6	32
17	Vehicle after test 401021-6	33
18	Interior of vehicle for test 401021-6	34
19	Details of the Ohio Type 1 thrie beam transition	40
20	Details of the Ohio Type 1 thrie beam transition – sections B-B, C-C, and D-D . . .	41
21	Details of the Ohio Type 1 thrie beam transition—notes and bending diagrams . . .	42
22	Ohio Type 1 thrie beam transition before test 401021-1	43
23	Vehicle/installation geometrics for test 401021-1	45
24	Vehicle before test 401021-1	46
25	Vehicle trajectory path after test 401021-1	48
26	Installation after test 401021-1	49
27	Vehicle after test 401021-1	50
28	Interior of vehicle for test 401021-1	51
29	Details of the Ohio Type 1 thrie beam transition with asphalt curb	58
30	Details of the Ohio Type 1 thrie beam transition with asphalt curb —sections B-B, C-C, and D-D	59
31	Details of the Ohio Type 1 thrie beam transition with asphalt curb – bending diagrams, detail B, and section E-E	60
32	Details of Ohio Type 1 thrie beam transition with asphalt curb—notes	61
33	Ohio Type 1 thrie beam transition with asphalt curb before test 401021-5	62
34	Vehicle/installation geometrics for test 401021-5	64
35	Vehicle before test 401021-5	65
36	Vehicle trajectory path after test 401021-5	67
37	Installation after test 401021-5	68

LIST OF FIGURES (continued)

<u>Figure</u>		<u>Page</u>
38	Vehicle after test 401021-5	69
39	Interior of vehicle for test 401021-5	70
40	Ohio Type 1 thrie beam transition with asphalt curb before test 401021-2a	76
41	Vehicle/installation geometrics for test 401021-2a	77
42	Vehicle before test 401021-2a	78
43	Vehicle trajectory path after test 401021-2a	80
44	Installation after test 401021-2a	81
45	Vehicle after test 401021-2a	82
46	Interior of vehicle for test 401021-2a	83
47	Details of the Type “M” tubular steel bridge rail—section through railing and section A-A	90
48	Details of the Type “M” tubular steel bridge rail—section through post	91
49	Details of the Type “M” tubular steel bridge rail—anchor details	92
50	Details of the Type “M” tubular steel bridge rail—end post details	93
51	Details of the Type “M” tubular steel bridge rail—legend for drawing and general notes	94
52	Anchor details as tested	95
53	Details of the thrie beam transition approach—overall details	96
54	Details of the thrie beam transition approach—connection and splice details	97
55	Details of the thrie beam transition approach—beam and post detail	98
56	Details of the thrie beam transition approach—general notes	99
57	Details of thrie beam transition connection to bridge rail —backup plate and anchor plate detail	100
58	Details of thrie beam transition connection to bridge rail —anchor and backup plate mounting to bridge railing	101
59	Details of thrie beam transition connection to bridge rail —thrie beam connection to tubular railing	102
60	Wisconsin transition installation before testing	103
61	Vehicle/installation geometrics for test 401021-3	104
62	Vehicle before test 401021-3	105
63	Vehicle trajectory path after test 401021-3	107
64	Installation after test 401021-3	108
65	Vehicle after test 401021-3	110
66	Interior of vehicle for test 401021-3	111
67	Simulation setup	118
68	Snagging of door edge on box-beam splice	119
69	Closeup of door deformation with parts of transition and vehicle removed	119
70	Model of modified New York box-beam transition and C2500 pickup truck	121
71	Door edge contact with the rail splice	121

LIST OF FIGURES (continued)

<u>Figure</u>		<u>Page</u>
72	Hood snagging with first bridge rail post	122
73	Overall damage to vehicle	123
74	Model of modified New York box-beam transition and single-unit truck	123
75	Single-unit truck simulation without suspension failure	124
76	Unrealistic deformation of single-unit truck after axle separation	125
77	Setup for transition impact with the original CIP	126
78	Door edge at downstream end of expansion splice	127
79	Pickup truck simulation at 0.2 s	127
80	Vehicle damage profile after impact	128
81	Setup for pickup simulation at alternate impact location	128
82	Door edge at downstream edge of expansion splice for alternate impact location .	129
83	Vehicle damage profile after impact at alternate location	129
84	Position of front left tire due to the presence of curb	130
85	Model of latest NYDOT box-beam transition system	131
86	Interaction of door edge with box-beam expansion splice	132
87	Interaction of tire with bridge rail post baseplate (original design Task B1)	133
88	Downstream view of interaction of tire with bend in rail element and bridge rail post baseplate (original design, Task B1)	133
89	Downstream view of interaction of tire with bridge rail post baseplate (modified design, Task B4)	134
90	Interaction of tire with bridge rail post baseplate (modified design, Task B4)	135
91	Vehicle frame deformation—original system (Task B1)	136
92	Vehicle frame deformation—latest modified system (Task B4)	136
93	Pickup truck deformed shape at 180 ms	137
94	Details of the NYSDOT box-beam transition—overall details	140
95	Details of the NYSDOT box-beam transition—expansion splice details	141
96	Details of the NYSDOT box-beam transition—fixed splice details	142
97	NYSDOT box-beam transition before testing	144
98	Impact point for <i>NCHRP Report 350</i> test 3-21 on the NYSDOT box-beam transition	145
99	Vehicle/installation geometrics for test 401021-7	146
100	Vehicle before test 401021-7	147
101	Vehicle trajectory path after test 401021-7	149
102	Installation after test 401021-7	150
103	Vehicle after test 401021-7	152
104	Interior of vehicle for test 401021-7	153
105	Typical instrumentation setup on the rail for test 401021-4	171
106	Typical instrumentation setup on the rail for test 401021-6	172
107	Typical instrumentation setup on the rail for test 404201-1	173

LIST OF FIGURES (continued)

<u>Figure</u>		<u>Page</u>
108	Typical instrumentation setup on the rail for test 401021-5	175
109	Typical instrumentation setup on the rail for test 401021-2a	176
110	Typical instrumentation setup on the rail for test 401021-3	177
111	Vehicle properties for test 401021-4	185
112	Occupant compartment measurements for test 401021-4	187
113	Vehicle properties for test 401021-6	188
114	Occupant compartment measurements for test 401021-6	190
115	Vehicle properties for test 401021-1	191
116	Occupant compartment measurements for test 401021-1	193
117	Vehicle properties for test 401021-5	194
118	Occupant compartment measurements for test 401021-5	196
119	Vehicle properties for test 401021-2a	197
120	Vehicle properties for test 401021-3	198
121	Occupant compartment measurements for test 401021-3	200
122	Vehicle properties for test 401021-7	201
123	Occupant compartment measurements for test 401021-7	203
124	Sequential photographs for test 401021-4 (overhead view)	205
125	Sequential photographs for test 401021-4 (frontal view)	206
126	Sequential photographs for test 401021-4 (rear view)	207
127	Sequential photographs for test 401021-6 (overhead view)	208
128	Sequential photographs for test 401021-6 (frontal view)	209
129	Sequential photographs for test 401021-6 (rear view)	210
130	Sequential photographs for test 401021-1 (overhead view)	211
131	Sequential photographs for test 401021-1 (frontal view)	212
132	Sequential photographs for test 401021-1 (rear view)	213
133	Sequential photographs for test 401021-5 (overhead view)	214
134	Sequential photographs for test 401021-5 (frontal view)	215
135	Sequential photographs for test 401021-5 (rear view)	216
136	Sequential photographs for test 401021-2a (overhead view)	217
137	Sequential photographs for test 401021-2a (frontal view)	218
138	Sequential photographs for test 401021-2a (rear view)	219
139	Sequential photographs for test 401021-3 (overhead view)	220
140	Sequential photographs for test 401021-3 (frontal view)	221
141	Sequential photographs for test 401021-3 (rear view)	222
142	Sequential photographs for test 401021-7 (overhead view)	223
143	Sequential photographs for test 401021-7 (frontal view)	224
144	Sequential photographs for test 401021-7 (rear view)	225
145	Vehicular sign convention and orientation diagram	227

LIST OF FIGURES (continued)

<u>Figure</u>		<u>Page</u>
146	Vehicle angular displacements for test 401021-4	228
147	Vehicle longitudinal accelerometer trace for test 401021-4 (accelerometer located at center of gravity)	229
148	Vehicle lateral accelerometer trace for test 401021-4 (accelerometer located at center of gravity)	230
149	Vehicle vertical accelerometer trace for test 401021-4 (accelerometer located at center of gravity)	231
150	Vehicle longitudinal accelerometer trace for test 401021-4 (accelerometer located over rear axle)	232
151	Vehicle lateral accelerometer trace for test 401021-4 (accelerometer located over rear axle)	233
152	Vehicle vertical accelerometer trace for test 401021-4 (accelerometer located over rear axle)	234
153	Vehicle longitudinal accelerometer trace for test 401021-4 (accelerometer located on top surface of instrument panel)	235
154	Vehicle longitudinal accelerometer trace for test 401021-4 (accelerometer located on right front brake caliper)	236
155	Vehicle lateral accelerometer trace for test 401021-4 (accelerometer located on left front brake caliper)	237
156	Vehicle longitudinal accelerometer trace for test 401021-4 (accelerometer located on top of engine block)	238
157	Vehicle longitudinal accelerometer trace for test 401021-4 (accelerometer located on bottom of engine block)	239
158	Vehicle angular displacements for test 401021-6	240
159	Vehicle longitudinal accelerometer trace for test 401021-6 (accelerometer located at center of gravity)	241
160	Vehicle lateral accelerometer trace for test 401021-6 (accelerometer located at center of gravity)	242
161	Vehicle vertical accelerometer trace for test 401021-6 (accelerometer located at center of gravity)	243
162	Vehicle longitudinal accelerometer trace for test 401021-6 (accelerometer located over rear axle)	244
163	Vehicle lateral accelerometer trace for test 401021-6 (accelerometer located over rear axle)	245
164	Vehicle vertical accelerometer trace for test 401021-6 (accelerometer located over rear axle)	246

LIST OF FIGURES (continued)

<u>Figure</u>	<u>Page</u>
165	Vehicle longitudinal accelerometer trace for test 401021-6 (accelerometer located on top surface of instrument panel) 247
166	Vehicle lateral accelerometer trace for test 401021-6 (accelerometer located on right front brake caliper) 248
167	Vehicle longitudinal accelerometer trace for test 401021-6 (accelerometer located on left front brake caliper) 249
168	Vehicle longitudinal accelerometer trace for test 401021-6 (accelerometer located on top of engine block) 250
169	Vehicle longitudinal accelerometer trace for test 401021-6 (accelerometer located on bottom of engine block) 251
170	Vehicular angular displacements for test 401021-1 252
171	Vehicle longitudinal accelerometer trace for test 401021-1 (accelerometer located at center of gravity) 253
172	Vehicle lateral accelerometer trace for test 401021-1 (accelerometer located at center of gravity) 254
173	Vehicle vertical accelerometer trace for test 401021-1 (accelerometer located at center of gravity) 255
174	Vehicle longitudinal accelerometer trace for test 401021-1 (accelerometer located over rear axle) 256
175	Vehicle lateral accelerometer trace for test 401021-1 (accelerometer located over rear axle) 257
176	Vehicle vertical accelerometer trace for test 401021-1 (accelerometer located over rear axle) 258
177	Vehicle longitudinal accelerometer trace for test 401021-1 (accelerometer located on top surface of instrument panel) 259
178	Vehicle longitudinal accelerometer trace for test 401021-1 (accelerometer located on right front brake caliper) 260
179	Vehicle lateral accelerometer trace for test 401021-1 (accelerometer located on left front brake caliper) 261
180	Vehicle longitudinal accelerometer trace for test 401021-1 (accelerometer located on top of engine block) 262
181	Vehicle longitudinal accelerometer trace for test 401021-1 (accelerometer located on bottom of engine block) 263
182	Vehicular angular displacements for test 401021-5 264
183	Vehicle longitudinal accelerometer trace for test 401021-5 (accelerometer located at center of gravity) 265

LIST OF FIGURES (continued)

<u>Figure</u>	<u>Page</u>
184	Vehicle lateral accelerometer trace for test 401021-5 (accelerometer located at center of gravity) 266
185	Vehicle vertical accelerometer trace for test 401021-5 (accelerometer located at center of gravity) 267
186	Vehicle longitudinal accelerometer trace for test 401021-5 (accelerometer located over rear axle) 268
187	Vehicle lateral accelerometer trace for test 401021-5 (accelerometer located over rear axle) 269
188	Vehicle vertical accelerometer trace for test 401021-5 (accelerometer located over rear axle) 270
189	Vehicle longitudinal accelerometer trace for test 401021-5 (accelerometer located on top surface of instrument panel) 271
190	Vehicle longitudinal accelerometer trace for test 401021-5 (accelerometer located on right front brake caliper) 272
191	Vehicle lateral accelerometer trace for test 401021-5 (accelerometer located on left front brake caliper) 273
192	Vehicle longitudinal accelerometer trace for test 401021-5 (accelerometer located on top of engine block) 274
193	Vehicle longitudinal accelerometer trace for test 401021-5 (accelerometer located on bottom of engine block) 275
194	Vehicular angular displacements for test 401021-2a 276
195	Vehicle longitudinal accelerometer trace for test 401021-2a (accelerometer located at center of gravity) 277
196	Vehicle lateral accelerometer trace for test 401021-2a (accelerometer located at center of gravity) 278
197	Vehicle vertical accelerometer trace for test 401021-2a (accelerometer located at center of gravity) 279
198	Vehicle longitudinal accelerometer trace for test 401021-2a (accelerometer located in vehicle cab) 280
199	Vehicle lateral accelerometer trace for test 401021-2a (accelerometer located in vehicle cab) 281
200	Vehicle longitudinal accelerometer trace for test 401021-2a (accelerometer located over rear axle) 282
201	Vehicle lateral accelerometer trace for test 401021-2a (accelerometer located over rear axle) 283
202	Vehicle longitudinal accelerometer trace for test 401021-2a (accelerometer located on top surface of instrument panel) 284
203	Vehicle longitudinal accelerometer trace for test 401021-2a (accelerometer located on right front brake caliper) 285

LIST OF FIGURES (continued)

<u>Figure</u>		<u>Page</u>
204	Vehicle lateral accelerometer trace for test 401021-2a (accelerometer located on left front brake caliper)	286
205	Vehicle longitudinal accelerometer trace for test 401021-2a (accelerometer located on top of engine block)	287
206	Vehicle longitudinal accelerometer trace for test 401021-2a (accelerometer located on bottom of engine block)	288
207	Vehicular angular displacements for test 401021-3	289
208	Vehicle longitudinal accelerometer trace for test 401021-3 (accelerometer located at center of gravity)	290
209	Vehicle lateral accelerometer trace for test 401021-3 (accelerometer located at center of gravity)	291
210	Vehicle vertical accelerometer trace for test 401021-3 (accelerometer located at center of gravity)	292
211	Vehicle longitudinal accelerometer trace for test 401021-3 (accelerometer located over rear axle)	293
212	Vehicle lateral accelerometer trace for test 401021-3 (accelerometer located over rear axle)	294
213	Vehicle vertical accelerometer trace for test 401021-3 (accelerometer located over rear axle)	295
214	Vehicle longitudinal accelerometer trace for test 401021-3 (accelerometer located on top surface of instrument panel)	296
215	Vehicle lateral accelerometer trace for test 401021-3 (accelerometer located on right front brake caliper)	297
216	Vehicle longitudinal accelerometer trace for test 401021-3 (accelerometer located on left front brake caliper)	298
217	Vehicle longitudinal accelerometer trace for test 401021-3 (accelerometer located on top of engine block)	299
218	Vehicle longitudinal accelerometer trace for test 401021-3 (accelerometer located on bottom of engine block)	300
219	Vehicular angular displacements for test 401021-7	301
220	Vehicle longitudinal accelerometer trace for test 401021-7 (accelerometer located at center of gravity)	302
221	Vehicle lateral accelerometer trace for test 401021-7 (accelerometer located at center of gravity)	303
222	Vehicle vertical accelerometer trace for test 401021-7 (accelerometer located at center of gravity)	304
223	Vehicle longitudinal accelerometer trace for test 401021-7 (accelerometer located over rear axle)	305
224	Vehicle lateral accelerometer trace for test 401021-7 (accelerometer located over rear axle)	306

LIST OF FIGURES (continued)

<u>Figure</u>	<u>Page</u>
225	Vehicle vertical accelerometer trace for test 401021-7 (accelerometer located over rear axle) 307
226	Lateral accelerometer trace for test 401021-4 (accelerometer located at center of post 13) 309
227	Axial strain, location 1, field side, for test 401021-4 310
228	Axial strain, location 2, field side, for test 401021-4 311
229	Axial strain, location 3, field side, for test 401021-4 312
230	Axial strain, location 4, field side, for test 401021-4 313
231	Axial strain, location 5, field side, for test 401021-4 314
232	Axial strain, location 6, field side, for test 401021-4 315
233	Lateral accelerometer trace for test 401021-6 (accelerometer located at center of post 11) 316
234	Axial strain, location 1, field side, for test 401021-6 317
235	Axial strain, location 2, field side, for test 401021-6 318
236	Axial strain, location 3, field side, for test 401021-6 319
237	Axial strain, location 4, field side, for test 401021-6 320
238	Axial strain, location 5, field side, for test 401021-6 321
239	Axial strain, location 6, field side, for test 401021-6 322
240	Lateral accelerometer trace for test 404201-1 (accelerometer located at center of post 13) 323
241	Axial strain, location 1, field side, for test 404201-1 324
242	Axial strain, location 2, field side, for test 404201-1 325
243	Axial strain, location 3, field side, for test 404201-1 326
244	Axial strain, location 4, field side, for test 404201-1 327
245	Axial strain, location 5, field side, for test 404201-1 328
246	Axial strain, location 6, field side, for test 404201-1 329
247	Lateral accelerometer trace for test 401021-5 (accelerometer located at center of post 13) 330
248	Axial strain, location 1, field side, for test 401021-5 331
249	Axial strain, location 2, field side, for test 401021-5 332
250	Axial strain, location 3, field side, for test 401021-5 333
251	Axial strain, location 4, field side, for test 401021-5 334
252	Axial strain, location 5, field side, for test 401021-5 335
253	Axial strain, location 6, field side, for test 401021-5 336
254	Lateral accelerometer trace for test 401021-2a (accelerometer located at center of post 13) 337
255	Axial strain, location 1, field side, for test 401021-2a 338
256	Axial strain, location 2, field side, for test 401021-2a 339

LIST OF FIGURES (continued)

<u>Figure</u>		<u>Page</u>
257	Axial strain, location 3, field side, for test 401021-2a	340
258	Axial strain, location 4, field side, for test 401021-2a	341
259	Axial strain, location 5, field side, for test 401021-2a	342
260	Axial strain, location 6, field side, for test 401021-2a	343
261	Lateral accelerometer trace for test 401021-3 (accelerometer located at center of post 18)	344
262	Axial strain, location 1, field side, for test 401021-3	345
263	Axial strain, location 2, field side, for test 401021-3	346
264	Axial strain, location 3, field side, for test 401021-3	347
265	Axial strain, location 4, field side, for test 401021-3	348
266	Axial strain, location 5, field side, for test 401021-3	349
267	Axial strain, location 6, field side, for test 401021-3	350

LIST OF TABLES

<u>Table No.</u>		<u>Page</u>
1	Transition testing performed	3
2	Performance evaluation summary for <i>NCHRP Report 350</i> test 3-21 on the Ohio 12-gauge nonsymmetrical Type 2 transition	158
3	Performance evaluation summary for <i>NCHRP Report 350</i> test 3-21 on the Ohio Type 2 10-gauge nonsymmetrical transition	159
4	Performance evaluation summary for <i>NCHRP Report 350</i> test 3-21 on the Ohio Type 1 transition without asphalt curb	160
5	Performance evaluation summary for <i>NCHRP Report 350</i> test 3-21 on the Ohio Type 1 transition with asphalt curb	161
6	Performance evaluation summary for <i>NCHRP Report 350</i> test 4-22 on the Ohio Type 1 transition with asphalt curb	163
7	Performance evaluation summary for <i>NCHRP Report 350</i> test 3-21 on the Wisconsin three beam transition to Type “M” tubular steel bridge rail	164
8	Performance evaluation summary for <i>NCHRP Report 350</i> test 3-21 on the modified NYSDOT box-beam transition to four-rail steel bridge rail	165
9	Results of transition testing	166
10	Locations of vehicle accelerometers for test 401021-4	178
11	Locations of vehicle accelerometers for test 401021-6	179
12	Locations of vehicle accelerometers for test 401021-1	179
13	Locations of vehicle accelerometers for test 401021-5	180
14	Locations of vehicle accelerometers for test 401021-2a	180
15	Locations of vehicle accelerometers for test 401021-3	181
16	Exterior crush measurements for test 401021-4	186
17	Exterior crush measurements for test 401021-6	189
18	Exterior crush measurements for test 401021-1	192
19	Exterior crush measurements for test 401021-5	195
20	Exterior crush measurements for test 401021-3	199
21	Exterior crush measurements for test 401021-7	202

INTRODUCTION

PROBLEM

Numerous concrete bridge parapets and tubular bridge railings have been successfully crash tested and meet the current standards of National Cooperative Highway Research Program (NCHRP) *Report 350*.⁽¹⁾ Likewise, several guardrail systems have been tested to *NCHRP Report 350* guidelines and meet the requirements for placement on the National Highway System. The Federal Highway Administration (FHWA), in its continuing efforts to promote and provide safer longitudinal barriers for all the Nation's roadways, recognizes that more information is needed on the transitions between guardrails and bridge railings.

BACKGROUND

The need for testing of transitions is becoming more evident. Tests performed on W-beam transitions to concrete bridge parapets had mixed results.⁽²⁾ A flared concrete parapet with nested W-beam, C152x12.2 rub rail, steel posts, and wood blockout transition experienced pocketing and subsequent vehicle rollover. A vertical wall transition employing nested W-beam guardrail and W-beam rub rail performed well. Recent testing by the Midwest Roadside Safety Facility (MwRSF) has been performed on three beam transitions with both steel and wood posts to concrete safety shape barriers.⁽³⁾ In both cases using the original design configuration, excessive deflections caused pocketing and subsequent vehicle rollover. When posts were lengthened to increase stiffness, successful test results were achieved.

In addition, under a previous study, FHWA, in cooperation with New York State Department of Transportation (NYSDOT), initiated a contract with the objective to crash test and evaluate the NYSDOT two- and four-rail bridge railings, and the box-beam transition. Under the first part of the study, the two- and four-rail bridge railings were evaluated to *NCHRP Report 350 TL-4*.⁽⁴⁾ To evaluate to TL-4, three full-scale crash tests on the length of need (LON) of the longitudinal barrier, or bridge railing, are required. These include an 820-kg passenger car impacting the critical impact point (CIP) at a nominal impact speed and angle of 100 km/h and 20 degrees; a 2000-kg pickup truck impacting the CIP at a nominal impact speed and angle of 100 km/h and 25 degrees; and an 8000-kg single-unit truck impacting the CIP at a nominal impact speed and angle of 80 km/h and 15 degrees.

The NYSDOT two-rail bridge railing met all specifications for *NCHRP Report 350* test designation 4-10, but the NYSDOT two-rail curbless bridge railing did not meet criteria for D and K of *NCHRP Report 350* test designation 4-11. Separation and deformation of the occupant compartment were judged to have potential for causing serious injury. Damage to the concrete deck at one post location was extensive and required major repairs. It was recommended that the post-to-deck connection be reviewed with the objective of reducing structural damage to the deck. No modifications were made to the deck and *NCHRP Report 350* test designation 4-12 was

performed. The NYSDOT two-rail bridge railing met all criteria for *NCHRP Report 350* test designation 4-12.

The NYSDOT four-rail curbless bridge railing performed acceptably during *NCHRP Report 350* test designations 4-12 and 4-11. The lower bridge railing geometry of the four-rail system was similar to the two-rail curbless bridge railing. Therefore, because *NCHRP Report 350* test designation 4-10 of the two-rail performed acceptably during crash testing, this test was not performed on the four-rail version.

After evaluation of the two bridge railings, NYSDOT and FHWA decided to evaluate a box-beam transition attached to the New York four-rail curbless bridge railing. *NCHRP Report 350* test designation 3-21: the 2000-kg pickup truck impacting the CIP of the transition at 100 km/h and 25 degrees. The box-beam transition did not meet occupant risk criterion D or vehicle trajectory criterion K for *NCHRP Report 350* test designation 3-21. Due to the significant amount of overall deformation of the occupant compartment, separation in the floor pan, and partial ejection of the dummy through the door (which was pulled open at the hinges), damage to the vehicle was judged to have potential for causing serious injury to occupants. This severe damage resulted when the vehicle snagged on the rail splice joints and bolt heads that protruded after the rail element was partially collapsed.⁽⁴⁾

OBJECTIVES

Several transitions were selected by the State Representatives for SP&R Pooled Fund Study No. 2-134, "Testing New Bridge Rail and Transition Designs." The objective of this study is to crash test and evaluate these transitions according to requirements of *NCHRP Report 350*. The scope of this study is as follows:

"This study will crash test a series of three beam transitions from guardrails to bridge rails in accordance with the appropriate test levels of *NCHRP Report 350*. These transition designs were selected by the State Representatives for SP&R Pooled Fund Study No. 2-134, 'Testing New Bridge Rail and Transition Designs.'

This requirement shall consist of using appropriate computer simulation codes to determine the critical impact point (CIP) of transition sections, conducting full-scale crash tests of transition designs, preparing test reports, preparing a final report in electronic format and storing test data on Bernoulli cartridges. This contract will provide the States with transition designs that have been crash tested and evaluated in accordance with National Cooperative Highway Research Program (NCHRP) Report No. 350."

The transitions tested under this project are listed in table 1.

Table 1. Transition testing performed.

Test Number	Description of Appurtenance	<i>NCHRP Report 350</i> Test Designation
401021-1	Ohio Type 1 Thrie Beam Transition to Concrete Parapet	3-21
401021-2a	Ohio Type 1 Thrie Beam Transition to Concrete Parapet with Asphalt Curb	4-22
401021-3	Thrie Beam Transition to Wisconsin Type “M” Tubular Steel Bridge Rail	3-21
401021-4	Ohio Non-symmetrical Type 2 12-Gauge W-beam to Thrie Beam Transition	3-21
401021-5	Ohio Type 1 Thrie Beam Transition to Concrete Parapet with Asphalt Curb	3-21
401021-6	Ohio Non-symmetrical Type 2 10-Gauge W-beam to Thrie Beam Transition	3-21
401021-7	New York State DOT Modified Box Beam Transition to Four-Rail Steel Bridge Rail	3-21

In addition to the thrie beam transitions tested in this study, under Modification No. 3 of this contract, FHWA requested that the contractor perform a finite-element analysis (FEA) of the NYSDOT box-beam transition to four-rail bridge railing that had failed the test with the pickup truck under the previous contract. *NCHRP Report 350* test designation 3-21 was previously performed on the box-beam transition to the NYSDOT four-rail steel bridge railing.⁽⁴⁾ Four tasks involving FEA were required. The first was to model/reproduce the snagging in the original test, and then subsequent tasks were performed to determine whether the modifications of the transition would perform acceptably. A full-scale crash test was then performed on the modification, which performed acceptably in the FEA. During the crash test, the transition section contained and redirected the pickup truck and all computed occupant risk values were within acceptable limits. However, occupant compartment deformation in the driver’s side floor pan area was 175 mm, and the door was pulled open at the hinges.

This report presents the construction details of each of the devices tested, the results of *NCHRP Report 350* crash tests performed, and the evaluation of the performance of each device according to the guidelines of *NCHRP Report 350*. Also included is the FEA requested by

FHWA to evaluate a box-beam transition attached to the NYSDOT four-rail bridge railing, and subsequent full-scale crash test, *NCHRP Report 350* test designation 3-21.

TEST PARAMETERS

TEST FACILITY

All testing performed under this contract was performed at an 809-hectare complex of research and training facilities situated 16 km northwest of the main campus of Texas A&M University. The site, formerly a U.S. Air Force base, has large expanses of concrete runways and parking aprons well suited for experimental research and testing in the areas of vehicle performance and handling, vehicle-roadway interaction, durability and efficacy of highway pavements, and safety evaluation of roadside safety hardware. The site selected for construction of the installations was along the edges of aprons and runways. The aprons and runways consist of an unreinforced jointed concrete pavement in 3.8-meter (m) by 4.6-m blocks nominally 203-305 millimeters (mm) deep. The aprons and runways are about 50 years old; the joints have some displacement, but are otherwise flat and level.

TEST ARTICLES

All test articles evaluated were constructed according to details and drawings provided by FHWA and/or States. Drawings of each installation are included with the description of each device in the following chapters.

TEST CONDITIONS

FHWA determined which *NCHRP Report 350* tests were to be performed on each of the test articles evaluated. Accordingly, the conditions specified in *NCHRP Report 350* for the specific tests chosen were used as target conditions. The target and actual test conditions for each test article are reported here. The vehicles in each of the tests were directed into the installation using the cable reverse tow and guidance system (detailed in appendix A), and were released to be free-wheeling and unrestrained just before the test.

The crash test and data analysis procedures were in accordance with guidelines presented in *NCHRP Report 350*. Brief descriptions of these procedures are presented in appendix A.

EVALUATION CRITERIA

The crash tests performed were evaluated in accordance with the criteria presented in *NCHRP Report 350*. As stated in *NCHRP Report 350*, "Safety performance of a highway appurtenance cannot be measured directly but can be judged on the basis of three factors: structural adequacy, occupant risk, and vehicle trajectory after collision." Safety evaluation criteria from table 5.1 of *NCHRP Report 350* were used to evaluate the crash tests reported

herein. An assessment of the criteria related to each particular test is included at the end of each test.

Also included at the end of each test are supplemental evaluation factors and terminology used for visual assessment of the test results as suggested by FHWA in a memorandum entitled: *Action: Identifying Acceptable Highway Safety Features*, dated July 25, 1997.⁽⁵⁾

OHIO THRIE BEAM TRANSITION AT THE 12-GAUGE NONSYMMETRICAL TYPE 2 TRANSITION SECTION

TEST ARTICLE—TEST 401021-4

Details for the Ohio Nonsymmetrical Thrie Beam transition were provided by Ohio DOT in a drawing designated GR3.3 Bridge Terminal Assembly, Type 3. The Ohio Nonsymmetrical Thrie Beam Transition consists of 3810 mm of nested (two) thrie beam guardrails; a 12-gauge nonsymmetric W-beam to thrie beam transition; and 3810 mm of standard W-beam guardrail. The total length of the transition is 9525 mm. In addition to the transition, 7620 mm of standard length-of-need guardrail was attached to the transition, which was anchored on the upstream end using a LET anchorage system. The height of the thrie beam transition immediately adjacent to the parapet was approximately 902 mm. The height of the W-beam guardrail in the transition was approximately 706 mm. TTI received drawing details for this transition from the Ohio DOT and these details were used for this project.

The downstream end of the transition was attached to a rigid concrete parapet that was previously constructed for another project at the testing facility. To eliminate any interaction effects between the parapet and the transition, the contractor added an additional 3810 mm segment of nested thrie beam with support posts between the transition and the concrete parapet. The nested thrie beam transition was attached to the concrete parapet with a 10-gauge thrie beam terminal connector. The parapet used for this project was not a standard design used to support this transition, so a special retrofit connection was required to attach the terminal connector to the parapet. This retrofit connection consisted of a piece of TS356x102x6.4 structural tube attached to the parapet using four A325 bolts that were bolted through the traffic side of the tube and through the preformed holes in the parapet. After the connection tube was attached to the parapet, the terminal connector was then attached to the tube using four 50 mm long A325 bolts through the traffic side of the tube only.

Posts 16 through 22 of the transition were W200x36 steel posts, 2438 mm in length and embedded approximately 1511 mm below grade. Post 15 was a W150x37 steel post, 2438 mm in length, and embedded approximately 1511 mm below grade. Posts 12 through 14 were W150x37 steel posts, 1830 mm in length, and embedded approximately 1100 mm below grade. Posts 7 through 11 were W150x13 steel posts, 1830 mm in length, and were embedded approximately 1100 mm below grade. Posts 1 through 6 were 150 mm x 200 mm wood posts as required for the LET anchorage system. Posts 1 through 13 were spaced approximately 1905 mm apart. Posts 13 through 22 (posts in the immediate transition area) were spaced approximately 952 mm apart.

Wood blockouts were used at all post locations. At posts 1 through 11, the nominal sizes of the blocks were 150 mm x 200 mm x 355 mm in length. At posts 6 through 11, the blocks were routed to a depth of approximately 7 mm to fit the flange width of each steel post. At posts 12 through 14, the nominal sizes of the blocks were 197 mm x 200 mm x 355 mm in length and were routed to a depth of approximately 7 mm to fit the flange of each post. At posts 16 through

22, the nominal sizes of the blocks were 203 mm x 200 mm x 572 mm in length and were routed to a depth of approximately 7 mm to fit the flange of each post. For additional information, please refer to figures 1 and 2. Photographs of the completed installation are shown in figure 3.

CRASH TEST 401021-4 (NCHRP REPORT 350 TEST NO. 3-11)

Test Conditions

This test corresponds to *NCHRP Report 350* test designation 3-21, which is the 2000 kg pickup truck impacting the CIP of the transition at a nominal speed and angle of 100 km/h and 25 degrees. The objective was to evaluate the performance in the nonsymmetrical section that transitions from W-beam guardrail to thrie beam. According to guidelines of *NCHRP Report 350*, the BARRIER VII simulation program was used to select the CIP for this test. The data generated indicated the CIP to be 2.3 m upstream of the first post in the nonsymmetrical transition section.

Test Vehicle

A 1996 Chevrolet 2500 pickup truck (figures 4 and 5) was used for the crash test. Test inertia weight of the vehicle was 2000 kg, and its gross static weight was 2077 kg. The height to the lower edge of the vehicle's front bumper was 365 mm and 593 mm to the upper edge of the front bumper. Additional dimensions and information on the vehicle are given in appendix B, figure 111. The vehicle was directed into the installation using the cable reverse tow and guidance system, and was released to be freewheeling and unrestrained just before impact.

Soil and Weather Conditions

The crash test was performed the morning of September 1, 2000. No rainfall was recorded for the 10 days before the test. Moisture content of the *NCHRP Report 350* standard soil in which the transition was installed was 5.0 percent, 5.4 percent, and 5.5 percent at posts 12, 13, and 14, respectively. Weather conditions at the time of testing were: windspeed: 11 km/h; wind direction: 190 degrees with respect to the vehicle (vehicle was traveling in a southeasterly direction); temperature: 37 °C; relative humidity: 37 percent.

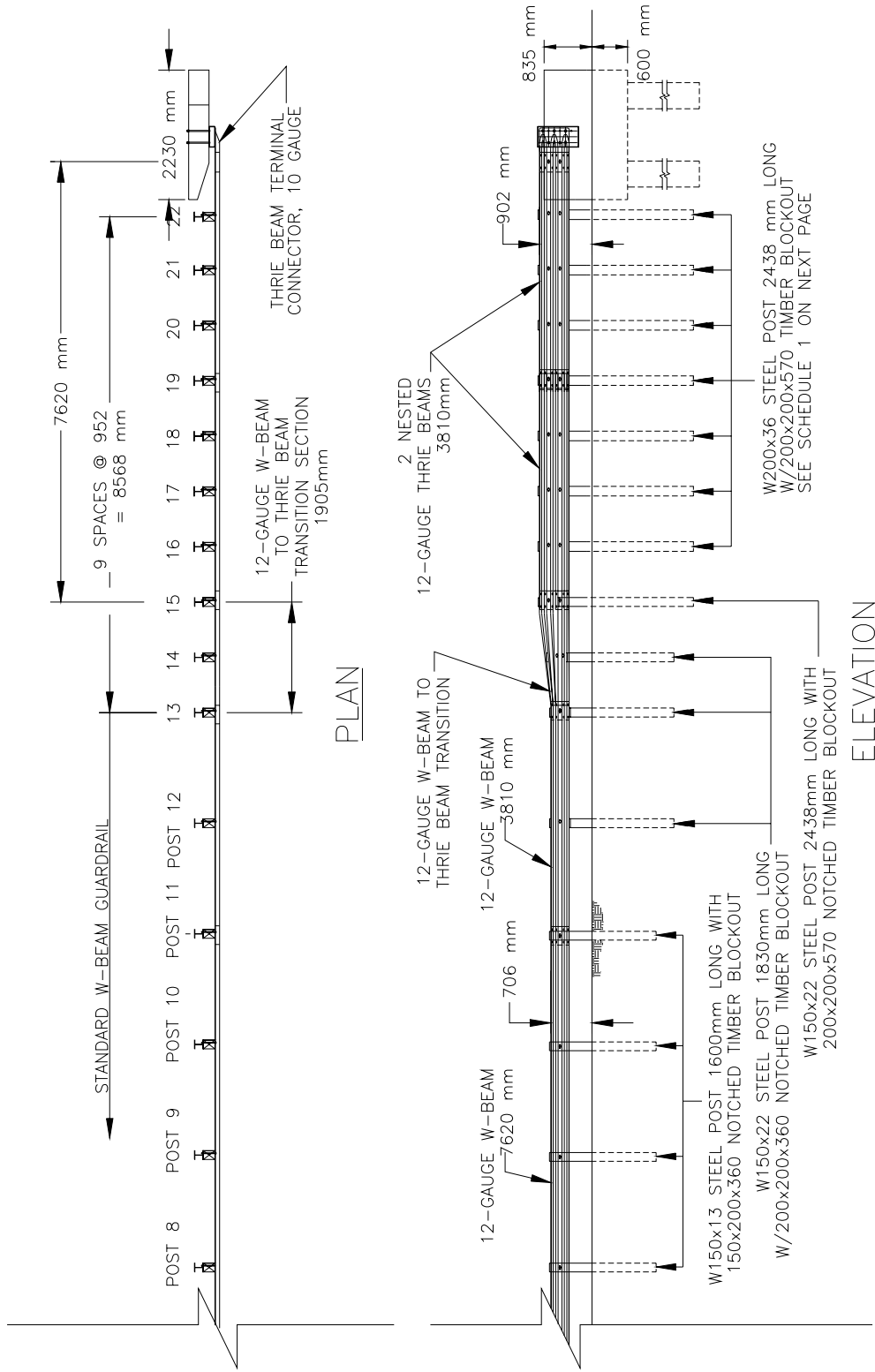


Figure 1. Details of the Ohio 12-gauge nonsymmetrical Type 2 thrie beam transition.

NOTES: (for diagrams in figure 1 and below)

GENERAL: For additional details, see Standard Construction Drawing (SCD) GR-1.1, GR-1.2 and other drawings pertaining to specific guardrails types.

APPLICATIONS: The Type 3 Bridge Terminal Assembly shall be used to connect guardrail runs to both the approach and trailing ends of Thrie-Beam Bridge Railings.

POSTS:

GENERAL—Posts may be set in drilled holes or driven to grade.

WOOD POSTS—shall be square-sawed pressure treated wood as per Certified Materials Specification (CMS) 710.14 and fabricated with square ends. Bolt holes shall be bored and tops of posts trimmed, if required, after posts are set.

ALTERNATE POSTS AND BLOCKOUTS for Type 3 Bridge Terminal Assemblies may be furnished according to the following chart. Plastic blockouts shall not be permitted for Type 3 Bridge Terminal Assemblies.

Wood Posts and Wood Blockouts	Posts	10" x 10" [250 mm x 250 mm]	8" x 8" [200 mm x 200 mm]
	Blockouts	6" x 8" [150 mm x 200 mm]	
Steel Posts and Wood Blockouts	Posts	W8x24 [W200x35.9]	W6x25 [W150x37.1]
	Notched Blockouts	8" x 7 7/8" [200 mm x 200 mm]	7 3/4" x 7 7/8" [197 mm x 200 mm]
	Notched Width (W) See Detail	6 1/2" (+3/8", -0) [165 mm (+10, -0)]	6 1/8" (+3/8", -0) [154 mm (+10, -0)]

SCHEDULE 1 POST AND BLOCKOUT DETAILS

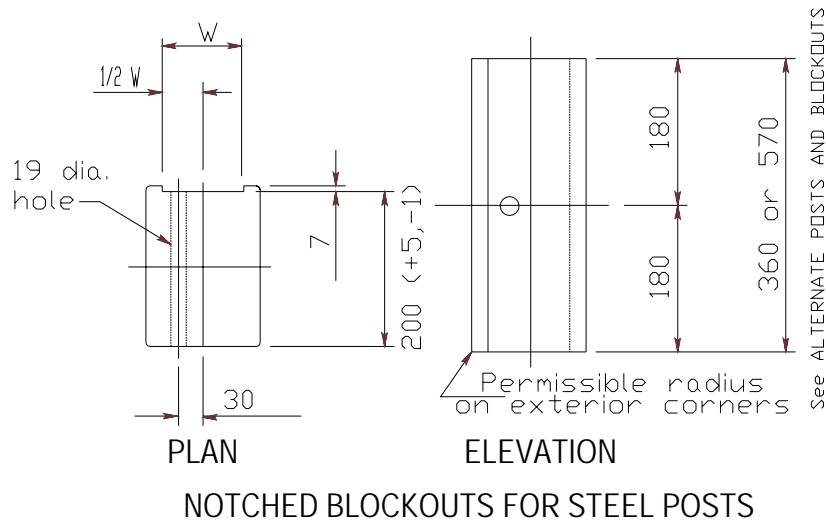


Figure 2. Details of the Ohio 12-gauge nonsymmetrical Type 2 thrie beam transition—notes.



a) Overall view of traffic side of transition.



b) Closeup view of Ohio transition section.

Figure 3. Ohio transition before test 401021-4.



a) Geometrics from traffic side.



b) Geometrics from field side.

Figure 4. Vehicle/installation geometrics for test 401021-4.



a) Front quarter view.



b) Overhead view.

Figure 5. Vehicle before test 401021-4.

Impact Description

The 2000 kg pickup truck impacted the transition at 850 mm upstream from post 12 at an impact angle of 24.5 degrees while traveling at a speed of 101.9 km/h. Posts 12, 11 and 13 moved rearward at 0.007 s, 0.020 s and 0.025 s, respectively. The vehicle began to redirect at 0.049 s. Posts 14, 15 and 16 moved at 0.062 s, 0.084 s and 0.113 s, respectively. At 0.108 s, the left front tire was cut on post 13; at 0.143 s it deflated. By 0.158 s the windshield shattered, and by 0.171 s the right front tire lost contact with the road surface. The right rear tire lost contact with the road surface at 0.174 s, and at 0.202 s the rear of the vehicle contacted the rail element. The vehicle became parallel with the rail element at 0.234 s and was traveling at a speed of 54.3 km/h. At 0.509 s the vehicle lost contact with the installation and was traveling at a speed of 50.2 km/h at an exit angle of 16.1 degrees. Brakes on the vehicle were not applied and the vehicle came to rest 45.8 m downstream from impact and 14.5 m behind the test installation. Sequential photographs of the test period are shown in appendix C, figures 124 through 126.

Damage to Test Article

The Ohio transition sustained moderate damage as shown in figures 6 and 7. Tire marks marred post 13 and the rail element was torn at the splice at post 13. The rail element was detached from post 14. Blockouts were chipped at posts 13 and 14. The blockout at post 15 was twisted and chipped. Posts 16 through 14 were pushed rearward 5 mm, 22 mm, and 80 mm, respectively. Posts 13 and 12 moved 170 mm and 53 mm rearward. Posts 11 to the end terminal were disturbed. Length of contact of the vehicle with the transition was 4.6 m. Maximum dynamic deflection of the rail element during the test was 439 mm and maximum permanent deformation was 190 mm to the rail element at post 13.

Vehicle Damage

Damage imparted to the vehicle is shown in figure 8. The following vehicle components received structural damage: left upper and lower A-arms, right side A and B pillars, left side ball joint, rod ends, steering arm, stabilizer arm, and left front frame. Also damaged were the bumper, hood, radiator, fan, left front and rear quarter panels, left door, left front wheel and rim, right front quarter panel, and right door. The floor pan and roof of the vehicle were deformed. Maximum exterior crush to the front bumper was 740 mm. The interior of the vehicle is shown in figure 9. Maximum deformation of the occupant compartment was 175 mm at the lower kick panel in the driver's foot well area. Exterior vehicle crush and occupant compartment measurements are shown in appendix B, table 16 and figure 112.



Figure 6. Vehicle trajectory path after test 401021-4.



a) Damage at impact.



b) Damage at post 13.

Figure 7. Installation after test 401021-4.



a) Front quarter view.



b) Overhead view.

Figure 8. Vehicle after test 401021-4.



a) Before test.



b) After test.

Figure 9. Interior of vehicle for test 401021-4.

Occupant Risk Factors

Data from the triaxial accelerometer, located at the vehicle center of gravity (c.g.), were digitized to compute occupant impact velocity and ridedown accelerations. The occupant impact velocity and ridedown accelerations in the longitudinal axis only are required from these data for evaluation of criterion L of *NCHRP Report 350*. In the longitudinal direction, occupant impact velocity was 7.2 m/s at 0.125 s, maximum 0.010-s ridedown acceleration was -11.7 g's from 0.171 to 0.181 s, and the maximum 0.050-s average was -11.1 g's between 0.078 and 0.128 s. In the lateral direction, the occupant impact velocity was 7.0 m/s at 0.125 s, the highest 0.010-s occupant ridedown acceleration was 12.4 g's from 0.173 to 0.183 s, and the maximum 0.050-s average was 9.2 g's between 0.063 and 0.113 s. Vehicle angular displacements and accelerations versus time traces are shown in appendix D, figures 146 through 157.

Rail Instrumentation Results

Six strain gauges and one accelerometer were installed on the Ohio transition to measure longitudinal strains in the steel rail and post acceleration during the crash test. Graphs of data from the strain gauges installed on the railing are shown in figures 226 through 232 of appendix E. These data were collected to at the request of FHWA. The data serve no purpose in determining acceptability of performance of the transition, but rather provide information for use in future computer simulation modeling and validation efforts.

Strain gauge bridges were located as follows: #1) 810 mm from the center of post 12 on the field side of the plate at 590 mm from ground level; #2) 810 mm from the center of post 12 on the field side of the plate at 460 mm from ground level; #3) 370 mm from the center of post 17 on the field side of the plate at 805 mm from ground level; #4) 370 mm from the center of post 17 on the field side of the plate at 670 mm from ground level; #5) 370 mm from the center of post 17 on the traffic side at 615 mm from ground level; #6) 370 mm from the center of post 17 on the field side of the plate at 485 mm from ground level. At these locations, the W-beam and thrie beam were prepared by first grinding away the mill scale to produce a clean and smooth surface in a 60 x 30 mm area where the gauges were spot welded to bond them to the steel. A complete description of the instrumentation is presented in appendix A, with photographs of typical setup shown in figure 105 of appendix A.

Assessment of Test Results

The following *NCHRP Report 350* safety evaluation criteria were used to evaluate this crash test:

Structural Adequacy

- A. *Test article should contain and redirect the vehicle; the vehicle should not penetrate, underride, or override the installation although controlled lateral deflection of the test article is acceptable.*

Result: The Ohio Transition contained and redirected the 2000 kg pickup truck. The vehicle did not penetrate, underride, or override the installation. Maximum dynamic deflection of the transition was 439 mm. (PASS)

Occupant Risk

- D. *Detached elements, fragments or other debris from the test article should not penetrate or show potential for penetrating the occupant compartment, or present an undue hazard to other traffic, pedestrians, or personnel in a work zone. Deformation of, or intrusions into, the occupant compartment that could cause serious injuries should not be permitted.*

Result: No detached elements, fragments, or other debris were present to penetrate or to show potential for penetrating the occupant compartment, nor to present undue hazard to others in the area. Maximum deformation of the occupant compartment was 175 mm to the center of the floor pan area. (FAIL)

- F. *The vehicle should remain upright during and after collision although moderate roll, pitching, and yawing are acceptable.*

Result: The 2000-kg pickup truck remained upright and stable during and after the collision period. (PASS)

Vehicle Trajectory

- K. *After collision it is preferable that the vehicle's trajectory not intrude into adjacent traffic lanes.*

Result: The vehicle did not intrude into adjacent traffic lanes. (PASS)

- L. *The occupant impact velocity in the longitudinal direction should not exceed 12 m/s and the occupant ridedown acceleration in the longitudinal direction should not exceed 20 g's.*

Result: Longitudinal occupant impact velocity was 7.2 m/s and longitudinal ridedown acceleration was -11.7 g's. (PASS)

- M. *The exit angle from the test article preferably should be less than 60 percent of the test impact angle, measured at time of vehicle loss of contact with the test device.*

Result: Exit angle at loss of contact was 16.1 degrees, which was 66 percent of the impact angle. (FAIL)

The following supplemental evaluation factors and terminology, as presented in the FHWA memo entitled "Action: Identifying Acceptable Highway Safety Features," were used for visual assessment of test results.⁽⁵⁾ The factors underlined below pertain to the results of the crash test reported here.

PASSENGER COMPARTMENT INTRUSION

1. Windshield Intrusion

- | | |
|---|---|
| <i>a. <u>No windshield contact</u> (stressed)</i> | <i>e. Complete intrusion into passenger compartment</i> |
| <i>b. Windshield contact, no damage</i> | <i>f. Partial intrusion into passenger compartment</i> |
| <i>c. Windshield contact, no intrusion</i> | |
| <i>d. Device embedded in windshield, no significant intrusion</i> | |

2. Body Panel Intrusion

yes or no

LOSS OF VEHICLE CONTROL

1. Physical loss of control

3. Perceived threat to other vehicles

2. Loss of windshield visibility

4. Debris on pavement

PHYSICAL THREAT TO WORKERS OR OTHER VEHICLES

1. Harmful debris that could injure workers or others in the area

2. Harmful debris that could injure occupants in other vehicles

No debris was present.

VEHICLE AND DEVICE CONDITION

1. Vehicle Damage

- a. None
- b. Minor scrapes, scratches or dents
- c. Significant cosmetic dents
- d. Major dents to grill and body panels
- e. Major structural damage

2. Windshield Damage

- a. None
- b. Minor chip or crack
- c. Broken, no interference with visibility
- d. Broken and shattered, visibility restricted but remained intact
- e. Shattered, remained intact but partially dislodged
- f. Large portion removed
- g. Completely removed

3. Device Damage

- a. None
- b. Superficial
- c. Substantial, but can be straightened
- d. Substantial, replacement parts needed for repair
- e. Cannot be repaired

Conclusions

All computed occupant risk values were within acceptable limits. However, occupant compartment deformation in the driver's floor pan area was 175 mm, which is deemed unacceptable (due to location) according to FHWA's *Draft Guidelines for Analysis of Passenger Compartment Intrusion*.⁽⁶⁾

OHIO THRIE BEAM TRANSITION AT THE 10-GAUGE NONSYMMETRICAL TYPE 2 TRANSITION SECTION

TEST ARTICLE—TEST 401021-6

Details for the Ohio Nonsymmetrical Thrie Beam Transition were provided by Ohio DOT. The Ohio drawing is designated GR3.3 Bridge Terminal Assembly, Type 3. The Ohio Nonsymmetrical Thrie Beam Transition consists of 3810 mm of 2 nested 12-gauge thrie beam guardrails, a 10-gauge nonsymmetric W-beam to thrie beam transition, and 1905 mm of standard W-beam guardrail. The total length of the transition is 7620 mm. In addition to the transition, 5715 mm of standard LON guardrail was attached to the transition, which was anchored on the upstream end using a LET anchorage system. The height of the thrie beam transition immediately adjacent to the parapet was approximately 902 mm. The height of the W-beam guardrail in the transition was approximately 706 mm.

The downstream end of the transition was attached to a rigid concrete parapet that was previously constructed for another project at the testing facility. To eliminate any interaction effects between the parapet and the transition, the contractor added an additional 3810 mm segment of nested thrie beam with support posts between the transition and the concrete parapet. The nested thrie beam transition was attached to the concrete parapet with a 10-gauge thrie beam terminal connector. The parapet used for this project was not a standard design used to support this transition, so a special retrofit connection was required to attach the terminal connector to the parapet. This retrofit connection consisted of a piece of TS356x102x6.4 structural tube attached to the parapet using five A325 bolts bolting through the traffic side of the tube and through the preformed holes in the parapet. After the connection tube was attached to the parapet, the terminal connector was then attached to the tube using five 50-mm long A325 bolts that were bolted through the traffic side of the tube only.

Posts 14 through 20 of the transition were W200x36 steel posts, 2438 mm in length and embedded approximately 1511 mm below grade. Post 13 was a W150x22 steel post, 2438 mm in length, and embedded approximately 1511 mm below grade. Posts 10 through 12 were W150x22 steel posts, 1830 mm in length, and embedded approximately 1100 mm below grade. Posts 7 through 9 were W150x13 steel posts, 1830 mm in length, and were embedded approximately 1100 mm below grade. Posts 1 through 4 were 150 mm x 200 mm wood posts as required for the LET anchorage system. Posts 1 through 11 were spaced approximately 1905 mm apart. Posts 11 through 20 (posts in the immediate transition area) were spaced approximately 952 mm apart.

Wood blockouts were used at all post locations. At posts 1 through 9, the nominal sizes of the blocks were 150 mm x 200 mm x 355 mm in length. At posts 7 through 9, the blocks were routed to a depth of approximately 7 mm to fit the flange width of the steel posts. At posts 10 through 13, the nominal sizes of the blocks were 197 mm x 200 mm x 355 mm in length and were routed to a depth of approximately 7 mm to fit the flange of the posts. At posts 14 through 20, the nominal sizes of the blocks were 203 mm x 200 mm x 572 mm in length and were routed

to a depth of approximately 7 mm to fit the flange of the posts. For additional information, please refer to figures 10 and 11. Photographs of the completed installation are shown in figure 12.

CRASH TEST 401021-6 (NCHRP REPORT 350 TEST NO. 3-21)

Test Conditions

This test corresponds to *NCHRP Report 350* test designation 3-21. The objective was to evaluate the performance in the nonsymmetrical section that transitions from W-beam guardrail to thrie beam. According to guidelines of *NCHRP Report 350*, the BARRIER VII simulation program was used to select the CIP for this test. The data generated by the program indicated the CIP to be 2.3 m upstream of the first post in the nonsymmetrical transition section, which was post 11.

Test Vehicle

A 1997 Chevrolet 2500 pickup truck, shown in figures 13 and 14, was used for the crash test. Test inertia weight of the vehicle was 2000 kg, and its gross static weight was 2076 kg. The height to the lower edge of the vehicle front bumper was 378 mm, and the height to the upper edge of the front bumper was 595 mm. Additional dimensions and information on the vehicle are given in appendix B, figure 113. The vehicle was directed into the installation using the cable reverse tow and guidance system, and was released to be freewheeling and unrestrained just before impact.

Soil and Weather Conditions

The crash test was performed the morning of March 7, 2002. Rainfall of 1 mm was recorded 6 days before the test. No other rainfall was recorded for the remaining 10 days before the test. Moisture content of the *NCHRP Report 350* soil in which the test article was installed was 6.9 percent, 6.3 percent, and 6.4 percent at posts 10, 12, and 13, respectively. Weather conditions at the time of testing were as follows: windspeed: 26 km/h; wind direction: 180 degrees with respect to the vehicle (vehicle was traveling in a southwesterly direction); temperature: 22 °C; relative humidity: 71 percent.

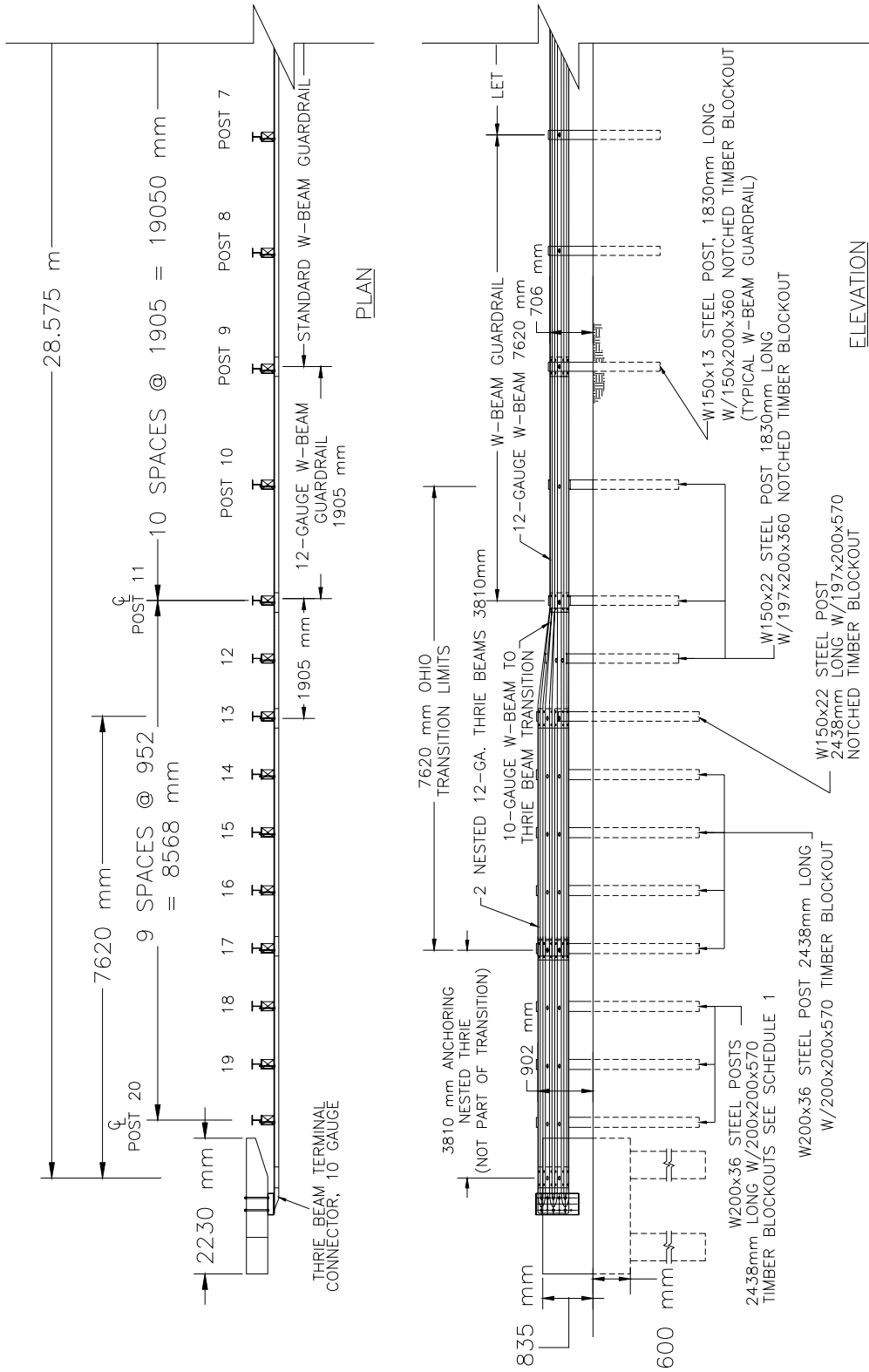


Figure 10. Details of the Ohio 10-gauge nonsymmetrical Type 2 thrie beam transition.

NOTES: (for diagrams in figure 10 and below)

GENERAL: For additional details, see SCD. GR-1.1, GR-1.2 and other drawings pertaining to specific guardrails types.

APPLICATIONS: The Type 3 Bridge Terminal Assembly shall be used to connect guardrail runs to both the approach and trailing ends of Thrie-Beam Bridge Railings.

POSTS:

GENERAL—Posts may be set in drilled holes or driven to grade.

WOOD POSTS—Shall be square-sawed pressure treated wood as per CMS 710.14 and fabricated with square ends. Bolt holes shall be bored and tops of posts trimmed, if required, after posts are set.

ALTERNATE POSTS AND BLOCKOUTS for Type 3 Bridge Terminal Assemblies may be furnished according to the following chart. Plastic Blockouts shall not be permitted for Type 3 Bridge Terminal Assemblies.

Wood Posts and Wood Blockouts	Posts	10" x 10" [250 mm x 250 mm]	8" x 8" [200 mm x 200 mm]
	Blockouts	6" x 8" [150 mm x 200 mm]	
Steel Posts and Wood Blockouts	Posts	W8x24 [W200x35.9]	W6x25 [W150x37.1]
	Notched Blockouts	8" x 7 7/8" [200 mm x 200 mm]	7 3/4" x 7 7/8" [197 mm x 200 mm]
	Notched Width (W) See Detail	6 1/2" (+3/8", -0) [165 mm (+10, -0)]	6 1/8" (+3/8", -0) [154 mm (+10, -0)]

SCHEDULE 1 POST AND BLOCKOUT DETAILS

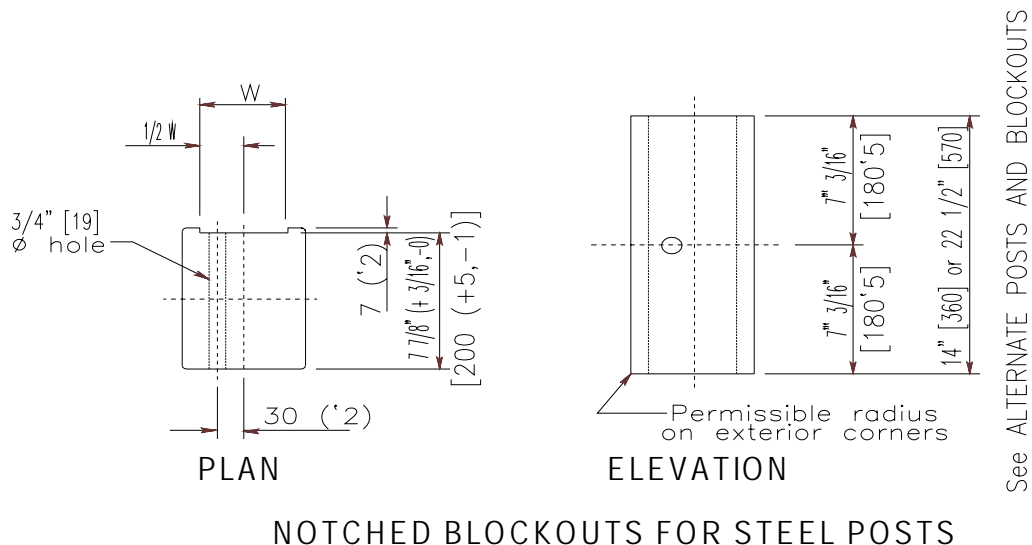


Figure 11. Details of the Ohio 10-gauge nonsymmetrical Type 2 thrie beam transition—notes.



a) Overall view of transition from traffic side.



b) Closeup view of transition section.

Figure 12. Ohio nonsymmetrical transition before test 401021-6.



a) Geometrics from traffic side.



b) Geometrics from field side.

Figure 13. Vehicle/installation geometrics for test 401021-6.



a) Front quarter view.



b) Overhead view.

Figure 14. Vehicle before test 401021-6.

Impact Description

The 2076-kg pickup truck, traveling at a speed of 100.2 km/h, impacted the nonsymmetrical transition 310 mm upstream of post 10 (2.21 m upstream of the first post in the nonsymmetrical section) at an impact angle of 25.4 degrees. Shortly after impact, post 10 began to deflect toward the field side and, at 0.025 s, post 9 began to deflect toward the field side. Post 11 began to deflect at 0.037 s and the vehicle began to redirect at 0.061 s. Posts 12 and 13 began to deflect toward the field side at 0.067 s and 0.084 s, respectively. At 0.111 s, the right front tire contacted the edge of the flange of post 11 and, at 0.124 s, post 14 began to deflect toward the field side. The rail element separated from the blockout at post 11 at 0.134 s. At 0.156 s the dummy's head contacted the side window, which shattered. At 0.248 s, the vehicle became parallel with the installation and was traveling at a speed of 52.8 km/h. The vehicle lost contact with the rail element at 0.592 s and was traveling at a speed of 46.9 km/h and an exit angle of 26.1 degrees. Brakes on the vehicle were applied at 2.5 s, and the vehicle began to yaw clockwise. The vehicle subsequently came to rest 27.45 m downstream of impact and 5.72 m forward of the traffic face of the rail. Sequential photographs of the test period are shown in appendix C, figures 127 through 129.

Damage to Test Article

Damage to the transition is shown in figures 15 and 16. Tire marks were on the impact edge of the flange and front faces of posts 11 and 12. The rail element was separated from the blockout at post 11; the rail element was torn around the lower right splice bolt. The upstream terminal was pulled longitudinally 25 mm. Maximum dynamic deflection of the rail during the test was 659 mm; maximum permanent deformation was 554 mm. The vehicle was in contact with the rail element for a distance of 6.67 m.

Vehicle Damage

The right front quarter of the pickup truck was damaged, as shown in figure 17. Structural damage included deformed right front frame member, stabilizer bar, right upper and lower A-arms, right side tie rod ends and spindle, floor pan, and firewall. Also damaged were the front bumper, fan, radiator, right front quarter panel, right door and window glass, right rear bed, and the right front tire and wheel rim. The windshield sustained stress cracks. Maximum exterior crush to the vehicle in the frontal plane was 680 mm at the right front corner at bumper height, and in the side plane was 470 mm at the right front corner. Maximum occupant compartment deformation was 52 mm in the kickpanel area near the passenger's feet. Photographs of the interior of the vehicle are shown in figure 18. Exterior vehicle crush and occupant compartment measurements are shown in appendix B, table 17 and figure 114.



Figure 15. Vehicle trajectory path after test 401021-6.



a) Damage at impact.



b) Damage from field side.

Figure 16. Installation after test 401021-6.

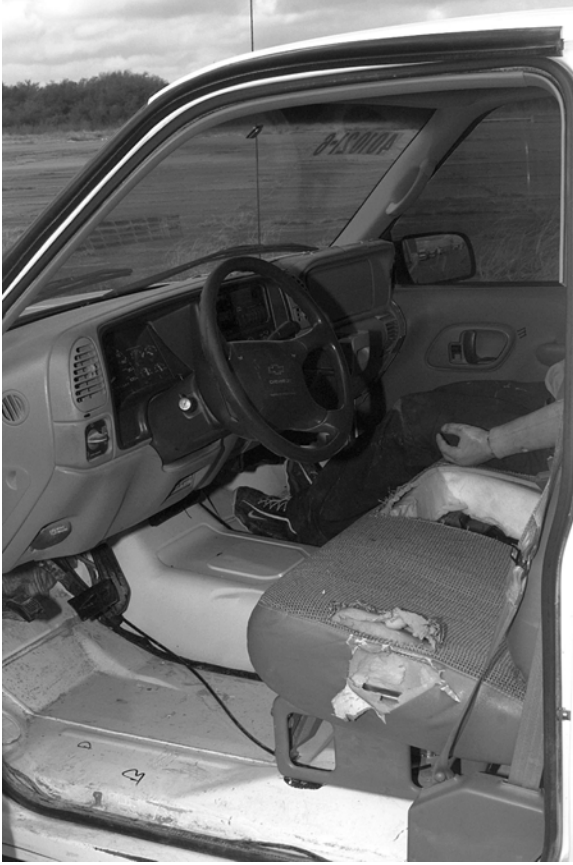


a) Front quarter view.



b) Overhead view.

Figure 17. Vehicle after test 401021-6.



a) Before test.



b) After test.

Figure 18. Interior of vehicle for test 401021-6.

Occupant Risk Factors

Data from the triaxial accelerometer, located at the vehicle c.g., were digitized to compute occupant impact velocity and ridedown accelerations. Only longitudinal occupant impact velocity and ridedown accelerations are required for this test for evaluation of criterion L of *NCHRP Report 350*. In the longitudinal direction, occupant impact velocity was 7.8 m/s at 0.133 s, maximum 0.010-s ridedown acceleration was -15.6 g's from 0.133 to 0.143 s, and the maximum 0.050-s average was -12.0 g's between 0.117 and 0.167 s. In the lateral direction, the occupant impact velocity was 6.9 m/s at 0.133 s, the highest 0.010-s occupant ridedown acceleration was 13.1 g's from 0.140 to 0.150 s, and the maximum 0.050-s average was -11.8 g's between 0.090 and 0.140 s. Vehicle angular displacements and accelerations versus time traces are shown in appendix D, figures 158 through 169.

Rail Instrumentation Results

Six strain gauges and one accelerometer were installed on the Ohio transition to measure longitudinal strains in the steel rail and post acceleration during the crash test. Graphs of data from the strain gauges installed on the railing are shown in figures 233 through 239 of appendix E. These data were collected at FHWA's request. The data serve no purpose in determining acceptability of performance of the transition, but rather intended to provide information for use in future computer simulation modeling and validation efforts.

Strain gauge bridges were located as follows: #1) 1330 mm upstream from the center of post 10 on the field side of the W-beam rail at 635 mm from ground level; #2) 1330 mm upstream from the center of post 10 on the field side of the W-beam rail at 510 mm from ground level; #3) 635 mm upstream from the center of post 16 on the field side of the thrie beam rail at 810 mm from ground level; #4) 635 mm upstream from the center of post 16 on the field side of the thrie beam rail at 675 mm from ground level; #5) 635 mm upstream from the center of post 16 on the traffic side of the thrie beam at 600 mm from ground level; #6) 635 mm upstream from the center of post 16 on the field side of the thrie beam at 480 mm from ground level. At these locations, the rail element was prepared by first grinding away the galvanized coating and the mill scale to produce a clean and smooth surface in a 60 x 30 mm area where the gauges were spot welded to bond them to the steel. A complete description of the instrumentation is presented in appendix A, with photographs of typical setup shown in figure 106 of appendix A.

Assessment of Test Results

An assessment of the test based on the applicable *NCHRP Report 350* safety evaluation criteria is provided below.

Structural Adequacy

- A. *Test article should contain and redirect the vehicle; the vehicle should not penetrate, underride, or override the installation, although controlled lateral deflection of the test article is acceptable.*

Result: The Ohio nonsymmetrical transition contained and redirected the pickup truck. The vehicle did not penetrate, underride, or override the installation. Maximum dynamic deflection during the test was 659 mm. (PASS)

Occupant Risk

- D. *Detached elements, fragments, or other debris from the test article should not penetrate or show potential for penetrating the occupant compartment, or present an undue hazard to other traffic, pedestrians, or personnel in a work zone. Deformation of, or intrusions into, the occupant compartment that could cause serious injuries should not be permitted.*

Result: No detached elements, fragments, or other debris was present to penetrate or to show potential for penetrating the occupant compartment, or to present undue hazard to others in the area. Maximum occupant compartment deformation was 52 mm at the kickpanel near the passenger's feet. (PASS)

- F. *The vehicle should remain upright during and after collision although moderate roll, pitching, and yawing are acceptable.*

Result: The pickup truck remained upright during and after the impact sequence. (PASS)

Vehicle Trajectory

- K. *After collision, it is preferable that the vehicle's trajectory not intrude into adjacent traffic lanes.*

Result: The vehicle came to rest 27.5 m downstream of impact and 5.7 m forward of the traffic face of the rail. (FAIL)

- L. *The occupant impact velocity in the longitudinal direction should not exceed 12 m/s and the occupant ridedown*

VEHICLE AND DEVICE CONDITION

1. Vehicle Damage

- a. None
- b. Minor scrapes, scratches or dents
- c. Significant cosmetic dents
- d. Major dents to grill and body panels
- e. Major structural damage

2. Windshield Damage

- a. None
- b. Minor chip or crack (stress)
- c. Broken, no interference with visibility
- d. Broken and shattered, visibility restricted but remained intact
- e. Shattered, remained intact but partially dislodged
- f. Large portion removed
- g. Completely removed

3. Device Damage

- a. None
- b. Superficial
- c. Substantial, but can be straightened
- d. Substantial, replacement parts needed for repair
- e. Cannot be repaired

Conclusions

The Ohio 10-gauge nonsymmetrical Type 2 transition section (from W-beam to thrie beam) met the required specifications for *NCHRP Report 350* test 3-21.

OHIO TYPE 1 THRIE BEAM TRANSITION TO CONCRETE PARAPET

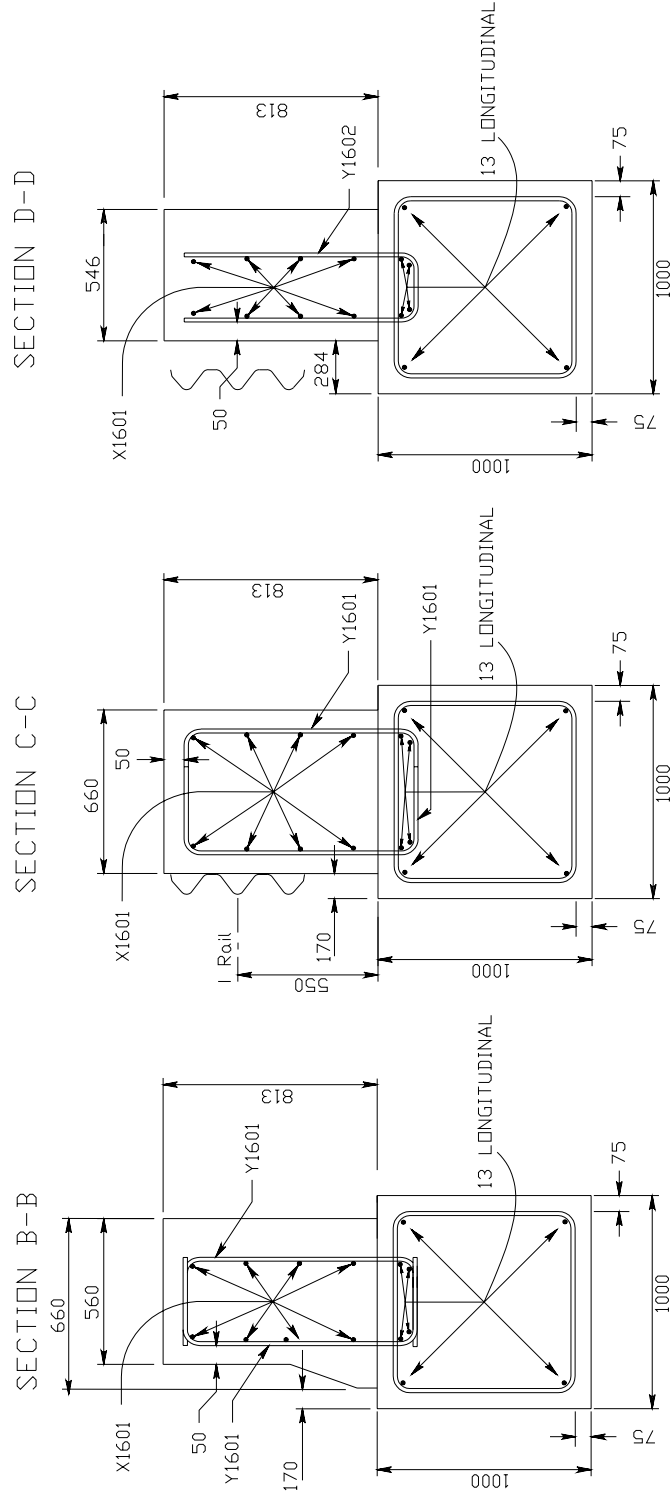
TEST ARTICLE—TEST 401021-1

The Ohio Type 1 Thrie Beam Transition to Concrete Parapet consists of 3810 mm nested (two thicknesses) thrie beam guardrails, a 12-gauge symmetric W-beam to thrie beam transition piece, and 3810 mm of standard W-beam guardrail. The total length of the transition is 6291 mm. In addition to the transition, 3658 mm of standard LON guardrail was attached to the transition, which was anchored on the upstream end using a LET anchorage system. The height of the thrie beam transition immediately adjacent to the parapet was approximately 803 mm. The height of the W-beam guardrail in the transition was approximately 706 mm. The contractor received several drawing details for this transition from Ohio DOT and these details were used for this project.

The downstream end of the transition was attached to a rigid concrete parapet that was fabricated to match the impact face of parapet shown in Ohio's drawing designated GR-3.5M. From conversation with Ohio DOT, the section shown on GR-3.5M is typically 9 m in length. The contractor increased the footing dimension because a shorter 5-m length is required for the test and a rigid concrete parapet provides a worst-case scenario. The nested thrie beam transition was attached to the concrete parapet with a 10-gauge thrie beam terminal connector. The terminal connector was attached to the parapet using four 22-mm diameter A325 bolts through the parapet.

Posts 8 through 10 of the transition were W150x37 steel posts, 1830 mm in length and embedded approximately 1040 mm below grade. Post 11 was a W150x37 steel post, 2440 mm in length, and embedded approximately 1612 mm below grade. Posts 12 and 13 were W200x36 steel posts, 2440 mm in length, and embedded approximately 1612 mm below grade. Posts 1 through 7 were 150 mm x 200 mm wood posts as required for the LET guardrail end treatment. Posts 1 through 9 were spaced approximately 1905 mm apart. Posts 9 through 13 (posts in the immediate transition area) were spaced approximately 952 mm apart.

Standard wood blockouts were used in the terminal and standard LON section. On posts 8 through 11, the nominal size of the blocks was 200 mm x 200 mm x 350 mm in length and the blocks were routed to a depth of 10 mm to fit the size of the steel posts. On posts 11 through 13, the blocks were 200 mm x 200 mm x 550 mm and routed to a depth of 10 mm to fit the size of the steel posts. For additional information, please refer to figures 19 through 21 of this report. Photographs of the completed installation are shown in figure 22.



All dimensions are in millimeters unless otherwise noted.

REFERENCE OHIO DOT DRAWING GR-3.5M FOR ORIGINAL DETAILS

Figure 20. Details of the Ohio Type 1 thrie beam transition – sections B-B, C-C, and D-D.

NOTES: (for diagrams in figure 19, 20, and below)

GENERAL: For additional details, see SCD GR-1.1M, GR-1.2M and other drawings pertaining to design of specific guardrail types. See SCD RM-4.3M for concrete barrier details.

APPLICATIONS: The Bridge Terminal Assembly, Type 1, Barrier Design, shall be used to connect Type 5 barrier design guardrail or Type 1 Impact Attenuators to concrete median barriers.

POSTS:

GENERAL—Posts may be set in drilled holes or driven to grade.

WOOD POSTS shall be square-sawed pressure treated wood as per Item 710.14 and fabricated with square ends. Bolt holes shall be bored and tops of posts trimmed, if required, after posts are set.

STEEL POSTS AND BLOCKOUTS may be furnished as an alternate. The steel alternates for wood posts are listed below.

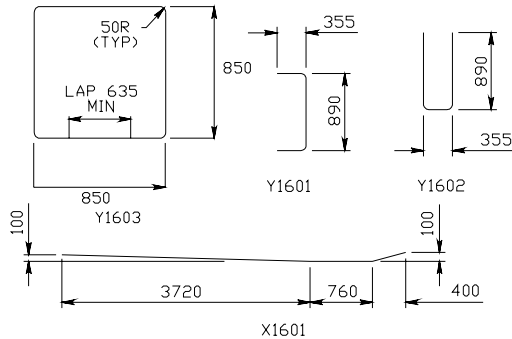
Wood Posts	250 mm x 250 mm	200 mm x 200 mm
Steel Posts	W200x35.9	W150x37.1

REINFORCING: All reinforcing bars shall be epoxy coated and included in the cost of Item 622.

PAYMENT: Payment for the guardrail transition section will be made at the unit price bid p Each for Item 606 – Bridge Terminal Assembly, Type 1, Barrier Design and shall include the extra cost, in excess of normal guardrail costs, for additional and different type posts and blockouts, nested thrie beam sections, terminal connectors, thrie beam transitions sections bolts, anchors, washers, and other hardware.

Payment for the concrete transition section will be made at the unit price bid per Meter for item 622 – Concrete Barrier, Type _ _ _ (A, Reinforced or B, Reinforced) and shall include materials, labor, and reinforcing steel required to construct the barrier as shown within the limits defined. (See Plan view.)

REFERENCE OHIO DOT DRAWING GR-3.5M FOR ORIGINAL DETAILS



NOT DRAWN TO SCALE
All dimensions are in millimeters unless otherwise noted.

REFERENCE OHIO DOT DRAWING GR-3.5M FOR ORIGINAL DETAILS

BENDING DIAGRAMS

REINFORCING BAR LIST

MARK	LENGTH (MM)	SHAPE	QUANTITY
X1601	4880	Bent	8 Each
Y1601	1530	Bent	20 Each
Y1602	2060	Bent	1 Each
Y1603	3400	Bent	11 Each

Figure 21. Details of the Ohio Type 1 thrie beam transition—notes and bending diagrams.



a) Transition from traffic side.



b) Transition from field side.

Figure 22. Ohio Type 1 three beam transition before test 401021-1.

CRASH TEST 401021-1 (NCHRP REPORT 350 TEST NO. 3-11)

Test Conditions

This test corresponds to *NCHRP Report 350* test designation 3-21; the pickup truck impacts the CIP of the transition at 100 km/h and 25 degrees. The objective was to evaluate the performance in the section that transitions from three beam to the concrete parapet. According to guidelines of *NCHRP Report 350*, the BARRIER VII simulation program was used to select the CIP for this test. The program indicated the CIP to be 1.676 m upstream of the concrete parapet.

Test Vehicle

A 1995 Chevrolet 2500 pickup truck, shown in figures 23 and 24, was used for the crash test. Test inertia weight of the vehicle was 2000 kg, and its gross static weight was 2075 kg. The height to the lower edge of the vehicle's front bumper was 445 mm and 595 mm to the upper edge of the front bumper. Additional dimensions and information on the vehicle are given in appendix B, figure 115. The vehicle was directed into the installation using the cable reverse tow and guidance system, and was released to be freewheeling and unrestrained just before impact.

Soil and Weather Conditions

The crash test was performed the morning of October 30, 2000. Seven days before the test, a total of 13 mm of rain was recorded, 8 days before the test, a total of 7 mm of rain was recorded, and 9 days before, a total of 2 mm of rain was recorded. No rainfall was recorded for the remaining 10 recording days before the test. Moisture content of the *NCHRP Report 350* standard soil in which the transition was installed was 3.9 percent. Weather conditions at the time of testing were as follows: windspeed: 6 km/h; wind direction: 25 degrees with respect to the vehicle (vehicle was traveling in a southeasterly direction); temperature: 28 °C; relative humidity: 72 percent.



a) Geometrics from traffic side.



b) Geometrics from field side.

Figure 23. Vehicle/installation geometrics for test 401021-1.



a) Front quarter view.



b) Overhead view.

Figure 24. Vehicle before test 401021-1.

Impact Description

The 2000 kg pickup truck impacted the transition at 1.7 m downstream from the end of the concrete parapet, while traveling at a speed of 101.7 km/h and an impact angle of 25.7 degrees. Post 13 and 12 moved at 0.012 s and 0.017 s, respectively. The vehicle began to redirect at 0.033 s. The left front tire pushed under the rail at 0.034 s; at 0.049 s, post 11 moved. At 0.076 s, the driver's seat began to move toward the door and the left front tire contacted the concrete parapet. By 0.093 s the driver's side window shattered, and by 0.103 s the hood latch released. The left front tire deflated at 0.110 s, and at 0.160 s the right front tire lost contact with the road surface. The rear of the vehicle contacted the rail element at 0.185 s. The vehicle became parallel with the rail element at 0.188 s and was traveling at a speed of 76.1 km/h. Post 13 moved at 0.193 s. At 0.301 s the vehicle lost contact with the installation and was traveling at a speed of 72.4 km/h and an exit angle of 7.5 degrees. The right front tire returned to the road surface at 0.371 s. Brakes on the vehicle were applied at 1.5 s and the vehicle came to rest 73.2 m downstream from impact and 12.2 m forward of the traffic face of the rail. Sequential photographs of the test period are shown in appendix C, figures 130 through 132.

Damage to Test Article

The Ohio Type 1 Thrie Beam Transition to Concrete Parapet sustained minimal damage as shown in figures 25 and 26. Tire marks marred the rail at post 13 and the end of the concrete parapet (which was chipped). The rail element remained attached at all posts. Post 13 moved 60 mm toward the field side and the rail deformed 78 mm. Post 12 moved 28 mm toward the field side and the rail deformed 15 mm. Posts 11 to the end terminal showed no movement. Length of contact of the vehicle with the transition was 3.2 m. Maximum dynamic deflection of the rail element during the test was 163 mm and maximum permanent deformation was 146 mm to the rail element between post 13 and the end of the concrete parapet.

Vehicle Damage

The 2000P vehicle sustained damage shown in figure 27. The following components received structural damage: left upper and lower A-arms, upper left side ball joint, left outer rod ends, and left side frame. Also damaged were the windshield (stress), front and rear bumpers, hood, grill, radiator, fan, left front and rear quarter panels, left door and glass, left rear wheel and rim, right front quarter panel, tailgate, and instrument panel. Maximum exterior crush to the front bumper was 550 mm. The interior is shown in figure 28. Maximum deformation of the occupant compartment was 140 mm at the center of the floor pan area and 129 mm in the kick panel area. The seam between the floor pan and fire wall opened. Exterior vehicle crush and occupant compartment measurements are shown in appendix B, table 18 and figure 116.



Figure 25. Vehicle trajectory path after test 401021-1.



a) Damage at impact.



b) Damage to parapet.

Figure 26. Installation after test 401021-1.



a) Front quarter view.



b) Overhead view.

Figure 27. Vehicle after test 401021-1.



a) Before test.



b) After test.

Figure 28. Interior of vehicle for test 401021-1.

Occupant Risk Factors

Data from the triaxial accelerometer, located at the vehicle c.g., were digitized to compute occupant impact velocity and ridedown accelerations. The occupant impact velocity and ridedown accelerations in the longitudinal axis only are required from these data for evaluation of criterion L of *NCHRP Report 350*. In the longitudinal direction, occupant impact velocity was 6.7 m/s at 0.097 s, maximum 0.010-s ridedown acceleration was -19.2 g's from 0.118 to 0.128 s, and the maximum 0.050-s average was -11.2 g's between 0.050 and 0.100 s. In the lateral direction, the occupant impact velocity was 8.2 m/s at 0.097 s, the highest 0.010-s occupant ridedown acceleration was 23.4 g's from 0.118 to 0.128 s, and the maximum 0.050-s average was 13.2 g's between 0.043 and 0.093 s. Vehicle angular displacements and accelerations versus time traces are shown in appendix D, figures 170 through 181.

Rail Instrumentation Results

Six strain gauges and one accelerometer were installed on the Ohio Type 1 Thrie Beam Transition to Concrete Parapet to measure longitudinal strains in the steel rail and post acceleration during the crash test. Graphs of data from the strain gauges installed on the railing are shown in figures 240 through 246 of appendix E. These data were collected at the request of FHWA. The data serve no purpose in determining acceptability of performance of the transition, but rather are intended to provide information for use in future computer simulation modeling and validation efforts.

Strain gauge bridges were located as follows: #1) 5540 mm downstream from the end of the concrete parapet on the field side of the plate at 625 mm from ground level; #2) 5540 mm downstream from the end of the concrete parapet on the field side of the plate at 505 mm from ground level; #3) 2745 mm downstream from the end of the concrete parapet on the field side of the plate at 715 mm from ground level; #4) 2745 mm downstream from the end of the concrete parapet on the field side of the plate at 520 mm from ground level; #5) 150 mm upstream from the end of the concrete parapet on the traffic side at 595 mm from ground level; #6) 150 mm upstream from the concrete parapet on the field side of the plate at 525 mm from ground level. At these locations, the steel rail was prepared by first grinding away the mill scale to produce a clean and smooth surface in a 60 x 30 mm area where the gauges were spot welded to bond them to the steel. A complete description of instrumentation is presented in appendix A, with photographs of typical setup shown in figure 107 of appendix A.

Assessment of Test Results

The following *NCHRP Report 350* safety evaluation criteria were used to evaluate this crash test:

Structural Adequacy

- A. *Test article should contain and redirect the vehicle; the vehicle should not penetrate, underide, or override the installation, although controlled lateral deflection of the test article is acceptable.*

Result: The Ohio Type 1 Thrie Beam Transition to Concrete Parapet contained and redirected the 2000-kg pickup truck. The vehicle did not penetrate or override the installation. The tire of the vehicle underrode the installation and overlapped on the concrete parapet 130 mm. Maximum dynamic deflection of the transition was 163 mm. (PASS)

Occupant Risk

- D. *Detached elements, fragments or other debris from the test article should not penetrate or show potential for penetrating the occupant compartment, or present an undue hazard to other traffic, pedestrians, or personnel in a work zone. Deformation of, or intrusions into, the occupant compartment that could cause serious injuries should not be permitted.*

Result: No detached elements, fragments, or other debris were present to penetrate or to show potential for penetrating the occupant compartment, nor to present undue hazard to others in the area. Maximum deformation of the occupant compartment was 140 mm to the center of the floor pan area, and the seam between the floor pan and firewall opened. Considerable deformation occurred in the driver floor pan area. No single dimension exceeded 150 mm but overall deformation indicates unacceptable performance. (FAIL)

- F. *The vehicle should remain upright during and after collision although moderate roll, pitching, and yawing are acceptable.*

Result: The 2000-kg pickup truck remained upright and stable during and after the collision period. (PASS)

Vehicle Trajectory

- K. *After collision, it is preferable that the vehicle's trajectory not intrude into adjacent traffic lanes.*

Result: The vehicle intruded 12.2 m forward of the traffic face of the installation. (FAIL)

- L. *The occupant impact velocity in the longitudinal direction should not exceed 12 m/s and the occupant ridedown acceleration in the longitudinal direction should not exceed 20 g's.*

Result: Longitudinal occupant impact velocity was 6.7 m/s and longitudinal ridedown acceleration was -19.2 g's. (PASS)

- M. *The exit angle from the test article preferably should be less than 60 percent of the test impact angle, measured at time of vehicle loss of contact with the test device.*

Result: Exit angle at loss of contact was 7.5 degrees, which was 29 percent of the impact angle. (PASS)

The following supplemental evaluation factors and terminology, as presented in the FHWA memo entitled "Action: Identifying Acceptable Highway Safety Features," were used for visual assessment of test results.⁽⁵⁾ Factors underlined below pertain to the crash test reported herein.

PASSENGER COMPARTMENT INTRUSION

1. Windshield Intrusion

- | | |
|---|---|
| <i>a. <u>No windshield contact (stressed)</u></i> | <i>e. Complete intrusion into passenger compartment</i> |
| <i>b. Windshield contact, no damage</i> | <i>f. <u>Partial intrusion into passenger compartment</u></i> |
| <i>c. Windshield contact, no intrusion</i> | |
| <i>d. Device embedded in windshield, no significant intrusion</i> | |

2. Body Panel Intrusion yes or no

LOSS OF VEHICLE CONTROL

- | | |
|--|---|
| <i><u>1. Physical loss of control</u></i> | <i><u>3. Perceived threat to other vehicles</u></i> |
| <i><u>2. Loss of windshield visibility</u></i> | <i>4. Debris on pavement</i> |

PHYSICAL THREAT TO WORKERS OR OTHER VEHICLES

- 1. Harmful debris that could injure workers or others in the area*
- 2. Harmful debris that could injure occupants in other vehicles*

No debris was present.

VEHICLE AND DEVICE CONDITION

1. Vehicle Damage

- a. None
- b. Minor scrapes, scratches or dents
- c. Significant cosmetic dents
- d. Major dents to grill and body panels
- e. Major structural damage

2. Windshield Damage

- a. None
- b. Minor chip or crack
- c. Broken, no interference with visibility
- d. Broken and shattered, visibility restricted but remained intact
- e. Shattered, remained intact but partially dislodged
- f. Large portion removed
- g. Completely removed

3. Device Damage

- a. None
- b. Superficial
- c. Substantial, but can be straightened
- d. Substantial, replacement parts needed for repair
- e. Cannot be repaired

Conclusions

The Ohio Type 1 Thrie Beam Transition to Concrete Parapet failed to meet occupant compartment deformation. The potential for serious injury existed due to large deformations. Individual dimensions did not exceed 150 mm, but overall occupant deformation was considerable and was judged to fail this criteria.

OHIO TYPE 1 THRIE BEAM TRANSITION TO CONCRETE PARAPET WITH ASPHALT CURB

TEST ARTICLE—TEST 401021-5 AND 2a

The Ohio Type 1 Thrie Beam Transition to Concrete Parapet with asphalt curb consists of 3810 mm of two nested thrie beam guardrails, a 12-gauge symmetric W-beam to thrie beam transition piece, and 3810 mm of standard W-beam guardrail. The total length of the transition is 6291 mm. In addition to the transition, 3658 mm of standard LON guardrail was attached to the transition, which was anchored on the upstream end using a LET anchorage system. The height of the thrie beam transition immediately adjacent to the parapet was approximately 803 mm. The height of the W-beam guardrail in the transition was approximately 706 mm. The contractor received several drawing details for this transition from Ohio DOT and these details were used for this project.

The downstream end of the transition was attached to a rigid concrete parapet that was fabricated to match the impact face of parapet shown in Ohio DOT's drawing designated GR-3.5M. From conversation with Ohio DOT, the section shown on GR-3.5M is typically 9 m in length. The contractor increased the footing dimension because a shorter 5-m length is allowed for the test, and a rigid concrete parapet provides a worst case scenario. The nested thrie beam transition was attached to the concrete parapet with a 10-gauge thrie beam terminal connector. The terminal connector was attached to the parapet using four 22-mm diameter A325 bolts through the parapet.

Posts 8 through 10 of the transition were W150x37 steel posts, 1830 mm in length and embedded approximately 1040 mm below grade. Post 11 was a W150x37 steel post, 2440 mm in length, and embedded approximately 1612 mm below grade. Posts 12 and 13 were W200x36 steel posts, 2440 mm in length, and embedded approximately 1612 mm below grade. Posts 1 through 7 were 150 mm x 200 mm wood posts as required for the LET guardrail end treatment. Posts 1 through 9 were spaced approximately 1905 mm apart. Posts 9 through 13 (posts in the immediate transition area) were spaced approximately 952 mm apart.

Standard wood blockouts were used in the terminal and standard LON section. On posts 8 through 11 the nominal size of the blocks was 200 mm x 200 mm x 350 mm in length and the blocks were routed to a depth of 10 mm to fit the size of the steel posts. On posts 11 through 13, the blocks were 200 mm x 200 mm x 550 mm and routed to a depth of 10 mm to fit the size of the steel posts.

A 7.1 m long x 100 mm high x 152 wide Type 2 asphaltic curb was installed in front of the Ohio Type 1 transition. The toe of the curb was placed 25 mm in front of the face of the thrie beam. The curb overlapped the lower edge of the concrete parapet for a distance of 1.2 m and tapered to ground level over 2.7 m on the upstream end (under the W-beam). For additional information, please refer to figures 29 through 32 of this report. Photographs of the completed installation are shown in figure 33.

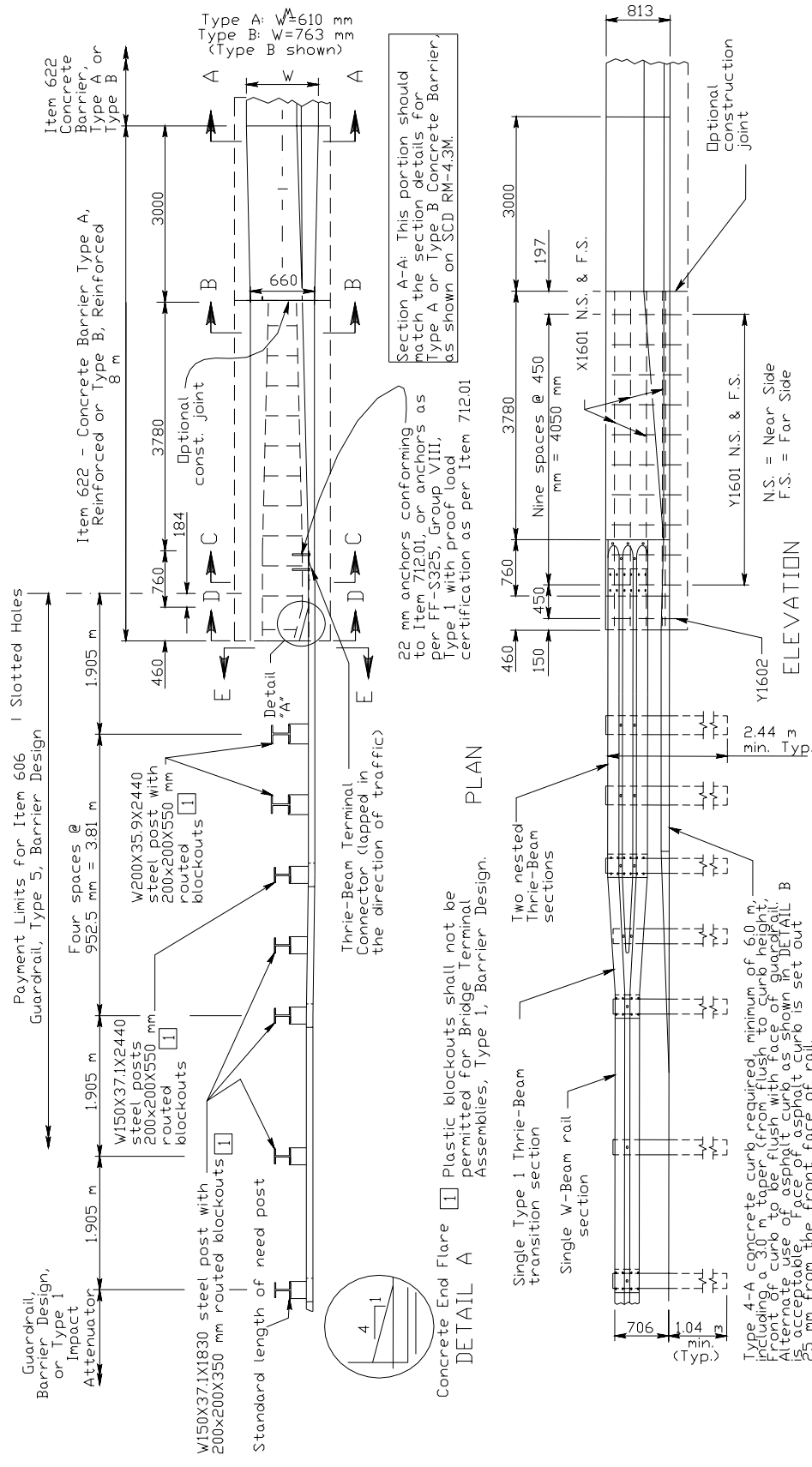


Figure 29. Details of the Ohio Type 1 thrie beam transition with asphalt curb.

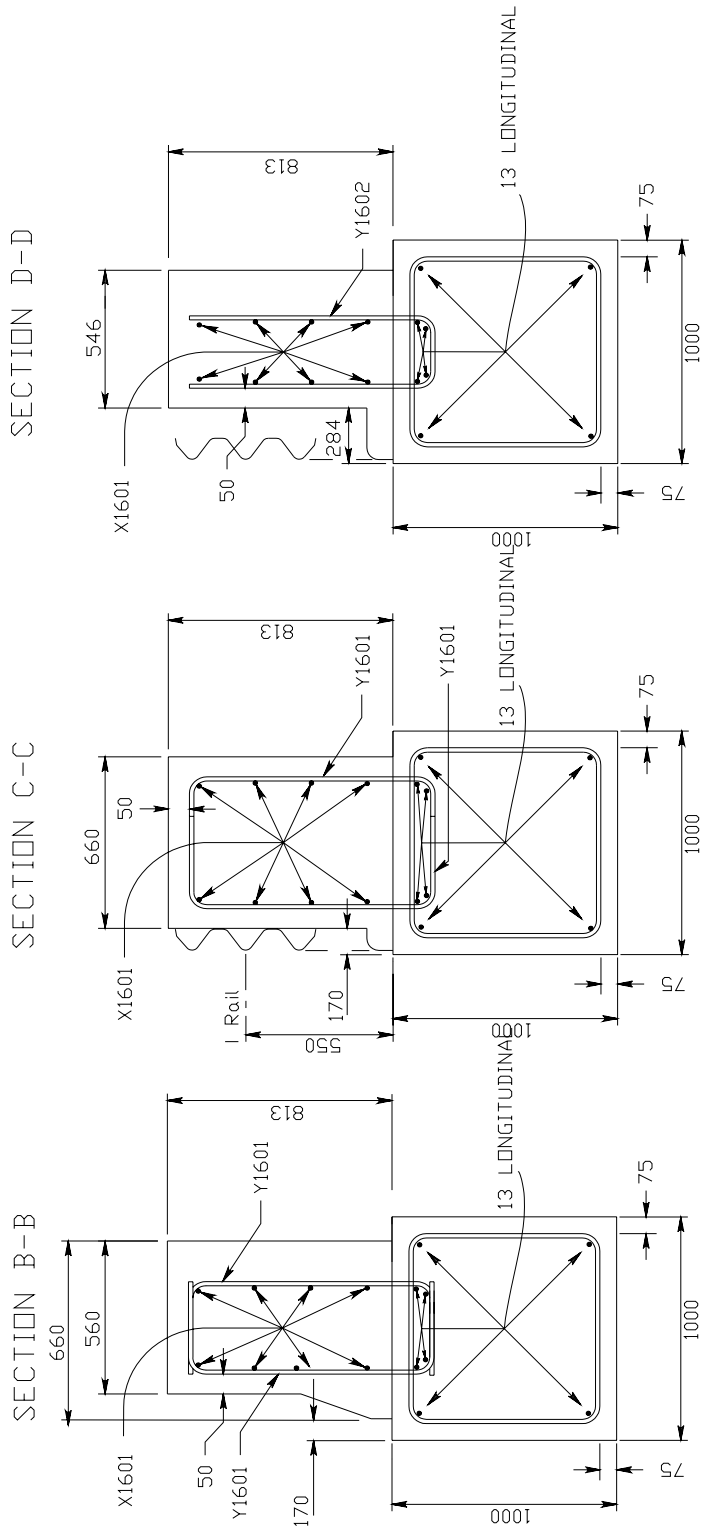


Figure 30. Details of the Ohio Type 1 thrie beam transition with asphalt curb—sections B-B, C-C, and D-D.

REFERENCE OHIO DOT DRAWING
GR-3.5M FOR ORIGINAL DETAILS

REINFORCING BAR LIST

MARK	LENGTH (mm)	SHAPE	QUANTITY
X1601	4880	Bent	8 Each
Y1601	1530	Bent	20 Each
Y1602	2060	Bent	1 Each
Y1603	3400	Bent	11 Each

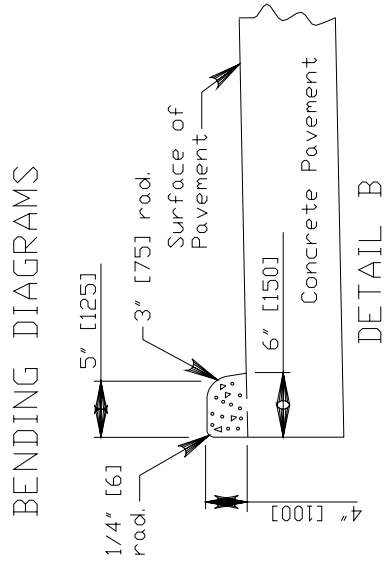
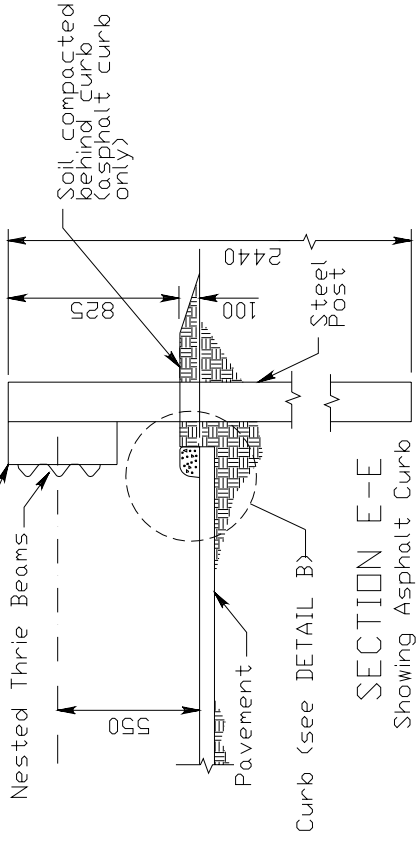
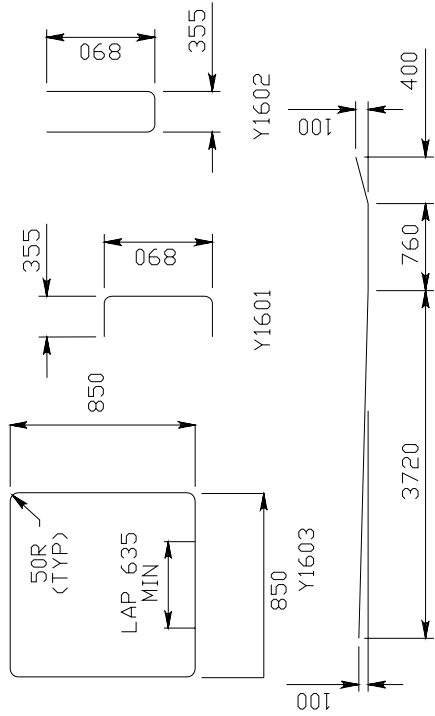


Figure 31. Details of the Ohio Type 1 thrie beam transition with asphalt curb – bending diagrams, detail B, and section E-E.

NOTES: (for diagrams in figures 29 through 31, and below)

GENERAL: For additional details, see SCD GR-1.1M, GR-1.2M and other drawings pertaining to design of specific guardrail types. See SCD RM-4.3M for concrete barrier details.

APPLICATIONS: The Bridge Terminal Assembly, Type 1, Barrier Design, shall be used to connect Type 5 barrier design guardrail or Type 1 Impact Attenuators to concrete median barriers.

POSTS:

GENERAL—Posts may be set in drilled holes or driven to grade.

WOOD POSTS shall be square-sawed pressure treated wood as per Item 710.14 and fabricated with square ends. Bolt holes shall be bored and tops of posts trimmed, if required, after posts are set.

STEEL POSTS AND BLOCKOUTS may be furnished as an alternate. The steel alternates for wood posts are listed below.

Wood Posts	250 mm x 250 mm	200 mm x 200 mm
Steel Posts	W200x35.9	W150x37.1

REINFORCING: All reinforcing bars shall be epoxy coated and included in the cost of Item 622.

PAYMENT: Payment for the guardrail transition section will be made at the unit price bid per Each for Item 606 – Bridge Terminal Assembly, Type 1, Barrier Design and shall include the extra cost, in excess of normal guardrail costs, for additional and different type posts and blockouts, nested thrie beam sections, terminal connectors, thrie beam transitions sections, bolts, anchors, washers, and other hardware.

Payment for the concrete transition section will be made at the unit price bid per Meter for item 622 – Concrete Barrier, Type _ _ _ (A, Reinforced or B, Reinforced) and shall include all materials, labor, and reinforcing steel required to construct the barrier as shown within the limits defined. (See Plan view.)

REFERENCE OHIO DOT DRAWING GR-3.5M FOR ORIGINAL DETAILS

Figure 32. Details of Ohio Type 1 thrie beam transition with asphalt curb—notes.



a) Transition from traffic side.



b) Transition from field side.

Figure 33. Ohio Type 1 thrie beam transition with asphalt curb before test 401021-5.

CRASH TEST 401021-5 (NCHRP REPORT 350 TEST NO. 3-11)

Test Conditions

This test corresponds to *NCHRP Report 350* test designation 3-21, which is the test with the pickup truck impacting the CIP of the transition at a nominal speed and angle of 100 km/h and 25 degrees. The objective was to evaluate the performance in the section that transitions from thrie beam to the concrete parapet. According to guidelines of *NCHRP Report 350*, the BARRIER VII simulation program was used to select the CIP for this test. The program indicated the CIP to be 1.676 m upstream of the concrete parapet.

Test Vehicle

A 1996 Chevrolet 2500 pickup truck, shown in figures 34 and 35, was used for the crash test. Test inertia weight of the vehicle was 2000 kg, and its gross static weight was 2075 kg. The height to the lower edge of the vehicle front bumper was 410 mm and to the upper edge of the front bumper was 620 mm. Additional dimensions and information on the vehicle are given in appendix B, figure 117. The vehicle was directed into the installation using the cable reverse tow and guidance system, and was released to be free-wheeling and unrestrained just before impact.

Soil and Weather Conditions

The crash test was performed the morning of July 2, 2001. Three days before the test, a total of 11 mm of rain was recorded. No rainfall was recorded for the remaining 10 recording days before the test. Moisture content of the *NCHRP Report 350* standard soil in which the transition was installed was 6.9 percent. Weather conditions at the time of testing were as follows: windspeed: 5 km/h; wind direction: 90 degrees with respect to the vehicle (vehicle was traveling in a southeasterly direction); temperature: 33 °C; relative humidity: 54 percent.

Impact Description

The 2000-kg pickup truck impacted the Ohio Type 1 transition at 1.67 m upstream from the end of the concrete parapet, while traveling at 100.4 km/h and an impact angle of 25.8 degrees. Shortly after the pickup contacted the thrie beam, posts 12 and 13 moved; at 0.042 s the vehicle began to redirect. The dummy's head shattered the left door glass at 0.102 s. At 0.180 s the vehicle was traveling parallel with the transition installation at 75.9 km/h. The rear of the vehicle contacted the thrie beam at 0.194 s. At 0.385 s, the vehicle lost contact with the transition and was traveling at 72.4 km/h and an exit angle of 16.0 degrees. Brakes on the vehicle were applied at 2.1 s, and the vehicle came to rest 41.1 m downstream from impact and 10.7 m forward of the traffic face of the rail. Sequential photographs of the test period are shown in appendix C, figures 133 through 135.



a) Geometrics from traffic side.



b) Geometrics from field side.

Figure 34. Vehicle/installation geometrics for test 401021-5.



a) Front quarter view.



b) Overhead view.

Figure 35. Vehicle before test 401021-5.

Damage to Test Article

The Ohio Type 1 transition with asphalt curb sustained minimal damage as shown in figures 36 and 37. The asphalt curb directly in front of the parapet separated into three pieces, with the initial separation at the end of the parapet. Tire marks marred the rail at post 13 and the end of the concrete parapet. The end of the concrete parapet was chipped; a tire mark on the end of the parapet near ground level extended 70 mm under the thrie beam. The rail element remained attached at all posts. Post 13 moved 55 mm toward field side and the rail deformed 55 mm. Post 12 moved 10 mm toward field side and the rail deformed 15 mm. Post 11 to the end terminal showed no movement. Length of contact of the vehicle with the transition was 2.52 m. Maximum dynamic deflection of the rail element during the test was 245 mm, and maximum permanent deformation was 155 mm to the rail element between post 13 and the end of the concrete parapet.

Vehicle Damage

The 2000P vehicle sustained damage as shown in figure 38. The following vehicle components received structural damage: upper left side ball joint, rear U-bolts, and the rear axle was separated from the vehicle. The roof was deformed and there was a hole in the floor pan. Also damaged were the windshield (stress), front and rear bumpers, hood, grill, radiator, fan, left front and rear quarter panels, left door and glass, left front and rear wheels and rims, right front quarter panel, tail gate, and instrument panel. Maximum exterior crush to the front bumper was 570 mm. The interior of the vehicle is shown in figure 39. Maximum deformation of the occupant compartment was 120 mm in the kick panel area. The seam between the floor pan and fire wall opened. Exterior vehicle crush and occupant compartment measurements are shown in appendix B, table 19 and figure 118.

Occupant Risk Factors

Data from the triaxial accelerometer, located at the vehicle c.g., were digitized to compute occupant impact velocity and ridedown accelerations. The occupant impact velocity and ridedown accelerations in the longitudinal axis only are required from these data for evaluation of criterion L of *NCHRP Report 350*. In the longitudinal direction, occupant impact velocity was 6.2 m/s at 0.094 s, maximum 0.010-s ridedown acceleration was -14.5 g's from 0.111 to 0.121 s, and the maximum 0.050-s average was -9.9 g's between 0.044 and 0.094 s. In the lateral direction, the occupant impact velocity was 8.9 m/s at 0.094 s, the highest 0.010-s occupant ridedown acceleration was 11.0 g's from 0.231 to 0.241 s, and the maximum 0.050-s average was 15.2 g's between 0.041 and 0.091 s. Vehicle angular displacements and accelerations versus time traces are shown in appendix D, figures 182 through 193.



Figure 36. Vehicle trajectory path after test 401021-5.



a) Overall view of damage.



b) Damage at transition.

Figure 37. Installation after test 401021-5.



a) Front quarter view.



b) Overhead view.

Figure 38. Vehicle after test 401021-5.



a) Before test.



b) After test.

Figure 39. Interior of vehicle for test 401021-5.

Rail Instrumentation Results

Six strain gauges and one accelerometer were installed on the Ohio transition to measure longitudinal strains in the steel rail and post acceleration during the crash test. Graphs of data from the strain gauges installed on the railing are shown in figures 247 through 253 of appendix E. These data were collected at FHWA's request. The data serve no purpose in determining acceptability of performance of the transition, but rather are intended to provide information for use in future computer simulation modeling and simulation efforts.

Strain gauge bridges were located as follows: #1) 5740 mm downstream from the end of the concrete parapet on the field side of the plate at 600 mm from ground level; #2) 5740 mm downstream from the end of the concrete parapet on the field side of the plate at 500 mm from ground level; #3) 2565 mm downstream from the end of the concrete parapet on the field side of the plate at 710 mm from ground level; #4) 2565 mm downstream from the end of the concrete parapet on the field side of the plate at 520 mm from ground level; #5) 120 mm upstream from the end of the concrete parapet on the traffic side at 625 mm from ground level; #6) 120 mm upstream from the concrete parapet on the field side of the plate at 550 mm from ground level. At these locations, the steel rail was prepared by first grinding away the mill scale to produce a clean and smooth surface in a 60 by 30 mm area where the gauges were spot welded to bond them to the steel. A complete description of instrumentation is presented in appendix A, with photographs of typical setup shown in figure 108 of appendix A.

Assessment of Test Results

The following *NCHRP Report 350* safety evaluation criteria were used to evaluate this crash test:

Structural Adequacy

- A. *Test article should contain and redirect the vehicle; the vehicle should not penetrate, underride, or override the installation although controlled lateral deflection of the test article is acceptable.*

Result: The Ohio Type 1 three beam transition with asphalt curb contained and redirected the 2000-kg pickup truck. The vehicle did not penetrate or override the installation. The tire of the vehicle underrode the installation and overlapped on the concrete parapet 70 mm. Maximum dynamic deflection of the transition was 245 mm. (PASS)

Occupant Risk

- D. *Detached elements, fragments, or other debris from the test article should not penetrate or show potential for penetrating the occupant compartment, or present an undue hazard to other traffic, pedestrians, or personnel in a work zone. Deformation of, or intrusions into, the occupant compartment that could cause serious injuries should not be permitted.*

Result: No detached elements, fragments, or other debris were present to penetrate or to show potential for penetrating the occupant compartment, nor to present undue hazard to others in the area. Maximum deformation of the occupant compartment was 120 mm in the kick panel, and the seam between the floor pan and firewall opened. Considerable deformation occurred in the driver floor pan area. No single dimension exceeded 150 mm, but overall deformation indicates marginal performance. (PASS)

- F. *The vehicle should remain upright during and after collision although moderate roll, pitching, and yawing are acceptable.*

Result: The 2000-kg pickup truck remained upright and stable during and after the collision period. (PASS)

Vehicle Trajectory

- K. *After collision it is preferable that the vehicle's trajectory not intrude into adjacent traffic lanes.*

Result: The vehicle intruded 10.7 m forward of the traffic face. (FAIL)

- L. *The occupant impact velocity in the longitudinal direction should not exceed 12 m/s and the occupant ridedown acceleration in the longitudinal direction should not exceed 20 g's.*

Result: Longitudinal occupant impact velocity was 6.2 m/s and longitudinal ridedown acceleration was -14.5 g's. (PASS)

- M. *The exit angle from the test article preferably should be less than 60 percent of the test impact angle, measured at time of vehicle loss of contact with the test device.*

Result: Exit angle at loss of contact was 16.0 degrees, which was 62 percent of the impact angle. (FAIL)

The following supplemental evaluation factors and terminology, as presented in the FHWA memo entitled “Action: Identifying Acceptable Highway Safety Features,” were used for visual assessment of test results.⁽⁵⁾ Factors underlined below pertain to the results of the test reported here.

PASSENGER COMPARTMENT INTRUSION

1. Windshield Intrusion

- | | |
|---|---|
| <i>a. <u>No windshield contact (stressed)</u></i> | <i>e. Complete intrusion into passenger compartment</i> |
| <i>b. Windshield contact, no damage</i> | <i>f. Partial intrusion into passenger compartment</i> |
| <i>c. Windshield contact, no intrusion</i> | |
| <i>d. Device embedded in windshield, no significant intrusion</i> | |

2. Body Panel Intrusion

yes or no

LOSS OF VEHICLE CONTROL

1. Physical loss of control

3. Perceived threat to other vehicles

2. Loss of windshield visibility

4. Debris on pavement

PHYSICAL THREAT TO WORKERS OR OTHER VEHICLES

1. Harmful debris that could injure workers or others in the area

2. Harmful debris that could injure occupants in other vehicles

No debris was present.

VEHICLE AND DEVICE CONDITION

1. Vehicle Damage

- | | |
|---|--|
| <i>a. None</i> | <i>d. Major dents to grill and body panels</i> |
| <i>b. Minor scrapes, scratches or dents</i> | <i>e. <u>Major structural damage</u></i> |
| <i>c. Significant cosmetic dents</i> | |

2. Windshield Damage

- | | |
|---|--|
| <i>a. None</i> | <i>e. Shattered, remained intact but partially dislodged</i> |
| <i>b. Minor chip or crack</i> | <i>f. Large portion removed</i> |
| <i>c. <u>Broken, no interference with visibility</u></i> | <i>g. Completely removed</i> |
| <i>d. Broken and shattered, visibility restricted but remained intact</i> | |

3. *Device Damage*

- a. *None*
- b. *Superficial*
- c. *Substantial, but can be straightened*
- d. *Substantial, replacement parts needed for repair*
- e. *Cannot be repaired*

Conclusions

The Ohio Type 1 Thrie Beam Transition to Concrete Parapet with Asphalt Curb met all occupant risk values and marginally met compartment deformation guidelines. Individual dimensions did not exceed 150 mm, but overall occupant deformation was considerable and was judged to be marginal for this criterion.

CRASH TEST 401021-2a (NCHRP REPORT 350 TEST NO. 4-22)

Test Conditions

This test corresponds to *NCHRP Report 350* test designation 4-22, which is the 8,000-kg single-unit truck impacting the CIP of the transition traveling at a nominal speed and angle of 80 km/h and 15 degrees. The objective was to evaluate the performance in the section that transitions from thrie beam to the concrete parapet. According to guidelines of *NCHRP Report 350*, the BARRIER VII simulation program was used to select the CIP for this test. The program indicated the CIP to be 1.7 m upstream of the end of the concrete parapet.

The installation used previously in test 401021-5 was repaired and used for this test. For details, see figures 29 through 32. Photographs of the Ohio Type 1 Thrie Beam Transition to Concrete Parapet with Asphalt Curb before this test is shown in figure 40.

Test Vehicle

A 1984 Chevrolet C70 single-unit truck, shown in figures 41 and 42, was used for the crash test. Test inertia weight of the vehicle was 8000 kg, and its gross static weight was 8000 kg. The height to the lower edge of the vehicle front bumper was 570 mm and the height to the upper edge of the front bumper was 850 mm. Additional dimensions and information on the vehicle are given in appendix B, figure 119. The vehicle was directed into the installation using the cable reverse tow and guidance system, and was released to be freewheeling and unrestrained just before impact.

Soil and Weather Conditions

The crash test was performed the afternoon of January 16, 2002. Five days before the test, a total of 31 mm of rain was recorded. No other rainfall was recorded during the 10 recording days before the test. Moisture content of the *NCHRP Report 350* standard soil in which the transition was installed was 6.8, 5.2, and 3.7 percent at posts 11, 13 and 15, respectively. Weather conditions at the time of testing were as follows: windspeed: 12 km/h; wind direction: 20 degrees with respect to the vehicle (vehicle was traveling in a southeasterly direction); temperature: 10 °C; relative humidity: 88 percent.



a) Closeup of transition.



b) Transition from field side.

Figure 40. Ohio Type 1 three beam transition with asphalt curb before test 401021-2a.



a) Geometrics from traffic side.



b) Frontal view of geometrics.

Figure 41. Vehicle/installation geometrics for test 401021-2a.



a) Front quarter view.



b) Overhead view.

Figure 42. Vehicle before test 401021-2a.

Impact Description

The 8000-kg single-unit truck impacted the transition 2.56 m upstream from the end of the concrete parapet, while traveling at 80.2 km/h and an impact angle of 14.6 degrees. At 0.020 s after impact, post 12 began to deflect toward the field side of the installation, and at 0.029 s posts 11 and 13 began to deflect toward the field side. The vehicle began to redirect at 0.051 s. The cab of the vehicle became parallel with the rail at 0.251 s as the vehicle was traveling at a speed of 75.3 km/h. The box of the vehicle became parallel with the rail at 0.277 s, and the rear of the box contacted the tops of the transition posts at 0.290 s. The bottom left side of the box contacted the top of the concrete parapet at 0.380 s. At 0.507 s, the vehicle lost contact with the parapet and was traveling at a speed of 69.4 km/h and an exit angle of 6.3 degrees. As the vehicle exited the parapet, it attained a maximum roll angle of 30 degrees at 0.864 s. The vehicle began to right itself; brakes on the vehicle were applied at 2.34 s. The vehicle came to rest in an upright position 77.8 m downstream of the point of impact and in line with the traffic face of the rail. Sequential photographs of the test period are shown in appendix C, figures 136 through 138.

Damage to Test Article

The Ohio Type 1 three beam transition sustained minimal damage as shown in figures 43 and 44. The asphalt in front of the curb was cracked, but the curb itself remained intact. Tire marks marred the rail from just upstream of post 13 to the end of the concrete parapet. The end of the concrete parapet was chipped. The rail element remained attached at all posts. Post 13 was displaced 50 mm toward field side, post 12 was displaced 30 mm toward field side, post 11 was displaced 15 mm toward field side, post 10 was disturbed, and post 9 to the end terminal showed no movement. Length of contact of the vehicle with the transition was 5.18 m. Maximum dynamic deflection of the rail element during the test was 120 mm and maximum permanent deformation was 70 mm to the rail element between post 13 and the end of the concrete parapet.

Vehicle Damage

The 8000S vehicle sustained damage shown in figure 45. The following vehicle components received structural damage: steering arm and linkage, box U-bolts, and floor pan. Also damaged were the front bumper, hood, grill, left front quarter panel, left front tire and wheel, left rear outside tire and wheel, and the lower left side of the box. Maximum exterior crush to the front bumper was 270 mm at the left front corner. The interior of the vehicle is shown in figure 46. There was no measurable deformation of the occupant compartment.



Figure 43. Vehicle trajectory path after test 401021-2a.



a) Overall view of damage.

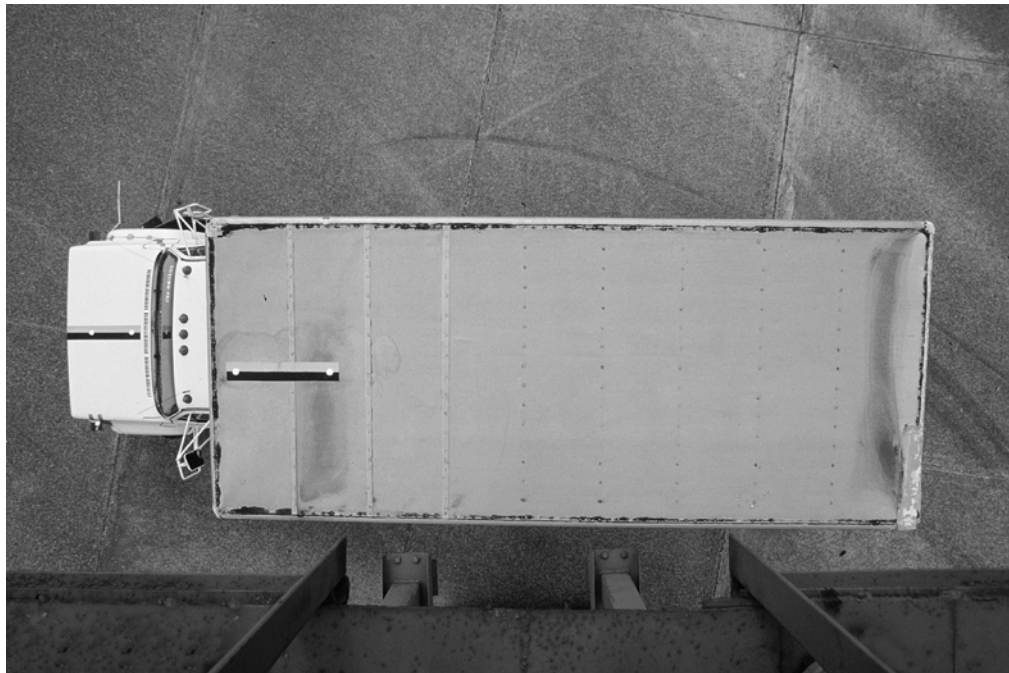


b) Damage at post 11.

Figure 44. Installation after test 401021-2a.



a) Front quarter view.



b) Overhead view.

Figure 45. Vehicle after test 401021-2a.



a) Before test.



b) After test.

Figure 46. Interior of vehicle for test 401021-2a.

Occupant Risk Factors

Data from the triaxial accelerometer, located at the vehicle c.g., were digitized to compute occupant impact velocity and ridedown accelerations. The occupant impact velocity and ridedown accelerations are not required for this test, but are reported for information purposes. In the longitudinal direction, occupant impact velocity was 2.7 m/s at 0.218 s, maximum 0.010-s ridedown acceleration was -5.2 g's from 1.586 to 1.596 s, and the maximum 0.050-s average was -2.0 g's between 0.373 and 0.423 s. In the lateral direction, the occupant impact velocity was 4.1 m/s at 0.217 s, the highest 0.010-s occupant ridedown acceleration was 8.1 g's from 0.413 to 0.423 s, and the maximum 0.050-s average was 3.7 g's between 0.385 and 0.435 s. Vehicle angular displacements and accelerations versus time traces are shown in appendix D, figures 194 through 206.

Rail Instrumentation Results

Six strain gauges and one accelerometer were installed on the Ohio transition to measure longitudinal strains in the steel rail and post acceleration during the crash test. Graphs of data from the strain gauges installed on the railing are shown in figures 254 through 260 of appendix E. The data serve no purpose in determining acceptability of performance of the transition, but rather are intended to be used in future computer simulation modeling and validation efforts.

Strain gauge bridges were located on the neutral axis for the normal plane of bending as follows: #1) 5700 mm upstream from the end of the concrete parapet on the field side of the rail at 635 mm from ground level; #2) 5700 mm upstream from the end of the concrete parapet on the field side of the rail at 505 mm from ground level; #3) 2840 mm upstream from the end of the concrete parapet on the field side of the rail at 605 mm from ground level; #4) 2840 mm downstream from the end of the concrete parapet on the field side of the rail at 535 mm from ground level; #5) at the end of the concrete parapet on the field side at 720 mm from ground level; #6) at the end the concrete parapet on the field side at 550 mm from ground level. At these locations, the steel rail was prepared by first grinding away the galvanized coating to produce a clean and smooth surface in a 60 x 30 mm area where the gauges were spot welded to bond them to the steel. The accelerometer located on the centerline of post 13 was 1300 mm downstream of the end of the parapet, 720 mm above ground level, and 480 mm behind the traffic face of the W-beam rail element. A complete description of instrumentation is presented in appendix A, with photos of typical setup shown in figure 109 of appendix A.

Assessment of Test Results

The following *NCHRP Report 350* safety evaluation criteria were used to evaluate this crash test:

Structural Adequacy

- A. *Test article should contain and redirect the vehicle; the vehicle should not penetrate, underride, or override the installation although controlled lateral deflection of the test article is acceptable.*

Result: The Ohio Thrie Beam Transition to Concrete Parapet with asphalt curb contained and redirected the 8000-kg single-unit truck. The vehicle did not penetrate, underride, or override the installation. Maximum dynamic deflection of the transition was 120 mm. (PASS)

Occupant Risk

- D. *Detached elements, fragments, or other debris from the test article should not penetrate or show potential for penetrating the occupant compartment, or present an undue hazard to other traffic, pedestrians, or personnel in a work zone. Deformation of, or intrusions into, the occupant compartment that could cause serious injuries should not be permitted.*

Result: No detached elements, fragments, or other debris were present to penetrate or to show potential for penetrating the occupant compartment, nor to present undue hazard to others in the area. No measurable deformation of the occupant compartment occurred. (PASS)

- G. *It is preferable, although not essential, that the vehicle remain upright during and after collision.*

Result: The 8000-kg single-unit truck remained upright during and after the collision period. (PASS)

Vehicle Trajectory

- K. *After collision it is preferable that the vehicle's trajectory not intrude into adjacent traffic lanes.*

Result: The vehicle did not intrude into adjacent traffic lanes. (PASS)

- M. *The exit angle from the test article preferably should be less than 60 percent of the test impact angle, measured at time of vehicle loss of contact with the test device.*

Result: Exit angle at loss of contact was 6.3 degrees, which was 43 percent of the impact angle. (PASS)

The following supplemental evaluation factors and terminology, as presented in the FHWA memo entitled “Action: Identifying Acceptable Highway Safety Features,” were used for visual assessment of test results.⁽⁵⁾ Factors underlined below pertain to the results of the test reported here.

PASSENGER COMPARTMENT INTRUSION

1. Windshield Intrusion

- | | |
|---|---|
| <i>a. <u>No windshield contact</u></i> | <i>e. Complete intrusion into passenger compartment</i> |
| <i>b. Windshield contact, no damage</i> | <i>f. Partial intrusion into passenger compartment</i> |
| <i>c. Windshield contact, no intrusion</i> | |
| <i>d. Device embedded in windshield, no significant intrusion</i> | |

2. Body Panel Intrusion

yes or no

LOSS OF VEHICLE CONTROL

1. Physical loss of control

3. Perceived threat to other vehicles

2. Loss of windshield visibility

4. Debris on pavement

PHYSICAL THREAT TO WORKERS OR OTHER VEHICLES

1. Harmful debris that could injure workers or others in the area

2. Harmful debris that could injure occupants in other vehicles

No debris was present.

VEHICLE AND DEVICE CONDITION

1. Vehicle Damage

- | | |
|---|--|
| <i>a. None</i> | <i>d. Major dents to grill and body panels</i> |
| <i>b. Minor scrapes, scratches or dents</i> | <i>e. <u>Major structural damage</u></i> |
| <i>c. Significant cosmetic dents</i> | |

2. Windshield Damage

- a. None*
- b. Minor chip or crack*
- c. Broken, no interference with visibility*
- d. Broken and shattered, visibility restricted but remained intact*
- e. Shattered, remained intact but partially dislodged*
- f. Large portion removed*
- g. Completely removed*

3. Device Damage

- a. None*
- b. Superficial*
- c. Substantial, but can be straightened*
- d. Substantial, replacement parts needed for repair*
- e. Cannot be repaired*

Conclusions

The Ohio Type 1 Thrie Beam Transition to Concrete Parapet with Asphalt Curb met required specifications for *NCHRP Report 350* test designation 4-22.

THRIE BEAM TRANSITION TO WISCONSIN TYPE “M” TUBULAR STEEL BRIDGE RAIL

TEST ARTICLE—TEST 401021-3

Details of the installation were provided by the State of Wisconsin DOT. The Wisconsin transition is constructed with nested 12-gauge thrie beams mounted on six 2.13-m-long, 150 x 200 mm wood posts spaced at 459 mm from the center end terminal connector bolt holes. Three posts are spaced at 918 mm through the 12-gauge W-beam to a thrie beam transition piece. The W-beam to thrie beam transition was attached to an extruder terminal for anchorage. A Type “M” tubular steel bridge rail was fabricated and attached to an existing structural slab with 25-mm-diameter mechanical anchor bolts. This deviates from the standard detail for post attachment as shown in the Wisconsin standard drawings for the Type “M” tubular bridge rail. However, the bridge rail is only providing anchorage for the transition test. The transition is attached to the Type “M” tubular bridge rail by a standard thrie beam terminal connector. Details of the installation are shown in figures 47 through 59, and photographs are shown in figure 60.

CRASH TEST 401021-3 (NCHRP REPORT 350 TEST NO. 3-21)

Test Conditions

This test corresponds to *NCHRP Report 350* test designation 3-21, which is the 2000-kg pickup truck impacting the CIP of the transition at a nominal speed and angle of 100 km/h and 25 degrees. The objective was to evaluate the performance in the Wisconsin transition section, which transitions from thrie beam guardrail to tubular steel bridge rail. Information provided in *NCHRP Report 350* was used to select the CIP for this test. According to this information, the target CIP was chosen as 1.92 m upstream of the first post of the bridge rail system.

Test Vehicle

A 1997 Chevrolet Cheyenne 2500 pickup truck, shown in figures 61 and 62, was used for the crash test. Test inertia weight of the vehicle was 2000 kg, and its gross static weight was 2078 kg. The height to the lower edge of the vehicle front bumper was 378 mm, and the height to the upper edge of the front bumper was 595 mm. Additional dimensions and information on the vehicle are given in appendix B, figure 120. The vehicle was directed into the installation using the cable reverse tow and guidance system, and was released to be freewheeling and unrestrained just before impact.

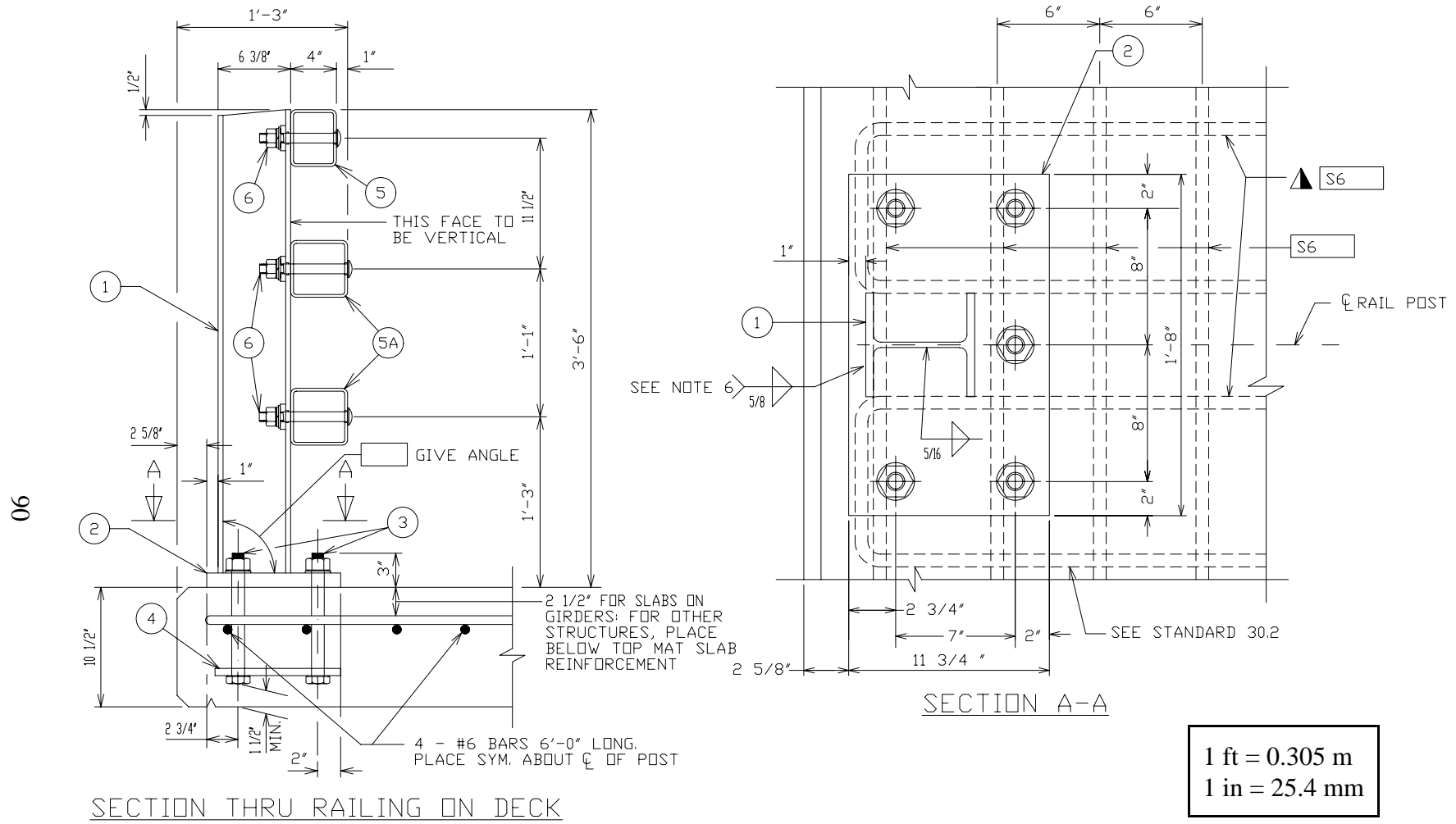
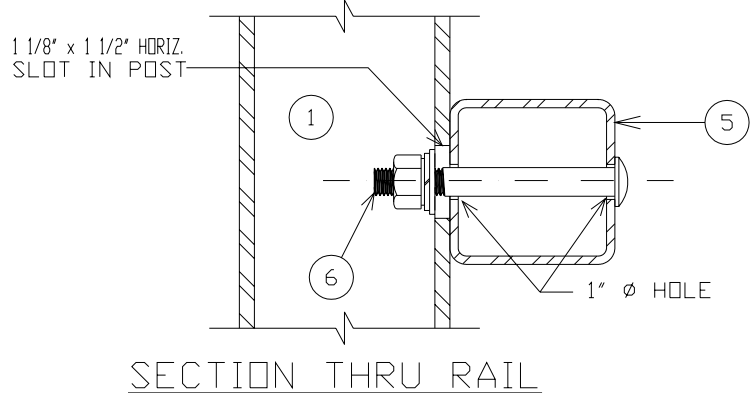
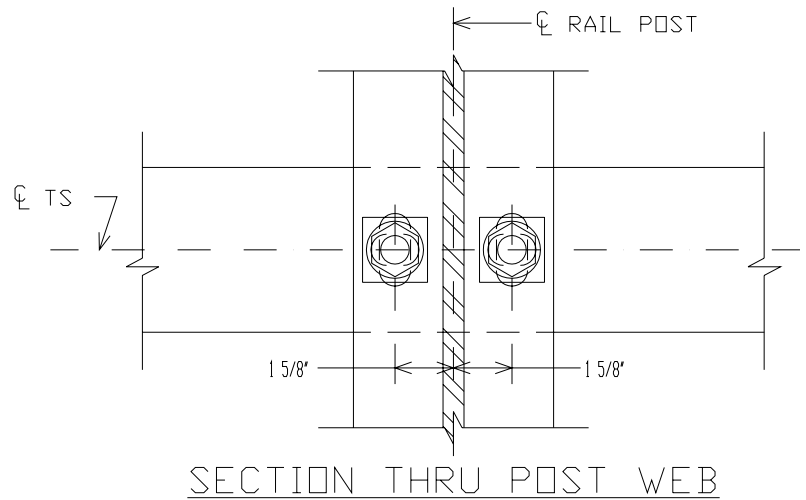


Figure 47. Details of the Type "M" tubular steel bridge rail—section through railing and section A-A.



NOTE: CONNECTIONS AT LOWER RAILS SHOWN.
 CONNECTIONS AT TOP RAIL SIMILAR.

TYPICAL RAIL TO POST CONNECTIONS

1 ft = 0.305 m
 1 in = 25.4 mm

Figure 48. Details of the Type “M” tubular steel bridge rail—section through post.

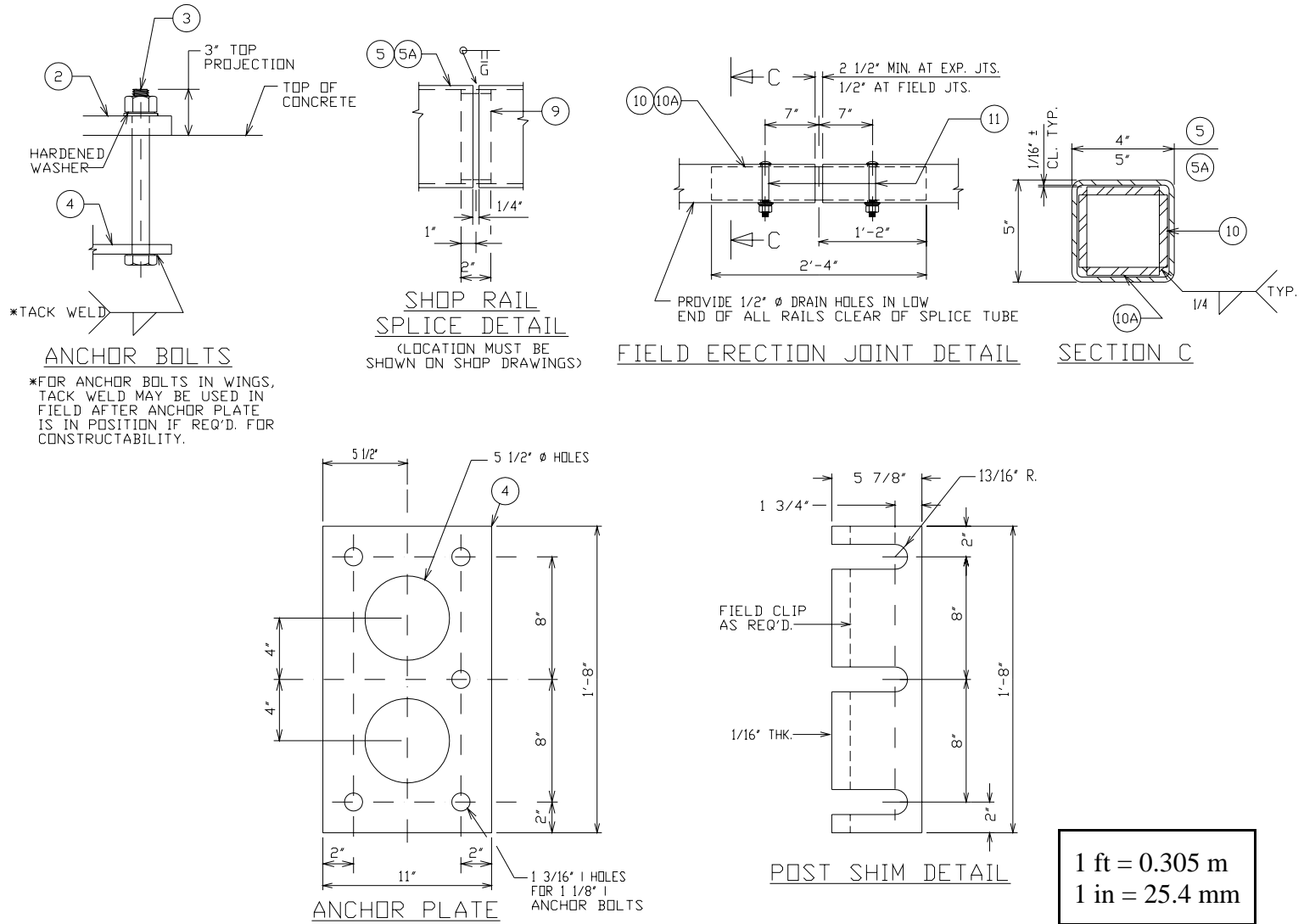
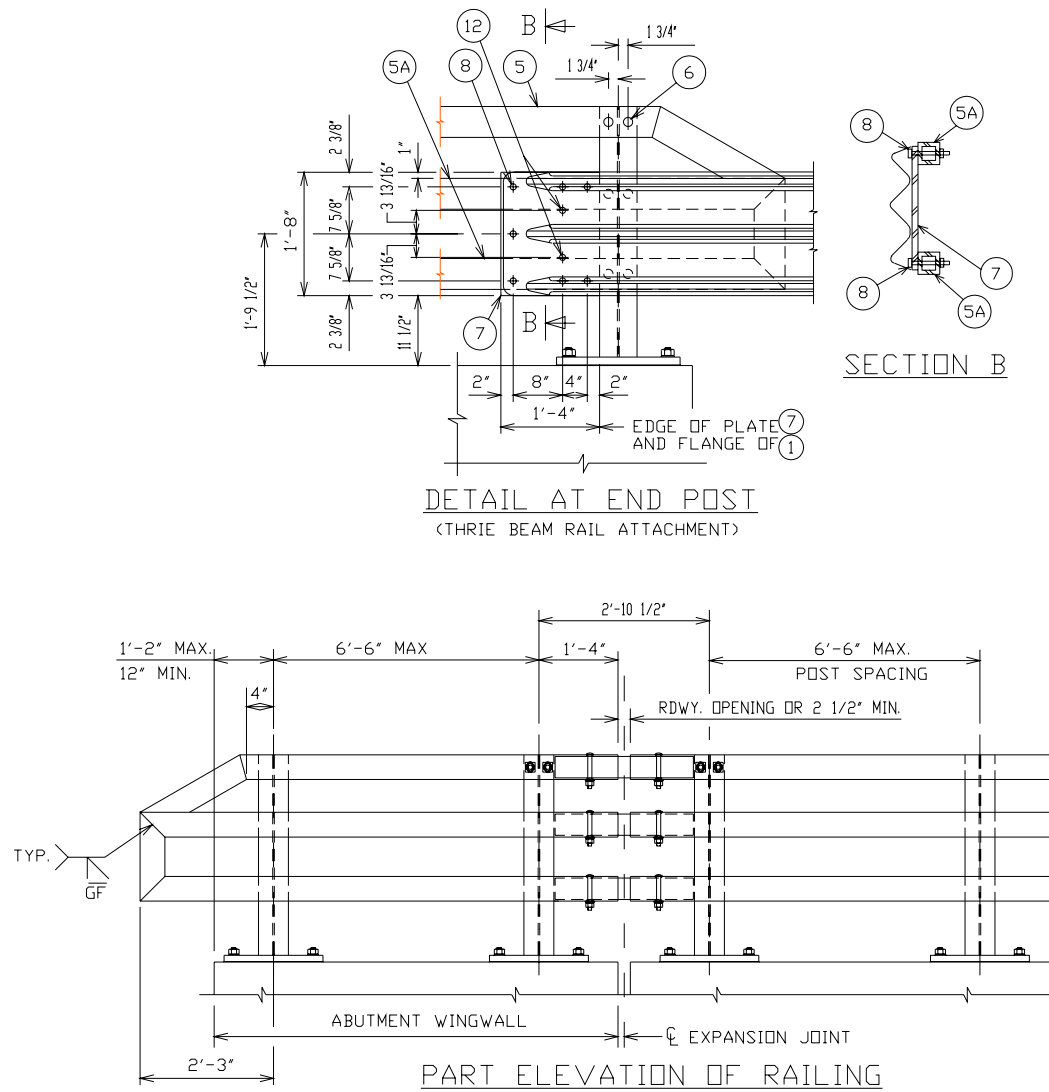


Figure 49. Details of the Type "M" tubular steel bridge rail—anchor details.



1 ft = 0.305 m
1 in = 25.4 mm

Figure 50. Details of the Type "M" tubular steel bridge rail—end post details.

Legend

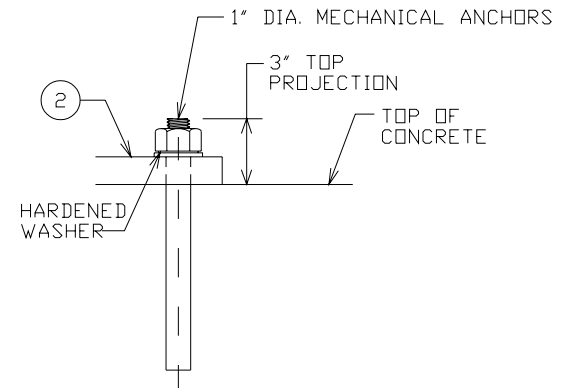
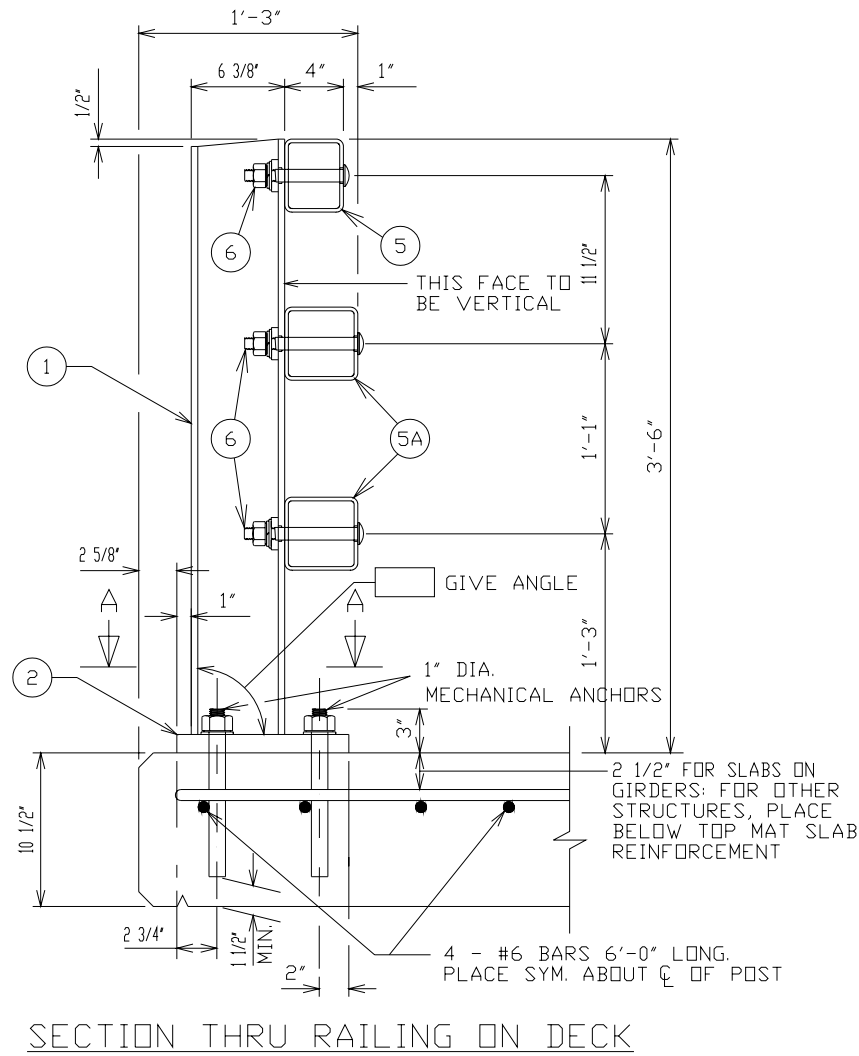
- ① W6x25 with 1-1/8" x 1-1/2" horizontal slots on each side of post for bolt No. 6. Cut bottom of post to match cross slope of roadway. Place post vertical. Place posts normal to grade line.
- ② Plate 1-1/4" x 11-3/4" x 1'-8" with 1-5/16" dia. slotted holes for anchor bolts No. 3. Weld to No. 1 as shown. Slots parallel to short side of plate.
- ③ ASTM A449 – 1-1/8" dia. anchor bolts with nut and hardened washer (all galvanized). 5 required per post. Thread 3" and place normal to plate No. 2. Chamfer top of bolts before threading. Use 1'-9" long in abutment wings. At posts on concrete slab superstructures where the slab thickness is >16", use 1'-3" long. Use 10-3/4" long at all other locations. (An equivalent threaded rod with nuts and hardened washers may be substituted for anchor bolts in wings if required for constructability.)
- ④ 5/8' x 11" x 1'-8" anchor plate (galvanized) with 1-3/16" dia. holes for anchor bolts No. 3.
- ⑤ TS5x4x0.25 structural tubing. Attach to No. 1 with No. 6.
- ⑤A TS5x5x0.25 structural tubing. Attach to No. 1 with No. 6.
- ⑥ 7/8" dia. A325 round head bolt with nut, 3/16" x 1-5/8" x 1-5/8" washer, and lock washer (2 required at each rail to post location).
- ⑦ Plate 3/8" x 1'-4" x 1'-8". Bolt to rail as shown in detail. Required at thrie beam guardrail attachments only. Place symmetrically about tubes No. 5A.
- ⑧ 1" dia. holes in plate No. 7 and tubes No. 5A for 7/8" dia. A325 bolts with hex nuts and washers. 6 holes in tubes and plate No. 7.
- ⑨ Splice sleeve fabricated from 1/4" plate. Provide "sliding fit."
- ⑩ 3/8" x 3-5/8" x 2'-4" plate. 2 per rail. Used in No. 5 & 5A.
- ⑩A 3/8" x 2-5/8" x 2'-4" plate used in No. 5, 3/8" x 3-5/8" x 2'-4" plate used in No. 5A. 2 per rail.
- ⑪ 7/8" dia. A325 round head bolt with nut, washer, and lock washer. Use 15/16" x 1-1/4" longitudinal slotted holes at field joints and 15/16" x 2-1/4" minimum longitudinal slotted holes at expansion joints in plate No. 10A.
- ⑫ 7/8" dia. x 1-1/2" long threaded shop welded studs (3 required). Tie to top of mat of steel.

GENERAL NOTES

1. Bid item shall be "Tubular Railing Type "M," which includes all items shown.
2. Rail post and base plates shall conform to the requirements of ASTM A709 Grade 50. Hollow railing structural tubing shall conform to the requirements of ASTM A500 Grade B or C with a certified FY = 50 ksi. Anchor plates and splice tube plates shall conform to the requirements of ASTM A709 Grade 36.
3. The nut securing the post base plate to the concrete shall be tightened to a snug fit and given an additional 1/8 turn.
4. Rails shall be continuous over a minimum of four (4) posts without splices where possible. Rails shall be spliced in a panel over expansion joints.
5. Ends of the tube sections shall be sawed. Grind smooth exposed edges. All cut ends shall be true and smooth.
6. Weld is the same on both flanges. Flange weld does not require magnetic particle testing.
7. Fill bolt slot openings in post shims and plate No. 2 and caulk around perimeter of plate no. 2 with non-staining gray non-bituminous joint sealer. Steel post shims may be used under posts where required for alignment.
8. Post base plates shall be flat with all surfaces smooth and free from warp and all edges smooth, straight, and vertical. All plate cuts shall be machine or machine flame cut.
9. For railing not to be painted, all material except anchorage detail (No. 4) shall be galvanized after fabrication. Prior to galvanizing, all steel railing posts and steel tubing shall be given a No. 6 blast cleaning by S.S.P.C. specifications.
10. For railing to be painted, all material except anchorage detail (No. 3 & 4) shall be painted with a three-coat zinc rich epoxy system. Prior to painting, all steel railing posts and steel tubing shall be given a No. 11 near white blast cleaning by S.S.P.C. specifications.
11. This railing meets *NCHRP Report 350* evaluation criteria for Test Level 4 (TL-4)

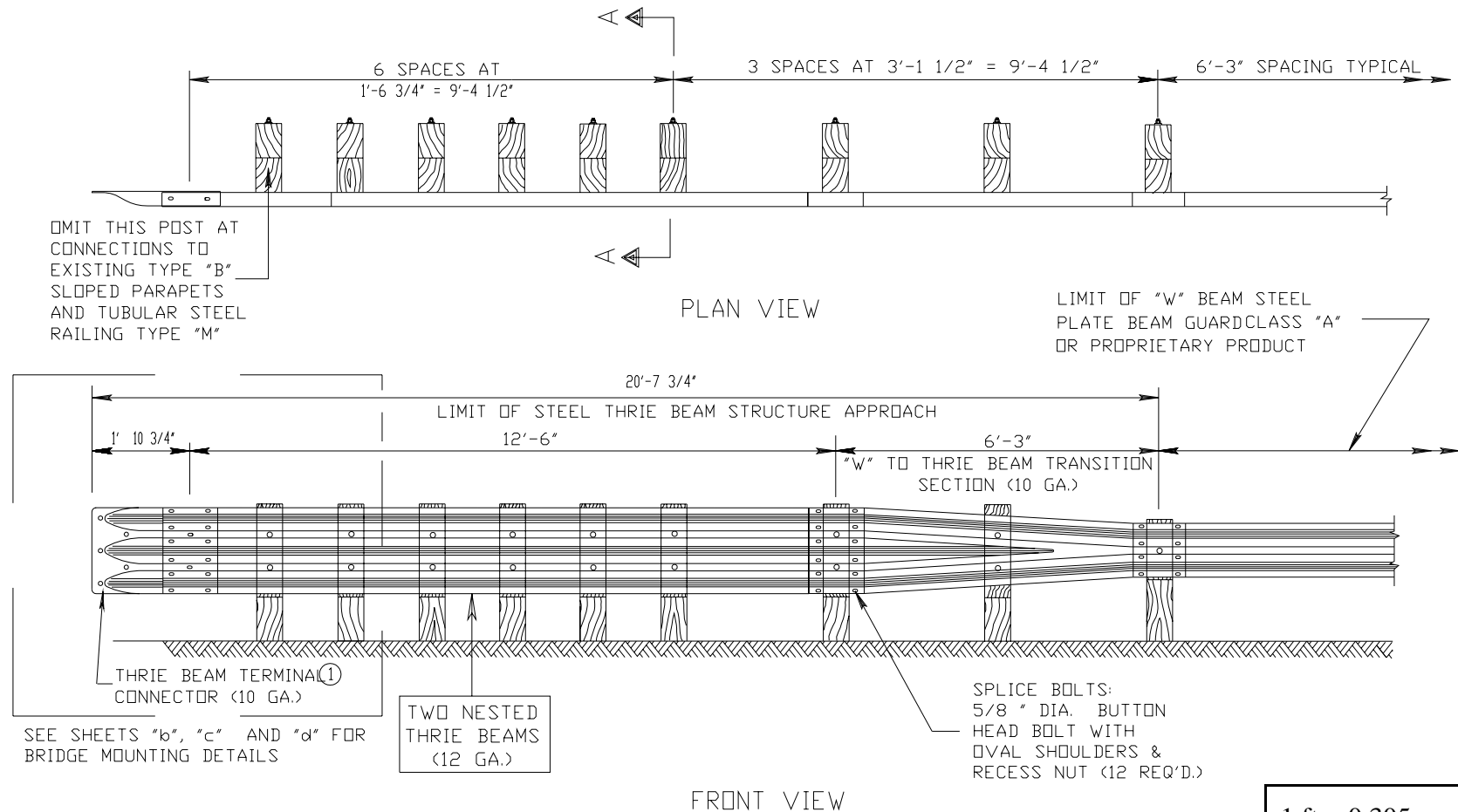
1 ft = 0.305 m
1 in = 25.4 mm

Figure 51. Details of the Type "M" tubular steel bridge rail—legend for drawing and general notes.



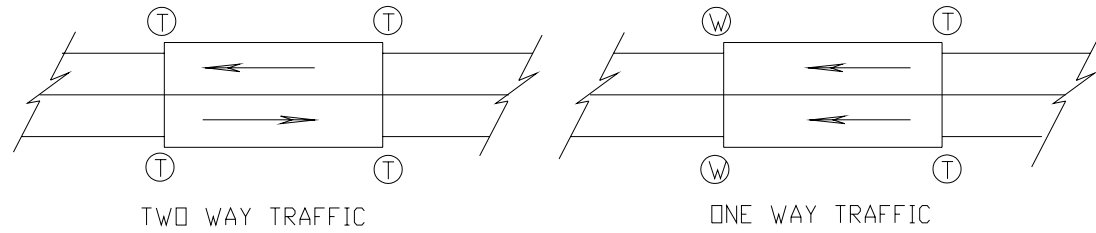
1 ft = 0.305 m
 1 in = 25.4 mm

Figure 52. Anchor details as tested.



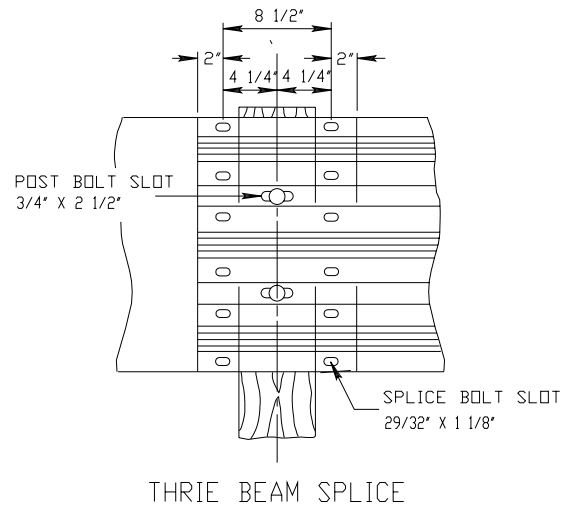
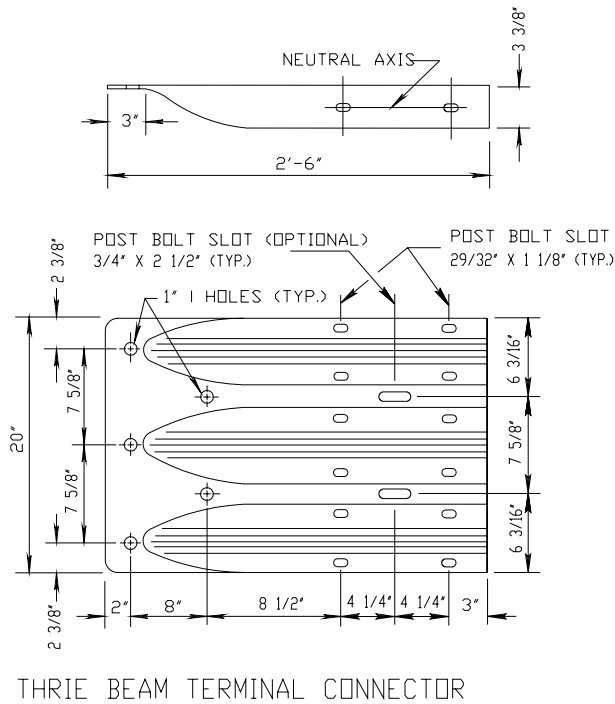
1 ft = 0.305 m
1 in = 25.4 mm

Figure 53. Details of the thrie beam transition approach—overall details.



Ⓣ THRIE BEAM CONNECTION
 Ⓜ W-BEAM CONNECTION WHEN REQUIRED

TYPICAL LOCATIONS OF THRIE BEAM AND W-BEAM CONNECTIONS TO BRIDGE



1 ft = 0.305 m
 1 in = 25.4 mm

Figure 54. Details of the thrie beam transition approach—connection and splice details.

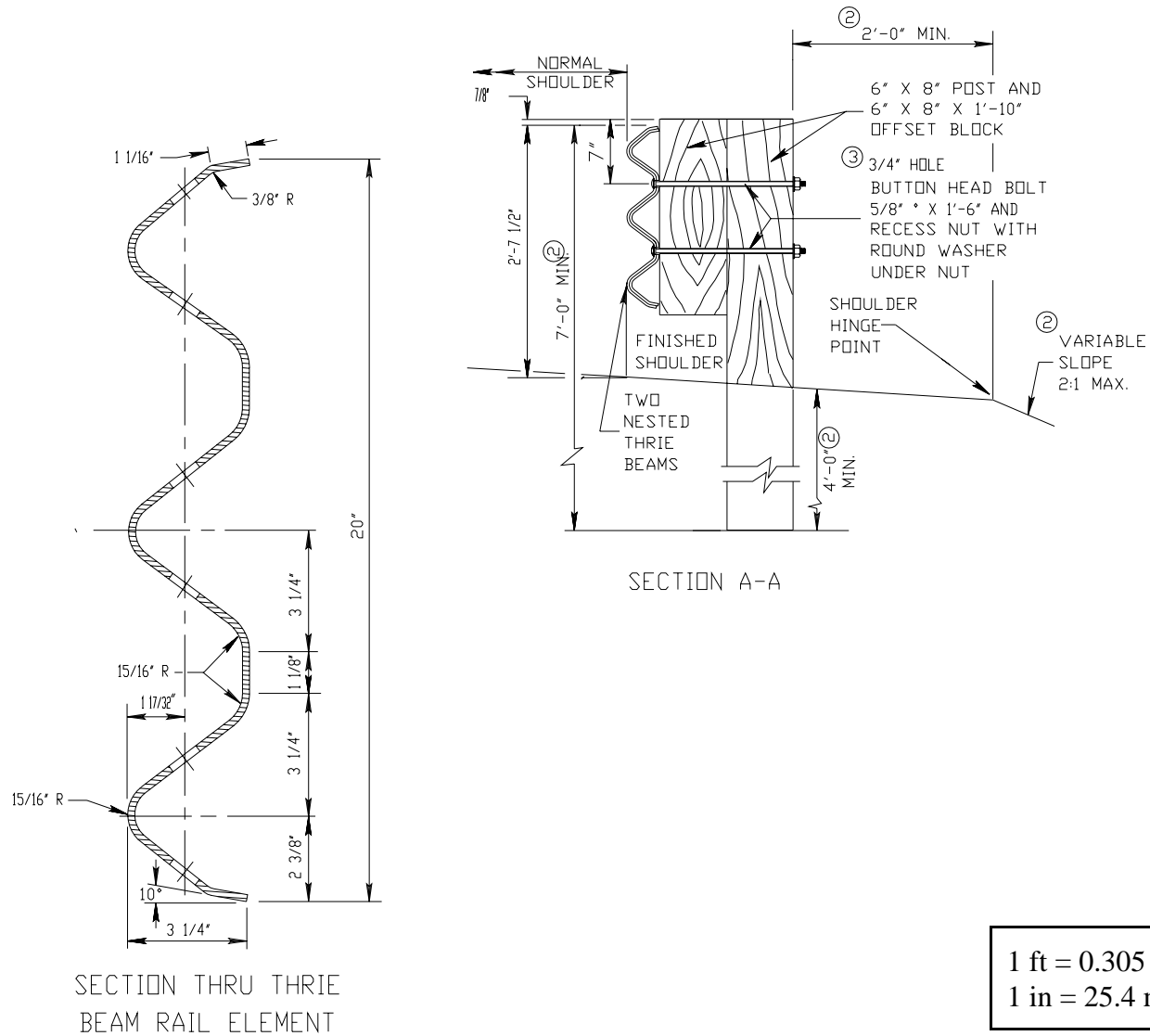


Figure 55. Details of the thrie beam transition approach—beam and post detail.

GENERAL NOTES

Details of construction, materials, and workmanship not shown on this drawing shall conform to the pertinent requirements of the Standard Specifications and the applicable special provisions.

Furnish and construct thrie beam structural approach according to the requirements of Section 614 of the Standard Specifications. Thrie beam sections shall conform to the requirements of AASHTO Designation M180, Class "A," Type 2.

Bolt the thrie beam to all posts and blockouts. Drill or punch bolt holes in the beam if the post spacing is less than 6'-3".

Do not use steel posts and notched plastic blockouts in the steel thrie beam structural approach and the transition section of steel plate beam guard, Class "A" installations.

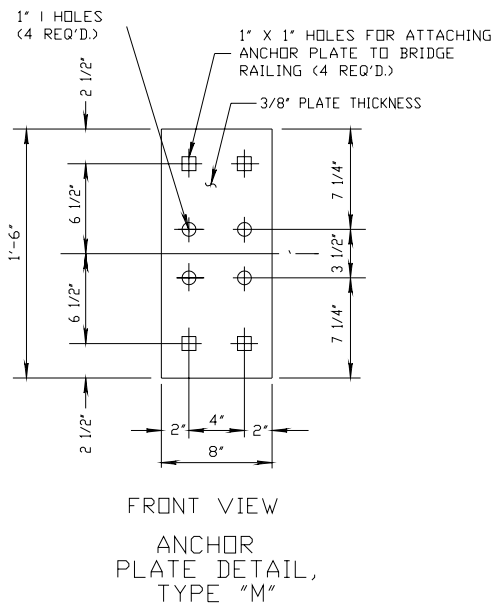
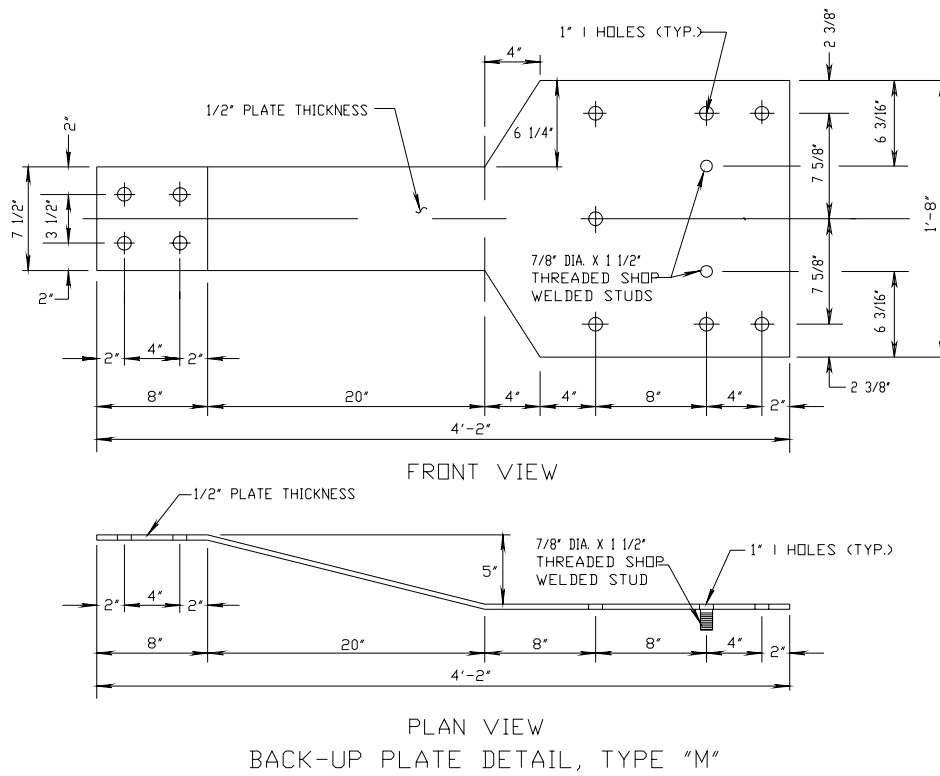
If rock is encountered during excavation, the engineer may approve using a 12-inch diameter post hole extending 20 inches deep into the rock. Place granular material in the bottom of the hole approximately 2-1/2 inches deep. Cut the posts to length and place in the hole. Backfill with material excavated from the hole and compact adequately. (See SDD 14 B 15-4a.)

Legend, figures 53-55

- ① Bridge Railing Type "W" do not require a terminal connector.
- ② Where existing conditions do not permit the appropriate earthwork shown on the plan, typical sections, or details, the engineer may allow the reduction or elimination of the 2-foot distance to the hinge point. Otherwise, build as the plan shows, or as the engineer directs. If the 2-foot distance to the hinge point is reduced or eliminated, increase the post embedment depth to 4'-6" or more.
- ③ Bolts shall conform to the requirements of ASTM F-1554, Grade 55. Nuts shall conform to the requirements of ASTM A-563 DH.

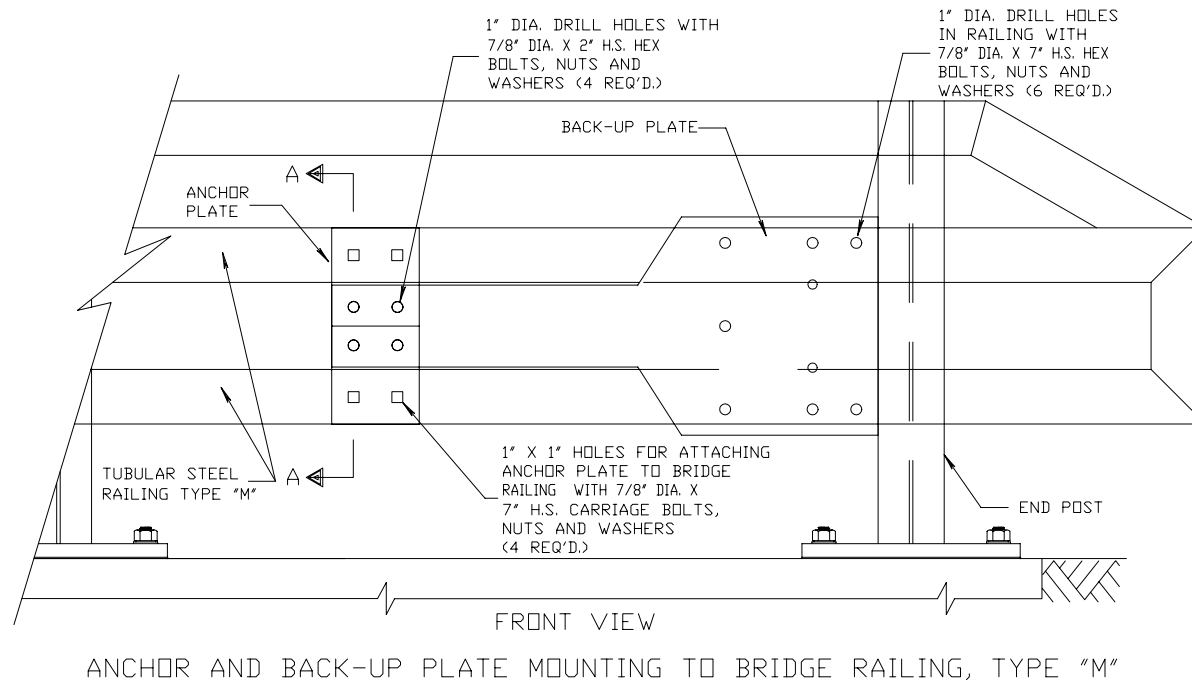
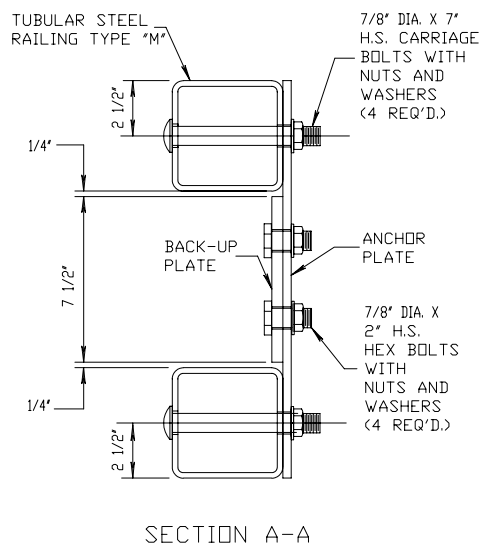
1 ft = 0.305 m 1 in = 25.4 mm

Figure 56. Details of the thrie beam transition approach—general notes.



1 ft = 0.305 m
1 in = 25.4 mm

Figure 57. Details of thrie beam transition connection to bridge rail —backup plate and anchor plate detail.

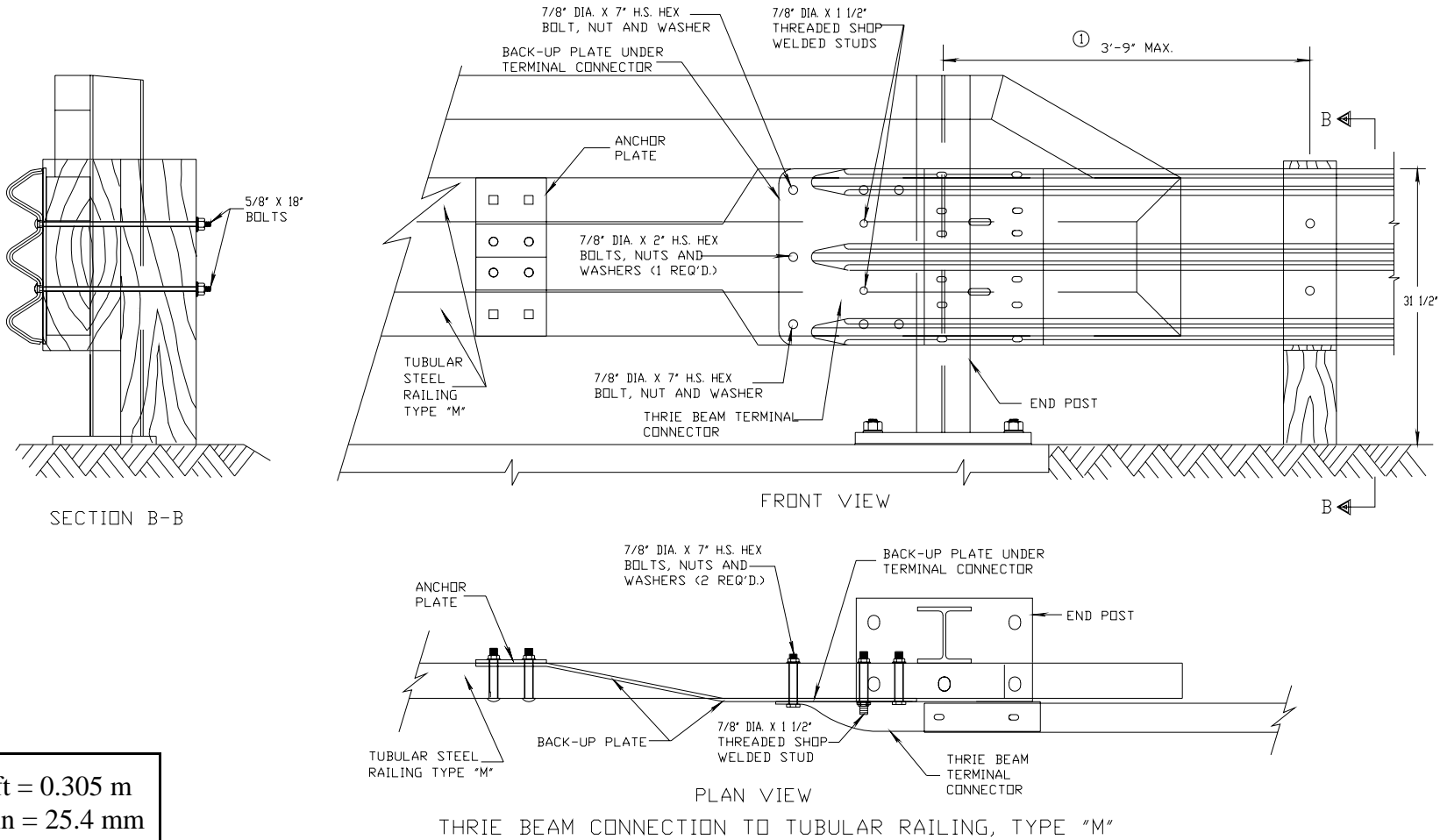


1 ft = 0.305 m
1 in = 25.4 mm

Figure 58. Details of thrie beam transition connection to bridge rail—anchor and backup plate mounting to bridge railing.

GENERAL NOTES

- ① VARY THIS DIMENSION DEPENDING ON ABUTMENT TYPE, WINGWALL DETAILS, AND ANGLE OF SKEW. PLACE THE FIRST WOOD POST OFF THE BRIDGE SHALL BE AS CLOSE AS FEASIBLE TO THE STEEL END POST.



1 ft = 0.305 m
1 in = 25.4 mm

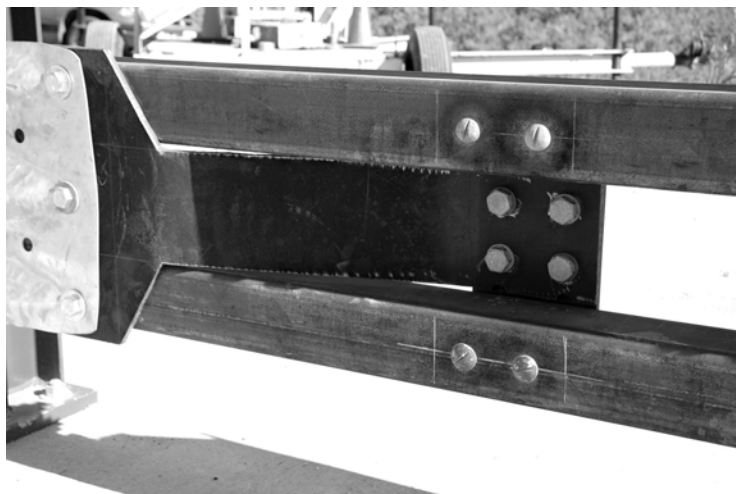
Figure 59. Details of thrie beam transition connection to bridge rail—thrie beam connection to tubular railing.



a) View of transition section.



b) Transition connection.



c) Front view of backup plate mounting.

Figure 60. Wisconsin transition installation before testing.



a) Vehicle/installation geometrics from traffic side.



b) Vehicle/installation geometrics from field side.

Figure 61. Vehicle/installation geometrics for test 401021-3.



a) Front quarter view.



b) Overhead view.

Figure 62. Vehicle before test 401021-3.

Soil and Weather Conditions

The crash test was performed the afternoon of November 22, 2002. Rainfall of 2.5 mm was recorded 8 days before the test. No other rainfall was recorded for the remaining 10 days before the date of the test. Moisture content of the *NCHRP Report 350* soil in which the test article was installed was 7.3 percent. Weather conditions at the time of testing were as follows: windspeed: 8 km/h; wind direction: 210 degrees with respect to the vehicle (vehicle was traveling in an easterly direction); temperature: 18 °C; relative humidity: 32 percent.

Impact Description

The pickup truck, traveling at a speed of 100.7 km/h, impacted the thrie beam transition 2090 mm downstream of the first bridge rail post (post 19) at an impact angle of 25.2 degrees. Shortly after impact, posts 14 through 19 began to deflect toward the field side. At 0.010 s after impact, the left front tire contacted the rail element and at 0.022 s the left front wheel turned toward the rail. Post 19 began to deflect toward the field side at 0.037 s, and the vehicle began to redirect at 0.046 s. At 0.052 s, the hood contacted the tapered box beam angling down from the first bridge rail post, and at 0.059 s post 20 began to deflect toward the field side. The dummy contacted and knocked out the side door glass at 0.111 s, and the rear view mirror contacted the tapered box beam at 0.121 s. At 0.183 s, the rear of the vehicle contacted the rail element, and at 0.186 s the vehicle was traveling parallel with the rail at a speed of 82.4 km/h. The exterior portion of the bed of the vehicle just above the rear wheel contacted the tapered box beam at 0.210 s. At 0.328 s, the vehicle lost contact with the transition as the vehicle was traveling at a speed of 81.0 km/h and an exit angle of 4.8 degrees. Brakes on the vehicle were applied at 1.5 s after impact, and the vehicle subsequently yawed 180 degrees and came to rest 73.2 m downstream from impact and 21.0 m forward of the traffic face of the rail. Sequential photographs of the test period are shown in appendix C, figures 139 through 141.

Damage to Test Article

There was minimal damage to the test installation as shown in figures 63 and 64. The top of the blackout at post 18 was gouged, and posts 15 through 18 were pushed toward the field side with a maximum permanent deflection of 45 mm at post 18 at the top thrie beam corrugation. Maximum dynamic deflection during the test was 49 mm. The mechanical anchor bolts were pulled up slightly on post 19 and the concrete deck surface around the front of the post was spalled. Total length of contact of the vehicle with the transition was 3.66 m and the working area was 0.52 m.



Figure 63. Vehicle trajectory path after test 401021-3.



a) Damage at impact.



b) Damage at end post.

Figure 64. Installation after test 401021-3.

Vehicle Damage

Damage to the vehicle is shown in figure 65. Structural damage was imparted to the left upper and lower A-arm, left upper ball joint, sway bar, and left front frame rail. Also damaged were the front bumper, hood, grill, radiator, fan, left front tire and wheel rim, left front quarter panel, left door and door glass, left rear exterior bed, left rear tire and wheel rim, and rear bumper. Maximum exterior crush to the vehicle was 650 mm in the frontal plane at the left front corner near bumper height. The windshield sustained stress cracks and the floor pan was deformed and separated from the firewall. Photographs of the interior of the vehicle are shown in figure 66. Maximum occupant compartment deformation was 74 mm in the kickpanel near the driver's feet. Exterior vehicle crush and occupant compartment measurements are shown in appendix B, table 20 and figure 121.

Occupant Risk Factors

Data from the triaxial accelerometer, located at the vehicle c.g., were digitized to compute occupant impact velocity and ridedown accelerations. Only the occupant impact velocity and ridedown accelerations in the longitudinal axis are required from these data for evaluation of criterion L of *NCHRP Report 350*. In the longitudinal direction, occupant impact velocity was 5.2 m/s at 0.095 s, maximum 0.010-s ridedown acceleration was -10.5 g's or acceleration (g's) from 0.204 to 0.214 s, and the maximum 0.050-s average was -9.1 g's between 0.050 and 0.100 s. In the lateral direction, the occupant impact velocity was 8.4 m/s at 0.095 s, the highest 0.010-s occupant ridedown acceleration was 13.8 g's from 0.213 to 0.223 s, and the maximum 0.050-s average was 13.2 g's between 0.043 and 0.093 s. Vehicle angular displacements and accelerations versus time traces are shown in appendix D, figures 207 through 218.

Results from Instrumentation of Test Article

Six strain gages and one accelerometer were installed on the thrie beam and W-beam rail elements to measure longitudinal strains and lateral acceleration during the crash test. Graphs of the data from the strain gages and accelerometer on the railing are shown in appendix E, figures 261 through 267 of appendix E. These data were collected at the request of FHWA. The data serve no purpose in determining acceptability of barrier performance, but rather are intended to provide information for use in future computer simulation modeling and validation efforts.



a) Front quarter view.



b) Overhead view.

Figure 65. Vehicle after test 401021-3.



a) Before test.



b) After test.

Figure 66. Interior of vehicle for test 401021-3.

Strain gage bridges were located as follows: (1) 590 mm downstream from the center of post 11 on the field side of the W-beam rail at 608 mm from ground level; (2) 590 mm downstream from the center of post 11 on the field side of the W-beam rail at 485 mm from ground level; (3) 460 mm downstream from the center of post 14 on the field side of the thrie beam rail at 703 mm from ground level; (4) 440 mm downstream from the center of post 14 on the field side of the thrie beam rail at 505 mm from ground level; (5) 435 mm downstream from the center of post 14 on the traffic side of the thrie beam at 320 mm from ground level; and (6) 230 mm downstream from the center of post 16 on the field side of the thrie beam at 500 mm from ground level. The accelerometer was installed on the back of post 18 in the longitudinal axis of the rail, at 530 mm above the ground surface. At these locations, the rail element was prepared by first grinding away the galvanized coating and the mill scale to produce a clean and smooth surface in a 60-mm x 30-mm area where the gages were spot-welded to bond them to the steel. A complete description of instrumentation is presented in appendix A, with photographs showing typical setup shown in figure 110 of appendix A.

Assessment of Test Results

An assessment of the test based on the applicable *NCHRP Report 350* safety evaluation criteria is provided below.

Structural Adequacy

- A. *Test article should contain and redirect the vehicle; the vehicle should not penetrate, underride, or override the installation although controlled lateral deflection of the test article is acceptable.*

Result: The Wisconsin transition contained and redirected the pickup truck. The vehicle did not penetrate, underride, or override the installation. Maximum dynamic deflection was 49 mm.
(PASS)

Occupant Risk

- D. *Detached elements, fragments, or other debris from the test article should not penetrate or show potential for penetrating the occupant compartment, or present an undue hazard to other traffic, pedestrians, or personnel in a work zone. Deformation of, or intrusions into, the occupant compartment that could cause serious injuries should not be permitted.*

Results: No detached elements, fragments, or other debris were present to penetrate or to show potential for penetrating the occupant compartment, or to present a hazard to others in the area. Maximum occupant compartment deformation was 74 mm in

the kickpanel area on the driver's side. (PASS)

- F. *The vehicle should remain upright during and after collision although moderate roll, pitching, and yawing are acceptable.*

Result: The vehicle remained upright during and after the collision event. (PASS)

Vehicle Trajectory

- K. *After collision, it is preferable that the vehicle's trajectory not intrude into adjacent traffic lanes.*

Result: The vehicle came to rest 73.2 m downstream of impact and 21.0 m forward of the traffic face of the rail. (FAIL)

- L. *The occupant impact velocity in the longitudinal direction should not exceed 12 m/s and the occupant ridedown acceleration in the longitudinal direction should not exceed 20 g's.*

Result: Longitudinal occupant impact velocity was 5.2 m/s and maximum longitudinal occupant ridedown acceleration was -10.5 g's. (PASS)

- M. *The exit angle from the test article preferably should be less than 60 percent of the test impact angle, measured at time of vehicle loss of contact with the test device.*

Result: Exit angle at loss of contact was 4.8 degrees, which was 19 percent of the impact angle. (PASS)

The following supplemental evaluation factors and terminology, as presented in the FHWA memo entitled "Action: Identifying Acceptable Highway Safety Features," were used for visual assessment of test results.⁽⁵⁾ Factors underlined below pertain to the results of the test reported here.

PASSENGER COMPARTMENT INTRUSION

1. Windshield Intrusion

- a. No windshield contact*
- b. Windshield contact, no damage*
- c. Windshield contact, no intrusion*
- d. Device embedded in windshield, no significant intrusion*
- e. Complete intrusion into passenger compartment*
- f. Partial intrusion into passenger compartment*

2. Body Panel Intrusion

yes or no

LOSS OF VEHICLE CONTROL

1. Physical loss of control

3. Perceived threat to other vehicles

2. Loss of windshield visibility

4. Debris on pavement

PHYSICAL THREAT TO WORKERS OR OTHER VEHICLES

1. Harmful debris that could injure workers or others in the area

2. Harmful debris that could injure occupants in other vehicles

No harmful debris present.

VEHICLE AND DEVICE CONDITION

1. Vehicle Damage

- a. None*
- b. Minor scrapes, scratches or dents*
- c. Significant cosmetic dents*
- d. Major dents to grill and body panels*
- e. Major structural damage*

2. Windshield Damage

- a. None*
- b. Minor chip or crack*
- c. Broken, no interference with visibility*
- d. Broken and shattered, visibility restricted but remained intact*
- e. Shattered, remained intact but partially dislodged*
- f. Large portion removed*
- g. Completely removed*

3. Device Damage

- a. None*
- b. Superficial*
- c. Substantial, but can be straightened*
- d. Substantial, replacement parts needed for repair*
- e. Cannot be repaired*

Conclusions

The Wisconsin transition to Type “M” tubular steel bridge rail was tested and evaluated according to *NCHRP Report 350* requirements and met the evaluation criteria for test 3-21.

COMPUTER SIMULATION OF THE NYSDOT BOX-BEAM TRANSITION AND MODIFIED BOX-BEAM TRANSITION

INTRODUCTION

Under Modification No. 3 of this contract, the contractor performed an FEA of the original NYSDOT box-beam transition to four-tube bridge rail that failed the pickup truck test (test 4-21) recommended in *NCHRP Report 350*.⁽⁴⁾ This transition was tested in 1999 as test no. 404531-7.

Task B1 required the modeling of the NYSDOT box-beam transition to four-tube bridge rail that failed the test with the pickup truck (test no. 404531-7). The purpose of this modeling effort was to attempt to capture the vehicle-to-barrier interactions that contributed to the deformation of the passenger compartment and caused the driver's side door to become detached from the pickup truck.

In Task B2, the research team was to construct a finite-element model of the modified NYSDOT box-beam transition to four-tube bridge rail. The model was then to be subjected to crash conditions that simulated those of Test Level 4 in *NCHRP Report 350*. Both the pickup truck test (test designation 4-21) and the single-unit van-truck test (test designation 4-22) were to be investigated.

For Task B3, the research team was to construct a finite-element model of the modified NYSDOT box-beam transition to concrete barrier. The single slope concrete barrier to which the transition model was attached was modeled as rigid material. The model was subjected to crash conditions that simulated those of Test level 4 in *NCHRP Report 350*. Both the pickup truck test (test designation 4-21) and the single-unit van-truck test (test designation 4-22) were to be investigated.

Task B4 required that after review of the FEA performed in Tasks B1 through B3, the Contracting Officer's Technical Representative (COTR) would request that the researchers communicate any desired changes to the box-beam transition to further improve performance for additional FEA.

TASK B1

The purpose of Task B1 was to develop a valid model of the original NYSDOT box-beam transition that replicated the failure events observed in test 404531-7 (New York Four-Rail Bridge Rail Transition). In this test, the leading edge of the driver's side door snagged on the edge of a box-beam rail element located at the downstream end of an expansion joint in the box-beam rail. The snagging was severe enough to cause the door to be ripped open at its hinges, permitting the lower extremities of the anthropomorphic dummy positioned in the driver's seat to be thrown from the occupant compartment.

The model of the transition system includes the transition section in the impact region, the first bridge rail post, and the four bridge rail members up to the second bridge rail (see figure 67). Appropriate boundary conditions were applied to account for the continuity of the system on both the upstream and downstream ends. Although the full test installation was initially modeled for this task, a subset of the model was found to be sufficient to capture the response of the system for the impact condition of interest. Reducing the size of the model had the added benefit of expediting the simulation runs.

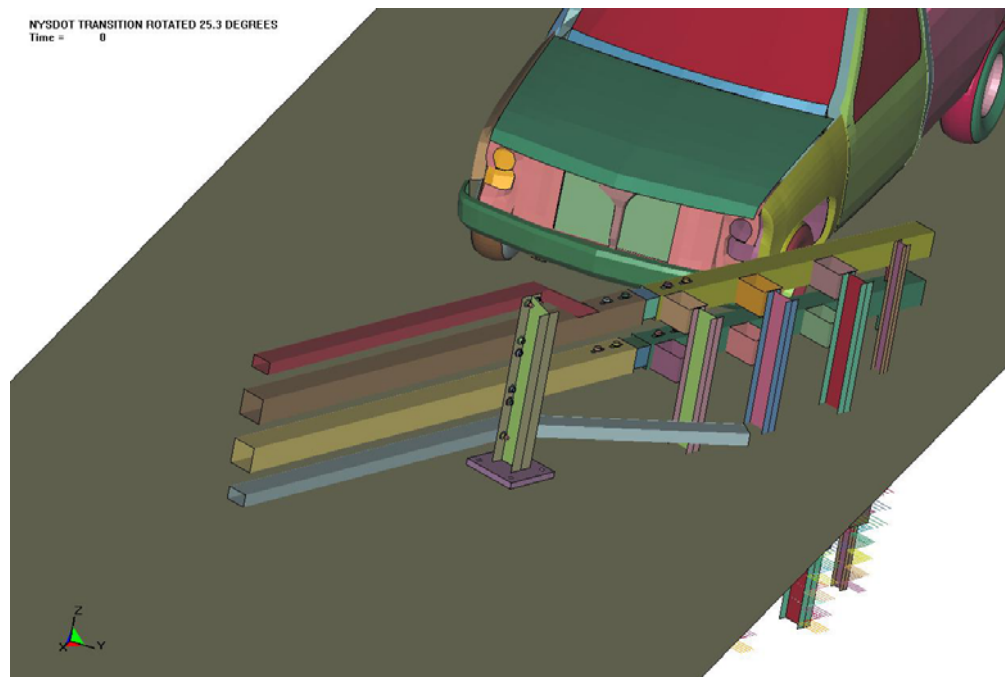


Figure 67. Simulation setup.

This specific problem of door edge snagging at the box-beam splice was a great challenge to simulate numerically in a reliable and stable manner. This phenomenon exhibits sensitivity in regard to several model parameters, including element formulations, hourglass controls, and contacts. Moreover, detailed models of both the barrier and vehicle are required to capture such a localized failure mechanism that has a consequence on the global performance of the test.

A model of a 2000-kg pickup truck developed by the National Crash Analysis Center (NCAC) under FHWA sponsorship was used in the simulation. Several changes were made to the vehicle model to enhance its capability to detect door edge snagging as well as the capability to fail (erode) elements associated with the door hinges. The revised vehicle model was used to simulate an impact with the original NYSDOT box-beam transition using the speed, angle, and impact location from the actual crash test. The model successfully captured the snagging of the door edge on the box-beam splice (see figure 68). As shown in figure 69, the resulting deformation of the door was excessive.

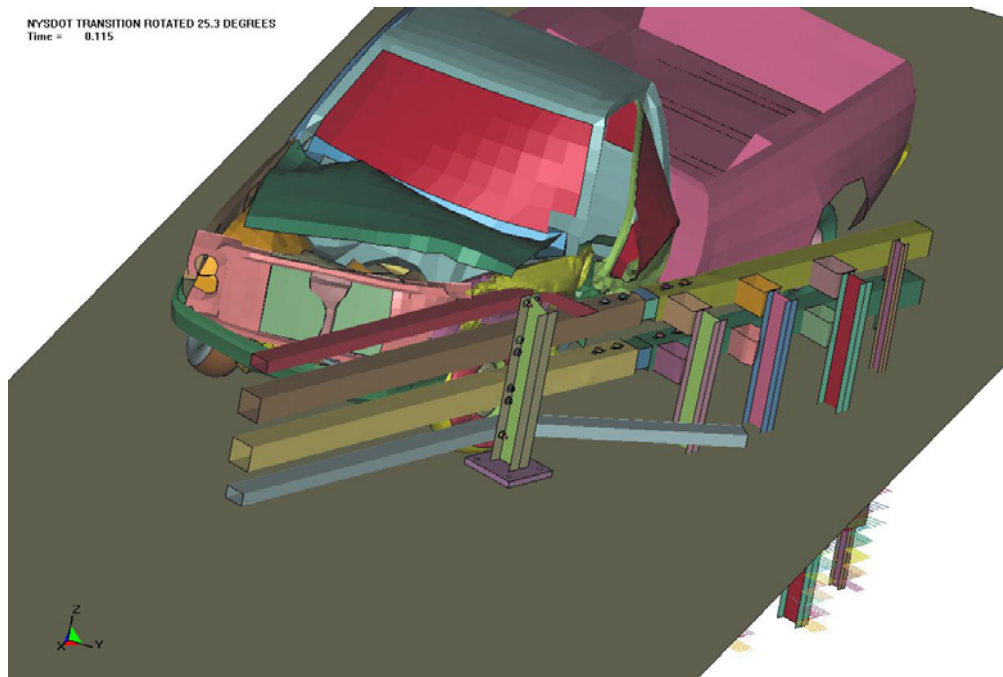


Figure 68. Snagging of door edge on box-beam splice.

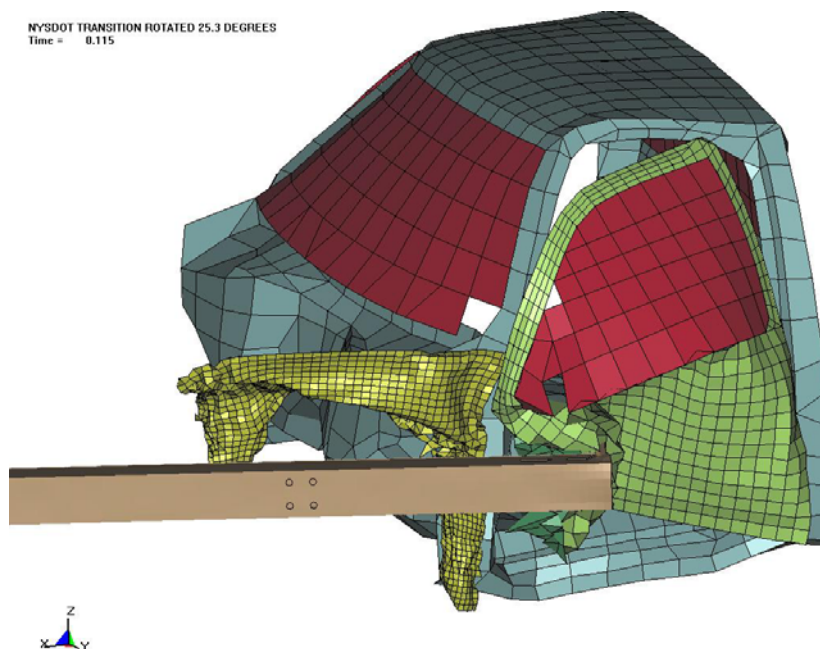


Figure 69. Closeup of door deformation with parts of transition and vehicle removed.

The simulation ended at 0.13 s, right after the left front wheel passed the first bridge rail post. The simulation energy balance was maintained within acceptable engineering limits. The profile of the vehicle damage and the vehicular motions were in general agreement with that observed in the full-scale crash test during the simulated time.

Given the correlation between the test and simulation, the model was considered sufficiently valid to proceed with a comparative evaluation to assess the effectiveness of the modified transition in mitigating the observed snagging behavior. However, given the sensitivity of these localized phenomena to changes in the model, the researchers expressed a word of caution regarding the use and interpretation of subsequent simulation results in assessing compliance of modified designs with *NCHRP Report 350*.

TASK B2

The purpose of Task B2 was to model the modified New York box-beam four-tube bridge rail transition and evaluate its impact performance based on simulations with both the 2000-kg pickup truck and 8000-kg single-unit truck.

The model of the transition system included the transition section in the impact region, the first bridge rail post, and the four bridge rail members up to the second bridge rail post. Appropriate boundary conditions were applied to account for the continuity of the system on both the upstream and downstream ends. The model developed under Task B1 was modified according to the NYSDOT drawing BD-RS4 R2 “Steel Bridge Railing to Box-Beam Guide Rail Transition.” The changes included flaring the top bridge rail element horizontally toward the field side, and adding a fourth heavy transition post, which decreased the distance between the last transition post and the first bridge post. All components in the impact region were explicitly modeled to provide more accurate assessment of their interaction with the vehicle models.

Simulations were conducted to examine the interaction of the 2000-kg pickup truck design test vehicle with the expansion splice and other components of the modified transition under *NCHRP Report 350* test 4-21 impact conditions. This test involves the 2000-kg pickup impacting the transition at its CIP at a speed of 100 km/h and an angle of 25 degrees. The finite-element model of the modified transition and vehicle before impact is shown in figure 70.

In the pickup truck simulation, the vehicle impacted the system the same distance upstream of the expansion joint as that used in the failed crash test of the original New York box-beam transition to four-tube bridge rail and the simulation studies conducted under Task B1. As expected in a transition impact of this severity, the front left corner of the vehicle experienced substantial damage. Some snagging contact occurred between the door and the downstream edge of the expansion splice. However, the resulting damage to the door was not as severe as that observed in the original system. Figure 71 shows the door edge contact as it reaches the downstream edge of the splice.

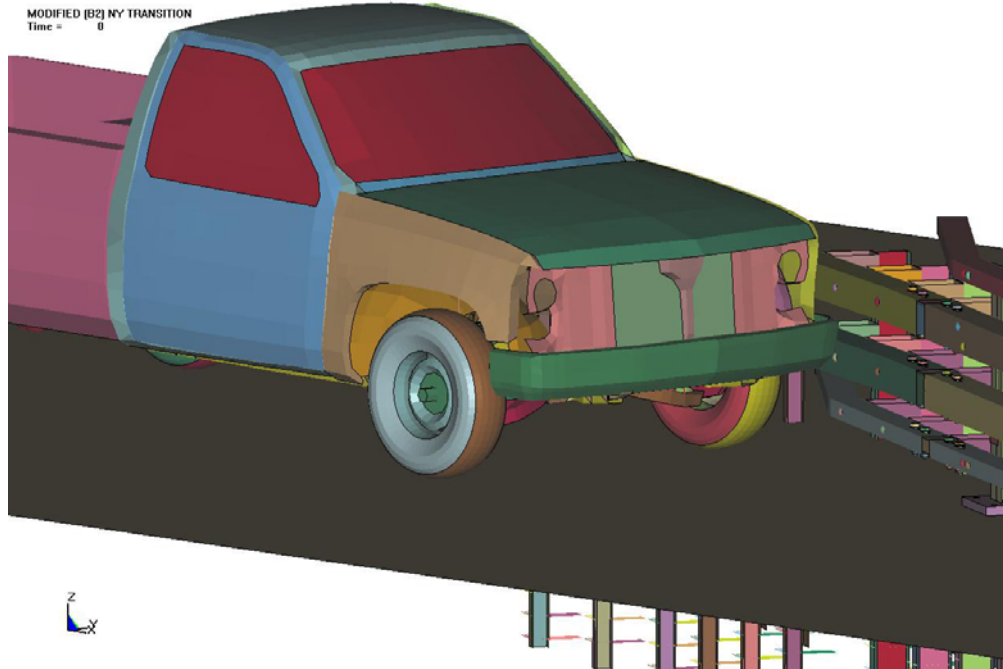


Figure 70. Model of modified New York box-beam transition and C2500 pickup truck.



Figure 71. Door edge contact with the rail splice.

The door-snagging problem is believed to be sensitive to a number of variables, including various vehicle characteristics, impact location, and impact conditions (i.e., speed and angle). Given the sensitivity of such localized phenomena to changes in the model, the researchers recommended that this aspect of the simulation results be interpreted with due caution.

As shown in figure 72, the modification to the termination of the upper bridge rail element permitted the hood of the pickup truck to severely snag on the first bridge rail post. Although hinge failure of the hood is not present in the vehicle model, the severity of the hood snagging raises a significant safety concern that needed to be addressed. The overall vehicle damage resulting from the impact is shown in figure 73.

Under Task B2, additional simulations were conducted in an attempt to examine the performance of the modified New York box-beam transition when impacted by an 8000-kg single-unit truck under *NCHRP Report 350* test 4-22 impact conditions. This test involves the 8000-kg single-unit truck impacting the transition at its CIP at a speed of 80 km/h and an angle of 15 degrees. A model of a Ford® F800 truck developed by the NCAC under FHWA sponsorship was used in the simulation. The finite-element model of the modified transition and vehicle before impact is shown in figure 74.

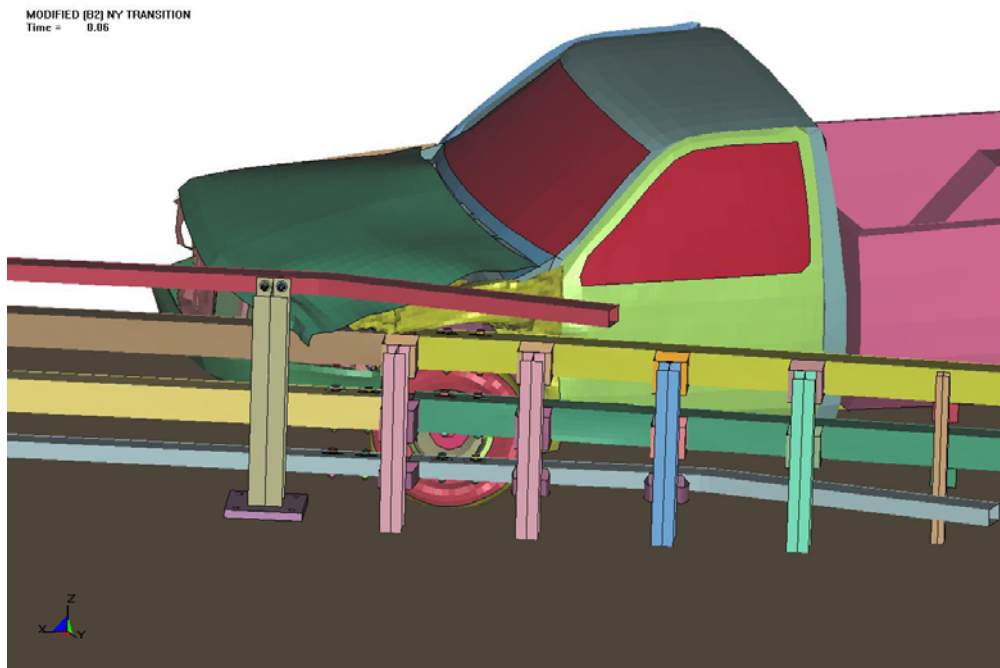


Figure 72. Hood snagging with first bridge rail post.

MODIFIED [B2] NY TRANSITION
Time = 0.12002

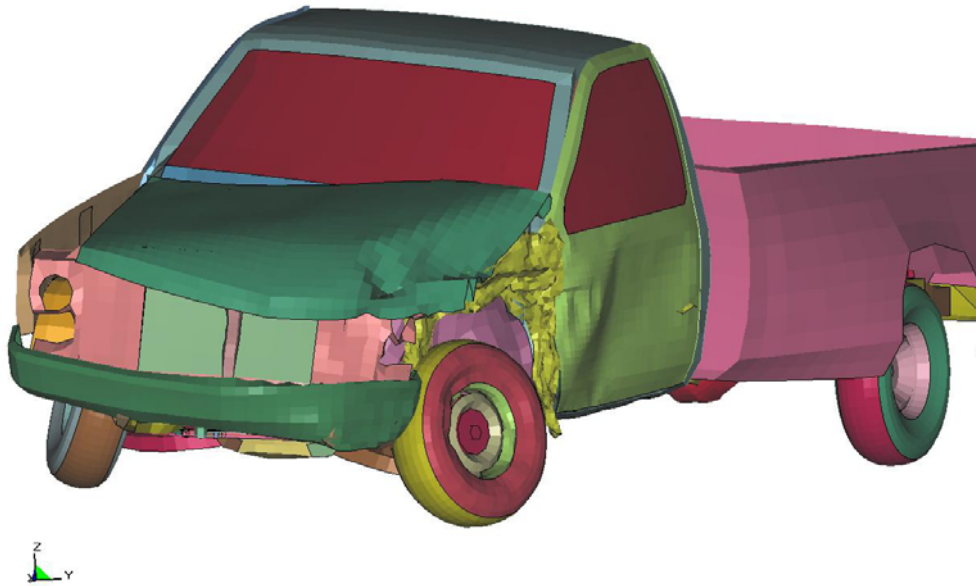


Figure 73. Overall damage to vehicle.

6KS 80 KM/H @ 15 DEG - NY TRANS
Time = 0

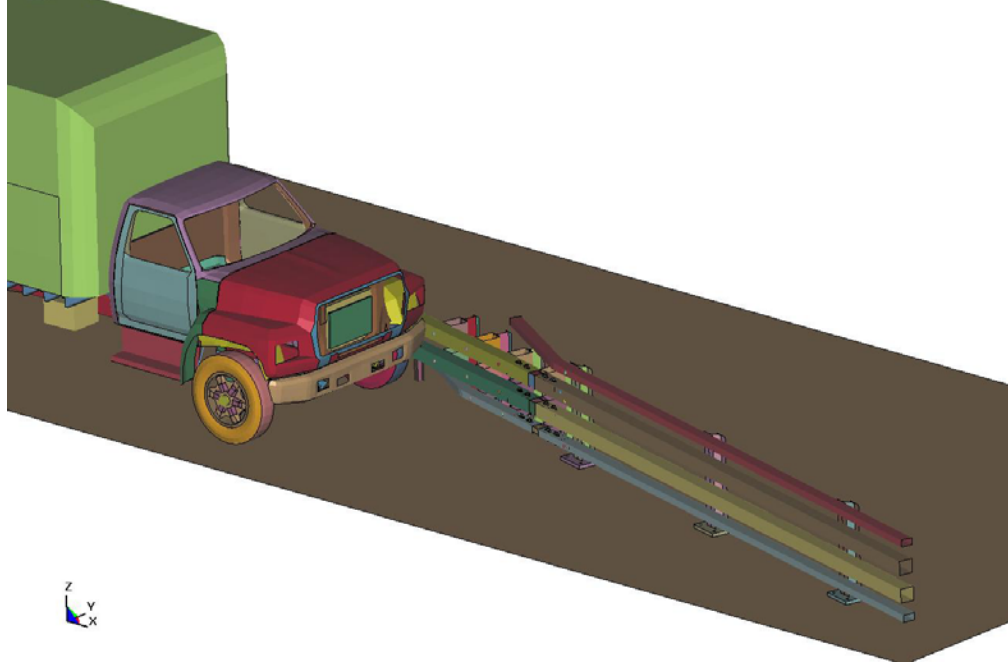


Figure 74. Model of modified New York box-beam transition and single-unit truck.

The researchers requested FHWA assistance in making selected revisions to the F800 model to provide more accurate and meaningful response. When FHWA was unable to comply with this request, the simulations were performed with the current F800 model without modification. The newest release of LS-DYNA (v. 970) was used for the simulations.

As shown in figure 75, the F800 model experienced significant structural deformation to the suspension, frame rails, and cab. The researchers felt this level of deformation was unrealistic for a redirection impact of this type and is at least partially attributable to the absence of failure in the model (e.g., axle-to-suspension connection). It is very common in redirection tests with single-unit trucks to have the front axle detach from the suspension during impact. If this failure mechanism is not accounted for in the model, the axle cannot release at the proper load level, and more force is transmitted into the suspension, frame rails, etc., resulting in excessive deformation.

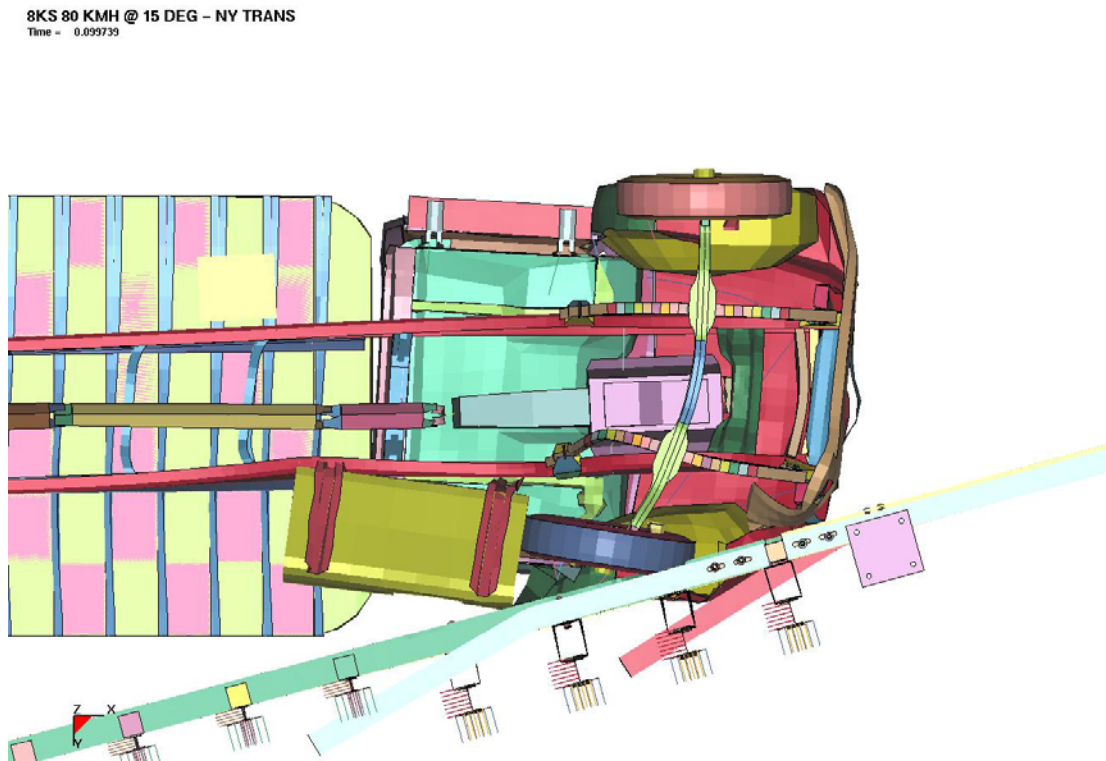


Figure 75. Single-unit truck simulation without suspension failure.

At the request of the COTR, an additional simulation with the single-unit truck model was performed. Just before inducing deformation to the frame rails, the connection of the axle to the suspension was released to simulate failure. With failure of this connection, it was hypothesized that the deformation to the truck frame and cab would be more realistic.

The subsequent simulation of the single-unit truck into the modified New York box-beam transition produced unrealistic vehicle response indicating that the truck model requires more

extensive modification than failure of the axle connection. Although deleting the nodal rigid bodies connecting the axle to the leaf springs at a specified time (70 ms) allowed the simulation to run further with more realistic behavior, other parts of the truck (e.g., gas tank), subsequently engaged the frame rails and produced what the researchers consider to be excessive and unrealistic deformations of the frame rails and cab later in the simulation. Figure 76 shows the associated vehicle deformation.

In the opinion of the researchers, the current F800 model was not providing realistic response, and any simulation results associated with its use in evaluating the New York box-beam transition were, therefore, highly suspect. The researchers and the COTR agreed that no further simulations with the F800 truck model should be conducted until revisions to the model can be completed by FHWA or others.

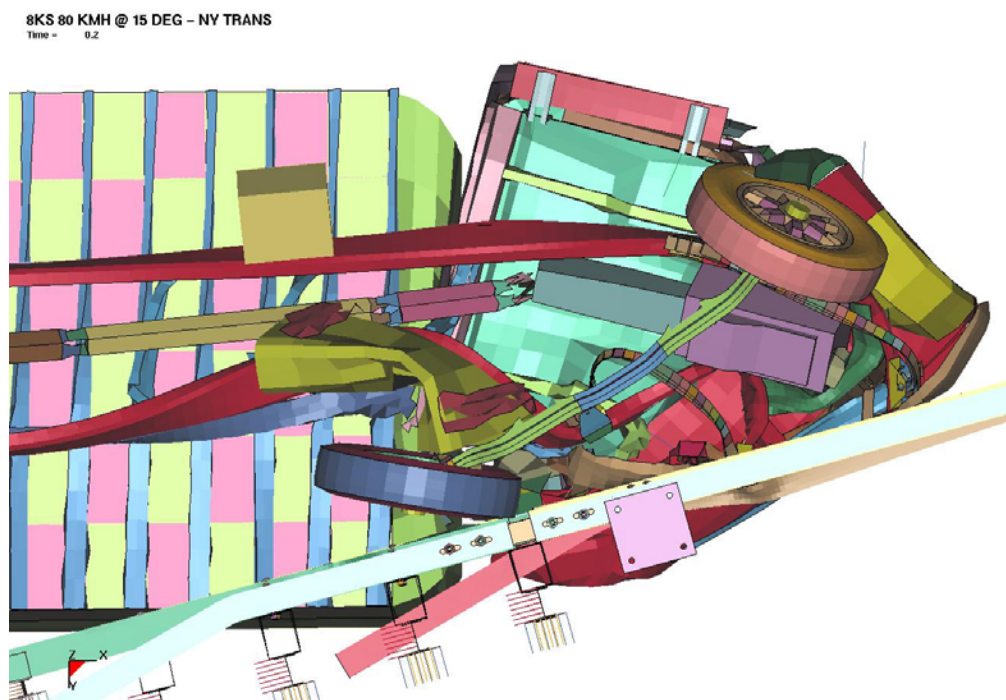


Figure 76. Unrealistic deformation of single-unit truck after axle separation.

TASK B3

The purpose of Task B3 was to model the New York box-beam transition to a single slope concrete parapet and evaluate its impact performance based on a simulation with a 2000-kg pickup truck. The specific transition system investigated in this task is detailed in NYDOT drawing BD-RC13 R1 “Concrete Bridge Barriers: Single Slope Barrier to Box-Beam Transition.”

The model of the transition system includes the concrete parapet and curb, box-beam rubrail, box-beam rail, posts, and associated connection hardware (bolts, splice tubes, etc.). All

components in the impact region were explicitly modeled to provide more accurate assessment of their interaction with the vehicle models.

Simulations were conducted to quantify the interaction of the 2000-kg pickup truck design test vehicle with the box-beam expansion joint, curb, and other components of the transition under *NCHRP Report 350* test 3-21 impact conditions. This test involves the 2000-kg pickup impacting the transition at its CIP at a speed of 100 km/h and an angle of 25 degrees. The finite-element model of the transition and vehicle before impact is shown in figure 77.

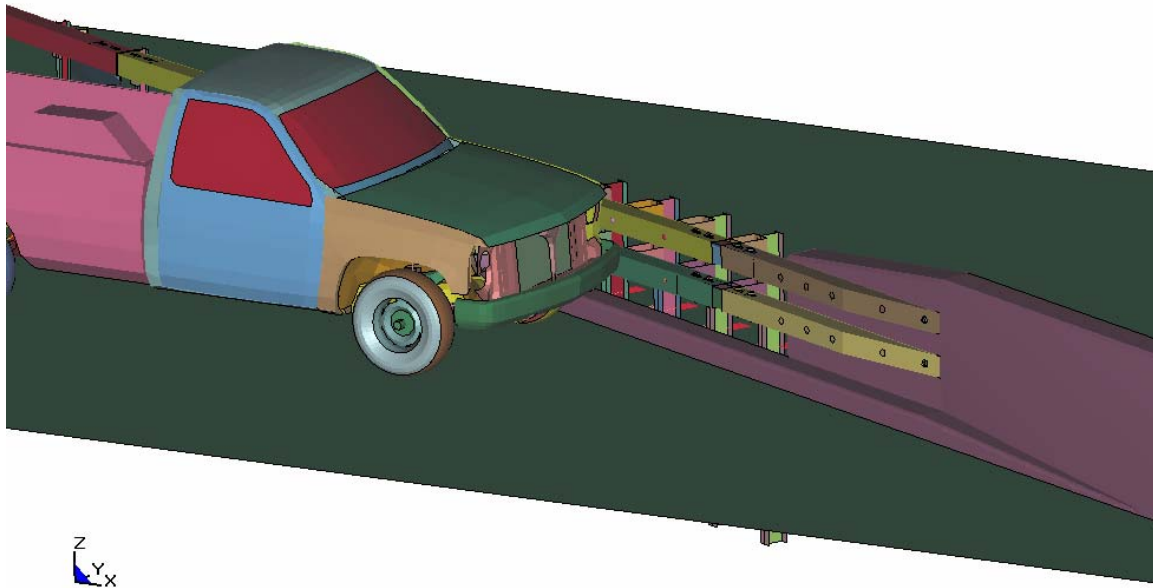


Figure 77. Setup for transition impact with the original CIP.

In the first analysis, the vehicle impacted the system at the same distance upstream of the expansion joint as was used in the failed crash test of the original New York box-beam transition to four-tube bridge rail and the simulation studies conducted under Tasks B1 and B2. As expected in a transition impact of this severity, the front left corner of the vehicle experienced substantial damage. Although some contact occurred between the door and the expansion splice, the door edge on the impact side did not exhibit severe snagging nor indicate a propensity to otherwise disengage from the vehicle cabin. Figure 78 shows the door edge (with other vehicle components removed for clarity) as it reaches the downstream edge of the splice. An image of the vehicle as it is exiting the transition system is shown in figure 79. The vehicle damage resulting from the impact is shown in figure 80.

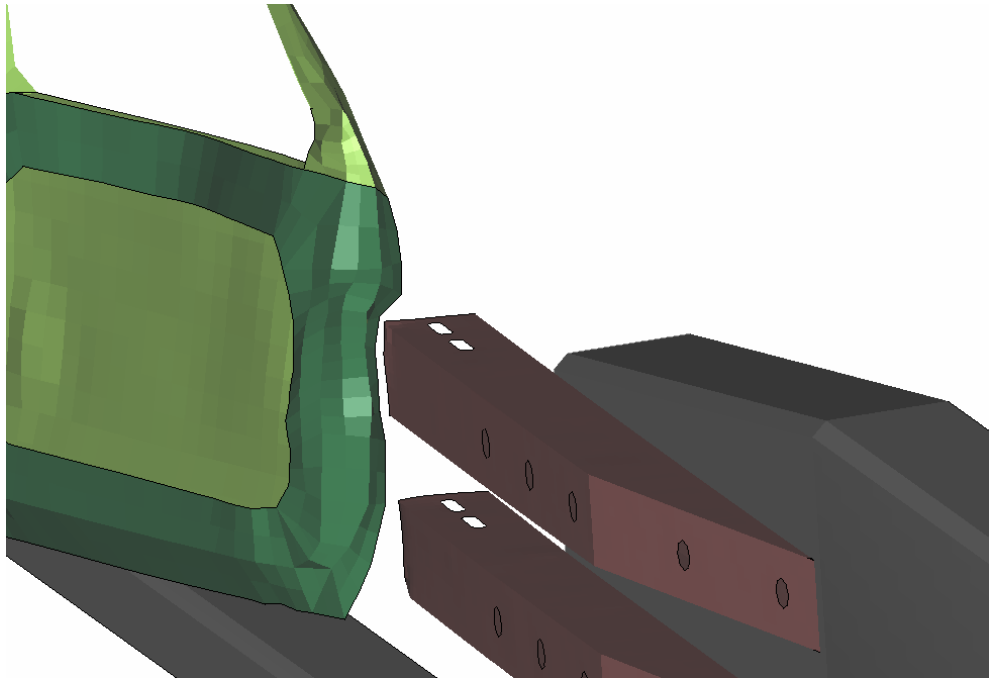


Figure 78. Door edge at downstream end of expansion splice.

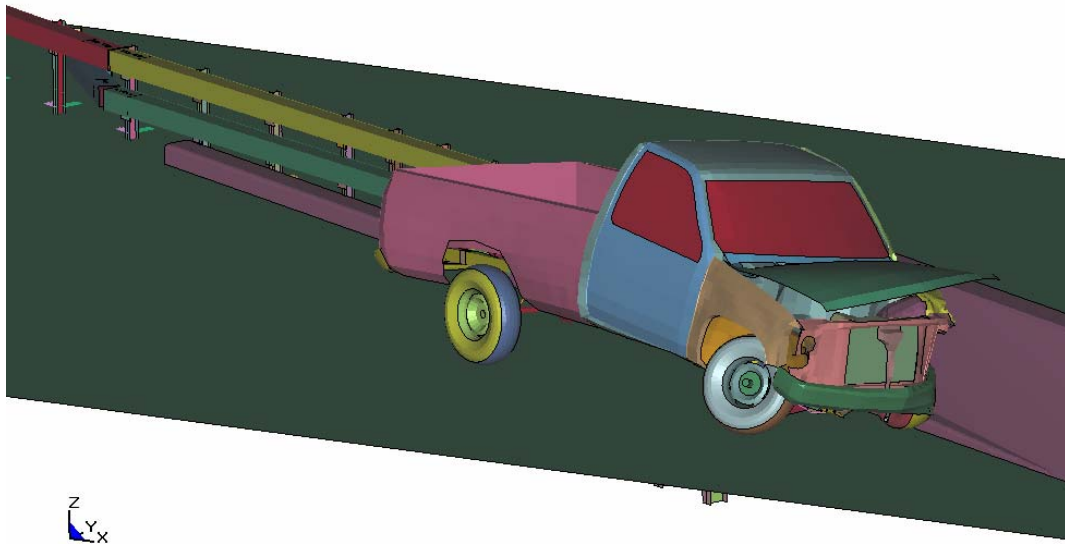


Figure 79. Pickup truck simulation at 0.2 s.

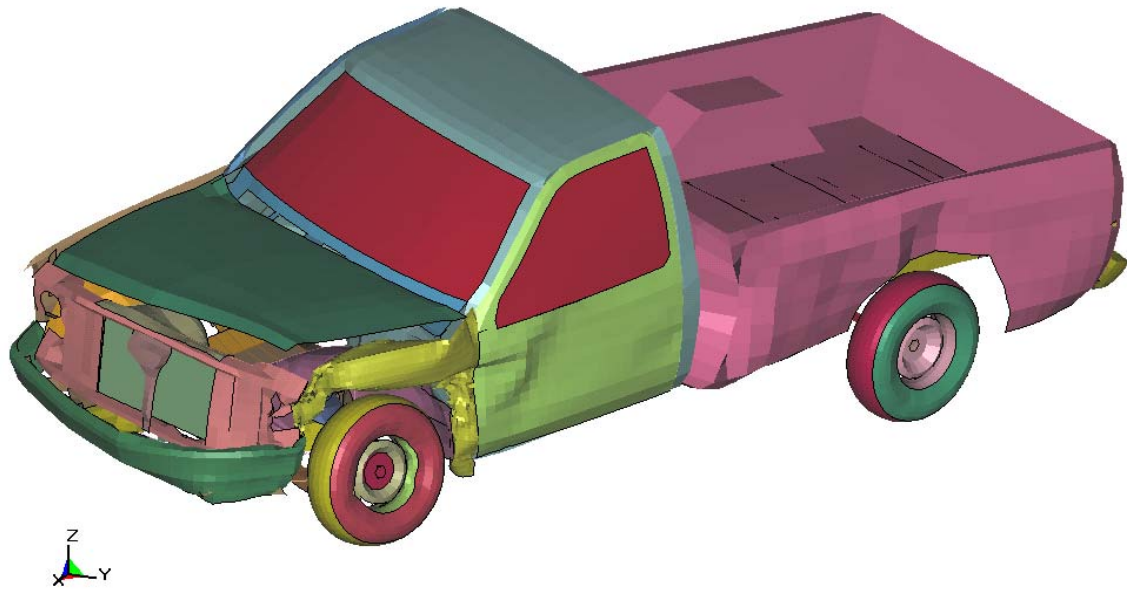


Figure 80. Vehicle damage profile after impact.

A second simulation was conducted to see whether changing the impact point would change the severity of the door edge interaction with the edge of the box beam on the downstream end of the expansion splice. In the second simulation, the impact point was shifted downstream (i.e., closer to the splice) a distance of 457 mm (see figure 81).

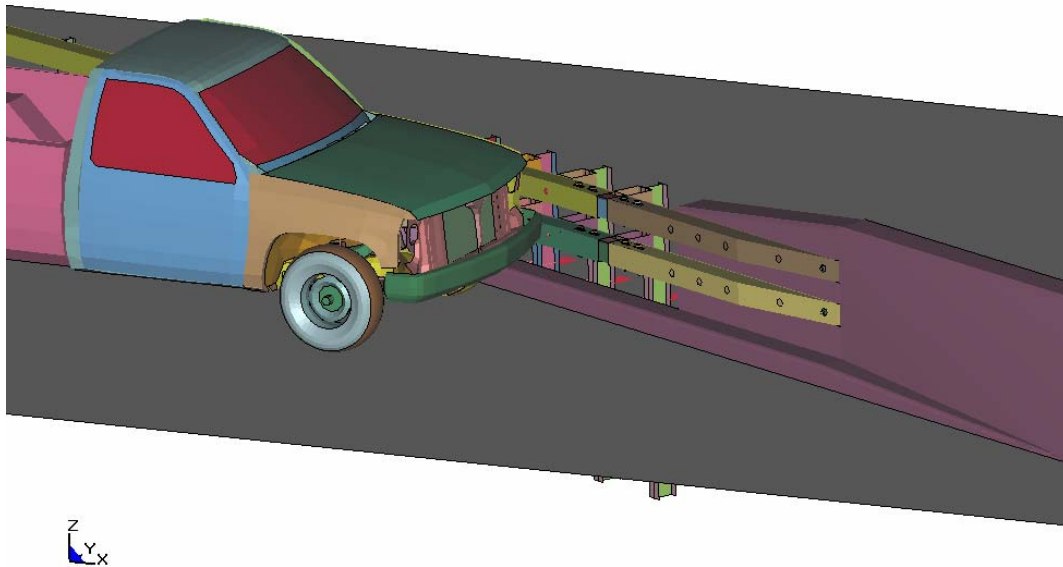


Figure 81. Setup for pickup simulation at alternate impact location.

In the second simulation, the damage to the door was more pronounced. The edge of the box beam engaged some “wrinkled” sheet metal on the door just past the door edge (see figure 82). However, the contact with the splice did not force the front door edge to separate from the cabin. The damage to the vehicle after impact is shown in figure 83.

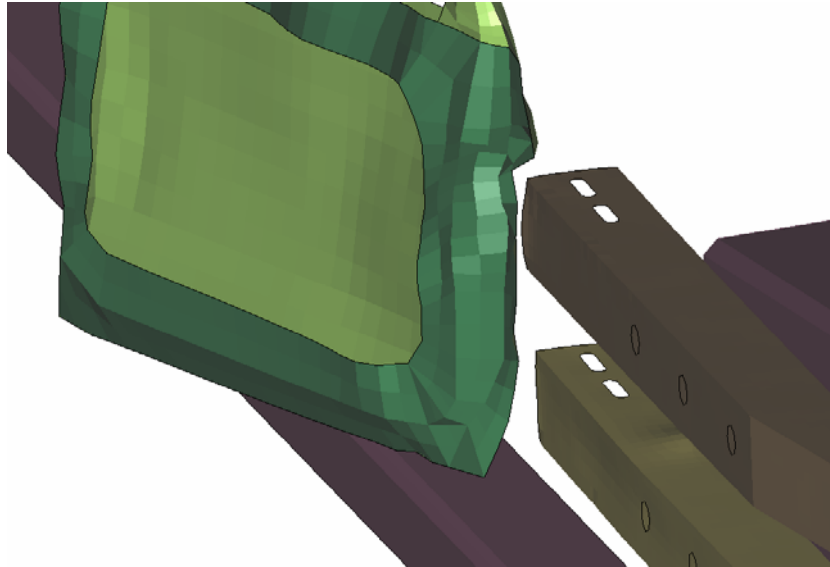


Figure 82. Door edge at downstream edge of expansion splice for alternate impact location.

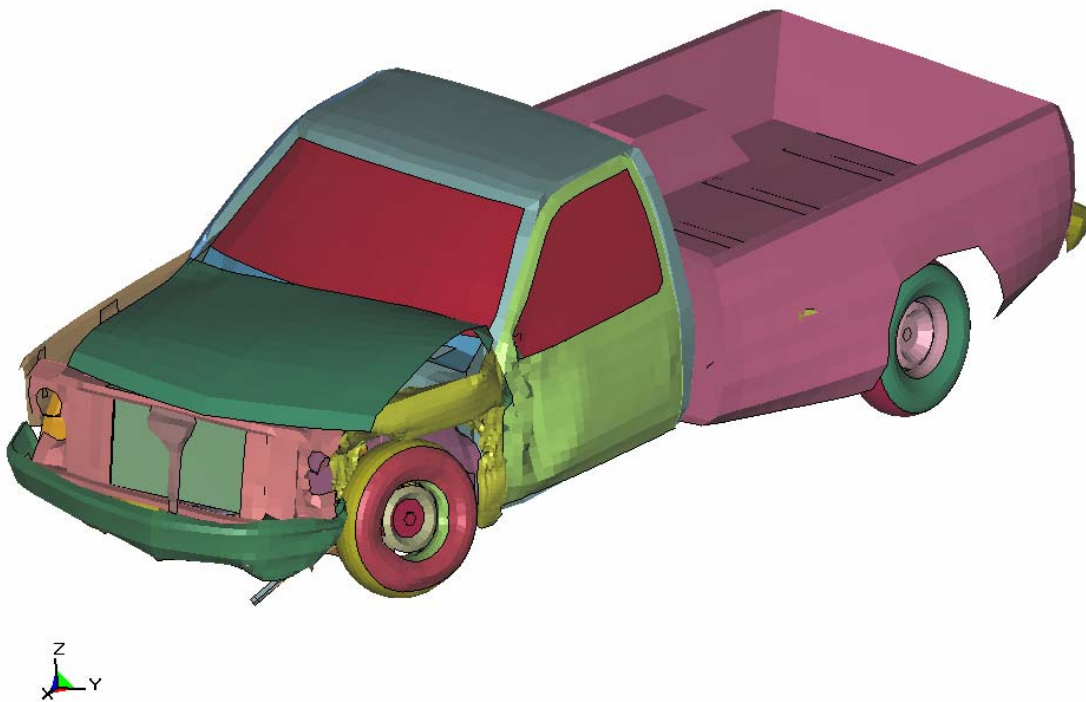


Figure 83. Vehicle damage profile after impact at alternate location.

As described previously, the door-snagging problem is believed to be sensitive to a number of variables, including various vehicle characteristics, impact location, and impact conditions (i.e., speed and angle). It was noted in both simulations conducted to evaluate the performance of the box-beam transition connected to a concrete parapet that the front left tire mounted the curb during the impact. This action raised the height of the tire, causing it to engage the upper box-beam rail element. This is illustrated in figure 84 (with various vehicle and rail components removed for clarity). The result is a different load transfer mechanism between the transition system and vehicle that, from a simulation standpoint, may have influenced the interaction of the door with the splice. In an actual impact of this severity, the impact-side tires will likely air out after contact with the curb. Because the modeled tires do not include this failure capability, their presence may unrealistically influence the interaction. However, the extent to which this occurred (if any) is difficult to ascertain.

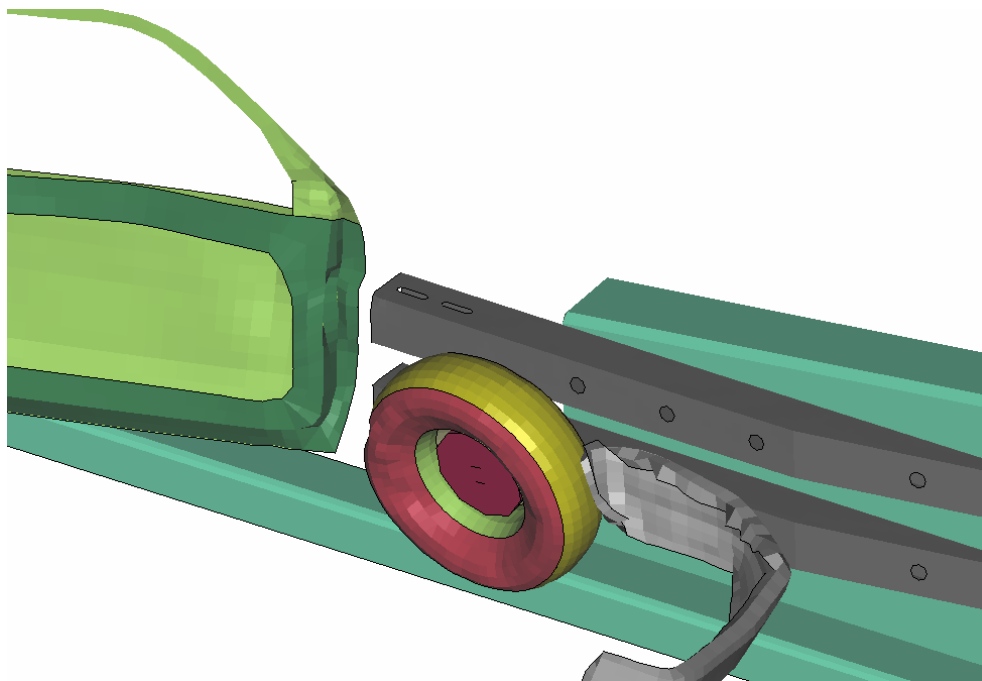


Figure 84. Position of front left tire due to the presence of curb.

In a comparative sense, it appears that the modified New York box-beam transition to single slope concrete barrier does not have the same propensity for door snagging on the expansion splice as the original transition to four-tube bridge rail. However, given the sensitivity of such localized phenomena to changes in the model, the researchers express a word of caution regarding the use of these simulation results in assessing the performance improvements associated with the modified design.

More common failure modes for transitions are rollover and excessive occupant compartment deformation. The pickup truck vehicle was redirected in a stable manner and rollover does not appear to be a concern. Further, the vehicle appears to be smoothly redirected

without significant damage. However, because current vehicle models have not been validated for assessment of occupant compartment deformation, the evaluation of this criterion cannot be made in an absolute sense. Thus, even though the severity of door snagging is mitigated, compliance with *NCHRP Report 350* may not be a certainty.

TASK B4

The purpose of Task B4 was to model modifications to the New York box-beam four-tube bridge rail transition proposed by NYSDOT and FHWA, and evaluate the impact performance of the modified design based on simulations with the 2000-kg pickup truck. The model was constructed per NYSDOT’s latest drawing sheet “Steel Bridge Railing to Box-Beam Guide Rail Transition” and BD-RS8 R2 “Splice Details for Box Beam and Rails on Bridge and Transitions.” The changes include turning the end of the top bridge rail element down and bolting it to the top of the third bridge rail element, adding a fourth heavy transition post that resulted in shortening the distance between the last transition post and the first bridge post, moving the box-beam expansion splice for the third and second rails upstream, extending the rub rail upstream with an expansion splice of its own, and changing the splice details to allow for a tighter yet constructable connection.

The model of the transition system includes the transition section in the impact region, the first bridge rail post, and the four bridge rail members up to the second bridge rail post. All components in the impact region were explicitly modeled to provide more accurate assessment of their interaction with the vehicle model. Appropriate boundary conditions were applied to account for the continuity of the system on both the upstream and downstream ends. Additionally, revisions were made to the pickup truck model to reflect selected characteristics of the vehicle purchased for a subsequent full-scale crash test planned on the modified transition system.

Simulations were conducted to examine the interaction of the 2000-kg pickup truck design test vehicle with the expansion splice and other components of the modified transition under *NCHRP Report 350* test 3-21 impact conditions. This test involves a 2000-kg pickup truck impacting the transition at its CIP at a speed of 100 km/h and an angle of 25 degrees. The finite-element model of the vehicle and the modified transition are shown in figure 85.

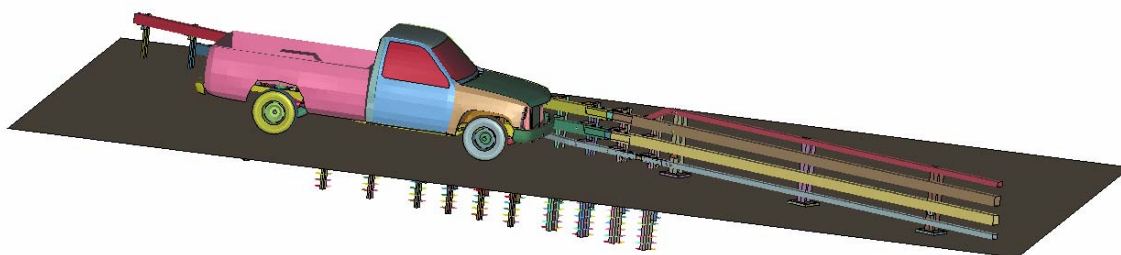


Figure 85. Model of latest NYDOT box-beam transition system.

Snagging Potential of Door Edge with Box-Beam Splice

In the Task B4 simulation, the pickup truck test vehicle impacted the modified transition system the same distance upstream of the expansion splice as previously used in the failed crash test of the original New York box-beam transition to four-tube bridge rail and the simulation studies conducted under Task B1. Since, as mentioned above, the splice for the third rail was moved upstream, the CIP was moved accordingly.

As expected in a transition impact of this severity, the front left corner of the vehicle experienced substantial damage. The deformed front fender of the pickup truck protected/shielded the door edge from the box beam, thereby allowing the door to avoid significant snagging with the expansion splice. The resulting damage to the door was, therefore, not as severe as observed in the original transition system. Figure 86 shows the door edge contact as it reaches the downstream edge of the splice.

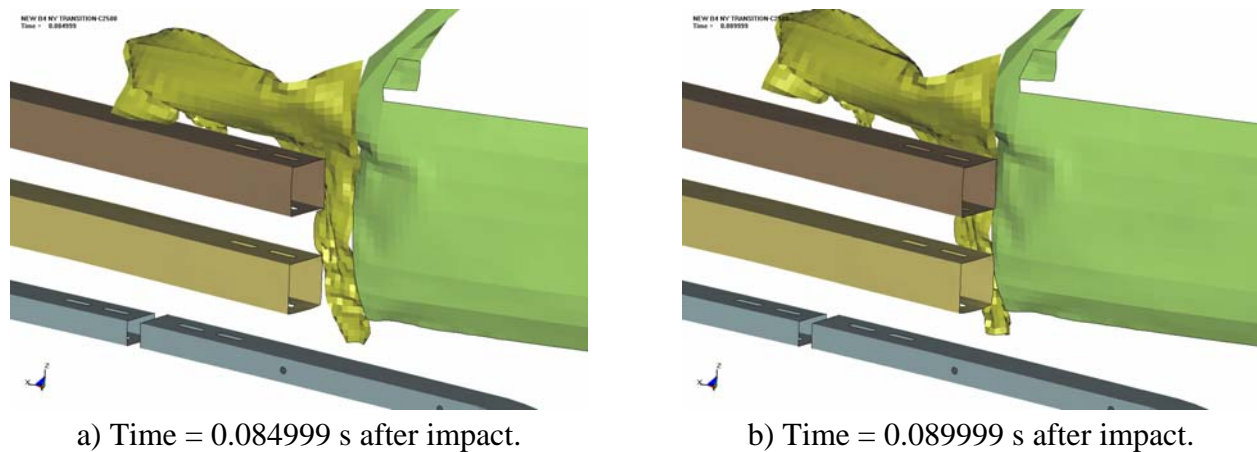


Figure 86. Interaction of door edge with box-beam expansion splice.

Tire Interaction with Rub Rail

In both the test and simulation of the original transition system, the front left tire of the pickup truck rotated out of plane underneath the second rail element after impact, subsequently contacting the bend point in the rub rail and the base plate of the first bridge rail post. This behavior was more pronounced in the test than in the simulation. Images from the Task B1 simulation depicting this behavior are shown in figures 87 and figure 88.

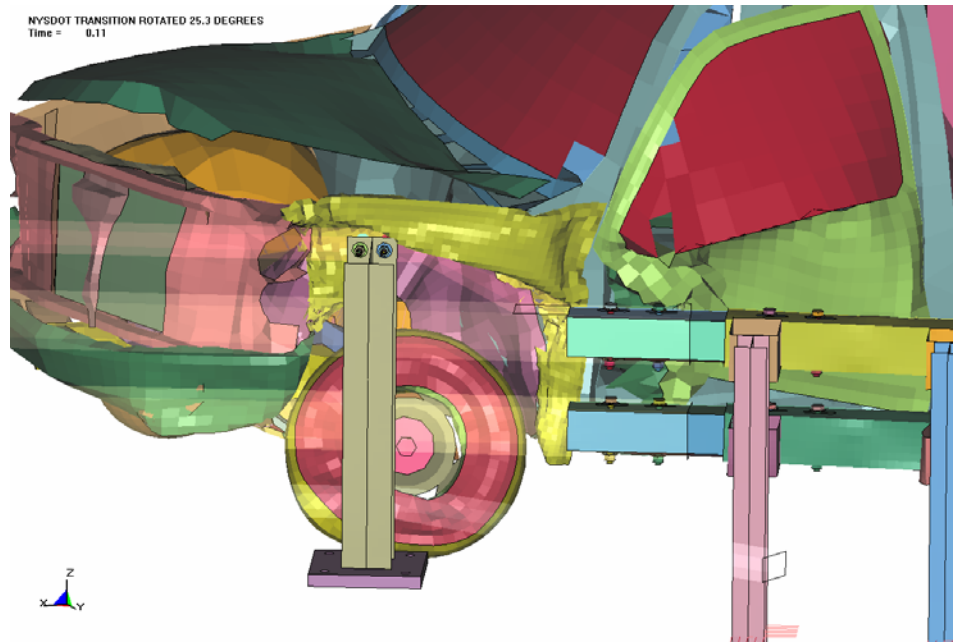


Figure 87. Interaction of tire with bridge rail post baseplate (original design, Task B1).

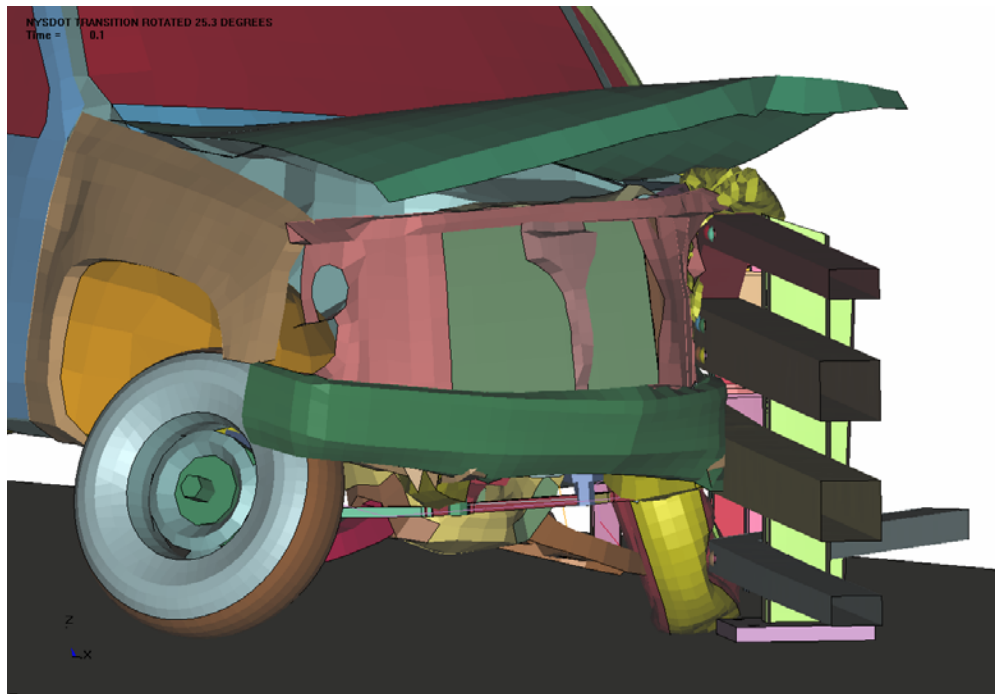


Figure 88. Downstream view of interaction of tire with bend in rail element and bridge rail post baseplate (original design, Task B1).

In the modified transition design evaluated under Task B4, the bend point in the rub rail was shifted further upstream. Consequently, the front left tire engaged the rub rail bend point as soon as the vehicle impacted the system and before any out-of-plane rotation of the wheel occurred. This indicates a more direct barrier-tire-vehicle force transfer mechanism that could influence the extent of occupant compartment deformation. The direct contact from the tire/wheel assembly caused the rub rail to deform toward the field side of the installation and contact the first transition post. Further, the rub rail was pushed downstream a short distance until the tolerance in the slots in the rub rail splice connection was expended. When the tire subsequently engaged the base plate of the first bridge rail post, it presented itself with a more vertically aligned profile as shown in figure 89 and figure 90 below.

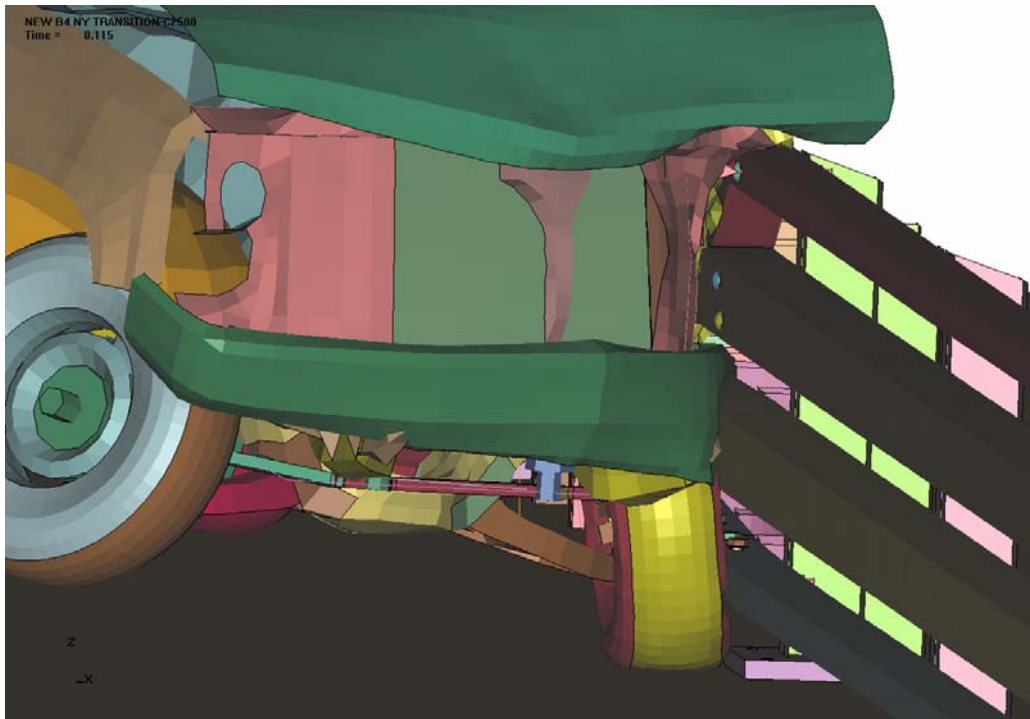


Figure 89. Downstream view of interaction of tire with bridge rail post baseplate (modified design, Task B4).

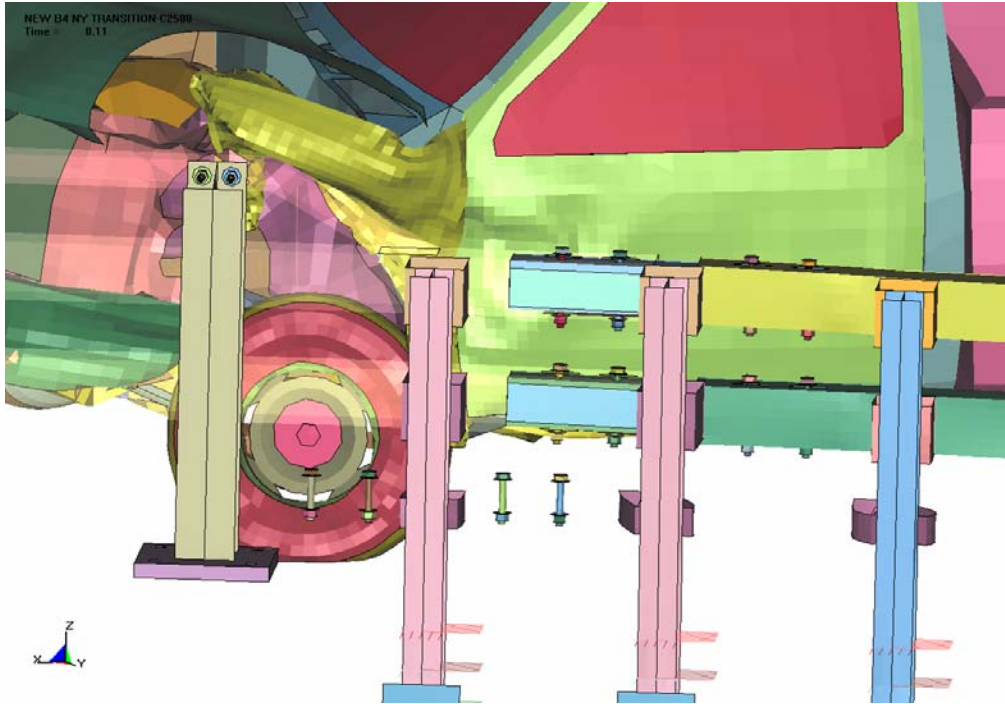


Figure 90. Interaction of tire with bridge rail post baseplate (modified design, Task B4).

Vehicle Frame Rail Deformation

Simulations of both the original transition system (Task B1) and the modified transition (Task B4) indicated what the researchers consider to be excessive vehicle frame deformation resulting when the impact force was transferred from the front left tire/wheel to the suspension assembly as shown in figures 91 and 92. It should be noted that some deformation of the front left frame rail was reported in the crash test of the original NYSDOT box-beam transition design and that the measured occupant compartment deformation was 158 mm (which is marginal based on FHWA evaluation criteria). Due to lack of connection failure in the suspension of the pickup truck model, it is not possible to accurately capture the load transfer from the tire/wheel to the frame rail or other parts of the vehicle (e.g., floor pan, firewall). However, since both simulations showed similar magnitudes of frame deformation (figures 91 and 92), it is reasonable to conclude that a vehicle impacting the latest modified transition system would sustain a similar level of occupant compartment deformation (OCD) as in the impact of the original system. Thus, the magnitude of the OCD associated with a pickup truck impact into the modified transition design is expected to be marginal.

NYS DOT TRANSITION ROTATED 25.3 DEGREES
Time = 0.13

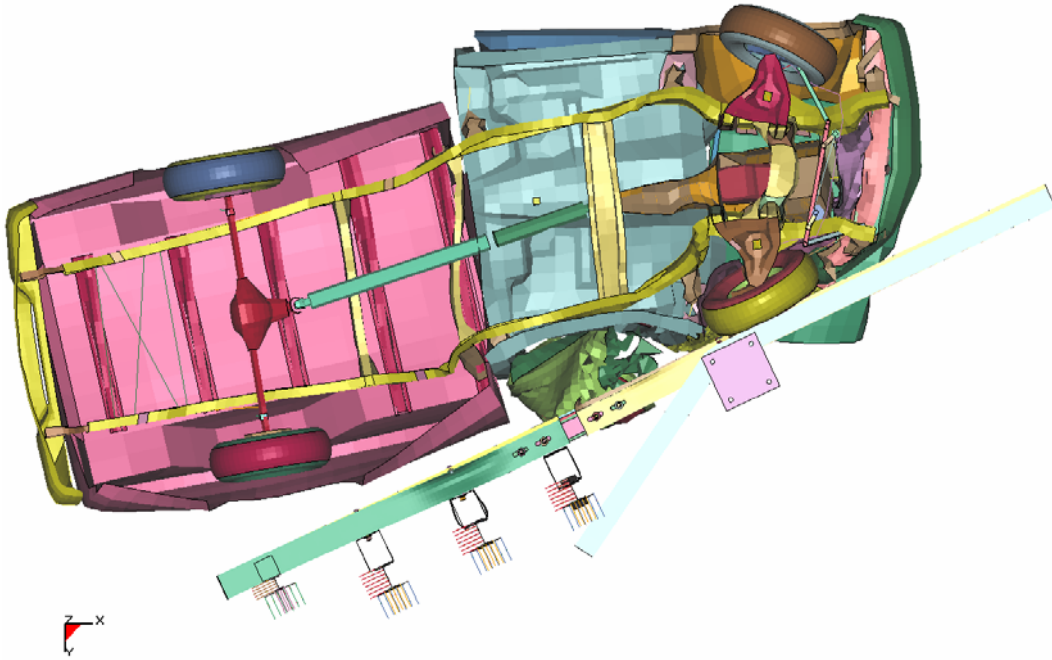


Figure 91. Vehicle frame deformation—original system (Task B1).

NEW B4 NY TRANSITION-C2500
Time = 0.13

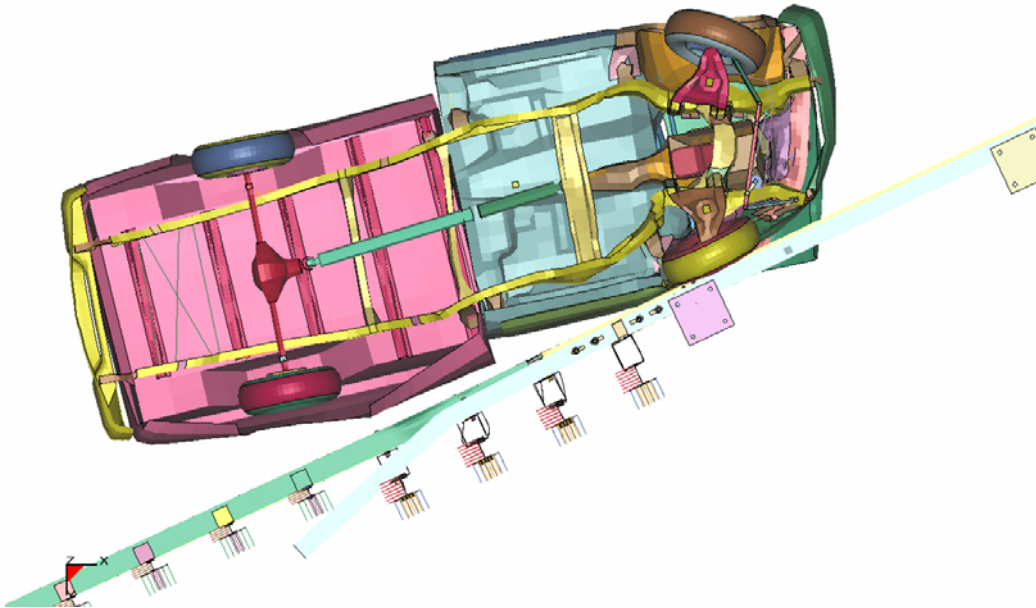


Figure 92. Vehicle frame deformation—latest modified system (Task B4).

Sensitivity and Stochastic Issues

The vehicle damage resulting from the simulated impact is shown in figure 93. The overall interpretation of this simulation is that the performance of the latest modified transition design would be marginally acceptable. The vehicle was redirected in a stable and upright manner. While the possibility of door snagging on the expansion splice is still present, the simulation indicates an improvement over the original design. However, the researchers express caution in the interpretation of this aspect of the simulation due to the sensitivity of the current models in capturing this behavior.

NEW B4 NY TRANSITION-C2500
Time = 0.18

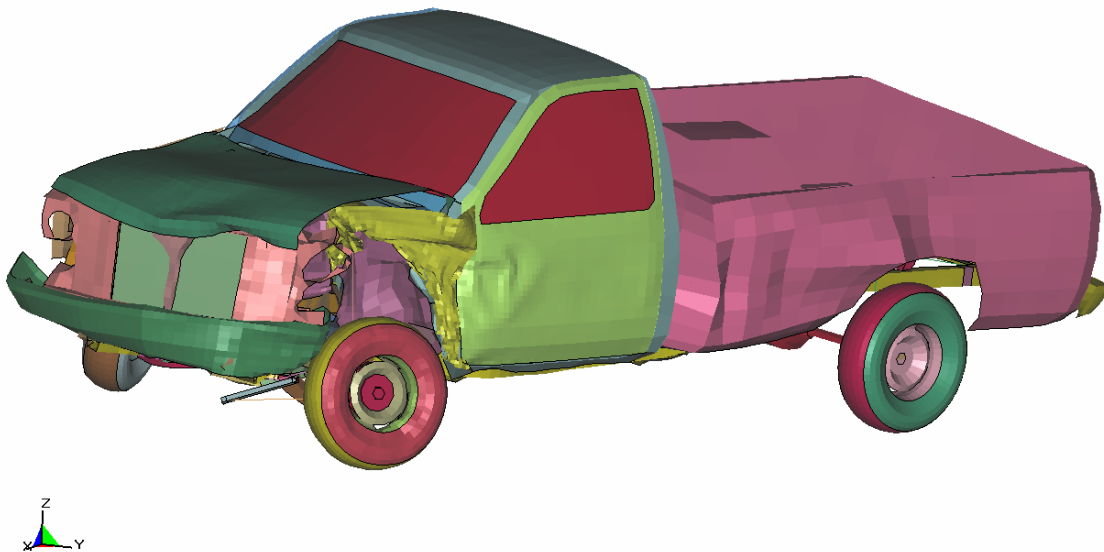


Figure 93. Pickup truck deformed shape at 180 ms.

Generally speaking, the limitations and scope of the models should be carefully considered when defining how accurately and in how much detail the crash test results can be predicted. For instance, the current vehicle model does not include failure mechanisms in the suspension or tire, which are known to occur in virtually every transition impact. Both of these failure modes occurred in the crash test of the original transition system, so the effect of their absence in the model is difficult to determine. For instance, the occupant compartment deformation is expected to be marginal based on a qualitative comparison between the Task B1 and Task B4 simulations. However, because the load transfer path cannot be precisely replicated, a more direct quantitative assessment of this evaluation criterion cannot be made.

Based on the results of the predictive simulation results presented herein, NYSDOT and FHWA decided to conduct a full-scale crash test on the modified NYSDOT box-beam transition to four-tube bridge rail described in Task B4. Details of this testing are described in the next section.

MODIFIED NYSDOT BOX-BEAM TRANSITION TO FOUR-RAIL BRIDGE RAIL

TEST ARTICLE—TEST 401021-7

The NYSDOT box-beam guardrail to steel bridge rail transition consists of two steel tubes connected to the New York standard four-rail bridge railing design that transitions into the New York standard box-beam guardrail. The contractor received a drawing from NYSDOT titled “Steel Bridge Railing to Box-Beam Guide Rail Transition.” The complete transition system, LON of guardrail, and Wyoming Box-Beam End Treatment (WYBET) were provided by a company that manufactures these transitions according to NYSDOT specifications and supplies these transitions to NYSDOT. Drawings are shown in figures 94 through 96.

The test installation consisted of a 10.4 m transition section, 14.7 m length of need of box-beam guardrail, and 1.1 m long Type 1 end assembly. The transition is connected to the two middle rails and the rub rail of the four-tube bridge rail. The transition tubes are connected with two 900-mm expansion splice tubes and the rub rail was connected with a 900-mm splice bar. Each tube and splice bar was connected with four M20 fully threaded bolts that bolted through the tubes and splices. The splice tubes were fabricated from TS127x127x7.9 tubes with two 100 mm x 6 mm x 875 mm fill plates welded to two adjoining sides of the tubes. These two splices were at the second post off the end of the bridge rail. The rub rail splice was at the first post off of the end of the bridge rail. A 110-mm gap was present between the transition tubes and bars and the bridge rail tubes.

The top TS127x76x6.4 rail of the bridge railing extended horizontally beyond the last bridge rail post 150 mm and was sloped downward over a distance of 460 mm. It was connected to the top TS152x152x4.8 tube with an M20 round head, square neck carriage bolt placed perpendicular to the surface of the top rail section. The bottom TS127x76x6.4 rail of the bridge railing extended horizontally beyond the third transition post. It was then angled at 15 degrees away from the roadway passing in front of the fourth post and behind post 5 of the transition. The rub rail then terminated behind post of the transition.

The 10.2 m transition consisted of two TS152x152x4.8 tubes supported by 14 posts. The first transition post was located 600 mm from the last bridge deck post. The first four posts in the transition away from the bridge deck were W150x14 heavy posts spaced at 600 mm on centers followed by four S75x8 transition posts spaced also at 600 mm on centers. The remaining length of transition consisted of six S75x8 transition posts spaced at 900 mm on centers. TS203x152x6.4 tubular blockouts were used on the W150x14 heavy posts. The blockouts were connected to the first and second posts by two M14x38-mm-long standard hex bolts. The rails were bolted to the third and fourth posts by one M20 round head, square neck bolt. The remaining transition and box-beam guardrail posts were connected to the transition tubular members by L127x89x9.5 shelf angles that connected to the posts with M12x38-mm-long standard hex bolts. The transition and box-beam tubes were supported by the shelf angles and bolted through the angles using M8 standard hex head bolts.

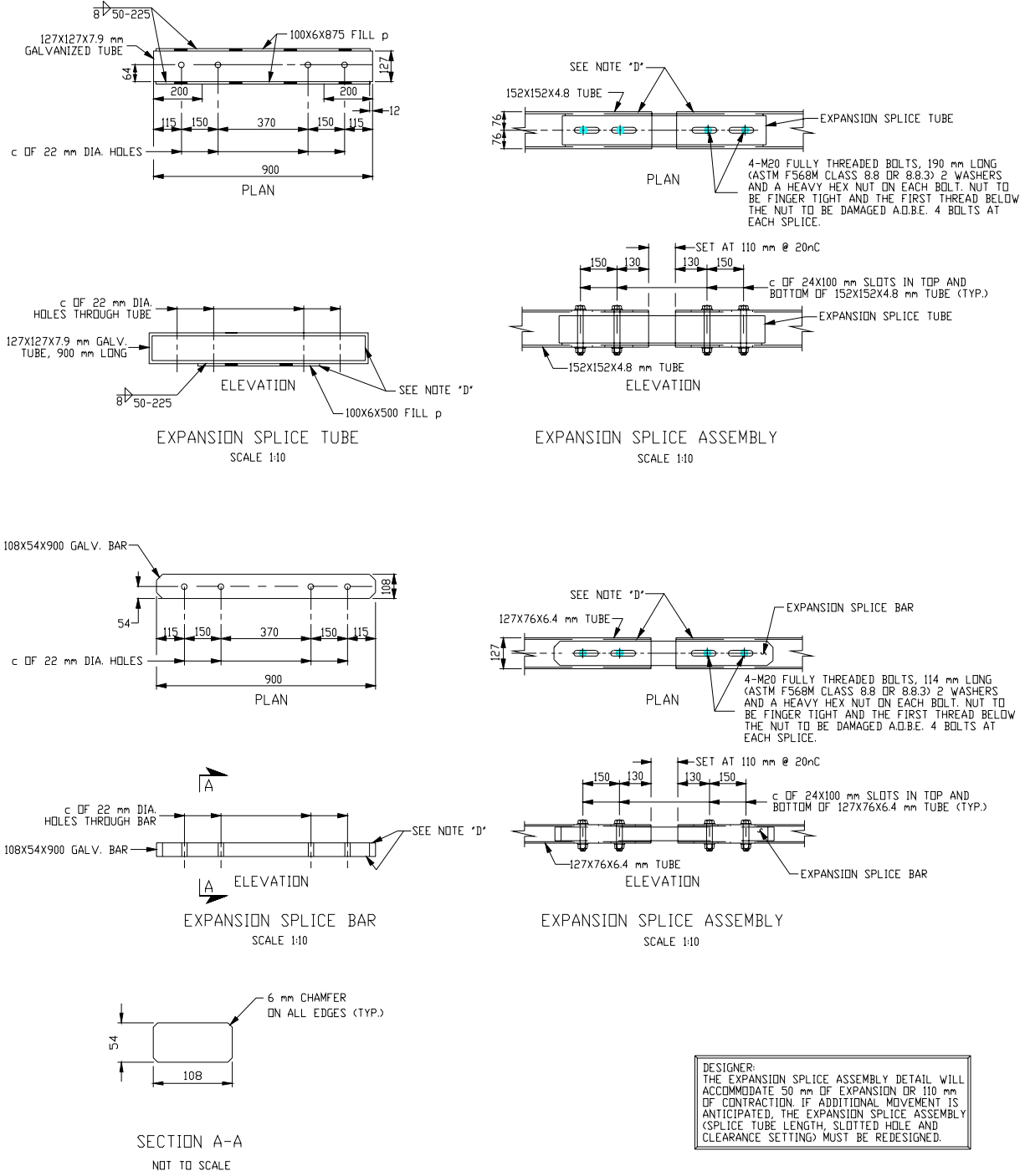


Figure 95. Details of the NYSDOT box-beam transition—expansion splice details.

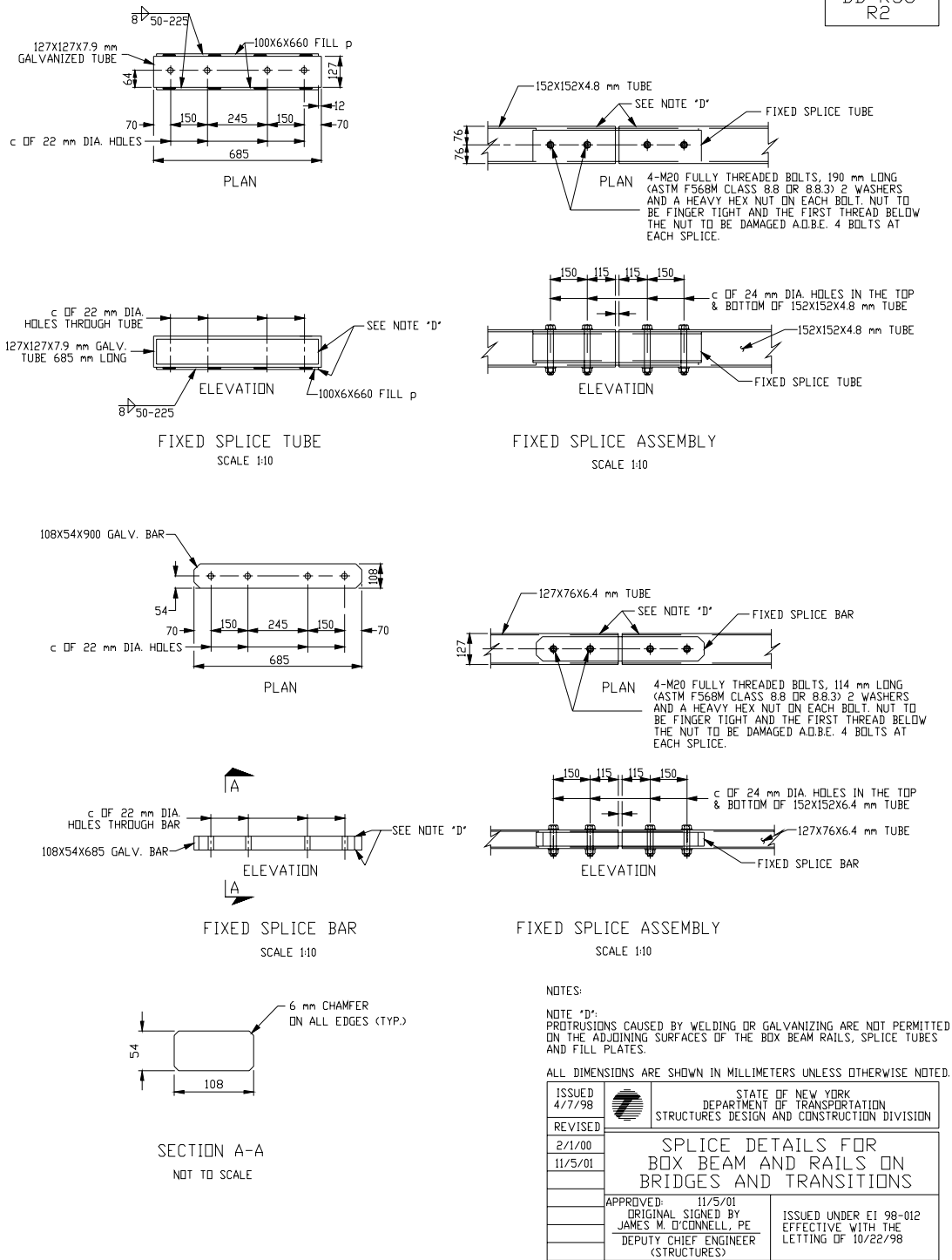


Figure 96. Details of the NYSDOT box-beam transition—fixed splice details.

The top TS152x152x4.8 transition tube attached to the bridge railing at a height of 830 mm above the deck surface and sloped to meet the box-beam guardrail height of 685 at post 14 of the transition. The lower TS152x152x4.8 transition tube attached to the bridge railing at 528 mm above the deck surface and sloped 380 mm above the ground surface at post 13. At post 11, the lower transition tube angled back 26 degrees behind post 12 through 14 and sloped downward from this point to the ground surface. Two posts supported the flared back portion of the lower transition tube.

The W150x14 heavy posts used in the transition were 2.14 m in length and utilized 200 mm x 6 mm x 600 mm soil plates attached 470 mm from the bottom of the posts. The S75x8 transition posts used in the installation were also 2.14 m in length and utilized 200 mm x 6 mm x 800 mm soil plates attached 400 mm from the bottom of the posts.

Approximately 2.7 m of standard New York box-beam guardrail extended beyond the transition. This guardrail system consisted of TS152x152x4.8 box beam with a mounting height of 685 mm. The guardrail was supported by S75x8 standard New York State highway posts 1.6 m in length with 200 mm x 6 mm x 600 mm soil plates attached to each post. The soil plates were located 100 mm from the bottom of the posts. The posts were spaced at 1830 mm on centers. A WYBET box-beam terminal was used to terminate the test installation.

Details of the installation are shown in figures 94 through 96, and photographs of the completed installation as tested are shown in figure 97.

CRASH TEST 401021-7 (NCHRP REPORT 350 TEST NO. 3-21)

Test Conditions

NCHRP Report 350 test designation 3-21 was performed on the NYSDOT box-beam transition. This test involves a 2000-kg pickup truck impacting the CIP of the transition at a nominal speed and angle of 100 km/h and 25 degrees. According to the computer simulation program the CIP was 961 mm from the left front corner of the vehicle to the splice edge (lip) of the upstream box-beam element (see figure 98).

Test Vehicle

A 1994 Chevrolet C2500 pickup truck, shown in figures 99 and 100, was used for the crash test. Test inertia weight of the vehicle was 2003 kg, and its gross static weight was 2077 kg. The height to the lower edge of the vehicle front bumper was 378 mm, and the height to the upper edge of the front bumper was 595 mm. Additional dimensions and information on the vehicle are given in appendix B, figure 122. The vehicle was directed into the installation using the cable reverse tow and guidance system, and was released to be freewheeling and unrestrained just before impact.



a) Traffic side of installation.



b) Field side of transition section.

Figure 97. NYSDOT box-beam transition before testing.

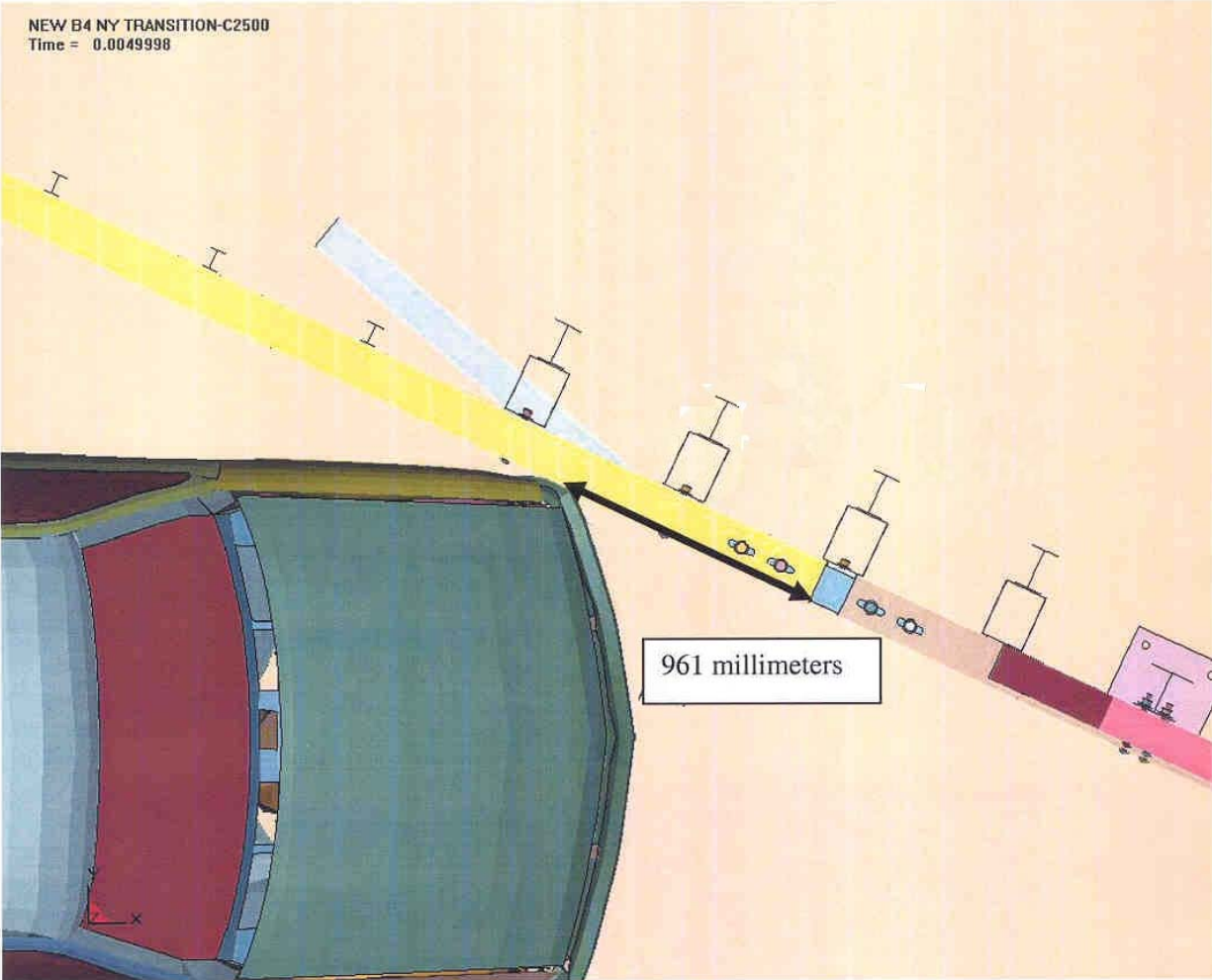


Figure 98. Impact point for *NCHRP Report 350* test 3-21 on the NYSDOT box-beam transition.



a) Traffic side view.



b) Field side view.

Figure 99. Vehicle/installation geometrics for test 401021-7.



a) Front quarter view.



b) Overhead view.

Figure 100. Vehicle before test 401021-7.

Soil and Weather Conditions

The crash test was performed the afternoon of March 15, 2004. Rainfall of 4 mm was recorded 2 days before the test. No other rainfall was recorded during the remaining 10 days before the date of the test. Moisture content of the *NCHRP Report 350* soil in which the test article was installed was 8.2 percent at post 3. Weather conditions at the time of testing were as follows: windspeed: 5 km/h; wind direction: 90 degrees with respect to the vehicle (vehicle was traveling in a northeasterly direction); temperature: 22 °C; relative humidity: 70 percent.

Impact Description

The pickup truck, traveling at an impact speed of 100.0 km/h, impacted the NYSDOT box-beam transition 1.46 m upstream of post 1, at an impact angle of 24.4 degrees. Shortly after impact, the vehicle hood and left front quarter panel began to deform. At 0.035 s, the driver's side door opened at the top of the door frame, and at 0.038 s, the vehicle began to redirect. Post 3 began to deflect toward the field side at 0.040 s, and the glass in the driver's side door shattered at 0.115 s. At 0.175 s, the vehicle was traveling parallel with the transition at a speed of 81.9 km/h. The right side of the tailgate separated from the vehicle at 0.180s. At 0.401 s, the vehicle lost contact with the transition and was traveling at a speed of 76.5 km/h and an exit angle of 7.0 degrees. Brakes on the vehicle were applied at 1.1 s after impact, and the vehicle subsequently came to rest upright 50.3 m downstream of impact and 3.7 m forward of the traffic face to the transition. Sequential photographs of the test period are shown in appendix C, figures 142 through 144.

Damage to Test Article

Moderate damage was imparted to the transition, as shown in figures 101 and 102. The anchor bolts on the first bridge rail post were pulled up 20 mm and the rear bolts 5 mm. The blockouts at posts 2 and 3 were partially collapsed. Maximum dynamic deflection of the transition rail was 124 mm. Maximum permanent deformation of the transition rail was 30 mm at the top rail element at post 3. The splice on the middle rail element just downstream of post 3 was pulled out 25 mm. Total length of contact of the vehicle with the transition was 3.24 m.



Figure 101. Vehicle trajectory path after test 401021-7.



a) Damage at lower splice.



b) Overall view of damage.



c) Damage at upper splice.

Figure 102. Installation after test 401021-7.

Vehicle Damage

Most of the damage to the vehicle was to the left front corner and rear axle, as shown in figure 103. Structural damage to the vehicle was sustained by the left upper and lower A-arm, left frame rail, left U-bolts, and rear axle; the drive shaft also pulled out. Also damaged were the front bumper, grill, hood, left front quarter panel, left tire and wheel rim, left door and glass, left rear exterior bed, and A-post; the windshield was shattered. Maximum exterior crush to the vehicle was 500 mm at the left front corner at bumper height. Maximum occupant compartment deformation was 60 mm at the left kickpanel area laterally across the front of the cab. Photographs of the interior of the vehicle are shown in figure 104. Exterior vehicle crush and occupant compartment measurements are shown in appendix B, table 21 and figure 123.

Occupant Risk Factors

Data from the triaxial accelerometer, located at the vehicle c.g., were digitized to compute occupant impact velocity and ridedown accelerations. The occupant impact velocity and ridedown accelerations in the longitudinal axis only are required from these data for evaluation of criterion L of *NCHRP Report 350*. In the longitudinal direction, occupant impact velocity was 4.4 m/s at 0.093 s, maximum 0.010-s ridedown acceleration was -12.6 g's from 0.097 to 0.107 s, and the maximum 0.050-s average was -8.1 g's between 0.041 and 0.091 s. In the lateral direction, the occupant impact velocity was 7.2 m/s at 0.093 s, the highest 0.010-s occupant ridedown acceleration was 15.4 g's from 0.206 to 0.216 s, and the maximum 0.050-s average was 13.8 g's between 0.023 and 0.073 s. Vehicle angular displacements and accelerations versus time traces are shown in appendix D, figures 219 through 225.

Assessment of Test Results

An assessment of the test based on the applicable *NCHRP Report 350* safety evaluation criteria is provided below.

Structural Adequacy

- A. *Test article should contain and redirect the vehicle; the vehicle should not penetrate, underride, or override the installation, although controlled lateral deflection of the test article is acceptable.*



a) Front quarter view.



b) Overhead view.

Figure 103. Vehicle after test 401021-7.



a) Before test.



b) After test.

Figure 104. Interior of vehicle for test 401021-7.

Result: The modified NYSDOT box-beam transition contained and redirected the pickup truck. The vehicle did not penetrate, underride, or override the installation. Maximum dynamic deflection during the test was 124 mm. (PASS)

Occupant Risk

D. *Detached elements, fragments, or other debris from the test article should not penetrate or show potential for penetrating the occupant compartment, or present an undue hazard to other traffic, pedestrians, or personnel in a work zone. Deformation of, or intrusions into, the occupant compartment that could cause serious injuries should not be permitted.*

Result: No detached elements, fragments, or other debris were present to penetrate or to show potential for penetrating the occupant compartment, or to present hazard to others in the area. Maximum occupant compartment deformation was 60 mm laterally at the kickpanel across the cab. (PASS)

F. *The vehicle should remain upright during and after collision although moderate roll, pitching, and yawing are acceptable.*

Result: The pickup truck remained upright during and after the collision event. (PASS)

Vehicle Trajectory

K. *After collision, it is preferable that the vehicle's trajectory not intrude into adjacent traffic lanes.*

Result: The vehicle came to rest 50.3 m downstream of impact and 3.6 m forward of the traffic face of the rail. (FAIL)

L. *The occupant impact velocity in the longitudinal direction should not exceed 12 m/s and the occupant ridedown acceleration in the longitudinal direction should not exceed 20 g's.*

Result: Longitudinal occupant impact velocity was 4.4 m/s, and longitudinal ridedown acceleration was -12.6 g's. (PASS)

M. *The exit angle from the test article preferably should be less than 60 percent of the test impact angle, measured at time of vehicle*

loss of contact with the test device.

Result: Exit angle at loss of contact with the transition was 7.0 degrees, which was 29 percent of the impact angle. (PASS)

The following supplemental evaluation factors and terminology, as presented in the FHWA memo titled “Action: Identifying Acceptable Highway Safety Features,” were used for visual assessment of test results.⁽⁵⁾ Factors underlined below pertain to the results of the test reported here.

PASSENGER COMPARTMENT INTRUSION

1. Windshield intrusion

- | | |
|---|---|
| <i>a. <u>No windshield contact</u></i> | <i>e. Complete intrusion into passenger compartment</i> |
| <i>b. Windshield contact, no damage</i> | <i>f. Partial intrusion into passenger compartment</i> |
| <i>c. Windshield contact, no intrusion</i> | |
| <i>d. Device embedded in windshield, no significant intrusion</i> | |

2. Body panel intrusion

yes or no

LOSS OF VEHICLE CONTROL

- | | |
|---|--|
| <i>1. <u>Physical loss of control</u></i> | <i>3. Perceived threat to other vehicles</i> |
| <i>2. Loss of windshield visibility</i> | <i>4. Debris on pavement</i> |

PHYSICAL THREAT TO WORKERS OR OTHER VEHICLES

- 1. Harmful debris that could injure workers or others in the area*
- 2. Harmful debris that could injure occupants in other vehicles*

No debris was present.

VEHICLE AND DEVICE CONDITION

1. Vehicle damage

- | | |
|---|--|
| <i>a. None</i> | <i>d. Major dents to grill and body panels</i> |
| <i>b. Minor scrapes, scratches or dents</i> | <i>e. <u>Major structural damage</u></i> |
| <i>c. Significant cosmetic dents</i> | |

2. *Windshield damage*

- a. *None*
- b. *Minor chip or crack*
- c. *Broken, no interference with visibility*
- d. *Broken and shattered, visibility restricted but remained intact*
- e. *Shattered, remained intact but partially dislodged*
- f. *Large portion removed*
- g. *Completely removed*

3. *Device Damage*

- a. *None*
- b. *Superficial*
- c. *Substantial, but can be straightened*
- d. *Substantial, replacement parts needed for repair*
- e. *Cannot be repaired*

Conclusions

Although the splice on the middle rail element just downstream of post 3 was pulled out 25 mm, there was no evidence that the door was snagged as in the previous test. The modified NYSDOT box-beam transition performed acceptably according to requirements for *NCHRP Report 350* test 3-21.

SUMMARY AND CONCLUSIONS

ASSESSMENT OF TEST RESULTS

FHWA initiated this contract with the objective of crash testing and evaluating several thrie beam transitions to *NCHRP Report 350*. FHWA determined which *NCHRP Report 350* tests should be performed on each of the test articles evaluated. In addition, FEA and subsequent crash testing of the modeled NYSDOT modified box-beam transition to four-rail steel bridge rail was performed.

Ohio Nonsymmetrical Type 2 W-Beam to Thrie Beam Transition

The first test (*NCHRP Report 350* test 3-21) on the Ohio thrie beam transition at the nonsymmetrical Type 2 transition section was performed with a 12-gauge nonsymmetrical section (from W-beam to thrie beam). During the test, all computed occupant risk values were within acceptable limits, as shown in table 2. However, occupant compartment deformation in the driver's side floor pan area was 175 mm, which is deemed unacceptable (due to location) according to FHWA's *Draft Guidelines for Analysis of Passenger Compartment Intrusion*.⁽⁵⁾

The second test was performed on an Ohio 10-gauge nonsymmetrical Type 2 transition section (from W-beam to thrie beam). As shown in table 3, the 10-gauge section met the required specifications for *NCHRP Report 350* test 3-21.

Ohio Type 1 Thrie Beam Transition to Concrete Parapet

Three tests were performed on the Ohio Type 1 thrie beam transition to concrete parapet. During the first test (*NCHRP Report 350* test 3-21), the Ohio Type 1 thrie beam transition failed to meet occupant compartment deformation (see table 4). The potential for serious injury existed due to large deformations. Individual dimensions did not exceed 150 mm, but overall occupant deformation (see figure 28) was considerable and was judged to fail this criterion.

For the second test (again *NCHRP Report 350* test 3-21), a 7.1-m long x 100 mm high x 152 mm wide Type 2 asphaltic curb was installed in front of the Ohio Type 1 transition. The toe of the curb was placed 25 mm in front of the face of the thrie beam. The curb overlapped the lower edge of the concrete parapet for a distance of 1.2 m and tapered to ground level over 2.7 m on the upstream end (under the W-beam). The Ohio Type 1 thrie beam transition to concrete parapet with asphalt curb met all occupant risk values and marginally met compartment deformation guidelines (see table 5). Individual dimensions did not exceed 150 mm, but overall occupant deformation was considerable and was judged to be marginal for this criterion.

Table 2. Performance evaluation summary for *NCHRP Report 350* test 3-21 on the Ohio 12-gauge nonsymmetrical Type 2 transition.

Test Agency: Texas Transportation Institute		Test No.: 401021-4	Test Date: 09/01/2000
NCHRP Report 350 Test 3-21 Evaluation Criteria		Test Results	Assessment
<u>Structural Adequacy</u>			
A.	<i>Test article should contain and redirect the vehicle; the vehicle should not penetrate, underide, or override the installation although controlled lateral deflection of the test article is acceptable.</i>	The Ohio 12-gauge nonsymmetrical Type 2 transition contained and redirected the pickup truck. The vehicle did not penetrate, underide, or override the installation. Maximum dynamic deflection of the transition was 439 mm.	Pass
<u>Occupant Risk</u>			
D.	<i>Detached elements, fragments, or other debris from the test article should not penetrate or show potential for penetrating the occupant compartment, or present an undue hazard to other traffic, pedestrians, or personnel in a work zone. Deformations of, or intrusions into, the occupant compartment that could cause serious injuries should not be permitted.</i>	No detached elements, fragments, or other debris were present to penetrate or to show potential for penetrating the occupant compartment, nor to present undue hazard to others in the area. Maximum deformation of the occupant compartment was 175 mm in the driver's floor pan area.	Fail
F.	<i>The vehicle should remain upright during and after collision although moderate roll, pitching, and yawing are acceptable.</i>	The 2000-kg pickup truck remained upright and stable during and after the collision period.	Pass
<u>Vehicle Trajectory</u>			
K.	<i>After collision, it is preferable that the vehicle's trajectory not intrude into adjacent traffic lanes.</i>	The vehicle did not intrude into adjacent traffic lanes.	Pass*
L.	<i>The occupant impact velocity in the longitudinal direction should not exceed 12 m/s and the occupant ridedown acceleration in the longitudinal direction should not exceed 20 g's.</i>	Longitudinal occupant impact velocity was 7.2 m/s and longitudinal ridedown acceleration was -11.7 g's.	Pass
M.	<i>The exit angle from the test article preferably should be less than 60 percent of test impact angle, measured at time of vehicle loss of contact with test device.</i>	Exit angle at loss of contact was 16.1 degrees, which was 66 percent of the impact angle.	Fail*

*Criteria K and M are preferable, not required.

Table 3. Performance evaluation summary for *NCHRP Report 350* test 3-21 on the Ohio Type 2 10-gauge nonsymmetrical transition.

Test Agency: Texas Transportation Institute		Test No.: 401021-6	Test Date: 03/07/2002
NCHRP Report 350 Test 3-21 Evaluation Criteria		Test Results	Assessment
<u>Structural Adequacy</u>			
A.	<i>Test article should contain and redirect the vehicle; the vehicle should not penetrate, underride, or override the installation although controlled lateral deflection of the test article is acceptable.</i>	The Ohio 10-gauge nonsymmetrical Type 2 transition contained and redirected the pickup truck. The vehicle did not penetrate, underride, or override the installation. Maximum dynamic deflection during the test was 659 mm.	Pass
<u>Occupant Risk</u>			
D.	<i>Detached elements, fragments, or other debris from the test article should not penetrate or show potential for penetrating the occupant compartment, or present an undue hazard to other traffic, pedestrians, or personnel in a work zone. Deformations of, or intrusions into, the occupant compartment that could cause serious injuries should not be permitted.</i>	No detached elements, fragments, or other debris was present to penetrate or to show potential for penetrating the occupant compartment, or to present undue hazard to others in the area. Maximum occupant compartment deformation was 52 mm at the kickpanel near the passenger's feet.	Pass
F.	<i>The vehicle should remain upright during and after collision although moderate roll, pitching, and yawing are acceptable.</i>	The pickup truck remained upright during and after the impact sequence.	Pass
<u>Vehicle Trajectory</u>			
K.	<i>After collision, it is preferable that the vehicle's trajectory not intrude into adjacent traffic lanes.</i>	The vehicle came to rest 27.5 m downstream of impact and 5.7 m forward of the traffic face of the rail.	Fail*
L.	<i>The occupant impact velocity in the longitudinal direction should not exceed 12 m/s and the occupant ridedown acceleration in the longitudinal direction should not exceed 20 g's.</i>	Longitudinal occupant impact velocity was 7.8 m/s and longitudinal ridedown acceleration was -15.6 g's.	Pass
M.	<i>The exit angle from the test article preferably should be less than 60 percent of test impact angle, measured at time of vehicle loss of contact with test device.</i>	Exit angle at loss of contact was 26.1 degree, which was over 100 percent of the impact angle.	Fail*

*Criteria K and M are preferable, not required.

Table 4. Performance evaluation summary for *NCHRP Report 350* test 3-21 on the Ohio Type 1 transition without asphalt curb.

Test Agency: Texas Transportation Institute	Test No.: 401021-1	Test Date: 10/30/2000
<i>NCHRP Report 350 Test 3-21 Evaluation Criteria</i>	Test Results	Assessment
<u>Structural Adequacy</u>		
A. <i>Test article should contain and redirect the vehicle; the vehicle should not penetrate, underide, or override the installation although controlled lateral deflection of the test article is acceptable.</i>	The Ohio Type 1 transition without asphalt curb contained and redirected the pickup truck. The vehicle did not penetrate or override the installation. The tire of the vehicle underrode the installation and overlapped the parapet 130 mm. Maximum dynamic deflection of the transition was 163 mm.	Pass
<u>Occupant Risk</u>		
D. <i>Detached elements, fragments, or other debris from the test article should not penetrate or show potential for penetrating the occupant compartment, or present an undue hazard to other traffic, pedestrians, or personnel in a work zone. Deformations of, or intrusions into, the occupant compartment that could cause serious injuries should not be permitted.</i>	No detached elements, fragments, or other debris were present to penetrate or to show potential for penetrating the occupant compartment, nor to present undue hazard to others in the area. Maximum deformation of the occupant compartment was 140 mm in the center of the floor pan area and the seam between the floor pan and firewall opened.	Fail
F. <i>The vehicle should remain upright during and after collision although moderate roll, pitching, and yawing are acceptable.</i>	The 2000-kg pickup truck remained upright and stable during and after the collision period.	Pass
<u>Vehicle Trajectory</u>		
K. <i>After collision, it is preferable that the vehicle's trajectory not intrude into adjacent traffic lanes.</i>	The vehicle intruded 12.2 m forward of the traffic face of the installation.	Fail*
L. <i>The occupant impact velocity in the longitudinal direction should not exceed 12 m/s and the occupant ridedown acceleration in the longitudinal direction should not exceed 20 g's.</i>	Longitudinal occupant impact velocity was 6.7 m/s and longitudinal ridedown acceleration was -19.2 g's.	Pass
M. <i>The exit angle from the test article preferably should be less than 60 percent of test impact angle, measured at time of vehicle loss of contact with test device.</i>	Exit angle at loss of contact was 7.5 degrees, which was 29 percent of the impact angle.	Pass*

*Criteria K and M are preferable, not required.

Table 5. Performance evaluation summary for *NCHRP Report 350* test 3-21 on the Ohio Type 1 transition with asphalt curb.

Test Agency: Texas Transportation Institute	Test No.: 401021-5	Test Date: 07/02/2001
NCHRP Report 350 Test 3-21 Evaluation Criteria	Test Results	Assessment
<u>Structural Adequacy</u>		
A. <i>Test article should contain and redirect the vehicle; the vehicle should not penetrate, underide, or override the installation although controlled lateral deflection of the test article is acceptable.</i>	The Ohio Type 1 transition with asphalt curb contained and redirected the pickup truck. The vehicle did not penetrate or override the installation. The tire of the vehicle underrode the installation and overlapped the parapet 70 mm. Maximum dynamic deflection of the transition was 245 mm.	Pass
<u>Occupant Risk</u>		
D. <i>Detached elements, fragments, or other debris from the test article should not penetrate or show potential for penetrating the occupant compartment, or present an undue hazard to other traffic, pedestrians, or personnel in a work zone. Deformations of, or intrusions into, the occupant compartment that could cause serious injuries should not be permitted.</i>	No detached elements, fragments, or other debris were present to penetrate or to show potential for penetrating the occupant compartment, nor to present undue hazard to others in the area. Maximum deformation of the occupant compartment was 120 mm in the kick panel area and the seam between the floor pan and firewall opened. No single dimension exceeded 150 mm, but overall deformation indicates marginal performance.	Pass
F. <i>The vehicle should remain upright during and after collision although moderate roll, pitching, and yawing are acceptable.</i>	The 2000-kg pickup truck remained upright and stable during and after the collision period.	Pass
<u>Vehicle Trajectory</u>		
K. <i>After collision, it is preferable that the vehicle's trajectory not intrude into adjacent traffic lanes.</i>	The vehicle intruded 10.7 m toward traffic lanes.	Fail*
L. <i>The occupant impact velocity in the longitudinal direction should not exceed 12 m/s and the occupant ridedown acceleration in the longitudinal direction should not exceed 20 g's.</i>	Longitudinal occupant impact velocity was 6.2 m/s and longitudinal ridedown acceleration was -14.5 g's.	Pass
M. <i>The exit angle from the test article preferably should be less than 60 percent of test impact angle, measured at time of vehicle loss of contact with test device.</i>	Exit angle at loss of contact was 16.0 degrees, which was 62 percent of the impact angle.	Fail*

*Criteria K and M are preferable, not required.

With the acceptable performance of *NCHRP Report 350* test 3-21 on the Ohio Type 1 Thrie Beam Transition to Concrete Parapet with Asphalt Curb, a third test, *NCHRP Report 350* test 4-22, was performed. The Ohio Type 1 transition with asphalt curb met required specifications for *NCHRP Report 350* test designation 4-22, as shown in table 6, making this transition acceptable for TL-4.

Thrie Beam Transition to Wisconsin Type “M” Tubular Steel Bridge Rail

One test was performed on the Wisconsin Thrie Beam Transition to Type “M” Tubular Steel Bridge Rail. The transition was tested and evaluated according to *NCHRP Report 350* requirements and met the evaluation criteria for test 3-21, as shown in table 7.

Modified NYSDOT Box-Beam Transition to Four-Rail Steel Bridge Rail

Under Modification No. 3 of this contract, FHWA requested an FEA of the NYSDOT box-beam transition to four-rail steel bridge rail that had failed the test with the pickup truck under the previous contract. *NCHRP Report 350* test designation 3-21 was previously performed on the box-beam transition to the NYSDOT four-rail steel bridge rail. During this test, the transition section contained and redirected the pickup truck, and all computed occupant risk values were within acceptable limits. However, occupant compartment deformation in the driver’s side floor pan area was 175 mm, and the door was pulled open at the hinges.

Four tasks were performed under the FEA on the New York box-beam transition. The first task required modeling of the New York box-beam transition and the failure that occurred during the previous testing. The next two tasks were to investigate the performance of modifications to the New York box-beam transition to determine performance at TL-4. After review of the FEA performed under Tasks B1 through B3, further changes were made to improve the performance of the transition. Changes included: turning the end of the top bridge rail element down and bolting it to the top of the third bridge rail element; adding a fourth heavy transition post that resulted in shortening the distance between the last transition post and the first bridge rail post; moving the box-beam expansion splice for the third and second rails upstream; extending the rub rail upstream with an expansion splice of its own; and changing the splice details to allow for a tighter yet constructable connection.

Based on the predictive simulation results of the FEA performed on the modified box-beam transition under Modification No. 3 of this contract, FHWA decided to perform a full-scale crash test on the modified transition based on the results of Task B4 of the analysis. *NCHRP Report 350* test 3-21 was performed on the modified transition. Although the splice on the middle rail element just downstream of post 3 was pulled out 25 mm, there was no evidence that the door snagged as in the previous test. The modified NYSDOT box-beam transition performed acceptably according to requirements for *NCHRP Report 350* test 3-21, as shown in table 8.

Table 6. Performance evaluation summary for *NCHRP Report 350* test 4-22 on the Ohio Type 1 transition with asphalt curb.

Test Agency: Texas Transportation Institute		Test No.: 401021-2a	Test Date: 01/16/2002
<i>NCHRP Report 350</i> Test 4-22 Evaluation Criteria		Test Results	Assessment
<u>Structural Adequacy</u>			
A.	<i>Test article should contain and redirect the vehicle; the vehicle should not penetrate, underride, or override the installation although controlled lateral deflection of the test article is acceptable.</i>	The Ohio Type 1 transition with asphalt curb contained and redirected the 8000-kg single-unit truck. The vehicle did not penetrate, underride, or override the installation. Maximum dynamic deflection of the transition was 120 mm.	Pass
<u>Occupant Risk</u>			
D.	<i>Detached elements, fragments, or other debris from the test article should not penetrate or show potential for penetrating the occupant compartment, or present an undue hazard to other traffic, pedestrians, or personnel in a work zone. Deformations of, or intrusions into, the occupant compartment that could cause serious injuries should not be permitted.</i>	No detached elements, fragments, or other debris were present to penetrate or to show potential for penetrating the occupant compartment, nor to present undue hazard to others in the area. No measurable deformation of the occupant compartment occurred.	Pass
F.	<i>The vehicle should remain upright during and after collision although moderate roll, pitching, and yawing are acceptable.</i>	The 8000-kg single-unit truck remained upright during and after the collision period.	Pass*
<u>Vehicle Trajectory</u>			
K.	<i>After collision, it is preferable that the vehicle's trajectory not intrude into adjacent traffic lanes.</i>	The vehicle did not intrude into adjacent traffic lanes.	Pass*
M.	<i>The exit angle from the test article preferably should be less than 60 percent of test impact angle, measured at time of vehicle loss of contact with test device.</i>	Exit angle at loss of contact was 6.8 degrees, which was 43 percent of the impact angle.	Pass*

*Criteria F, K, and M are preferable, not required.

Table 7. Performance evaluation summary for *NCHRP Report 350* test 3-21 on the Wisconsin three beam transition to Type “M” tubular steel bridge rail.

Test Agency: Texas Transportation Institute		Test No.: 401021-3	Test Date: 11/22/2002
NCHRP Report 350 Test 3-21 Evaluation Criteria		Test Results	Assessment
<u>Structural Adequacy</u>			
A.	<i>Test article should contain and redirect the vehicle; the vehicle should not penetrate, underide, or override the installation although controlled lateral deflection of the test article is acceptable.</i>	The Wisconsin three beam transition to Type “M” tubular steel bridge rail contained and redirected the pickup truck. The vehicle did not penetrate, underide, or override the installation. Maximum dynamic deflection was 49 mm.	Pass
<u>Occupant Risk</u>			
D.	<i>Detached elements, fragments, or other debris from the test article should not penetrate or show potential for penetrating the occupant compartment, or present an undue hazard to other traffic, pedestrians, or personnel in a work zone. Deformations of, or intrusions into, the occupant compartment that could cause serious injuries should not be permitted.</i>	No detached elements, fragments, or other debris were present to penetrate or to show potential for penetrating the occupant compartment, or to present a hazard to others in the area. Maximum occupant compartment deformation was 74 mm in the kickpanel area on the driver’s side.	Pass
F.	<i>The vehicle should remain upright during and after collision although moderate roll, pitching, and yawing are acceptable.</i>	The vehicle remained upright during and after the collision event.	Pass
<u>Vehicle Trajectory</u>			
K.	<i>After collision, it is preferable that the vehicle's trajectory not intrude into adjacent traffic lanes.</i>	The vehicle came to rest 73.2 m downstream of impact and 21.0 m forward of the traffic face of the rail.	Fail*
L.	<i>The occupant impact velocity in the longitudinal direction should not exceed 12 m/s and the occupant ridedown acceleration in the longitudinal direction should not exceed 20 g’s.</i>	Longitudinal occupant impact velocity was 5.2 m/s and maximum longitudinal occupant ridedown acceleration was -10.5 g’s.	Pass
M.	<i>The exit angle from the test article preferably should be less than 60 percent of test impact angle, measured at time of vehicle loss of contact with test device.</i>	Exit angle at loss of contact was 4.8 degrees, which was 19 percent of the impact angle.	Pass*

*Criteria K and M are preferable, not required.

Table 8. Performance evaluation summary for *NCHRP Report 350* test 3-21 on the modified NYSDOT box-beam transition to four-rail steel bridge rail.

Test Agency: Texas Transportation Institute		Test No.: 401021-7	Test Date: 03/15/2004
NCHRP Report 350 Test 3-21 Evaluation Criteria		Test Results	Assessment
<u>Structural Adequacy</u>			
A.	<i>Test article should contain and redirect the vehicle; the vehicle should not penetrate, underride, or override the installation although controlled lateral deflection of the test article is acceptable.</i>	The modified NYSDOT box-beam transition to four-rail steel bridge rail contained and redirected the pickup truck. The vehicle did not penetrate, underride, or override the installation. Maximum dynamic deflection during the test was 124 mm.	Pass
<u>Occupant Risk</u>			
D.	<i>Detached elements, fragments, or other debris from the test article should not penetrate or show potential for penetrating the occupant compartment, or present an undue hazard to other traffic, pedestrians, or personnel in a work zone. Deformations of, or intrusions into, the occupant compartment that could cause serious injuries should not be permitted.</i>	No detached elements, fragments, or other debris was present to penetrate or to show potential for penetrating the occupant compartment, or to present hazard to others in the area. Maximum occupant compartment deformation was 60 mm laterally at the kickpanel across the cab.	Pass
F.	<i>The vehicle should remain upright during and after collision although moderate roll, pitching, and yawing are acceptable.</i>	The pickup truck remained upright during and after the collision event.	Pass
<u>Vehicle Trajectory</u>			
K.	<i>After collision, it is preferable that the vehicle's trajectory not intrude into adjacent traffic lanes.</i>	The vehicle came to rest 50.3 m downstream of impact and 3.6 m forward of the traffic face of the rail.	Fail*
L.	<i>The occupant impact velocity in the longitudinal direction should not exceed 12 m/s and the occupant ridedown acceleration in the longitudinal direction should not exceed 20 g's.</i>	Longitudinal occupant impact velocity was 4.4 m/s, and longitudinal ridedown acceleration was -12.6 g's.	Pass
M.	<i>The exit angle from the test article preferably should be less than 60 percent of test impact angle, measured at time of vehicle loss of contact with test device.</i>	Exit angle at loss of contact with the transition was 7.0 degrees, which was 29 percent of the impact angle.	Pass*

*Criteria K and M are preferable, not required.

CONCLUSIONS

Table 9 provides a brief assessment of the full-scale crash testing performed on the transitions under this contract.

Table 9. Results of transition testing.

Description of Appurtenance	Test Number	<i>NCHRP Report 350</i> Test Designation	Assessment
Ohio Nonsymmetrical Type 2 W-beam to Thrie Beam Transition With 12-gauge section With 10-gauge section	401021-4 401021-6	3-21 3-21	Fail Pass
Ohio Type 1 Thrie Beam Transition to Concrete Parapet Type 1 without curb Type 1 with asphalt curb Type 1 with asphalt curb	401021-1 401021-5 401021-2a	3-21 3-21 4-22	Fail Pass Pass
Thrie Beam Transition to Wisconsin Type "M" Tubular Steel Bridge Rail	401021-3	3-21	Pass
NYSDOT Modified Box-Beam Transition to Four-Rail Steel Bridge Rail	401021-7	3-21	Pass

REFERENCES

1. H. E. Ross, Jr., D. L. Sicking, R. A. Zimmer and J. D. Michie, *Recommended Procedures for the Safety Performance Evaluation of Highway Features*, National Cooperative Highway Research Program Report 350, Transportation Research Board, National Research Council, Washington, DC, 1993.
2. C. E. Buth, W. L. Menges, and Sandra K. Schoeneman, *NCHRP Report 350 Assessment of Existing Roadside Safety Hardware*, Report No. FHWA-RD-01-042, Contract No. DTFH61-97-C-00039, Federal Highway Administration, Texas Transportation Institute, The Texas A&M University System, College Station, TX, November 2000.
3. R. K. Faller et al., *Two-Approach Guardrail Transition for Concrete Safety Shape Barriers*, Research Report No. TRP-03-69-98, Midwest Roadside Safety Facility, University of Nebraska-Lincoln, Lincoln, NE, May 1998.
4. C. E. Buth, W. L. Menges, and W. F. Williams, *Testing and Evaluation of the New York Two-Rail Curbless and Four-Rail Curbless Bridge Railing and Box-Beam Transition*, Research Report 404531-F, Texas Transportation Institute, The Texas A&M University System, College Station, TX, September 1999.
5. Federal Highway Administration Memorandum from the Director, Office of Engineering, entitled "ACTION: Identifying Acceptable Highway Safety Features," dated July 25, 1997.
6. R. Powers, *Draft Guidelines for Analysis of Passenger Compartment Intrusion*, Federal Highway Administration, Washington, DC, January 1999.

APPENDIX A. CRASH TEST PROCEDURES AND DATA ANALYSIS

The crash test and data analysis procedures were in accordance with guidelines presented in *NCHRP Report 350*. Following are brief descriptions of these procedures.

ELECTRONIC INSTRUMENTATION AND DATA PROCESSING FOR THE TEST INSTALLATION

Six strain gauges and one accelerometer were installed on the transitions to measure longitudinal strains in the steel rail and post acceleration during the crash test; locations for each test are noted below. Tensile strains were reported as millionths of a mm per mm of strain or microstrain, every 0.0001 s during the impact along with the acceleration values in g's.

Two single, active-arm, weldable strain gauges were installed on the neutral bending axis of the metal beam, and four were installed on the neutral axis of the metal beam. All six of these locations were on the field side of the rail elements, which would produce strain in tension during impact. Strain gauges were then connected, through cables, as quarter active-arm, full-bridge circuits using completion resistors in the amplifier units. This arrangement provided for measurement of surface strain, in the longitudinal direction, of the steel backing during the vehicle impact.

Once wired and tested, each strain gauge bridge was calibrated by placing a precision resistor across the gauge to produce a microstrain value based on calculations using the published values included with each strain gauge. The resulting values then were used to produce a microstrain calibration step at the amplifier when a precision resistor was switched across one leg of the bridge, which is referred to as a resistance calibration (R-cal) or shunt cal.

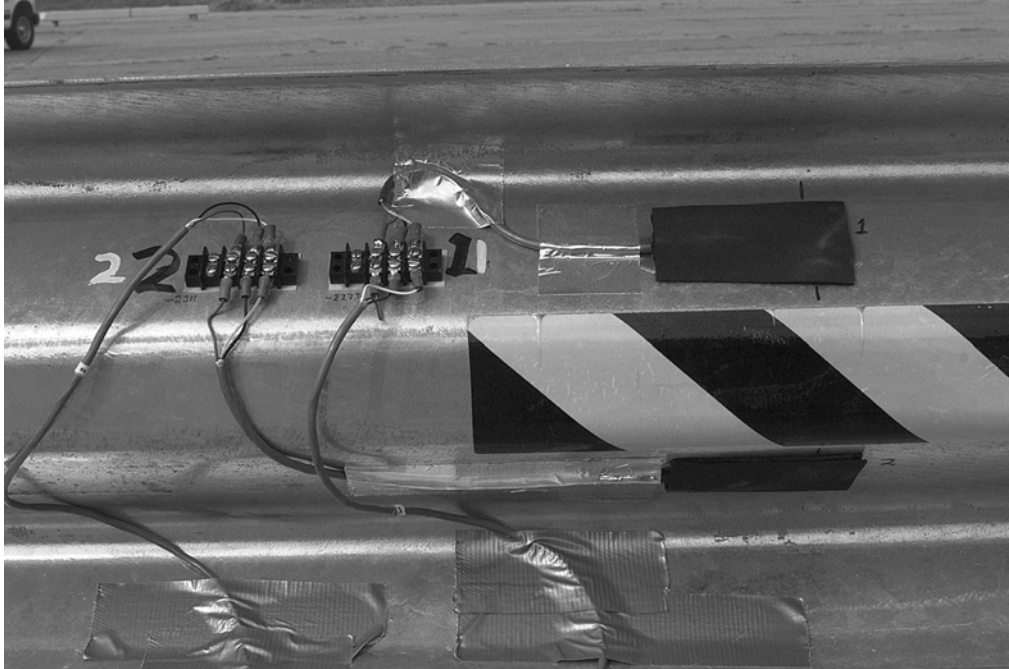
Approximately 100 m of cable connected the strain gauges to the strain gauge amplifiers located in a vehicle behind the installation with appropriate compensation calculations made for cable lengths. The output of the strain gauge amplifiers fed a P-band telemetry transmitter in the instrumentation vehicle. Just before the impact the R-cal data were sent over the telemetry link to provide subsequent correction values to the data. In the base station, these calibration and impact data signals were recorded simultaneously on a 28-track instrumentation tape recorder, with all of the vehicle data to provide time synchronization. These analog data then were digitized at 10,000 samples per second to produce force data in engineering units.

For test 401021-4, the accelerometer was installed on the back of post 13 in the longitudinal axis of the rail. Strain gauge bridges were located as follows: #1) 810 mm from the center of post 12 on the field side of the plate at 590 mm from ground level; #2) 810 mm from the center of post 12 on the field side of the plate at 460 mm from ground level; #3) 370 mm from the center of post 17 on the field side of the plate at 805 mm from ground level; #4) 370 mm from the center of post 17 on the field side of the plate at 670 mm from ground level; #5) 370 mm from the center of post 17 on the traffic side at 615 mm from ground level; #6)

370 mm from the center of post 17 on the field side of the plate at 485 mm from ground level. At these locations, the steel rail was prepared by first grinding away the mill scale to produce a clean and smooth surface in a 60 x 30 mm area where the gauges were spot welded to bond them to the steel. Photographs showing typical setup for this test are shown in figure 105.

For test 401021-6, the accelerometer was installed on the back of post 11 in the longitudinal axis of the rail, at 685 mm above the ground surface. Strain gauge bridges were located as follows: #1) 1330 mm upstream from the center of post 10 on the field side of the W-beam rail at 635 mm from ground level; #2) 1330 mm upstream from the center of post 10 on the field side of the W-beam rail at 510 mm from ground level; #3) 635 mm upstream from the center of post 16 on the field side of the thrie beam rail at 810 mm from ground level; #4) 635 mm upstream from the center of post 16 on the field side of the thrie beam rail at 675 mm from ground level; #5) 635 mm upstream from the center of post 16 on the traffic side of the thrie beam at 600 mm from ground level; #6) 635 mm upstream from the center of post 16 on the field side of the thrie beam at 480 mm from ground level. At these locations, the rail element was prepared by first grinding away the galvanized coating and the mill scale to produce a clean and smooth surface in a 60 x 30 mm area where the gauges were spot welded to bond them to the steel. Photographs showing typical setup for this test are shown in figure 106.

For test 401021-1, the accelerometer was installed on the back of post 13 (150 mm from the end of the parapet and 72 mm above the ground) in the lateral axis of the rail. Strain gauge bridges were located as follows: #1) 5540 mm downstream from the end of the concrete parapet on the field side of the rail element at 625 mm from ground level; #2) 5540 mm downstream from the end of the concrete parapet on the field side of the rail element at 505 mm from ground level; #3) 2745 mm downstream from the end of the concrete parapet on the field side of the rail element at 715 mm from ground level; #4) 2745 mm downstream from the end of the concrete parapet on the field side of the rail element at 520 mm from ground level; #5) 150 mm upstream from the end of the concrete parapet on the traffic side at 595 mm from ground level; #6) 150 mm upstream from the concrete parapet on the field side of the rail element at 525 mm from ground level. At these locations, the steel rail was prepared by first grinding away the mill scale to produce a clean and smooth surface in a 60 x 30 mm area where the gauges were spot welded to bond them to the steel. Photographs showing typical setup for this test are shown in figure 107.

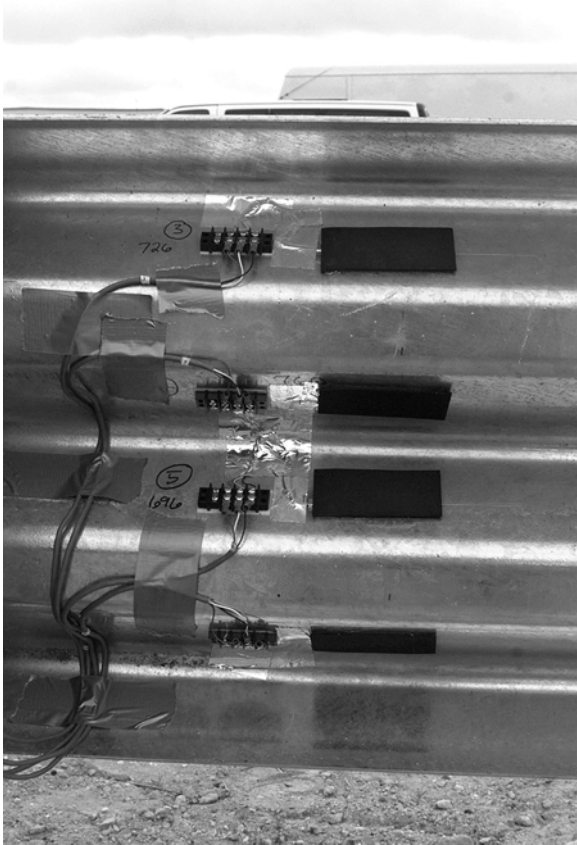


a) Strain gauge on rail.

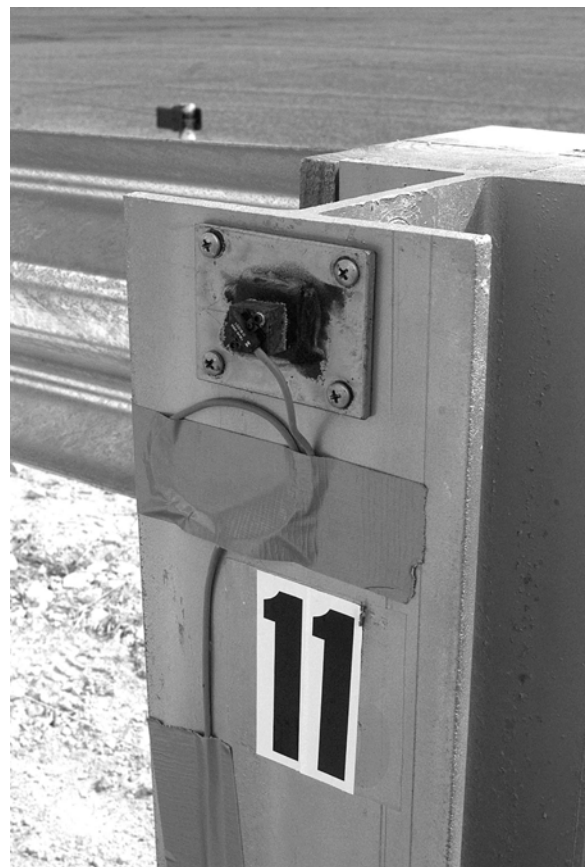


b) Accelerometer on post 13.

Figure 105. Typical instrumentation setup on the rail for test 401021-4.



a) Strain gauges on rail.

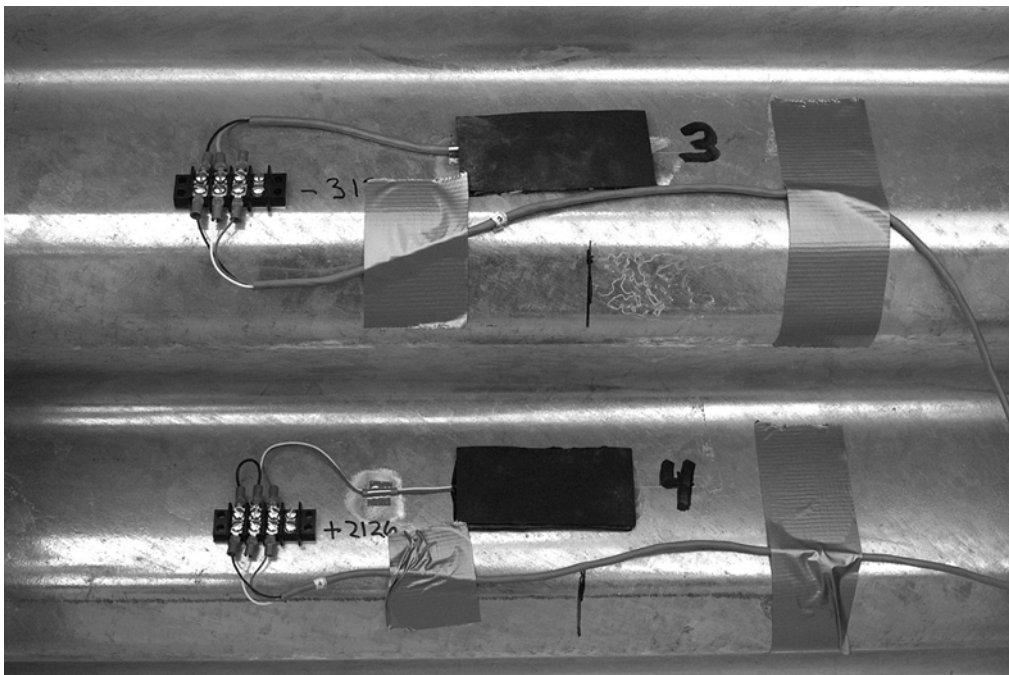


b) Accelerometer on post 11.

Figure 106. Typical instrumentation setup on the rail for test 401021-6.



a) Strain gauges on W-beam rail element.



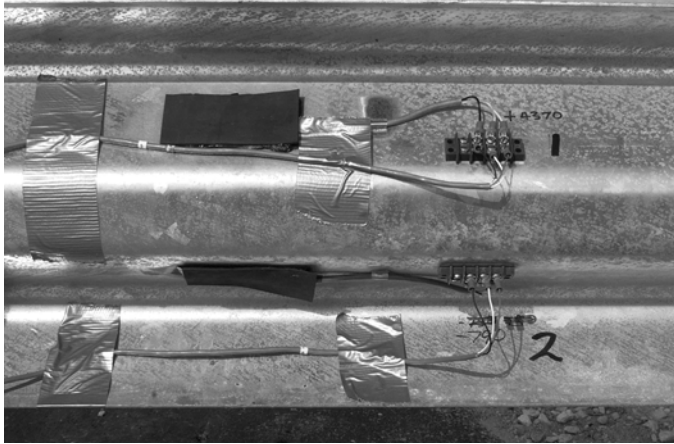
b) Closeup of strain gauges.

Figure 107. Typical instrumentation setup on the rail for test 404201-1.

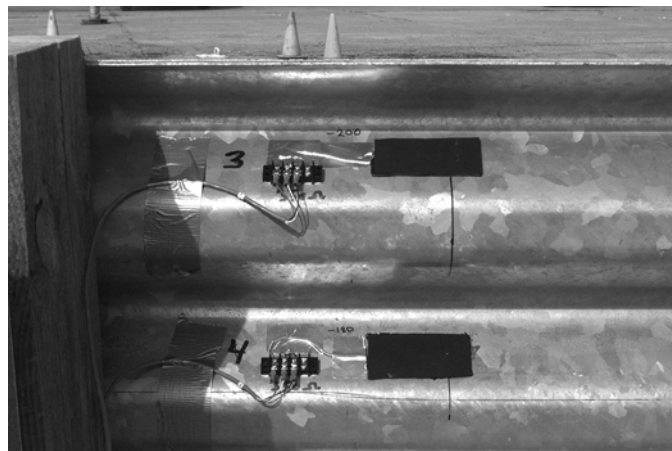
For test 401021-5, the accelerometer was installed on the back of post 13 in the longitudinal axis of the rail. Strain gauge bridges were located as follows: #1) 5740 mm upstream from the end of the concrete parapet on the field side of the plate at 600 mm from ground level; #2) 5740 mm upstream from the end of the concrete parapet on the field side of the plate at 500 mm from ground level; #3) 2565 mm upstream from the end of the concrete parapet on the field side of the plate at 710 mm from ground level; #4) 2565 mm upstream from the end of the concrete parapet on the field side of the plate at 520 mm from ground level; #5) 120 mm upstream from the end of the concrete parapet on the traffic side at 625 mm from ground level; #6) 120 mm upstream from the concrete parapet on the field side of the plate at 550 mm from ground level. At these locations, the steel rail was prepared by first grinding away the mill scale to produce a clean and smooth surface in a 60 x 30 mm area where the gauges were spot welded to bond them to the steel. Photographs showing typical setup for this test are shown in figure 108.

For test 401021-2a, the accelerometer was installed on the back of post 13. Strain gauge bridges on the neutral axis for the normal plane of bending were located as follows: #1) 5700 mm upstream from the end of the concrete parapet on the field side of the rail at 635 mm from ground level; #2) 5700 mm upstream from the end of the concrete parapet on the field side of the rail at 505 mm from ground level; #3) 2840 mm upstream from the end of the concrete parapet on the field side of the rail at 605 mm from ground level; #4) 2840 mm downstream from the end of the concrete parapet on the field side of the rail at 535 mm from ground level; #5) at the end of the concrete parapet on the field side at 720 mm from ground level; #6) at the end the concrete parapet on the field side at 550 mm from ground level. At these locations, the rail was prepared by first grinding away the galvanized coating to produce a clean and smooth surface in a 60 x 30 mm area where the gauges were spot welded to bond them to the steel. The accelerometer located on the centerline of post 13 was 1300 mm downstream of the end of the parapet, 720 mm above ground level, and 480 mm behind the traffic face of the W-beam rail element. Photographs showing typical setup for this test are shown in figure 109.

For test 401021-3, the accelerometer was installed on the back of post 18 in the longitudinal axis of the rail, at 530 mm above the ground surface. Strain gauge bridges were located as follows: #1) 590 mm downstream from the center of post 11 on the field side of the W-beam rail at 608 mm from ground level; #2) 590 mm downstream from the center of post 11 on the field side of the W-beam rail at 485 mm from ground level; #3) 460 mm downstream from the center of post 14 on the field side of the thrie beam rail at 703 mm from ground level; #4) 440 mm downstream from the center of post 14 on the field side of the thrie beam rail at 505 mm from ground level; #5) 435 mm downstream from the center of post 14 on the traffic side of the thrie beam at 320 mm from ground level; and #6) 230 mm downstream from the center of post 16 on the field side of the thrie beam at 500 mm from ground level. At these locations, the rail element was prepared by first grinding away the galvanize coating and the mill scale to produce a clean and smooth surface in a 60 x 30 mm area where the gauges were spot-welded to bond them to the steel. Photographs showing typical setup for this test are shown in figure 110.



a) Strain gauges 1 and 2.



b) Strain gauges 3 and 4.



c) Strain gauge 5.

Figure 108. Typical instrumentation setup on the rail for test 401021-5.

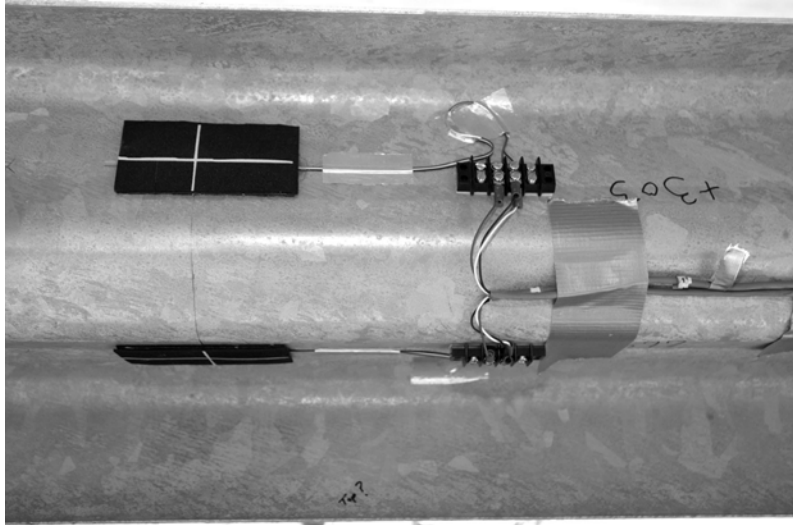


a) Strain gauges on rail.

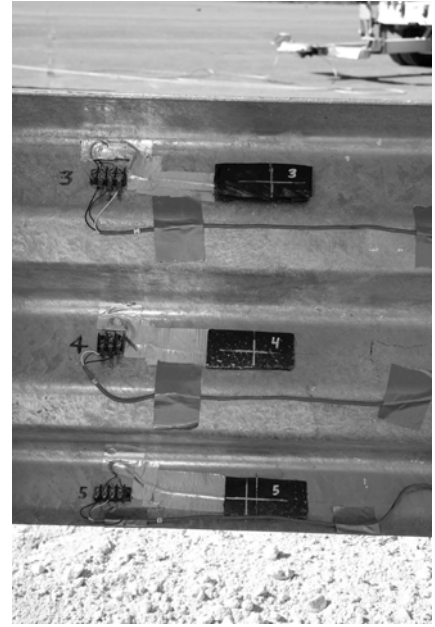


b) Accelerometer on post 13.

Figure 109. Typical instrumentation setup on the rail for test 401021-2a.



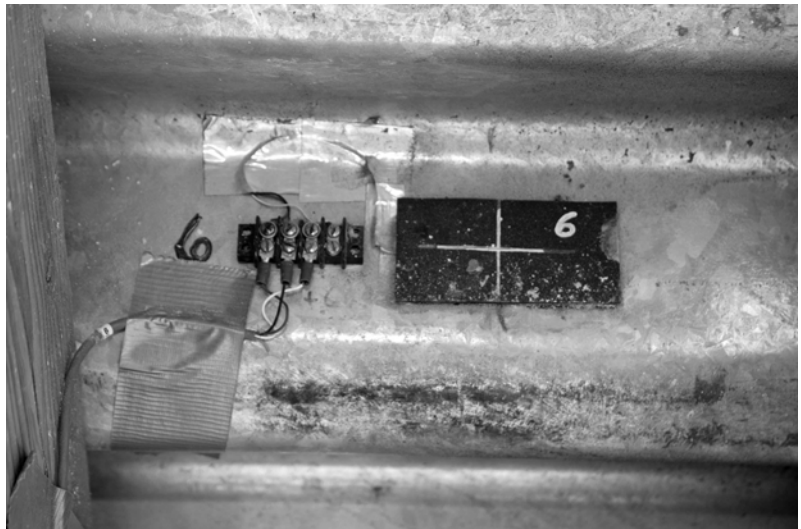
a) Strain gauges 1 and 2.



b) Strain gauges 3, 4, and 5.



d) Accelerometer location.



c) Strain gauge 6.

Figure 110. Typical instrumentation setup on the rail for test 401021-3.

**ELECTRONIC INSTRUMENTATION AND DATA PROCESSING
FOR THE TEST VEHICLE**

The test vehicle was instrumented with five uniaxial accelerometers mounted in the following locations: (1) center top surface of the instrument panel; (2) inside end of right front wheel spindle; (3) inside end of left front wheel spindle; (4) top of engine block; and (5) bottom of engine block. The location of each accelerometer for each test is reported in tables 10 through 15. These accelerometers were Endevco® Model 7264A low-mass piezoresistive accelerometers with a ± 2000 g range.

Table 10. Locations of vehicle accelerometers for test 401021-4.

Location	X (mm) (distance from front axle)*	Y (mm) (distance from centerline)*	Z (mm) (distance from ground)*	Data Axis
Instrument panel	-870	0	+1350	+X
Right front wheel spindle	0	+700	+361	+X
Left front wheel spindle	0	-700	+361	+Y
Top of engine block	+170	+90	+970	+X
Bottom of engine block	-370	+180	+416	+X
Vehicle c.g.	-1420	0	+640	+X,+Y,+Z
Vehicle rear axle	-3340	0	+850	+X,+Y,+Z

*Reference point: X = 0 at front axle Y = 0 at centerline Z = 0 at ground
Sign convention: +X = forward +Y = right +Z = down

Table 11. Locations of vehicle accelerometers for test 401021-6.

Location	X (mm) (distance from front axle)*	Y (mm) (distance from centerline)*	Z (mm) (distance from ground)*	Data Axis
Instrument panel	-820	0	-1290	+X
Right front wheel spindle	0	+690	-360	-Y
Left front wheel spindle	0	-690	-360	+X
Top of engine block	+215	100	-940	+X
Bottom of engine block	-210	105	-430	+X
Vehicle c.g.	-1394	0	-630	+X,+Y,+Z
Vehicle rear axle	-3360	0	-860	+X,+Y,+Z

*Reference point: X = 0 at front axle Y = 0 at centerline Z = 0 at ground
 Sign convention: +X = forward +Y = right +Z = down

Table 12. Locations of vehicle accelerometers for test 401021-1.

Location	X (mm) (distance from front axle)*	Y (mm) (distance from centerline)*	Z (mm) (distance from ground)*	Data Axis
Instrument panel	-820	0	-1350	+X
Right front wheel spindle	0	+700	-361	+X
Left front wheel spindle	0	-700	-361	+Y
Top of engine block	-165	+90	-416	+X
Bottom of engine block	-360	+170	-640	+X
Vehicle c.g.	-1450	0	-640	+X,+Y,+Z
Vehicle rear axle	-3350	0	-850	+X,+Y,+Z

*Reference point: X = 0 at front axle Y = 0 at centerline Z = 0 at ground
 Sign convention: +X = forward +Y = right +Z = down

Table 13. Locations of vehicle accelerometers for test 401021-5.

Location	X (mm) (distance from front axle)*	Y (mm) (distance from centerline)*	Z (mm) (distance from ground)*	Data Axis
Instrument panel	-850	0	-1345	+X
Right front wheel spindle	0	+720	-355	+X
Left front wheel spindle	0	-720	-355	+Y
Top of engine block	+150	-70	-930	+X
Bottom of engine block	-290	+100	-415	+X
Vehicle c.g.	-1460	0	-660	+X,+Y,+Z
Vehicle rear axle	-3340	0	-880	+X,+Y,+Z

*Reference point: X = 0 at front axle Y = 0 at centerline Z = 0 at ground
 Sign convention: +X = forward +Y = right +Z = down

Table 14. Locations of vehicle accelerometers for test 401021-2a.

Location	X (mm) (distance from front axle)*	Y (mm) (distance from centerline)*	Z (mm) (distance from ground)*	Data Axis
Instrument panel	-530	0	-1740	+X
Right front wheel spindle	90	+955	-495	+X
Left front wheel spindle	90	-955	-495	+Y
Top of engine block	+275	-100	-1270	+X
Bottom of engine block	0	0	-620	+X
Vehicle c.g.	-3150	0	-1100	+X,+Y,+Z
Vehicle cab	-1240	+210	-1050	+X, +Y
Vehicle rear axle	-5270	0	-1120	+X, +Y

*Reference point: X = 0 at front axle Y = 0 at centerline Z = 0 at ground
 Sign convention: +X = forward +Y = right +Z = down

Table 15. Locations of vehicle accelerometers for test 401021-3.

Location	X (mm) (distance from front axle)*	Y (mm) (distance from centerline)*	Z (mm) (distance from ground)*	Data Axis
Instrument panel	-840	0	-3400	+X
Right front wheel spindle	0	+730	-360	+X
Left front wheel spindle	0	-730	-360	+Y
Top of engine block	+110	+110	-940	+X
Bottom of engine block	-410	+105	-430	+X
Vehicle c.g.	-1450	+80	-610	+X,+Y,+Z
Vehicle rear axle	-3350	0	-870	+X,+Y,+Z

*Reference point: X = 0 at front axle Y = 0 at centerline Z = 0 at ground
 Sign convention: +X = forward +Y = right +Z = down

Onboard data acquisition is provided by a 16-channel, Diversified Technical Systems, Tiny Data Acquisition System Professional (TDAS PRO) hardware. Each analog channel has integral signal conditioning, fixed frequency antialias filtering, and a programmable transducer bridge power supply; these meet Society of Automotive Engineers (SAE) J211 specifications. Each 8-channel module contains 16 megabytes of battery-backed memory, allowing for more than 10 seconds of storage at 10,000 samples per second per channel. All channels are synchronized by a common external clock. The accuracy of this system is ± 0.1 percent.

In addition, the test vehicle was instrumented with: three solid-state angular rate transducers to measure roll, pitch, and yaw rates; a triaxial accelerometer near the vehicle c.g. to measure longitudinal, lateral, and vertical acceleration levels; and a backup biaxial accelerometer in the rear of the vehicle to measure longitudinal and lateral acceleration levels. These accelerometers were Endevco Model 2262CA, piezoresistive accelerometers with a ± 100 g range.

The accelerometers are strain gauge type with a linear millivolt output proportional to acceleration. Angular rate transducers are solid-state, gas-flow units designed for high-g service. Signal conditioners and amplifiers in the test vehicle increase the low-level signals to a ± 2.5 volt maximum level. The signal conditioners also provide the capability of an R-Cal or shunt calibration for the accelerometers and a precision voltage calibration for the rate transducers. The electronic signals from the accelerometers and rate transducers are transmitted to a base station by means of a 15-channel, constant-bandwidth, Inter-Range Instrumentation Group (IRIG), FM/FM telemetry link for recording on magnetic tape and for display on a real-time strip chart. Calibration signals from the test vehicle are recorded before the test and immediately afterwards. A crystal-controlled time reference signal is simultaneously recorded with the data.

Pressure-sensitive switches on the bumper of the impacting vehicle are actuated by wooden dowels before impact to indicate the elapsed time over a known distance to provide a measurement of impact velocity. The initial contact also produces an “event” mark on the data record to establish the instant of contact with the installation.

The multiplex of data channels, transmitted on one radio frequency, is received and demultiplexed onto separate tracks of a 28-track IRIG tape recorder. After the test, the data are played back from the tape machine and digitized. A proprietary software program (WinDigit) converts the analog data from each transducer into engineering units using the R-cal and pre-zero values at 10,000 samples per second per channel. This program also provides Society of Automotive Engineers (SAE) J211 class 180 phaseless digital filtering and vehicle impact velocity.

All accelerometers are calibrated annually according to SAE J211 Mar95 4.6.1 by means of a Endevco® 2901, precision primary-vibration standard. This device and its support instruments are returned to the factory annually for a National Institute of Standards and Technology (NIST) traceable calibration. The subsystems of each data channel also are evaluated annually, using instruments with current NIST traceability, and the results factored into the accuracy of the total data channel, per SAE J211. Calibrations and evaluations are made any time that data are suspect.

The Test Risk Assessment Program (TRAP) uses the data from WinDigit to compute occupant compartment impact velocities, time of occupant compartment impact after vehicle impact, and the highest 0.010-s average ridedown acceleration. WinDigit calculates change in vehicle velocity at the end of a given impulse period. In addition, maximum average accelerations over 0.050-s intervals in each of the three directions are computed. For reporting purposes, the data from the vehicle-mounted accelerometers are filtered with a 60-hertz (Hz) digital filter, and acceleration-versus-time curves for the longitudinal, lateral, and vertical directions are plotted using TRAP.

TRAP uses the data from the yaw, pitch, and roll rate transducers to compute angular displacement in degrees at 0.0001-s intervals and then plots: yaw, pitch, and roll versus time. These displacements refer to the vehicle-fixed coordinate system with the initial position and orientation of the vehicle-fixed coordinate system being initial impact.

ANTHROPOMORPHIC DUMMY INSTRUMENTATION

A 50th-percentile male anthropomorphic dummy, restrained with lap and shoulder belts, was placed in the driver’s position of the pickup trucks. The dummy was not instrumented.

PHOTOGRAPHIC INSTRUMENTATION AND DATA PROCESSING

Photographic coverage of the test included three high-speed cameras: one overhead with a field of view perpendicular to the ground and directly over the impact point; one placed behind the installation at an angle; and a third placed to have a field of view parallel to and aligned with the installation at the downstream end. A flash bulb activated by pressure-sensitive tape switches was positioned on the impacting vehicle to indicate the instant of contact with the installation and was visible from each camera. The films from these high-speed cameras were analyzed on a computer-linked motion analyzer to observe phenomena occurring during the collision and to obtain event time, displacement, and angular data. A 16-mm movie cine, a BetaCam™, a VHS-format video camera, and still cameras were used to document conditions of the test vehicle and installation before and after the test.

TEST VEHICLE PROPULSION AND GUIDANCE

The test vehicle was towed into the test installation using a steel cable guidance and reverse tow system. A steel cable for guiding the test vehicle is tensioned along the path, anchored at each end, and threaded through an attachment to the front wheel of the test vehicle. An additional steel cable is connected to the test vehicle, passed around a pulley near the impact point, through a pulley on the tow vehicle, and then anchored to the ground so the tow vehicle moves away from the test site. A two-to-one speed ratio between the test and tow vehicle exists with this system. Just before impact with the installation, the test vehicle was released to be freewheeling and unrestrained. The vehicle remains freewheeling, i.e., no steering or braking inputs, until the vehicle clears the immediate area of the test site, at which time brakes on the vehicle are activated, bringing it to a safe and controlled stop.

APPENDIX B. TEST VEHICLE PROPERTIES AND INFORMATION

DATE: <u>09/01/00</u>	TEST NO.: <u>401201-4</u>	VIN NO.: <u>1GCFC24M2TZ134339</u>
YEAR: <u>1996</u>	MAKE: <u>Chevrolet</u>	MODEL: <u>Cheyenne 2500 Pickup Truck</u>
TIRE INFLATION PRESSURE: _____	ODOMETER: <u>176871</u>	TIRE SIZE: <u>LT 225 75R16</u>

MASS DISTRIBUTION (kg)	LF <u>563</u>	RF <u>575</u>	LR <u>437</u>	RR <u>425</u>
------------------------	---------------	---------------	---------------	---------------

DESCRIBE ANY DAMAGE TO VEHICLE PRIOR TO TEST:

● Denotes accelerometer location.

NOTES: _____

ENGINE TYPE: 8 CYL

ENGINE CID: 5.0L

TRANSMISSION TYPE:

AUTO

MANUAL

OPTIONAL EQUIPMENT:

6 LUGS

DUMMY DATA:

TYPE: 50th percentile male

MASS: 76 kg

SEAT POSITION: Driver

GEOMETRY - (mm)

A <u>1900</u>	E <u>1305</u>	J <u>1030</u>	N <u>1590</u>	R <u>640</u>
B <u>775</u>	F <u>5420</u>	K <u>593</u>	O <u>1625</u>	S <u>850</u>
C <u>3340</u>	G <u>1439.5</u>	L <u>78</u>	P <u>730</u>	T <u>1424</u>
D <u>1760</u>	H _____	M <u>365</u>	Q <u>445</u>	U <u>3340</u>

MASS - (kg)	CURB	TEST INERTIAL	GROSS STATIC
M ₁	<u>1145</u>	<u>1138</u>	<u>1182</u>
M ₂	<u>784</u>	<u>862</u>	<u>895</u>
M _T	<u>1929</u>	<u>2000</u>	<u>2077</u>

Figure 111. Vehicle properties for test 401021-4.

Table 16. Exterior crush measurements for test 401021-4.

VEHICLE CRUSH MEASUREMENT SHEET¹

Complete When Applicable	
End Damage	Side Damage
Undeformed end width _____ Corner shift: A1 _____ A2 _____ End shift at frame (CDC) (check one) < 4 inches _____ ≥ 4 inches _____	Bowing: B1 ____ X1 ____ B2 ____ X2 ____ Bowing constant $\frac{X1 + X2}{2} = \underline{\hspace{2cm}}$

Note: Measure C1 to C6 from driver to passenger side in front or rear impacts—rear to front in side impacts.

Specific Impact Number	Plane* of C-Measurements	Direct Damage		Field L**	C ₁	C ₂	C ₃	C ₄	C ₅	C ₆	±D
		Width ** (CDC)	Max*** Crush								
1	Front bumper	1000	-740	1400	-740	-650	-500	-160	-10	+140	0
2	750 mm above ground	1000	-415	-1640	-90	-170	-250	-350	-N/A	-415	+650

¹Table taken from National Accident Sampling System (NASS).

*Identify the plane at which the C-measurements are taken (e.g., at bumper, above bumper, at sill, above sill, at beltline) or label adjustments (e.g., free space).

Free space value is defined as the distance between the baseline and the original body contour taken at the individual C locations. This may include the following: bumper lead, bumper taper, side protrusion, side taper, etc. Record the value for each C-measurement and maximum crush.

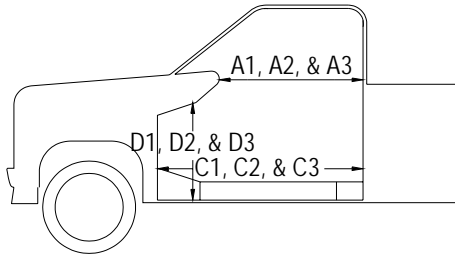
**Measure and document on the vehicle diagram the beginning or end of the direct damage width and field L (e.g., side damage with respect to undamaged axle).

***Measure and document on the vehicle diagram the location of the maximum crush.

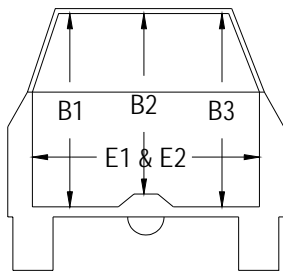
Note: Use as many lines/columns as necessary to describe each damage profile.

Truck

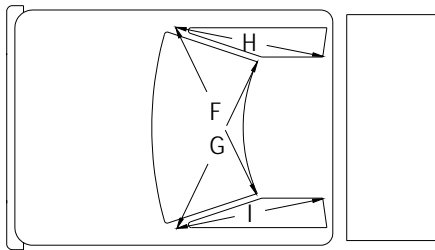
Occupant Compartment Deformation



a) Side view of truck.



b) Front or rear view of truck.



c) Top view of truck.

	BEFORE (mm)	AFTER (mm)
A1	906	780
A2	915	862
A3	934	938
B1	1080	1230
B2	1105	950
B3	1085	1049
C1	1375	1240
C2	1260	1240
C3	1371	1370
D1	320	376
D2	161	148
D3	312	319
E1	1585	1640
E2	1592	1710
F	1460	1545
G	1460	1385
H	1000	1010
I	1000	870
J*	1525	1350

* J = Lateral measurement across cab floor
kickpanel to kickpanel.

Figure 112. Occupant compartment measurements for test 401021-4.

DATE: 03/07/02 TEST NO.: 401021-6 VIN NO.: 1GCFC24M6VZ249657
YEAR: 1997 MAKE: Chevrolet MODEL: 2500 Pickup
TIRE INFLATION PRESSURE: _____ ODOMETER: 169404 TIRE SIZE: 225 75R16

MASS DISTRIBUTION (kg) LF 572 RF 561 LR 428 RR 439

DESCRIBE ANY DAMAGE TO VEHICLE PRIOR TO TEST:

● Denotes accelerometer location.
NOTES: _____

ENGINE TYPE: 8 CYL
ENGINE CID: 5.0 L
TRANSMISSION TYPE:
 AUTO
 MANUAL
OPTIONAL EQUIPMENT:
6 LUGS

DUMMY DATA:
TYPE: 50th percentile male
MASS: 76 kg
SEAT POSITION: passenger

GEOMETRY - (mm)

A	<u>1880</u>	E	<u>1310</u>	J	<u>1038</u>	N	<u>1590</u>	R	<u>665</u>
B	<u>810</u>	F	<u>5470</u>	K	<u>595</u>	O	<u>1610</u>	S	<u>870</u>
C	<u>3350</u>	G	<u>1452.2</u>	L	<u>70</u>	P	<u>725</u>	T	<u>1460</u>
D	<u>1770</u>	H	_____	M	<u>378</u>	Q	<u>440</u>	U	<u>3420</u>

MASS - (kg)	CURB	TEST INERTIAL	GROSS STATIC
M ₁	<u>1153</u>	<u>1133</u>	<u>1178</u>
M ₂	<u>829</u>	<u>867</u>	<u>898</u>
M _T	<u>1982</u>	<u>2000</u>	<u>2076</u>

Figure 113. Vehicle properties for test 401021-6.

Table 17. Exterior crush measurements for test 401021-6.

VEHICLE CRUSH MEASUREMENT SHEET¹

Complete When Applicable	
End Damage	Side Damage
Undeformed end width _____ Corner shift: A1 _____ A2 _____ End shift at frame (CDC) (check one) < 4 inches _____ ≥ 4 inches _____	Bowing: B1 ____ X1 ____ B2 ____ X2 ____ Bowing constant $\frac{X1 + X2}{2} = \underline{\hspace{2cm}}$

Note: Measure C1 to C6 from driver to passenger side in front or rear impacts–rear to front in side impacts.

Specific Impact Number	Plane* of C-Measurements	Direct Damage		Field L**	C ₁	C ₂	C ₃	C ₄	C ₅	C ₆	±D
		Width ** (CDC)	Max*** Crush								
1	Front bumper	900	680	1350	+120	+30	-20	-150	-370	-680	0
2	720mm above ground	900	470	1400	0	40	150	200	Wheel Well	470	+1200

¹Table taken from NASS.

*Identify the plane at which the C-measurements are taken (e.g., at bumper, above bumper, at sill, above sill, at beltline) or label adjustments (e.g., free space).

Free space value is defined as the distance between the baseline and the original body contour taken at the individual C locations. This may include the following: bumper lead, bumper taper, side protrusion, side taper, etc. Record the value for each C-measurement and maximum crush.

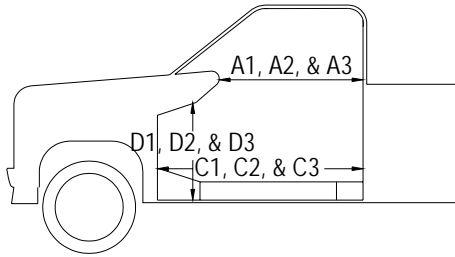
**Measure and document on the vehicle diagram the beginning or end of the direct damage width and field L (e.g., side damage with respect to undamaged axle).

***Measure and document on the vehicle diagram the location of the maximum crush.

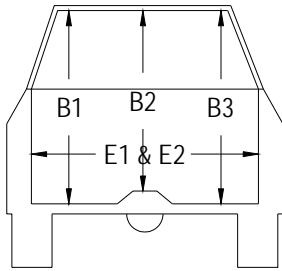
Note: Use as many lines/columns as necessary to describe each damage profile.

Truck

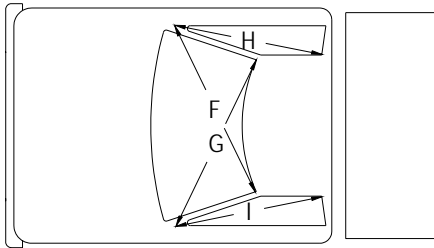
Occupant Compartment Deformation



a) Side view of truck.



b) Front or rear view of truck.



c) Top view of truck.

	BEFORE (mm)	AFTER (mm)
A1	872	883
A2	940	847
A3	935	896
B1	1092	1076
B2	983	963
B3	1077	1100
C1	1372	1372
C2	1368	1360
C3	1374	1360
D1	315	310
D2	158	126
D3	318	350
E1	1591	1615
E2	1595	1620
F	1464	1464
G	1464	1460
H	1100	1100
I	1100	1100
J	1522	1470

* J = Lateral measurement across cab floor kickpanel to kickpanel.

Figure 114. Occupant compartment measurements for test 401021-6.

DATE: 10/30/00 TEST NO.: 401021-1 VIN NO.: 1GCGC24K8SZ276188
 YEAR: 1995 MAKE: Chevrolet MODEL: 2500 Pickup Truck
 TIRE INFLATION PRESSURE: _____ ODOMETER: 210211 TIRE SIZE: LT 225 75R16

MASS DISTRIBUTION (kg) LF 573 RF 529 LR 453 RR 445

DESCRIBE ANY DAMAGE TO VEHICLE PRIOR TO TEST:

● Denotes accelerometer location.
 NOTES: _____

ENGINE TYPE: 8 CYL
 ENGINE CID: 5.7L
 TRANSMISSION TYPE:
 AUTO
 MANUAL

OPTIONAL EQUIPMENT:
6 LUGS

DUMMY DATA:
 TYPE: 50th percentile male
 MASS: 75 kg
 SEAT POSITION: Driver

GEOMETRY - (mm)

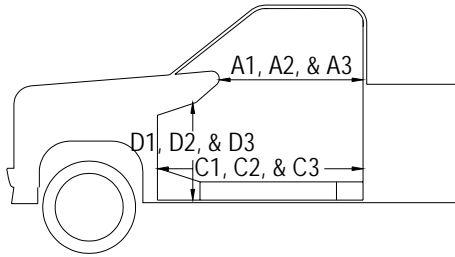
A	<u>1900</u>	E	<u>1305</u>	J	<u>1030</u>	N	<u>1590</u>	R	<u>640</u>
B	<u>775</u>	F	<u>542</u>	K	<u>595</u>	O	<u>1625</u>	S	<u>850</u>
C	<u>3350</u>	G	<u>1504.1</u>	L	<u>75</u>	P	<u>730</u>	T	<u>1450</u>
D	<u>1760</u>	H	_____	M	<u>445</u>	Q	<u>445</u>	U	<u>3350</u>

MASS - (kg)	CURB	TEST INERTIAL	GROSS STATIC
M ₁	<u>1110</u>	<u>1102</u>	<u>1152</u>
M ₂	<u>787</u>	<u>898</u>	<u>923</u>
M _T	<u>1897</u>	<u>2000</u>	<u>2075</u>

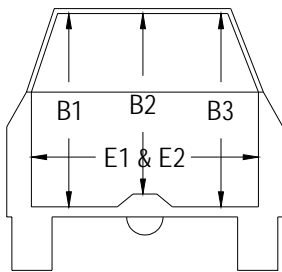
Figure 115. Vehicle properties for test 401021-1.

Truck

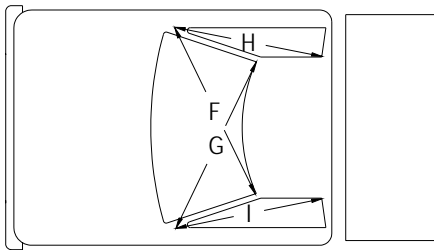
Occupant Compartment Deformation



a) Side view of truck.



b) Front or rear view of truck.



c) Top view of truck.

	BEFORE (mm)	AFTER (mm)
A1	867	850
A2	898	880
A3	912	910
B1	1076	1178
B2	1100	960
B3	1074	1071
C1	1377	1308
C2	1263	1220
C3	1373	1375
D1	322	420
D2	156	130
D3	310	335
E1	1580	1627
E2	1588	1670
F	1465	1460
G	1465	1455
H	900	900
I	900	900
J	1524	1395

* J = Lateral measurement across cab floor
kickpanel to kickpanel.

Figure 116. Occupant compartment measurements for test 401021-1.

DATE: 07-03-01 TEST NO.: 401021-5 VIN NO.: 1GCFC24MSTZ136604
 YEAR: 1996 MAKE: Chevrolet MODEL: 2500 Pickup Truck
 TIRE INFLATION PRESSURE: _____ ODOMETER: 168961 TIRE SIZE: LT 225 75R16

MASS DISTRIBUTION (kg) LF 577 RF 568 LR 433 RR 422

DESCRIBE ANY DAMAGE TO VEHICLE PRIOR TO TEST:

● Denotes accelerometer location.
 NOTES: _____

ENGINE TYPE: 8 CYL
 ENGINE CID: 5.7L
 TRANSMISSION TYPE:
 _____ AUTO
 _____ MANUAL

OPTIONAL EQUIPMENT:
6 LUGS

DUMMY DATA:
 TYPE: 50th percentile male
 MASS: 76 kg
 SEAT POSITION: Driver

GEOMETRY - (mm)

A	<u>1870</u>	E	<u>1320</u>	J	<u>1050</u>	N	<u>1600</u>	R	<u>670</u>
B	<u>850</u>	F	<u>5520</u>	K	<u>620</u>	O	<u>1615</u>	S	<u>850</u>
C	<u>3350</u>	G	<u>1432.1</u>	L	<u>65</u>	P	<u>760</u>	T	<u>1470</u>
D	<u>1790</u>	H	_____	M	<u>410</u>	Q	<u>440</u>	U	<u>3400</u>

MASS - (kg)	CURB	TEST INERTIAL	GROSS STATIC
M ₁	<u>1129</u>	<u>1145</u>	<u>1191</u>
M ₂	<u>768</u>	<u>855</u>	<u>885</u>
M _T	<u>1897</u>	<u>2000</u>	<u>2076</u>

Figure 117. Vehicle properties for test 401021-5.

Table 19. Exterior crush measurements for test 401021-5.

VEHICLE CRUSH MEASUREMENT SHEET¹

Complete When Applicable	
End Damage	Side Damage
Undeformed end width _____ Corner shift: A1 _____ A2 _____ End shift at frame (CDC) (check one) < 4 inches _____ ≥ 4 inches _____	Bowing: B1 ____ X1 ____ B2 ____ X2 ____ Bowing constant $\frac{X1 + X2}{2} = \underline{\hspace{2cm}}$

Note: Measure C1 to C6 from driver to passenger side in front or rear impacts–rear to front in side impacts.

Specific Impact Number	Plane* of C-Measurements	Direct Damage		Field L**	C ₁	C ₂	C ₃	C ₄	C ₅	C ₆	±D
		Width ** (CDC)	Max*** Crush								
1	Front bumper	800	570	700	570	420	350	230	130	40	-350
2	680 mm above ground	800	440	2000	0	60	100	150	270	440	+880

¹Table taken from NASS.

*Identify the plane at which the C-measurements are taken (e.g., at bumper, above bumper, at sill, above sill, at beltline) or label adjustments (e.g., free space).

Free space value is defined as the distance between the baseline and the original body contour taken at the individual C locations. This may include the following: bumper lead, bumper taper, side protrusion, side taper, etc. Record the value for each C-measurement and maximum crush.

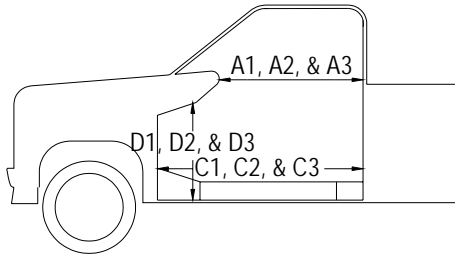
**Measure and document on the vehicle diagram the beginning or end of the direct damage width and field L (e.g., side damage with respect to undamaged axle).

***Measure and document on the vehicle diagram the location of the maximum crush.

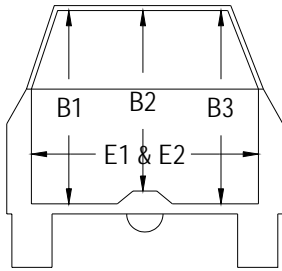
Note: Use as many lines/columns as necessary to describe each damage profile.

Truck

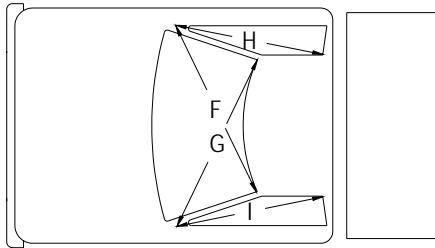
Occupant Compartment Deformation



a) Side view of truck.



b) Front or rear view of truck.



c) Top view of truck.

	BEFORE (mm)	AFTER (mm)
A1	868	820
A2	877	860
A3	918	914
B1	1072	1185
B2	1095	977
B3	1070	1074
C1	1370	1270
C2	1260	1238
C3	1373	1373
D1	323	426
D2	158	95
D3	315	325
E1	1587	1645
E2	1590	1720
F	1465	1460
G	1465	1439
H	900	900
I	900	890
J	1525	1405

* J = Lateral measurement across cab floor kickpanel to kickpanel.

Figure 118. Occupant compartment measurements for test 401021-5.

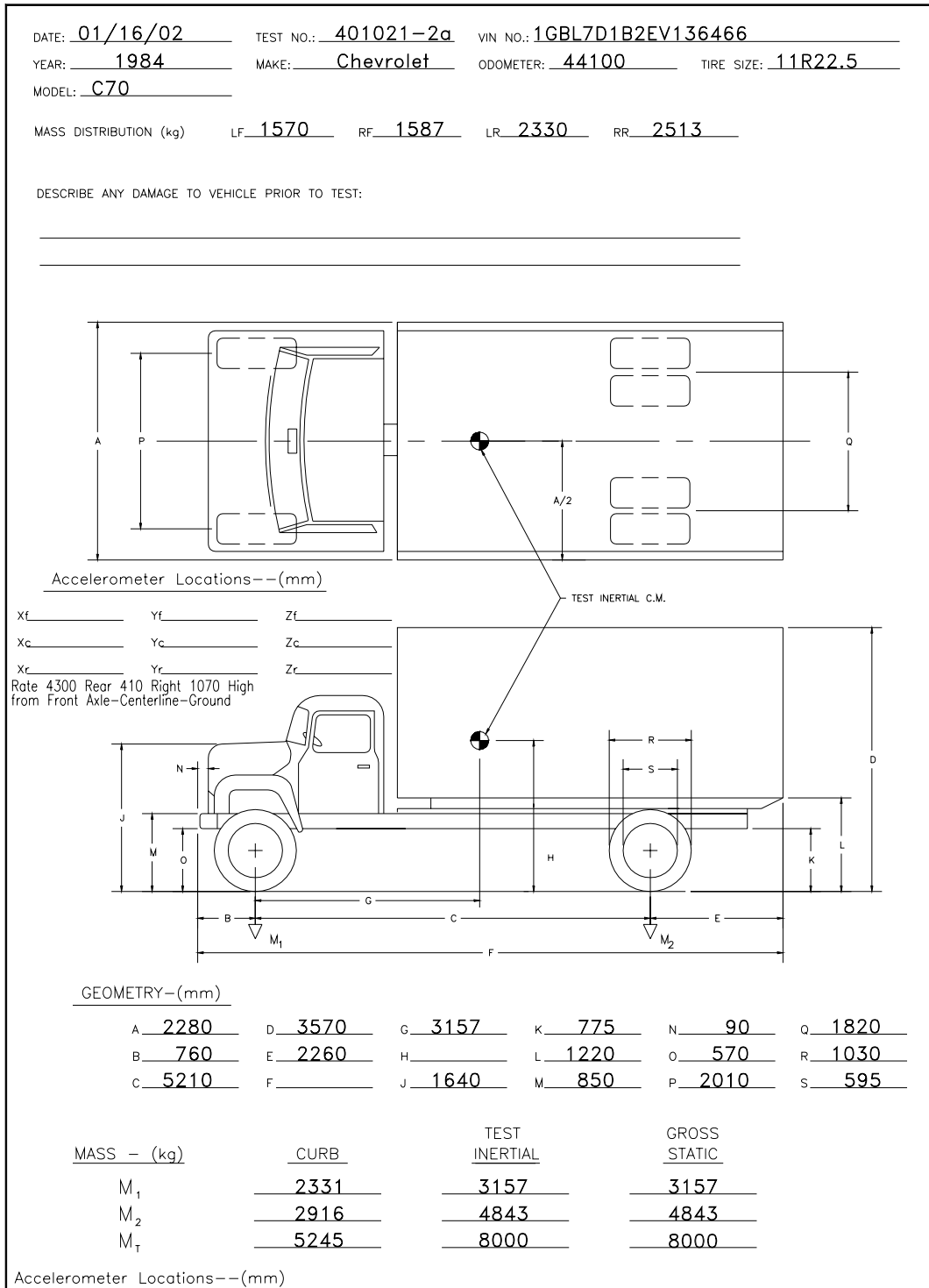


Figure 119. Vehicle properties for test 401021-2a.

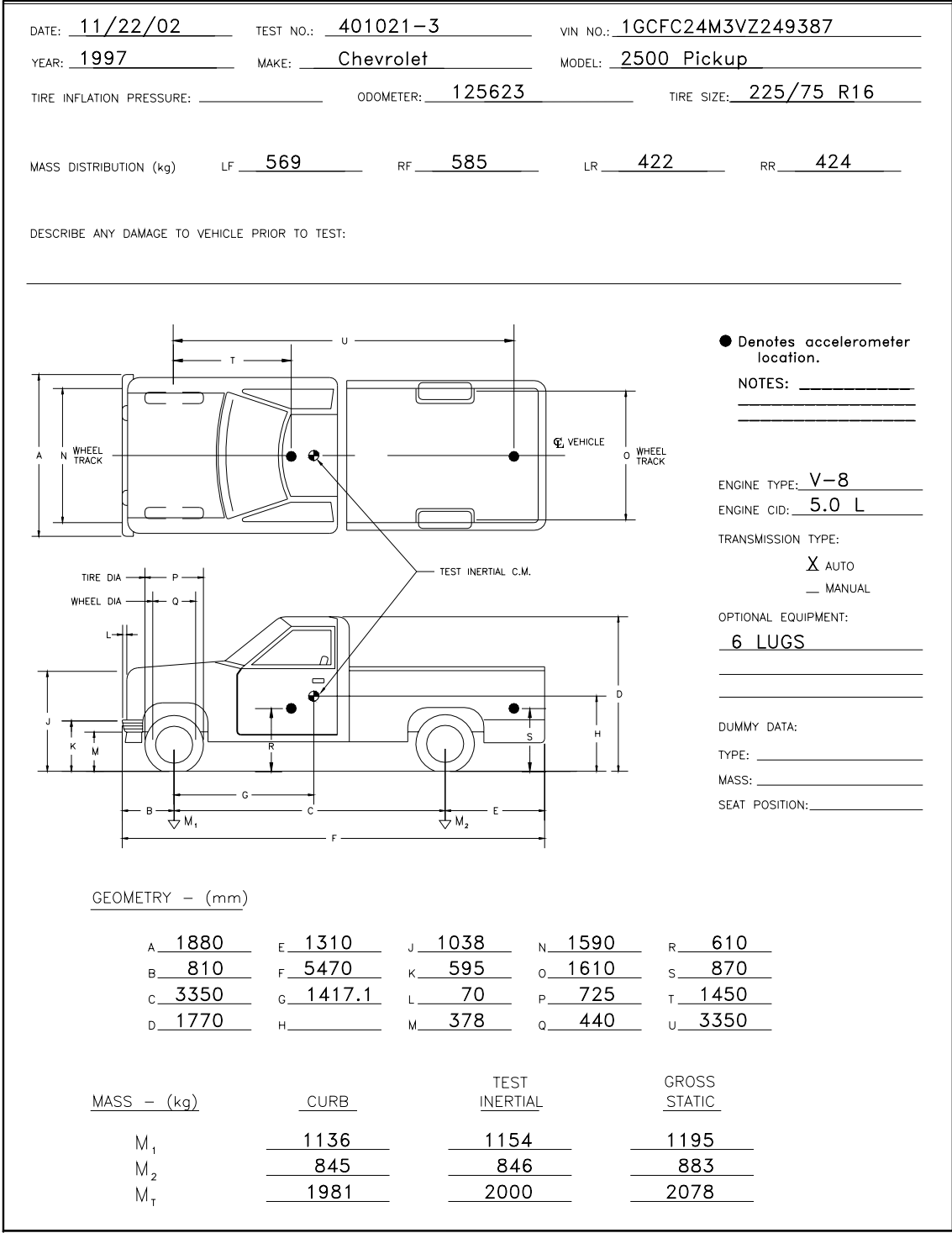
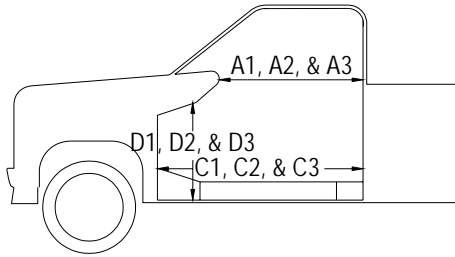


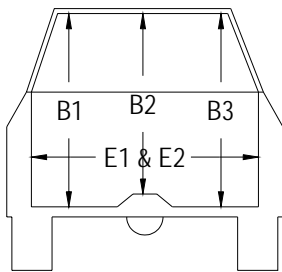
Figure 120. Vehicle properties for test 401021-3.

Truck

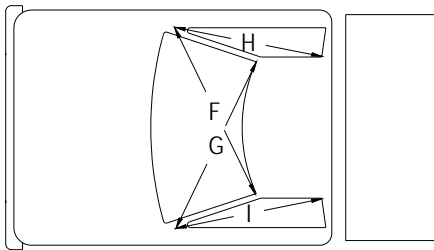
Occupant Compartment Deformation



a) Side view of truck.



b) Front or rear view of truck.



c) Top view of truck.

	BEFORE (mm)	AFTER (mm)
A1	869	843
A2	938	940
A3	910	913
B1	1075	1137
B2	951	900
B3	1085	1085
C1	1373	1360
C2	----	----
C3	1373	1373
D1	315	365
D2	156	125
D3	315	325
E1	1595	1625
E2	1590	1635
F	1480	1465
G	1480	1460
H	1240	1230
I	1254	1250
J	1522	1448

* J = Lateral measurement across cab floor kickpanel to kickpanel.

Figure 121. Occupant compartment measurements for test 401021-3.

DATE: 03/15/04 TEST NO.: 401021-7 VIN NO.: 1GCFC24K0R246990
 YEAR: 1994 MAKE: Chevrolet MODEL: Cheyenne 1500
 TIRE INFLATION PRESSURE: _____ ODOMETER: 138166 TIRE SIZE: LT 225/75 R16

MASS DISTRIBUTION (kg) LF 563 RF 551 LR 453 RR 436

DESCRIBE ANY DAMAGE TO VEHICLE PRIOR TO TEST:

● Denotes accelerometer location.
 NOTES: _____

ENGINE TYPE: V-8
 ENGINE CID: 5.7 L
 TRANSMISSION TYPE:
 AUTO
 MANUAL

OPTIONAL EQUIPMENT:
6 LUG

DUMMY DATA:
 TYPE: 50th percentile male
 MASS: 74 kg
 SEAT POSITION: driver

GEOMETRY - (mm)

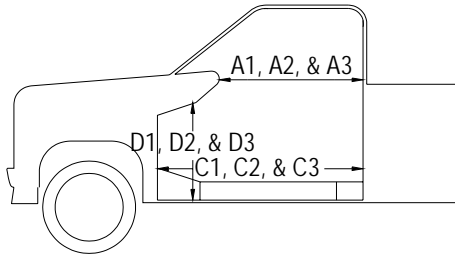
A	<u>1880</u>	E	<u>1310</u>	J	<u>1038</u>	N	<u>1590</u>	R	<u>610</u>
B	<u>810</u>	F	<u>5470</u>	K	<u>595</u>	O	<u>1610</u>	S	<u>860</u>
C	<u>3350</u>	G	<u>1486.8</u>	L	<u>70</u>	P	<u>725</u>	T	<u>1480</u>
D	<u>1770</u>	H	_____	M	<u>378</u>	Q	<u>440</u>	U	<u>3390</u>

MASS - (kg)	CURB	TEST INERTIAL	GROSS STATIC
M ₁	<u>1127</u>	<u>1115</u>	<u>1156</u>
M ₂	<u>828</u>	<u>889</u>	<u>921</u>
M _T	<u>1955</u>	<u>2003</u>	<u>2077</u>

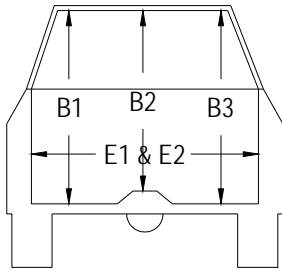
Figure 122. Vehicle properties for test 401021-7.

Truck

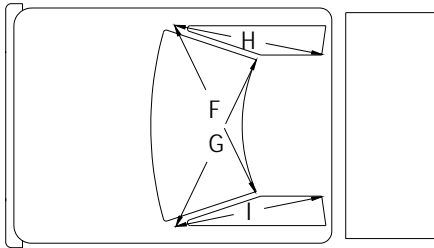
Occupant Compartment Deformation



a) Side view of truck.



b) Front or rear view of truck.



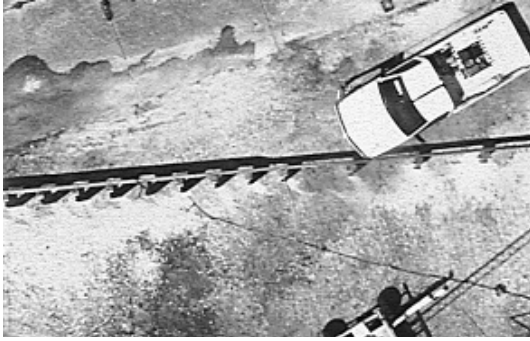
c) Top view of truck.

	BEFORE (mm)	AFTER (mm)
A1	892	875
A2	1085	1091
A3	1034	1042
B1	1075	1100
B2	950	971 - 897
B3	1067	1067
C1	1384	1360
C2	1250	1250
C3	1383	1383
D1	322	330
D2	80	70
D3	305	315
E1	1625	1631
E2	1620	1678
F	1453	1445
G	1453	1444
H	1250	1230
I	1250	1245
J	1505	1445

* J = Lateral measurement across cab floor kickpanel to kickpanel.

Figure 123. Occupant compartment measurements for test 401021-7.

APPENDIX C. SEQUENTIAL PHOTOGRAPHS



a) Overhead at 0.000 s.



e) Overhead at 0.287 s.



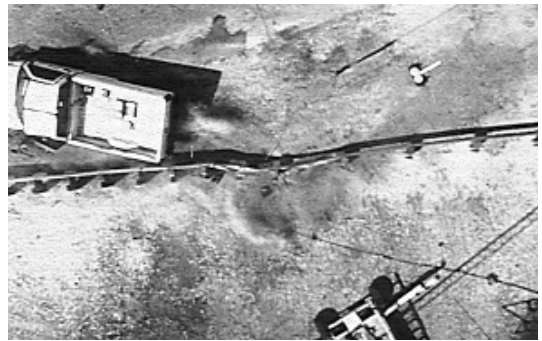
b) Overhead at 0.041 s.



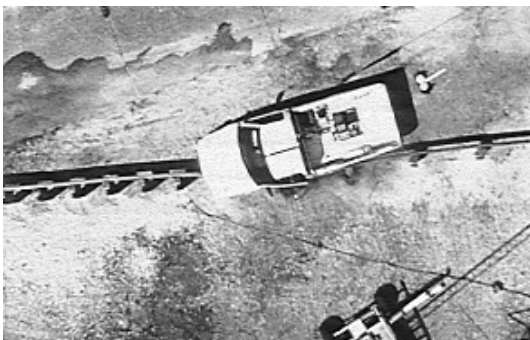
f) Overhead at 0.410 s.



c) Overhead at 0.103 s.



g) Overhead at 0.575 s.



d) Overhead at 0.164 s.



h) Overhead at 0.821 s.

Figure 124. Sequential photographs for test 401021-4 (overhead view).



a) Frontal at 0.000 s.



b) Frontal at 0.041 s.



c) Frontal at 0.103 s.



d) Frontal at 0.164 s.



e) Frontal at 0.287 s.



f) Frontal at 0.410 s.

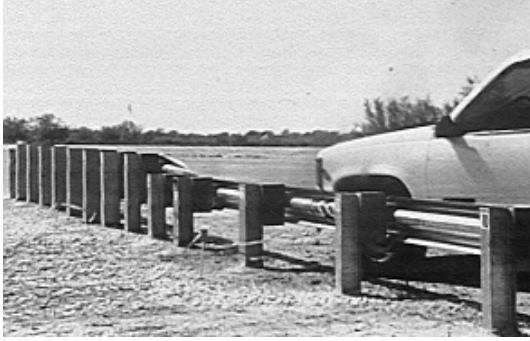


g) Frontal at 0.575 s.



h) Frontal at 0.821 s.

Figure 125. Sequential photographs for test 401021-4 (frontal view).



a) Rear at 0.000 s.



e) Rear at 0.287 s.



b) Rear at 0.041 s.



f) Rear at 0.410 s.



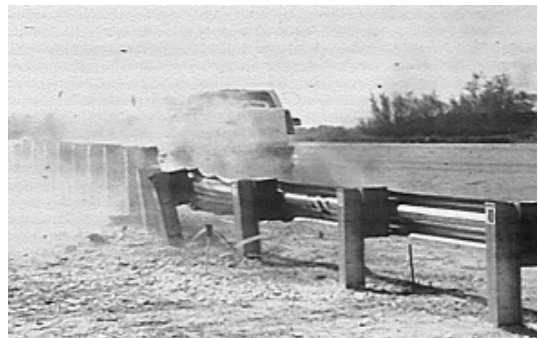
c) Rear at 0.103 s.



g) Rear at 0.575 s.



d) Rear at 0.164 s.



h) Rear at 0.821 s.

Figure 126. Sequential photographs for test 401021-4 (rear view).



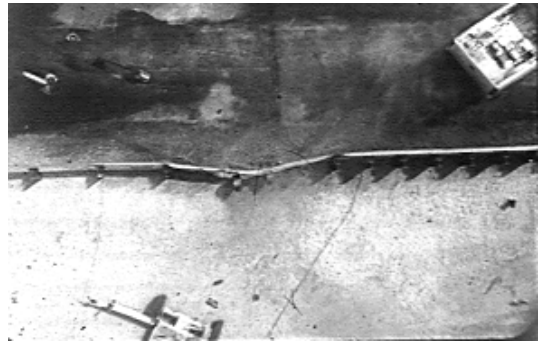
a) Overhead at 0.000 s.



e) Overhead at 0.473 s.



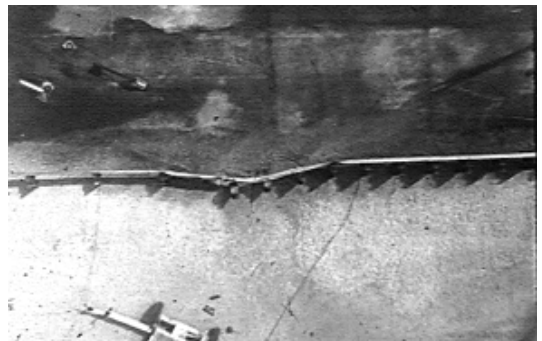
b) Overhead at 0.047 s.



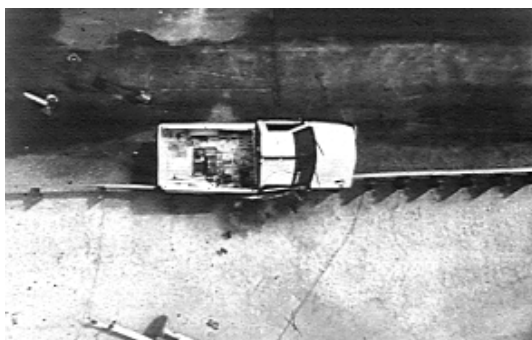
f) Overhead at 0.946 s.



c) Overhead at 0.118 s.



g) Overhead at 1.892 s.



d) Overhead at 0.237 s.



h) Overhead at 4.145 s.

Figure 127. Sequential photographs for test 401021-6 (overhead view).



a) Frontal at 0.000 s.



e) Frontal at 0.473 s.



b) Frontal at 0.047 s.



f) Frontal at 0.946 s.



c) Frontal at 0.118 s.



g) Frontal at 1.892 s.



d) Frontal at 0.237 s.

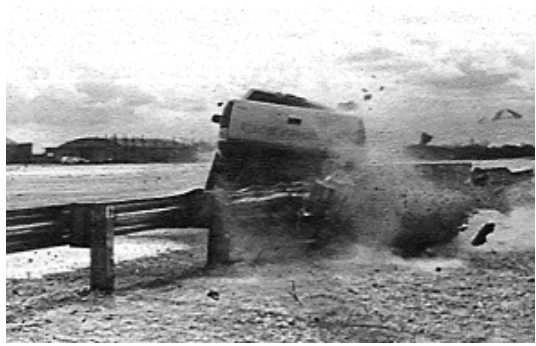


h) Frontal at 4.145 s.

Figure 128. Sequential photographs for test 401021-6 (frontal view).



a) Rear at 0.000 s.



e) Rear at 0.473 s.



b) Rear at 0.047 s.



f) Rear at 0.946 s.



c) Rear at 0.118 s.



g) Rear at 1.892 s.

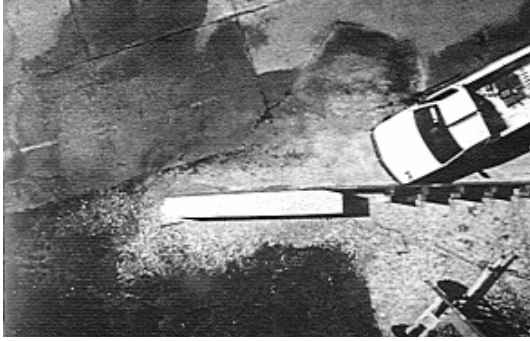


d) Rear at 0.237 s.



h) Rear at 4.145 s.

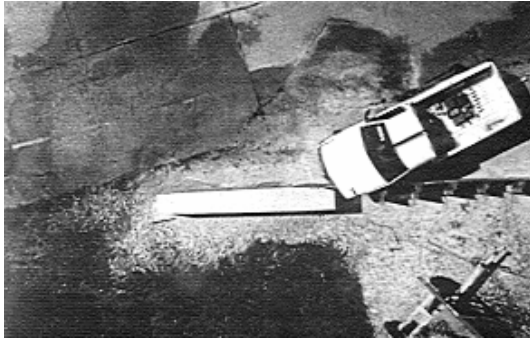
Figure 129. Sequential photographs for test 401021-6 (rear view).



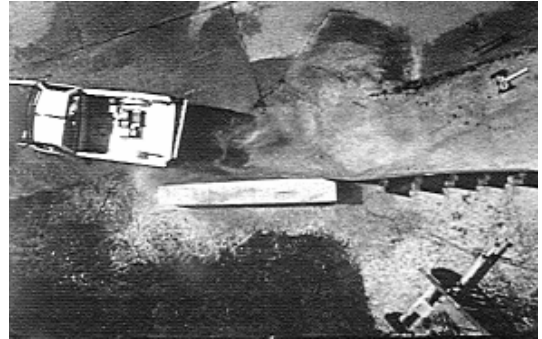
a) Overhead at 0.000 s.



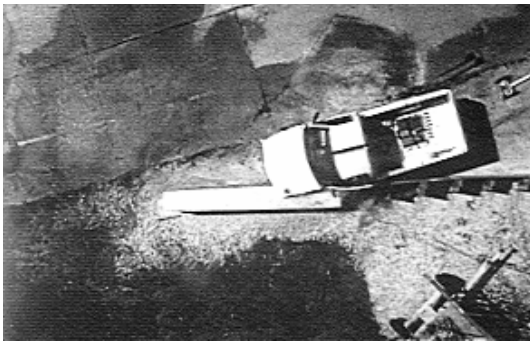
e) Overhead at 0.344 s.



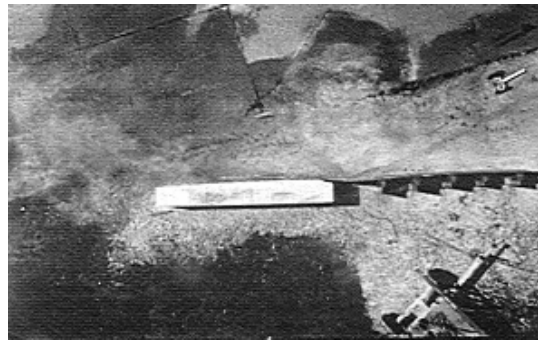
b) Overhead at 0.049 s.



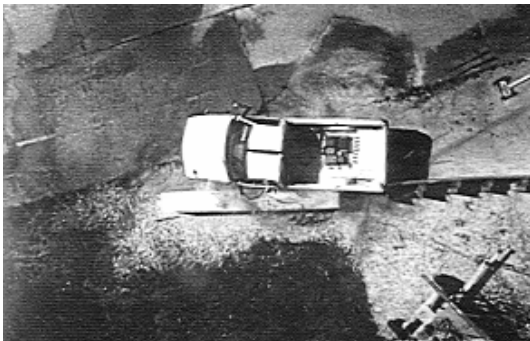
f) Overhead at 0.492 s.



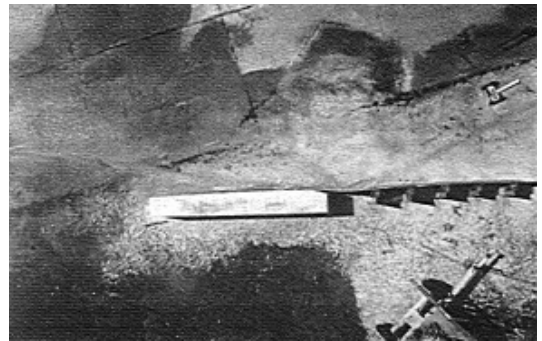
c) Overhead at 0.123 s.



g) Overhead at 0.861 s.



d) Overhead at 0.221 s.



h) Overhead at 1.476 s.

Figure 130. Sequential photographs for test 401021-1 (overhead view).



a) Frontal at 0.000 s.



e) Frontal at 0.344 s.



b) Frontal at 0.049 s.



f) Frontal at 0.492 s.



c) Frontal at 0.123 s.



g) Frontal at 0.861 s.



d) Frontal at 0.221 s.



h) Frontal at 1.476 s.

Figure 131. Sequential photographs for test 401021-1 (frontal view).



a) Rear at 0.000 s.



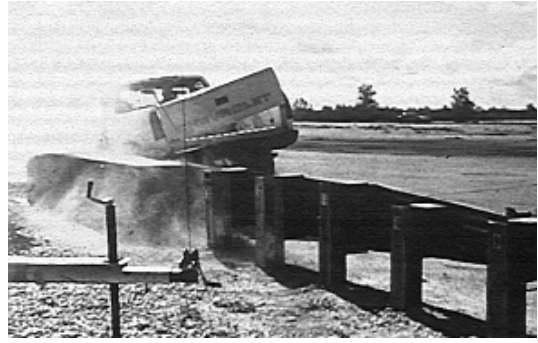
b) Rear at 0.049 s.



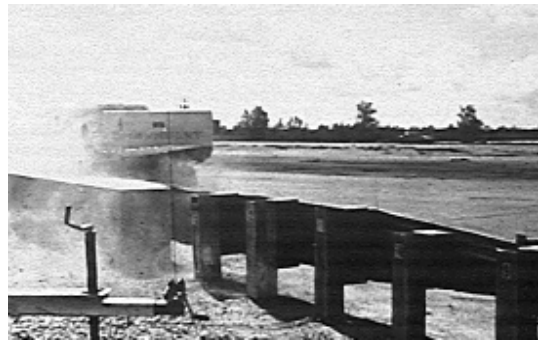
c) Rear at 0.123 s.



d) Rear at 0.221 s.



e) Rear at 0.344 s.



f) Rear at 0.492 s.



g) Rear at 0.861 s.



h) Rear at 1.476 s.

Figure 132. Sequential photographs for test 401021-1 (rear view).



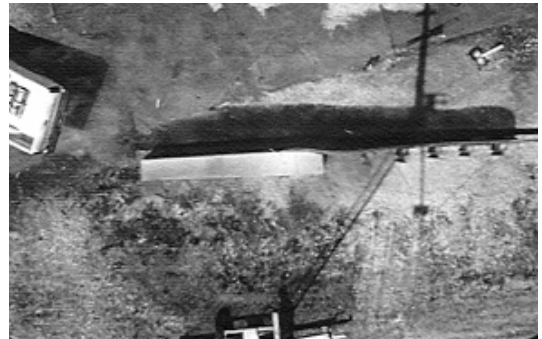
a) Overhead at 0.000 s.



e) Overhead at 0.370 s.



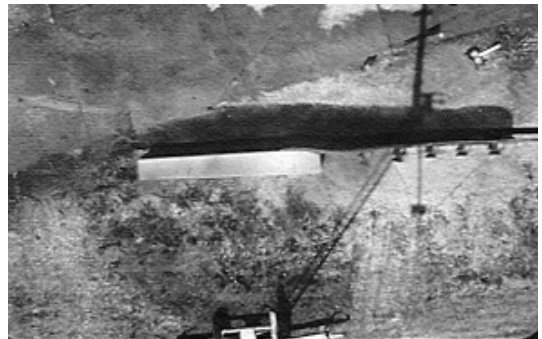
b) Overhead at 0.074 s.



f) Overhead at 0.617 s.



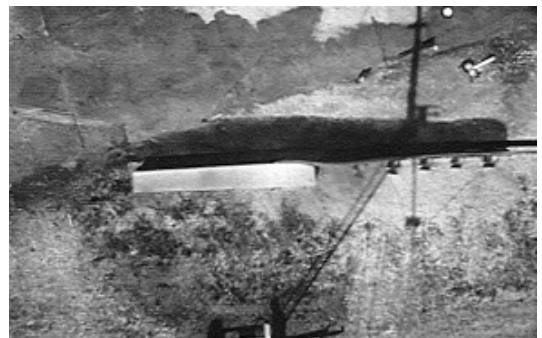
c) Overhead at 0.148 s.



g) Overhead at 0.987 s.



d) Overhead at 0.247 s.



h) Overhead at 1.727 s.

Figure 133. Sequential photographs for test 401021-5 (overhead view).



a) Frontal at 0.000 s.



e) Frontal at 0.370 s.



b) Frontal at 0.074 s.



f) Frontal at 0.617 s.



c) Frontal at 0.148 s.



g) Frontal at 0.987 s.



d) Frontal at 0.247 s.



h) Frontal at 1.727 s.

Figure 134. Sequential photographs for test 401021-5 (frontal view).



a) Rear at 0.000 s.



e) Rear at 0.370 s.



b) Rear at 0.074 s.



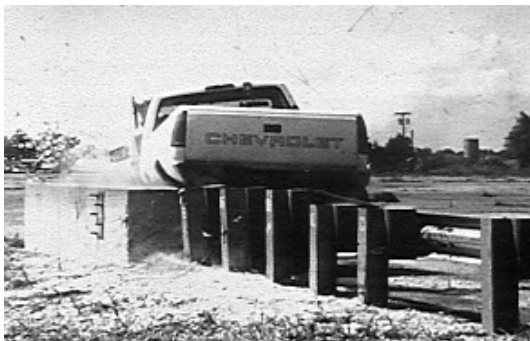
f) Rear at 0.617 s.



c) Rear at 0.148 s.



g) Rear at 0.987 s.



d) Rear at 0.247 s.



h) Rear at 1.727 s.

Figure 135. Sequential photographs for test 401021-5 (rear view).



a) Overhead at 0.000 s.



e) Overhead at 0.726 s.



b) Overhead at 0.121 s.



f) Overhead at 1.209 s.



c) Overhead at 0.242 s.



g) Overhead at 1.935 s.



d) Overhead at 0.435 s.



h) Overhead at 2.902 s.

Figure 136. Sequential photographs for test 401021-2a (overhead view).



a) Frontal at 0.000 s.



e) Frontal at 0.726 s.



b) Frontal at 0.121 s.



f) Frontal at 1.209 s.



c) Frontal at 0.242 s.



g) Frontal at 1.935 s.



d) Frontal at 0.435 s.



h) Frontal at 2.902 s.

Figure 137. Sequential photographs for test 401021-2a (frontal view).



a) Rear at 0.000 s.



e) Rear at 0.726 s.



b) Rear at 0.121 s.



f) Rear at 1.209 s.



c) Rear at 0.242 s.



g) Rear at 1.935 s.

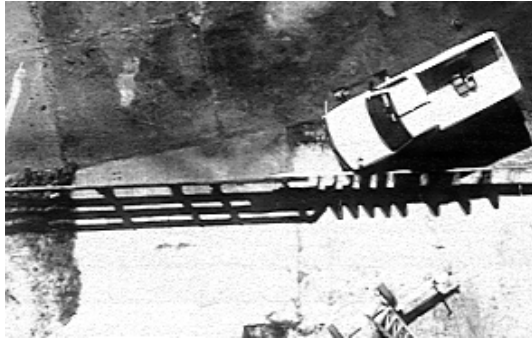


d) Rear at 0.435 s.

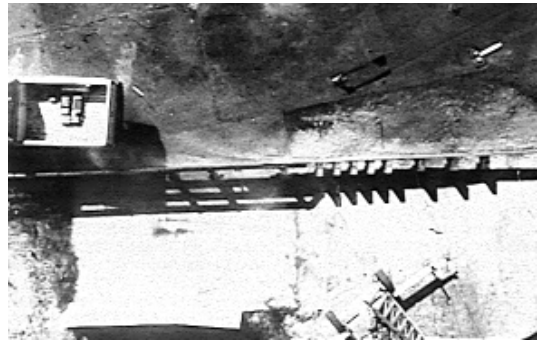


h) Rear at 2.902 s.

Figure 138. Sequential photographs for test 401021-2a (rear view).



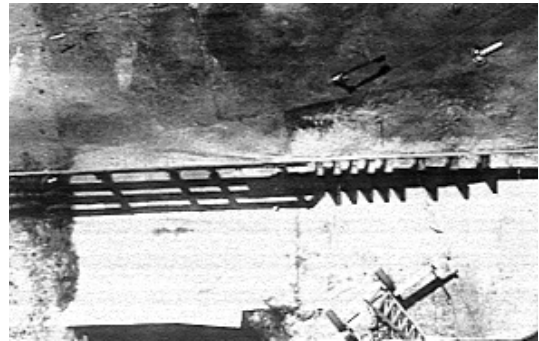
a) Overhead at 0.000 s.



e) Overhead at 0.486 s.



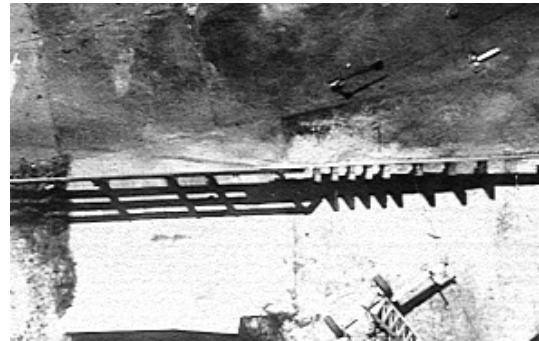
b) Overhead at 0.049 s.



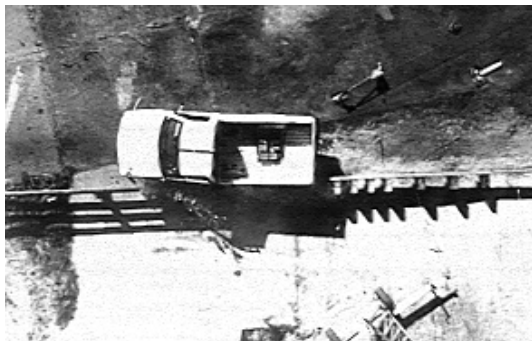
f) Overhead at 0.729 s.



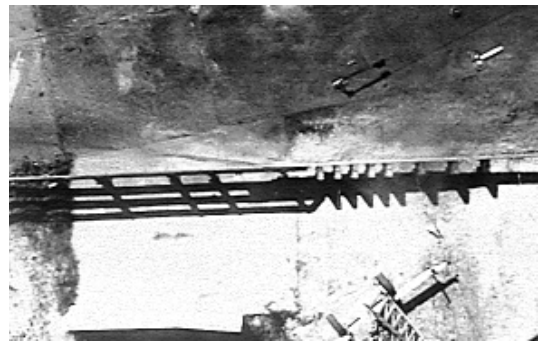
c) Overhead at 0.122 s.



g) Overhead at 1.215 s.



d) Overhead at 0.243 s.



h) Overhead at 1.945 s.

Figure 139. Sequential photographs for test 401021-3 (overhead view).



a) Frontal at 0.000 s.



e) Frontal at 0.486 s.



b) Frontal at 0.049 s.



f) Frontal at 0.729 s.



c) Frontal at 0.122 s.



g) Frontal at 1.215 s.



d) Frontal at 0.243 s.

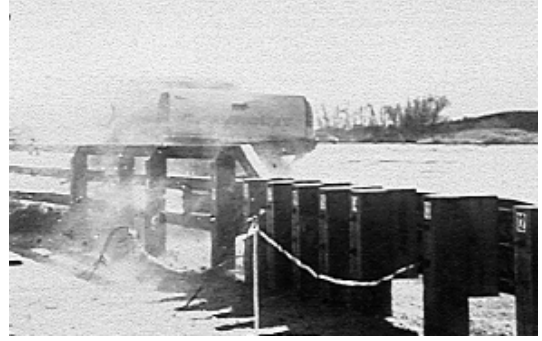


h) Frontal at 1.945 s.

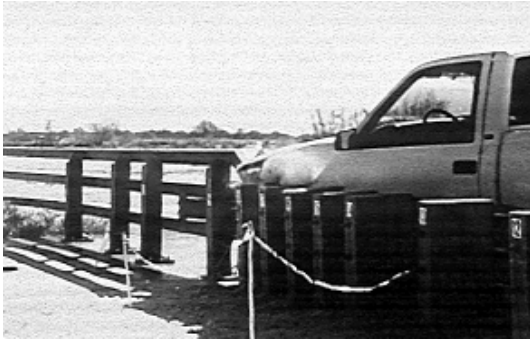
Figure 140. Sequential photographs for test 401021-3 (frontal view).



a) Rear at 0.000 s.



e) Rear at 0.486 s.



b) Rear at 0.049 s.



f) Rear at 0.729 s.



c) Rear at 0.122 s.



g) Rear at 1.215 s.

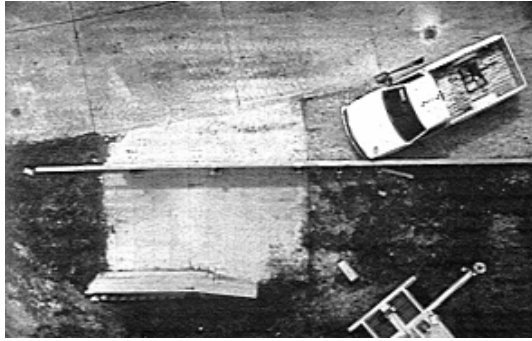


d) Rear at 0.243 s.

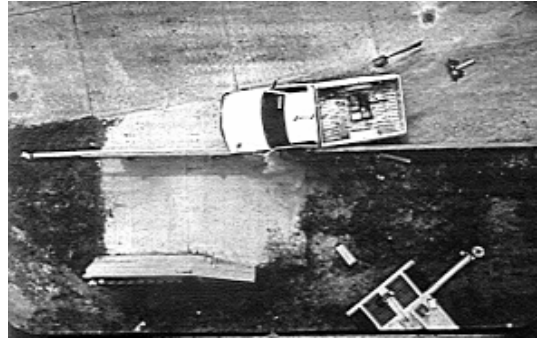


h) Rear at 1.945 s.

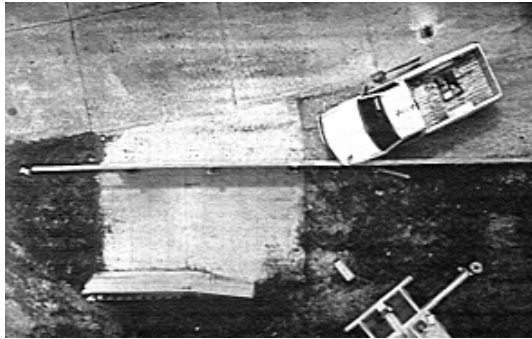
Figure 141. Sequential photographs for test 401021-3 (rear view).



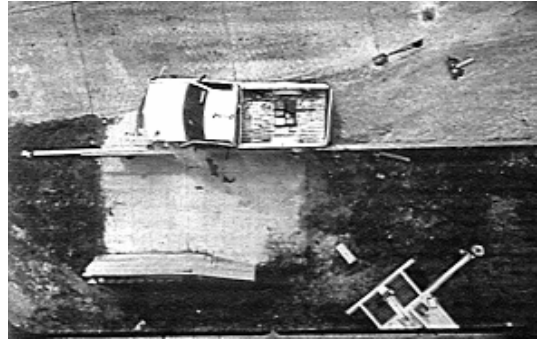
a) Overhead at 0.000 s.



e) Overhead at 0.150 s.



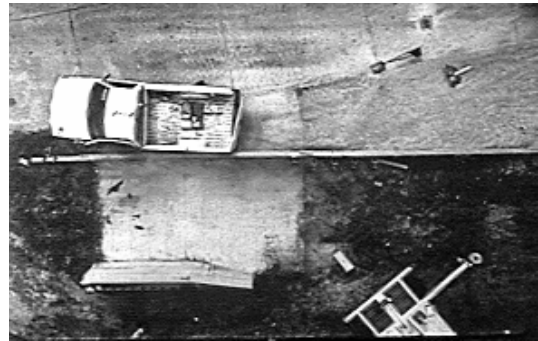
b) Overhead at 0.025 s.



f) Overhead at 0.251 s.



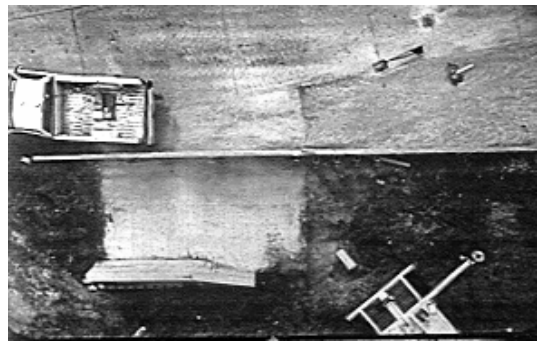
c) Overhead at 0.050 s.



g) Overhead at 0.376 s.



d) Overhead at 0.100 s.



h) Overhead at 0.501 s.

Figure 142. Sequential photographs for test 401021-7 (overhead view).



a) Frontal at 0.000 s.



e) Frontal at 0.150 s.



b) Frontal at 0.025 s.



f) Frontal at 0.251 s.



c) Frontal at 0.050 s.



g) Frontal at 0.376 s.

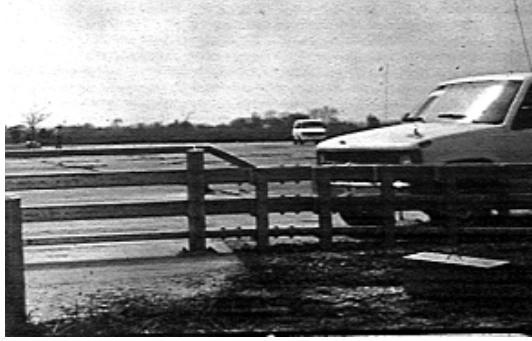


d) Frontal at 0.100 s.



h) Frontal at 0.501 s.

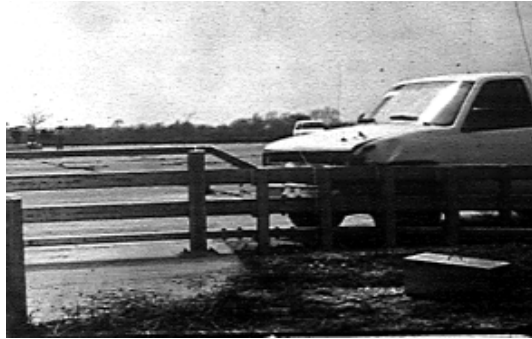
Figure 143. Sequential photographs for test 401021-7 (frontal view).



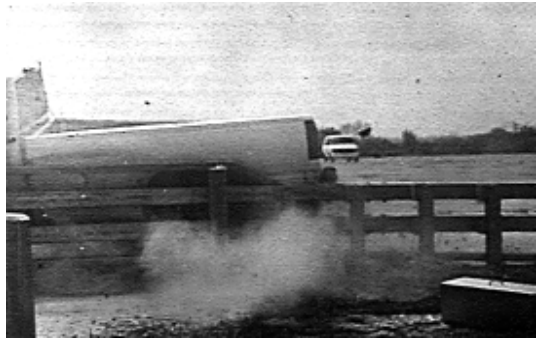
a) Rear at 0.000 s.



e) Rear at 0.150 s.



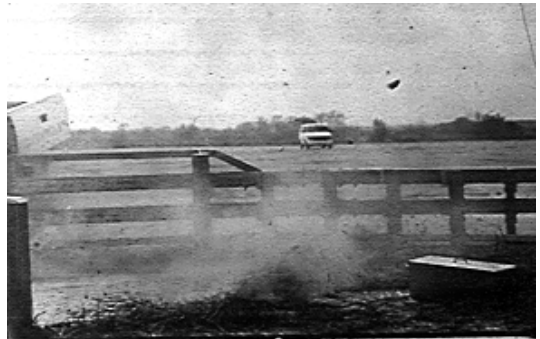
b) Rear at 0.025 s.



f) Rear at 0.251 s.



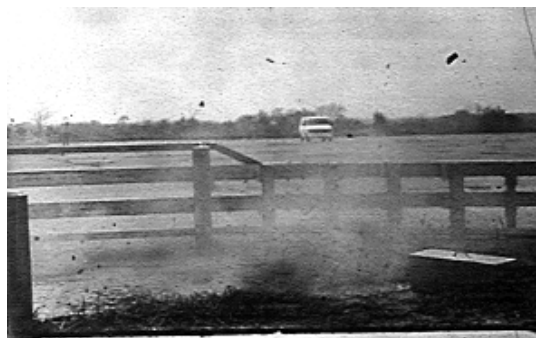
c) Rear at 0.050 s.



g) Rear at 0.376 s.



d) Rear at 0.100 s.



h) Rear at 0.501 s.

Figure 144. Sequential photographs for test 401021-7 (rear view).

APPENDIX D. VEHICLE ANGULAR DISPLACEMENTS AND ACCELERATIONS

This appendix contains graphs of vehicle angular displacements and vehicle accelerations from each test. These displacements and accelerations refer to the vehicle-fixed coordinate system (see figure 145) with the initial position of the vehicle-fixed coordinate system being initial impact. In accordance with SAE J211 OCT88, the convention for the vehicle is as follows:

- x—Positive in the normal forward motion direction.
- y—Positive toward the right.
- z—Positive vertically downward.

Sequence for determining orientation is:

1. Yaw.
2. Pitch.
3. Roll.

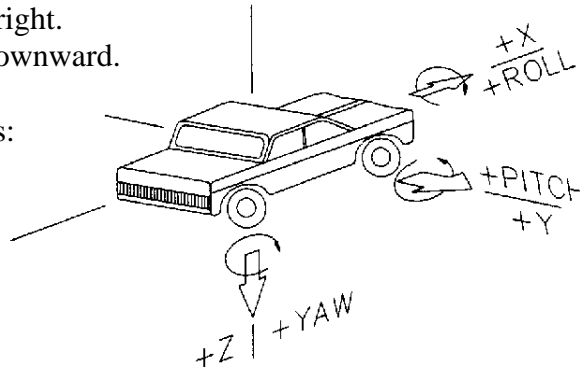


Figure 145. Vehicular sign convention and orientation diagram.

Roll, Pitch, and Yaw Angles

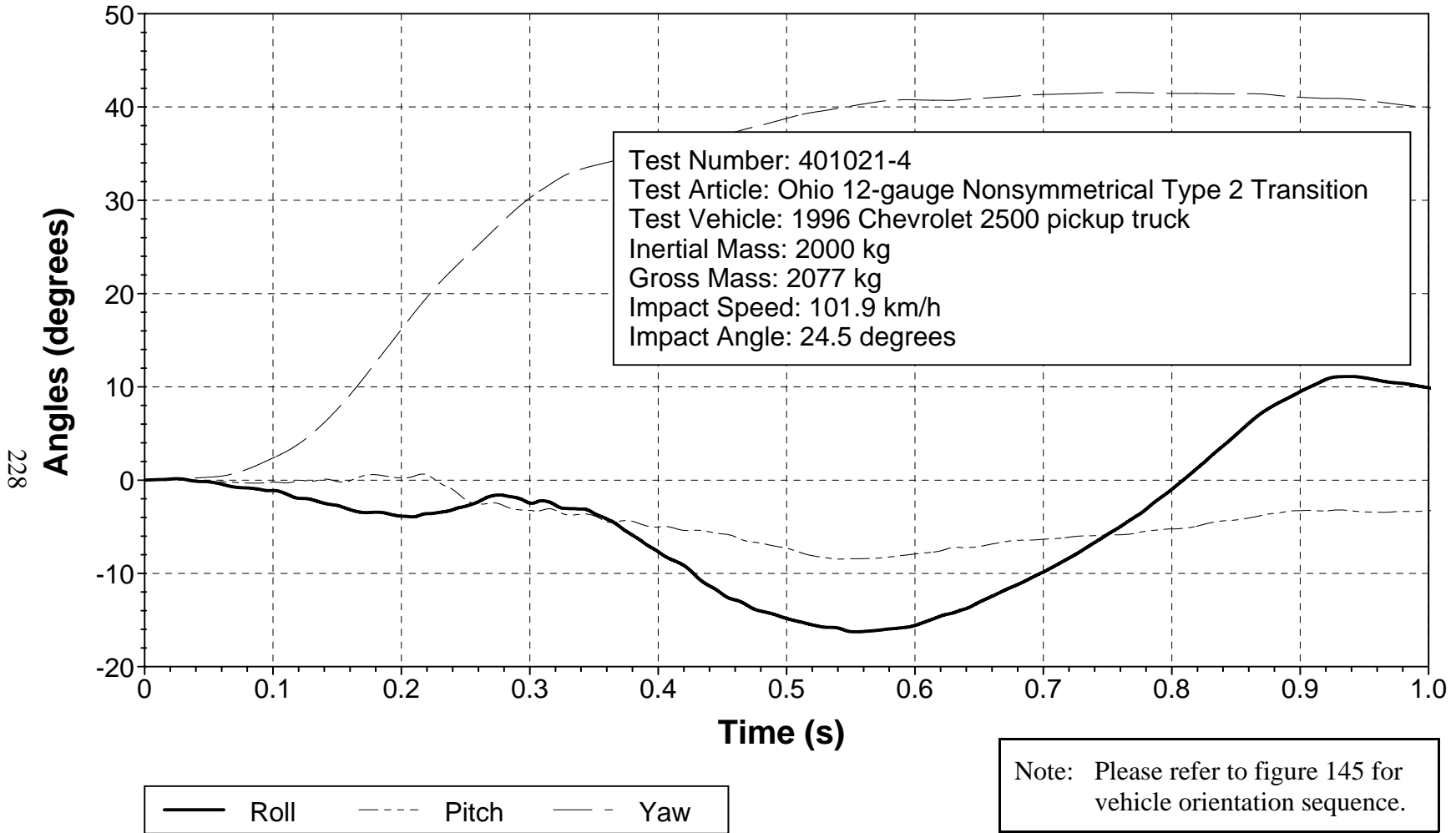


Figure 146. Vehicular angular displacements for test 401021-4.

X Acceleration at C.G.

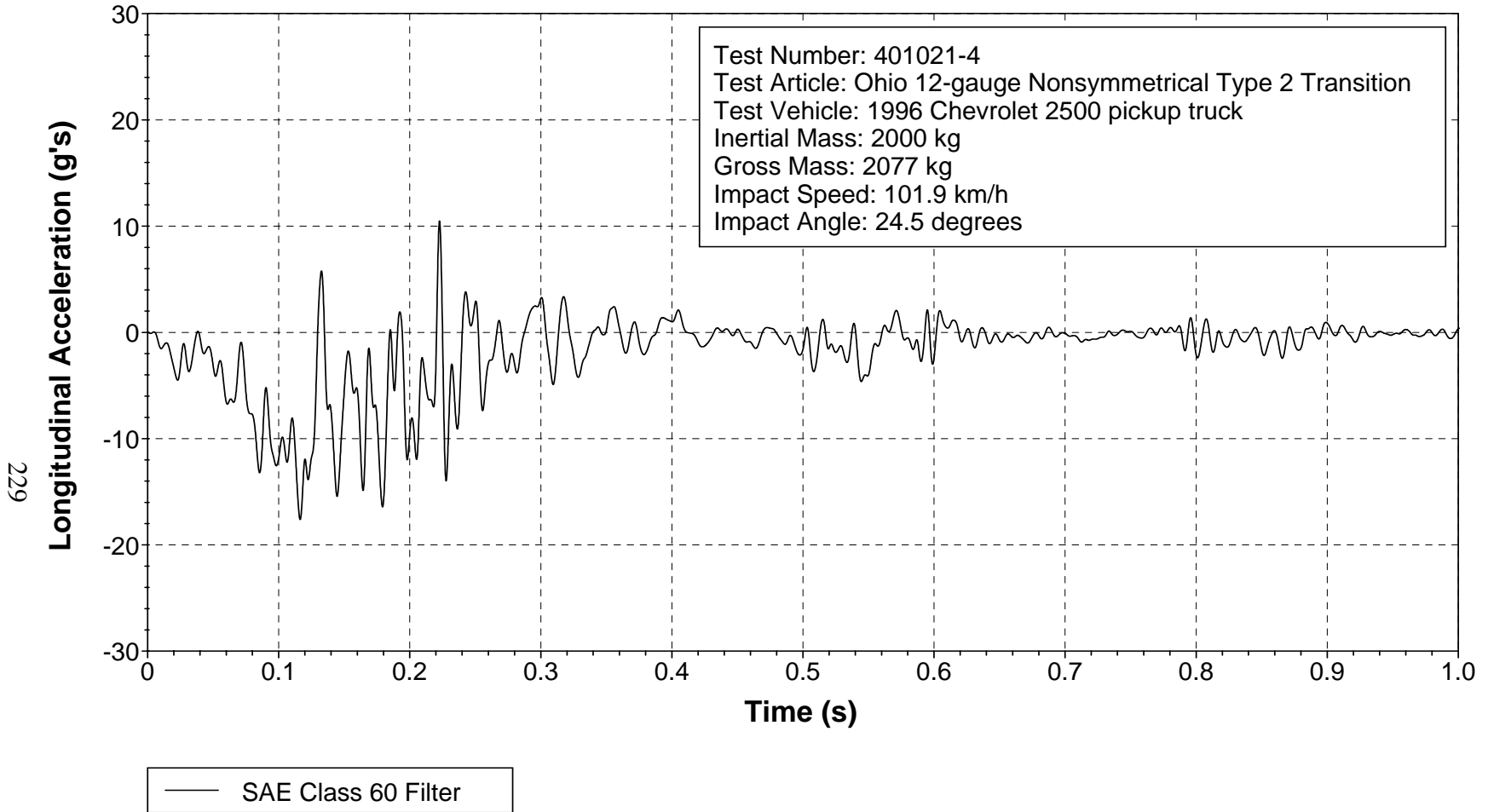


Figure 147. Vehicle longitudinal accelerometer trace for test 401021-4 (accelerometer located at center of gravity).

Y Acceleration at C.G.

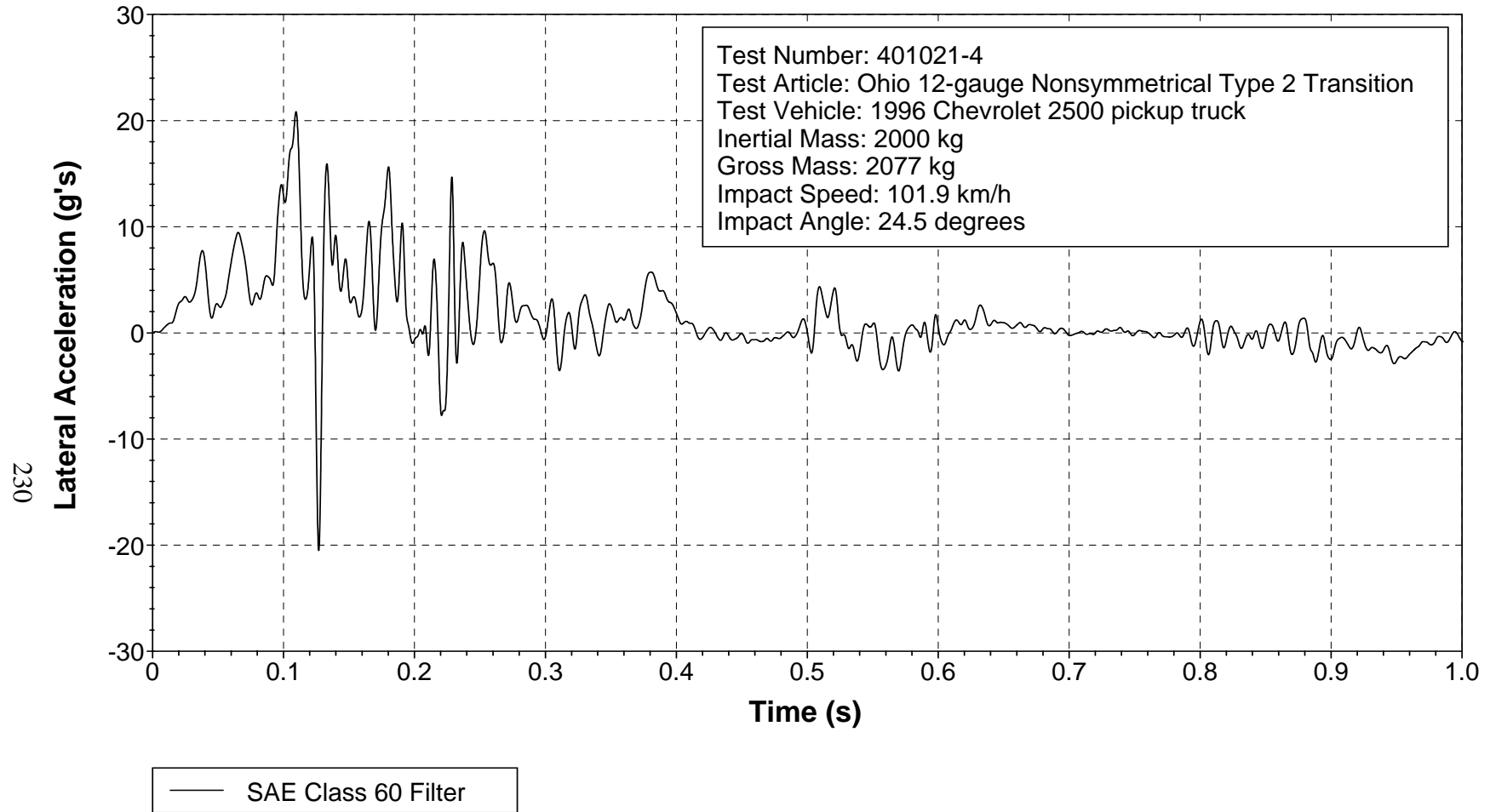


Figure 148. Vehicle lateral accelerometer trace for test 401021-4 (accelerometer located at center of gravity).

Z Acceleration at C.G.

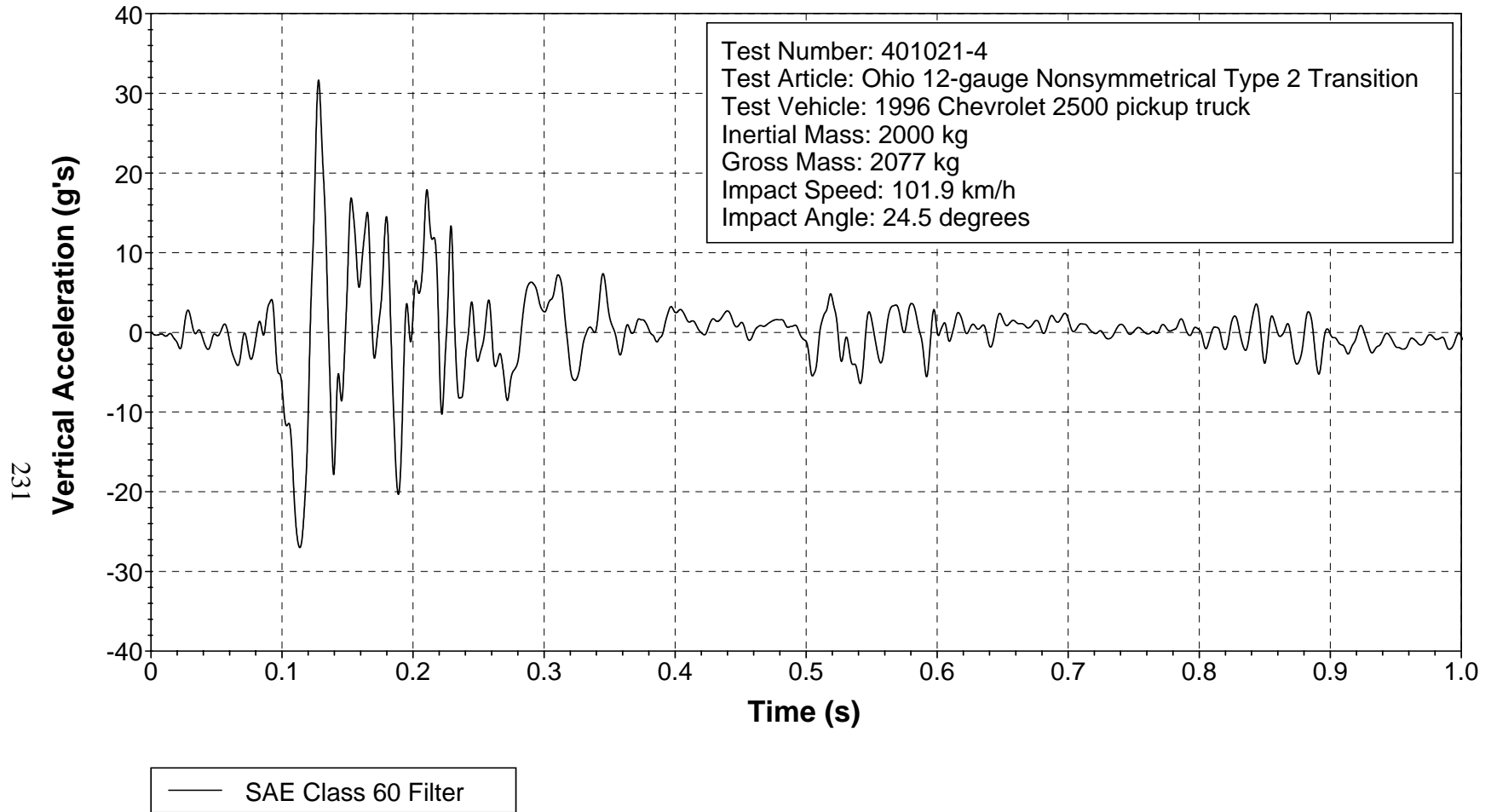


Figure 149. Vehicle vertical accelerometer trace for test 401021-4 (accelerometer located at center of gravity).

X Acceleration over Rear Axle

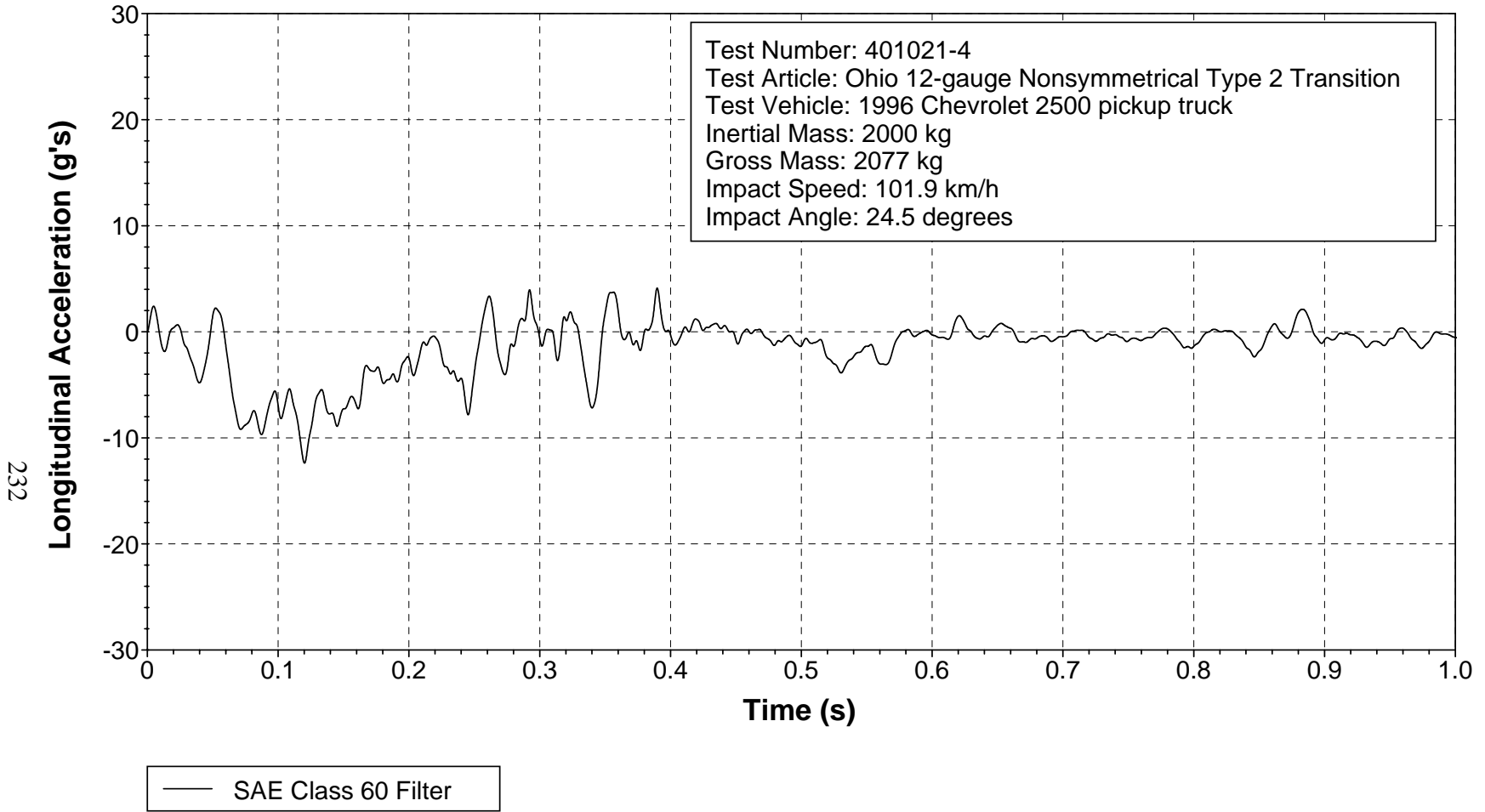


Figure 150. Vehicle longitudinal accelerometer trace for test 401021-4 (accelerometer located over rear axle).

Y Acceleration over Rear Axle

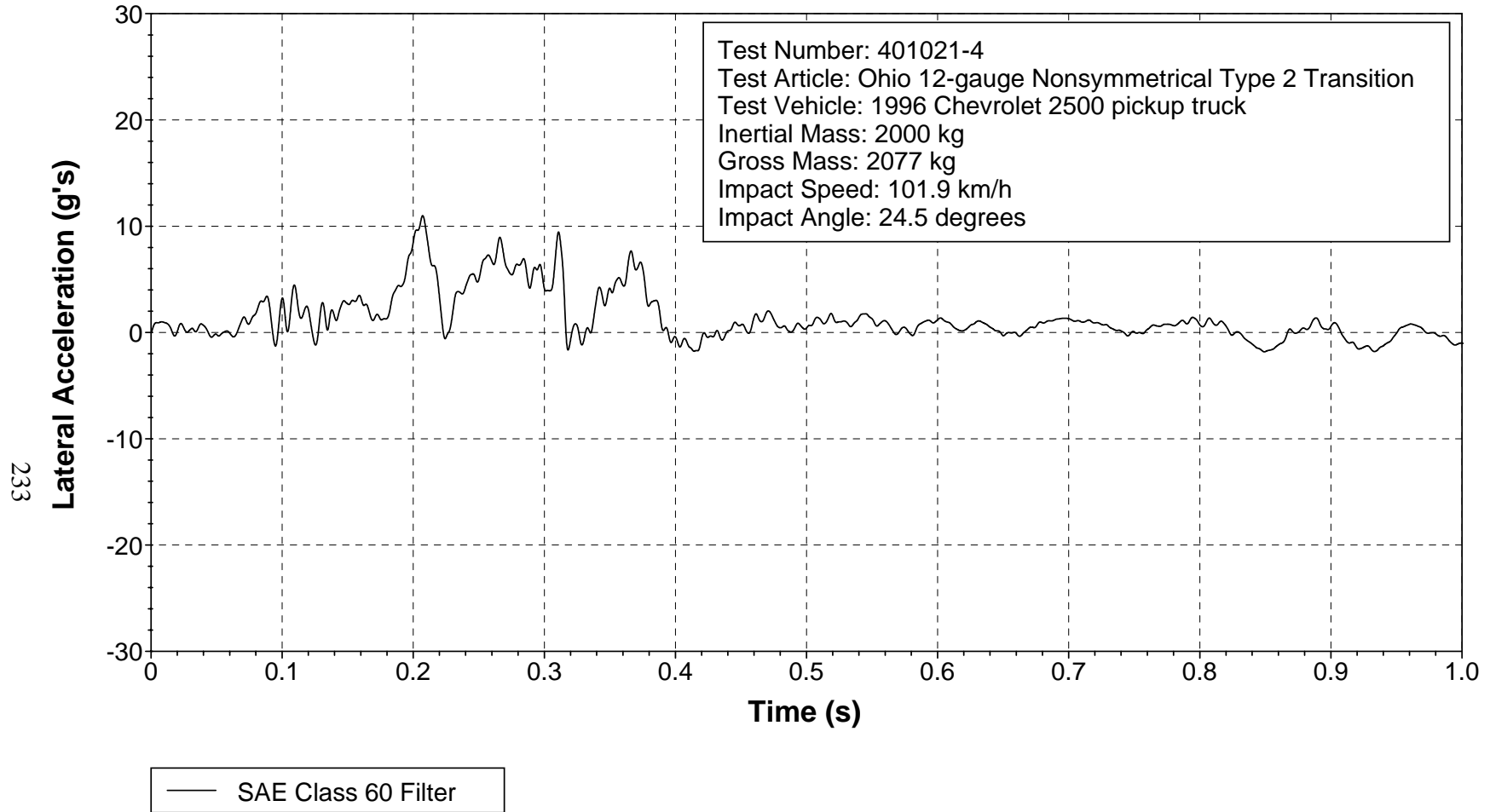


Figure 151. Vehicle lateral accelerometer trace for test 401021-4 (accelerometer located over rear axle).

Z Acceleration over Rear Axle

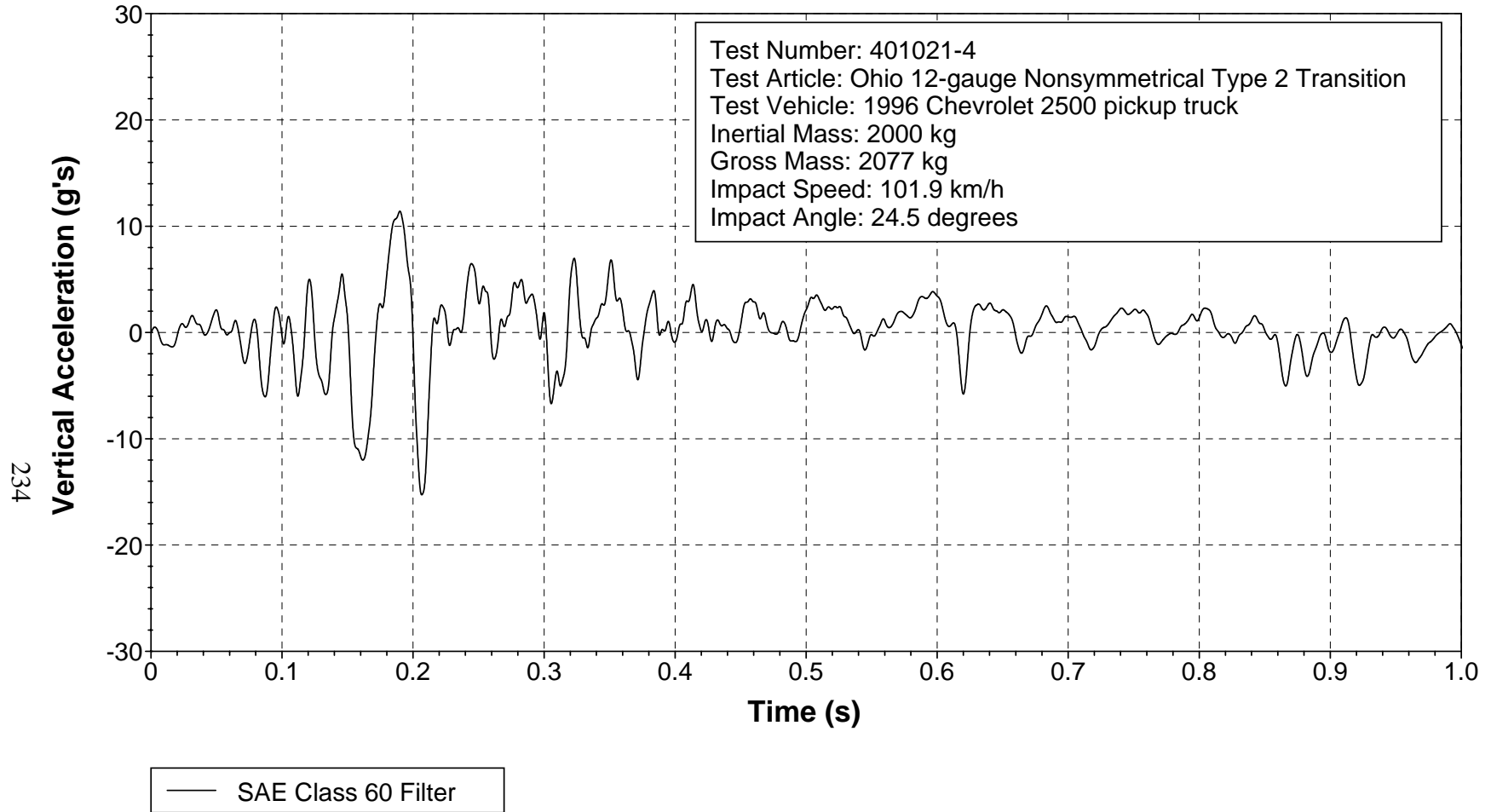


Figure 152. Vehicle vertical accelerometer trace for test 401021-4 (accelerometer located over rear axle).

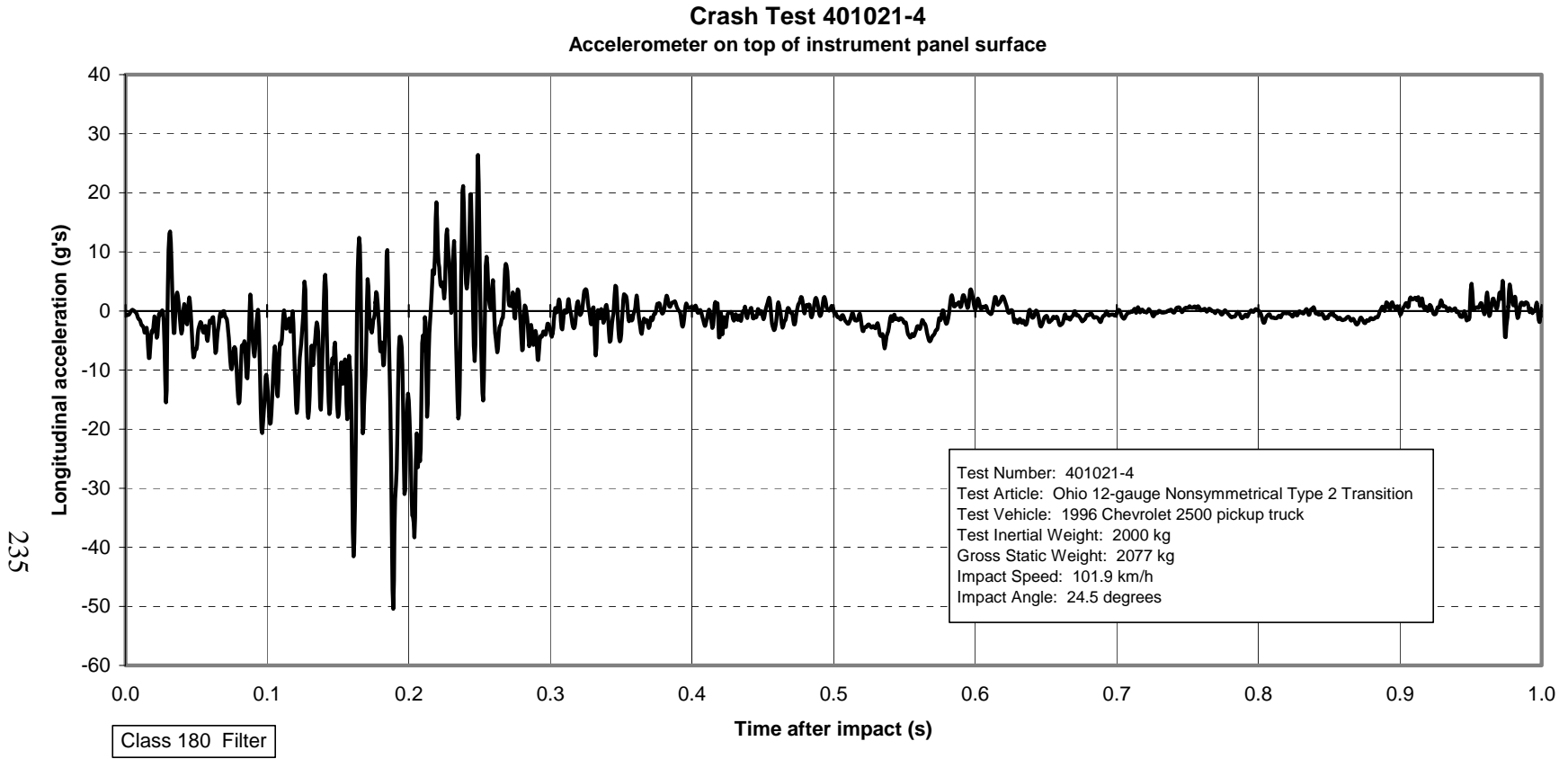


Figure 153. Vehicle longitudinal accelerometer trace for test 401021-4 (accelerometer located on top surface of instrument panel).

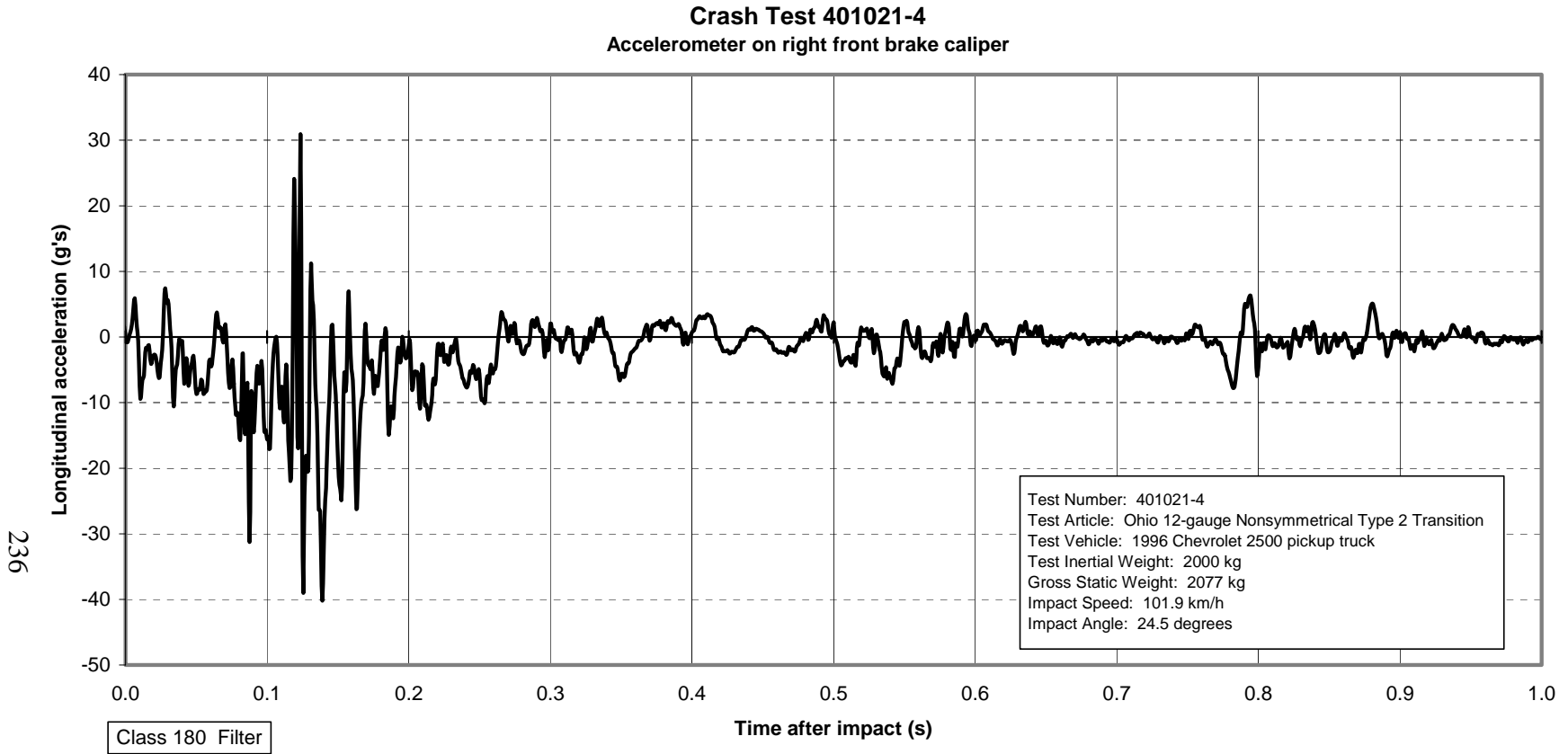


Figure 154. Vehicle longitudinal accelerometer trace for test 401021-4 (accelerometer located on right front brake caliper).

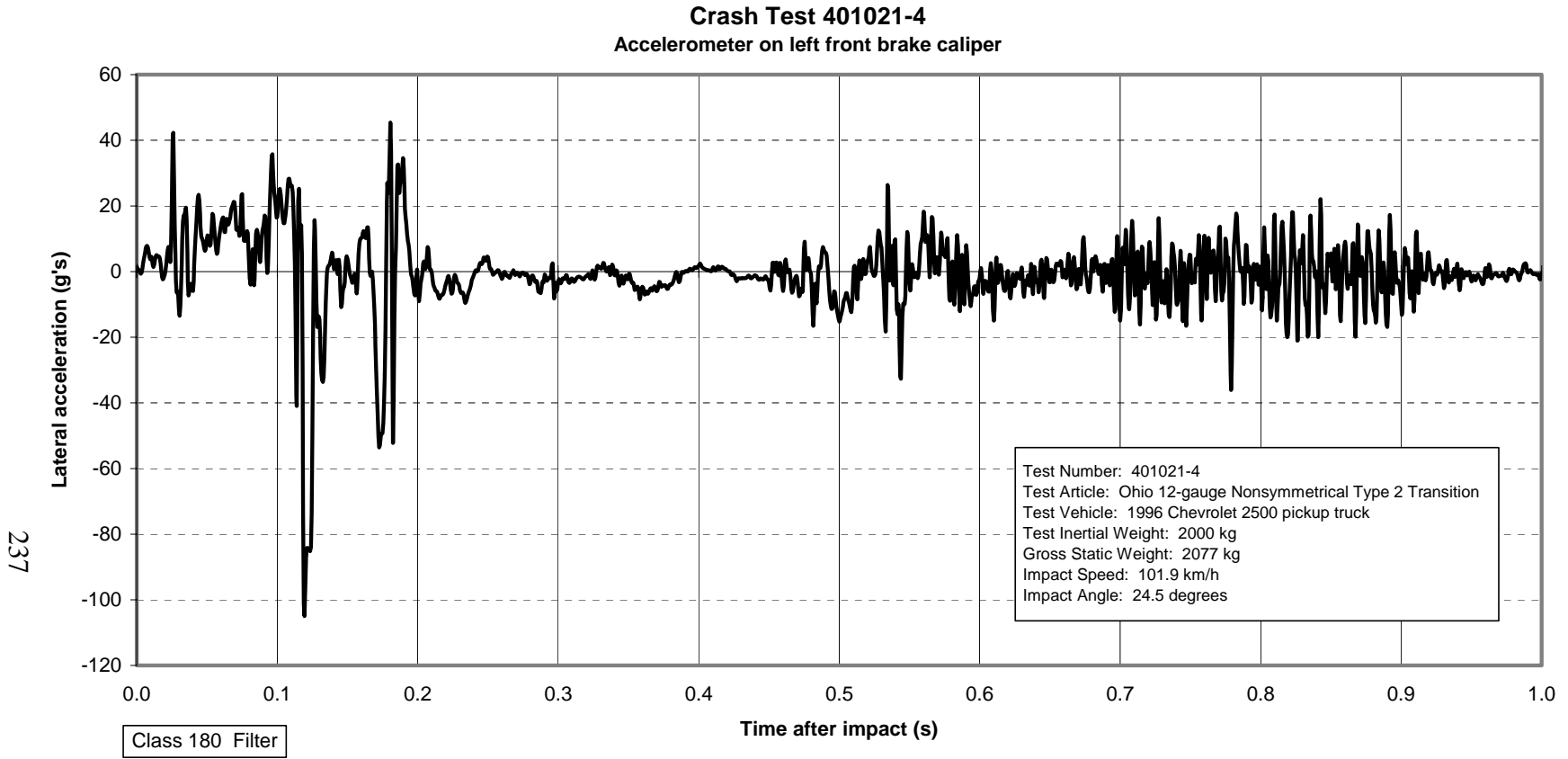


Figure 155. Vehicle lateral accelerometer trace for test 401021-4 (accelerometer located on left front brake caliper).

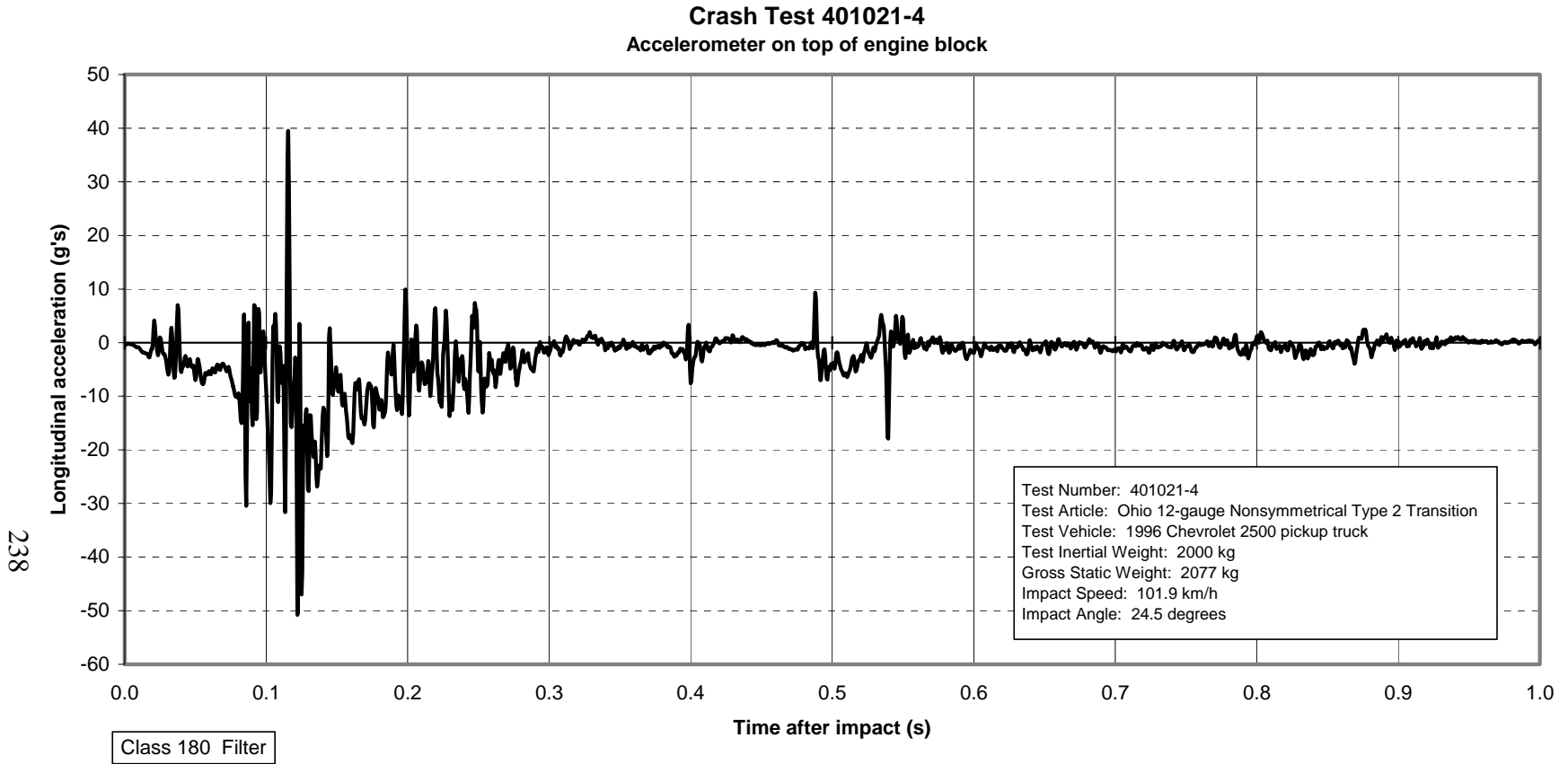


Figure 156. Vehicle longitudinal accelerometer trace for test 401021-4 (accelerometer located on top of engine block).

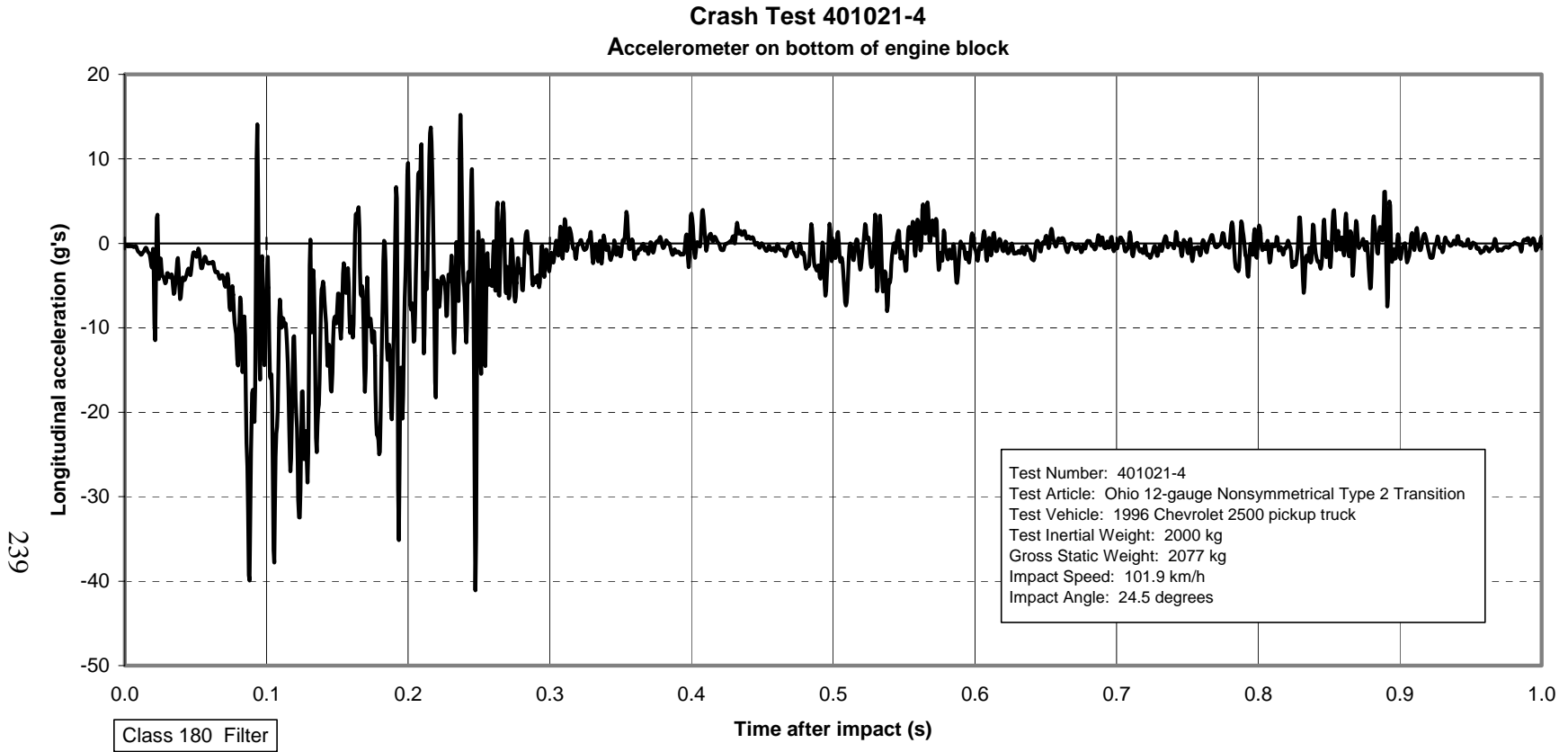


Figure 157. Vehicle longitudinal accelerometer trace for test 401021-4 (accelerometer located on bottom of engine block).

Roll, Pitch, and Yaw Angles

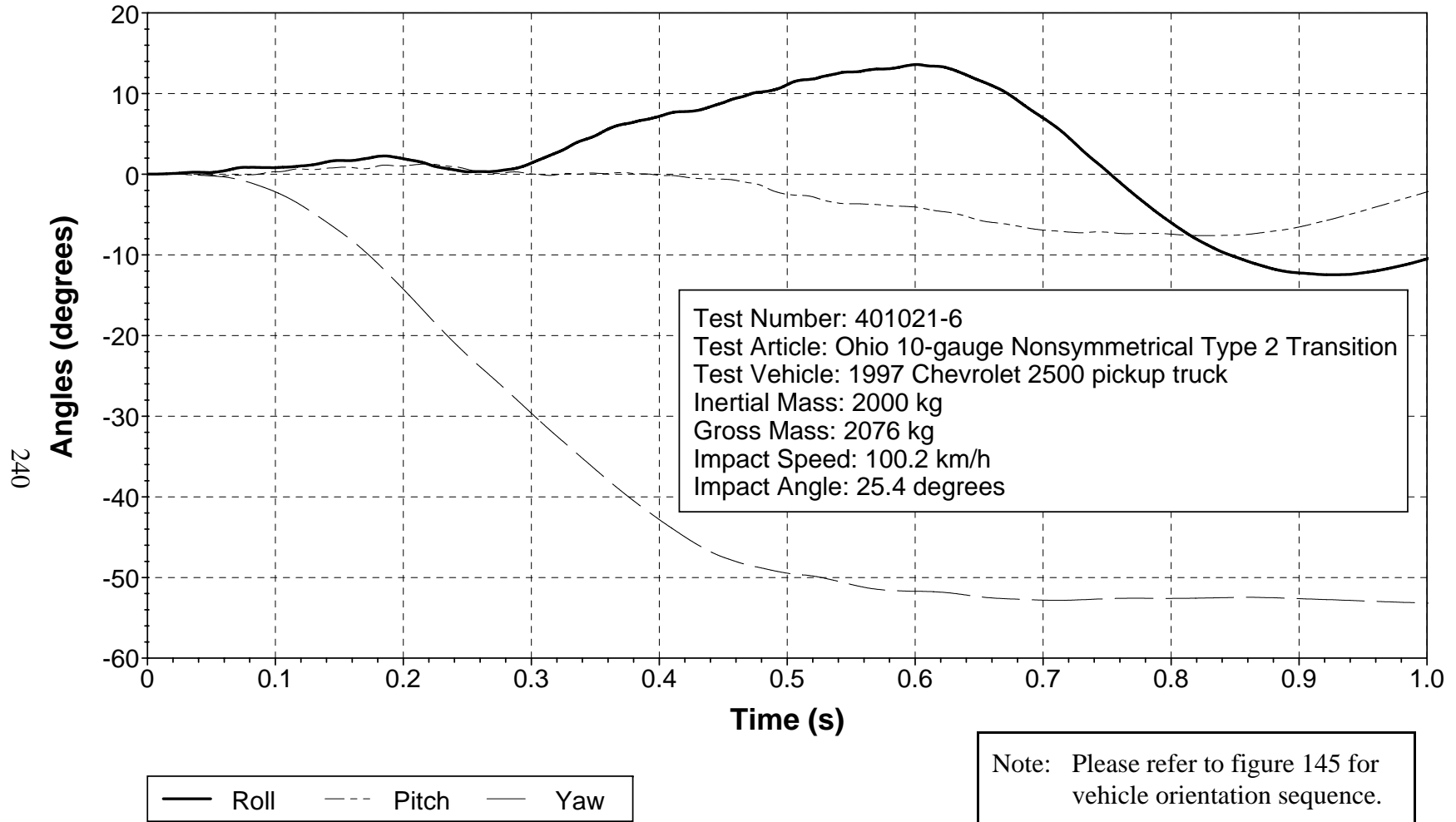


Figure 158. Vehicular angular displacements for test 401021-6.

X Acceleration at C.G.

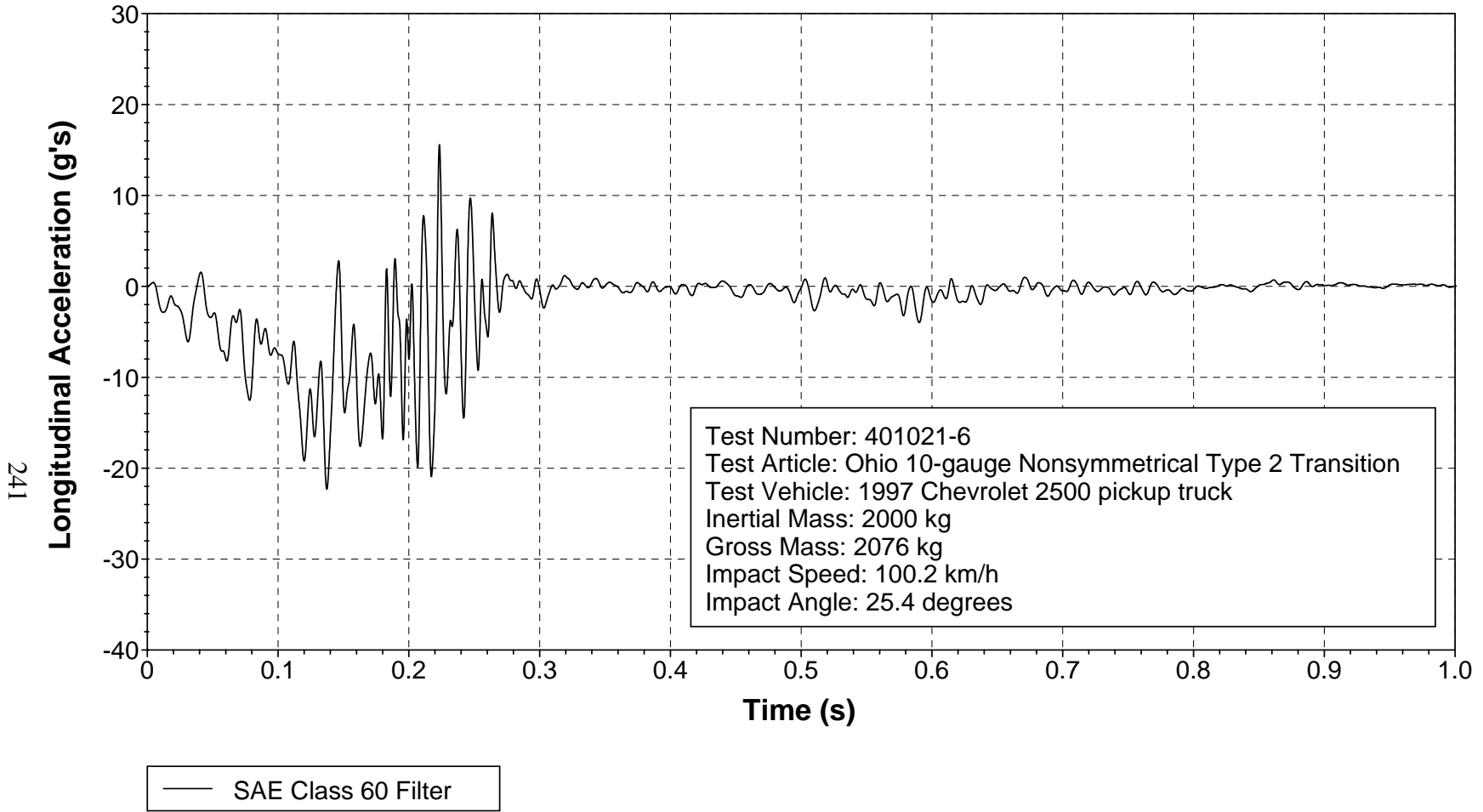


Figure 159. Vehicle longitudinal accelerometer trace for test 401021-6 (accelerometer located at center of gravity).

Y Acceleration at C.G.

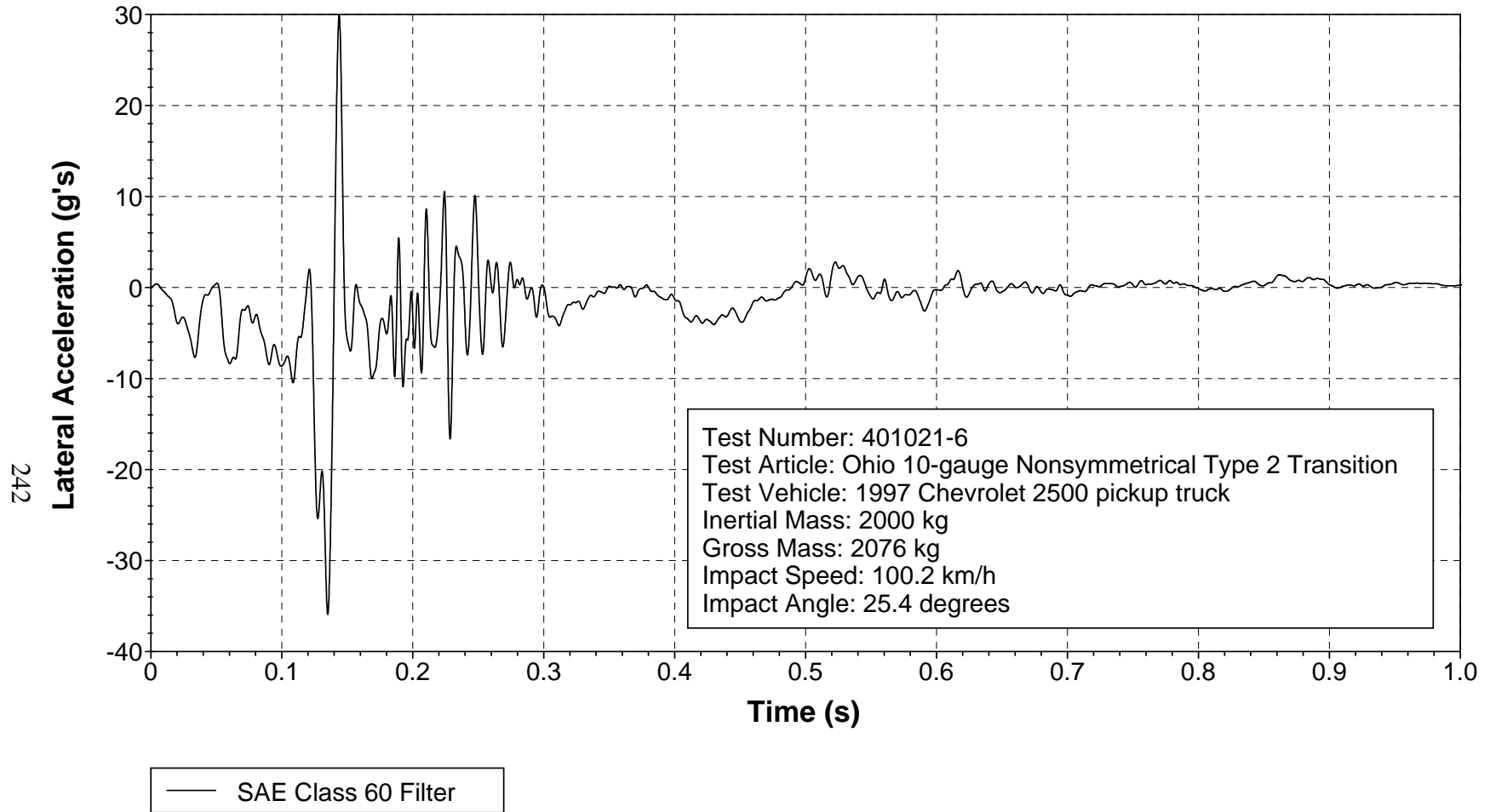


Figure 160. Vehicle lateral accelerometer trace for test 401021-6 (accelerometer located at center of gravity).

Z Acceleration at C.G.

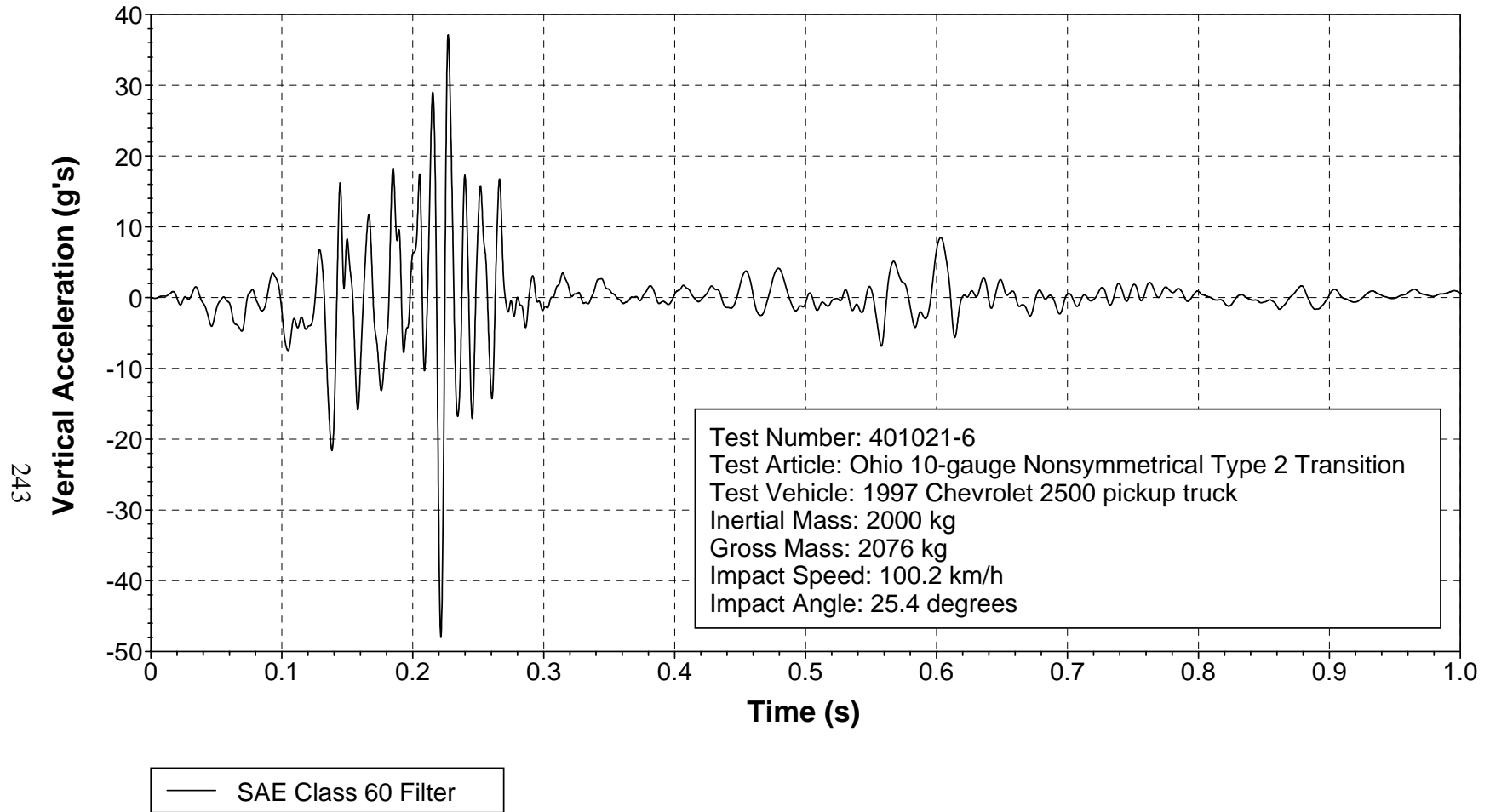


Figure 161. Vehicle vertical accelerometer trace for test 401021-6 (accelerometer located at center of gravity).

X Acceleration over Rear Axle

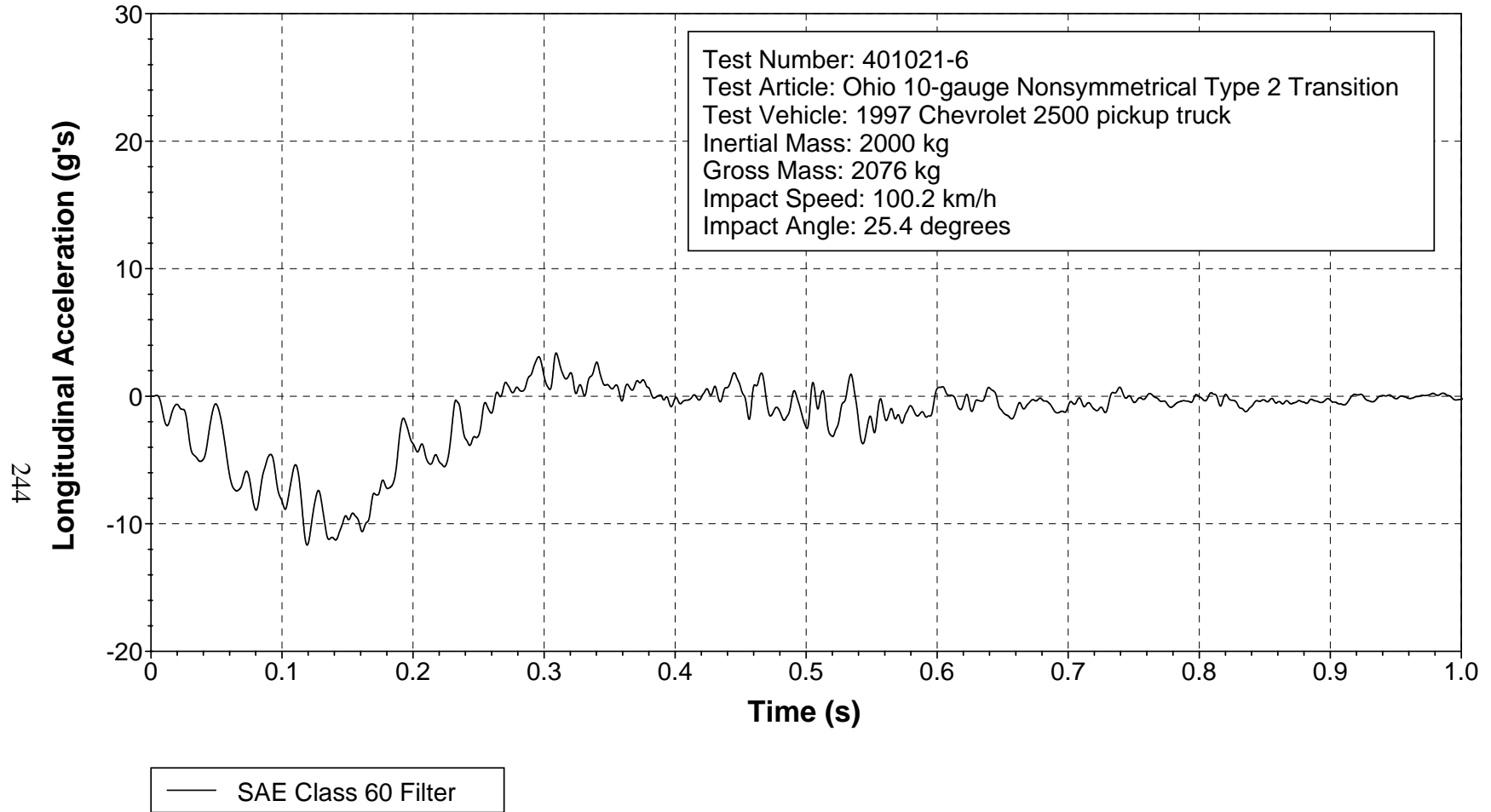


Figure 162. Vehicle longitudinal accelerometer trace for test 401021-6 (accelerometer located over rear axle).

Y Acceleration over Rear Axle

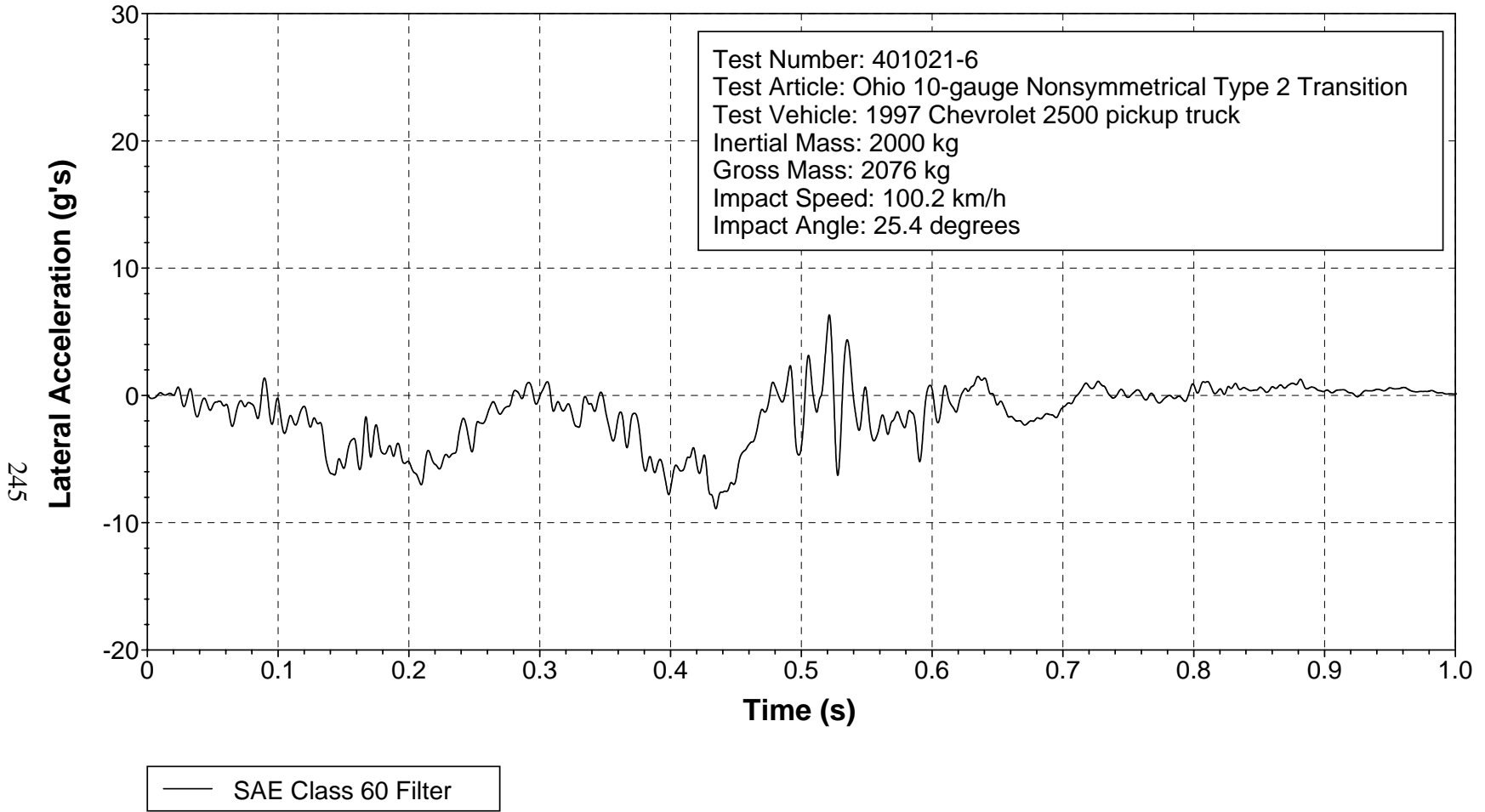


Figure 163. Vehicle lateral accelerometer trace for test 401021-6 (accelerometer located over rear axle).

Z Acceleration over Rear Axle

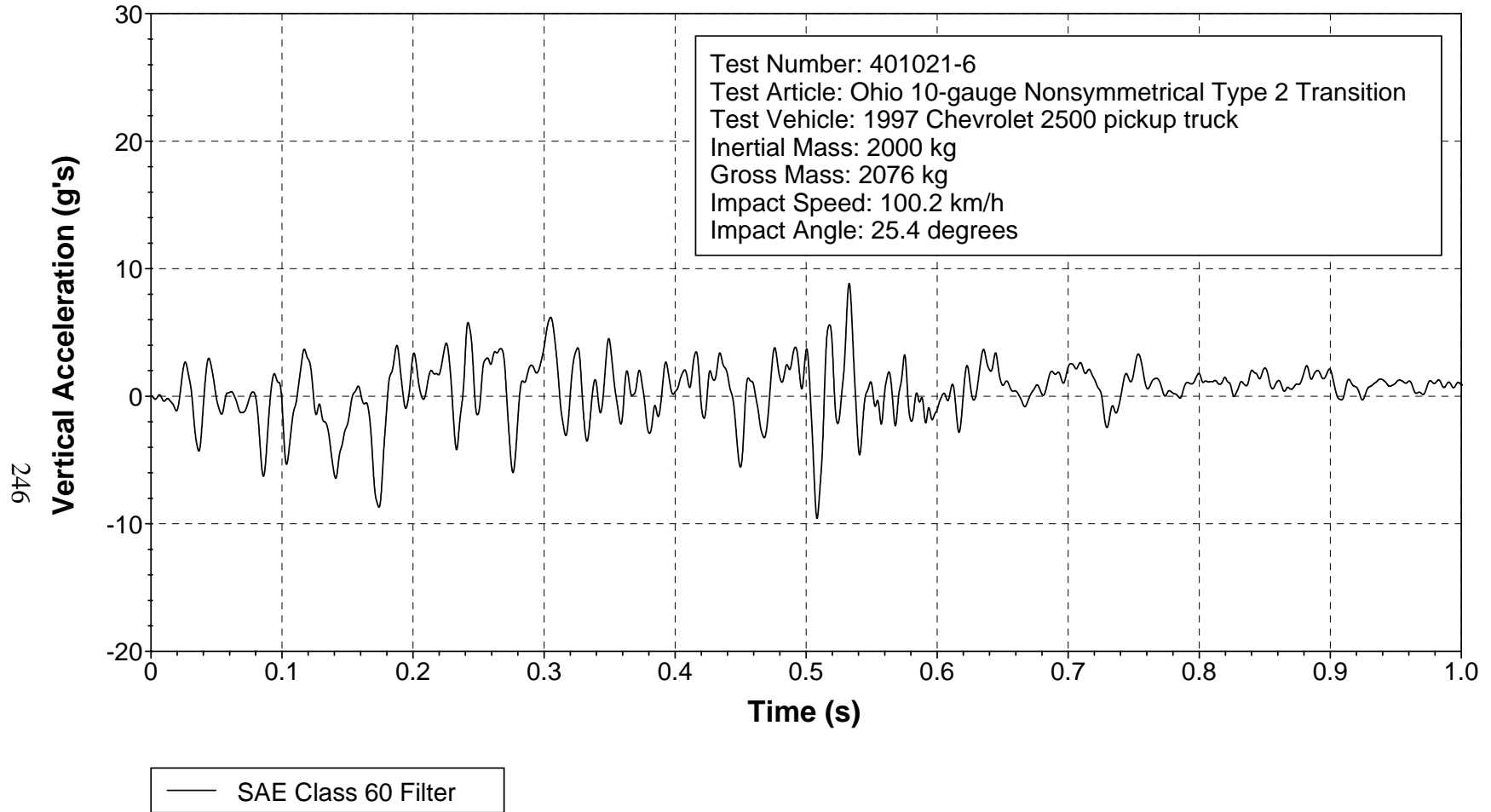


Figure 164. Vehicle vertical accelerometer trace for test 401021-6 (accelerometer located over rear axle).

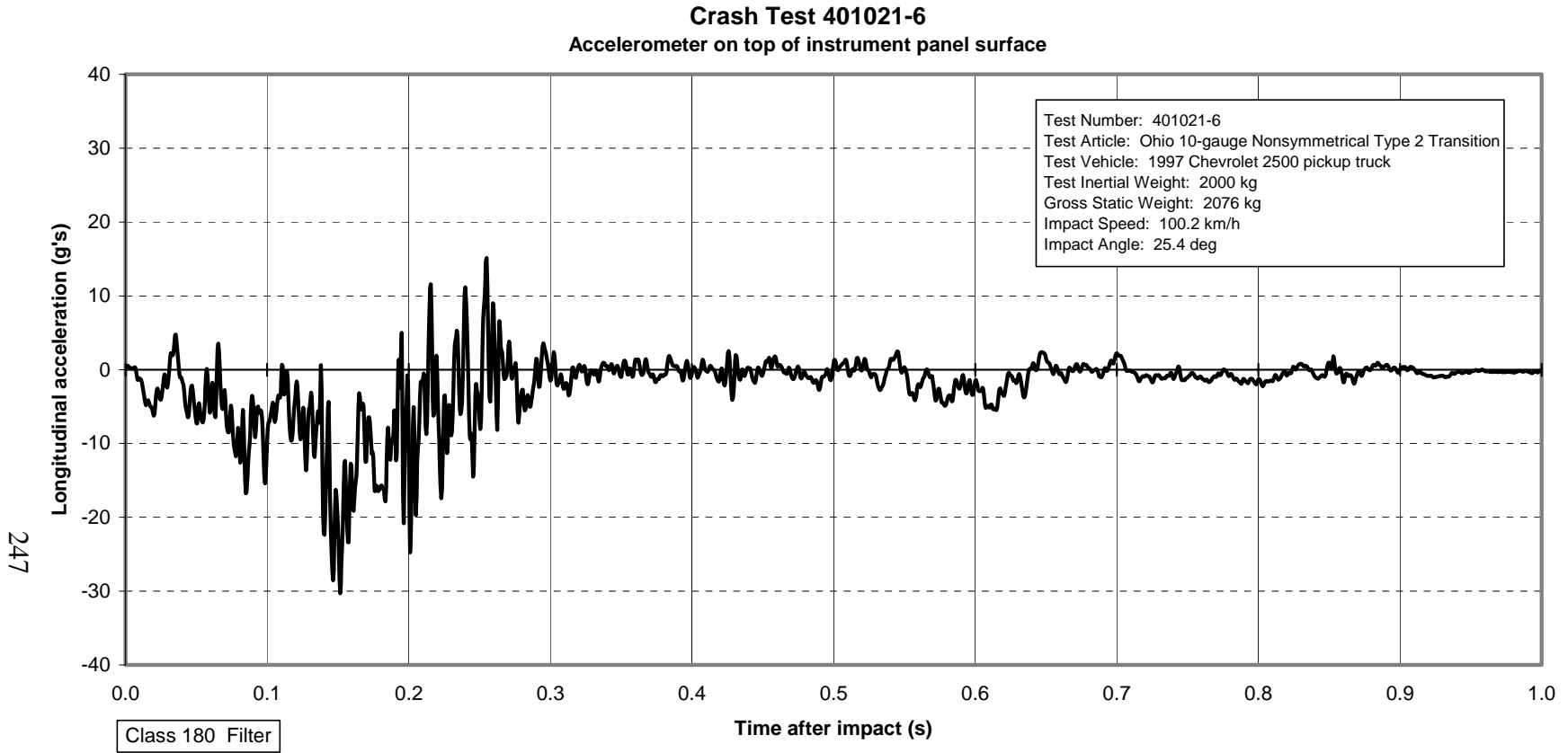


Figure 165. Vehicle longitudinal accelerometer trace for test 401021-6 (accelerometer located on top surface of instrument panel).

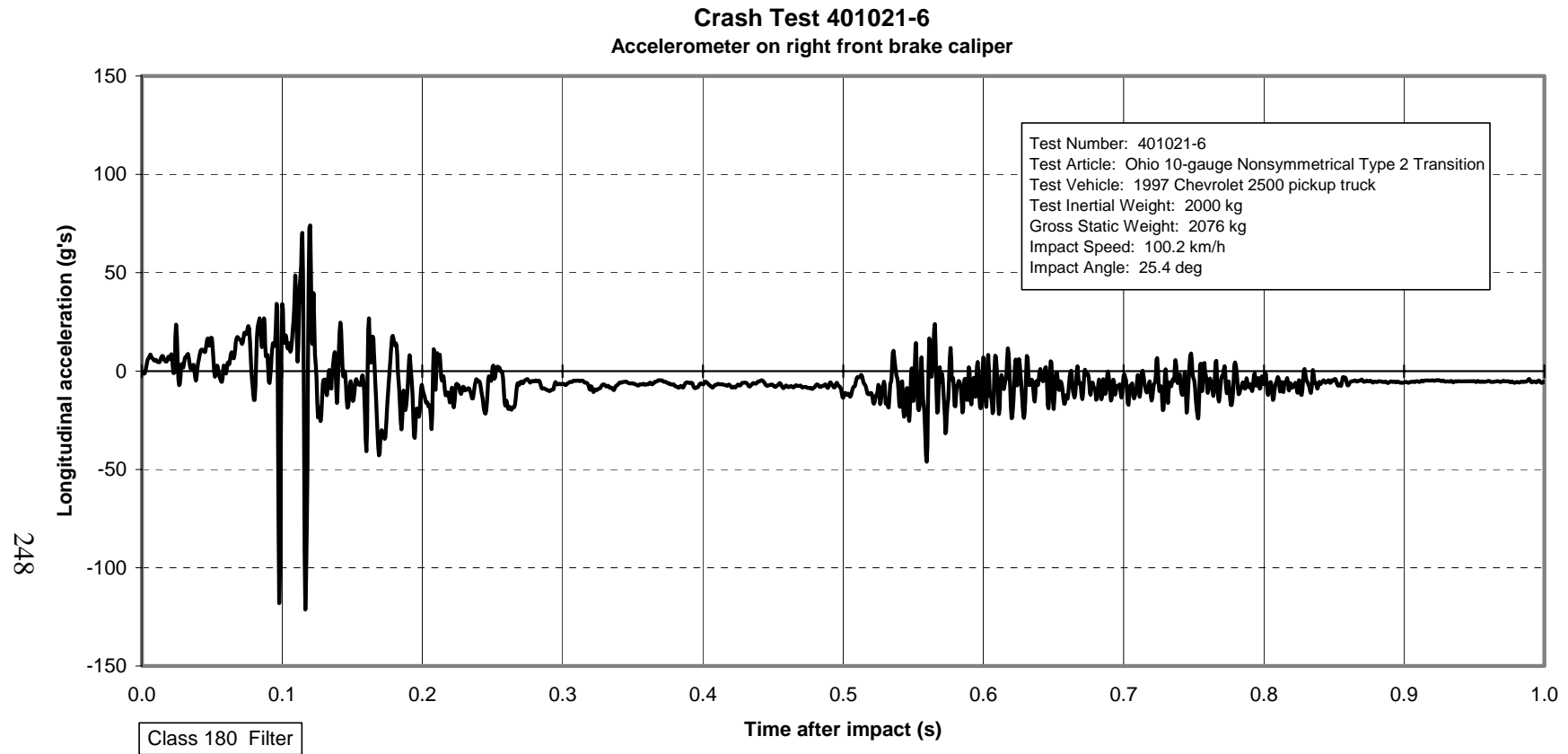


Figure 166. Vehicle lateral accelerometer trace for test 401021-6 (accelerometer located on right front brake caliper).

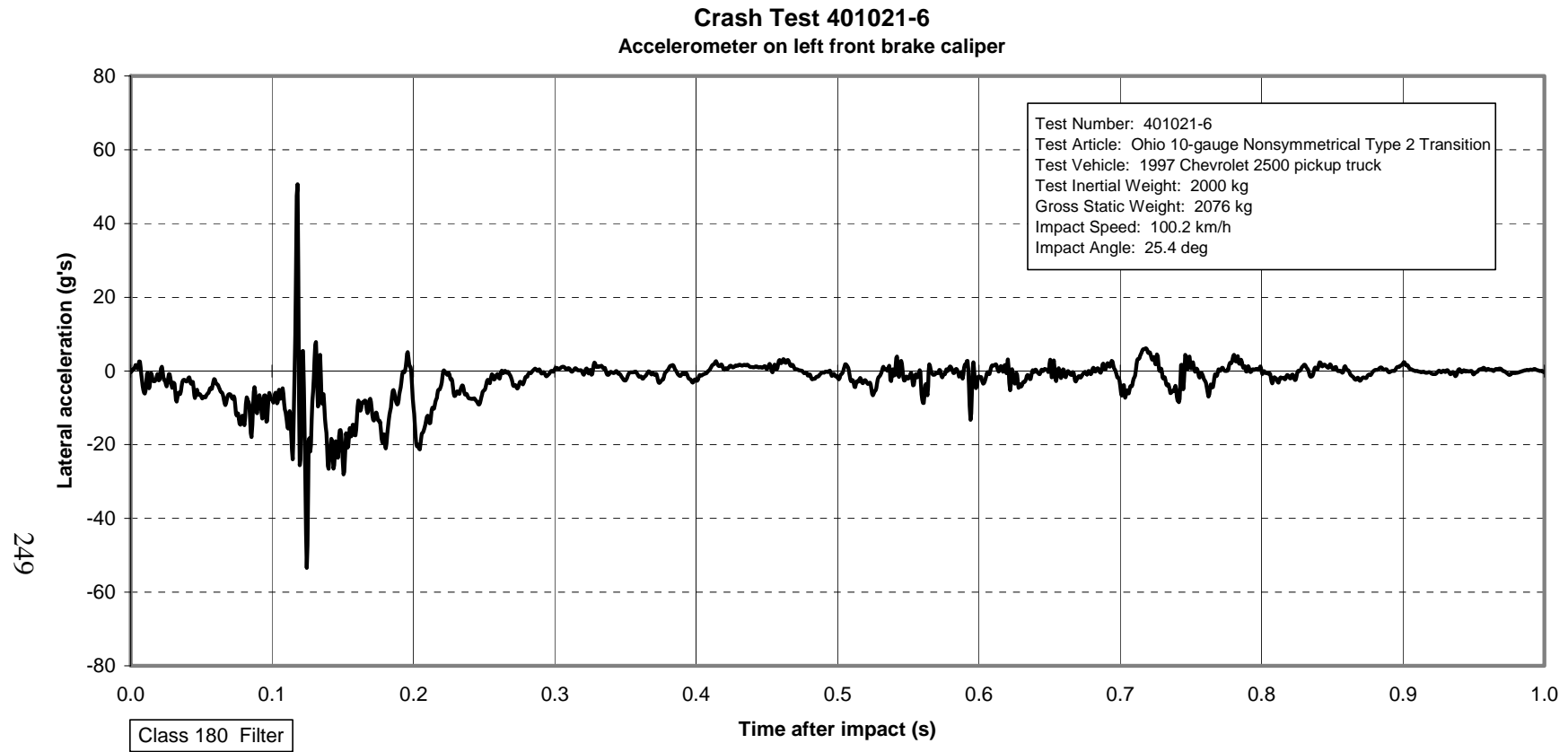


Figure 167. Vehicle longitudinal accelerometer trace for test 401021-6 (accelerometer located on left front brake caliper).

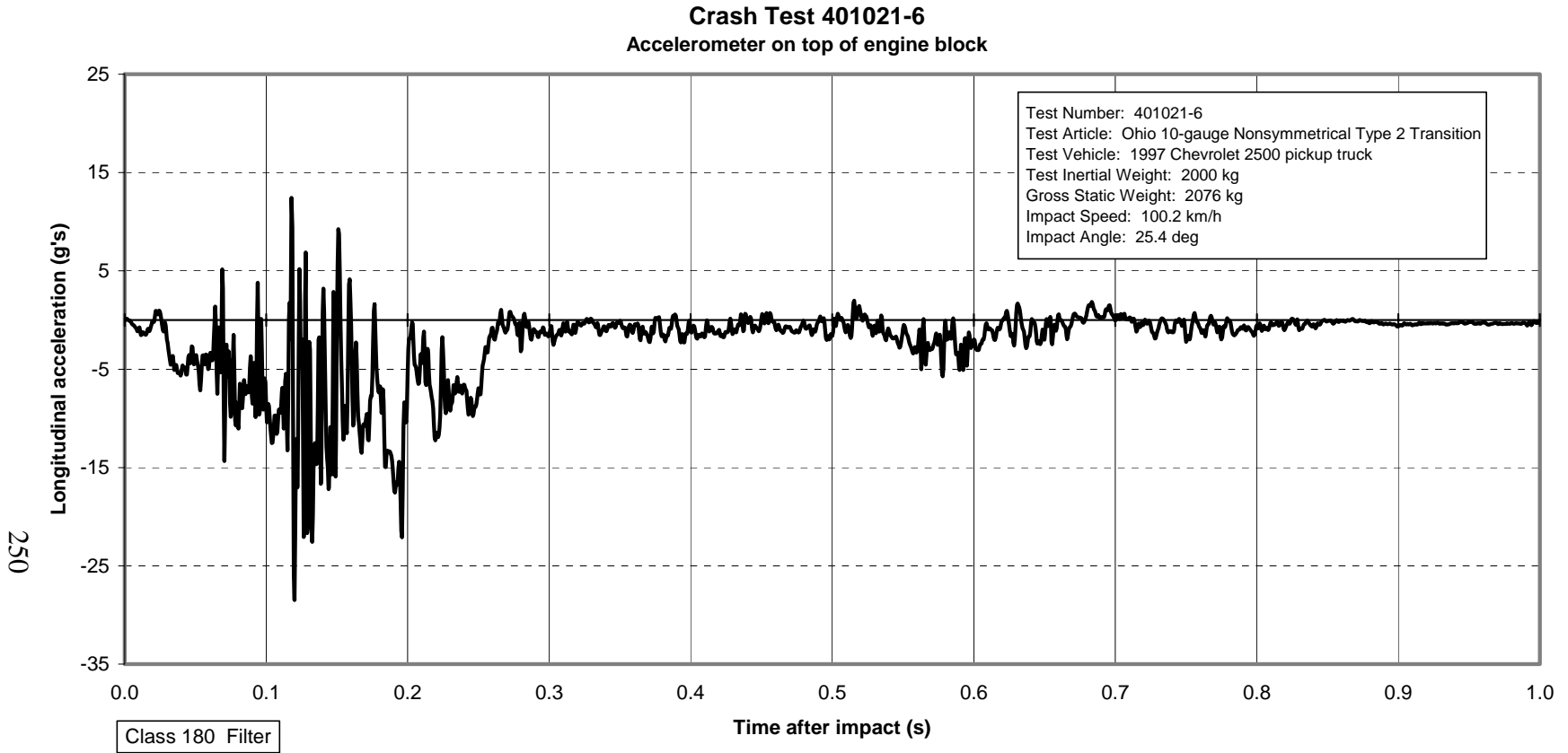


Figure 168. Vehicle longitudinal accelerometer trace for test 401021-6 (accelerometer located on top of engine block).

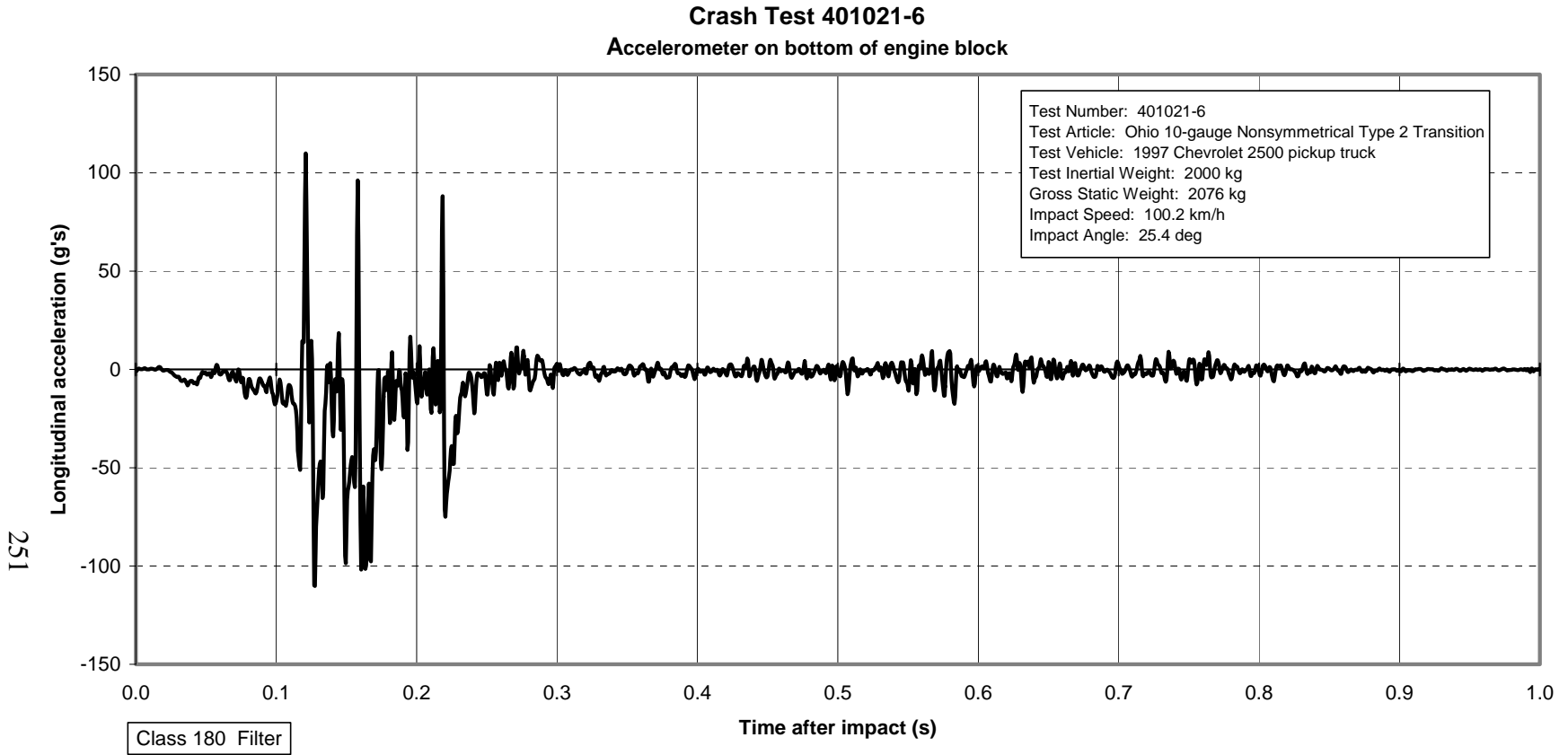


Figure 169. Vehicle longitudinal accelerometer trace for test 401021-6 (accelerometer located on bottom of engine block).

Roll, Pitch, and Yaw Angles

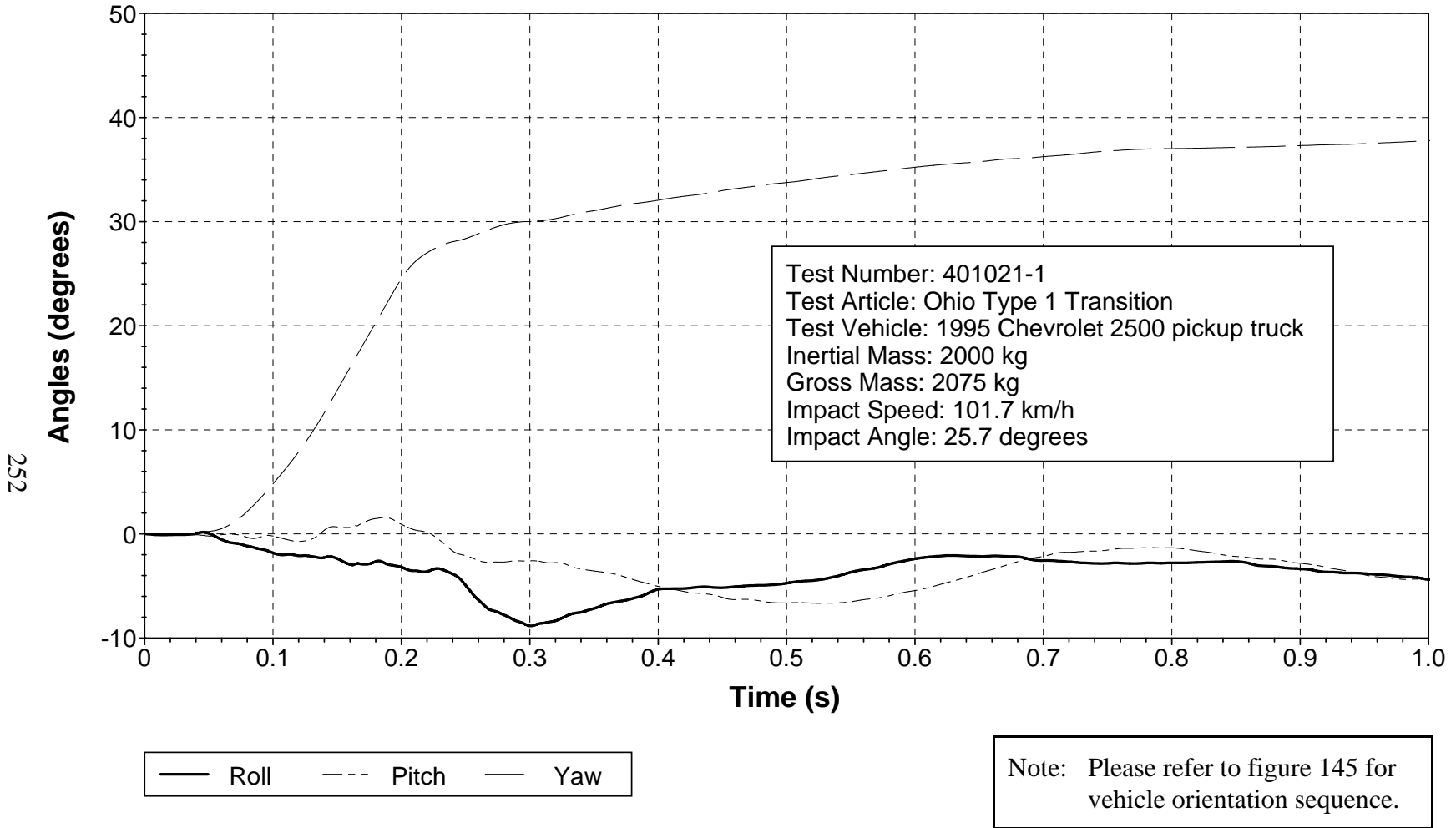


Figure 170. Vehicular angular displacements for test 401021-1.

X Acceleration at C.G.

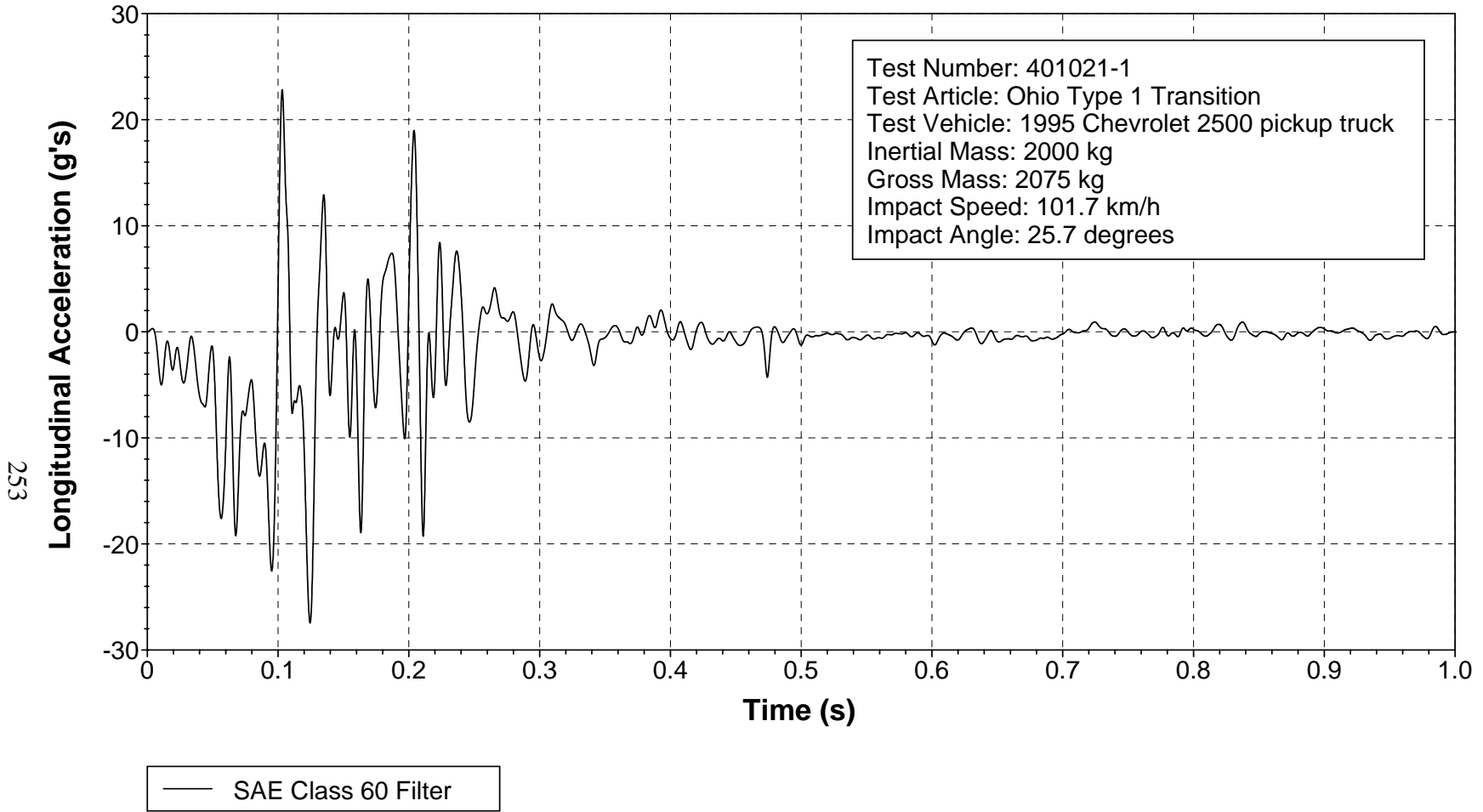


Figure 171. Vehicle longitudinal accelerometer trace for test 401021-1 (accelerometer located at center of gravity).

Y Acceleration at C.G.

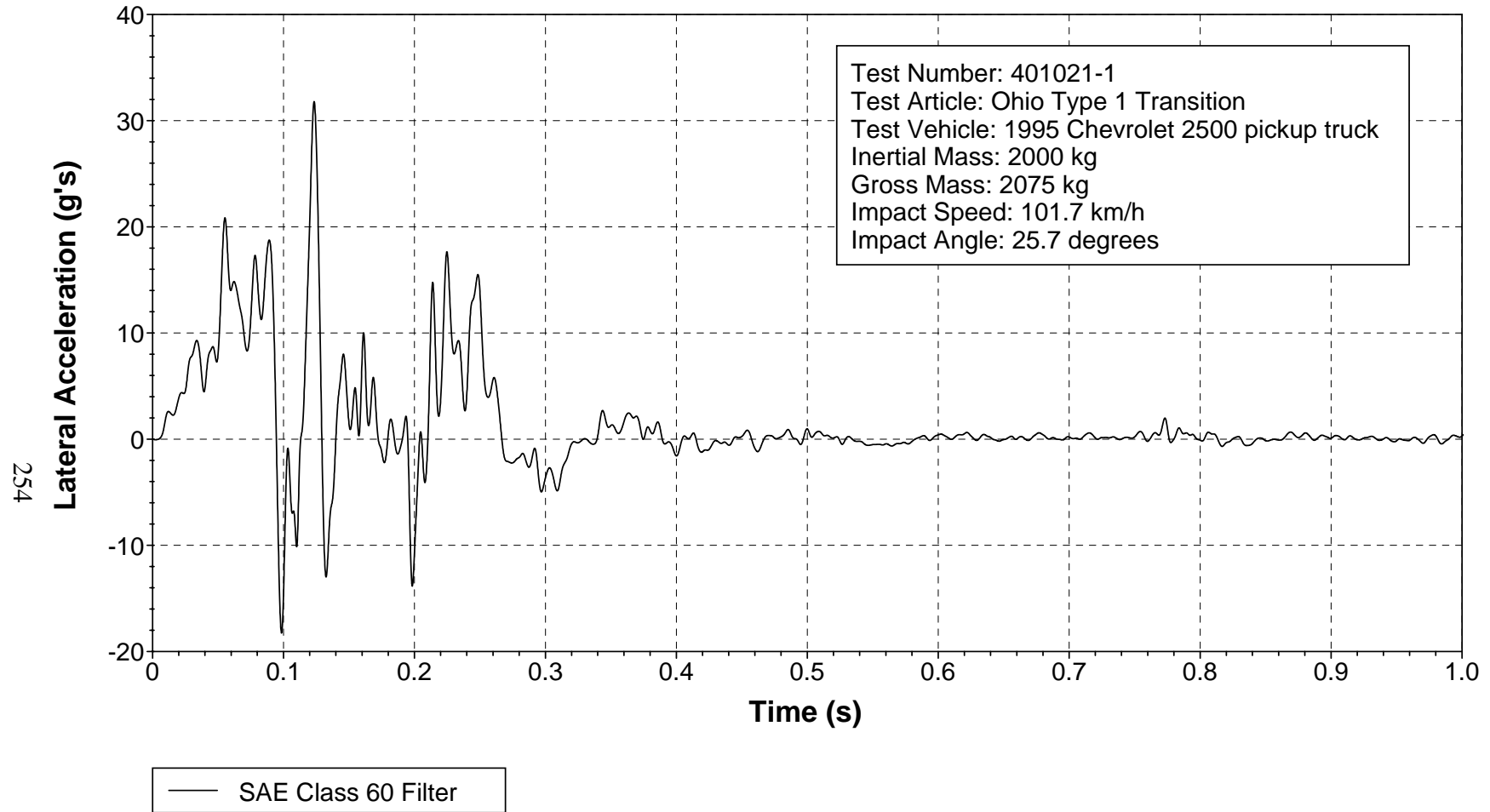


Figure 172. Vehicle lateral accelerometer trace for test 401021-1 (accelerometer located at center of gravity).

Z Acceleration at C.G.

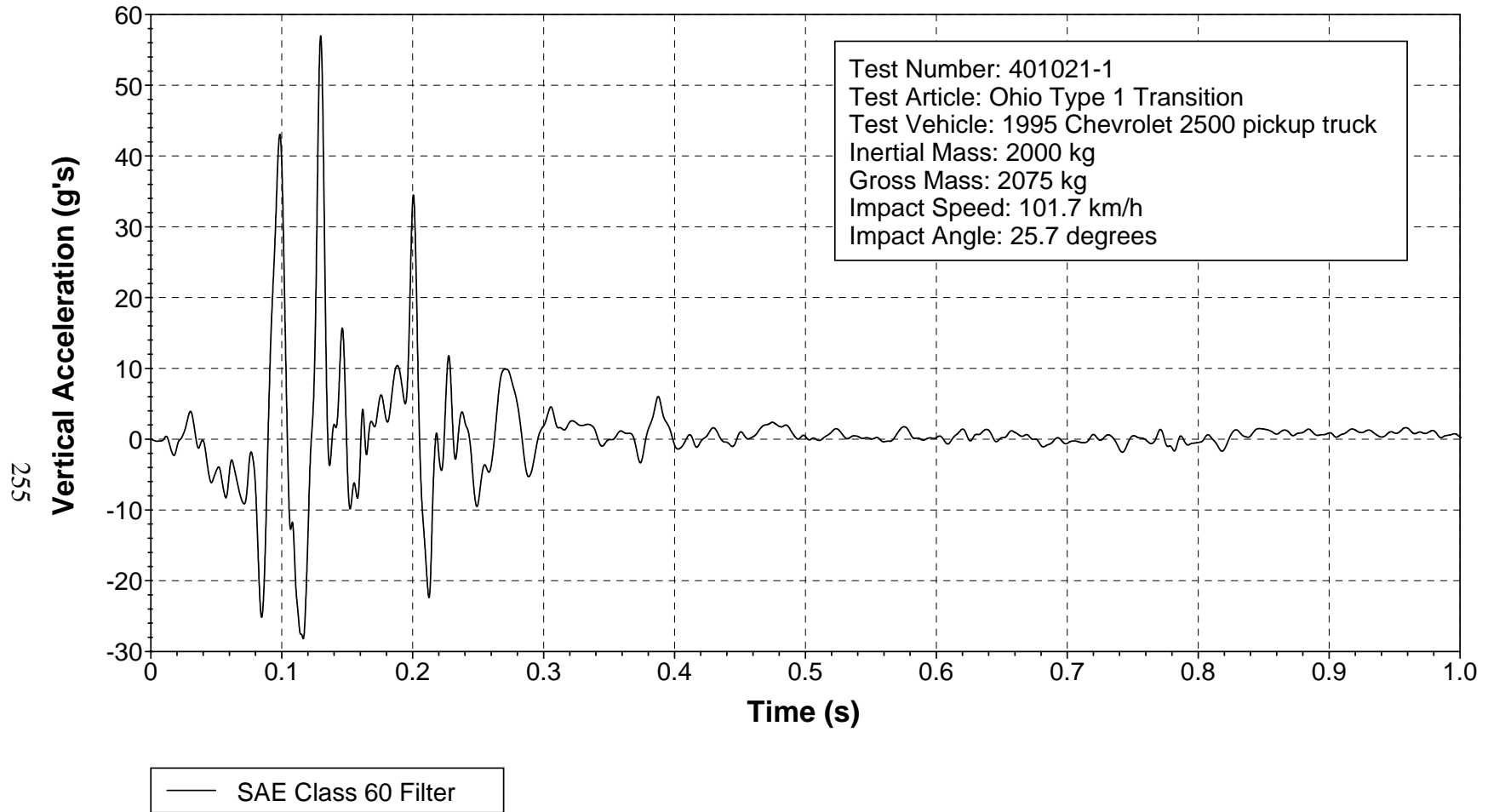


Figure 173. Vehicle vertical accelerometer trace for test 401021-1 (accelerometer located at center of gravity).

X Acceleration over Rear Axle

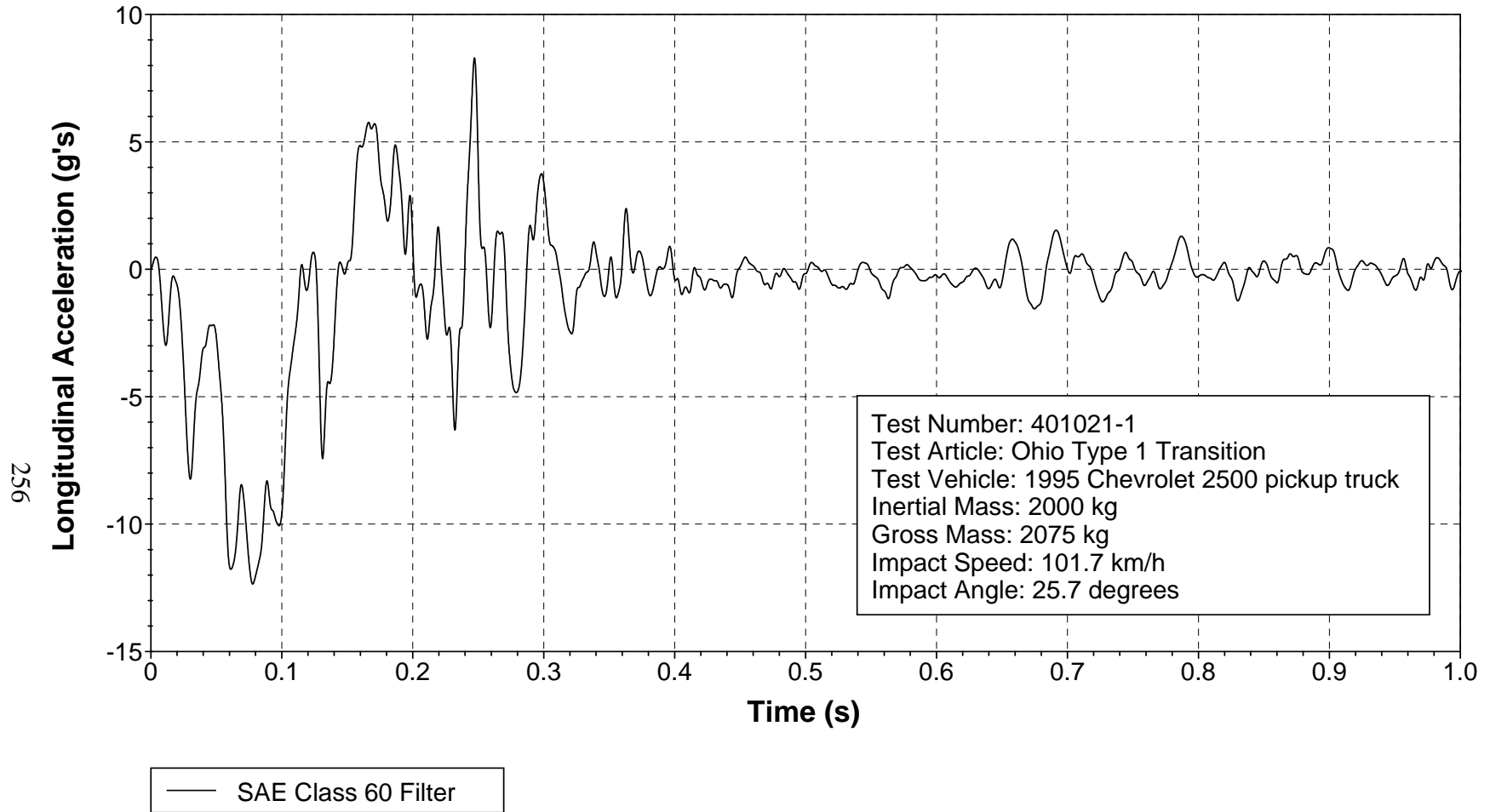


Figure 174. Vehicle longitudinal accelerometer trace for test 401021-1 (accelerometer located over rear axle).

Y Acceleration over Rear Axle

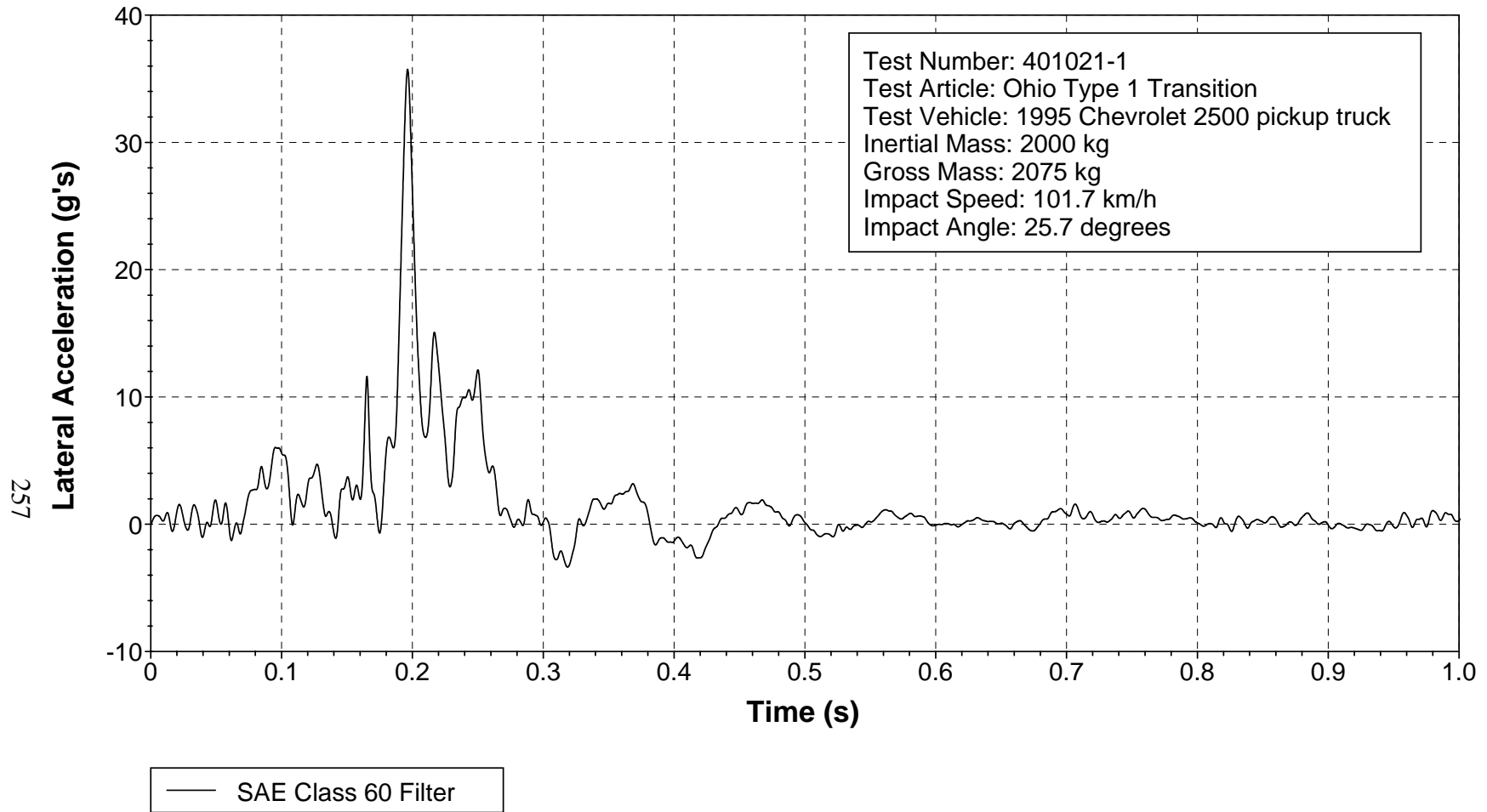


Figure 175. Vehicle lateral accelerometer trace for test 401021-1 (accelerometer located over rear axle).

Z Acceleration over Rear Axle

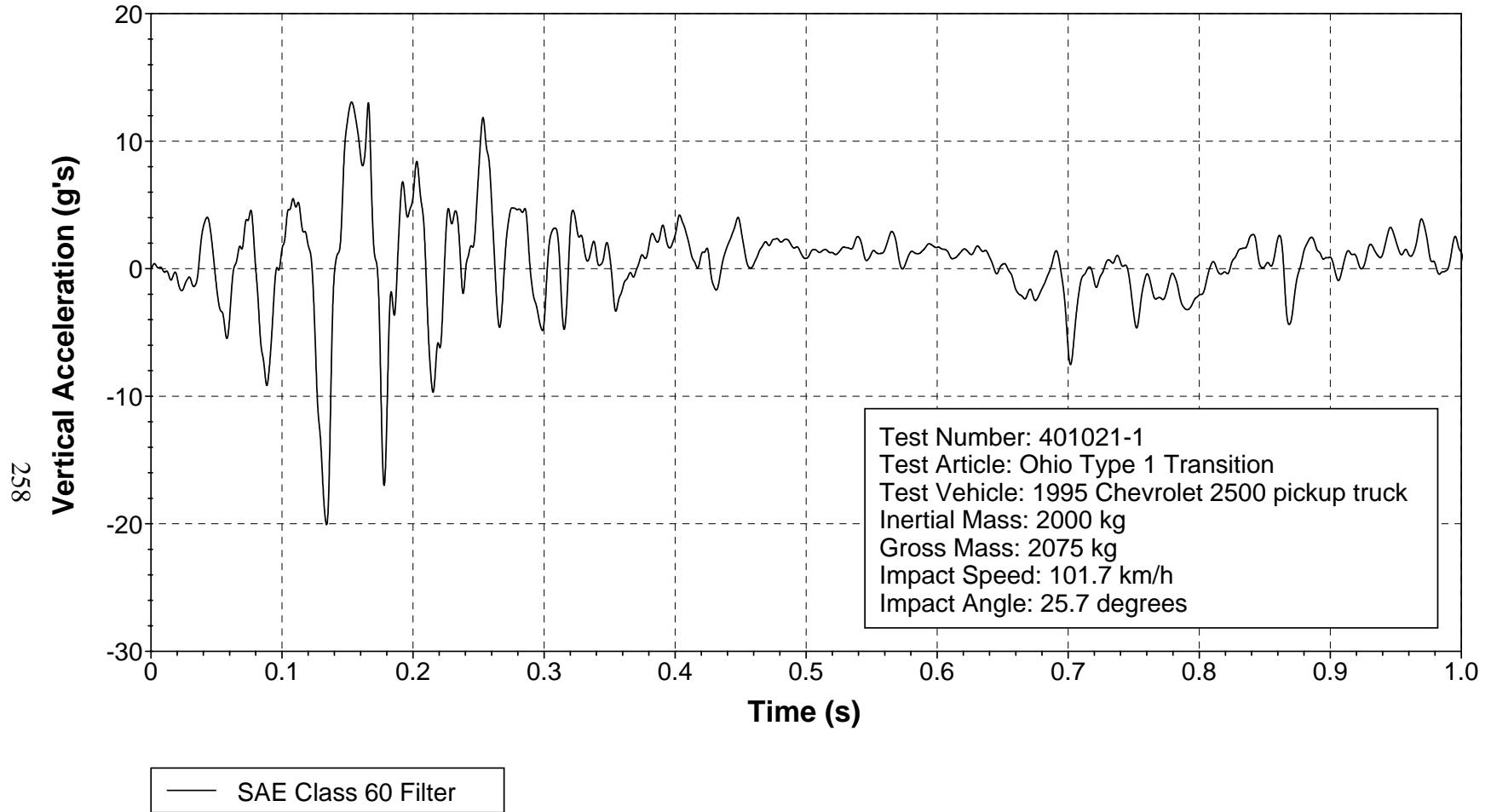


Figure 176. Vehicle vertical accelerometer trace for test 401021-1 (accelerometer located over rear axle).

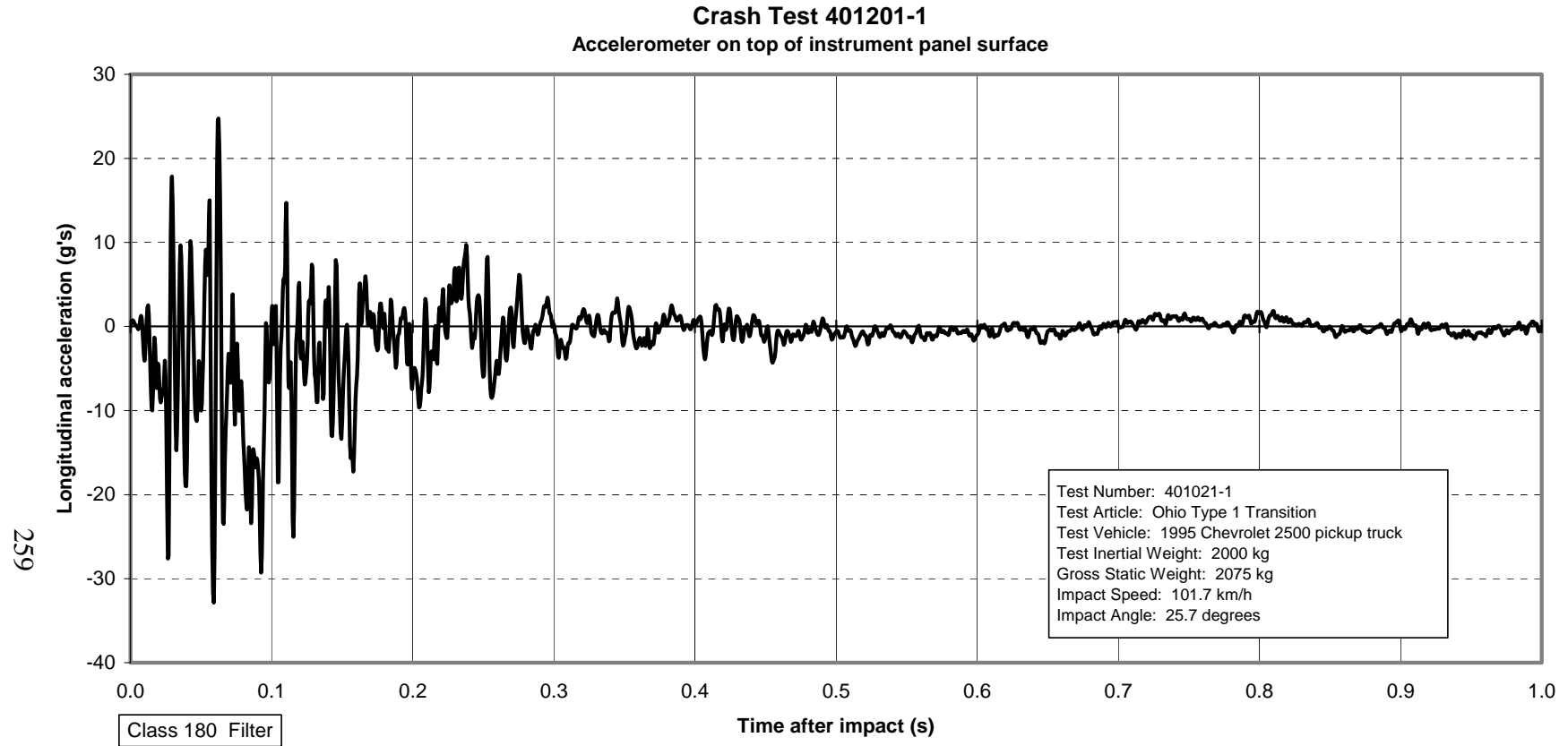


Figure 177. Vehicle longitudinal accelerometer trace for test 401021-1 (accelerometer located on top surface of instrument panel).

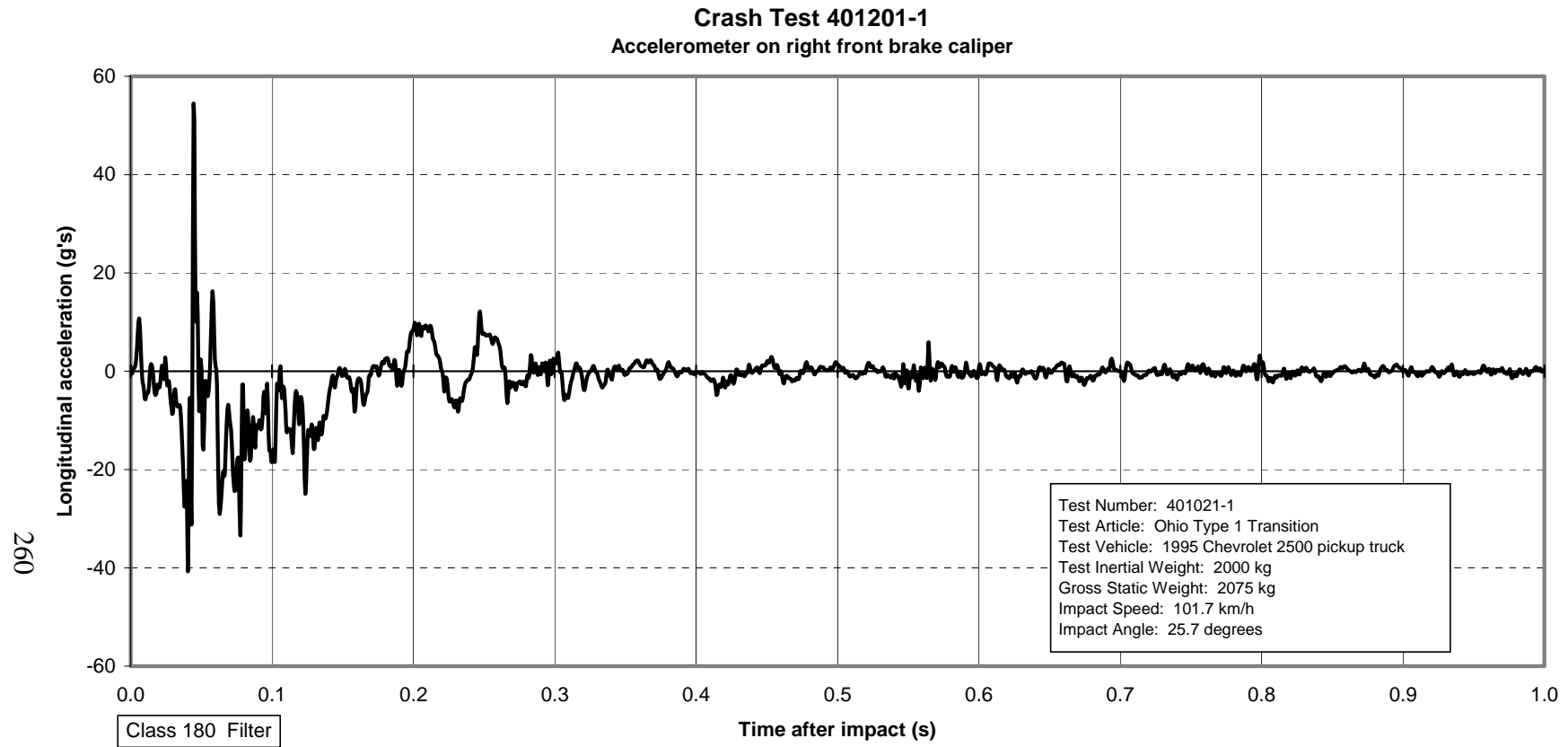


Figure 178. Vehicle longitudinal accelerometer trace for test 401021-1 (accelerometer located on right front brake caliper).

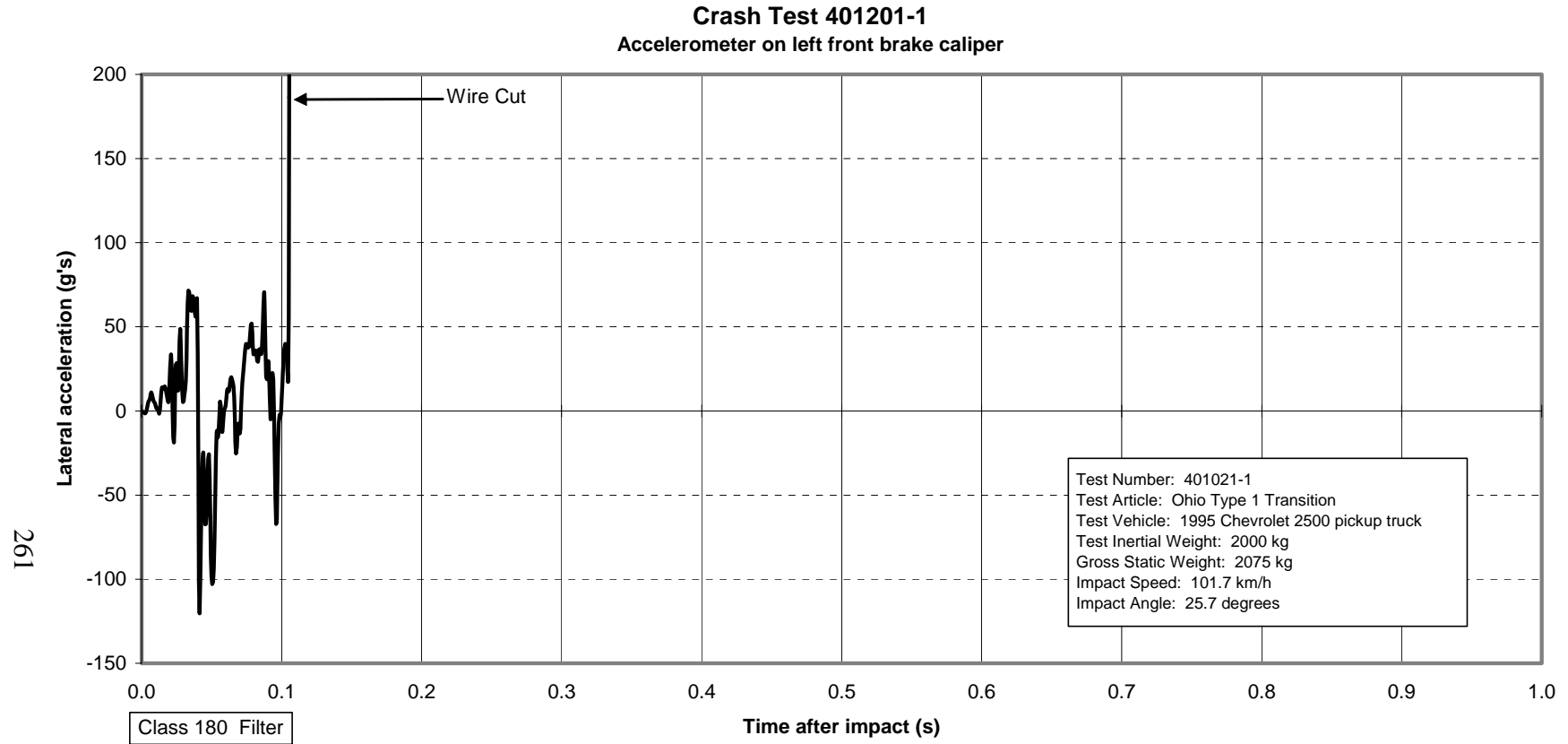


Figure 179. Vehicle lateral accelerometer trace for test 401021-1 (accelerometer located on left front brake caliper).

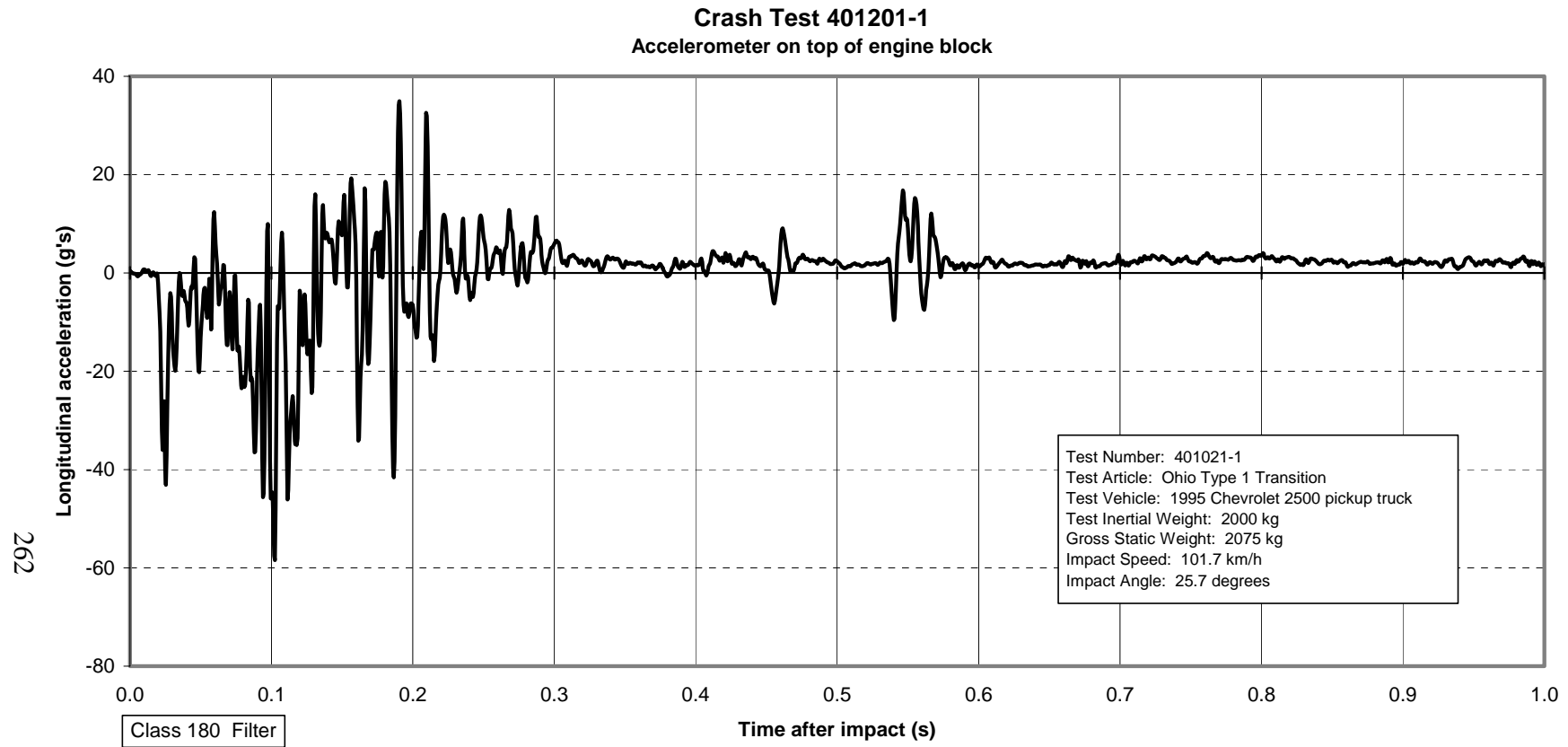


Figure 180. Vehicle longitudinal accelerometer trace for test 401021-1 (accelerometer located on top of engine block).

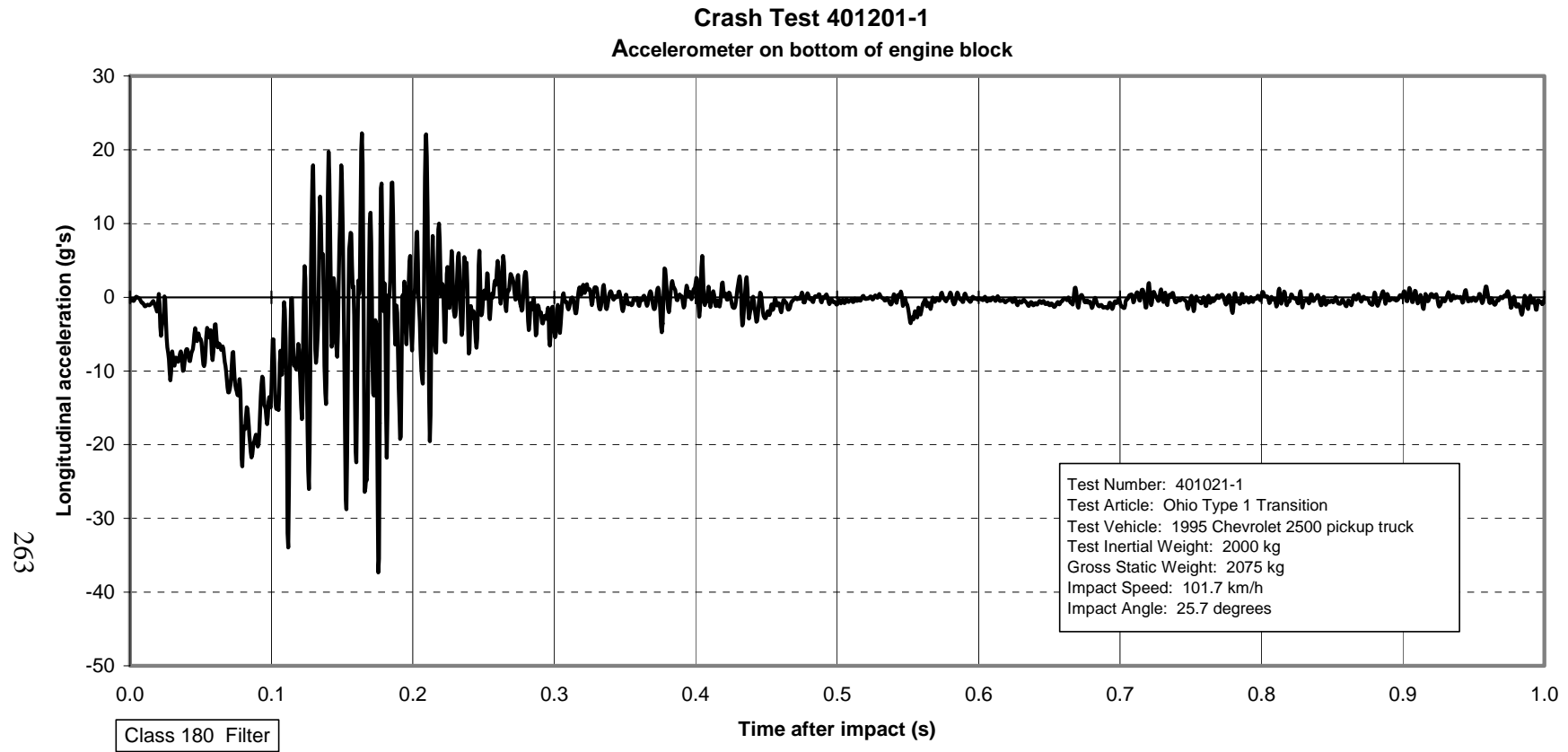


Figure 181. Vehicle longitudinal accelerometer trace for test 401021-1 (accelerometer located on bottom of engine block).

Roll, Pitch, and Yaw Angles

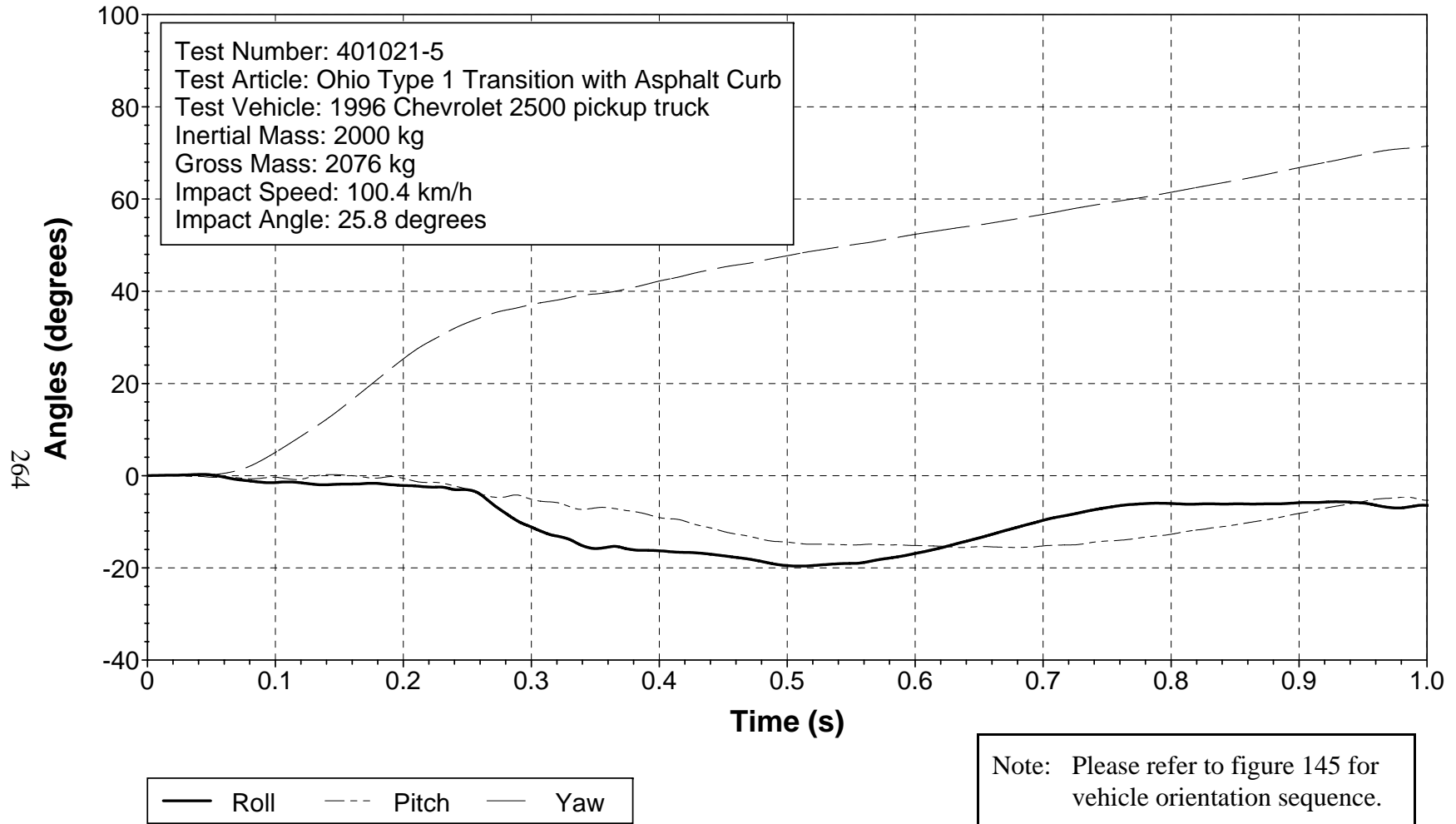


Figure 182. Vehicular angular displacements for test 401021-5.

X Acceleration at C.G.

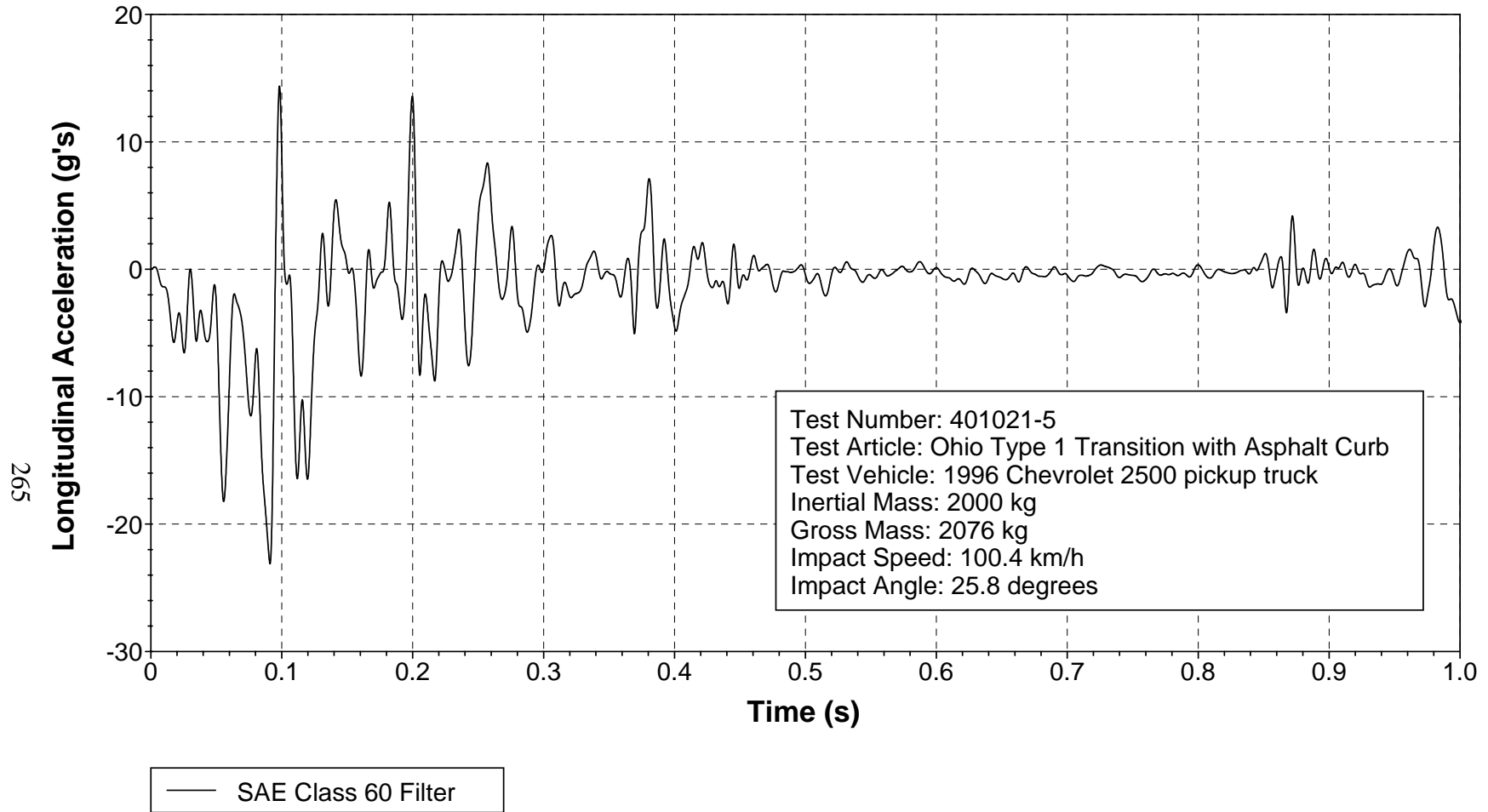


Figure 183. Vehicle longitudinal accelerometer trace for test 401021-5 (accelerometer located at center of gravity).

Y Acceleration at C.G.

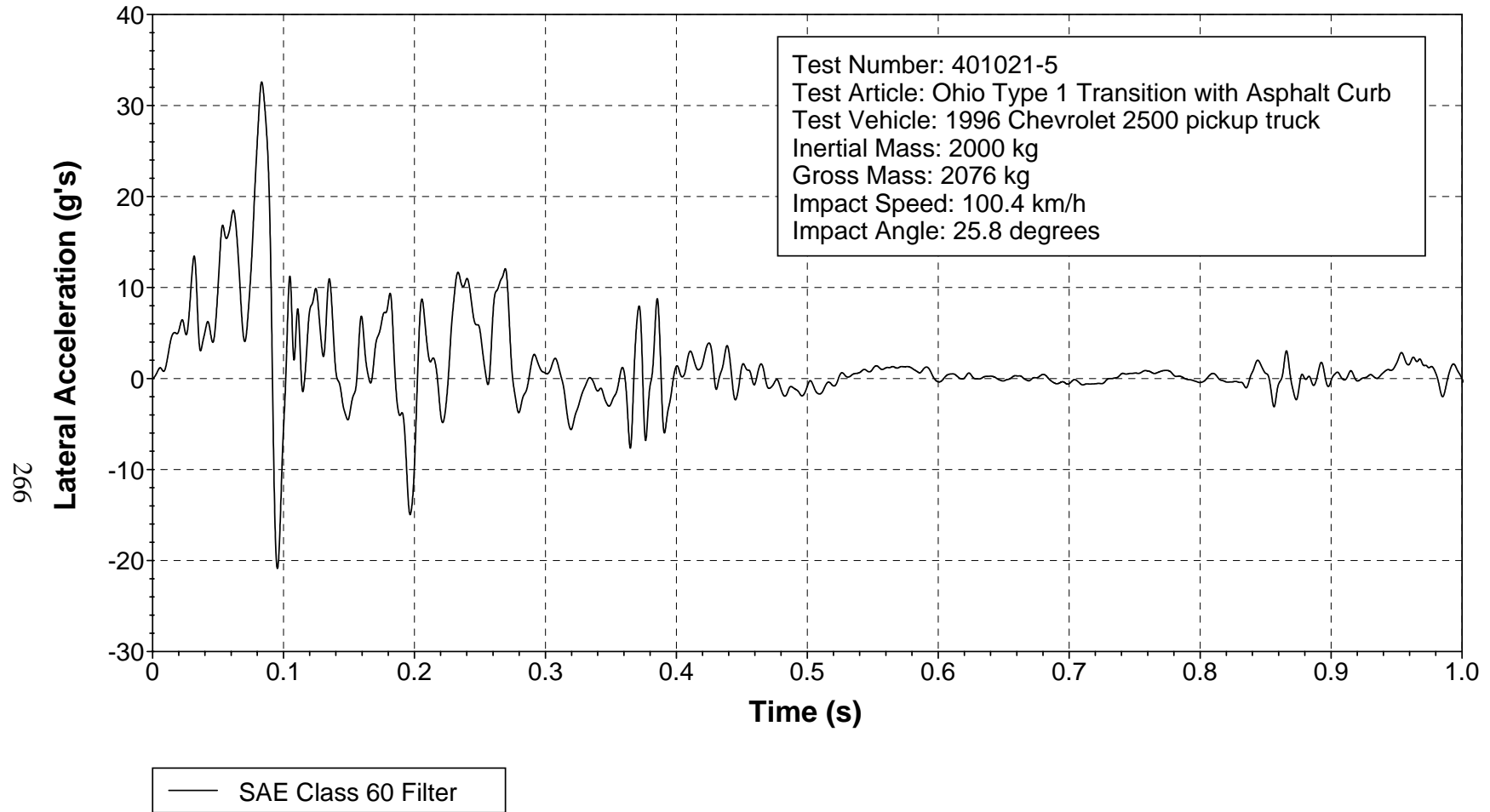


Figure 184. Vehicle lateral accelerometer trace for test 401021-5 (accelerometer located at center of gravity).

Z Acceleration at C.G.

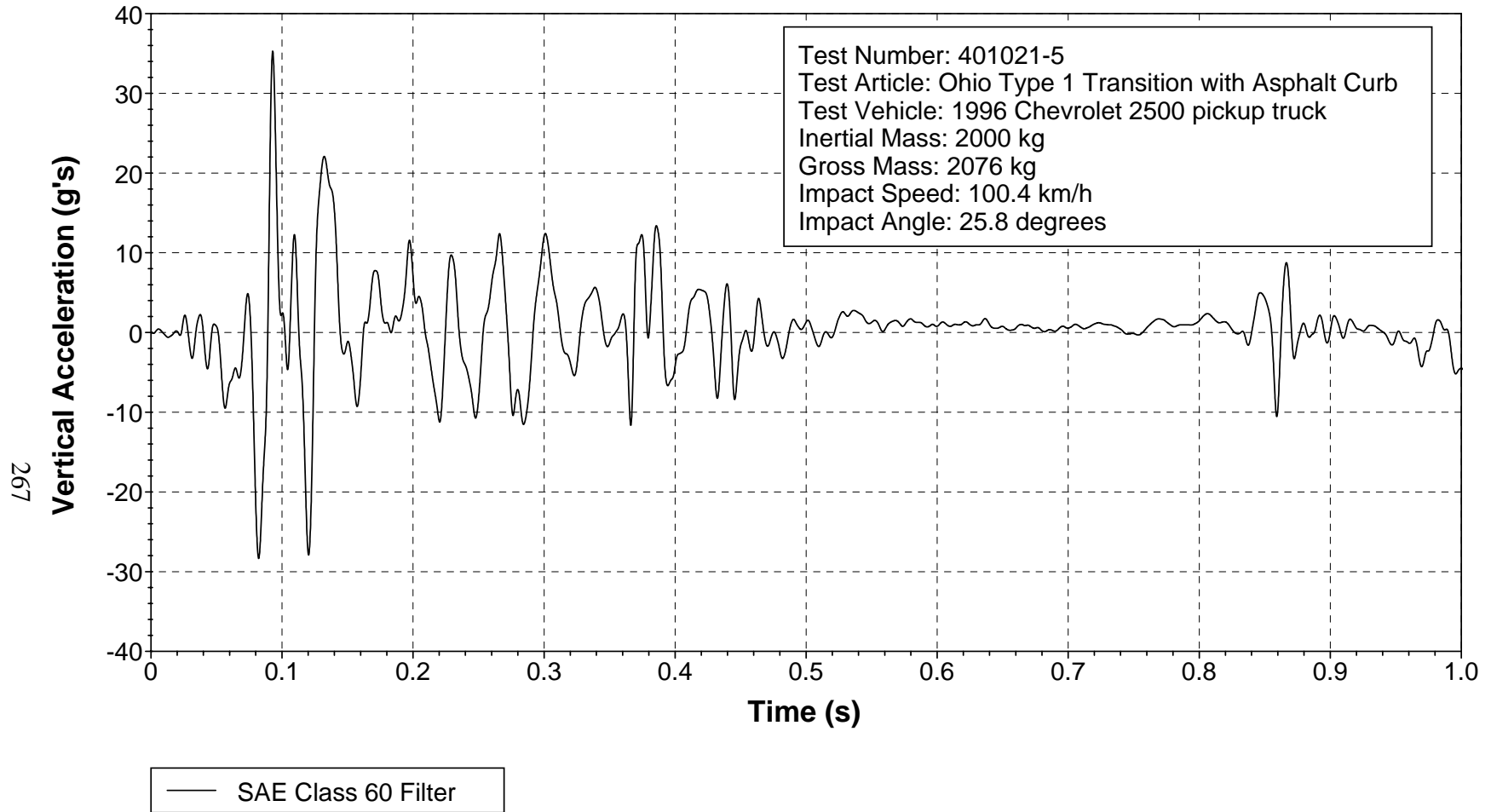


Figure 185. Vehicle vertical accelerometer trace for test 401021-5 (accelerometer located at center of gravity).

X Acceleration over Rear Axle

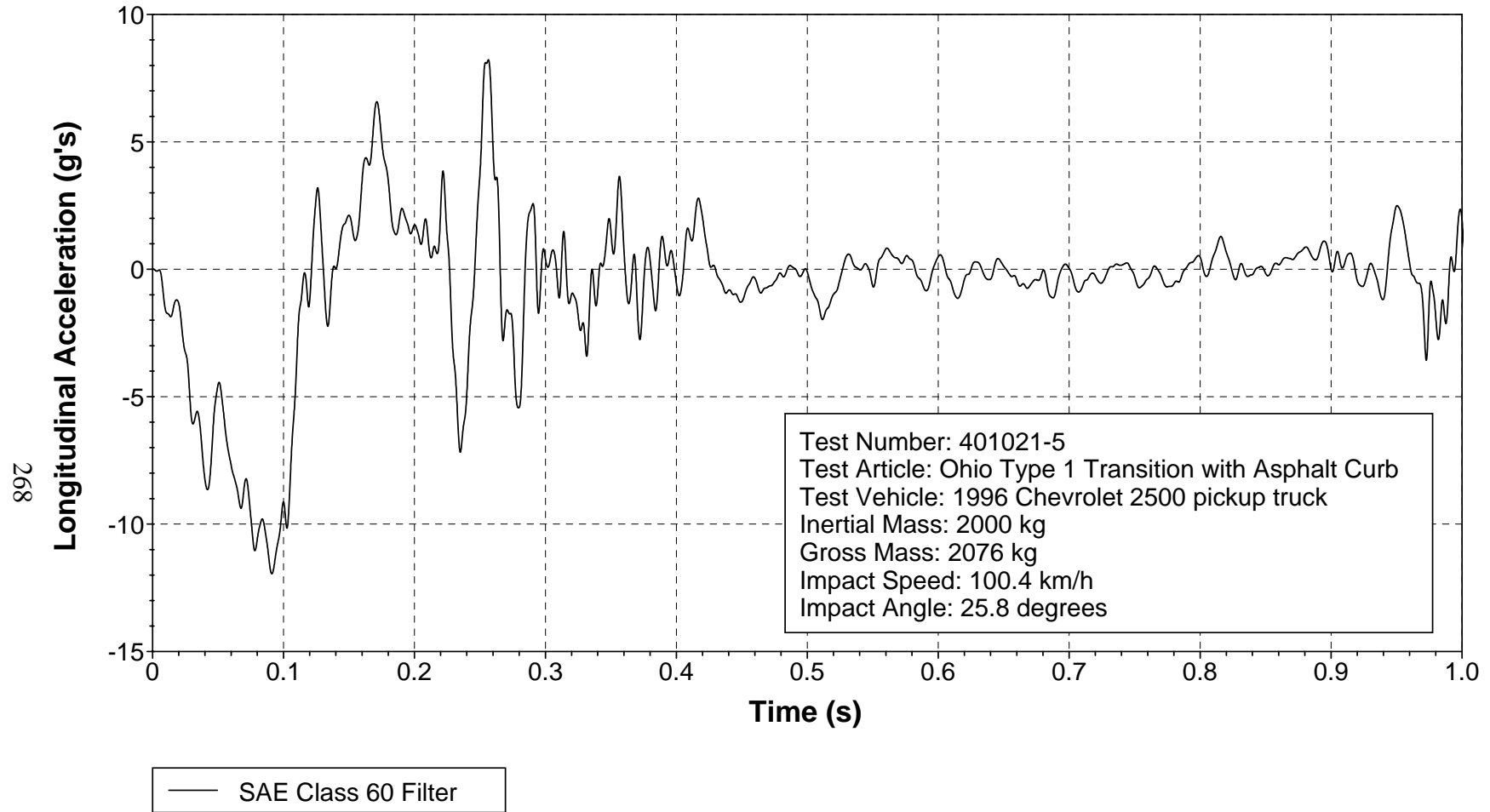


Figure 186. Vehicle longitudinal accelerometer trace for test 401021-5 (accelerometer located over rear axle).

Y Acceleration over Rear Axle

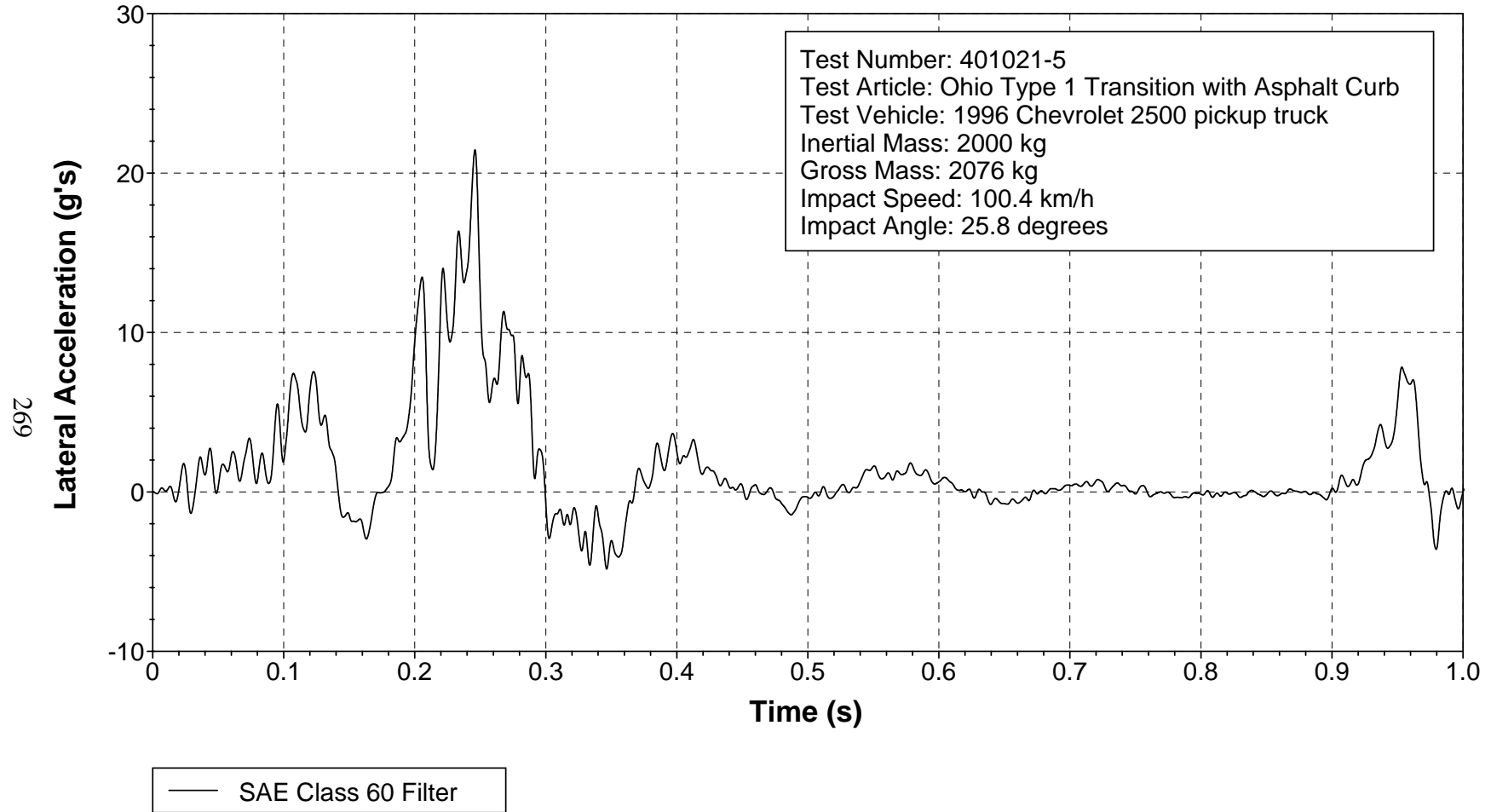


Figure 187. Vehicle lateral accelerometer trace for test 401021-5 (accelerometer located over rear axle).

Z Acceleration over Rear Axle

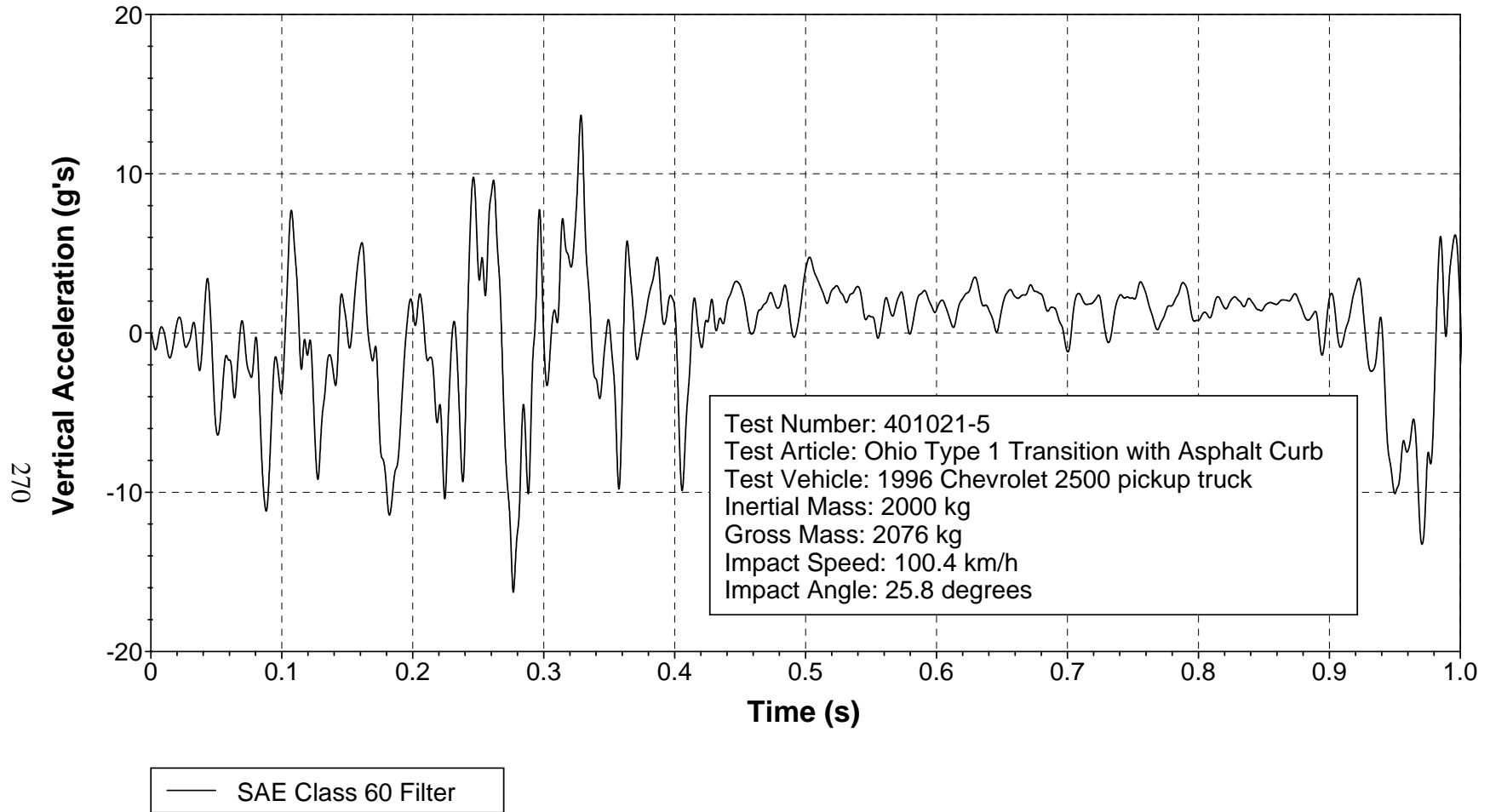


Figure 188. Vehicle vertical accelerometer trace for test 401021-5 (accelerometer located over rear axle).

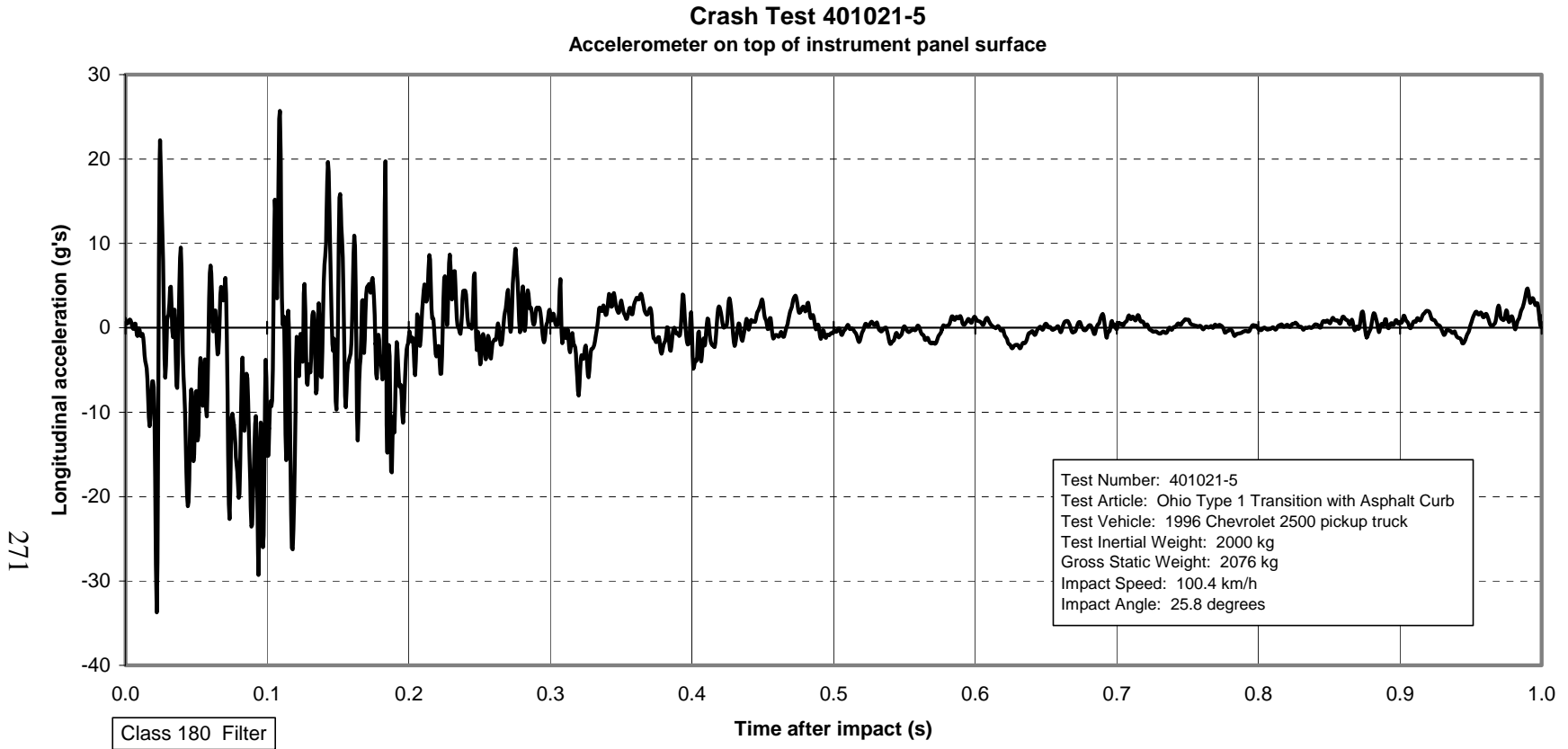


Figure 189. Vehicle longitudinal accelerometer trace for test 401021-5 (accelerometer located on top surface of instrument panel).

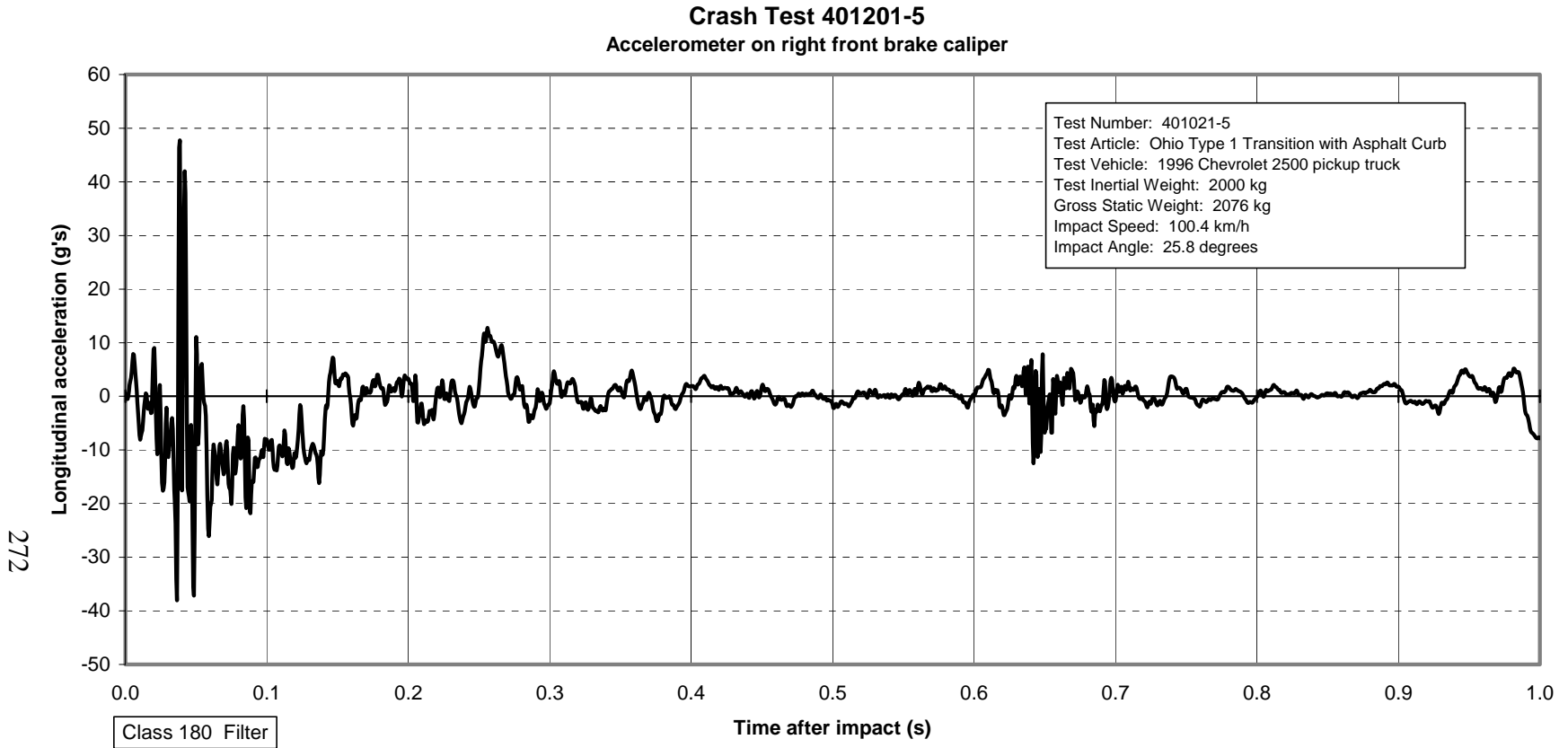


Figure 190. Vehicle longitudinal accelerometer trace for test 401021-5 (accelerometer located on right front brake caliper).

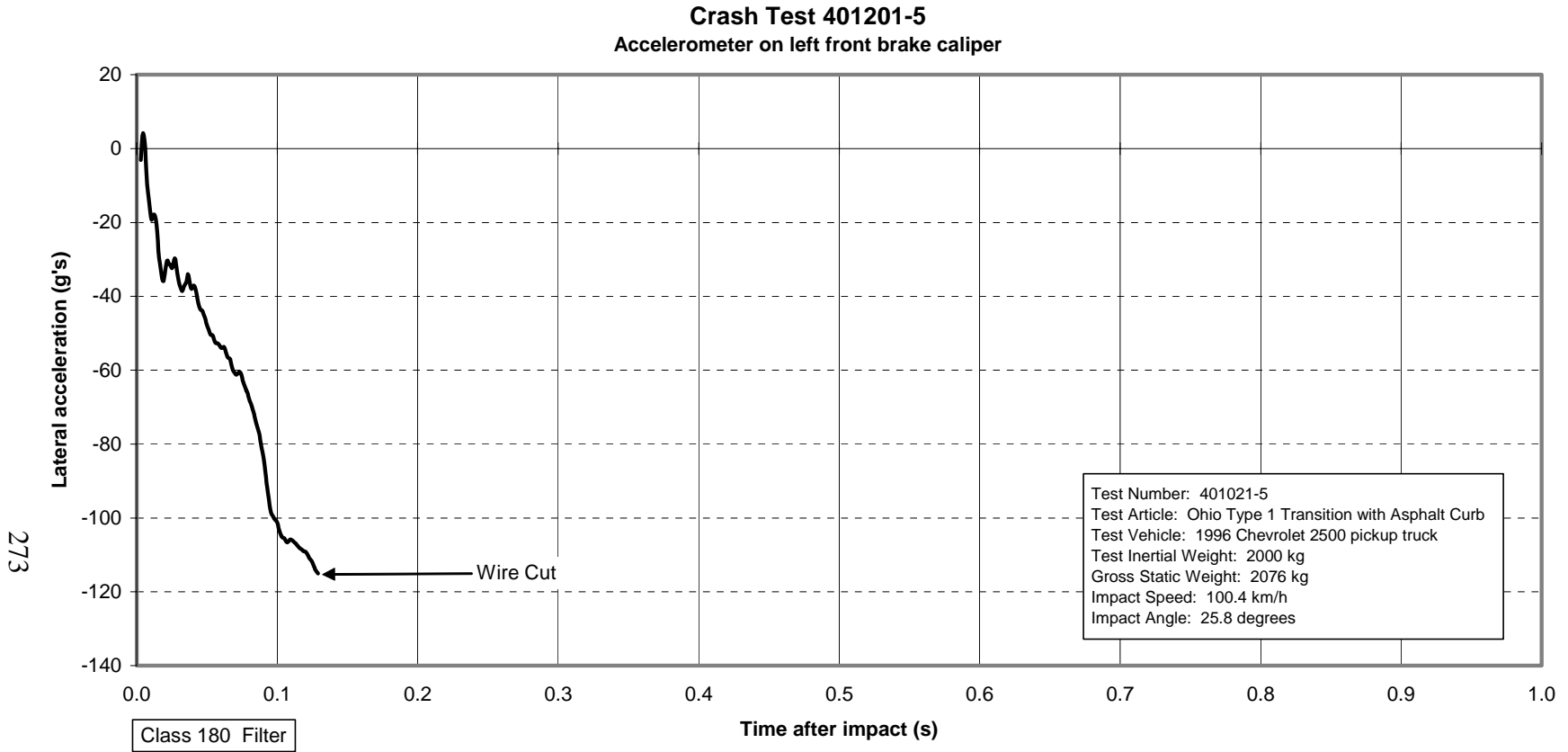


Figure 191. Vehicle lateral accelerometer trace for test 401021-5 (accelerometer located on left front brake caliper).

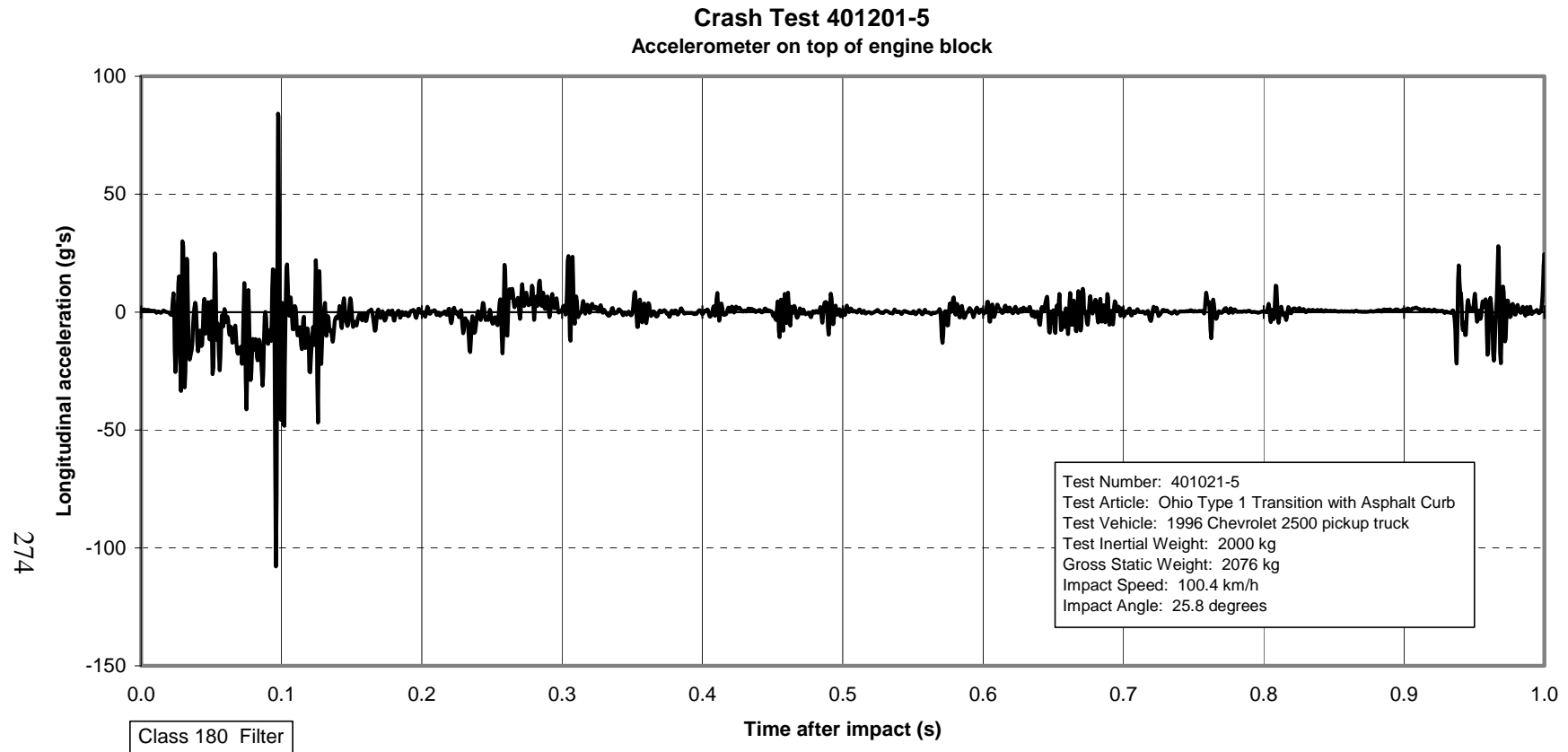


Figure 192. Vehicle longitudinal accelerometer trace for test 401021-5 (accelerometer located on top of engine block).

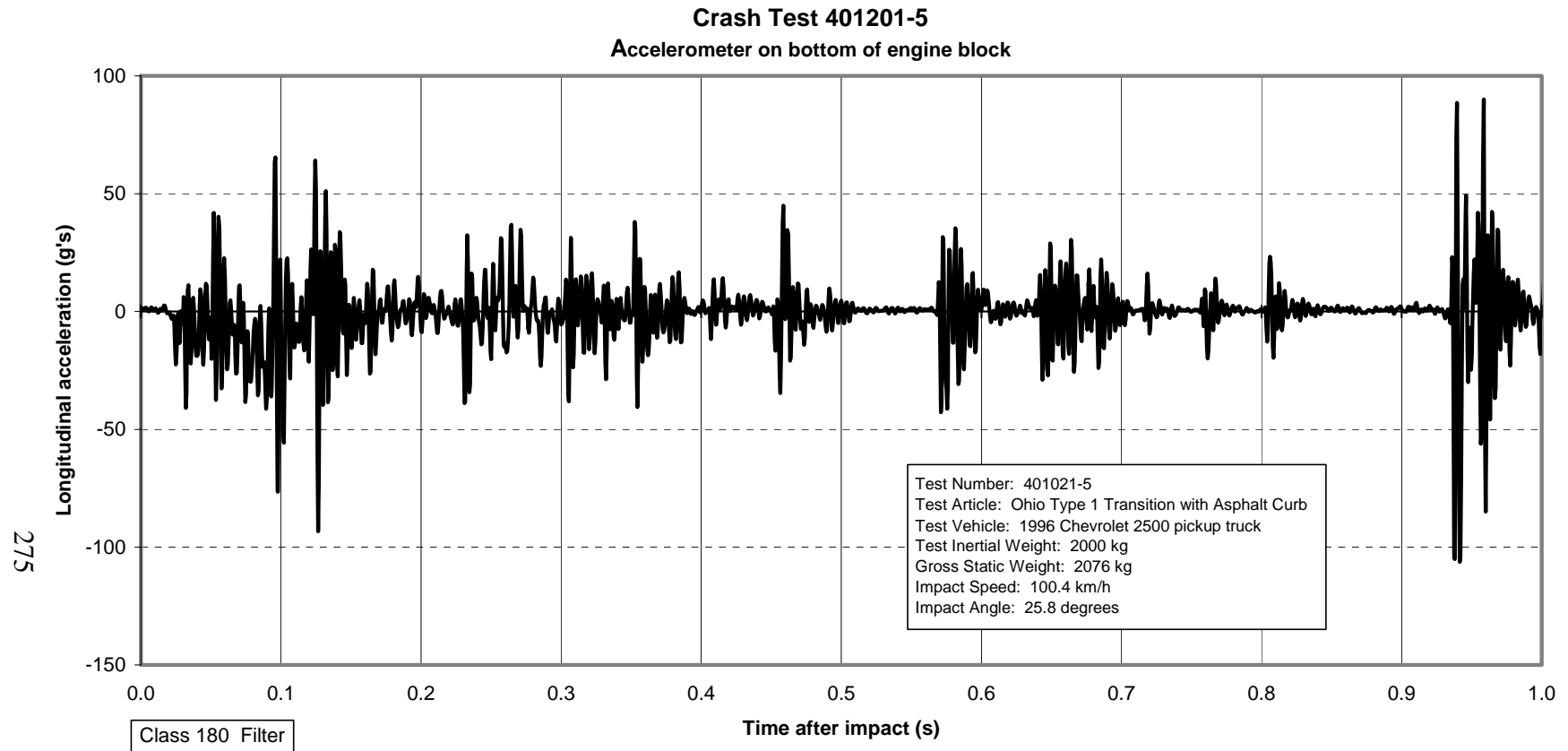


Figure 193. Vehicle longitudinal accelerometer trace for test 401021-5 (accelerometer located on bottom of engine block).

Roll, Pitch, and Yaw Angles

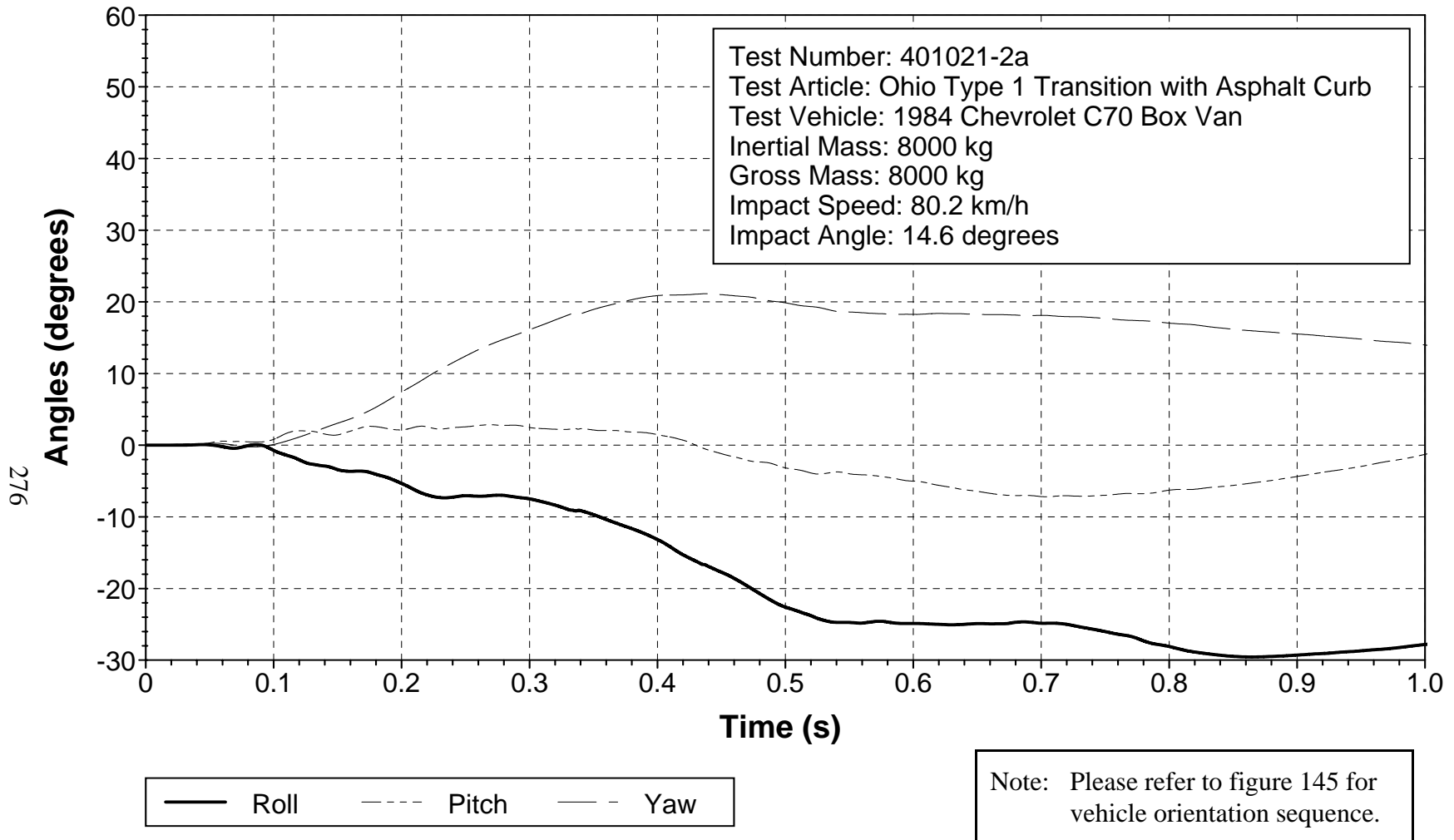


Figure 194. Vehicular angular displacements for test 401021-2a.

X Acceleration at C.G.

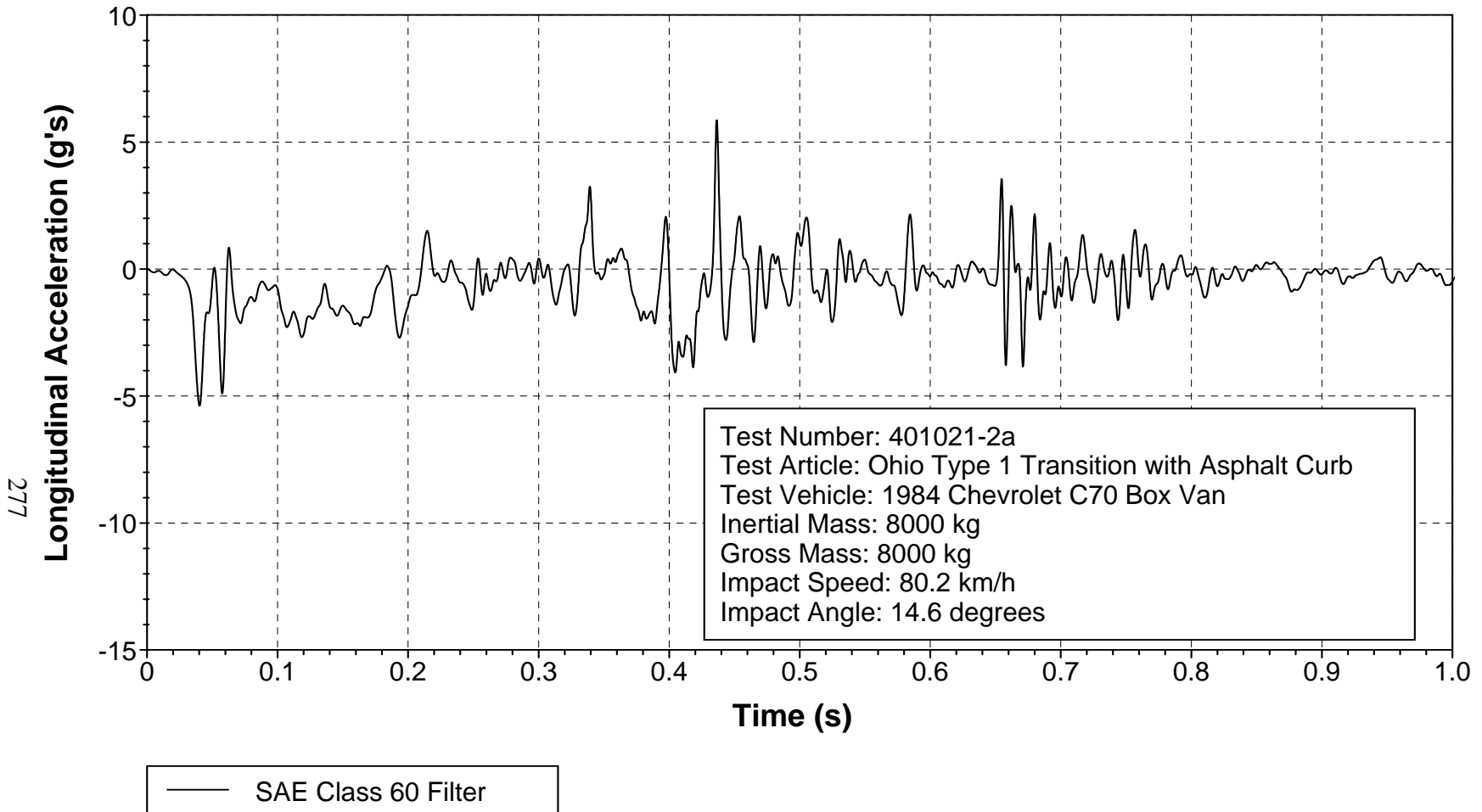


Figure 195. Vehicle longitudinal accelerometer trace for test 401021-2a (accelerometer located at center of gravity).

Y Acceleration at C.G.

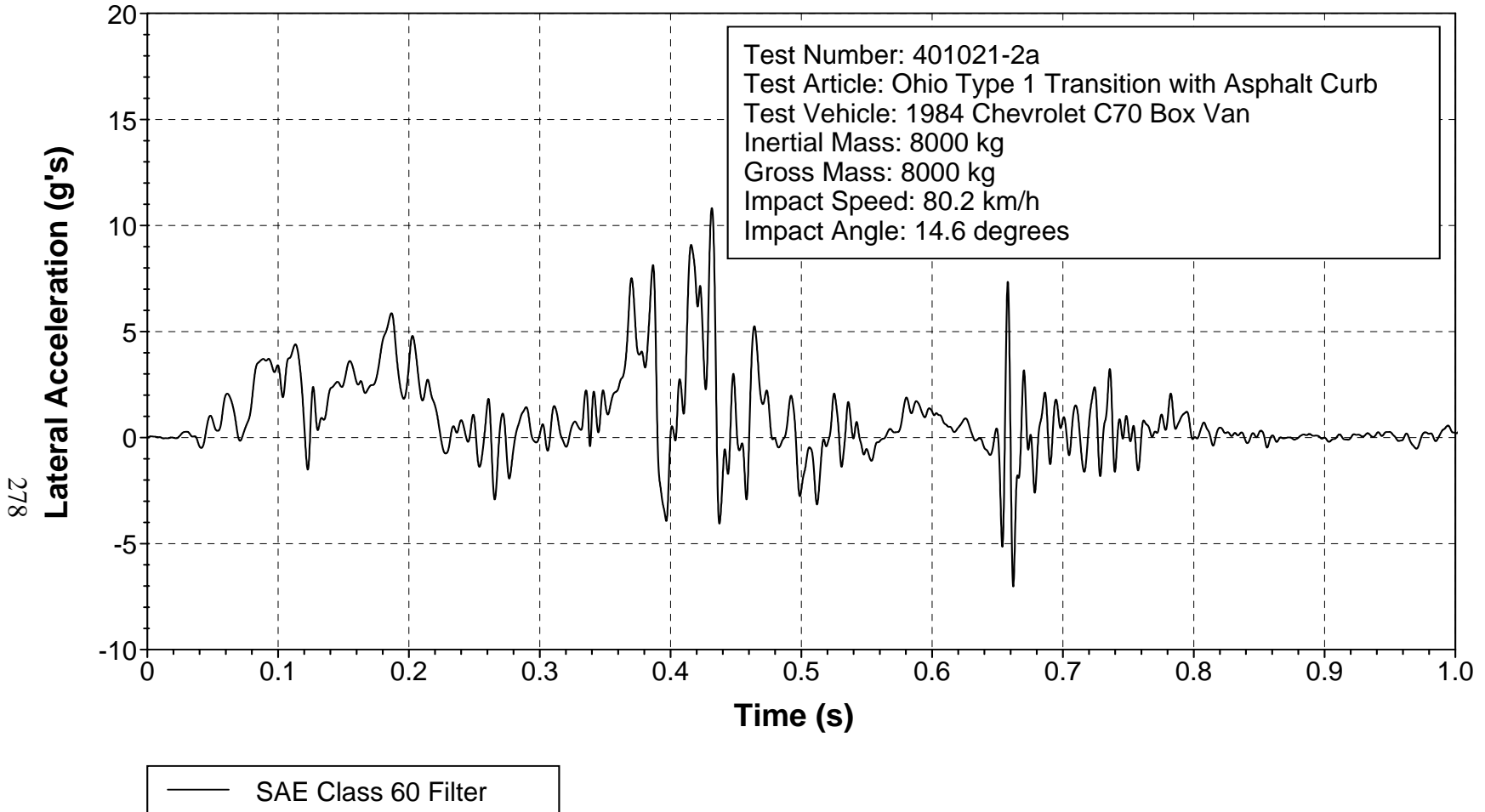


Figure 196. Vehicle lateral accelerometer trace for test 401021-2a (accelerometer located at center of gravity).

Z Acceleration at C.G.

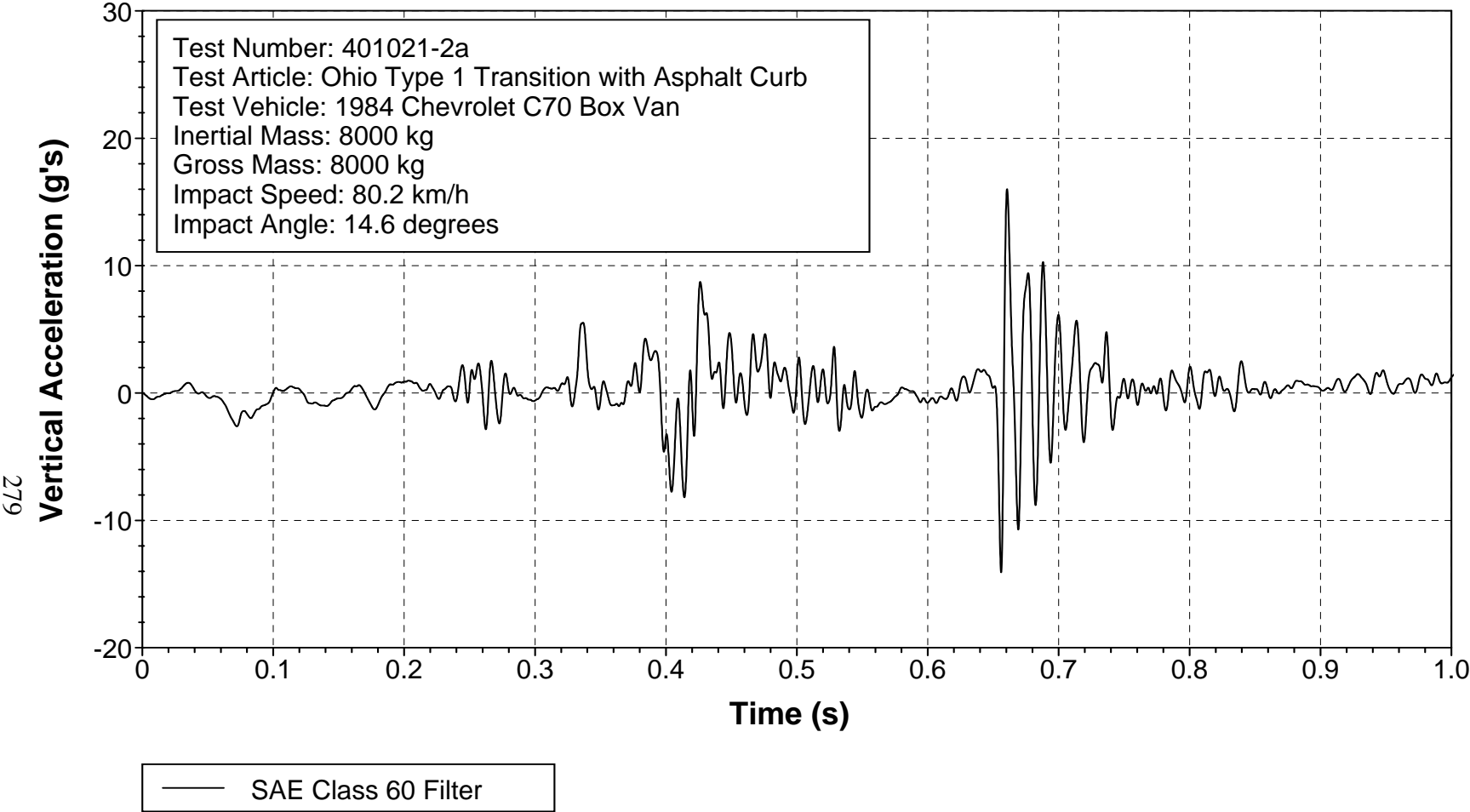


Figure 197. Vehicle vertical accelerometer trace for test 401021-2a (accelerometer located at center of gravity).

X Acceleration in Vehicle Cab

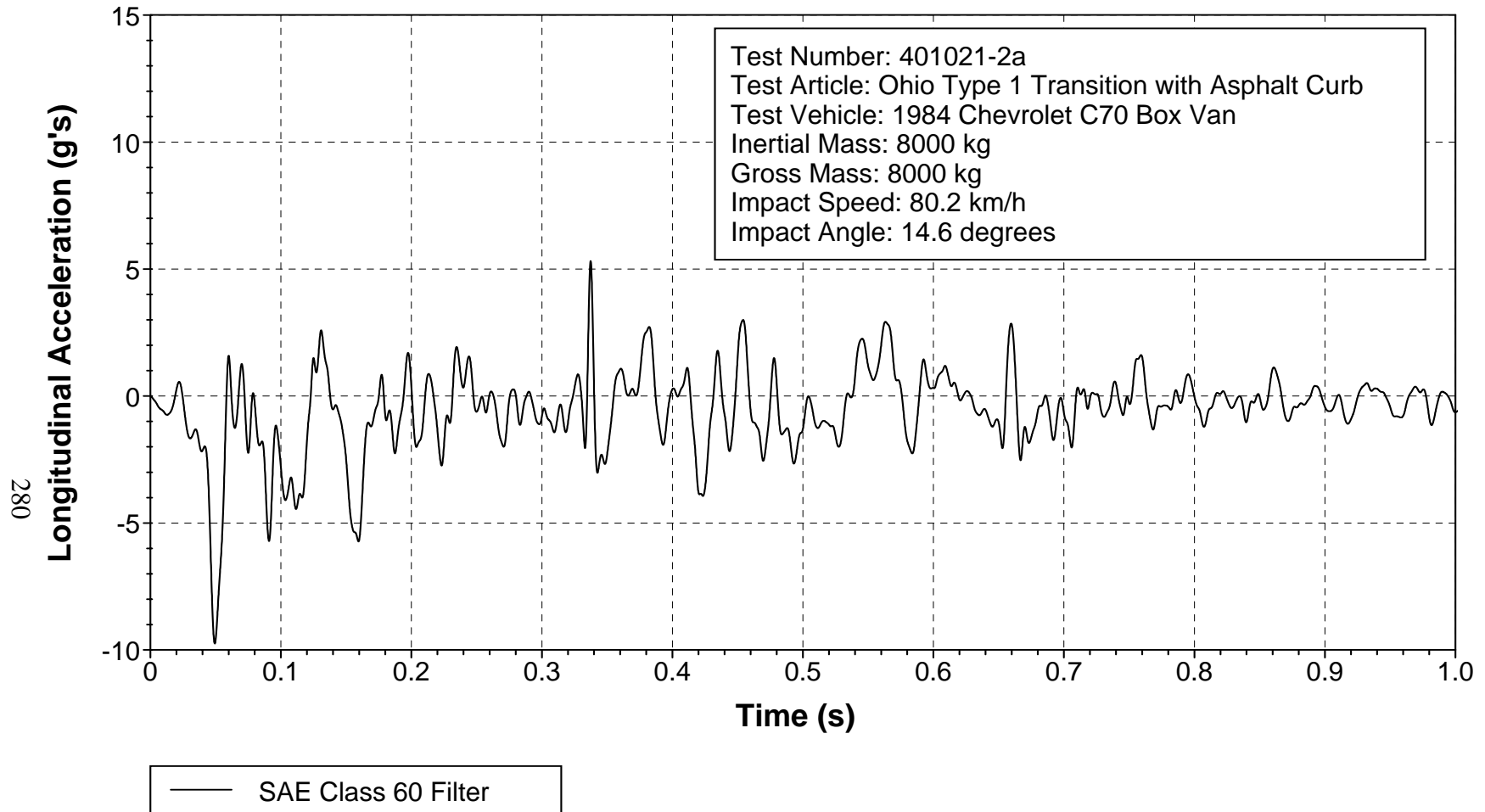


Figure 198. Vehicle longitudinal accelerometer trace for test 401021-2a
(accelerometer located in vehicle cab).

Y Acceleration in Vehicle Cab

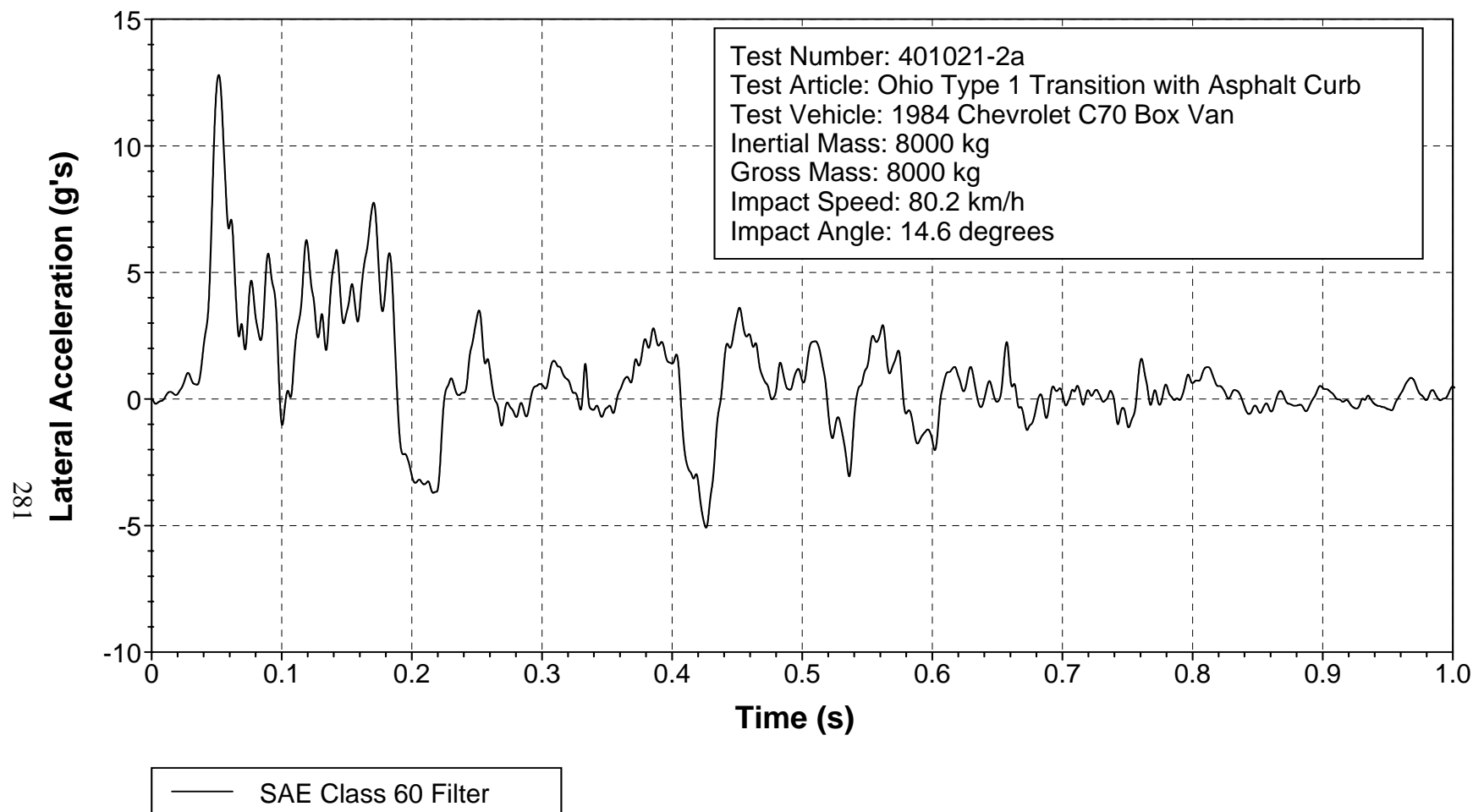


Figure 199. Vehicle lateral accelerometer trace for test 401021-2a (accelerometer located in vehicle cab).

X Acceleration over Rear Axle

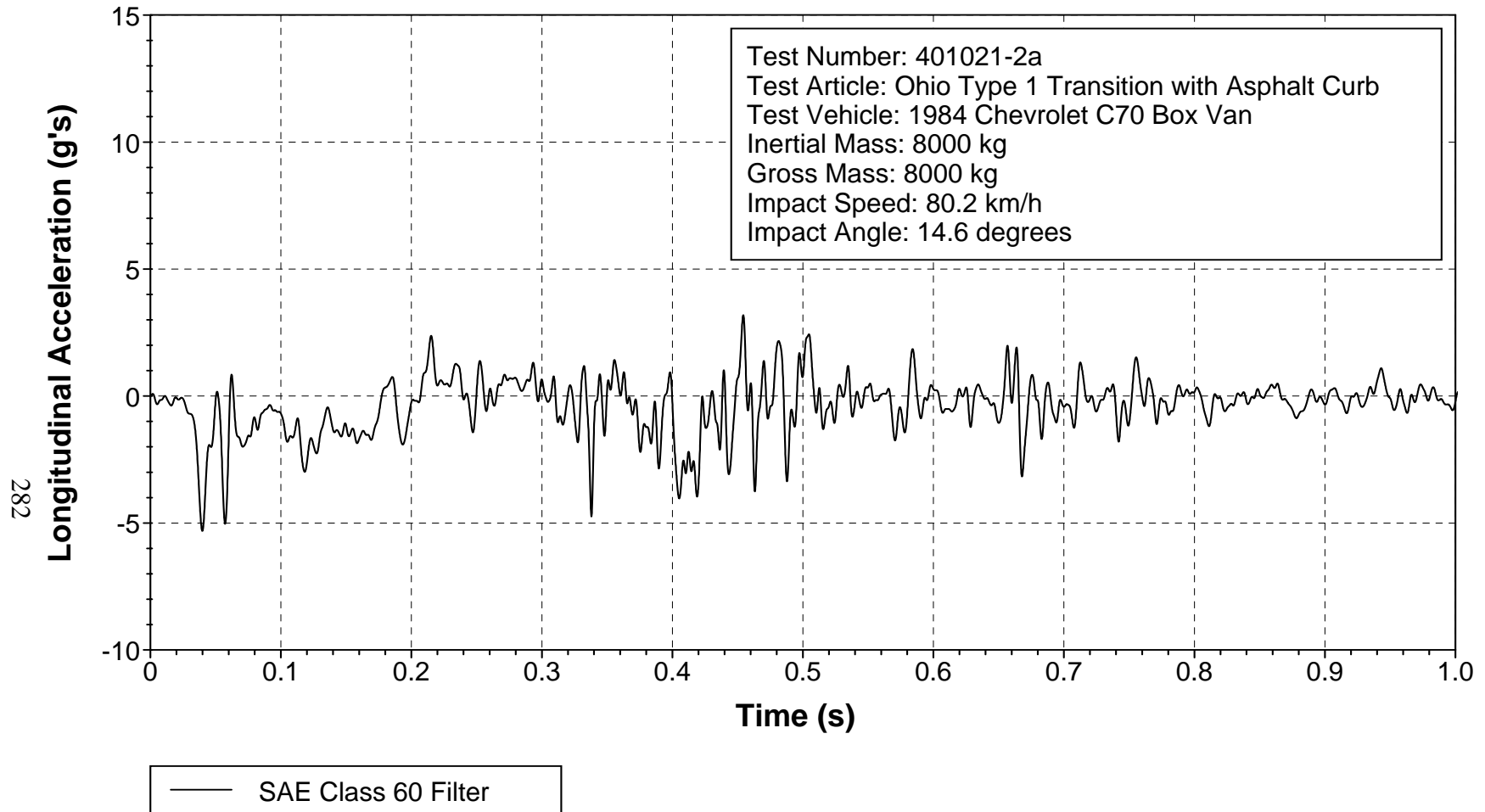


Figure 200. Vehicle longitudinal accelerometer trace for test 401021-2a (accelerometer located over rear axle).

Y Acceleration over Rear Axle

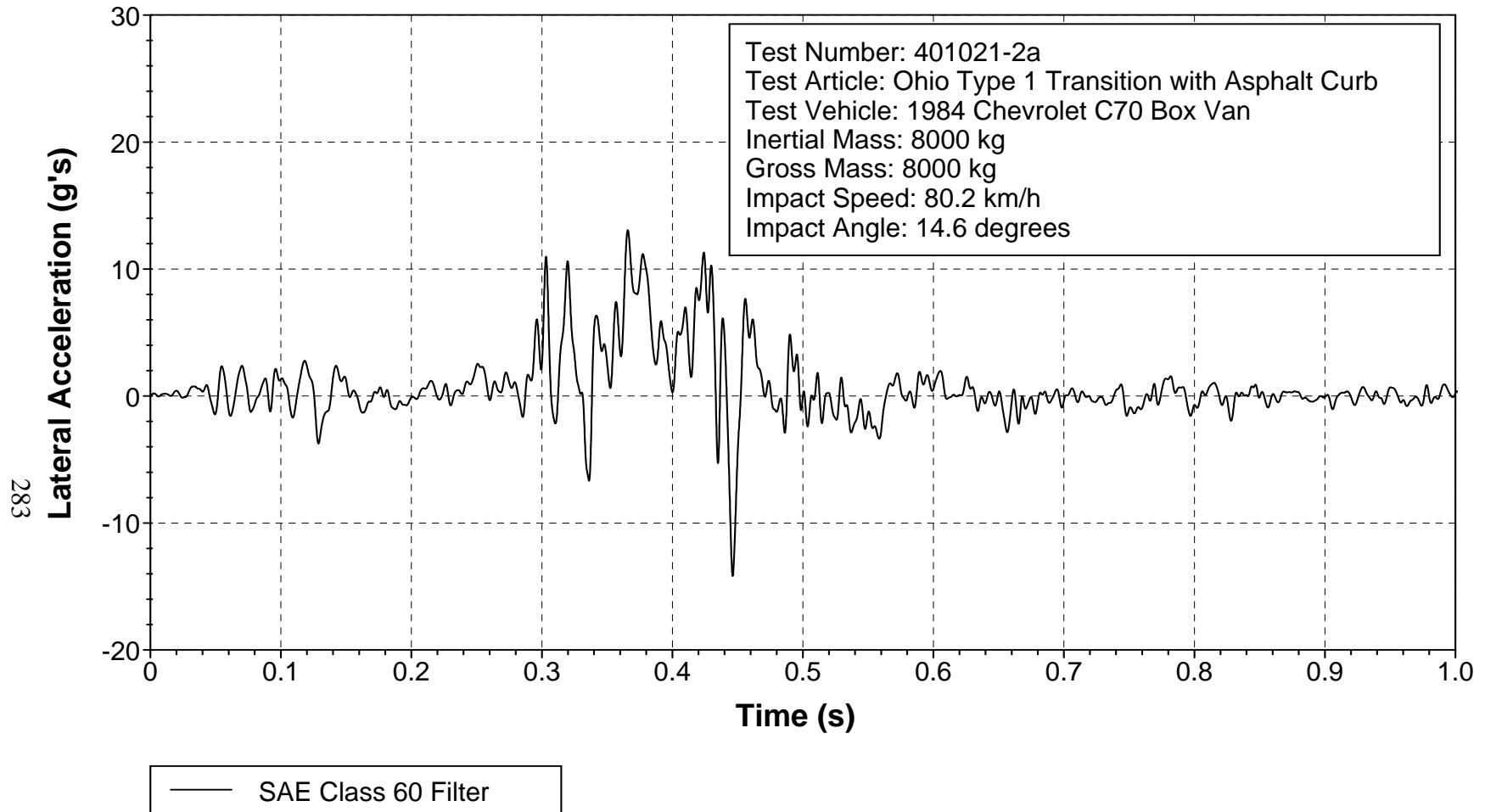


Figure 201. Vehicle lateral accelerometer trace for test 401021-2a (accelerometer located over rear axle).

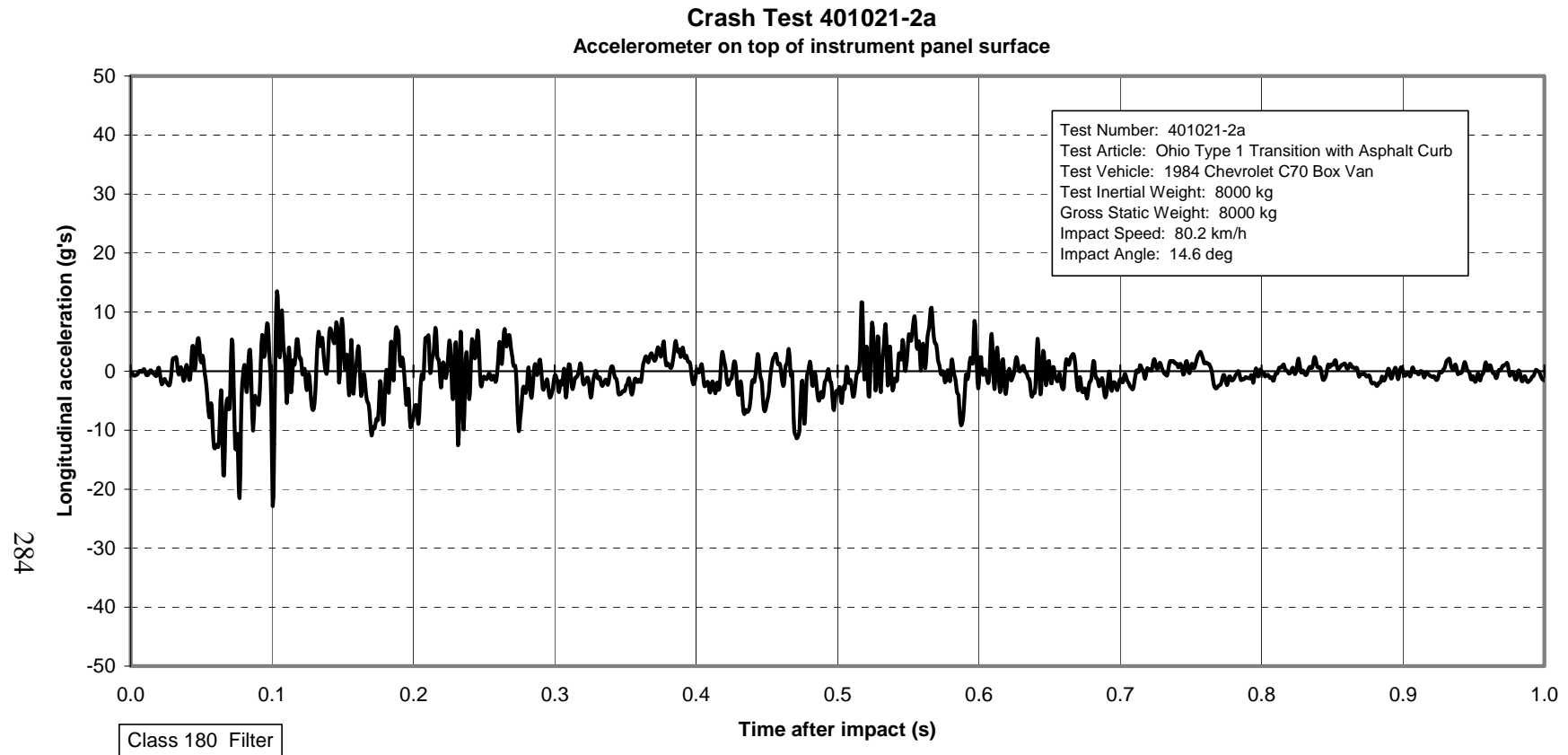


Figure 202. Vehicle longitudinal accelerometer trace for test 401021-2a (accelerometer located on top surface of instrument panel).

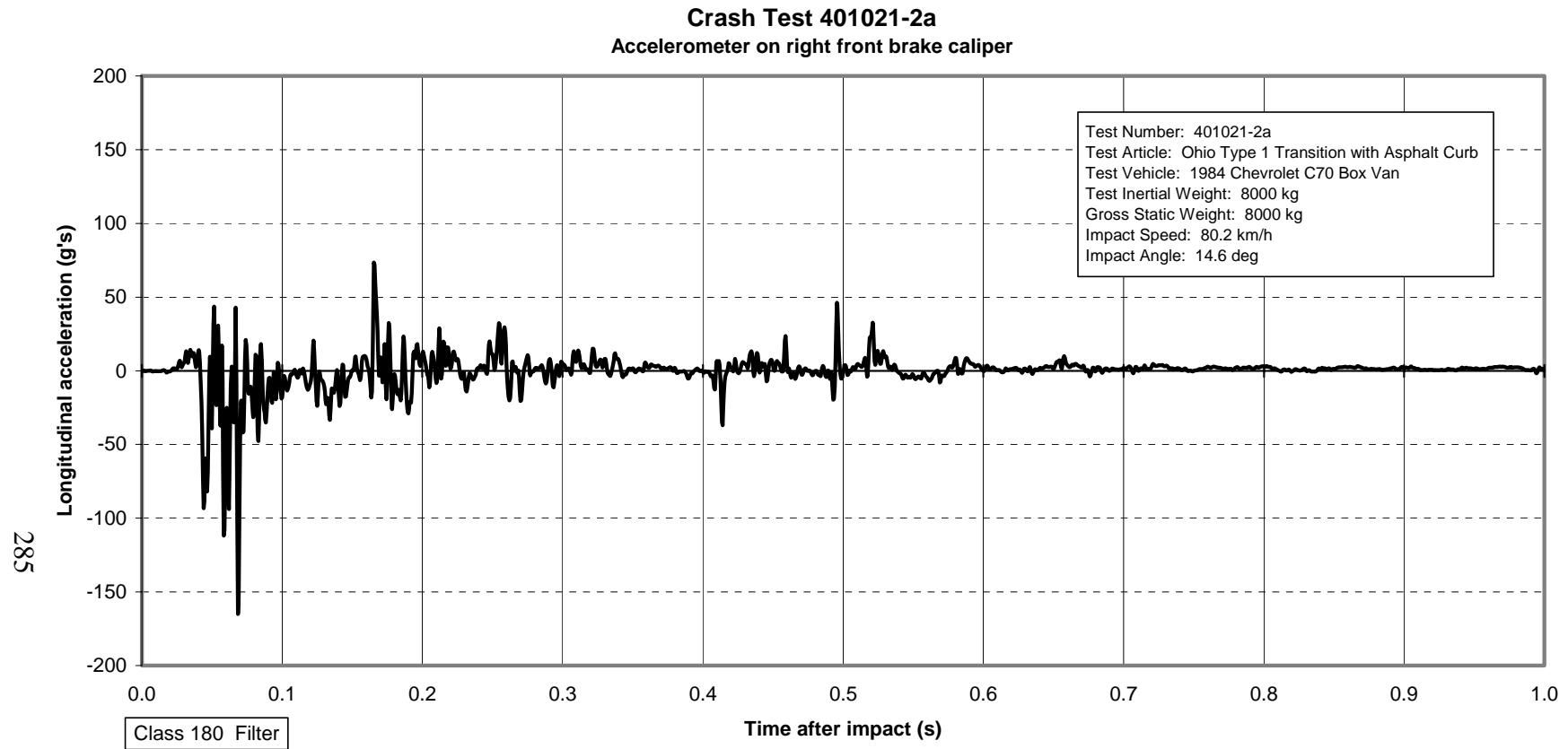


Figure 203. Vehicle longitudinal accelerometer trace for test 401021-2a (accelerometer located on right front brake caliper).

Crash Test 401021-2a
Accelerometer on left front brake caliper

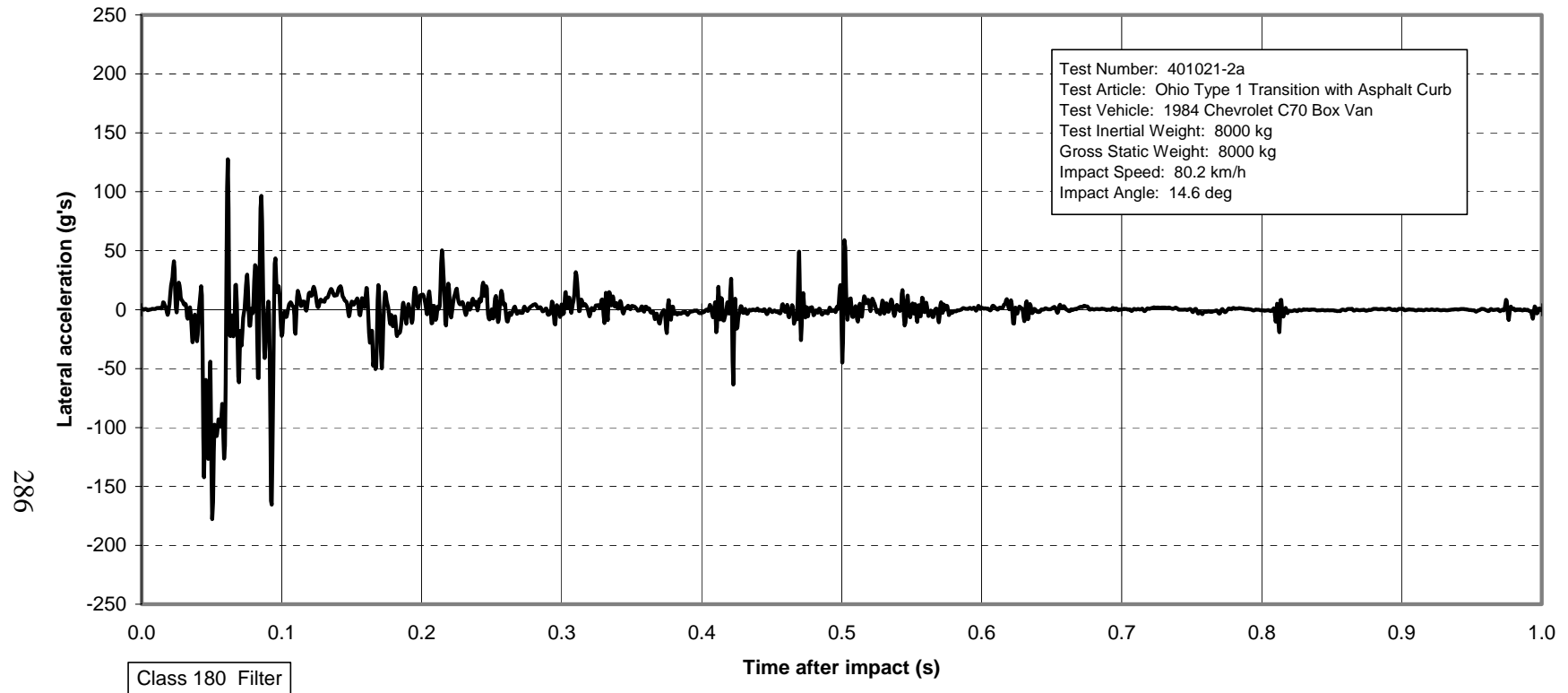


Figure 204. Vehicle lateral accelerometer trace for test 401021-2a
(accelerometer located on left front brake caliper).

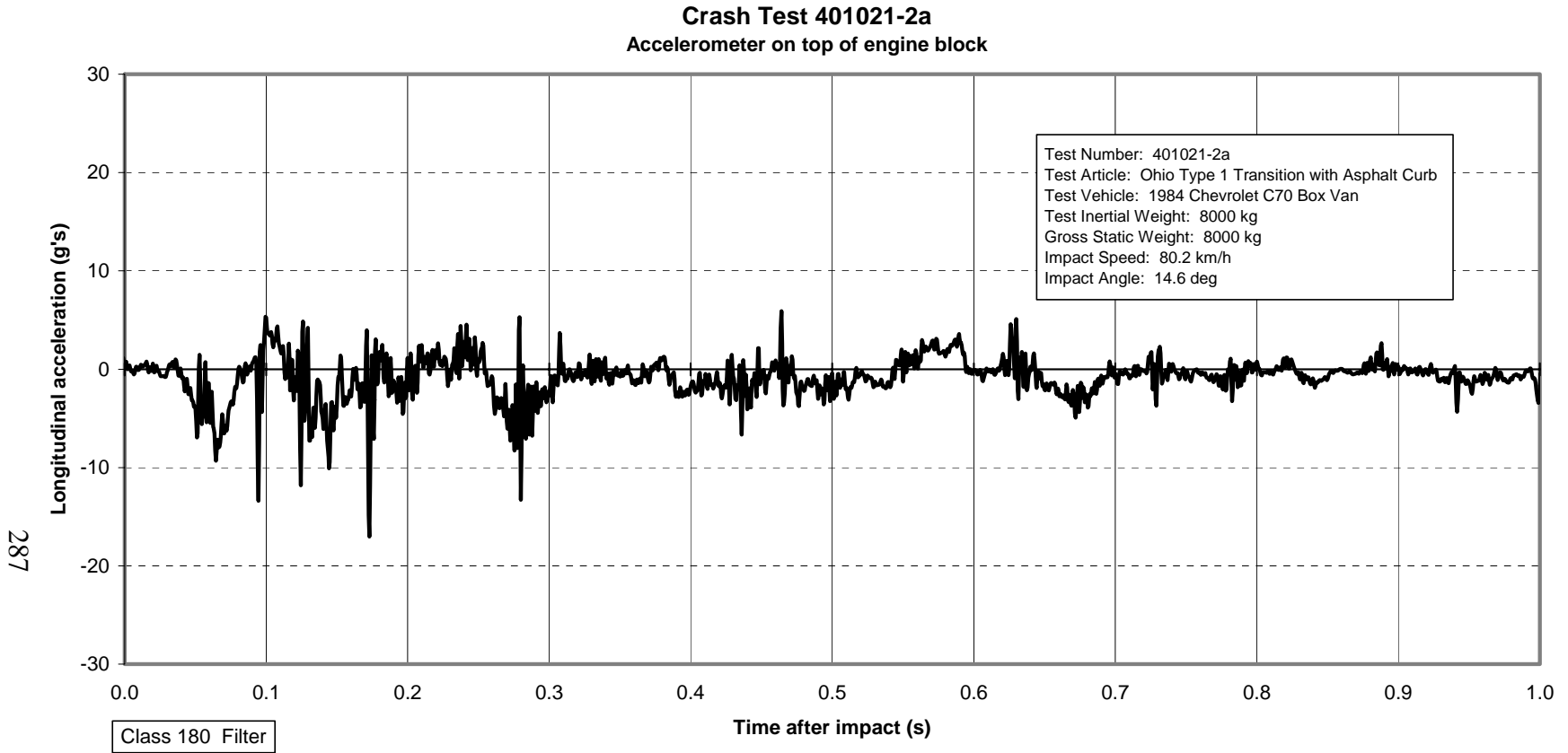


Figure 205. Vehicle longitudinal accelerometer trace for test 401021-2a (accelerometer located on top of engine block).

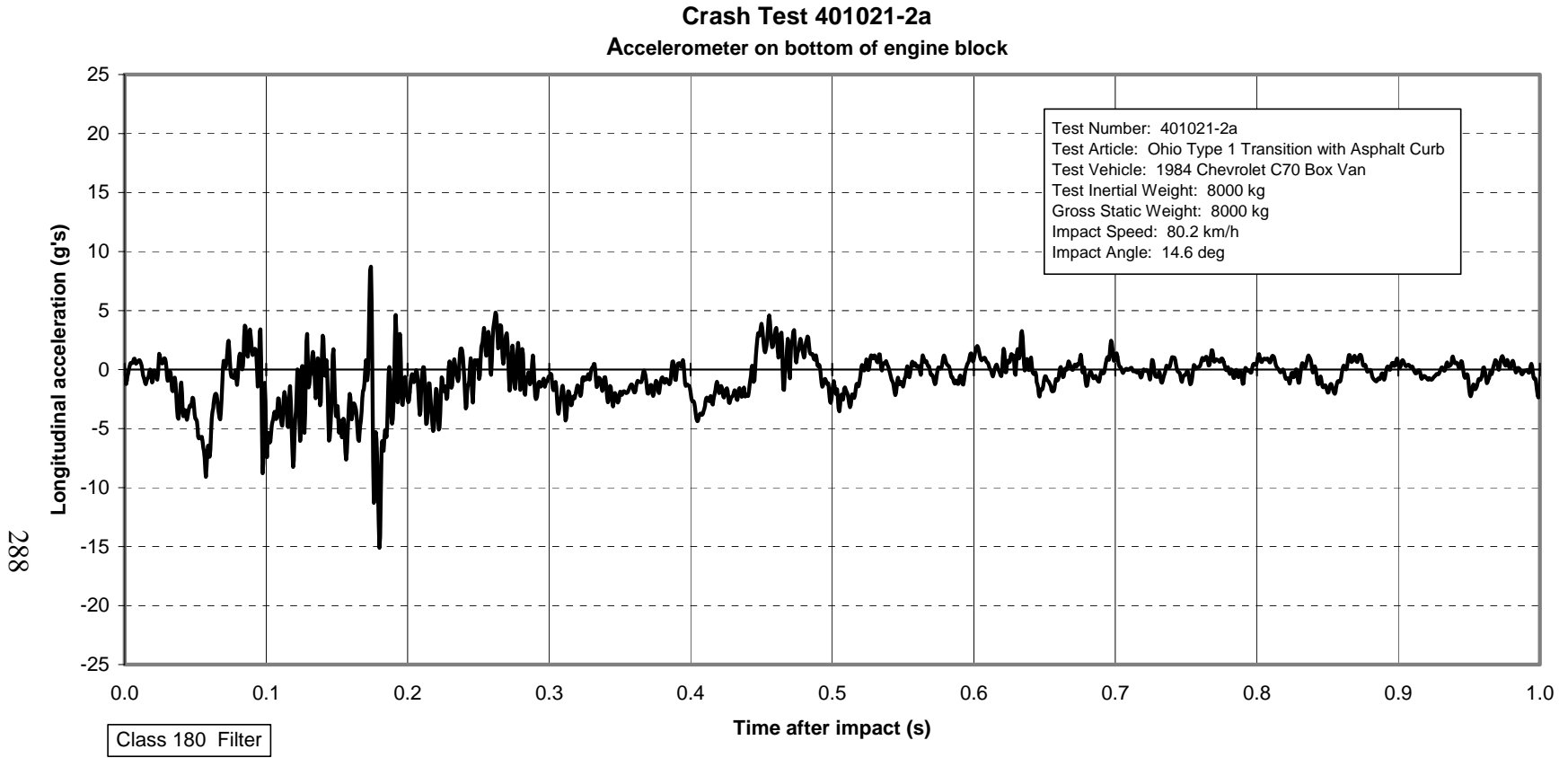


Figure 206. Vehicle longitudinal accelerometer trace for test 401021-2a (accelerometer located on bottom of engine block).

Roll, Pitch, and Yaw Angles

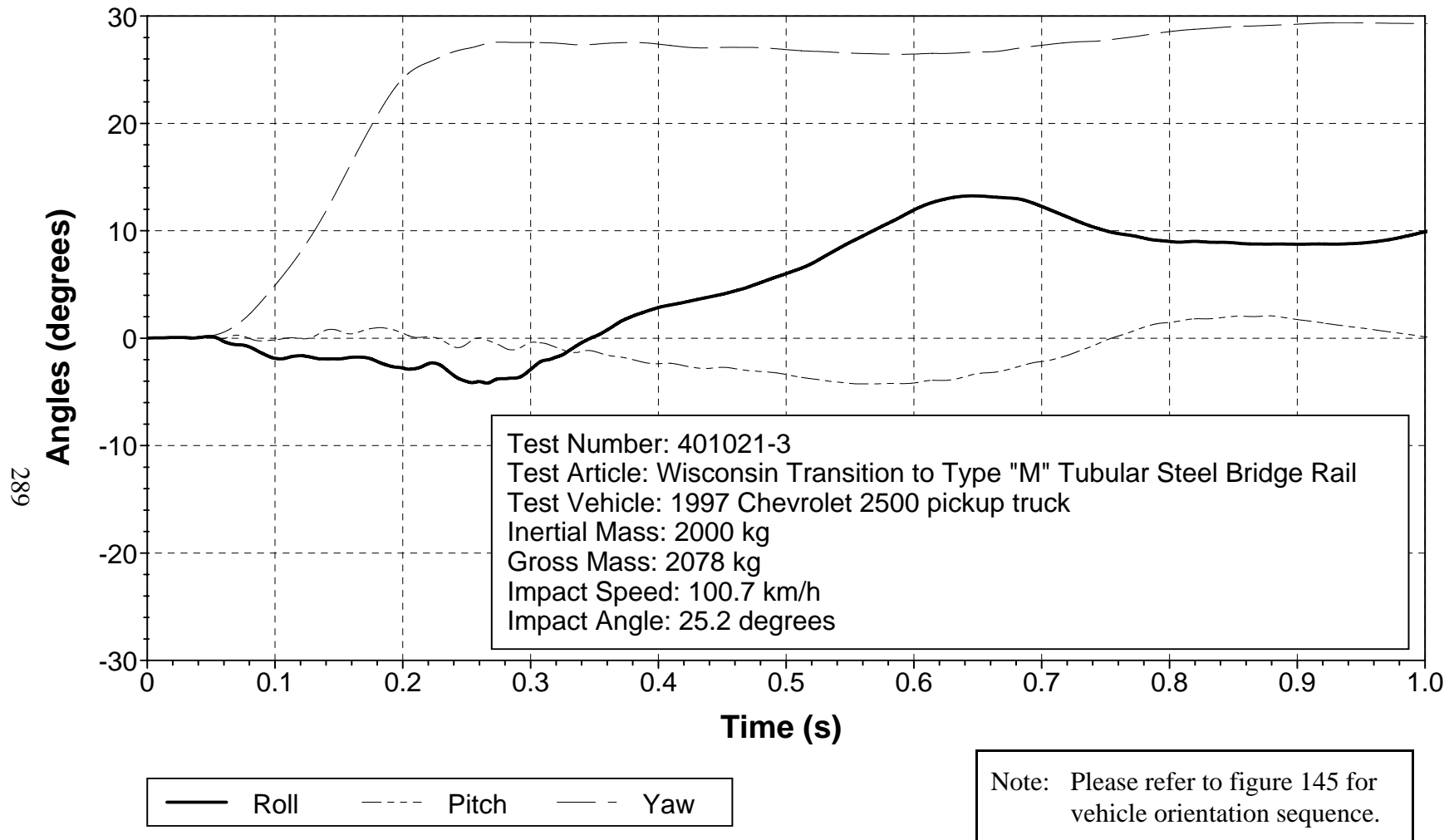


Figure 207. Vehicular angular displacements for test 401021-3.

X Acceleration at C.G.

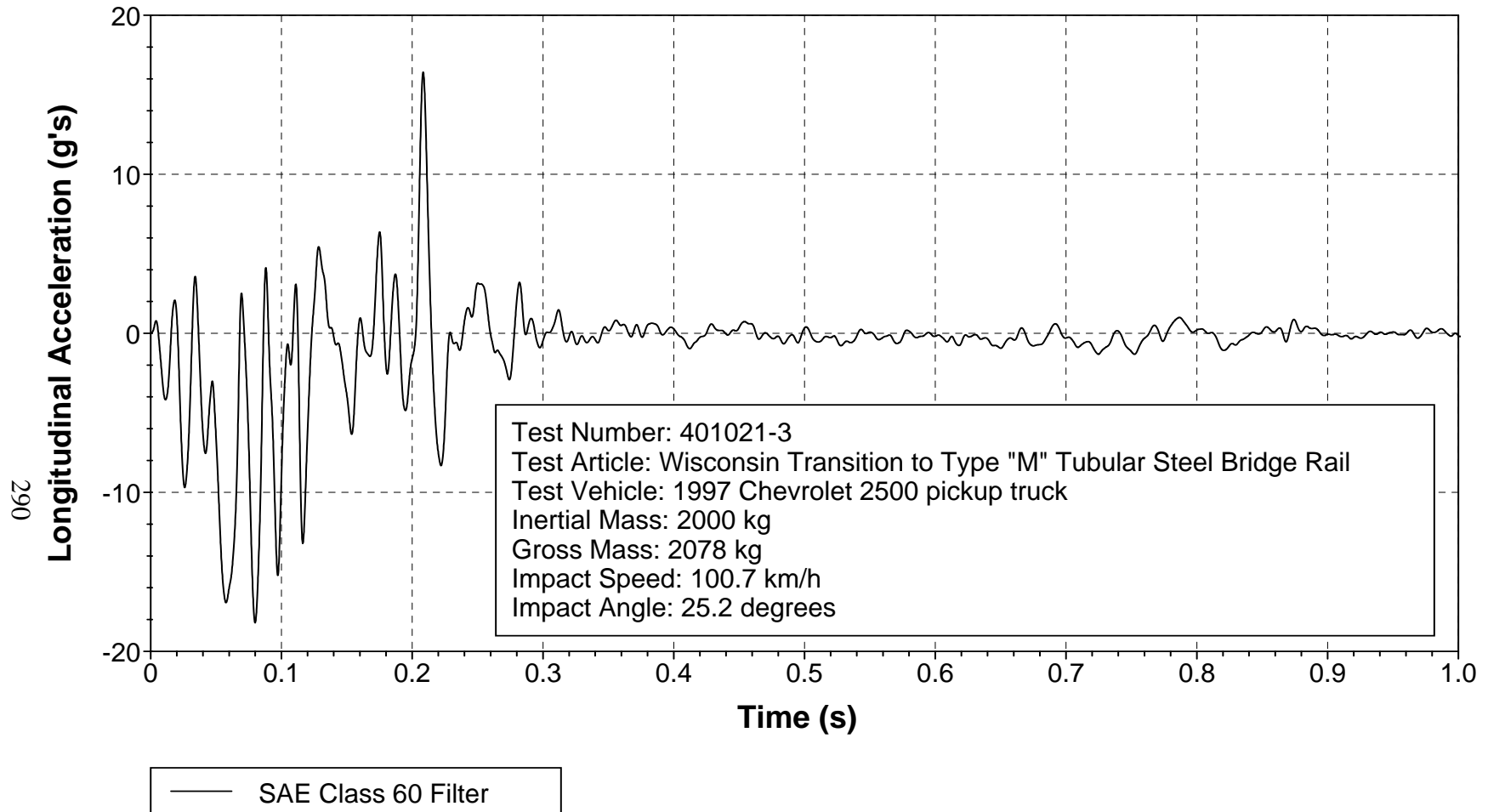


Figure 208. Vehicle longitudinal accelerometer trace for test 401021-3 (accelerometer located at center of gravity).

Y Acceleration at C.G.

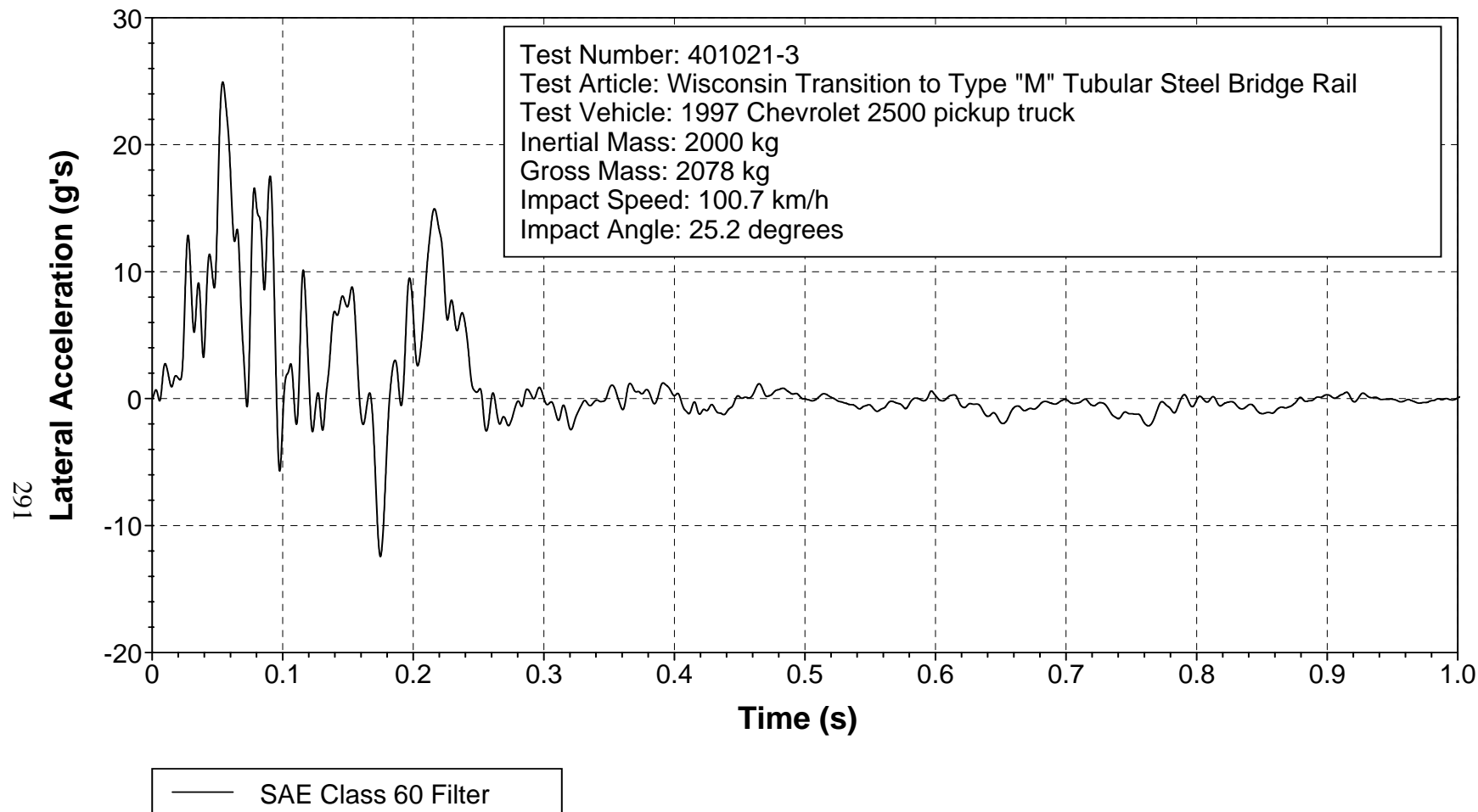


Figure 209. Vehicle lateral accelerometer trace for test 401021-3 (accelerometer located at center of gravity).

Z Acceleration at C.G.

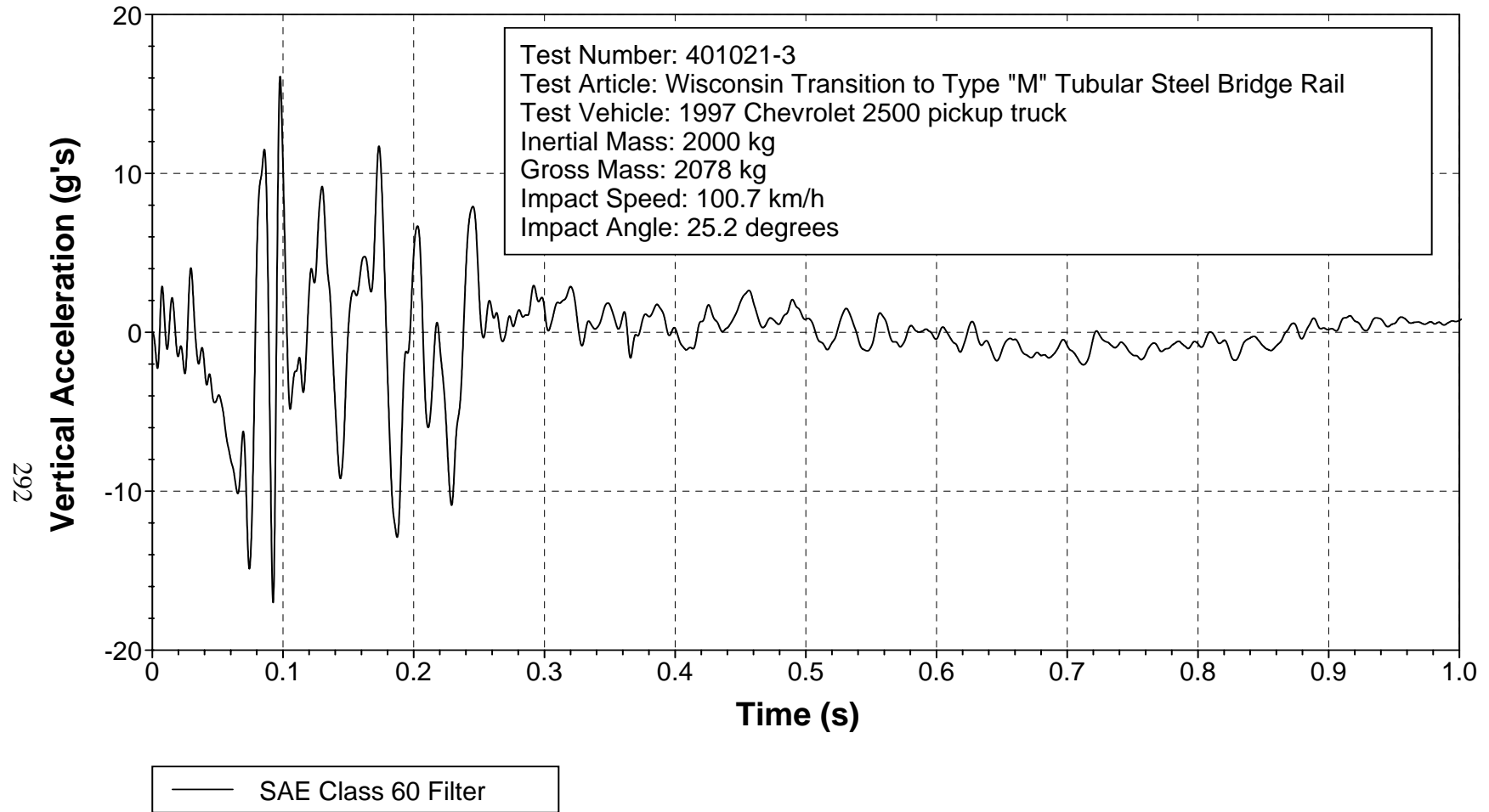


Figure 210. Vehicle vertical accelerometer trace for test 401021-3 (accelerometer located at center of gravity).

X Acceleration over Rear Axle

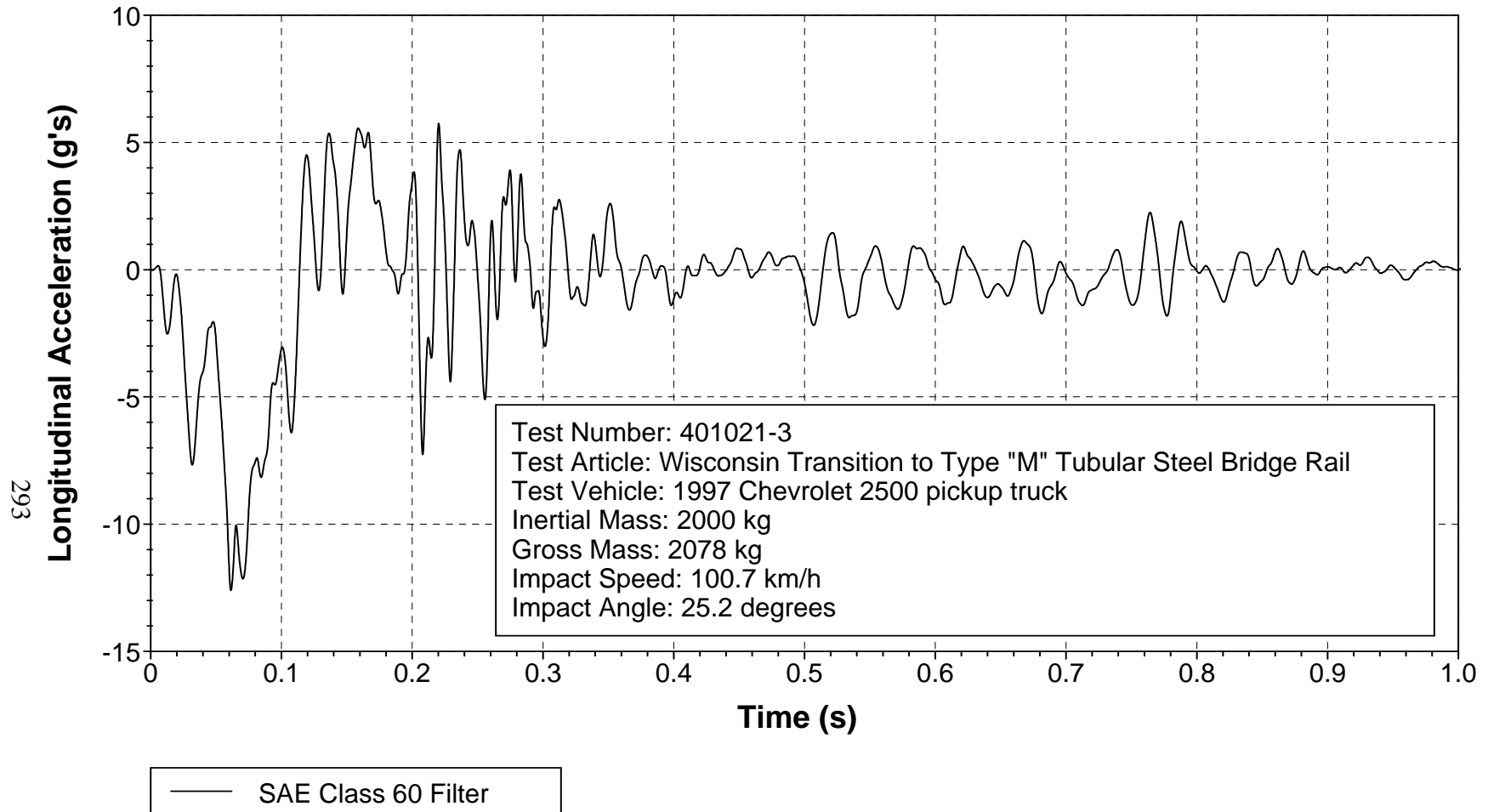


Figure 211. Vehicle longitudinal accelerometer trace for test 401021-3
(accelerometer located over rear axle).

Y Acceleration over Rear Axle

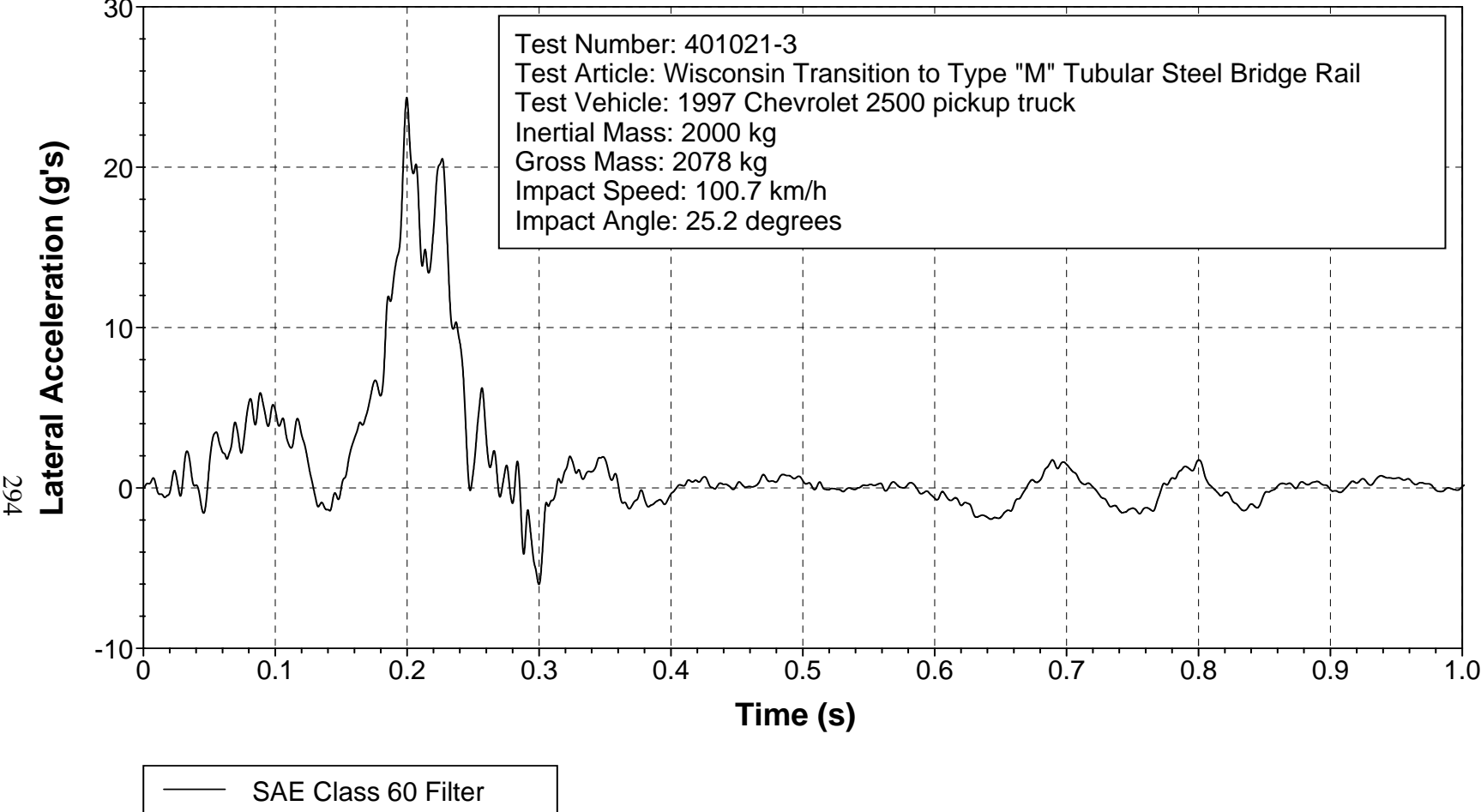


Figure 212. Vehicle lateral accelerometer trace for test 401021-3 (accelerometer located over rear axle).

Z Acceleration over Rear Axle

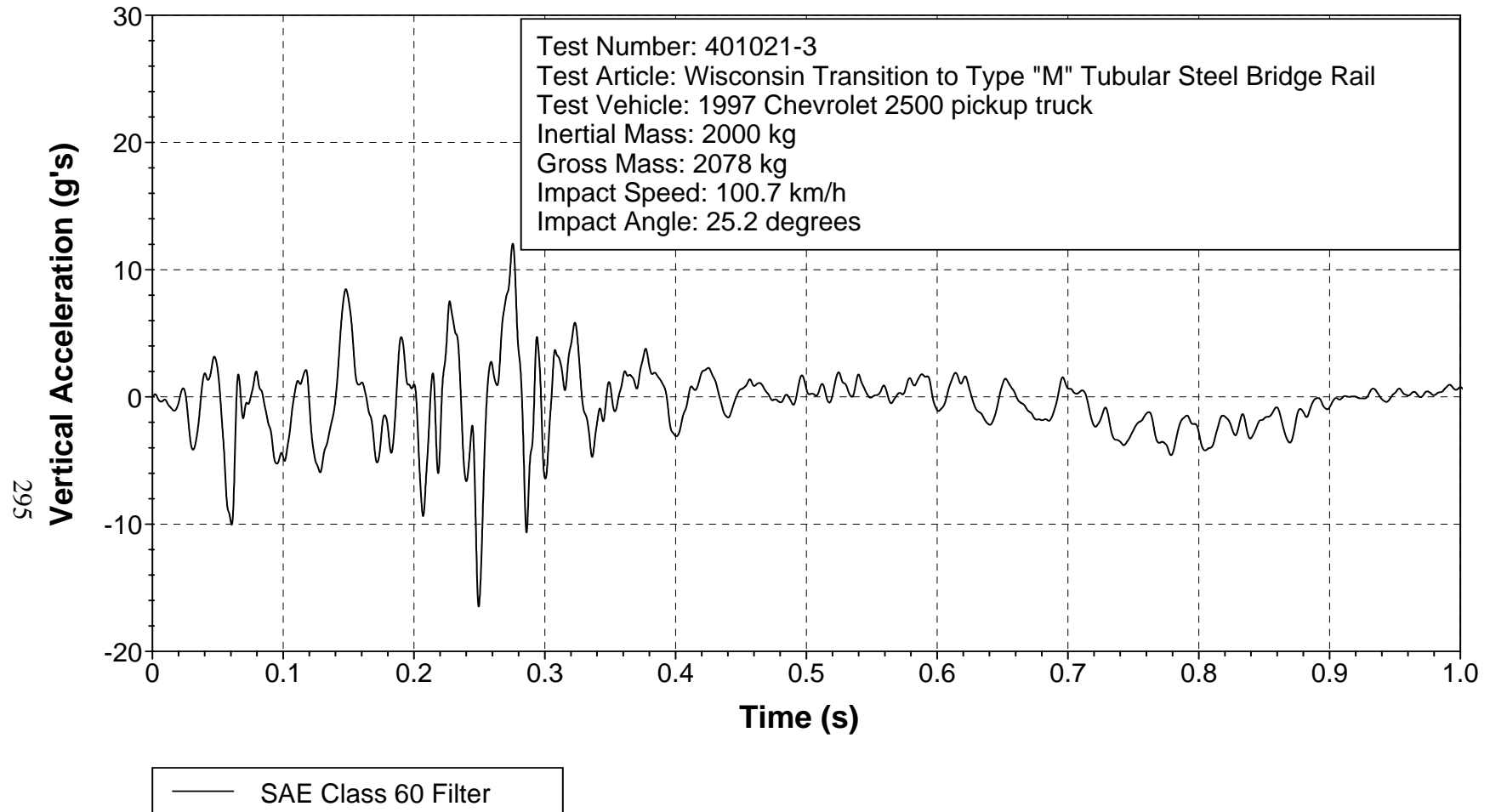


Figure 213. Vehicle vertical accelerometer trace for test 401021-3 (accelerometer located over rear axle).

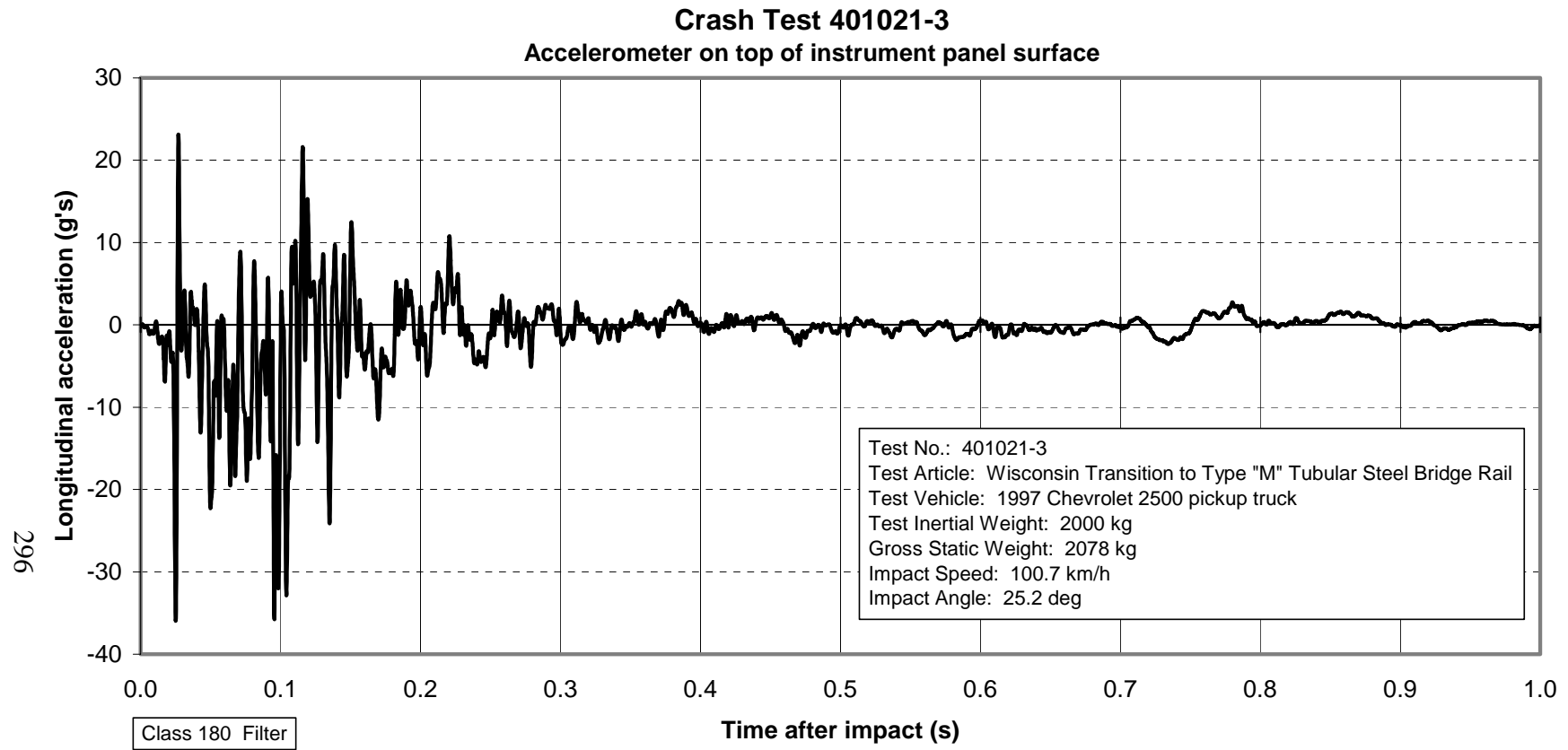


Figure 214. Vehicle longitudinal accelerometer trace for test 401021-3
(accelerometer located on top surface of instrument panel).

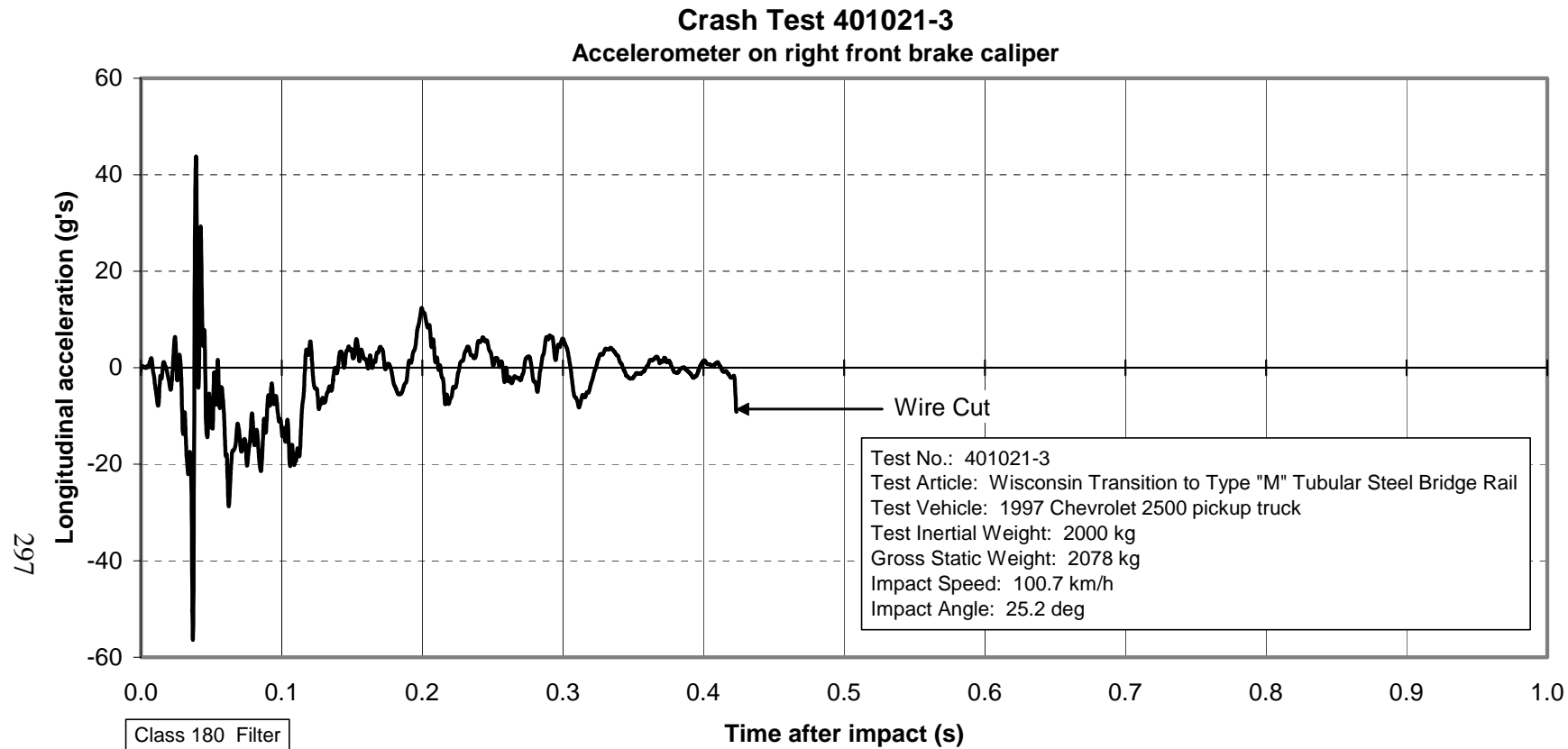


Figure 215. Vehicle lateral accelerometer trace for test 401021-3
(accelerometer located on right front brake caliper).

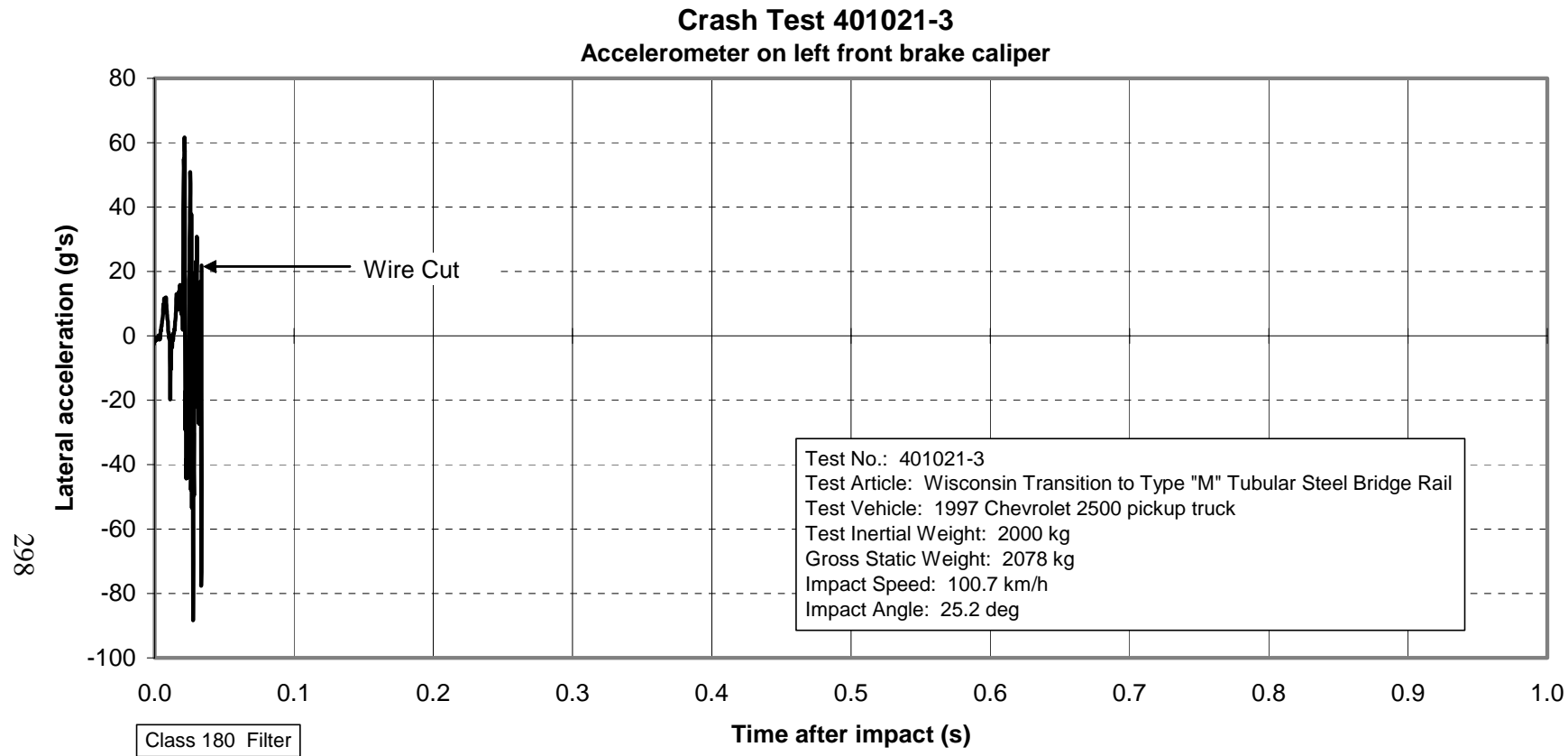


Figure 216. Vehicle longitudinal accelerometer trace for test 401021-3
(accelerometer located on left front brake caliper).

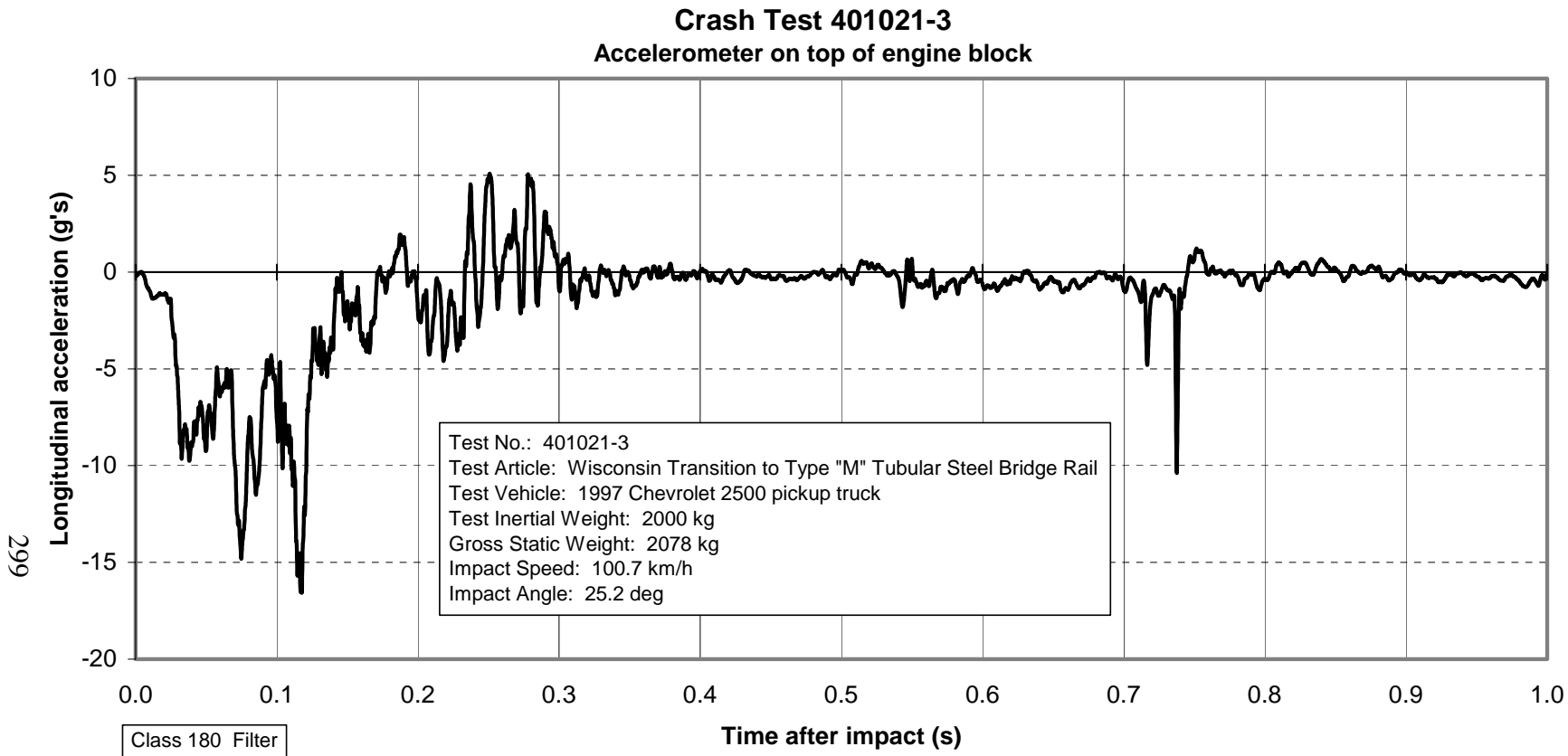


Figure 217. Vehicle longitudinal accelerometer trace for test 401021-3 (accelerometer located on top of engine block).

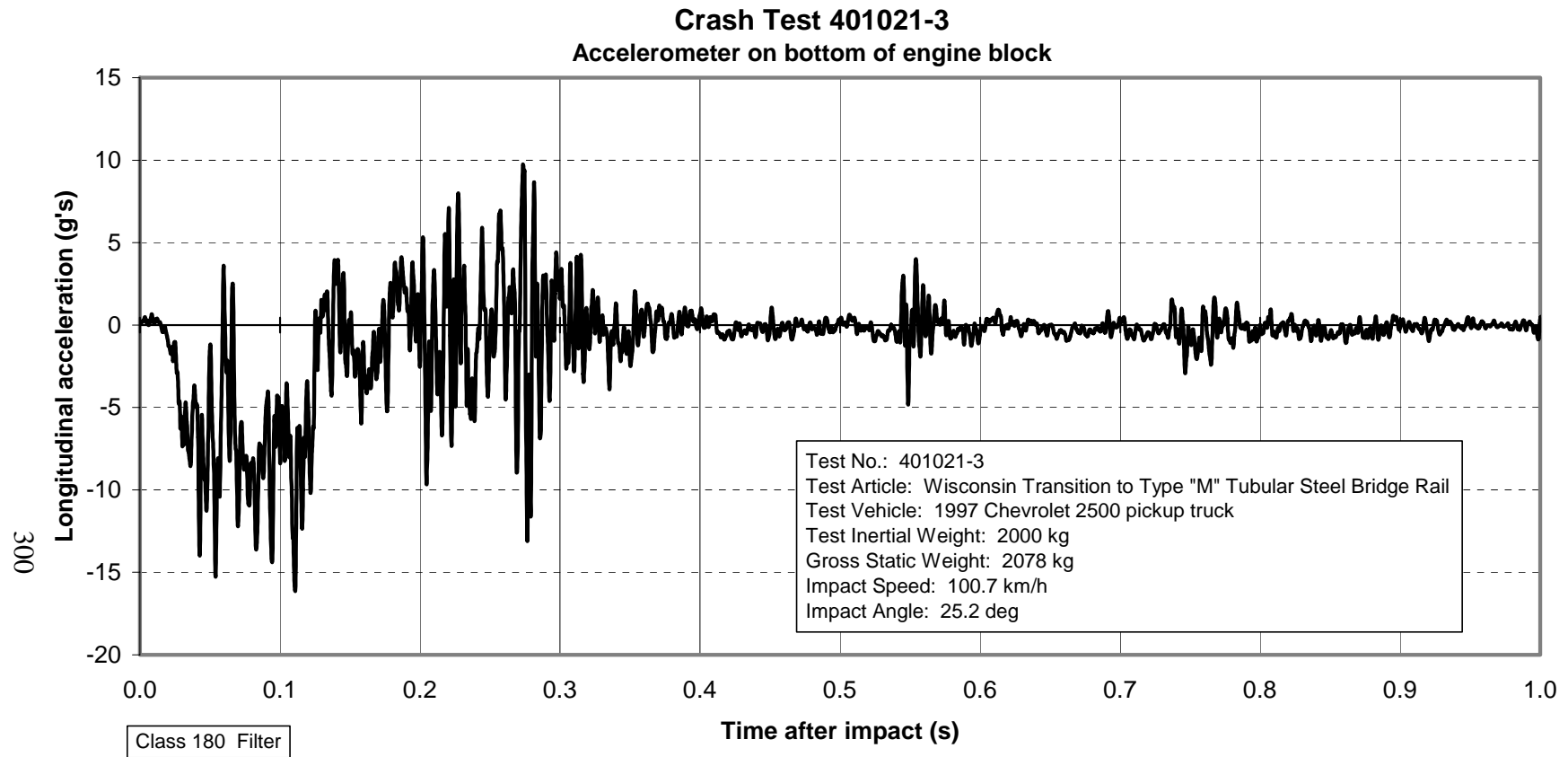


Figure 218. Vehicle longitudinal accelerometer trace for test 401021-3
(accelerometer located on bottom of engine block).

Roll, Pitch, and Yaw Angles

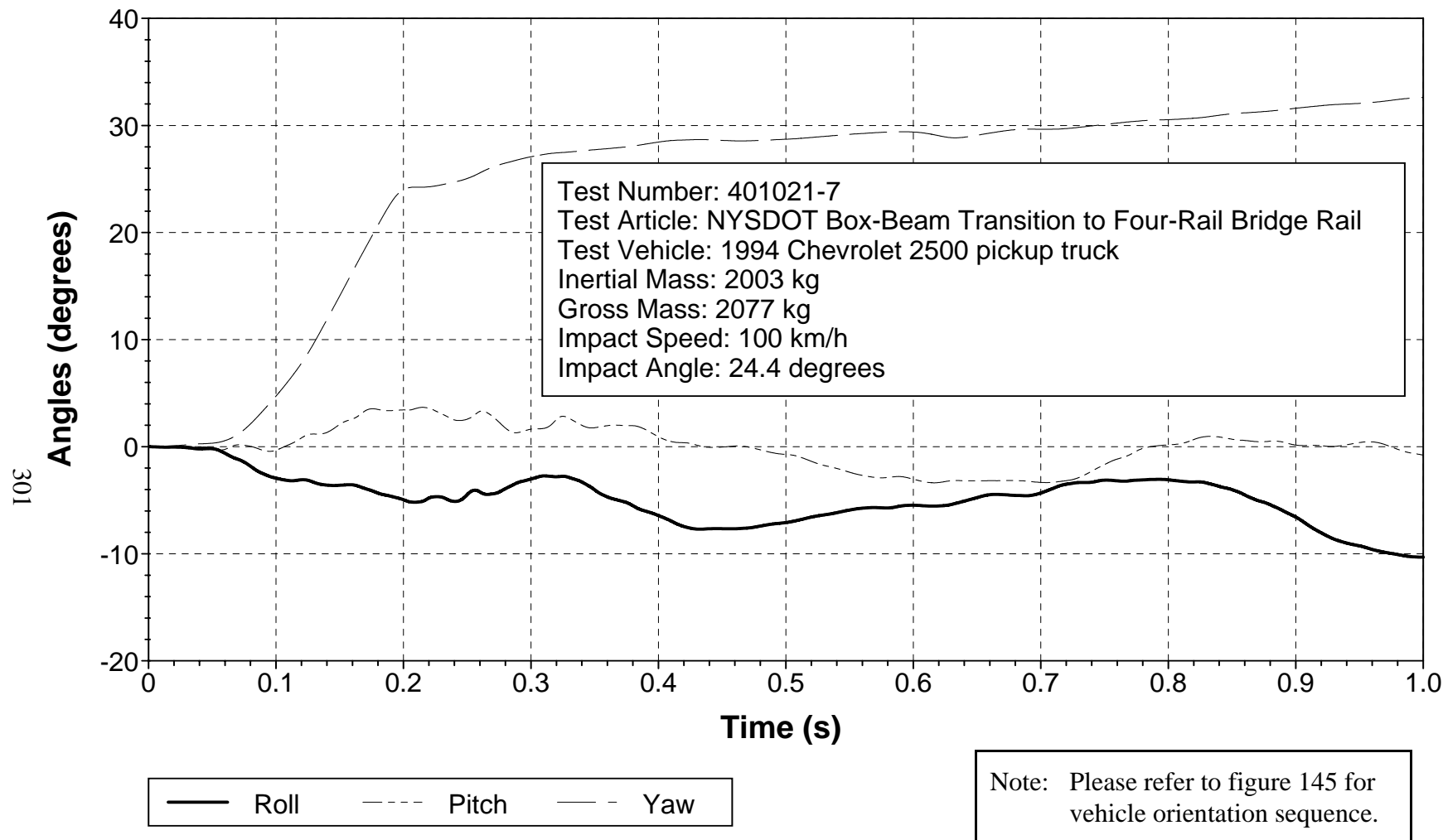


Figure 219. Vehicular angular displacements for test 401021-7.

X Acceleration at C.G.

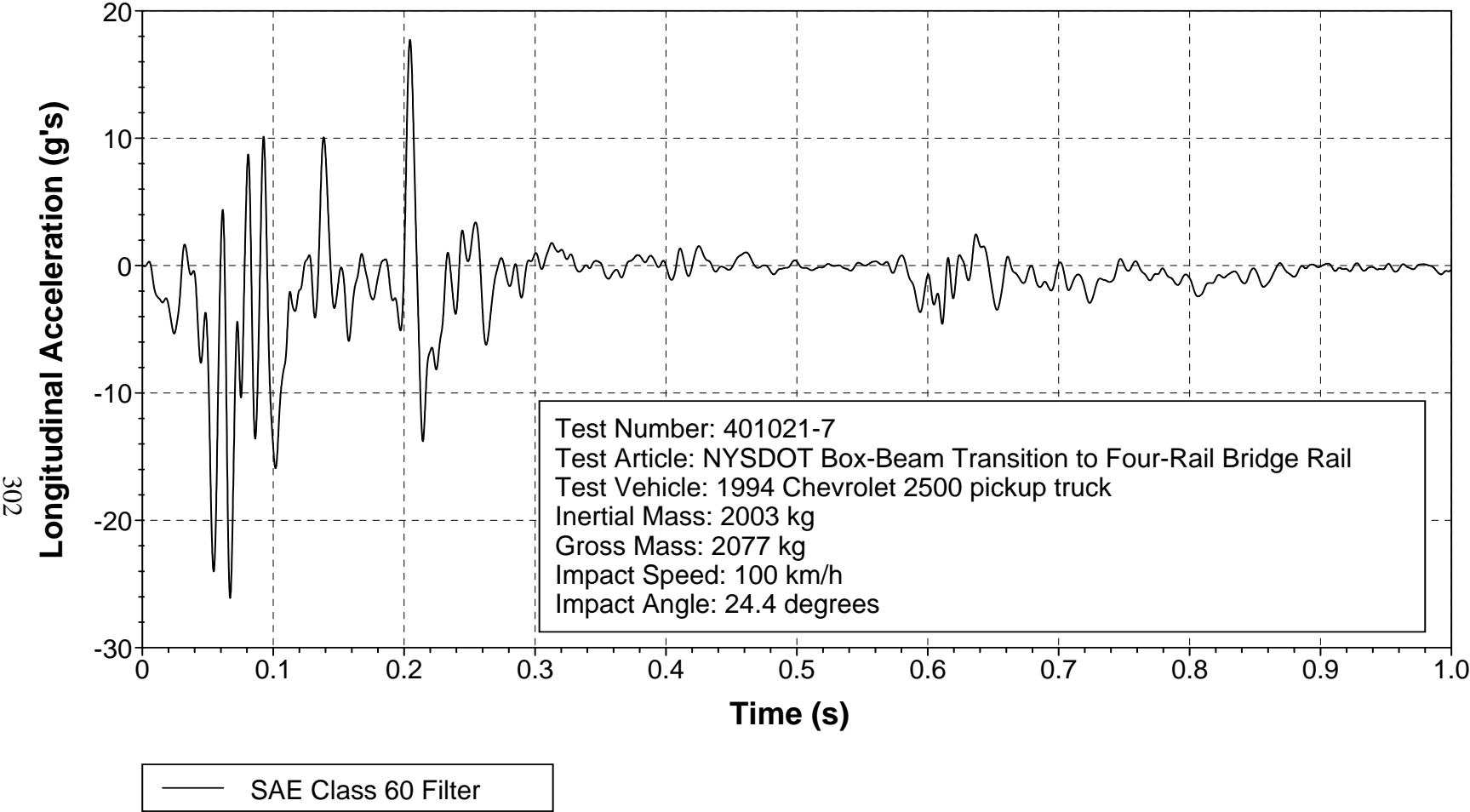


Figure 220. Vehicle longitudinal accelerometer trace for test 401021-7 (accelerometer located at center of gravity).

Y Acceleration at C.G.

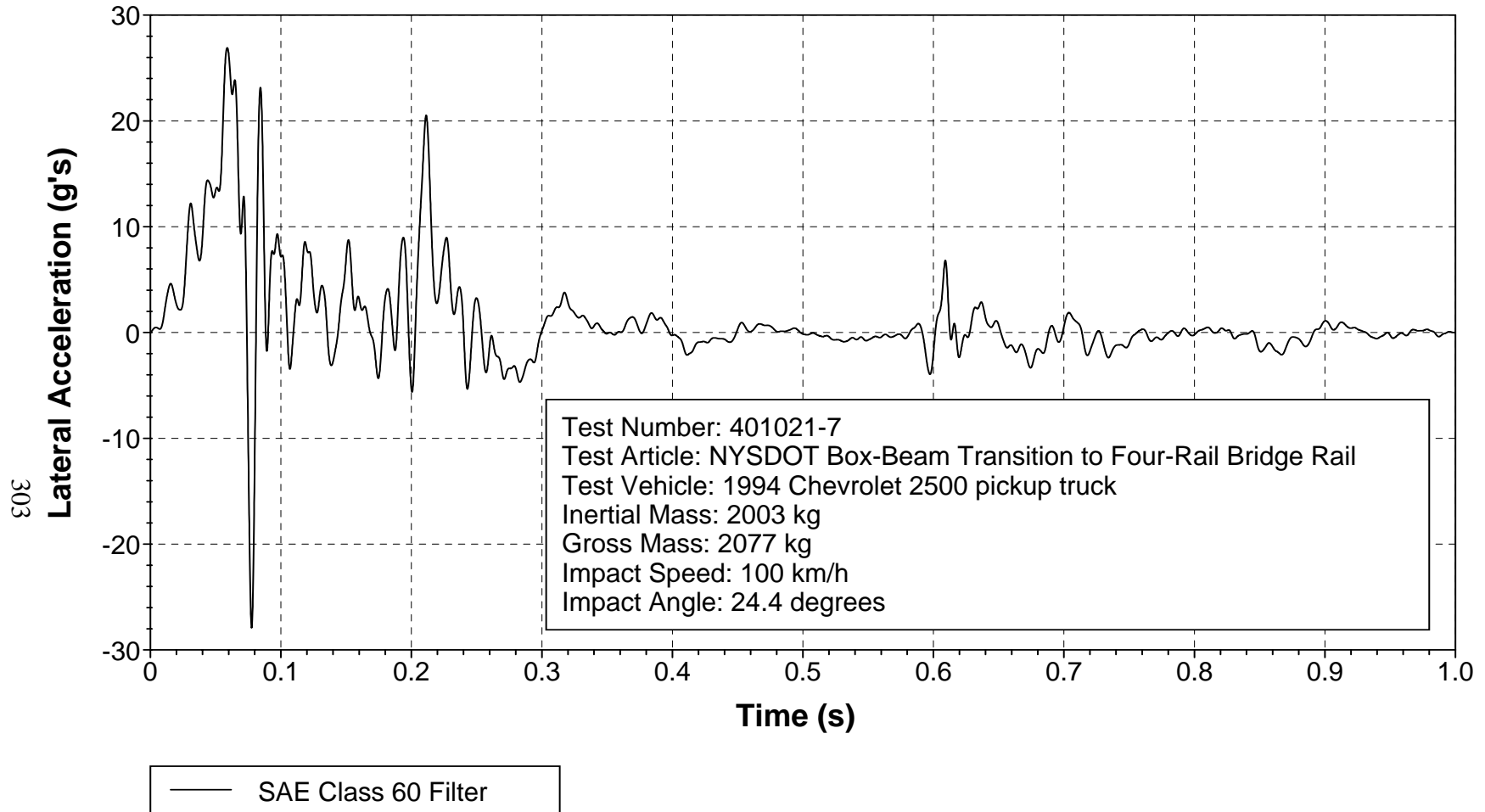


Figure 221. Vehicle lateral accelerometer trace for test 401021-7 (accelerometer located at center of gravity).

Z Acceleration at C.G.

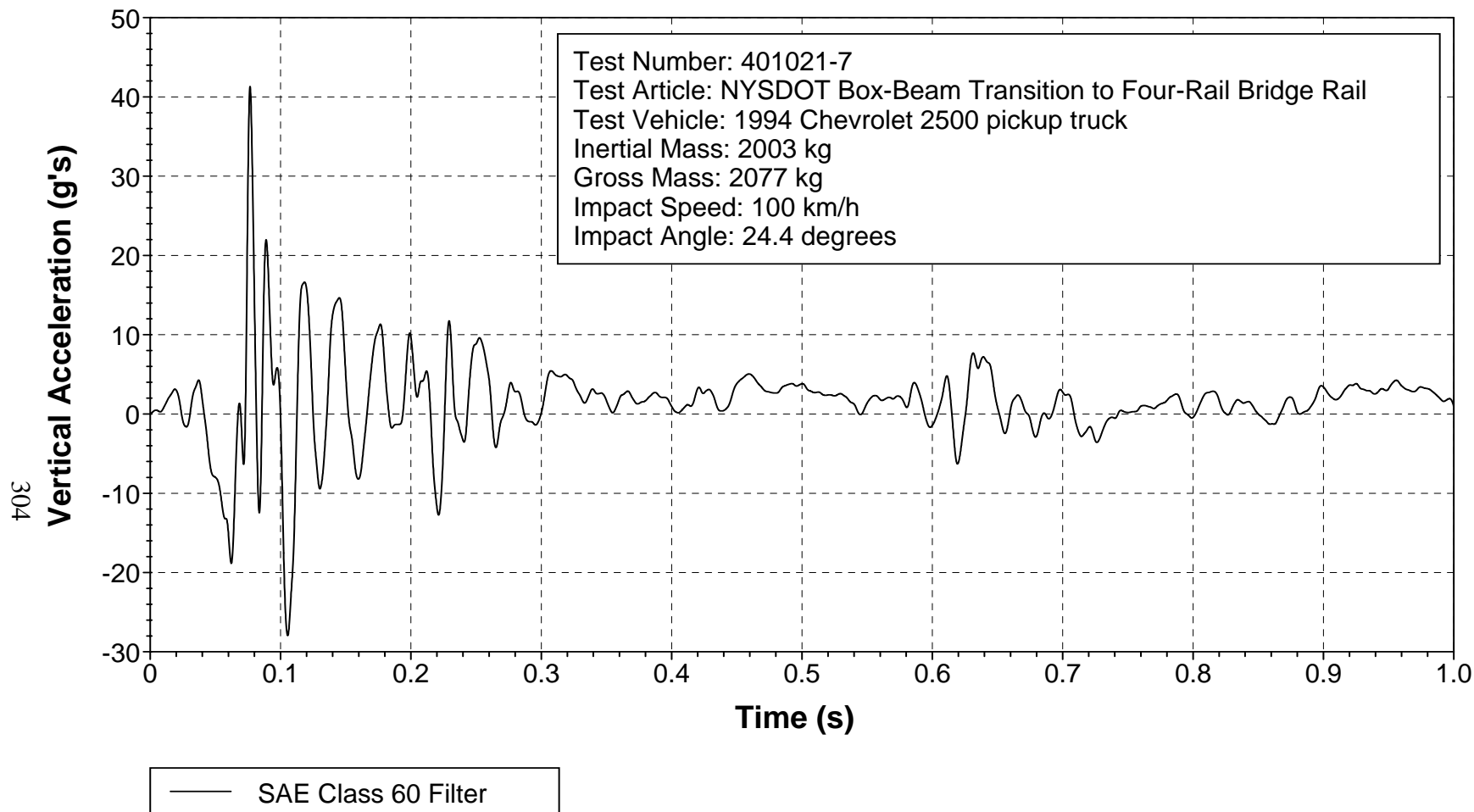


Figure 222. Vehicle vertical accelerometer trace for test 401021-7 (accelerometer located at center of gravity).

X Acceleration over Rear Axle

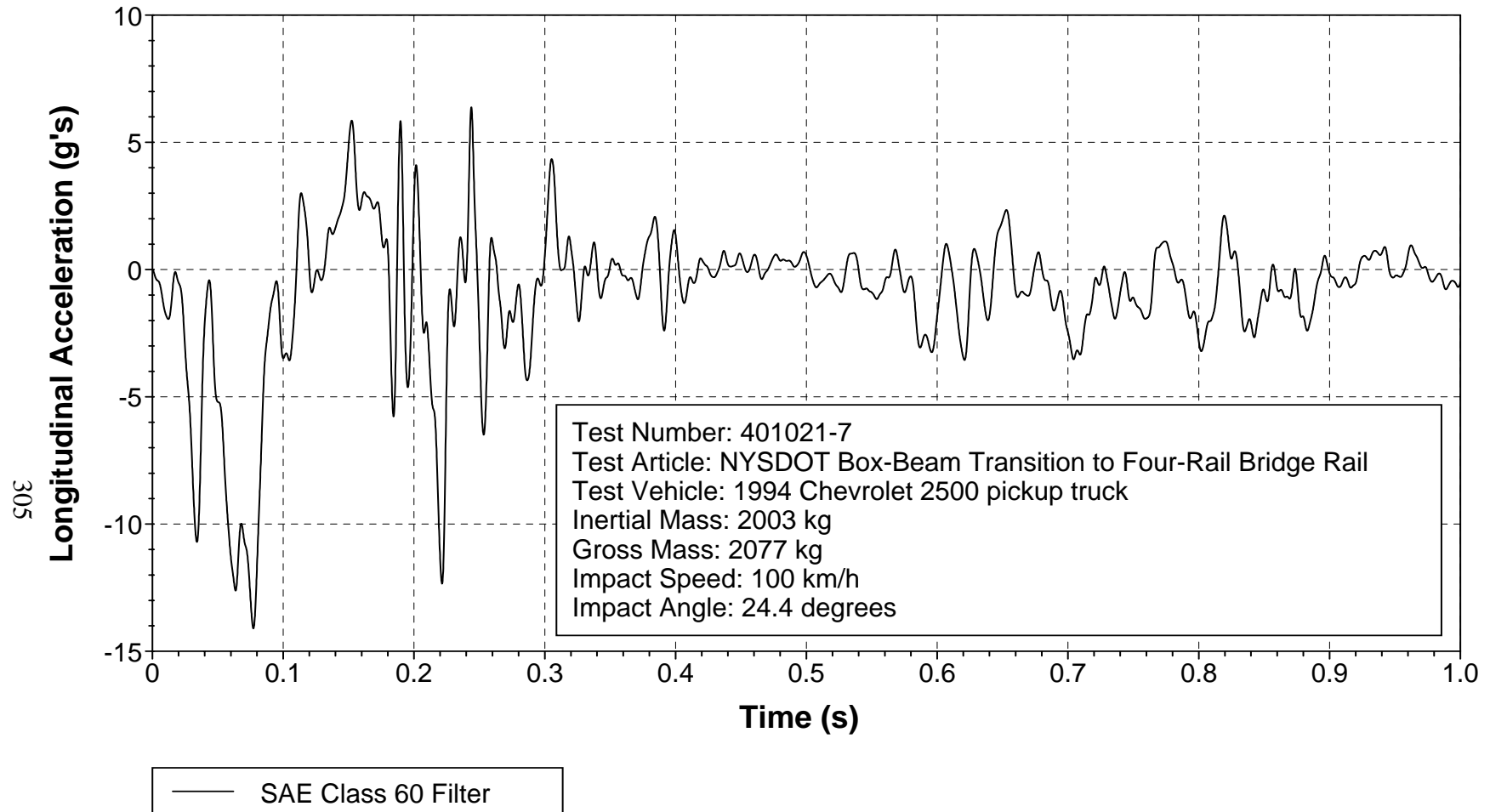


Figure 223. Vehicle longitudinal accelerometer trace for test 401021-7 (accelerometer located over rear axle).

Y Acceleration over Rear Axle

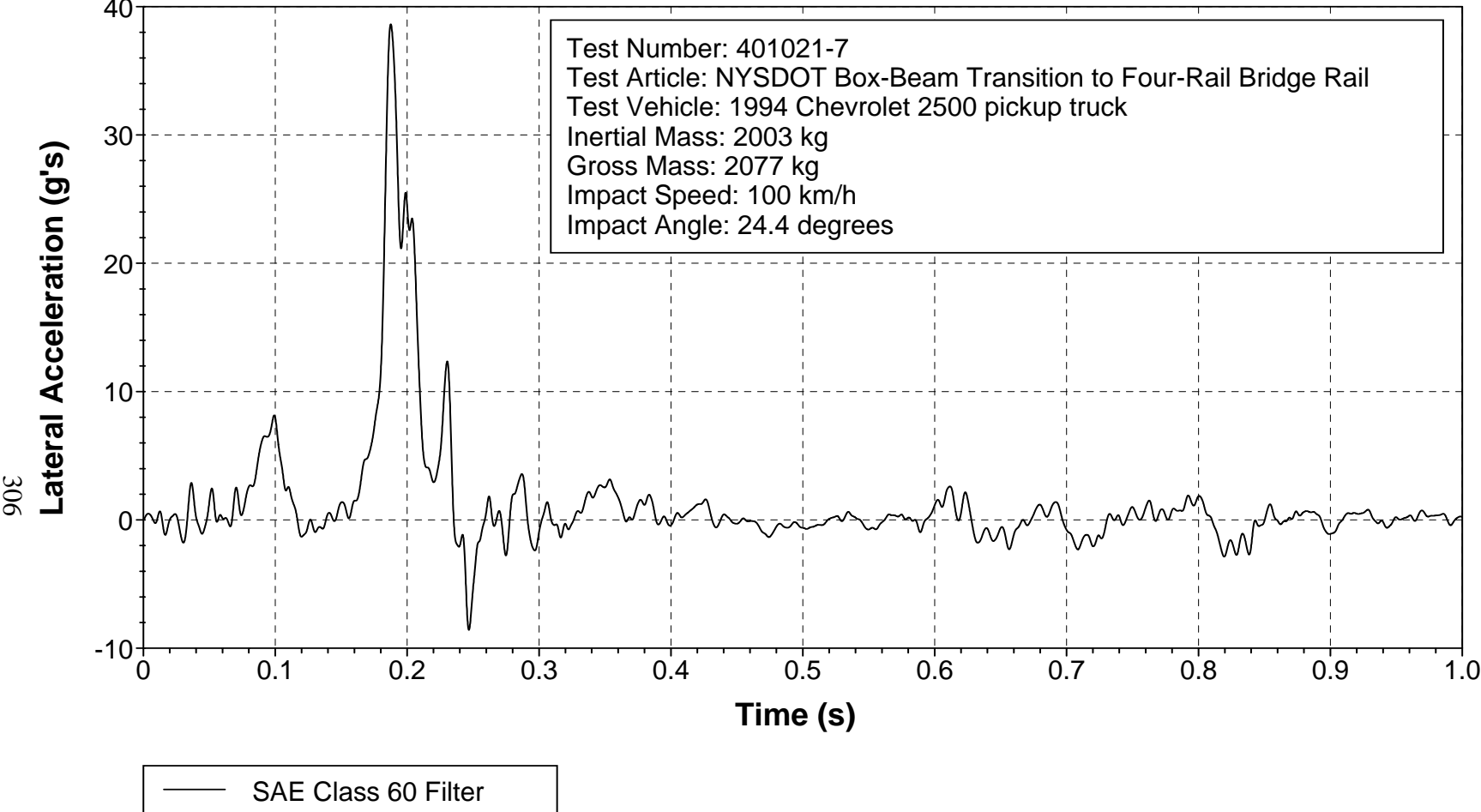


Figure 224. Vehicle lateral accelerometer trace for test 401021-7 (accelerometer located over rear axle).

Z Acceleration over Rear Axle

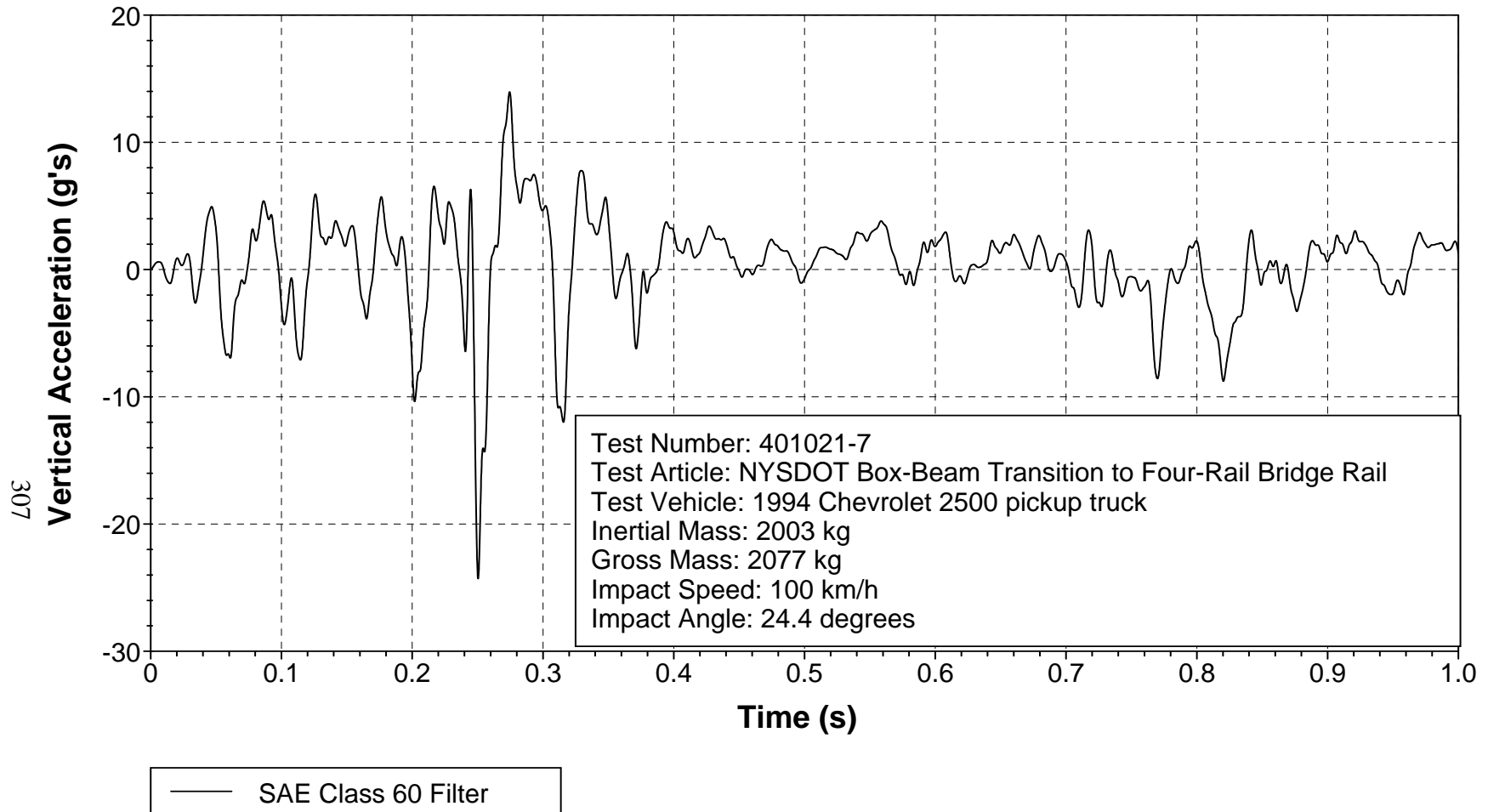


Figure 225. Vehicle vertical accelerometer trace for test 401021-7 (accelerometer located over rear axle).

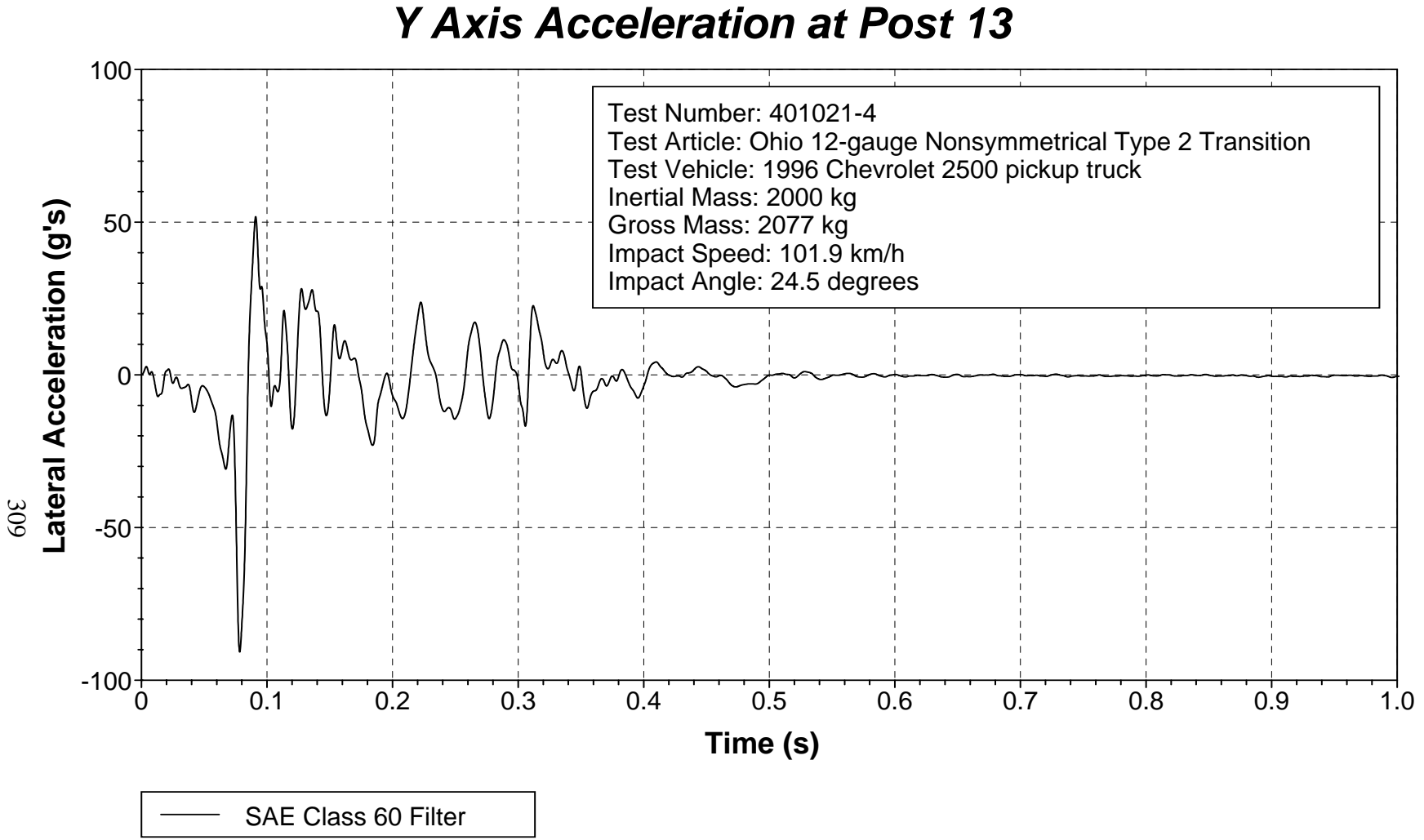


Figure 226. Lateral accelerometer trace for test 401021-4 (accelerometer located at center of post 13).

Gauge Location 1

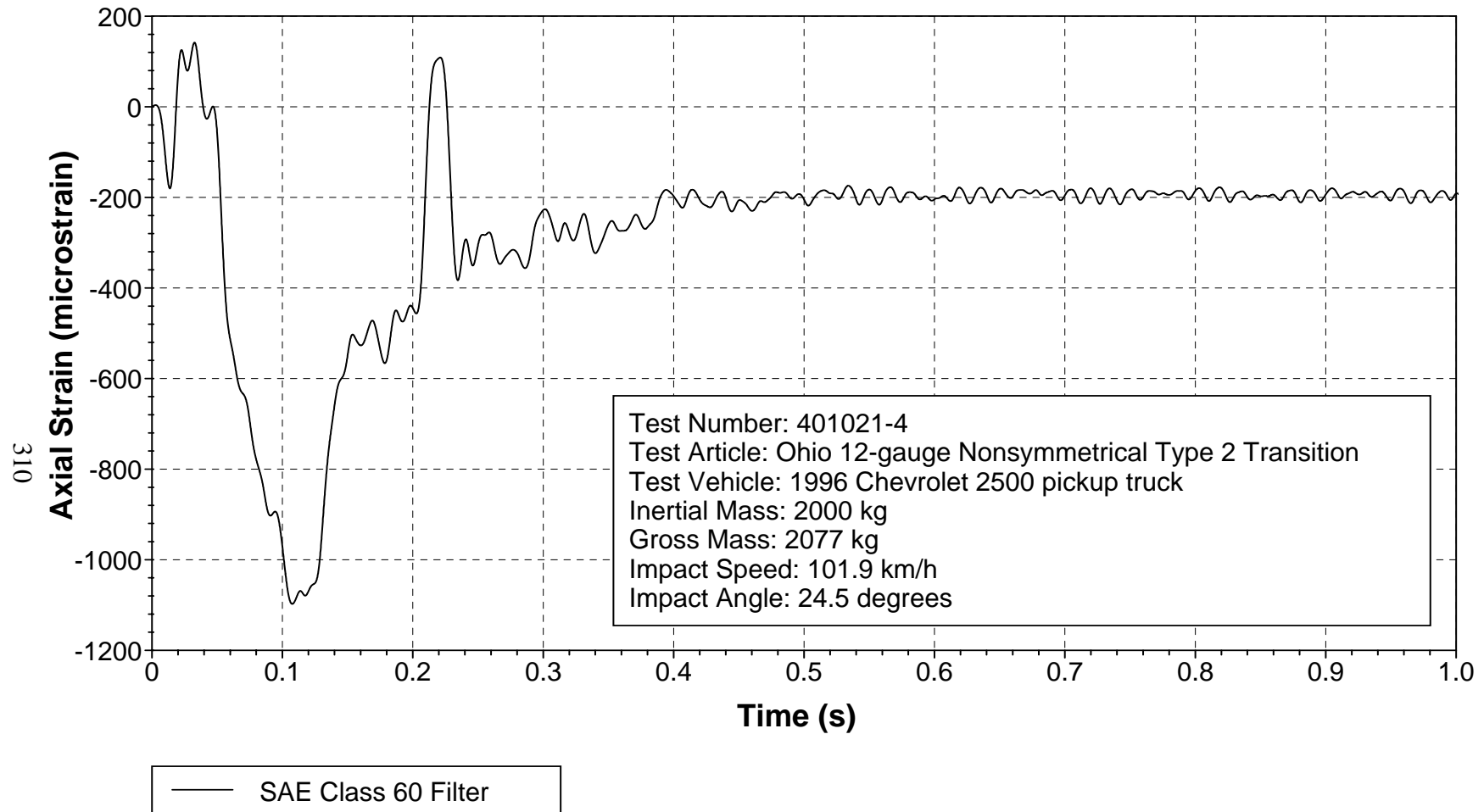


Figure 227. Axial strain, location 1, field side, for test 401021-4.

Gauge Location 2

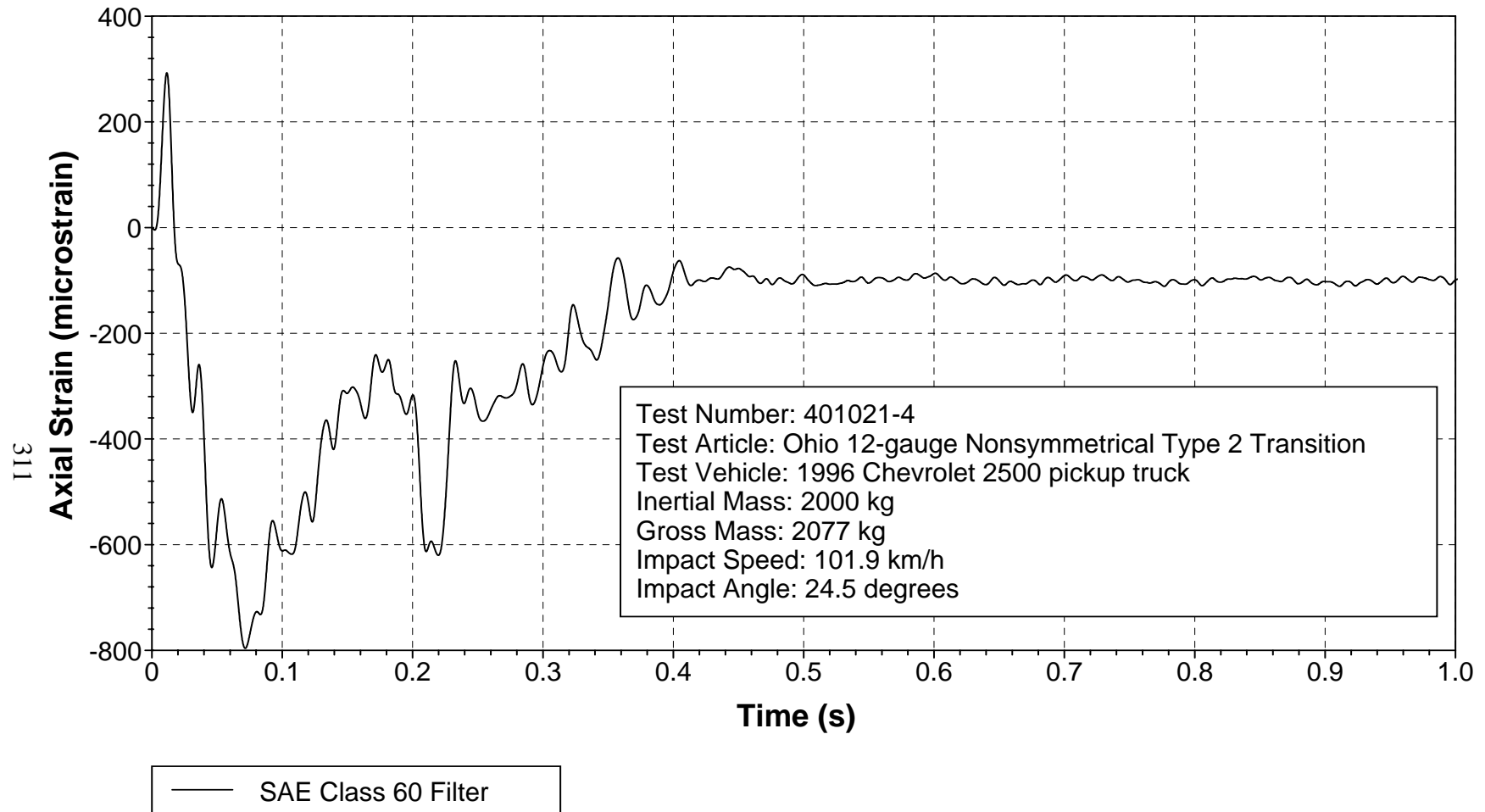


Figure 228. Axial strain, location 2, field side, for test 401021-4.

Gauge Location 3

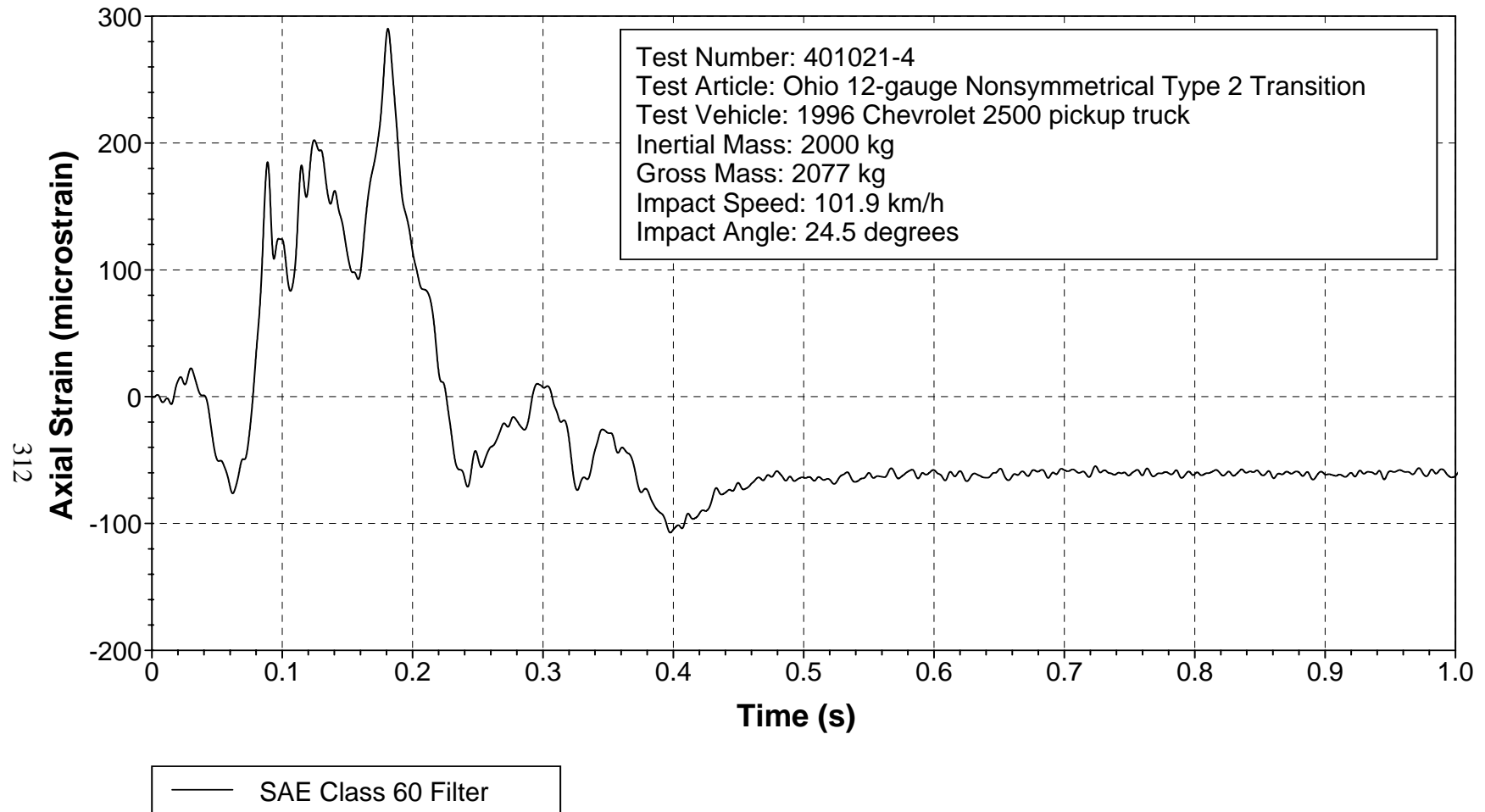


Figure 229. Axial strain, location 3, field side, for test 401021-4.

Gauge Location 4

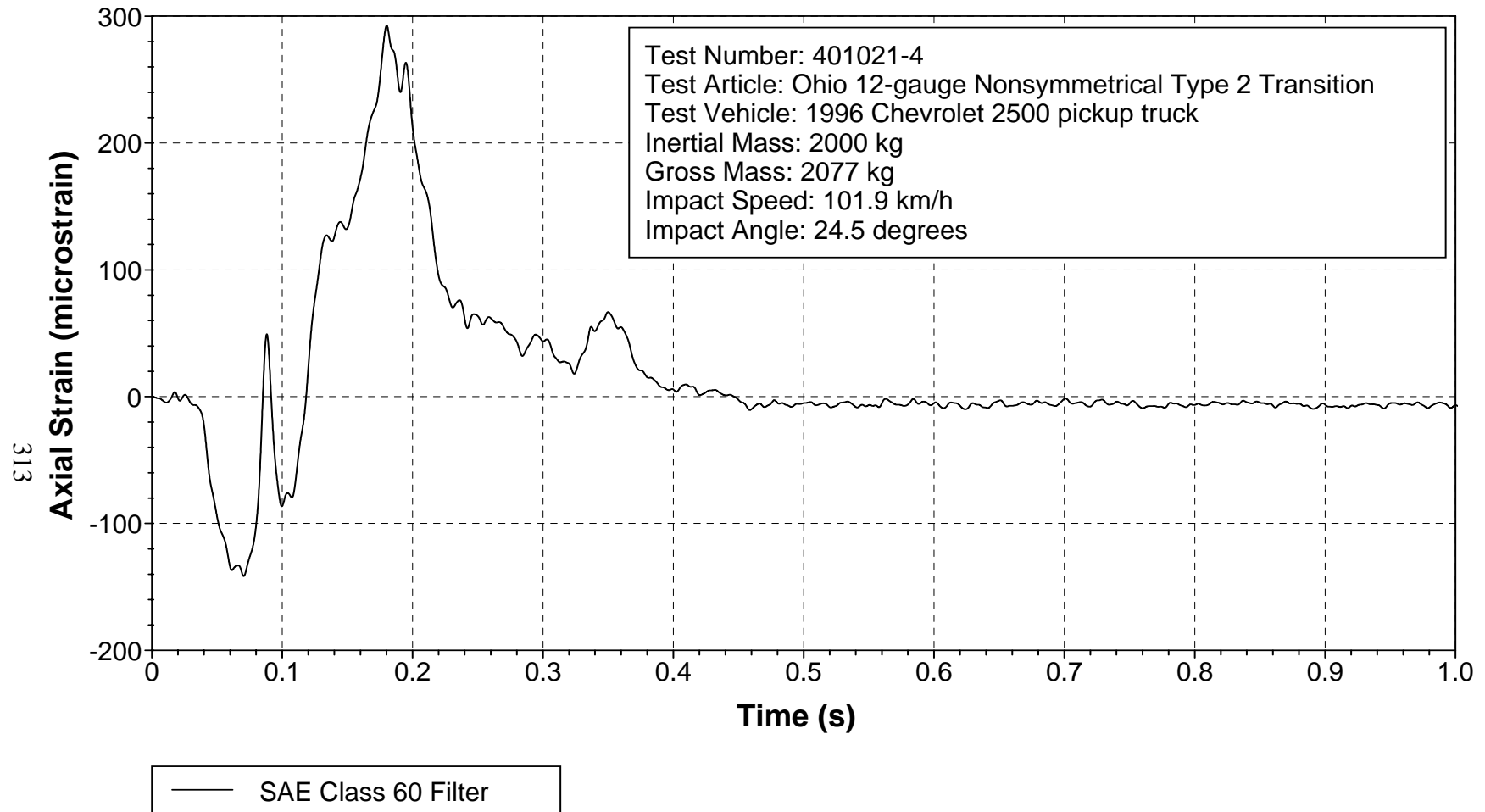


Figure 230. Axial strain, location 4, field side, for test 401021-4.

Gauge Location 5

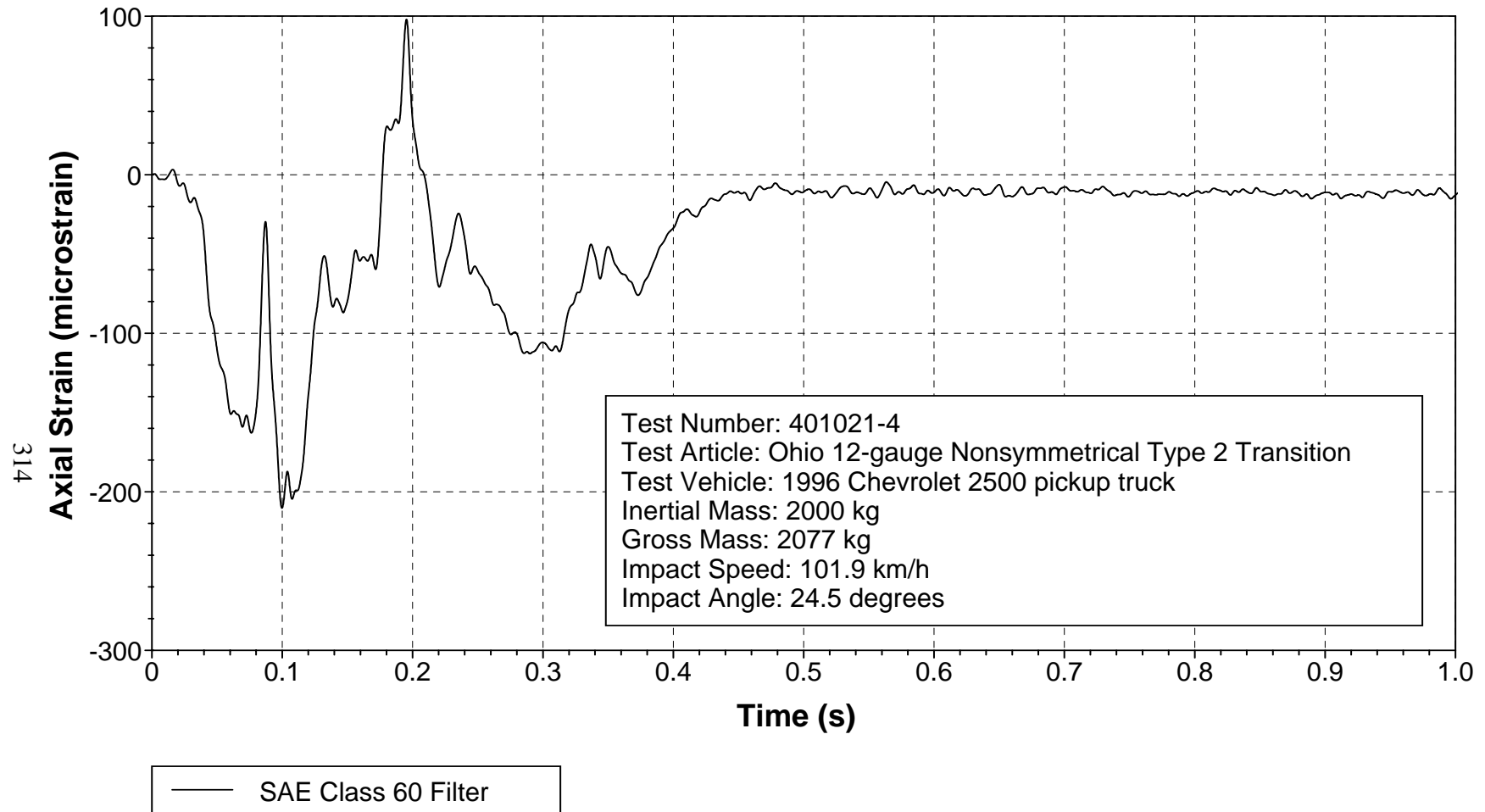


Figure 231. Axial strain, location 5, field side, for test 401021-4.

Gauge Location 6

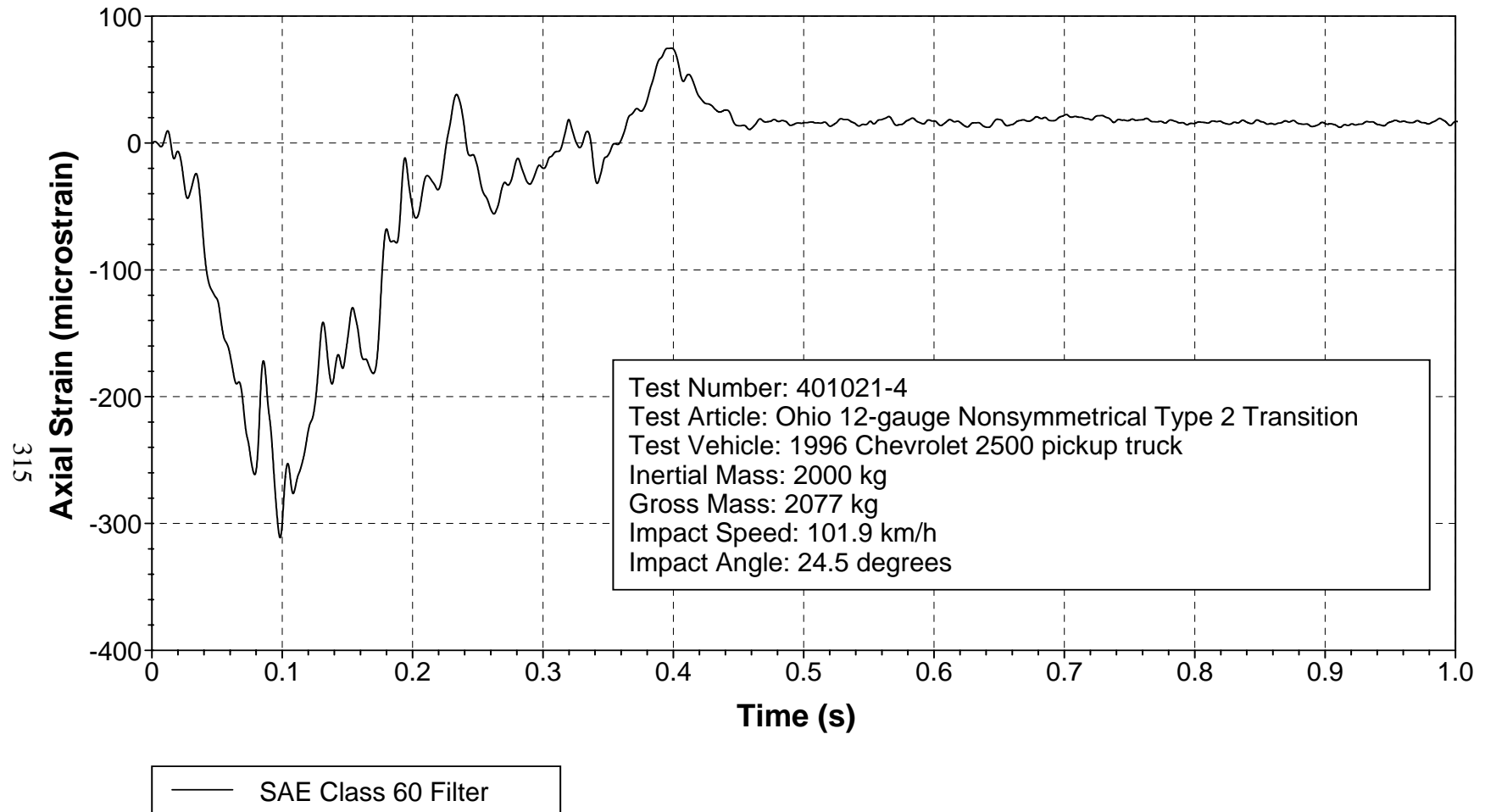


Figure 232. Axial strain, location 6, field side, for test 401021-4.

Y Axis Acceleration at Post 11

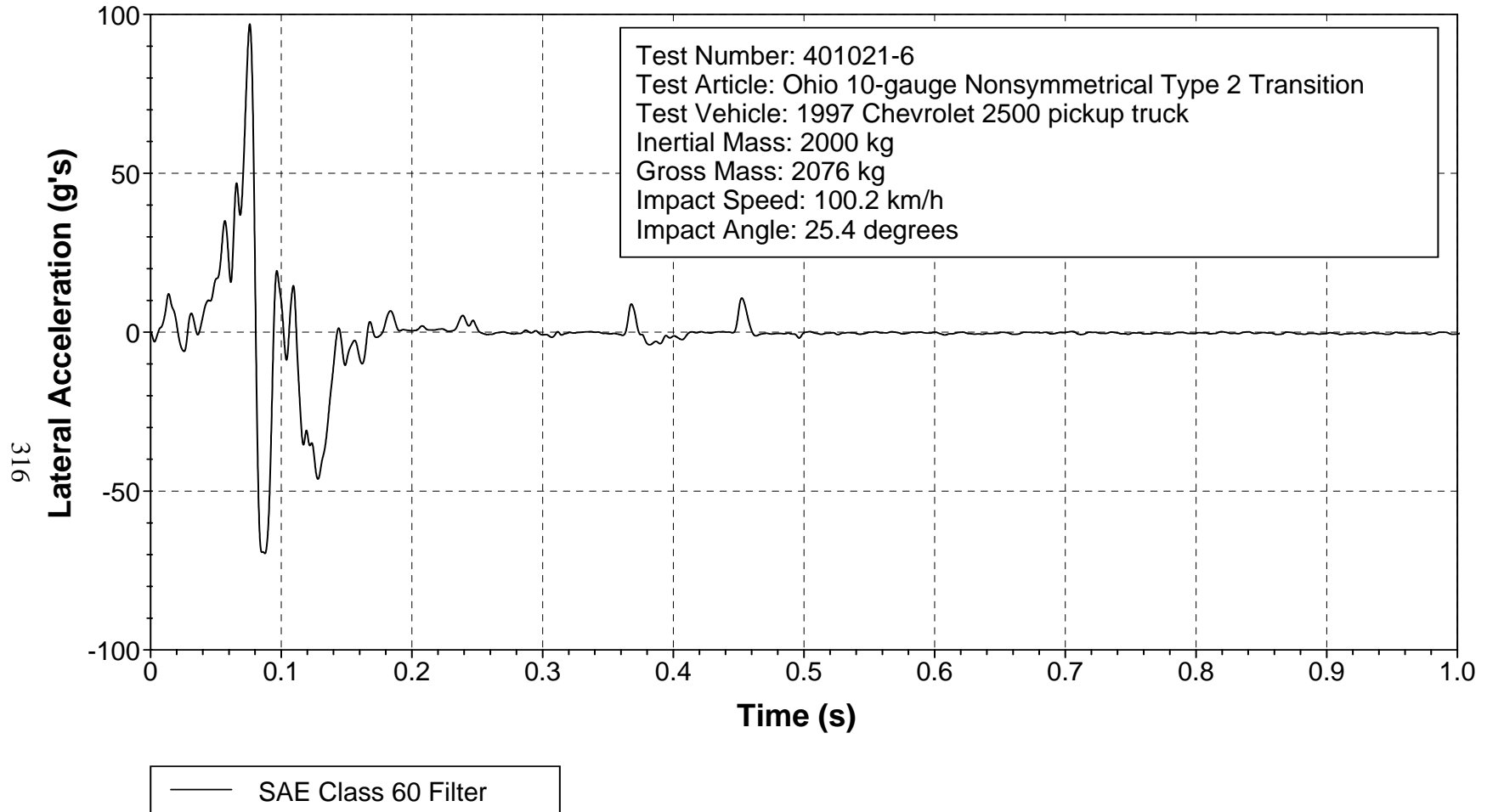


Figure 233. Lateral accelerometer trace for test 401021-6 (accelerometer located at center of post 11).

Gauge Location 1

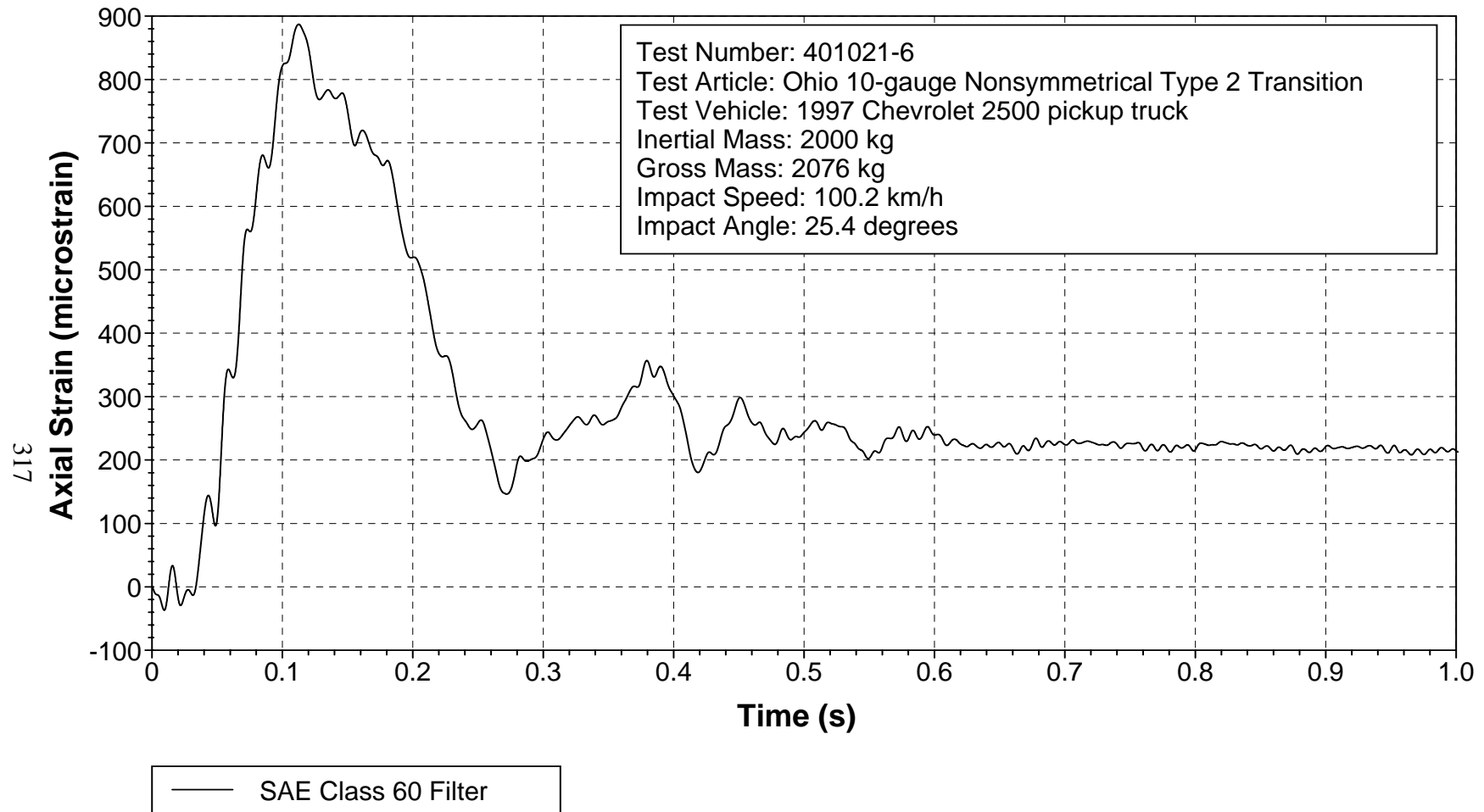


Figure 234. Axial strain, location 1, field side, for test 401021-6.

Gauge Location 2

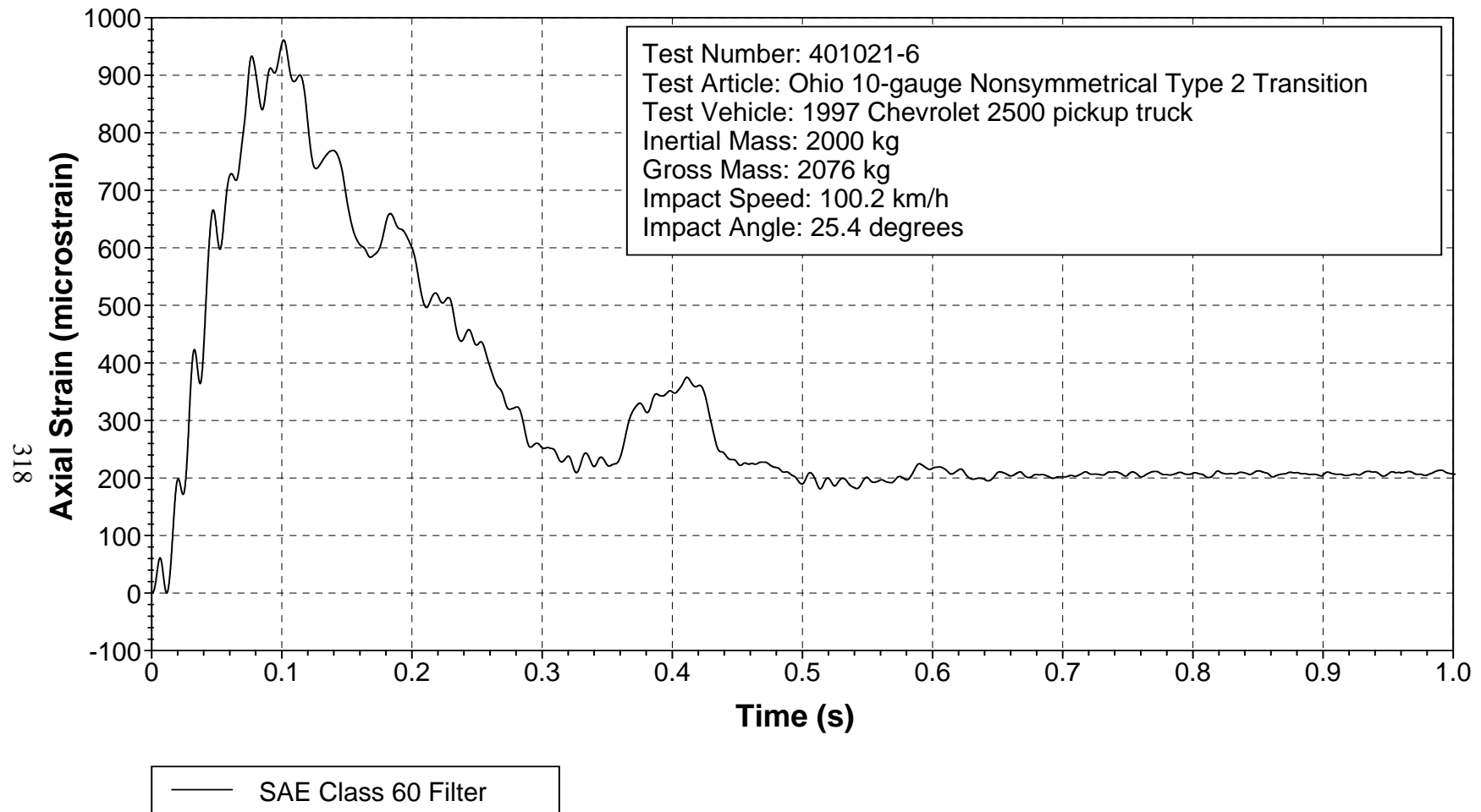


Figure 235. Axial strain, location 2, field side, for test 401021-6.

Gauge Location 3

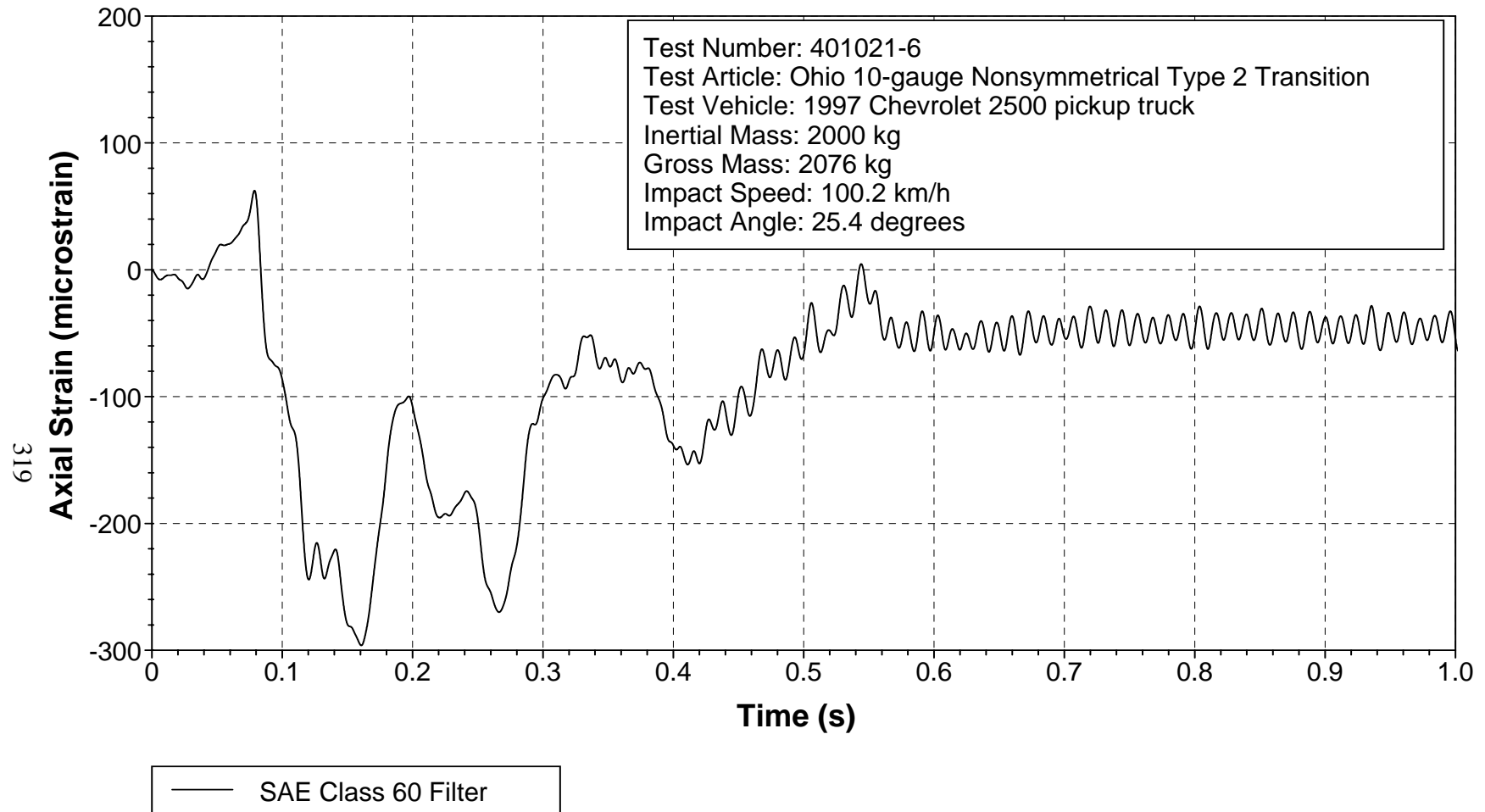


Figure 236. Axial strain, location 3, field side, for test 401021-6.

Gauge Location 4

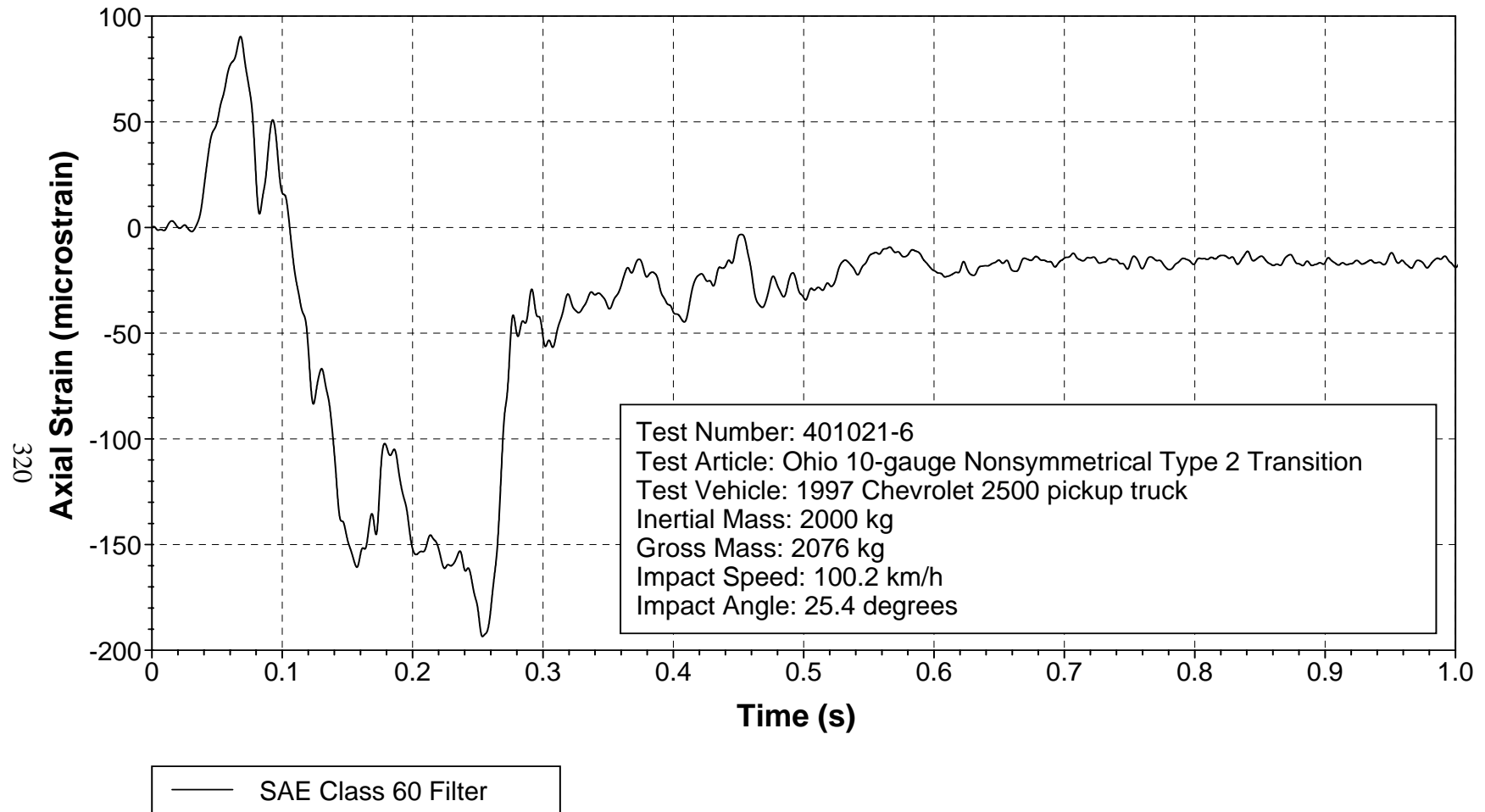


Figure 237. Axial strain, location 4, field side, for test 401021-6.

Gauge Location 5

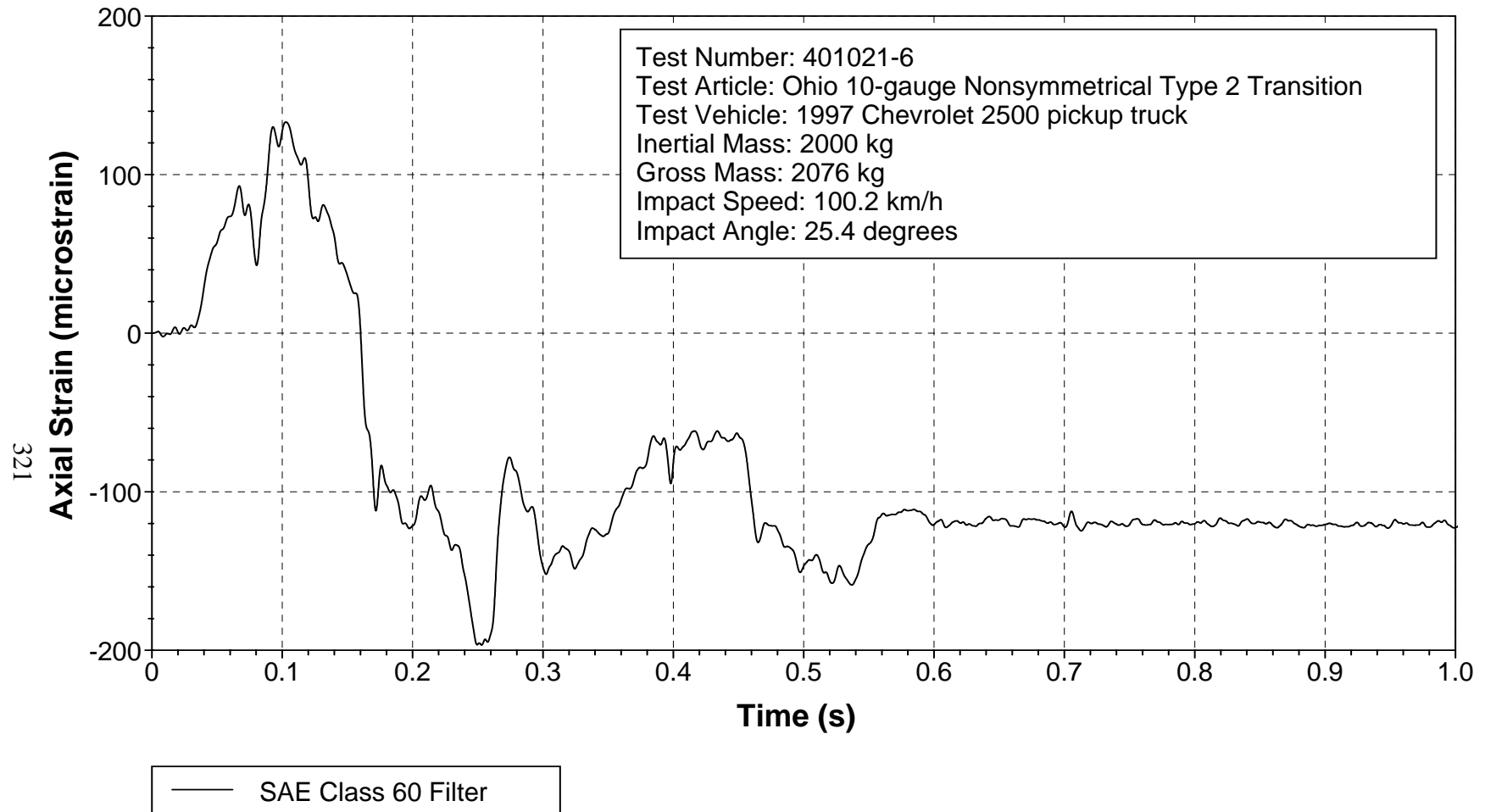


Figure 238. Axial strain, location 5, field side, for test 401021-6.

Gauge Location 6

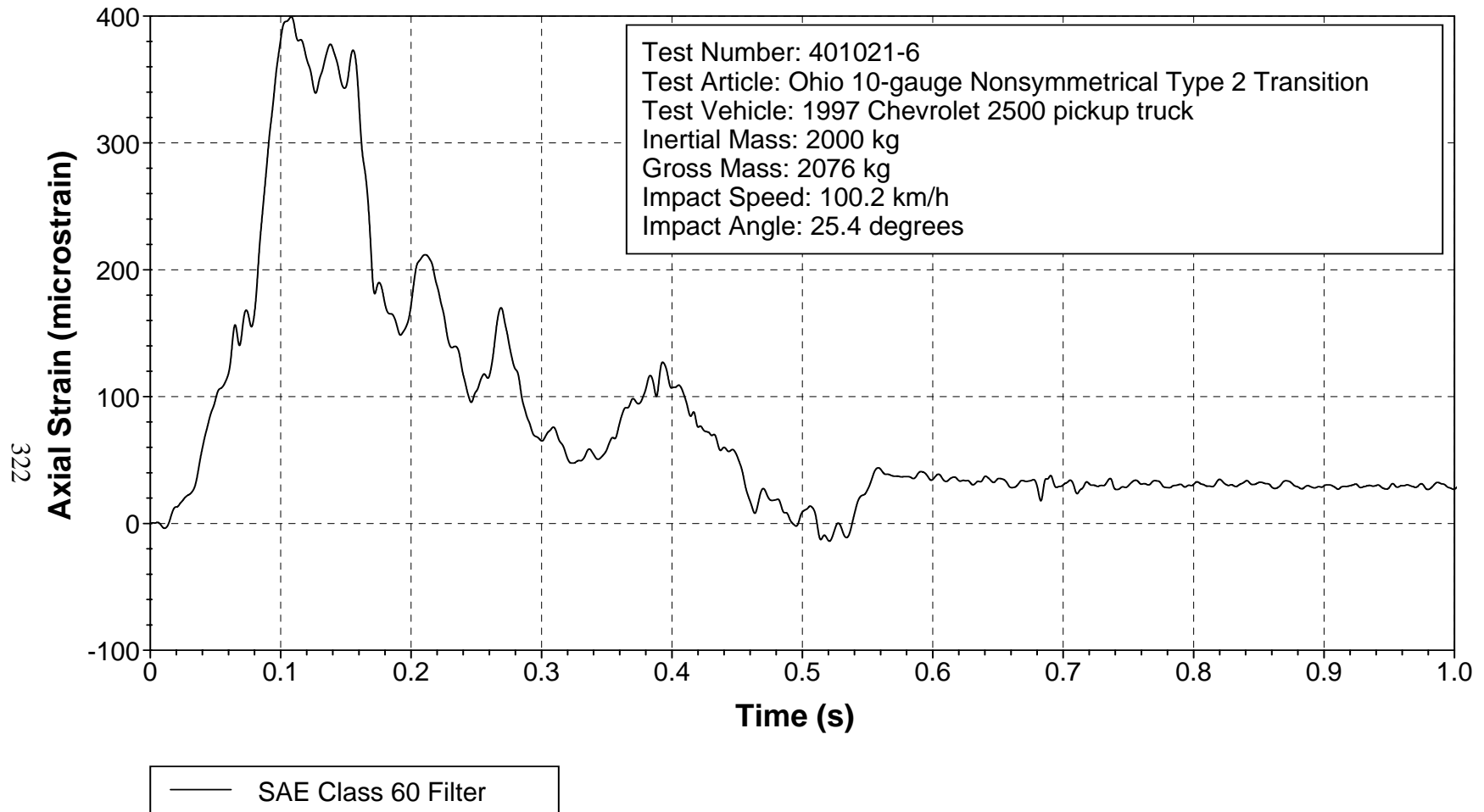


Figure 239. Axial strain, location 6, field side, for test 401021-6.

Y Axis Acceleration at Post 13

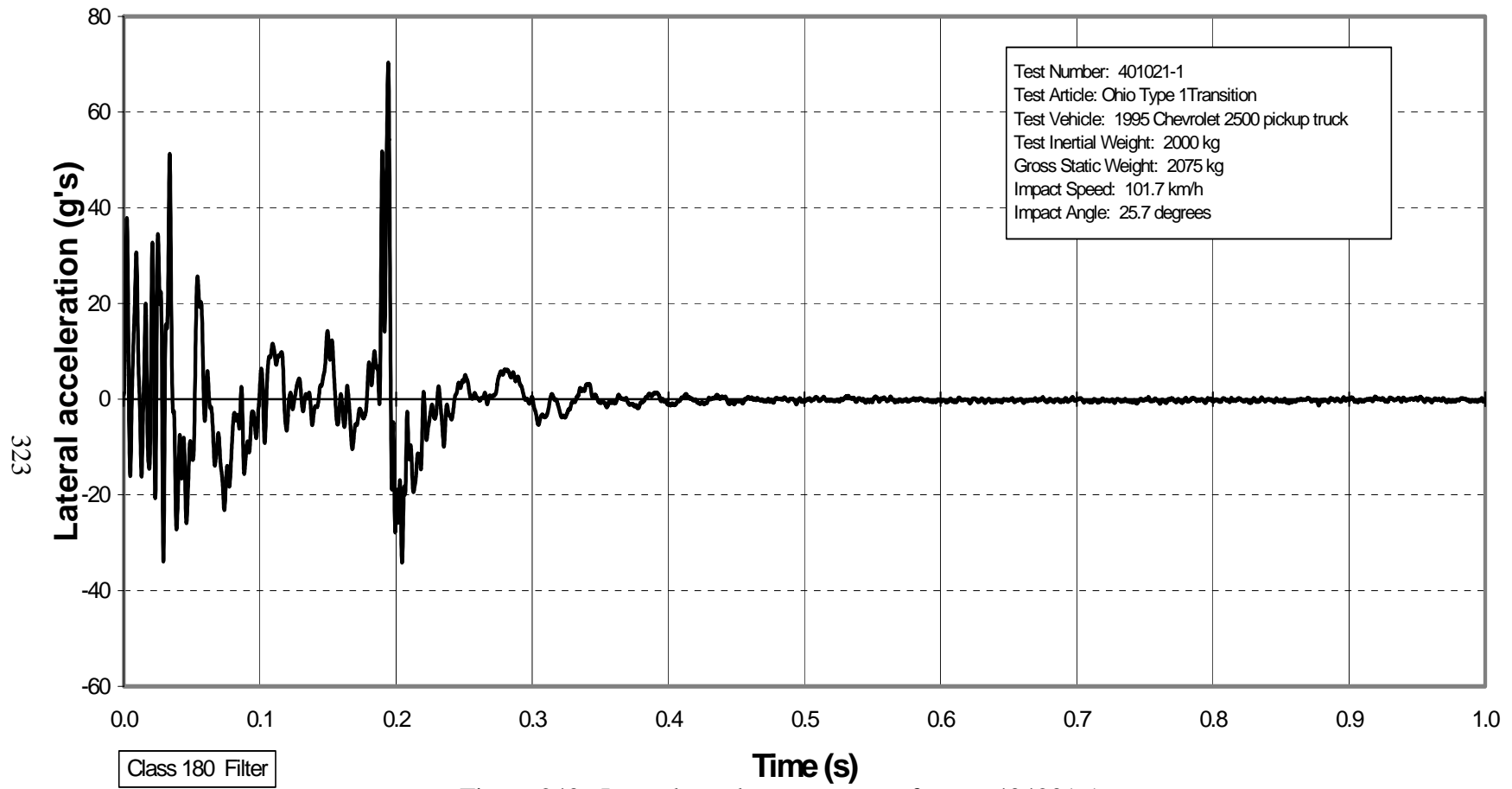


Figure 240. Lateral accelerometer trace for test 404201-1 (accelerometer located at center of post 13).

Gauge Location 1

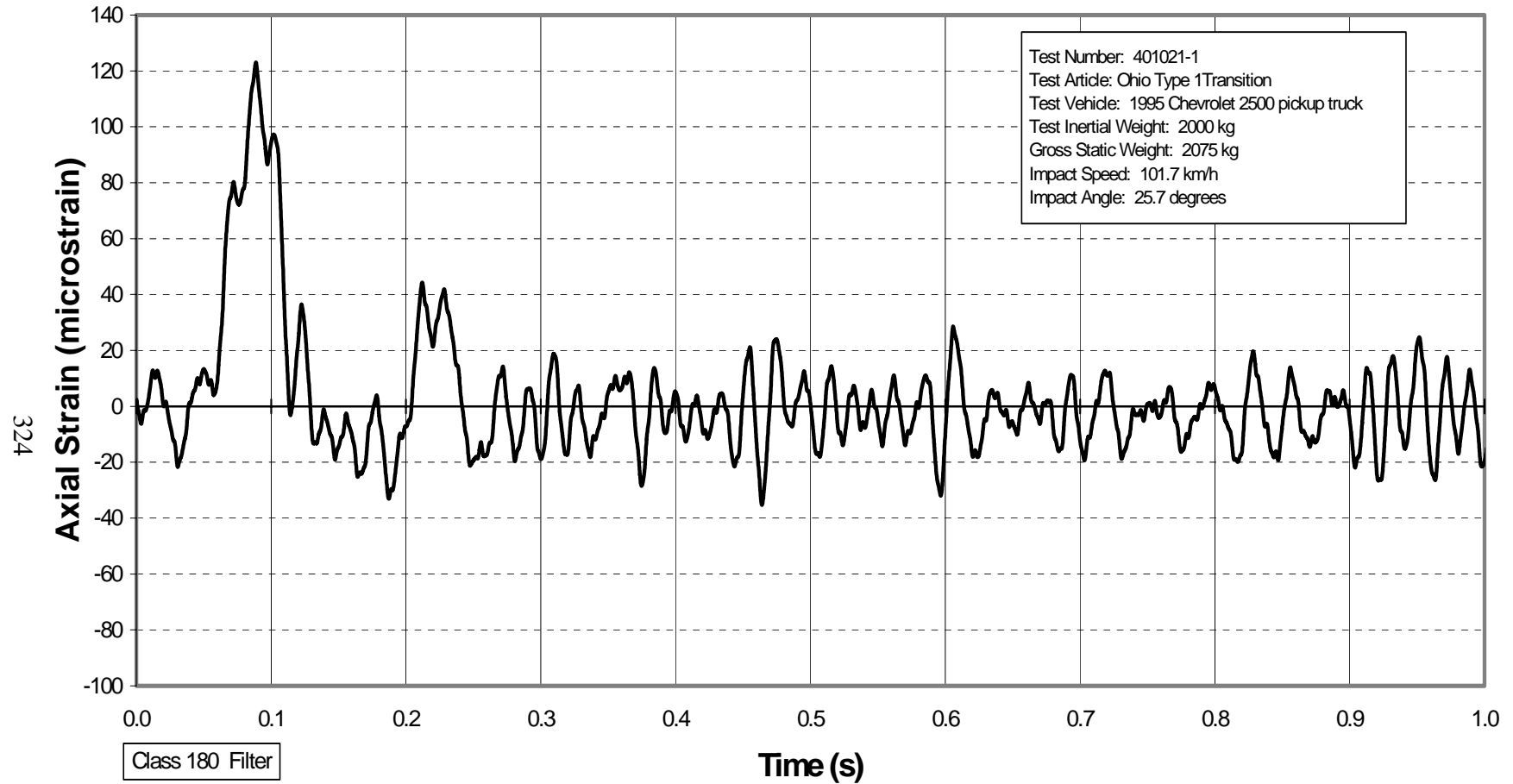


Figure 241. Axial strain, location 1, field side, for test 404201-1.

Gauge Location 2

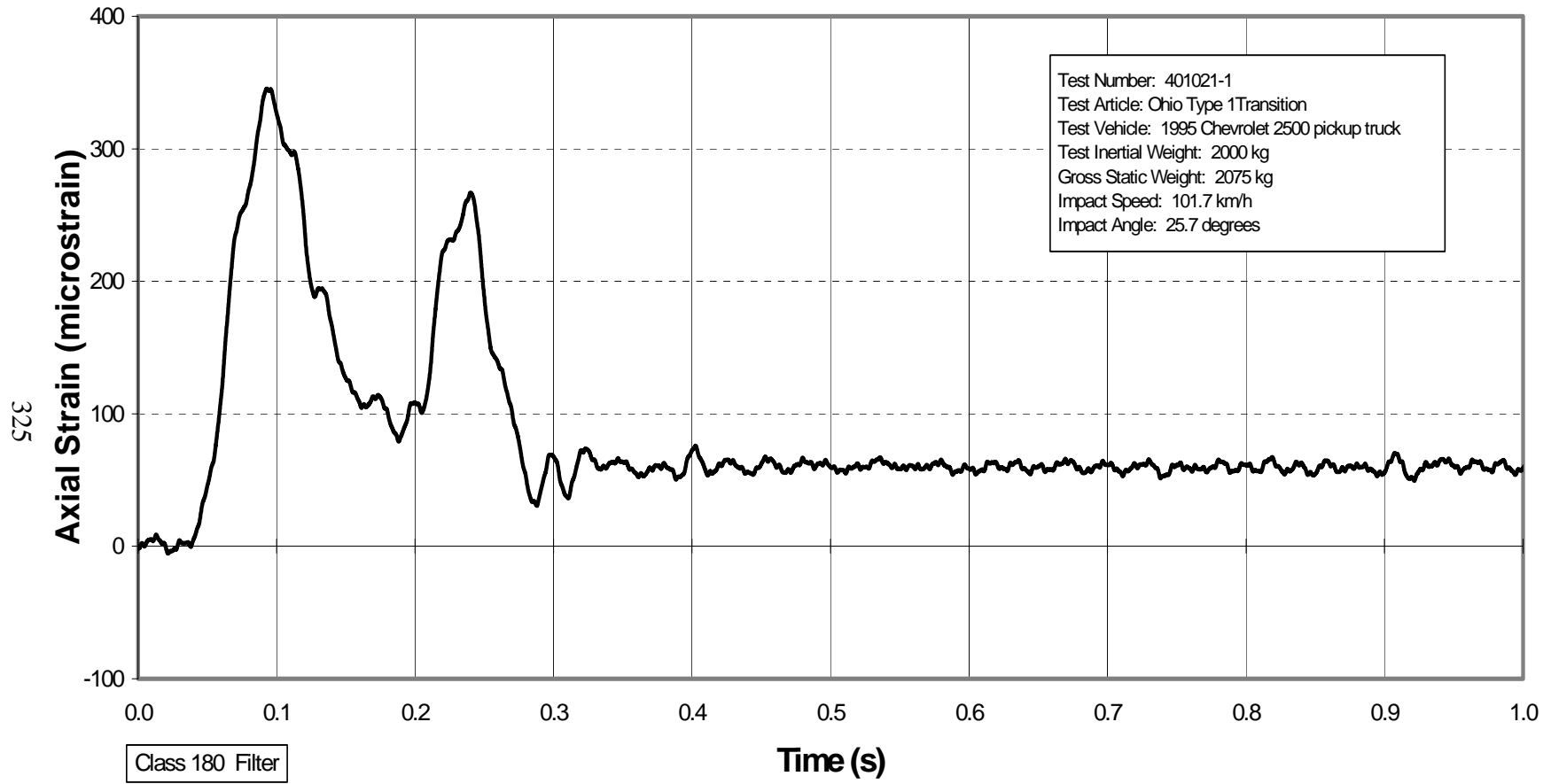


Figure 242. Axial strain, location 2, field side, for test 404201-1.

Gauge Location 3

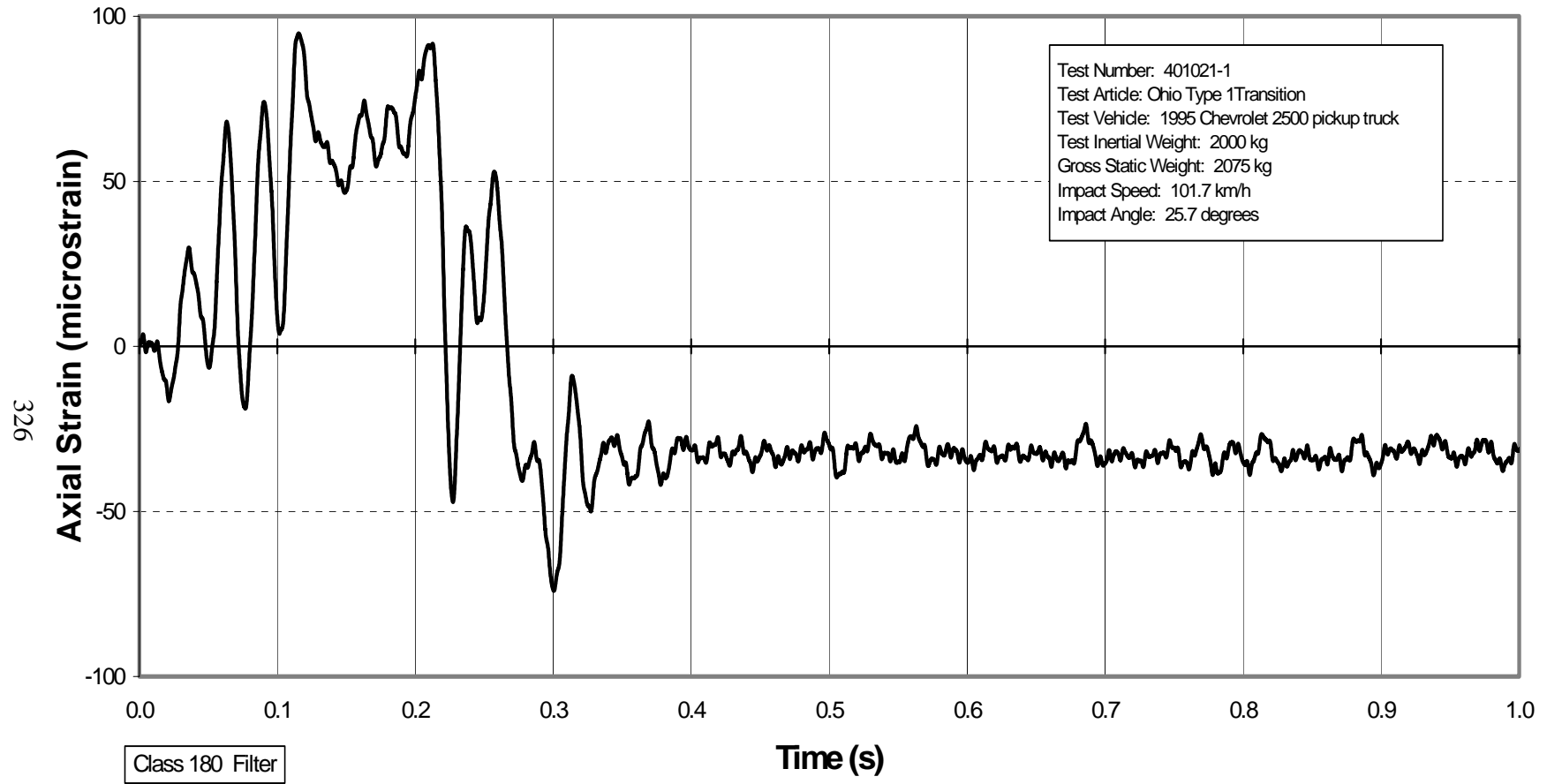


Figure 243. Axial strain, location 3, field side, for test 404201-1.

Gauge Location 4

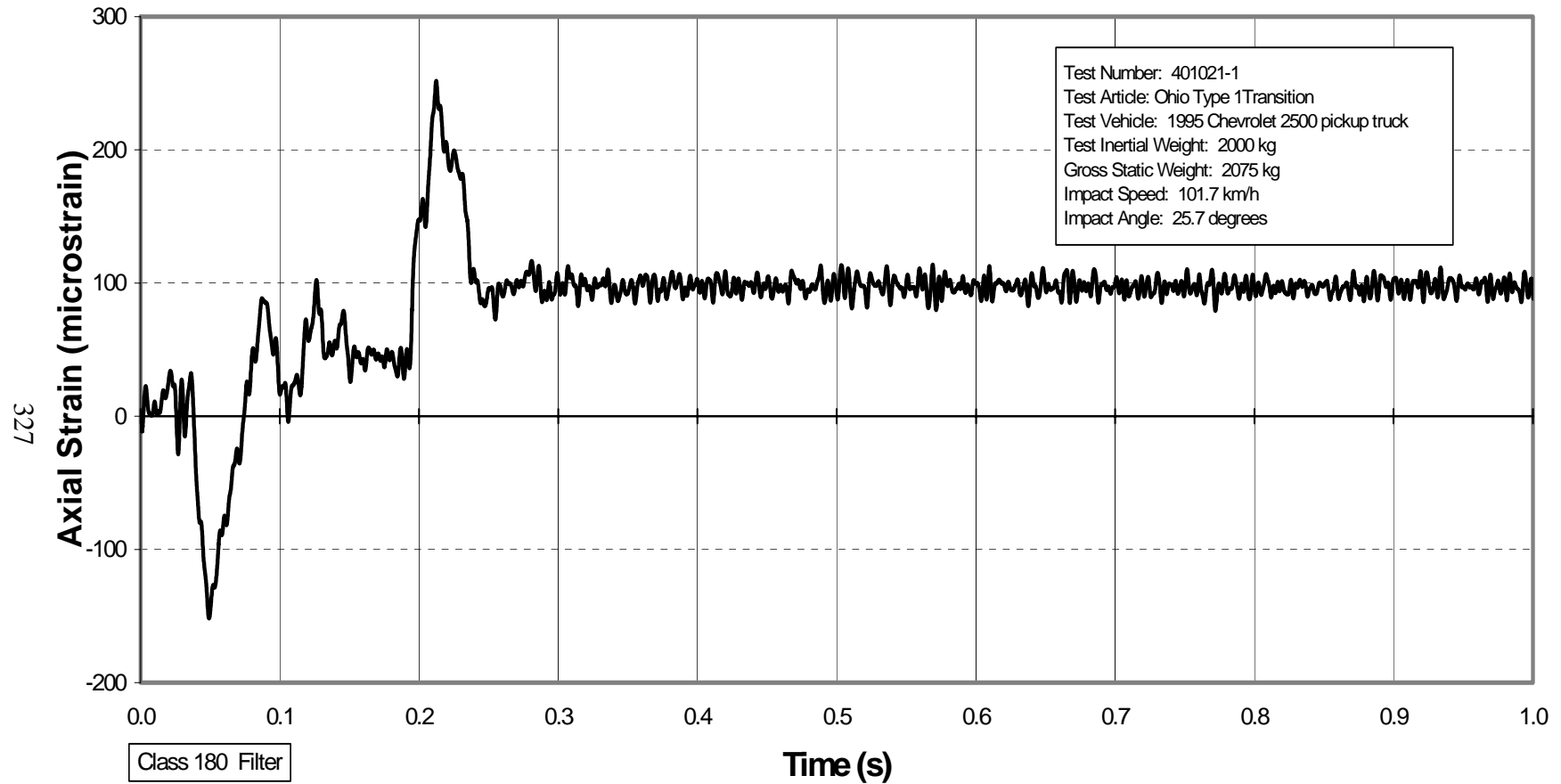


Figure 244. Axial strain, location 4, field side, for test 404201-1.

Gauge Location 5

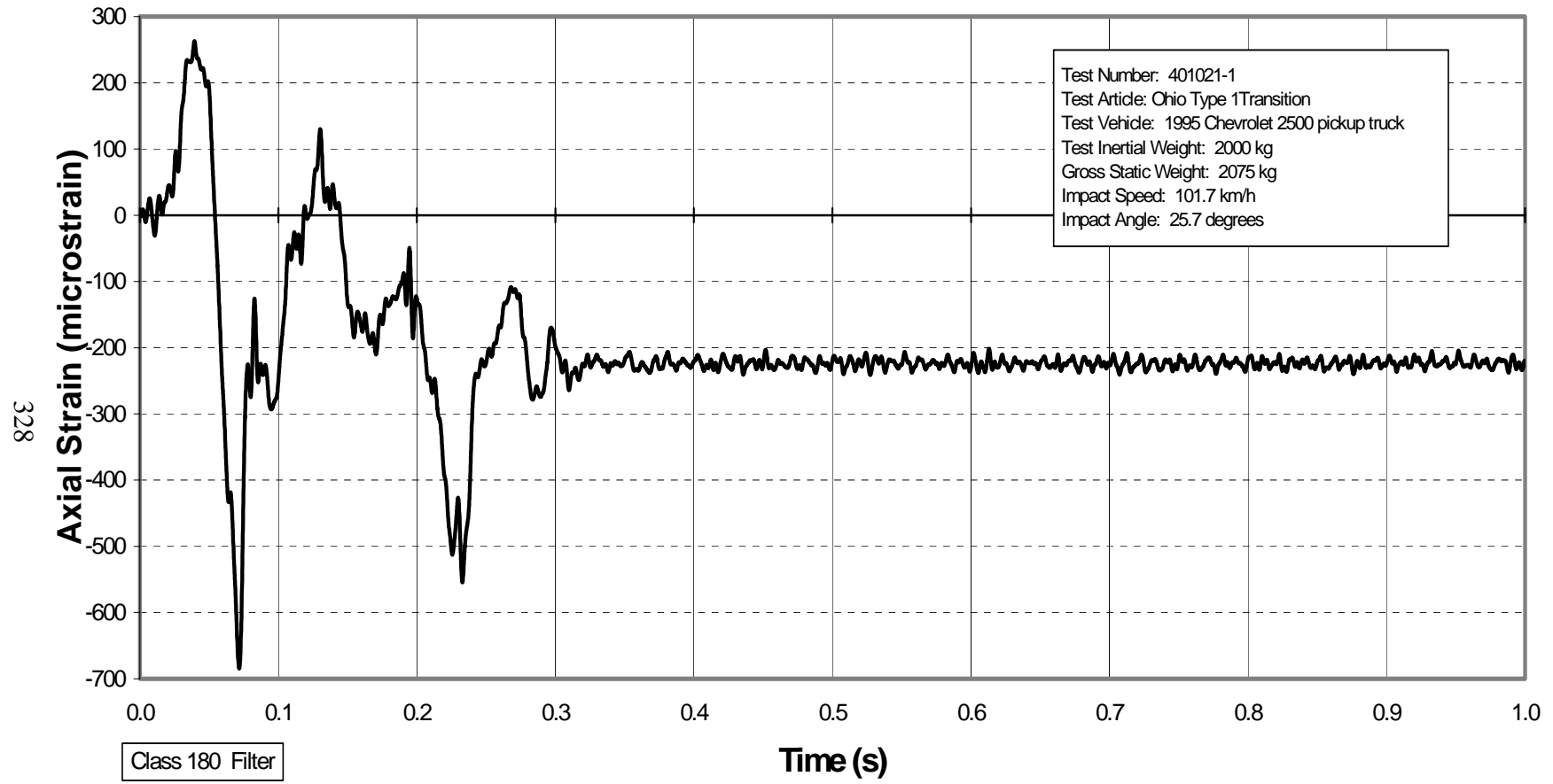


Figure 245. Axial strain, location 5, field side, for test 404201-1.

Gauge Location 6

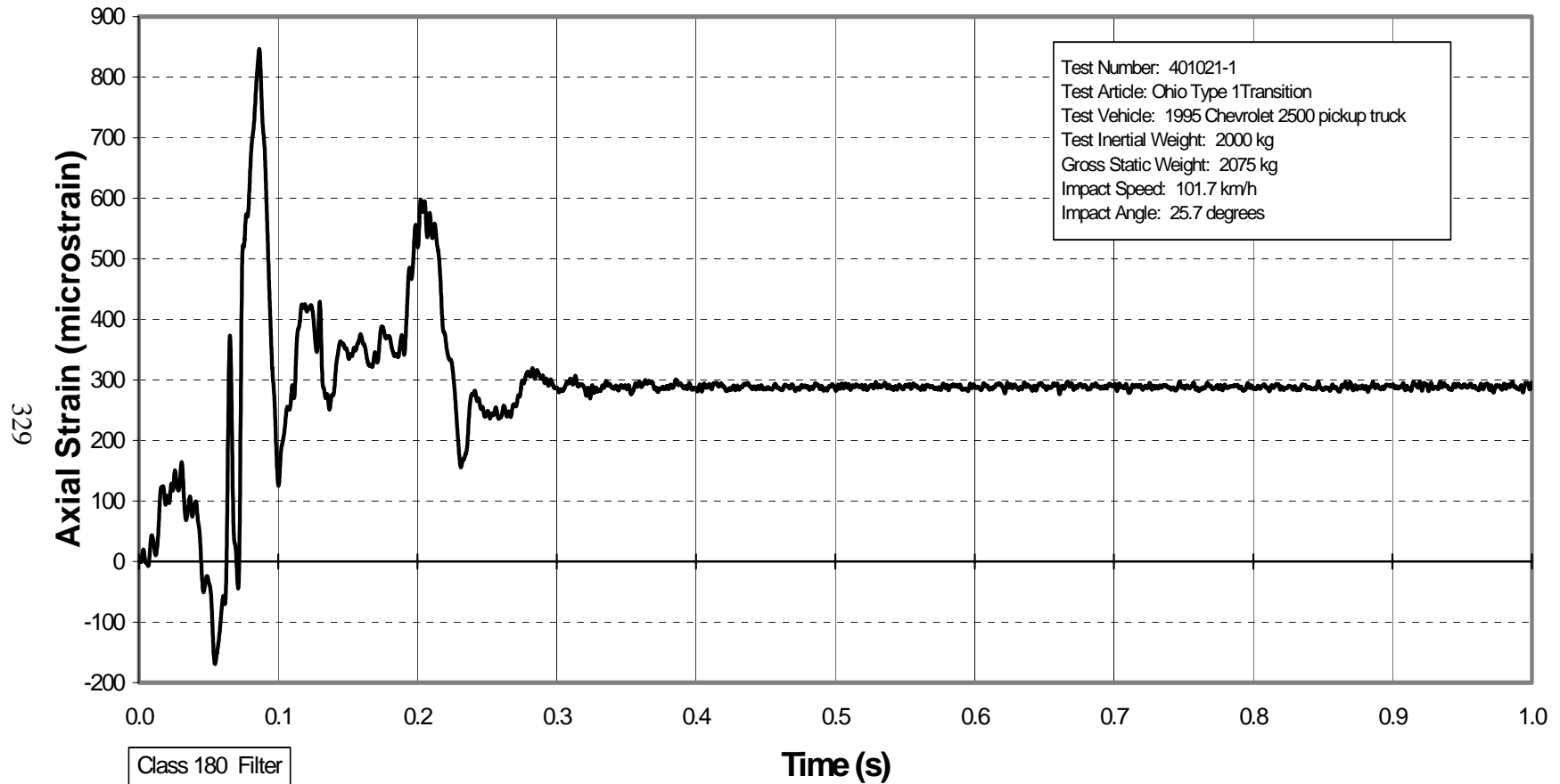


Figure 246. Axial strain, location 6, field side, for test 404201-1.

Y Axis Acceleration at Post 13

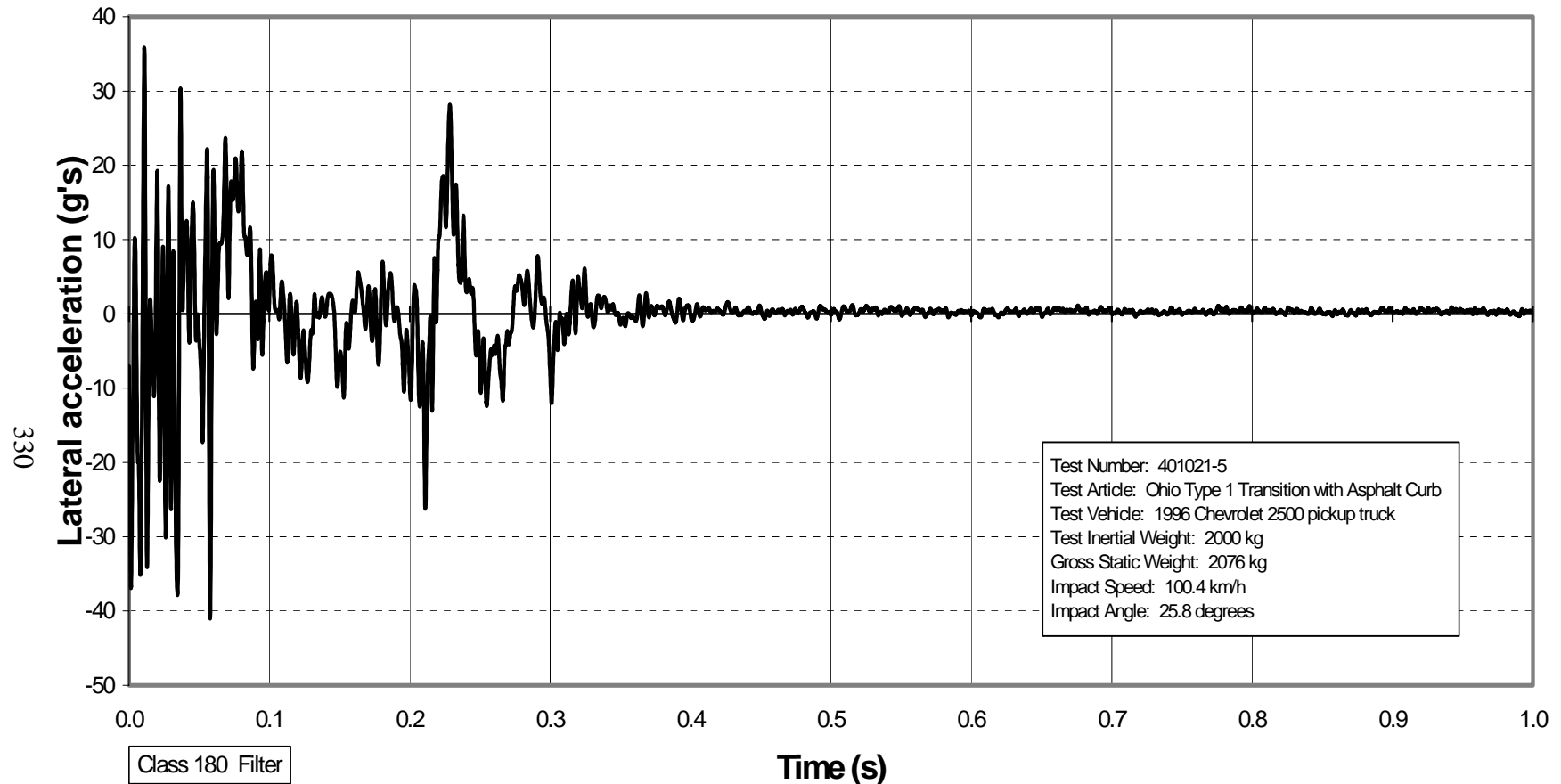


Figure 247. Lateral accelerometer trace for test 401021-5 (accelerometer located at center of post 13).

Gauge Location 1

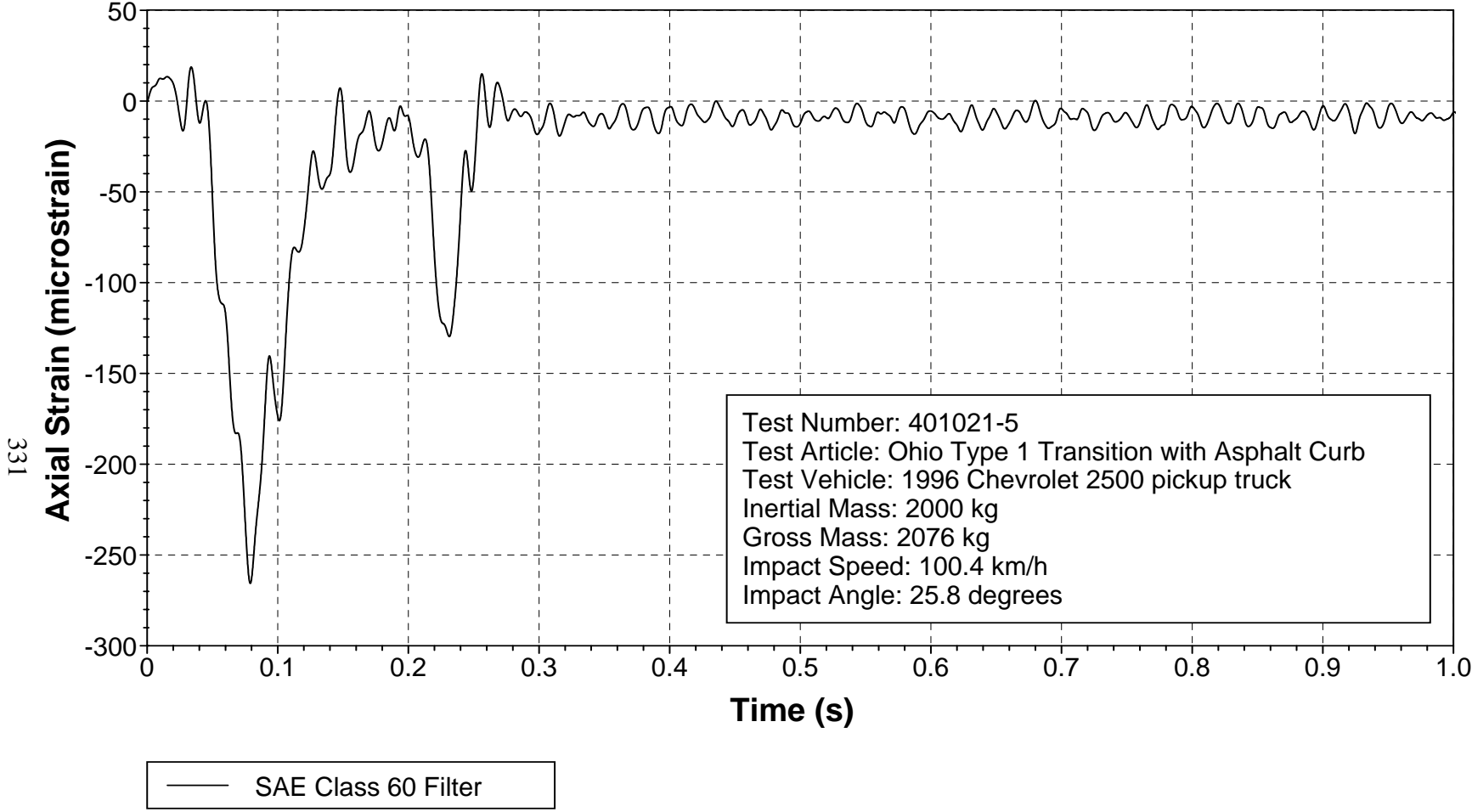


Figure 248. Axial strain, location 1, field side, for test 401021-5.

Gauge Location 2

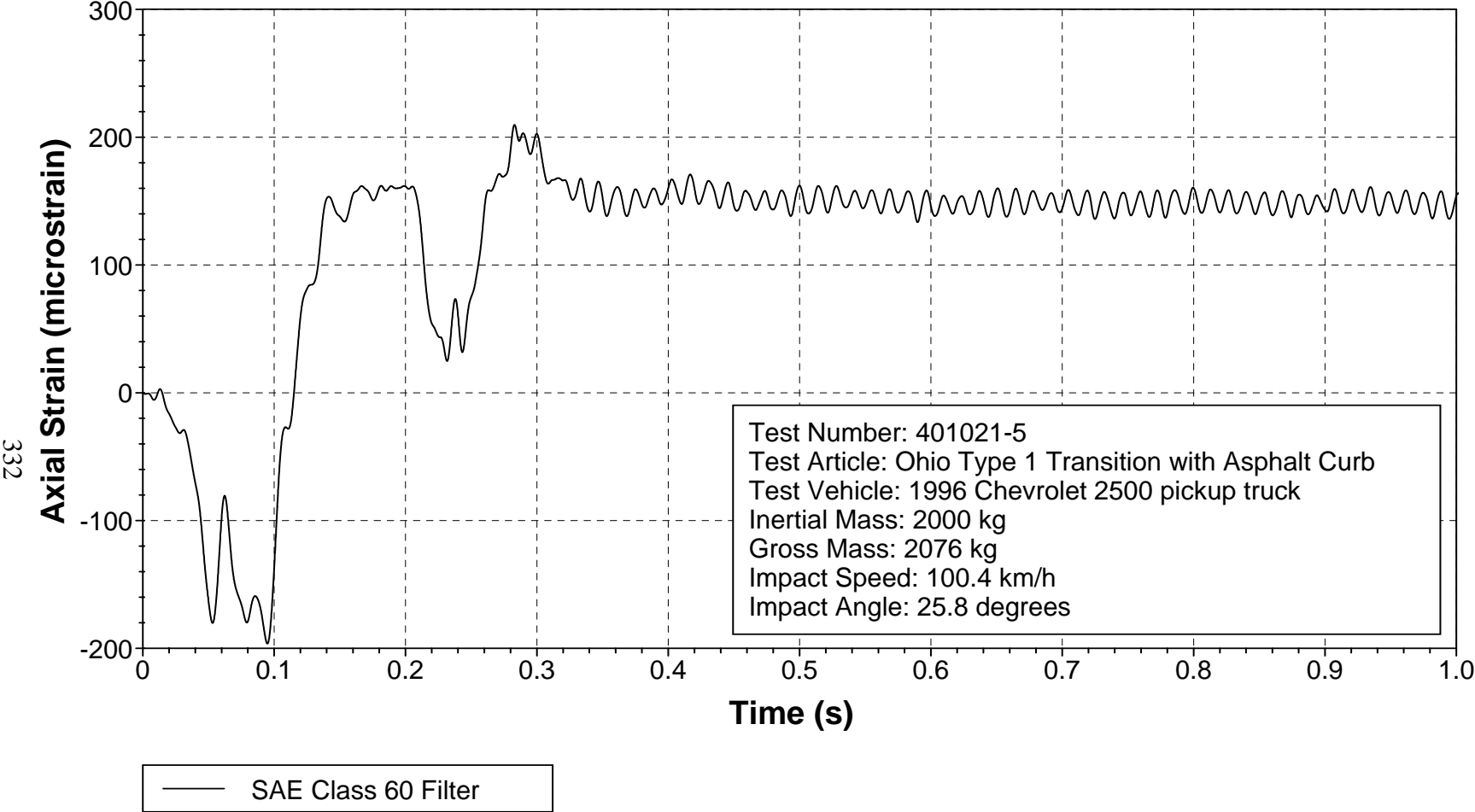


Figure 249. Axial strain, location 2, field side, for test 401021-5.

Gauge Location 3

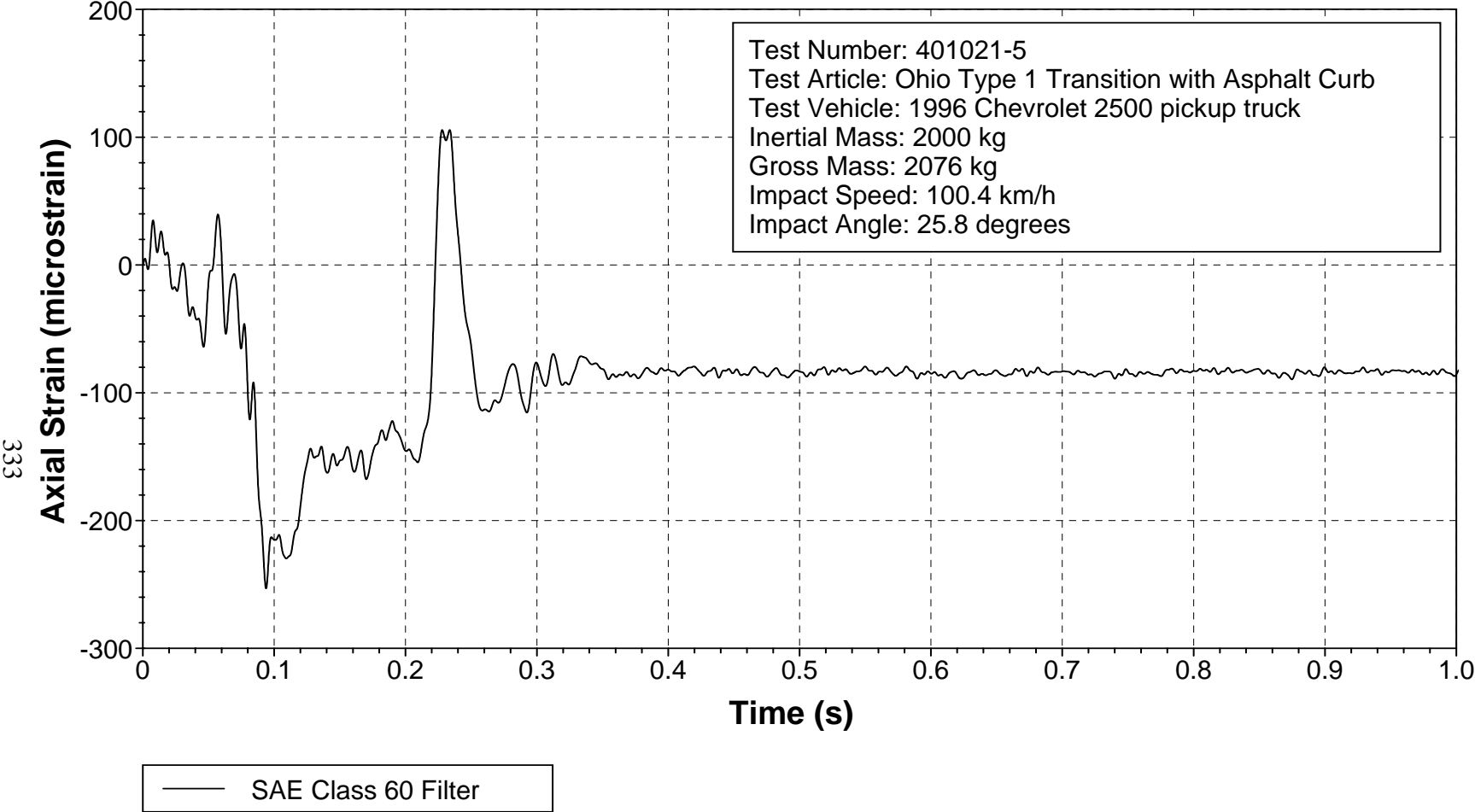


Figure 250. Axial strain, location 3, field side, for test 401021-5.

Gauge Location 4

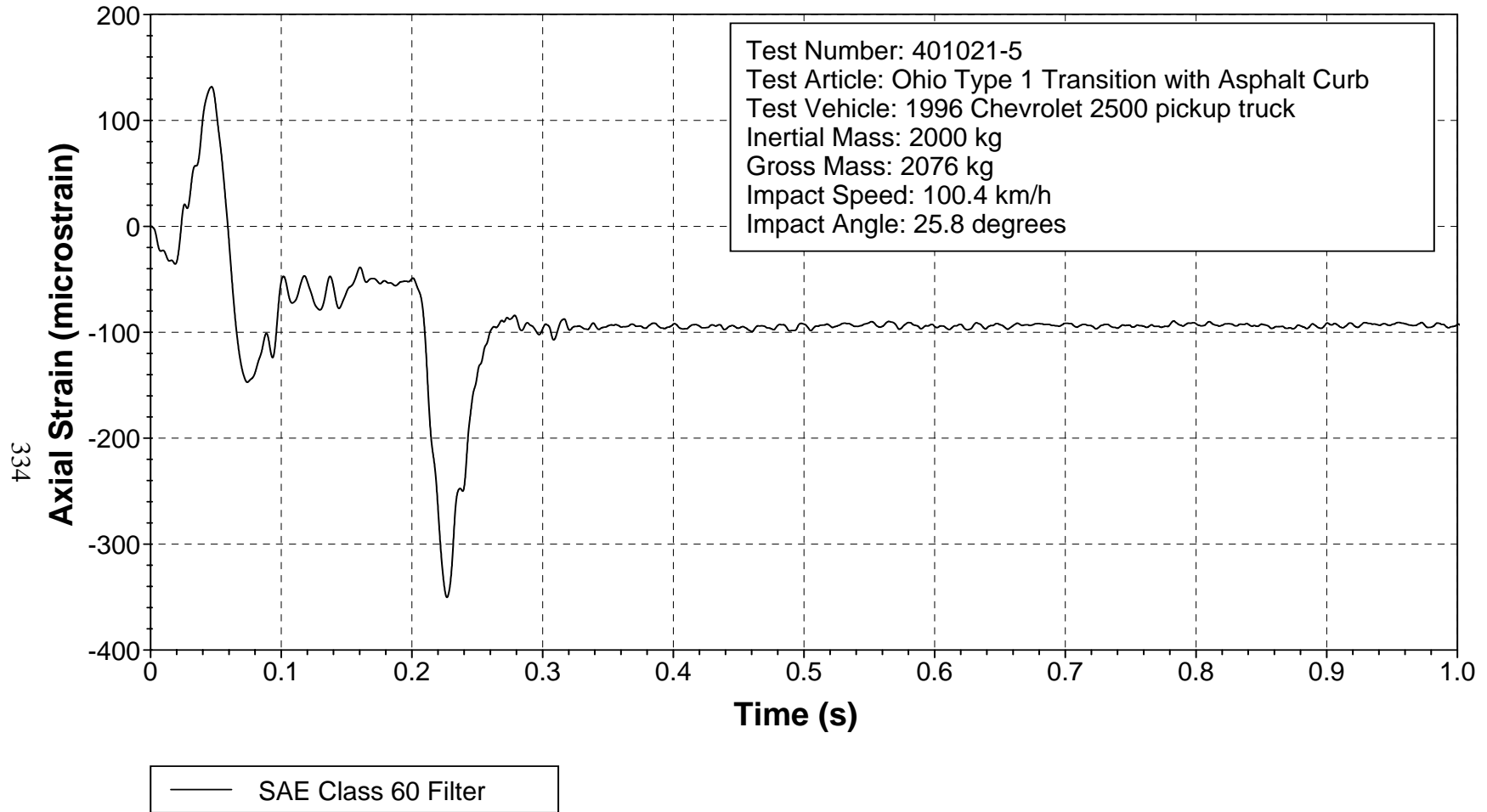


Figure 251. Axial strain, location 4, field side, for test 401021-5.

Gauge Location 5

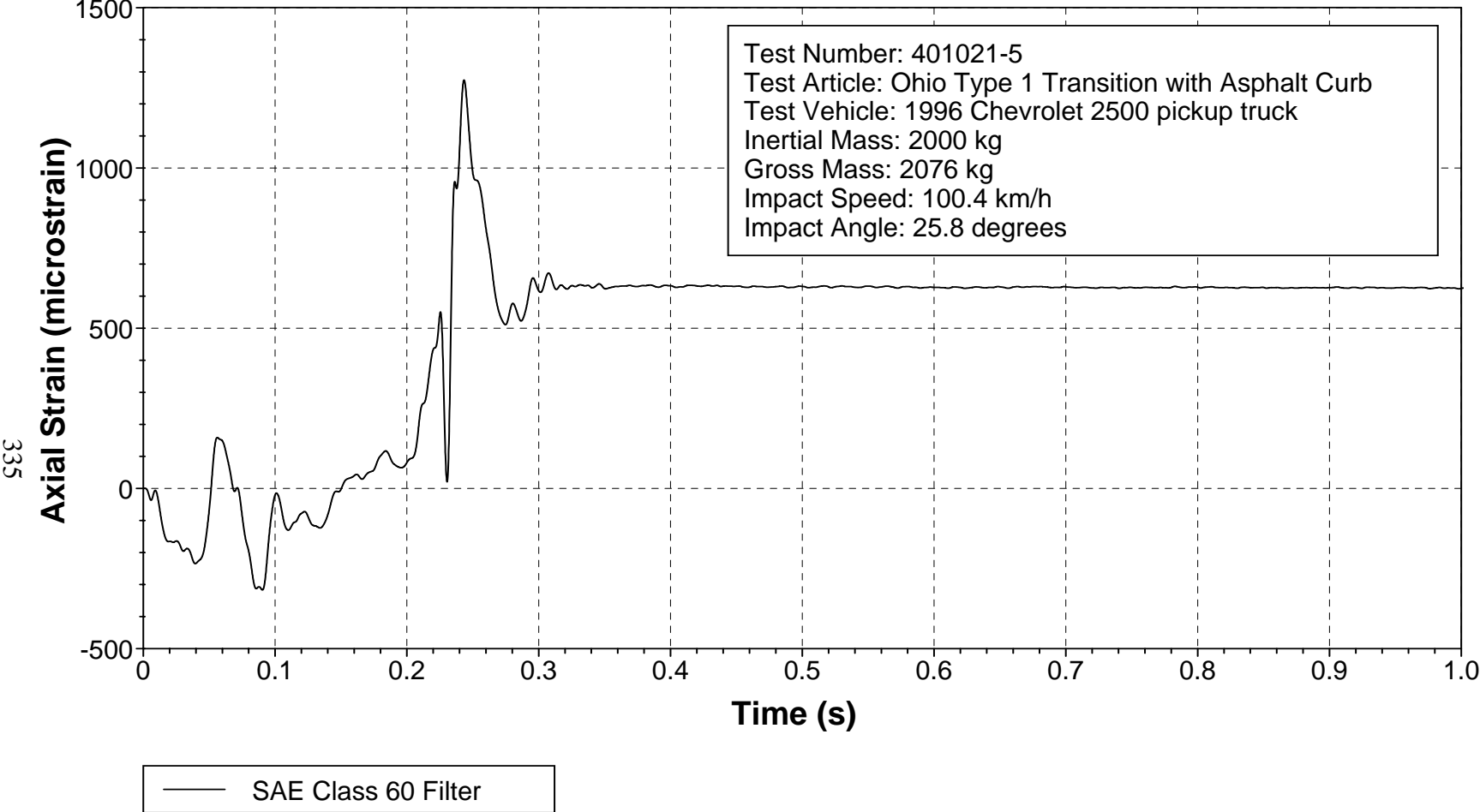


Figure 252. Axial strain, location 5, field side, for test 401021-5.

Gauge Location 6

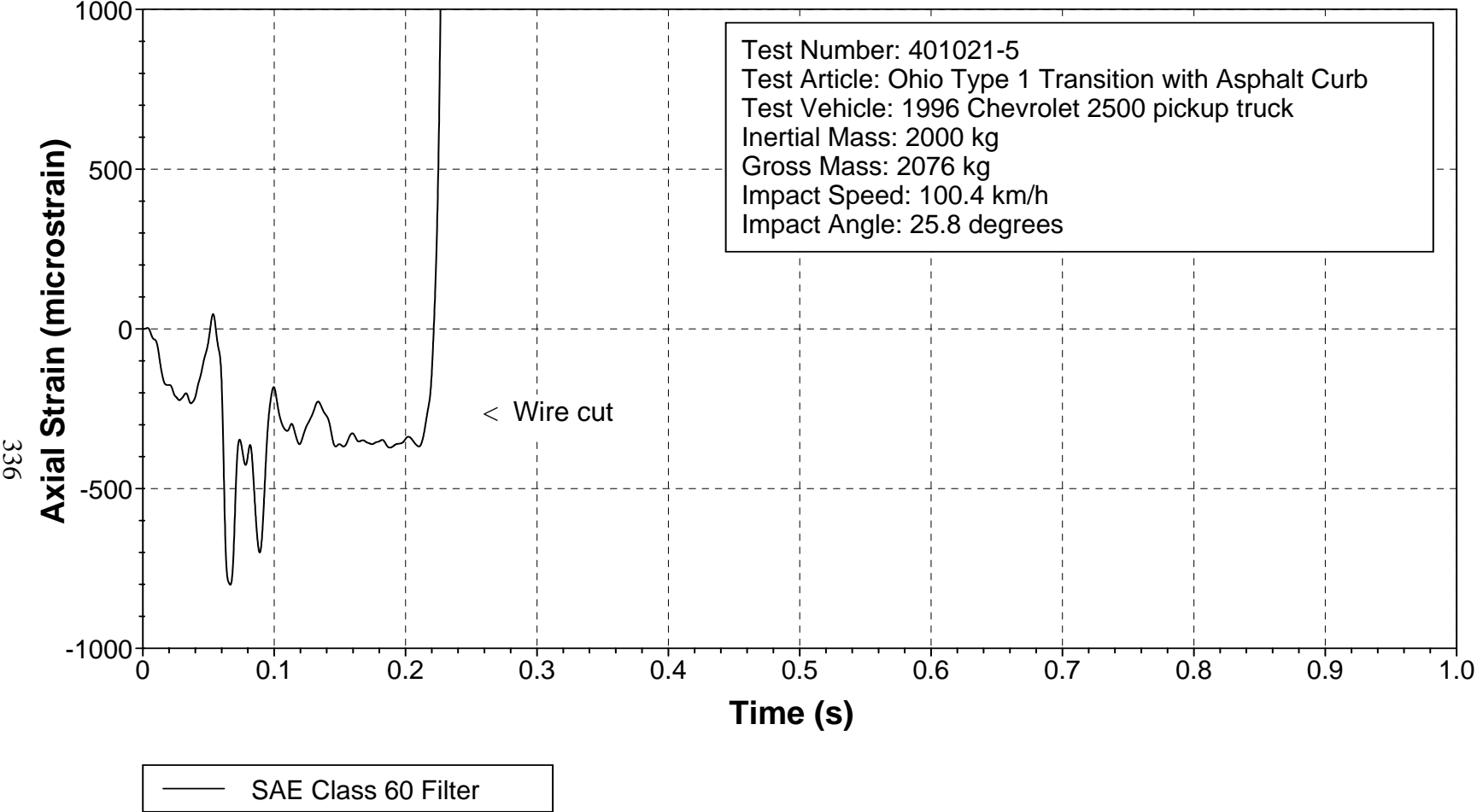


Figure 253. Axial strain, location 6, field side, for test 401021-5.

Y Axis Acceleration at Post 13

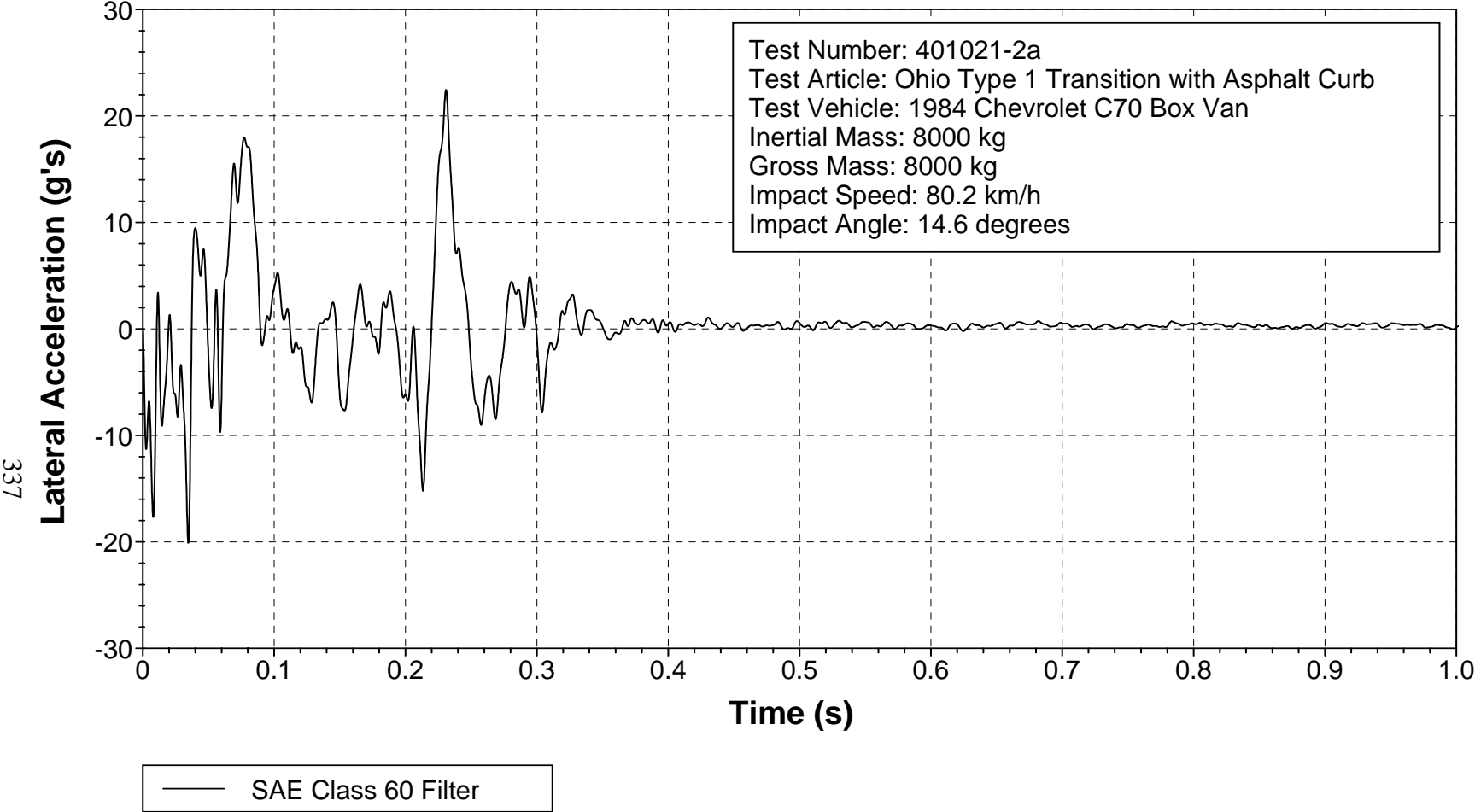


Figure 254. Lateral accelerometer trace for test 401021-2a (accelerometer located at center of post 13).

Gauge Location 1

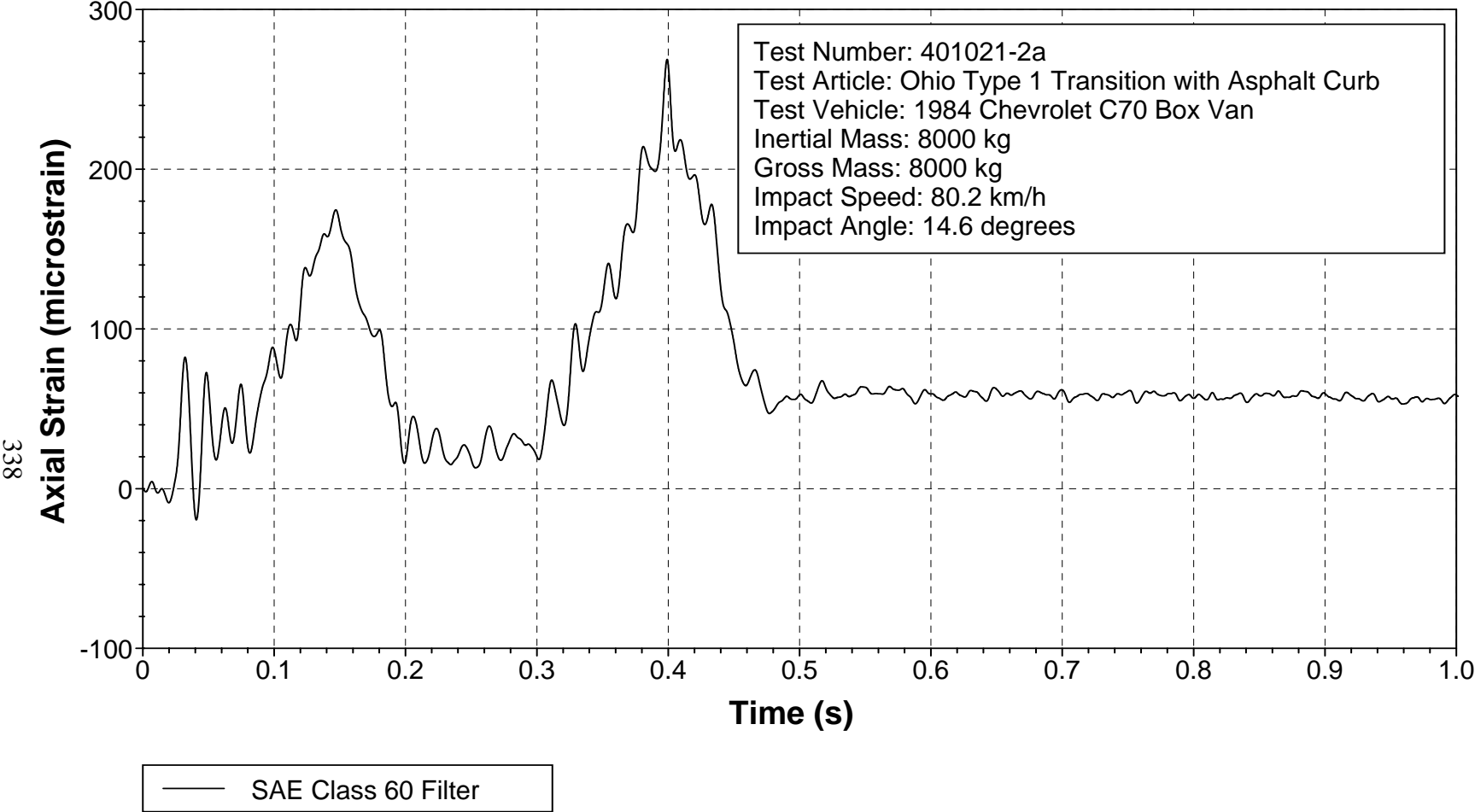


Figure 255. Axial strain, location 1, field side, for test 401021-2a.

Gauge Location 2

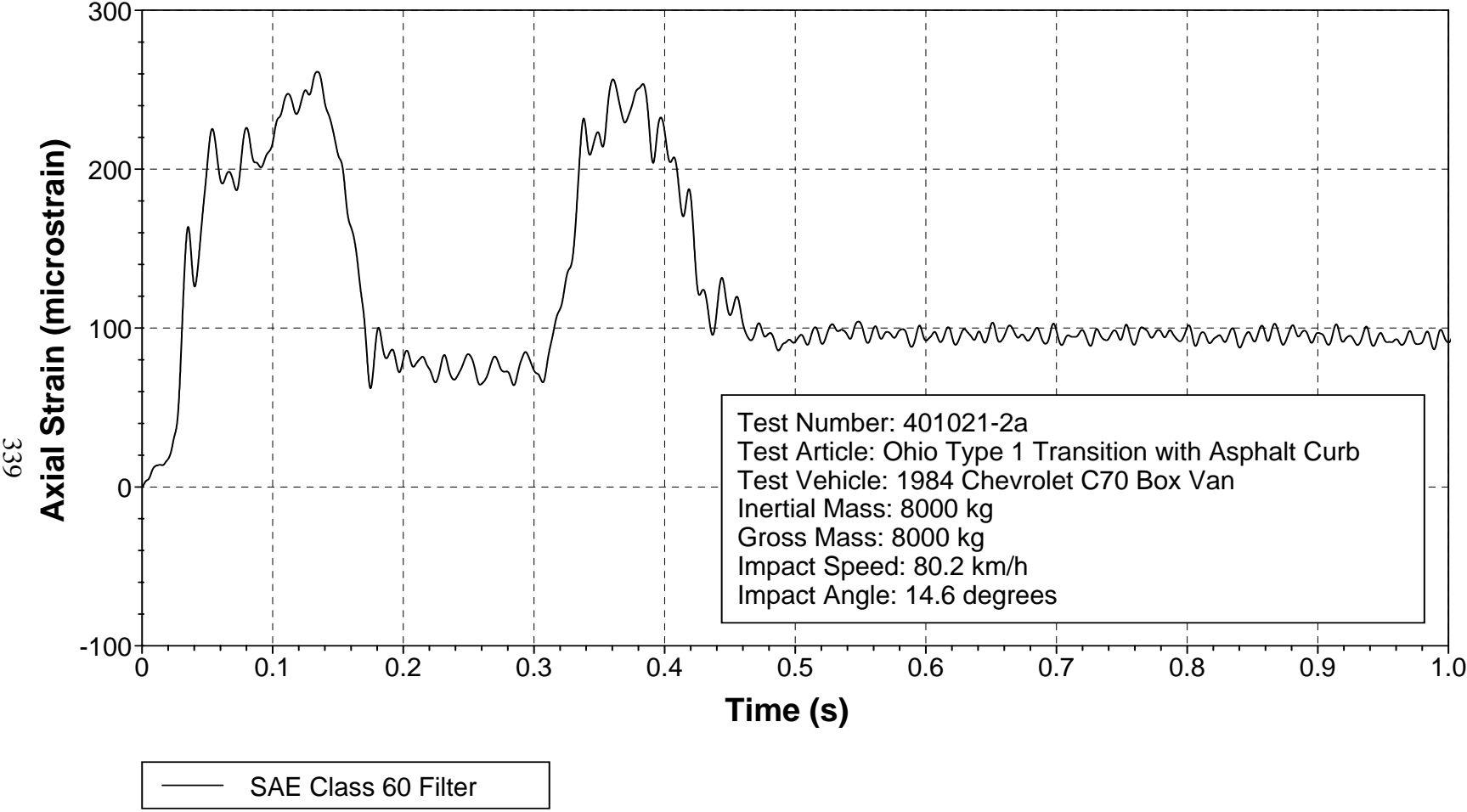


Figure 256. Axial strain, location 2, field side, for test 401021-2a.

Gauge Location 3

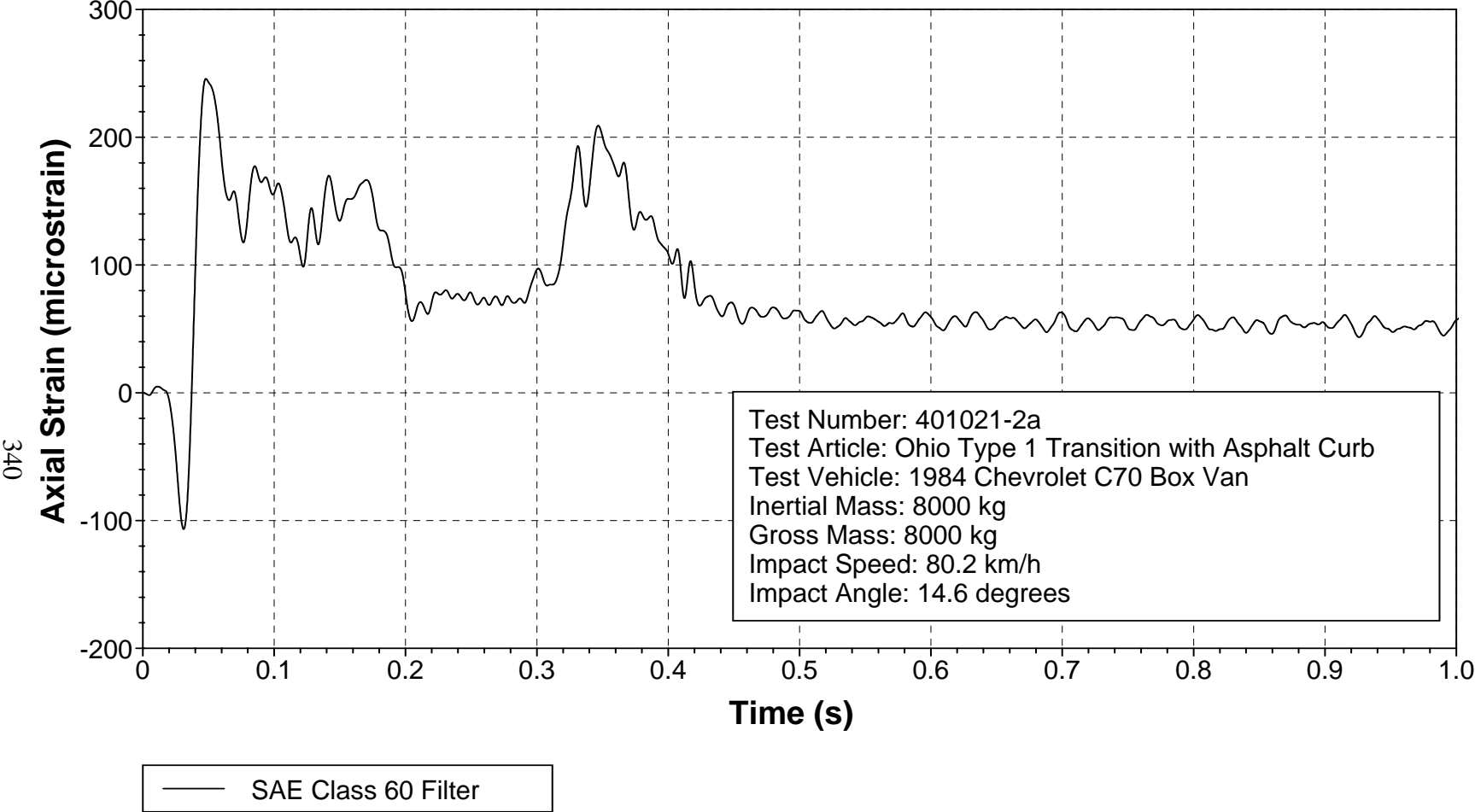


Figure 257. Axial strain, location 3, field side, for test 401021-2a.

Gauge Location 4

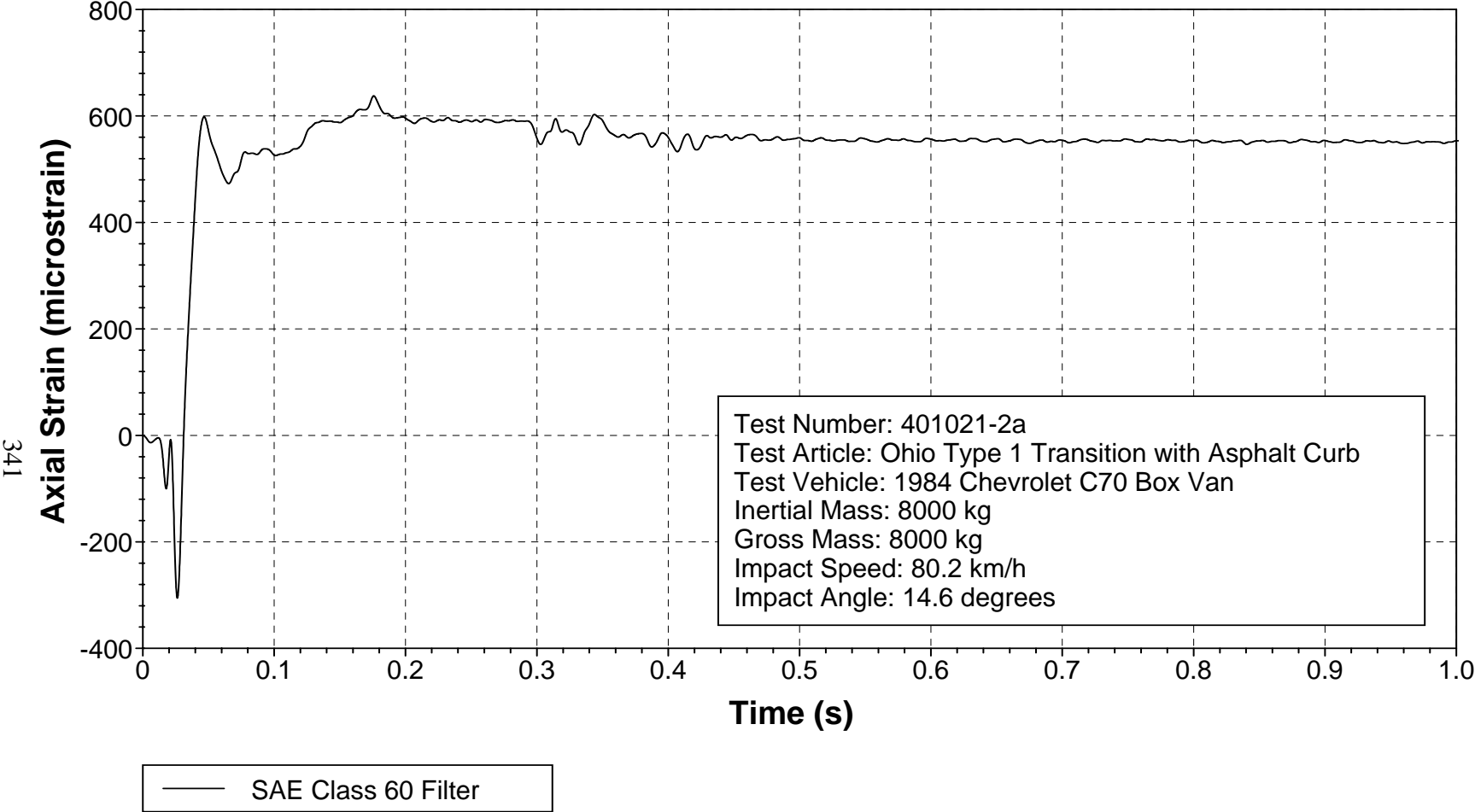


Figure 258. Axial strain, location 4, field side, for test 401021-2a.

Gauge Location 5

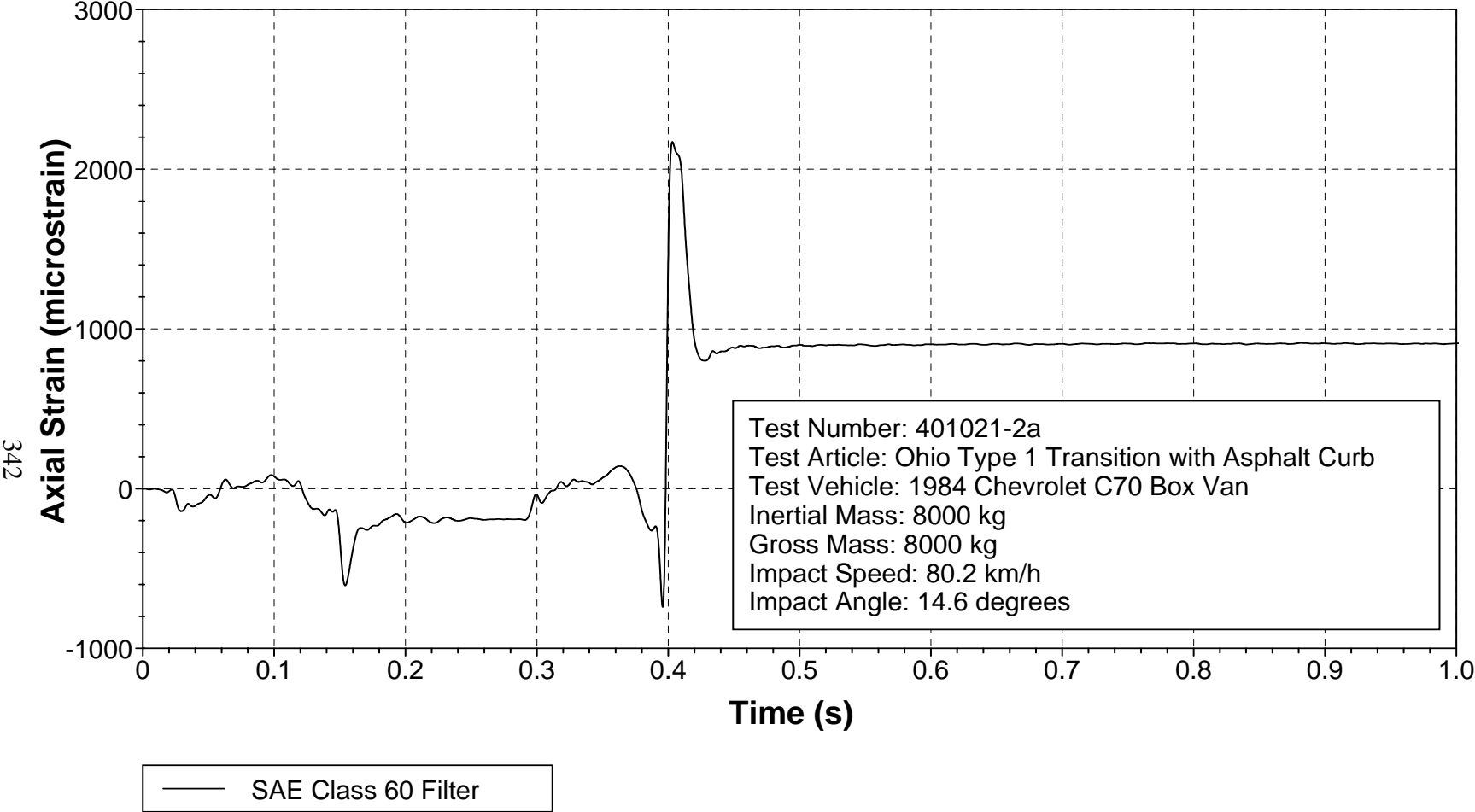


Figure 259. Axial strain, location 5, field side, for test 401021-2a.

Gauge Location 6

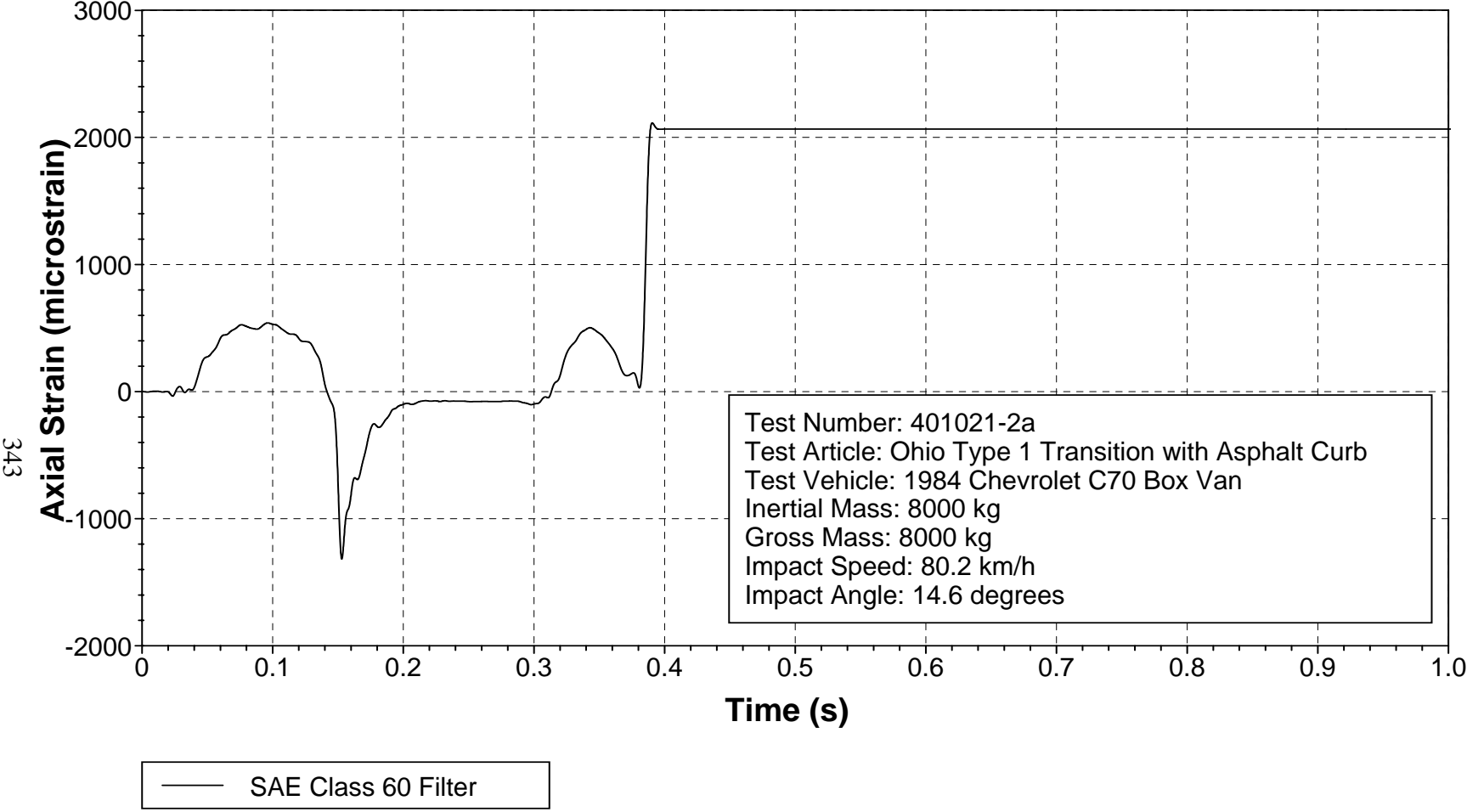


Figure 260. Axial strain, location 6, field side, for test 401021-2a.

Y Axis Acceleration at Post 18

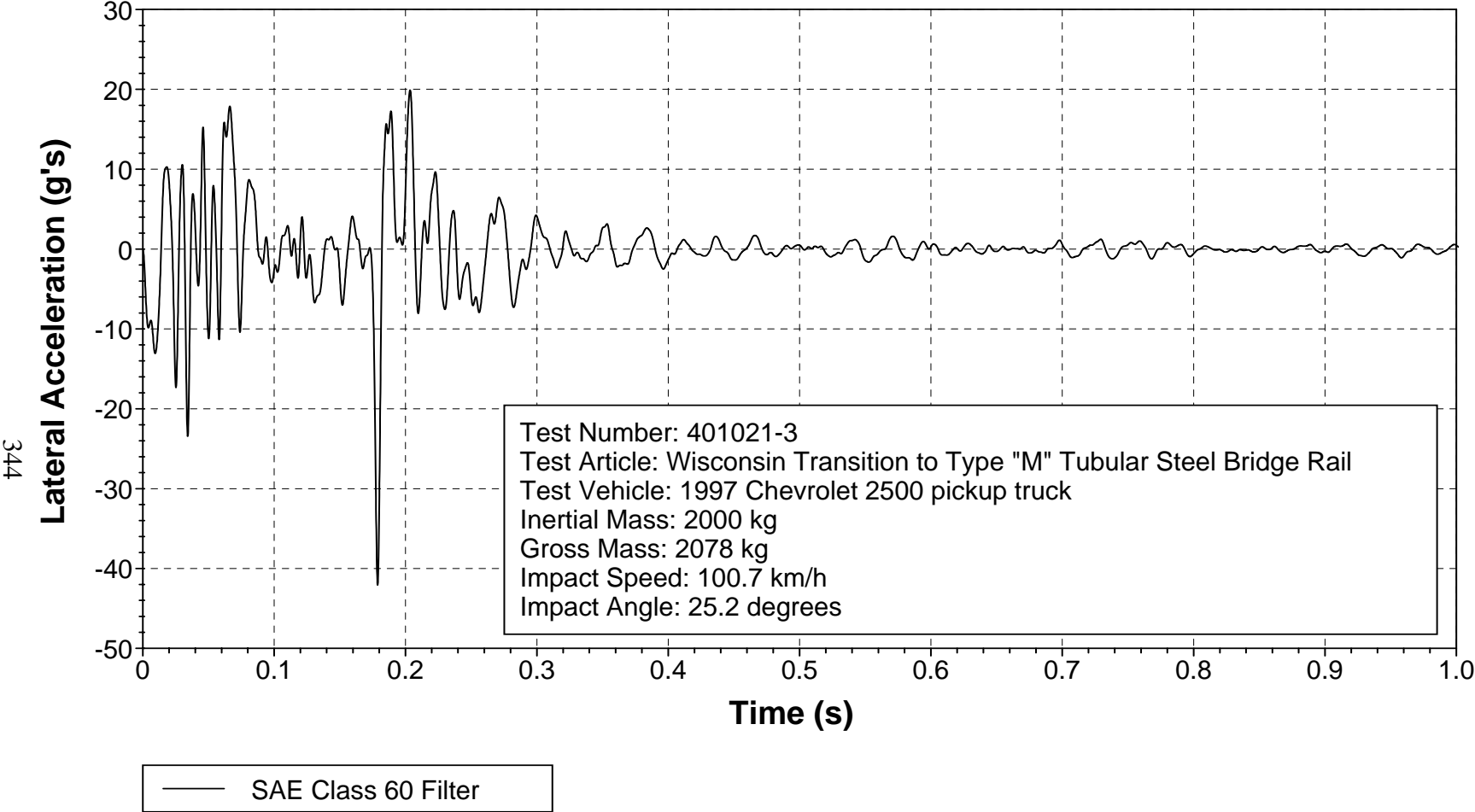


Figure 261. Lateral accelerometer trace for test 401021-3 (accelerometer located at center of post 18).

Gauge Location 1

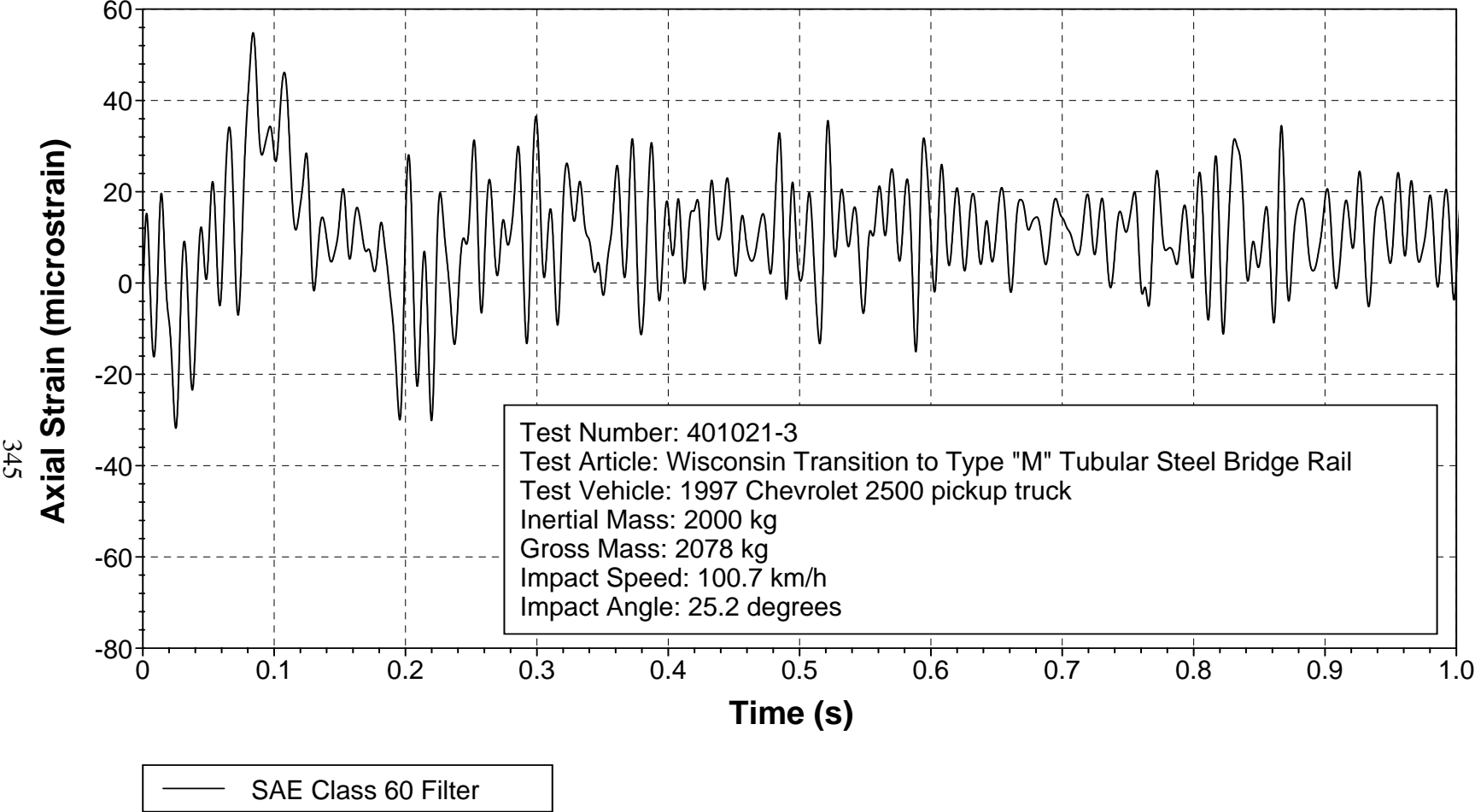


Figure 262. Axial strain, location 1, field side, for test 401021-3.

Gauge Location 2

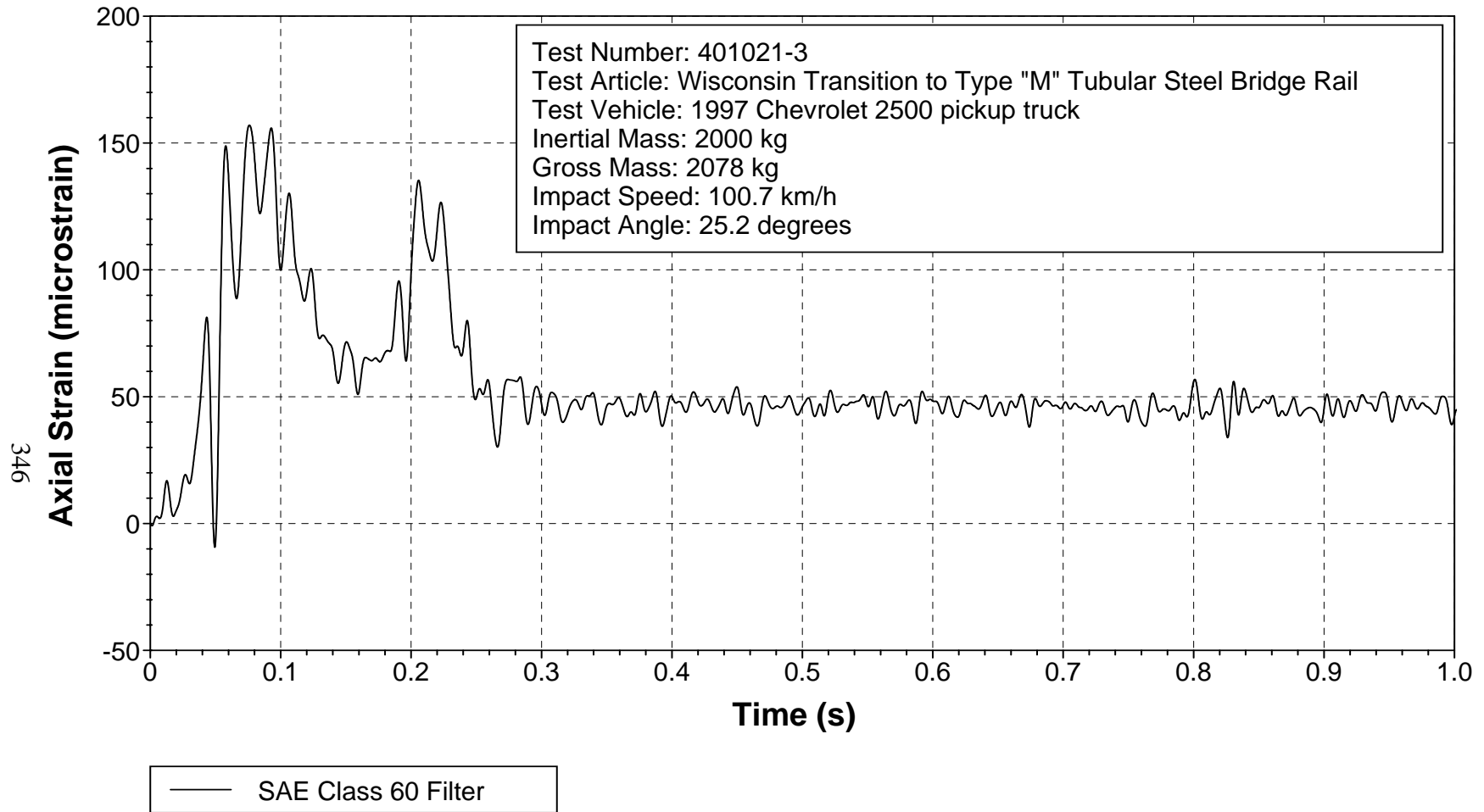


Figure 263. Axial strain, location 2, field side, for test 401021-3.

Gauge Location 3

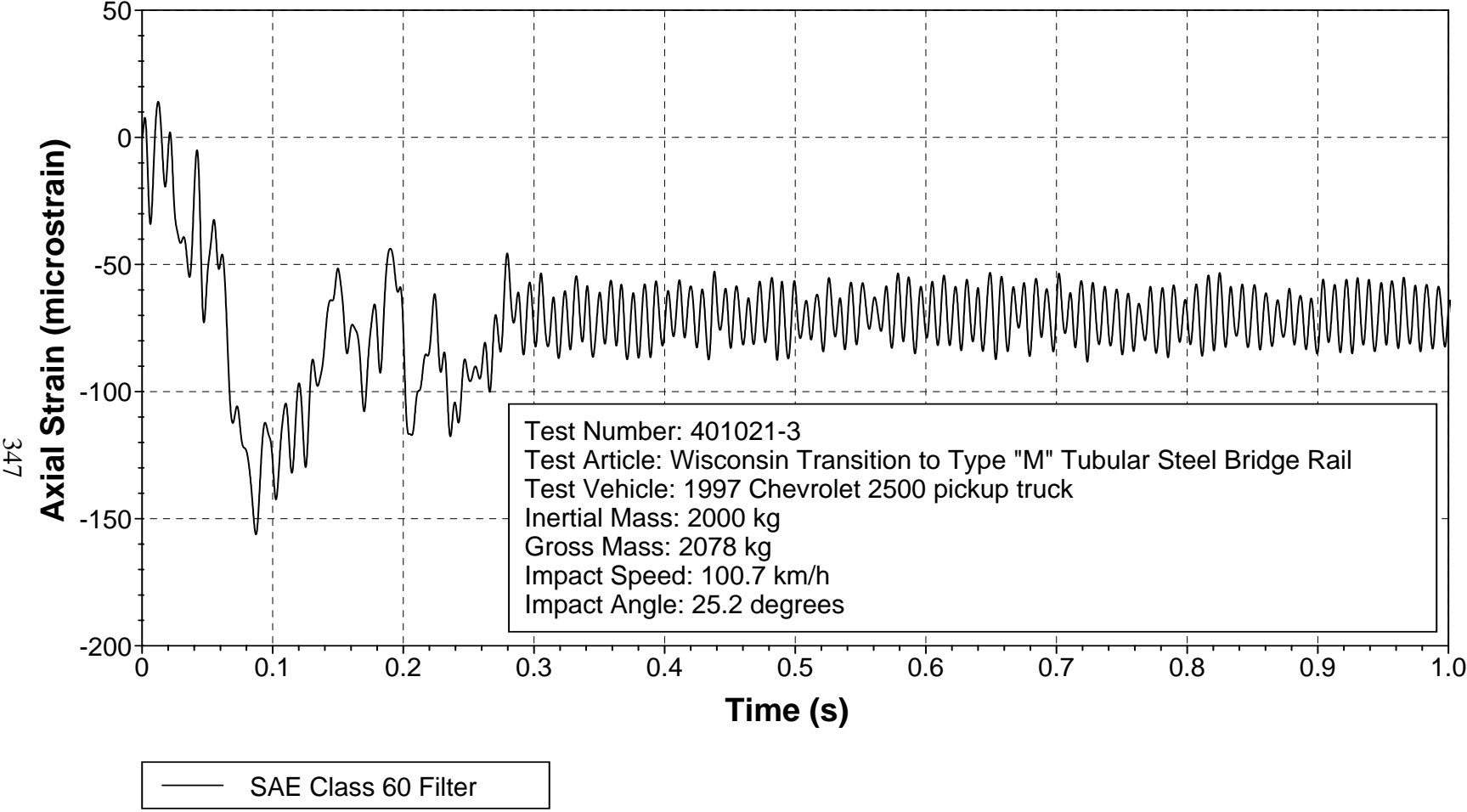


Figure 264. Axial strain, location 3, field side, for test 401021-3.

Gauge Location 4

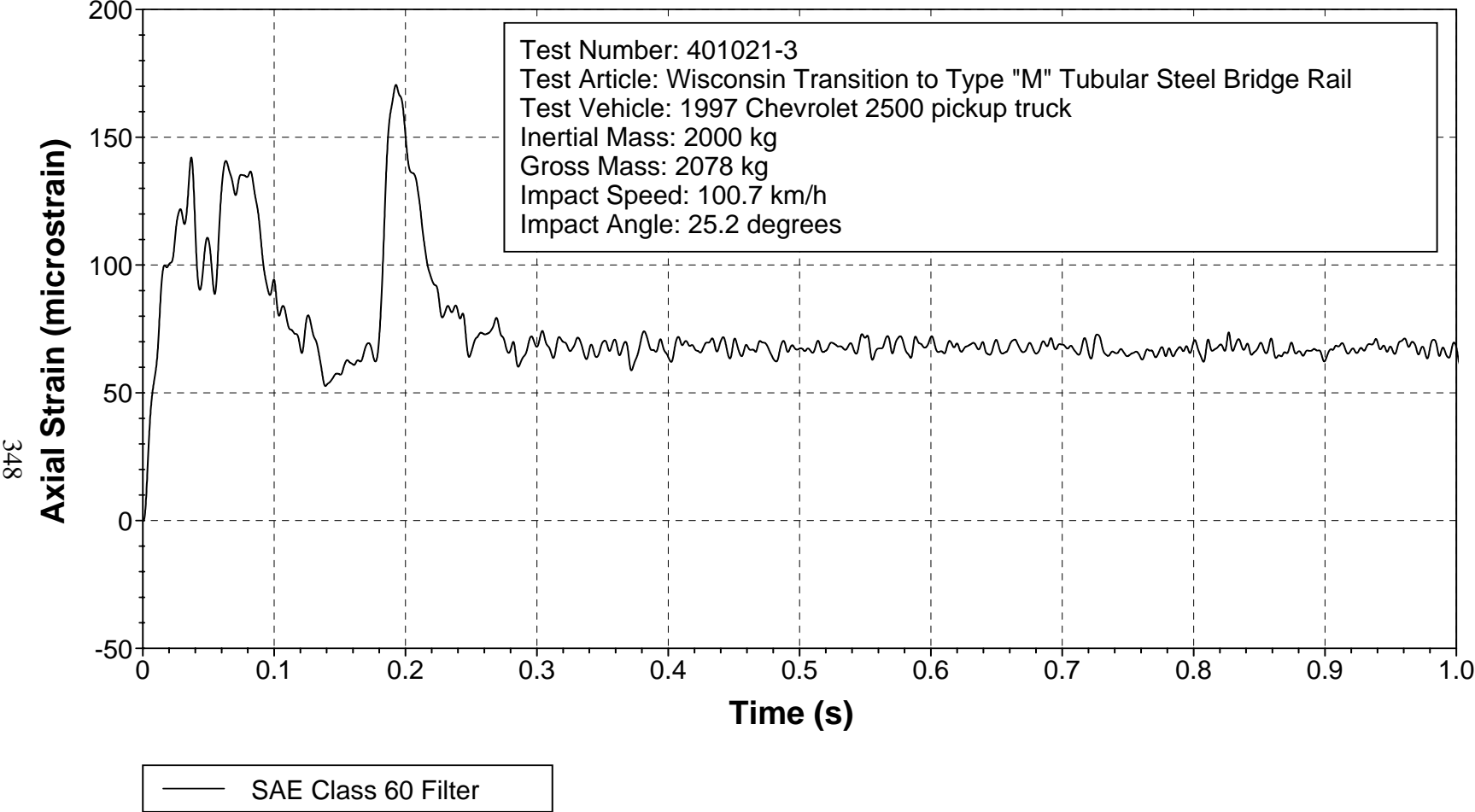


Figure 265. Axial strain, location 4, field side, for test 401021-3.

Gauge Location 5

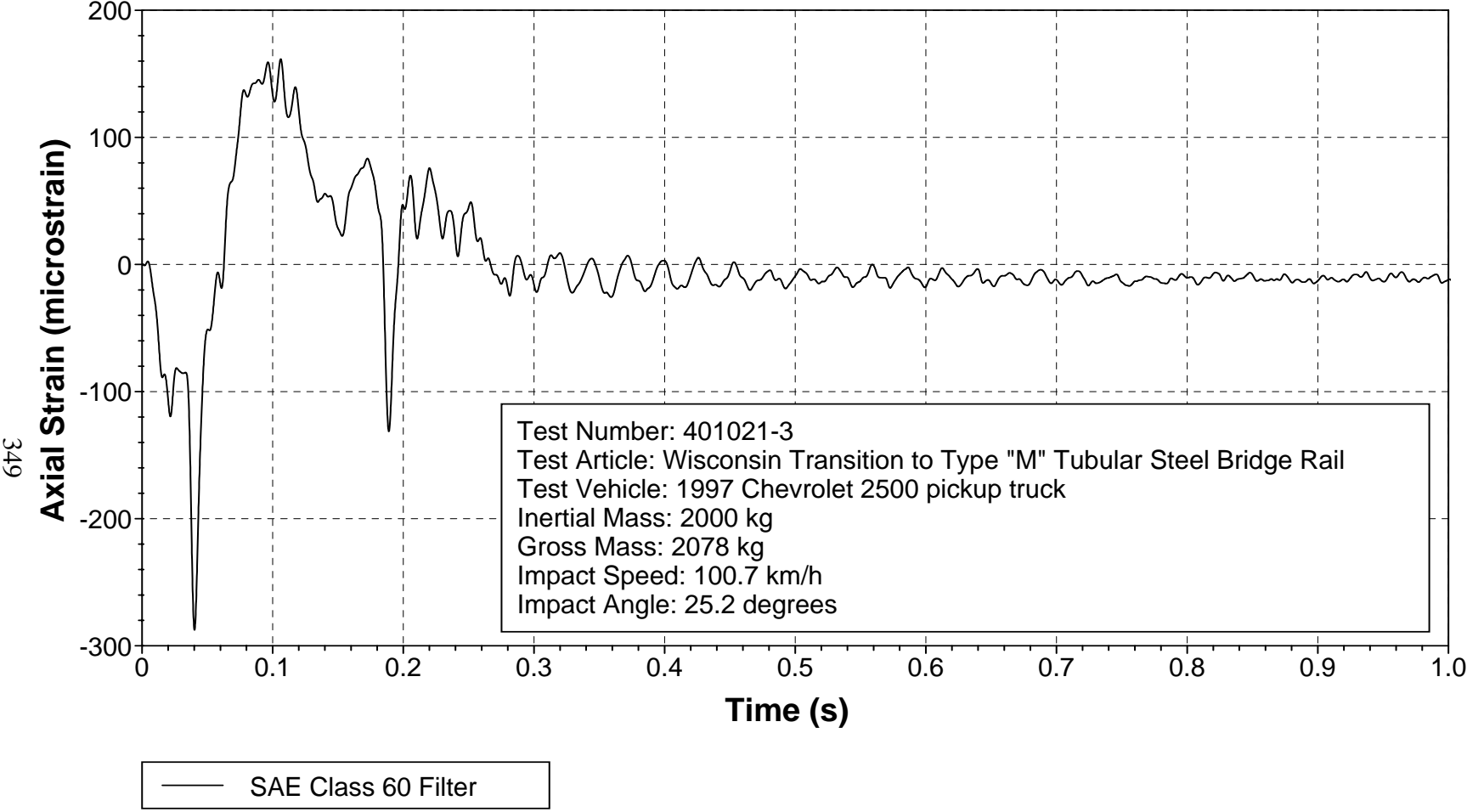


Figure 266. Axial strain, location 5, field side, for test 401021-3.

Gauge Location 6

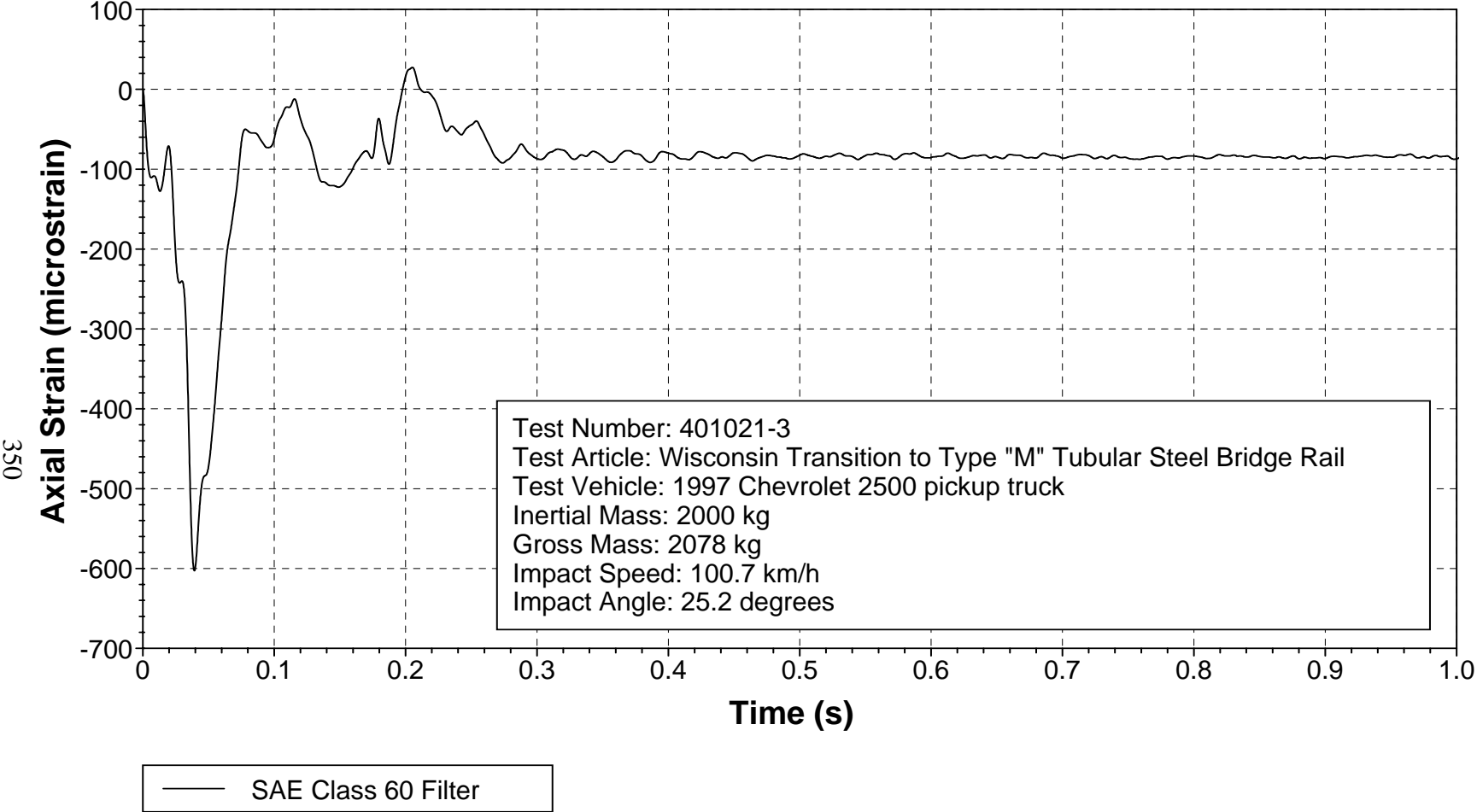


Figure 267. Axial strain, location 6, field side, for test 401021-3.